ORAL IMMUNE-ENHANCING RESEARCH IN FISH

EDITED BY: Jorge Galindo-Villegas, Peter Bossier and Felipe E. Reyes-López
PUBLISHED IN: Frontiers in Immunology

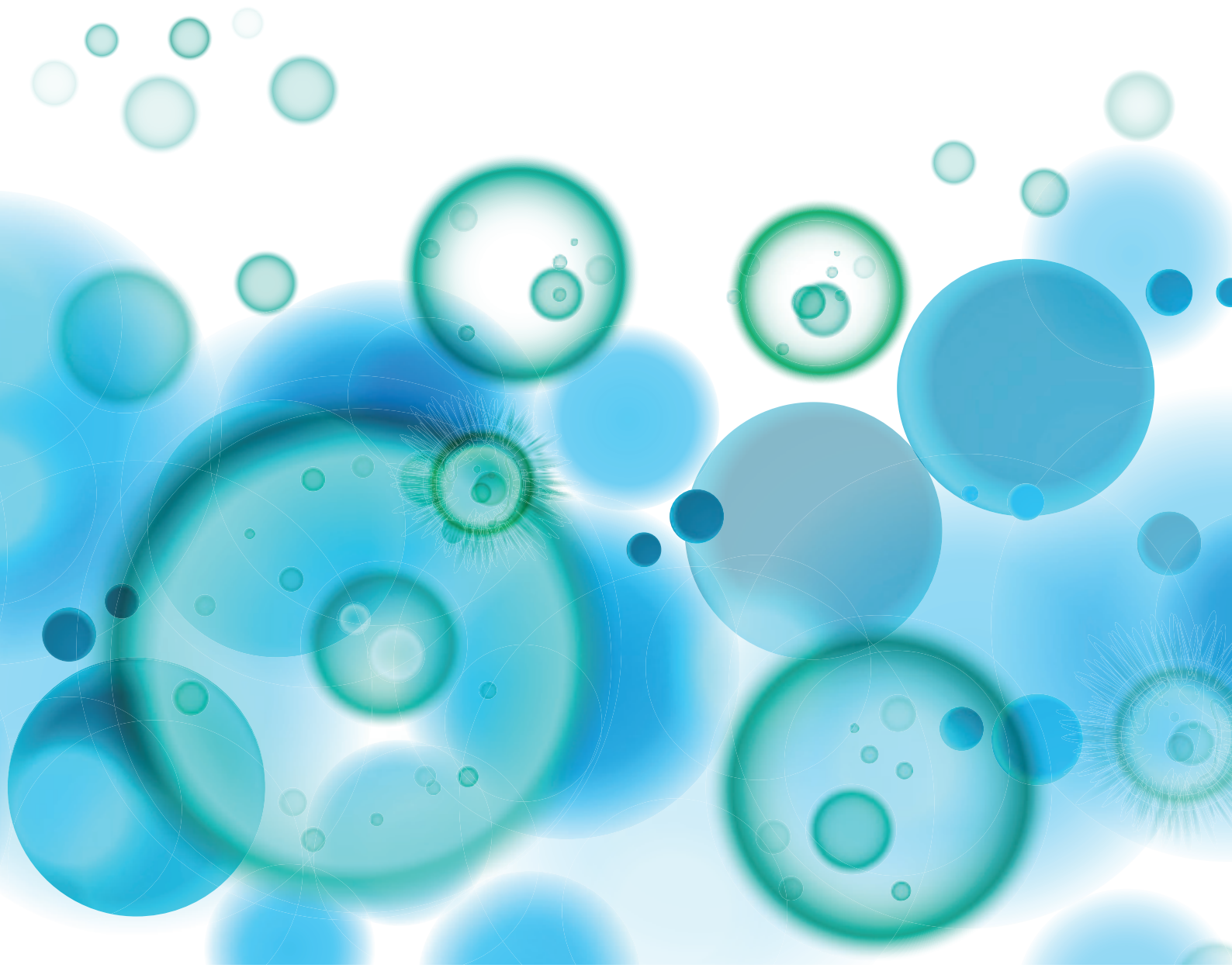

frontiers Research Topics

frontiers

ISSN 1664-8714
ISBN 978-2-88974-875-4
DOI 10.3389/978-2-88974-875-4

About Frontiers

Frontiers is more than just an open-access publisher of scholarly articles: it is a pioneering approach to the world of academia, radically improving the way scholarly research is managed. The grand vision of Frontiers is a world where all people have an equal opportunity to seek, share and generate knowledge. Frontiers provides immediate and permanent online open access to all its publications, but this alone is not enough to realize our grand goals.

Frontiers Journal Series

The Frontiers Journal Series is a multi-tier and interdisciplinary set of open-access, online journals, promising a paradigm shift from the current review, selection and dissemination processes in academic publishing. All Frontiers journals are driven by researchers for researchers; therefore, they constitute a service to the scholarly community. At the same time, the Frontiers Journal Series operates on a revolutionary invention, the tiered publishing system, initially addressing specific communities of scholars, and gradually climbing up to broader public understanding, thus serving the interests of the lay society, too.

Dedication to Quality

Each Frontiers article is a landmark of the highest quality, thanks to genuinely collaborative interactions between authors and review editors, who include some of the world's best academicians. Research must be certified by peers before entering a stream of knowledge that may eventually reach the public - and shape society; therefore, Frontiers only applies the most rigorous and unbiased reviews.
Frontiers revolutionizes research publishing by freely delivering the most outstanding research, evaluated with no bias from both the academic and social point of view. By applying the most advanced information technologies, Frontiers is catapulting scholarly publishing into a new generation.

What are Frontiers Research Topics?

Frontiers Research Topics are very popular trademarks of the Frontiers Journals Series: they are collections of at least ten articles, all centered on a particular subject. With their unique mix of varied contributions from Original Research to Review Articles, Frontiers Research Topics unify the most influential researchers, the latest key findings and historical advances in a hot research area! Find out more on how to host your own Frontiers Research Topic or contribute to one as an author by contacting the Frontiers Editorial Office: frontiersin.org/about/contact

ORAL IMMUNE-ENHANCING RESEARCH IN FISH

Topic Editors:
Jorge Galindo-Villegas, Nord University, Norway
Peter Bossier, Ghent University, Belgium
Felipe E. Reyes-López, Universitat Autònoma de Barcelona, Spain

Citation: Galindo-Villegas, J., Bossier, P., Reyes-López, F. E., eds. (2022). Oral Immune-Enhancing Research in Fish. Lausanne: Frontiers Media SA.
doi: 10.3389/978-2-88974-875-4

Table of Contents

frontiers in Immunology

EDITORIAL
published: 17 March 2022
doi: 10.3389/fimmu.2022.850026

Editorial: Oral Immune-Enhancing Research in Fish

Jorge Galindo-Villegas[1*], *Peter Bossier*[2*] *and Felipe E. Reyes-López*[3,4,5*]

[1] Faculty of Biosciences and Aquaculture, Nord University, Bodø, Norway, [2] Laboratory of Aquaculture & Artemia Reference Center, Department of Animal Science and Aquatic Ecology, Faculty of Bioscience Engineering, Ghent University, Ghent, Belgium, [3] Centro de Biotecnología Acuícola, Facultad de Química y Biología, Universidad de Santiago de Chile, Santiago, Chile, [4] Facultad de Medicina Veterinaria y Agronomía, Universidad de Las Américas, Santiago, Chile, [5] Department of Cell Biology, Physiology and Immunology, Universitat Autònoma de Barcelona, Bellaterra, Chile

Keywords: teleost fish model, Omics, probiotics-immunobiotics, disease enhancement, endobolome, holistic analysis, selective manipulation, microbiome

Editorial on the Research Topic

Oral Immune-Enhancing Research in Fish

INTRODUCTION

Aquaculture is recognized globally as the fastest growing food-producing sector for human consumption (1). However, to satisfy increasing international demand, it is predicted that current production must be doubled by 2030 while improving the biosafety protocols (2). Such an expansion will necessarily involve implementing innovative actions in aquaculture production while also targeting effective health control measures and considering animal welfare.

Diet, environment, and host genotype have been repeatedly demonstrated to play an essential role in defining the fish gut composition (3). However, only a few studies have examined the association between disease severity and degree of dysbiosis in fish. Likewise, the management of pathogens and parasites remains a sustainability challenge industry-wide due to poor understanding of the associated fish immune mechanism across species, and the effects of climate change on aquaculture remain uncertain and complex to validate (4). While these concepts are not necessarily new, applying modern high-throughput sequencing approaches and state-of-the-art immune techniques will accelerate our understanding of the complex trophic (e.g., prokaryotic, eukaryotic) structures, the host recognition systems within aquaculture species and systems, and the effect of an intervention on eventual health outcomes allowing aquaculture to benefit from parallel advances in related disciplines (5).

Among the latest therapies developed, orally administered health promoters have demonstrated a strong ability as critical mediators in enhancing the fish immune system. However, the interaction between each element per fish species is highly complex and not always homogeneous along the different developmental stages. Therefore, to assess the expected potential immunological promotion and enhancement capacity, the use of dedicated, robust, and innovative molecular tools accompanied by keen strategies of analysis devoted to elucidating the mode of action for the tested compounds are required.

By collating evidence, eleven exciting research papers written by 79 authors in our Research Topic entitled "Oral Immune-Enhancing Research in Fish" are presented in this *ebook*. Together, they will provide a platform of discussion in the advancement of the actual knowledge and

OPEN ACCESS

Edited and reviewed by:
Gaetano Isola,
University of Catania, Italy

***Correspondence:**
Jorge Galindo-Villegas
Jorge.galindo-villegas@nord.no
Peter Bossier
peter.bossier@ugent.be
Felipe E. Reyes-López
felipe.reyes@uab.cat

Specialty section:
This article was submitted to Comparative Immunology, a section of the journal Frontiers in Immunology

Received: *07 January 2022*
Accepted: *25 February 2022*
Published: *17 March 2022*

Citation:
Galindo-Villegas J, Bossier P and Reyes-López FE (2022) Editorial: Oral Immune-Enhancing Research in Fish. Front. Immunol. 13:850026. doi: 10.3389/fimmu.2022.850026

understanding beyond the immediate immune effects and the corresponding immune mechanisms in fish fed with functional feed additives, live supplemented feed, or even exposed to oral pollutants that stimulates a differential immune response in the animals under experimental or fish farm settings.

PHYTOGENICS AS SUSTAINABLE HEALTH ENHANCERS IN AQUACULTURE PRODUCTION

The implementation of innovative and sustainable production strategies has proven that plants have the potential to enhance the general physiology of animals. Phytogenics, defined as environmentally friendly plant-derived bioactive compounds, are used as functional feed additives that benefit animal growth and health. These elements often comprise aromatic plants extracts and essential oils rich in biologically active compounds. In farmed fish, a broad spectrum of phytogenics has been studied mainly due to their vast repertoire of properties, including growth promotion, antimicrobial, immunostimulant, antioxidant, anti-inflammatory, and sedative activities. Nevertheless, a pressing issue from using a phytogenic is the impact generated in the mucosal barrier and thus in the fish defense. Despite its enormous potential, establishing the phytogenics mode of action in mucosal tissues is essential for their proper use and safe administration Firmino et al..

Firmino et al. used feed microcapsules containing a blend of garlic essential oil, carvacrol, and thymol. They analyzed the Gilthead seabream skin transcriptional profile with some key skin mucus biomarkers and the resulting pathogenic bacterial growth capacity in the fish external live epithelium. Their results suggest that the phytogen-supplemented diet promoted the secretion of non-specific immune molecules into the skin mucus, causing the decrease of bacterial growth capacity. Likewise, novel transcriptomic enrichment analysis is presented, showing some cellular elements like the phagocytosis linked to the phytogenic treatment. Unfortunately, the exact mechanisms behind the action of the tested elements were not yet unveiled. Lastly, their results suggest that the tested additive could directly affect the intestinal host-microbial community composition that may influence the stress and immunological response in the skin. This observation suggests that the effect of the experimental diet on skin phagocytes and phagocytosis potential are a hot research line that deserves further evaluation.

Torrecillas et al. investigated the effect of two commercial additives in gill health of European sea bass fed with a low fish meal (FM)/low oil (FO) diet. The diets contained galactomannan oligosaccharides (Gmos) and a blend of garlic and labiatae-plant oils (Phyto), while an unsupplemented group served as a control. The morphological, histopathological, immunohistochemical, and biochemical parameters of the fish gills of sea bass given supplemented diets were protected from oxidative stress by modulating the expression patterns of oxidative enzyme-related genes. The diets also lowered the Pcna+ cell counts. It was argued that the reduction in Pcna counts in the gills of the fish-fed Phyto- and Gmos-supplemented diets might be associated with reduced levels of oxidative species via modulation of the endogenous antioxidant capacity. Moreover, Phyto supplementation reduced lamellar fusion, whereas Gmos supplementation reduced goblet cell count by 11% but did not affect the distribution of goblet cells along the primary lamellae. These protective effects could be considered in future prevention strategies against gill mucosal diseases in fish species, especially those sensitive to gill-associated pathogens.

In a different animal model, the gnotobiotic brine shrimp (*Artemia franciscana*), Zheng et al. showed that essential oils of *M. alternifolia* (containing mainly terpinen-4-ol and terpinene) and *L. citrata* (containing mainly citral and limonene) could significantly improve the survival of brine shrimp larvae when bath challenged with pathogenic *V. campbellii*. At the concentrations tested, no direct effect of the essential oils on the pathogen could be detected as revealed by life/dead staining and regrowth tests. The results rather indicated that supplementation of these two EOs enhanced immune gene expression, possibly contributing to protective immunity in brine shrimp larvae against *V. campbellii*. Furthermore, the EOs-regulate the expression of bacterial virulence factors, including decreased swimming motility and biofilm formation *in vitro*. This might contribute in part to protecting of the brine shrimp larvae against pathogenic *V. campbellii in vivo* However, further studies are needed to investigate the underlying protective mechanism of EOs, such as analyzing the expression of a larger panel of immune-related genes. Taken together, this study seems to indicate that essential oils can be part of disease intervention and/or prevention strategy in aquaculture.

SELECTIVE DIETARY MANIPULATION OF THE MICROBIOTA ANALYZED *IN VITRO* AND *IN VIVO* UNDER VARIATED CONTEXTS

Complex microbial communities colonize virtually every surface exposed to the external environment. They include prokaryotes, eukaryotes, and viruses, which provide enormous enzymatic capacity and play a key role in controlling many aspects of host physiology. Remarkably, the aquatic environment possesses an intrinsic aggressiveness due to the impressive number and diversity of microorganisms that coexist per square millimeter. Therefore, understanding the complex relationship between commensal microbes and fish is vital in maintaining healthy physiological homeostasis. Any disruption of this symbiosis (i.e., dysbiosis) can drive inflammation, and even worse, the development of inflammatory diseases (6). Indeed, studies using the 16s rRNA amplicon sequencing strategy have provided evidence that some pathologies are complex multifactorial diseases characterized by a profound dysbiosis of the microbial community. As a good example, in Atlantic salmon, it has been demonstrated that yellow mouth disease is dominated by distinct amplicon sequenced variants of

Tenacibaculum maritimum, together with opportunistic taxa, including *Vibrio* spp., play a role in the clinical disease progression (7). Several strategies to generate a positive loop in maintaining host health through microbiota management have been proposed. Among the diverse strategies to selectively manipulate host-microbe interactions, diet is a significant factor that shapes the proportional representation of the microbiota present, particularly in the gut and their relative gene content (8). Reciprocally, the microbiota configuration influences the nutritional value of food Montalban-Arques et al. Although these approaches are particularly promissory, a critical issue determining a successful output from the potential promoters expected on providing solid immune indicators and showing a reliable disease enhancement at the time of dissecting responses is the robustness of the employed assays. In this special issue, we put forward solid pieces of research providing reliable evidence on the host-microbe relationships and the dietary manipulatory capacity.

The study performed by Firmino et al. presents an integrative analysis linking the gene transcriptional activity with the microbiota responses in the gut of gilthead seabream. The fish were fed with a regular diet supplemented with a functional feed containing microencapsulated essential oils from garlic, carvacrol, and thymol. The formula displayed an extensive holistic capacity of modulating the immune response and the microbial composition towards a beneficial profile characterized by the decrease in the classes *Bacteroidia* and *Clostridia*. Likewise, the feed additives increased the bacterial sequences associated with glutathione and lipid metabolism. Therefore, the study provides new insights into host-microbial metabolism's shared role in building up a local immune response and crosstalk between gut and microbiota.

So far, the major challenge has been to understand the poorly studied signals and mechanisms of leukocytes after the addition of novel feed ingredients and their interaction with the microbiome at mucosal interphases in fish. Due to the unique characteristics displayed by the zebrafish model, exciting and solid progress in the recognition of new dietary elements and the associated mechanisms in the complex development and function of leukocytes and other types of cells with immune capacity has been documented (9). Here, Xie et al. using the powerful zebrafish as a model of intestinal inflammation show that excessive recruitment of leukocytes triggered by soybean meal can be reverted by applying a dietary sinomenine therapy. Sinomenine is an agonist of alpha7 nicotinic acetylcholine receptor (α7nAchR), a critical mediator controlling neuro-immune functions with anti-inflammatory properties through nicotine. Treated animals resulted with a higher proportion of CD4+ or Foxp3+ lymphocytes in the base of the intestinal folds, suggesting a synergy between α7nAchR and regulatory T-cells (Treg) in the response. Moreover, reduced enteritis and increased glucose metabolism were associated with the shift of *Sphingomonas* and *Shigella* composition and the increase in *Cetobacterium* biomass, suggesting that sinomenine can prevent fish foodborne enteritis at the immune or microbiota levels.

To gain further insights on the impact that dietary modulators have over the host commensal microorganisms and immunity, Castejón et al. investigated the integral role of the microbiota upon immunity and antibody processing in response to an extended endocrine disruptor in the aquatic environment in the Gilthead seabream. Specifically, the 17α-ethinylestradiol (EE_2) and the agonist G protein-coupled estrogen receptor agonist G-1 (G1) in the gut of gilthead seabream. Humoral lytic and oxidative stress response, essential mucosal inflammatory marker genes, and goblet cells contribution to immunity at the gut mucosal surface were explored. Additionally, the microbiome landscape on the immune repertoire following the dietary treatment and a priming immunization protocol using a model antigen (KLH) was revealed. Minor changes were observed on the stress markers or the gene expressions. However, the dietary treatment with EE2 combined with the immunization promoted remarkable changes in the bacterial class Betaproteobacteria and, unexpectedly, on the estrogen-degrading genus *Novosphingobium* a major member of the endobolome. Overall, this study highlighted the intrinsic relationship between xenoestrogens and their associated receptors in the ubiquitous fish immune regulation. Moreover, the subtle but significant crosstalk with the fish gut endobolome was described in fish for the first time.

There is an increasing consensus of the relevance for evaluating *in vitro* the biological mode of action of isolated compounds before moving forward to *in vivo* trials Firmino et al.. From the immunomodulatory point of view, amino acids (AA) are crucial components in the biosynthesis of immune support-associated molecules. In fish, several articles reported the effect of the dietary administration of AA on a spectrum of immune-related functions (10), with no particular attention on the cell-specific modulatory mechanisms. Thus, this necessitates *in vitro* studies that provide fast lights about the response dynamic for specific immune cell subsets prior to the *in vivo* stage. Machado et al. showed that methionine and tryptophan perform distinct roles in the immune response of head kidney leukocytes (HKL). While L-methionine increased the modulation of the expression of pro-inflammatory gene markers, tryptophan augmented the expression of the anti-inflammatory counterparts. However, the increase was only perceived when the HKL were exposed to lipopolysaccharides-extracted or UV-inactivated *Photobacterium damselae* subsp. *pisicida (Phdp)*. Exposing HKL to *Phdp* produces and releases an exotoxin that induces apoptosis. Therefore, the exposure of HKL to the exotoxin resulted in a diminished signal of apoptosis in the L-methionine-incubated cells. Meanwhile, the L-tryptophan group showed a pro-apoptotic activity by the elevated expression of the initiator *caspase 8* and an increased activity of caspase 3, suggesting a lowered resilience in the L-tryptophan-treated HKL in response to the infection by *Phdp*.

CLASSIC PROBIOTIC BACTERIA, IMMUNOSTIMULANTS, AND NOVEL RECOMBINANT PROTEINS

Probiotics and immunostimulants have been used as preventive strategies for limiting and controlling fish diseases. Probiotics

supplementation is aimed to maximize the profit from the crosstalk between the host and the commensal microbiota for improving the fish robustness and resilience. The study of Muñoz et al. used the *Lactococcus lactis* – a commensal bacteria found in mammals and salmonids, for producing the recombinant type Ia interferon (rIFN-Ia). Likewise, its role in protecting against the infectious pancreatic necrosis virus (IPNV) following *in vitro* and *in vivo* strategies was assessed. The study showed *in vitro* upregulation of antiviral genes (*mx*; *pkr*) after the administration of different doses of rIFN-IA and a reduction of the IPNV viral load determined through qPCR. The oral administration of Atlantic salmon (*Salmo salar*) with the *L. lactis* rIFN-Ia, revealed a higher expression of antiviral-related genes in spleen rather than head kidney. In addition, it showed a lower IPNV load in live Atlantic salmon even up to 60 days post-infection, suggesting that this oral strategy improved the antiviral response. Adopting a similar strategy, Santibañez et al. evaluated the effect of the *L. lactis* recombinant rIFN-γ-producer oral administration on rainbow trout (*Oncorhynchus mykiss*) through a challenge against 10^8 CFU of *F. psychrophilum*. The higher survival rate on rainbow trout fed *L. lactis* rIFN-γ suggests that this application would be a useful novel strategy for conferring oral protection to fish against the infection of some extracellular bacterial pathogens. However, further evaluations of the system *in vivo* and using variated developmental stages are required.

On the other hand, yeasts are considered immune modulators since they contain β-glucan, mannans, chitin, and nucleic acids, that can be recognized as microbial-associated molecular patterns (MAMPs) by pattern recognition receptors (PRRs) with high capacity of training the innate memory in fish myelocytes Zhang et al. The study of Morales-Lange et al. used the *Cyberlindnera jadinii* yeast in a 40% soybean meal (SBM) diet. The perspective of the study is interesting because they propose the use of the spleen to evaluate the effect of the novel diet fed in Atlantic salmon (*Salmo salar*). The study includes the evaluation of the immune response by RNAseq and indirect ELISA. Furthermore, the *C. jadinii* was exposed to two different down-stream processing conditions: heat-inactivated (ICJ), or autolysation (ACJ). In line with previous effects reported in the intestine after the dietary administration of SBM, these authors confirmed the pro-inflammatory status in spleen, being characterized by the increased TNFα and IFNγ levels recorded. Notably, ACJ response was characterized by the increasing level of IL-10 and the diminished content of TNFα. hus, the authors suggest using ACJ as a component in the formulation of diets for sustainable Atlantic salmon farming.

β-glucans have been extensively used in the aquaculture industry. However, the species-specificity, length of their side chains, and frequency of administration have depicted a variable role in immunomodulation, showing differences between short- and long-treatments, including the modulation of stress-associated mechanisms and immunosuppression. Cornet et al. proposed the use of Gas1a β-glucan produced by the null-mutant yeasts Gas1 of *Saccharomyces cerevisiae*, as new immunostimulant to protect rainbow trout (*Oncorhynchus mykiss*) juveniles against *Aeromonas salmonicida achromogenes* infection. For comparison purposes, the study included three β-glucan preparations: wild-type (WT), MacroGard, and the novel Gas1, evaluated at two time points after feeding the animals. Unexpectedly, after 36 days, the dietary supplementation with MacroGard resulted in the downregulation of immune genes and the lysozyme activity, immunoglobulin production and neutrophils proliferation in comparison to Gas1. The resulting immune status produced by Gas1 correlated with a higher survival rate against *A. salmonicida*. Moreover, the survival rate difference between Gas1 and WT suggests lower degree of branching and shorter side chain length may be the responsible in the differences observed in the efficiency of the immuno-stimulation between both β-glucan preparations.

Overall, the contributions gathered in this Research Topic provide holistic evidence on various mechanisms associated with oral immune enhancement of fish at the cellular and immune level, propose methods on the selective manipulation of the gut microbiota, and more importantly, deal on how to provide an increased health status and disease resistance in cultured teleost fish. By putting this information together, we hope to contribute to improving fish aquaculture by providing new concepts and research trends. Notably, we intend to provide evidence that by utilizing robust methodologies accompanied with robust analytical strategies, functional, exciting novel findings and future research perspectives could undoubtedly be achieved.

AUTHOR CONTRIBUTIONS

All authors listed have made a substantial, direct, and intellectual contribution to the work, and approved it for publication.

ACKNOWLEDGMENTS

To the Frontiers in Immunology Journal for allowing us to serve as guest editors on the present special issue targeting the oral immune-enhancing research in fish. To all the different international authors who independently of the output showed interest and participated with the external reviewers and appointed editors in this exciting journey.

REFERENCES

1. FAO. The State of World Fisheries and Aquaculture 2020. In:. *Sustainability in Action* Rome. (2020). doi: 10.4060/ca9229en
2. Acosta F, Montero D, Izquierdo M, Galindo-Villegas J. High-Level Biocidal Products Effectively Eradicate Pathogenic γ-Proteobacteria Biofilms From Aquaculture Facilities. *Aquaculture* (2021) 532:736004. doi: 10.1016/j.aquaculture.2020.736004
3. Bozzi D, Rasmussen JA, Carøe C, Sveier H, Nordøy K, Gilbert MTP, et al. Salmon Gut Microbiota Correlates With Disease Infection Status: Potential for Monitoring Health in Farmed Animals. *Anim Microbiome* (2021) 3:30. doi: 10.1186/s42523-021-00096-2
4. Naylor RL, Hardy RW, Buschmann AH, Bush SR, Cao L, Klinger DH, et al. Troell M. A 20-Year Retrospective Review of Global Aquaculture. *Nature* (2021) 591:551–63. doi: 10.1038/s41586-021-03308-6

5. Stentiford GD, Sritunyalucksana K, Flegel TW, Williams BAP, Withyachumnarnkul B, Itsathitphaisarn O, et al. New Paradigms to Help Solve the Global Aquaculture Disease Crisis. *PloS Pathog* (2017) 13:e1006160. doi: 10.1371/journal.ppat.1006160
6. Galindo-Villegas J, García-Moreno D, de Oliveira S, Meseguer J, Mulero V. Regulation of Immunity and Disease Resistance by Commensal Microbes and Chromatin Modifications During Zebrafish Development. *Proc Natl Acad Sci USA* (2012) 109:E2605–14. doi: 10.1073/pnas.1209920109
7. Wynne JW, Thakur KK, Slinger J, Samsing F, Milligan B, Powell JFF, et al. Microbiome Profiling Reveals a Microbial Dysbiosis During a Natural Outbreak of Tenacibaculosis (Yellow Mouth) in Atlantic Salmon. *Front Microbiol* (2020) 11:586387:586387. doi: 10.3389/fmicb.2020.586387
8. Ngowi EE, Wang Y-Z, Khattak S, Khan NH, Mahmoud SSM, Helmy YASH, et al. Impact of the Factors Shaping Gut Microbiota on Obesity. *J Appl Microbiol* (2021) 131:2131–47. doi: 10.1111/jam.15036
9. Galindo-Villegas J. Recent Findings on Vertebrate Developmental Immunity Using the Zebrafish Model. *Mol Immunol* (2016) 69:106–12. doi: 10.1016/j.molimm.2015.10.011
10. Oliva-Teles A. Nutrition and Health of Aquaculture Fish. *J Fish Dis* (2012) 35:83–108. doi: 10.1111/j.1365-2761.2011.01333.x

Conflict of Interest: The authors declare that the research was conducted without any commercial or financial relationships that could be construed as a potential conflict of interest.

Publisher's Note: All claims expressed in this article are solely those of the authors and do not necessarily represent those of their affiliated organizations, or those of the publisher, the editors and the reviewers. Any product that may be evaluated in this article, or claim that may be made by its manufacturer, is not guaranteed or endorsed by the publisher.

frontiers in Immunology

ORIGINAL RESEARCH
published: 04 March 2021
doi: 10.3389/fimmu.2021.625297

Diet, Immunity, and Microbiota Interactions: An Integrative Analysis of the Intestine Transcriptional Response and Microbiota Modulation in Gilthead Seabream (*Sparus aurata*) Fed an Essential Oils-Based Functional Diet

Joana P. Firmino[1,2,3], Eva Vallejos-Vidal[4], M. Carmen Balebona[5], Yuliaxis Ramayo-Caldas[6], Isabel M. Cerezo[5], Ricardo Salomón[1,3], Lluis Tort[7], Alicia Estevez[1], Miguel Ángel Moriñigo[5], Felipe E. Reyes-López[7,8,9] and Enric Gisbert[1]**

[1] IRTA, Centre de Sant Carles de la Ràpita (IRTA-SCR), Aquaculture Program, Sant Carles de la Ràpita, Spain, [2] TECNOVIT–FARMFAES, S.L. Alforja, Spain, [3] Ph.D. Program in Aquaculture, Universitat Autònoma de Barcelona, Barcelona, Spain, [4] Departamento de Biología, Facultad de Química y Biología, Centro de Biotecnología Acuícola, Universidad de Santiago de Chile, Santiago, Chile, [5] Department of Microbiology, Faculty of Science, University of Malaga, Málaga, Spain, [6] Animal Breeding and Genetics Program, Institute of Agrifood Research and Technology, Torre Marimon, Caldes de Montbui, Spain, [7] Department of Cell Biology, Physiology and Immunology, Universitat Autònoma de Barcelona, Barcelona, Spain, [8] Facultad de Medicina Veterinaria y Agronomía, Universidad de Las Américas, Santiago, Chile, [9] Consorcio Tecnológico de Sanidad Acuícola, Ictio Biotechnologies S. A., Santiago, Chile

Essential oils (EOs) are promising alternatives to chemotherapeutics in animal production due to their immunostimulant, antimicrobial, and antioxidant properties, without associated environmental or hazardous side effects. In the present study, the modulation of the transcriptional immune response (microarray analysis) and microbiota [16S Ribosomal RNA (rRNA) sequencing] in the intestine of the euryhaline fish gilthead seabream (*Sparus aurata*) fed a dietary supplementation of garlic, carvacrol, and thymol EOs was evaluated. The transcriptomic functional analysis showed the regulation of genes related to processes of proteolysis and inflammatory modulation, immunity, transport and secretion, response to cyclic compounds, symbiosis, and RNA metabolism in fish fed the EOs-supplemented diet. Particularly, the activation of leukocytes, such as acidophilic granulocytes, was suggested to be the primary actors of the innate immune response promoted by the tested functional feed additive in the gut. Fish growth performance and gut microbiota alpha diversity indices were not affected, while dietary EOs promoted alterations in bacterial abundances in terms of phylum, class, and genus. Subtle, but significant alterations in microbiota composition, such as the decrease in *Bacteroidia* and *Clostridia* classes, were suggested to participate in the modulation of the intestine transcriptional immune profile observed in fish fed the EOs diet. Moreover, regarding microbiota functionality, increased bacterial sequences associated with glutathione and lipid metabolisms, among others, detected in fish fed the EOs supported the metabolic alterations suggested to potentially affect the observed

OPEN ACCESS

Edited by:
Michiko Oyoshi,
Boston Children's Hospital and Harvard Medical School, United States

Reviewed by:
Yue Zhang,
Johns Hopkins Medicine, United States
Martha Reyes-Becerril,
Centro de Investigación Biológica del Noroeste (CIBNOR), Mexico
Francisco Guardiola,
University of Murcia, Spain

***Correspondence:**
Enric Gisbert
Enric.Gisbert@irta.cat
Felipe E. Reyes-López
Felipe.Reyes@uab.cat

Specialty section:
This article was submitted to Nutritional Immunology, a section of the journal Frontiers in Immunology

Received: 02 November 2020
Accepted: 28 January 2021
Published: 04 March 2021

Citation:
Firmino JP, Vallejos-Vidal E, Balebona MC, Ramayo-Caldas Y, Cerezo IM, Salomón R, Tort L, Estevez A, Moriñigo MÁ, Reyes-López FE and Gisbert E (2021) Diet, Immunity, and Microbiota Interactions: An Integrative Analysis of the Intestine Transcriptional Response and Microbiota Modulation in Gilthead Seabream (Sparus aurata) Fed an Essential Oils-Based Functional Diet. Front. Immunol. 12:625297. doi: 10.3389/fimmu.2021.625297

immune-related transcriptional response. The overall results indicated that the tested dietary EOs may promote intestinal local immunity through the impact of the EOs on the host-microbial co-metabolism and consequent regulation of significant biological processes, evidencing the crosstalk between gut and microbiota in the inflammatory regulation upon administration of immunostimulant feed additives.

Keywords: gut-associated lymphoid tissue, microbiota, additive, functional feed, aquaculture, oral immmunization, teleost, gut immune crosstalk

INTRODUCTION

In the post-antibiotics era, concerns about the potential loss of productivity due to an increase of infectious diseases are a reality within the animal production sector. The production of aquatic protein through aquaculture is not an exception. Regarding the aquaculture industry, the increasing pathogen resistance to chemotherapeutic treatments and their use restrictions, along with the rising public awareness regarding food safety, environmental impact, and animal welfare, have encouraged the development of alternative dietary treatments, such as functional feeds (1). Similarly, to livestock, functional feed additives may benefit farmed fish through the regulation of the host metabolism, nutrient absorption, and enhancement of host performance. Furthermore, it may activate the immunity of the host either by direct stimulation of the innate immune system or through the sustenance of commensal microorganisms and inhibition of pathogens in the intestinal tract (2). These factors, either individually or combined, may have a profound impact on key performance indicators. For instance, fish farmers recognize the direct effect of health promotion through feed in their economic gain by the improvement of key performance indicators (i.e., improving somatic growth, reducing feed conversion rates, promoting host welfare, and diminishing morbidity, among others). The wide array of potential benefits derived from functional feed additives and nutraceuticals has focused the light on their study and validation in aquafeeds. Among functional feed additives, phytogenics consist of a heterogeneous group of plant-derived products widely used in animal nutrition. Essential oils (EOs), a blend of organic substances synthesized by aromatic plants during secondary metabolism, whose chemical composition may vary according to plant and environment characteristics and/or extraction procedures, are the most common class of phytogenics used in livestock nutrition as well as in aquafeeds. EOs have been increasingly studied as promising chemotherapeutic alternatives due to their antimicrobial, immunostimulant, antioxidant, anti-stress, and growth-promoting properties, without associated environmental or hazardous side effects. In addition, there is also evidence that EOs may exert a positive impact on the gut health of livestock, including aquaculture relevant fish species (3). Particularly, some studies have recently reported the advantageous outcomes of the dietary administration of garlic (4), carvacrol, and/or thymol (5) in the gut health of aquatic species, which suggest them as interesting phytogenic targets for aquafeed additive development.

During the last years, the concept of "gut health" has become a trending topic due to its significance on the nutrition, metabolism, immunity, pathogen control, welfare, behavior, and performance of the host. Despite the term not being well-defined in the literature and perhaps having a subjective definition, the key components of this term in animal production are: (i) the diet, (ii) the functional structure of the mucosal barrier, (iii) an effective digestion and absorption of nutrients, (iv) an appropriate and stable microbiota, and (v) an effective immunity (6). Similar to higher vertebrates, teleost fish have a specialized and sophisticated gut immune system, although a significant variation is observed in the gastrointestinal tract of different species according to their nutritional requirements (7). The intestinal mucosal layer (including the mucus and the epithelial cells) form an important physical and biochemical defense barrier against exogenous substances, such as bacteria, toxins, and allergens. It also participates in the local immune response through the recognition and processing of antigens, the recruitment of innate and adaptive immune cells, and the secretion of cytokines, chemokines, antimicrobial peptides, and mucins through the gut-associated lymphoid tissue (GALT) (2).

A key actor in gut integrity and functionality is the microbial community that colonizes it. In this sense, the gut commensal microbiota, besides protecting the host against pathogenic bacteria invasion, are able to modulate the gene expression of processes involved in the stimulation of epithelial proliferation, nutrient metabolism, and innate immune responses, promoting intestinal homeostasis (3). Under this context, any interference on the intestinal mucosal barrier integrity and/or the microbiota composition may impair gut condition and health, leading to disease-related dysbiosis (8). An increasing body of evidence supports the general assumption that feed additives can influence considerably the fish gut condition, affecting the intestinal epithelium, microbiota, and mucosal immunity (2). There is also evidence that fish innate and adaptive immune system may influence the regulation and composition of the gut microbiota and *vice versa*. Such interactions are not clearly deciphered so far, especially in lower vertebrates (8). In this way, functional genomics studies provide a wide range of applications that allows an increased and better understanding of the mechanisms underlying this symbiosis. Consequently, this information is of paramount importance for deciphering the mode of action of feed additives and their proper dietary administration.

Under this context, the present study aimed to evaluate the intestinal tissue transcriptional activity and microbiota responses in the gut of the euryhaline fish gilthead seabream (*Sparus aurata*)

fed a functional feed additive consisting of a microencapsulated blend of garlic, carvacrol, and thymol EOs. Additionally, the authors also sought to provide new insights about the shared role of host-microbial co-metabolism in building-up a local immune response promoted by the tested feed additive.

MATERIALS AND METHODS

Rearing Conditions

Gilthead seabream fry (body weight, BW = 5.0 ± 0.2 g; mean ± SD) were purchased from Piscicultura Marina Mediterránea S.L. (Andromeda Group, Valencia, Spain) and transported to the research facilities of the Institute of Agrifood Research and Technology (IRTA) in Sant Carles de La Ràpita (Tarragona, Spain). Fish were randomly distributed among six tanks (450 L capacity) connected to the IRTAmar® recirculation system (5–10% water replacement per day for compensating evaporation and siphoning losses) in order to keep water quality through UV, biological, and mechanical filtration. At the beginning of the trial, 150 juveniles (25 fish per tank; initial density = 2 kg m^{-3}) were individually measured in body weight (BW, g) and standard length (SL, mm) to the nearest 0.1 g and 1 mm, respectively (BW = 40.3 ± 0.1 g; SL = 12.0 ± 0.2 mm). This assay took place under natural photoperiod, with daily monitoring of the water temperature (25.1 ± 1.5°C), oxygen (6.8 ± 1.7 mg/L; >80% saturation) (OXI330, Crison Instruments, Barcelona, Spain), and pH (7.5 ± 0.01) (pHmeter 507, Crison Instruments), whereas salinity (35‰) (MASTER-20 T; ATAGO Co. Ltd), ammonia (0.13 ± 0.1 mg NH_4^+/L), and nitrite (0.18 ± 0.1 mg NO_2^-/L) levels (HACH DR9000 Colorimeter, Hach®, Spain) were weekly controlled.

Diets and Feeding Trial

Diets were manufactured by Sparos Lda. (Olhão, Portugal) as follows: main ingredients were ground (below 250 μm) in a micropulverizer hammer mill (SH1; Hosokawa Micron, B.V., Doetinchem, The Netherlands). Powder ingredients and oils were then mixed according to the target formulation in a paddle mixer (RM90; Mainca, S.L., Granollers, Spain). After extrusion (2 mm pellet size), all feed batches were dried in a convection oven (OP 750-UF; LTE Scientifics, Oldham, UK) for 4 h at 45°C.

A basal (control) diet was formulated with high levels of marine-derived protein sources to contain 46% crude protein, 18% crude fat, and 21.5 MJ/kg gross energy (**Table 1**) as described in Firmino et al. (9). The second experimental diet was the control diet supplemented with 0.5% of the functional additive composed of a blend of microencapsulated garlic, carvacrol, and thymol synthetic EOs (AROTEC-G®, TECNOVIT-FARMFAES, S.L., Spain). When dealing with feed additives, especially EOs, their proper and controlled administration is of special importance. Thus, encapsulation technology was used for EOs incorporation into the experimental diet in order to improve its bioavailability and efficacy, as well as the standardization of its dosing in order to avoid variability and discrepancies among studies (10).

Diets were tested for 65 days in a feeding trial carried out in triplicate tanks. Fish were hand-fed two times per day at the daily rate of 3.0% of the stocked biomass, which approached apparent satiation. At the end of the trial, all the fish in each tank were netted, anesthetized (buffered 150 mg/L MS-222, Sigma-Aldrich, Spain), and measured for BW and SL. We calculated different performance parameters: specific growth rate (SGR; % BW/day) = 100 × (ln BWf – ln BWi)/days (where BWf and BWi represented the final and the initial body weights, respectively). Fulton's condition factor (K) = (BWf/SLf ^{3}) × 100 (where SLf was the final SL). This is a morphometric index that estimates the body condition of fish, assuming that heavier fish of a given length are in better condition (11).

In addition, four fish were randomly selected from each tank, euthanized with an overdose of the abovementioned anesthetic, and their gut removed. For transcriptional analysis purposes, a small section of the mid-anterior intestine from each fish was dissected, placed in RNAlater™ (Invitrogen, Thermo Fisher Scientific, Lithuania), incubated overnight (4°C), and stored at −80°C until further RNA extraction. There is evidence that the mid-anterior section of the fish intestine has a specialized immunological functionality when compared with other intestinal sections (12). The remaining sections of the anterior and posterior intestine were frozen separately in dry ice and stored at −80°C for further microbiota analysis.

Transcriptional Analysis

RNA Isolation and Quality Control

Gilthead seabream mid-anterior intestine samples were randomly selected per dietary treatment. Total RNA was extracted individually using the RNeasy® Mini Kit (Qiagen, Germany) and eluted (final volume = 35 μl) in nuclease-free water and treated with DNAse (DNA-free™ DNA Removal Kit; Invitrogen, Lithuania). Total RNA concentration and purity were quantified using a Nanodrop-2000® spectrophotometer (Thermo Scientific, USA) and stored at −80°C. Prior to hybridization with microarrays, RNA samples were checked for RNA integrity (Agilent 2100 Bioanalyzer; Agilent Technologies, Spain) and selected by the criteria of a RIN value >8.5. Three different pools of samples per dietary treatment were established ($n = 4$ fish each).

Microarrays

A transcriptional analysis for the intestine from both experimental groups was carried out using the Aquagenomics *S. aurata* oligonucleotide microarray v2.0 (4 × 44 K) (SAQ) platform. Detailed information and transcriptomic raw data are available at the Gene Expression Omnibus (GEO) public repository at the U.S. National Center for Biotechnology Information (NCBI), accession numbers GPL13442 and GSE159643, respectively. The sampling labeling, hybridization, washes, and scanning were performed as described before (9). For this purpose, a one-color RNA labeling was used (Agilent One-Color RNA Spike-In Kit; Agilent Technologies, USA). RNA from each sample pool (200 ng) was reverse-transcribed together with the RNA spike-in. Then, total RNA was used as a template for Cyanine-3 (Cy3) labeled cRNA synthesis and amplification with the Quick Amp Labeling Kit (Agilent Technologies). cRNA samples were purified using the RNeasy Micro Kit (Qiagen). Dye

TABLE 1 | Formulation and proximate composition of the basal diet.

Ingredients	Basal diet (%)
Fishmeal 70 LT FF Skagen	20.0
Fishmeal CORPESCA Super Prime	10.0
CPSP 90	2.5
Squid meal	2.5
Soy protein concentrate (Soycomil)	5.0
Wheat gluten	5.0
Corn gluten	8.0
Korfeed 60	4.5
Soybean meal 48	8.0
Rapeseed meal	4.0
Sunflower meal	3.0
Wheat meal	7.0
Whole peas	2.5
Fish oil—COPPENS	9.0
Soybean oil	1.5
Rapeseed oil	2.5
Vitamin and mineral Premix PV01	2.0
Soy lecithin—powder	2.0
Antioxidant powder (Paramega)	0.4
Dicalcium phosphate	0.6
TOTAL	100.0
Proximate composition, % in dry basis	
Crude protein	46.2
Crude fat	18.4
Gross Energy	21.5

incorporation and cRNA yield were checked (NanoDrop ND-2000® spectrophotometer). Then, Cy3-labeled cRNA (1.5 mg) with specific activity > 6.0 pmol Cy3/mg cRNA was fragmented at 60°C for 30 min, and hybridized with the array in presence of a hybridization buffer (Gene Expression Hybridization Kit, Agilent Technologies) at 65°C for 17 h. For washes, microarrays were incubated with Gene Expression wash buffers and stabilization and drying solution according to the manufacturer's instructions (Agilent Technologies). Microarray slides were then scanned (Agilent G2505B Microarray Scanner System), and spot intensities and other quality control features were extracted (Agilent Feature Extraction software version 10.4.0.0).

Intestine Functional Analysis: The Search Tool for the Retrieval of Interacting Genes

The Search Tool for the Retrieval of Interacting Genes (STRING) public repository version 11.0 (https://string-db.org) was used to generate the transcripteractome that takes place in the intestine of fish fed the EOs-supplemented diet. A Protein–Protein interaction (PPI) Networks Functional Enrichment Analysis for all the differentially expressed genes (DEGs) was conducted with a high-confidence interaction score (0.9) using *Homo sapiens* as model organism. Gene ontology (GO) enrichment analysis ($p < 0.05$) was also assessed including all the DEGs obtained. To confirm gene orthologs and match gene acronyms between both *H. sapiens* and gilthead seabream species, protein BLAST was run, and the GeneCards (www.genecards.org) and UniProt (www.uniprot.org) databases were accessed as described in Firmino et al. (9).

Intestinal Microbiota

DNA Extraction

Samples were thawed gradually on ice, and the intestinal contents were extracted by pressing toward the ends with a sterile object. After homogenizing the content, a sample (50 mg) was taken for DNA extraction following the protocol based on saline precipitation (13). DNA concentration was quantified fluorometrically with the Qubit™ dsDNA HS Assay Kit (Thermo Fisher Scientific, Waltham, MA, USA) and its purity and integrity assessed using a NanoDrop™ One UV-Vis Spectrophotometer WiFi (Thermo Scientific, USA) and through an agarose gel electrophoresis.

Amplicon Sequencing of 16S Ribosomal RNA and Sequence Data Processing

The 16S rRNA of samples were sequenced on an Illumina® MiSeq platform (Illumina, San Diego, CA, USA) with 2 × 300 bp paired-end sequencing in the Ultrasequencing Service of the Bioinnovation Center of University of Málaga (Málaga, Spain). Sequencing was carried out using the sense forward 5′ TCGTCG GCAGCGTCAGATGTGTATAAGAGACAGCCTACGGGNGG CWGCAG 3′ and 5′ GTCTCGTGGGCTCGGAGATGTGTAT AAGAGACAGGACTACHVGGGTATCTAATCC 3′ reverse primers directed to the variable regions V3–V4 of the 16S rRNA gene. All Illumina reads were analyzed using the FastaQC software in order to assess sequence quality. Further data processing including trimming and 16S rRNA analysis and visualization was performed with a workflow based on the mothur software package (1.39.5 version). Briefly, chimeras were detected using the software UCHIME version 4.2 (https://drive5.com/uchime, effective tags obtained) and sequences were aligned and clustered into operational taxonomic units (OTUs) with an identity cut of 80%. The total count threshold was set at 0.005% using the Greengenes database (13).

Microbial Functional Analysis: PICRUSt

Within the metagenomic study, the analysis of the most represented functions of the microbial community was conducted. For this purpose, PICRUSt (version 1.1.3) was used for comparing the predicted functional profiles from the anterior and posterior intestines of gilthead seabream fed both administered diets. PICRUSt is a bioinformatics software designed to predict the functional profile of a microbial community based on the study of the 16S rRNA. Reads from 12 samples (three samples from intestine sample and treatment) were filtered by rarefaction curves from 46,331 reads, and singletons were removed. A total of 45,844 sequences, which clustered into 103 OTUs identified in the Greengenes database, were used for additional bioinformatics analysis (**Supplementary Figure 1**). Sequencing data were introduced into the PICRUSt bioinformatics software, and samples were normalized to the number of copies of the 16S rRNA. Functional

metagenomes for each sample were predicted from the Kyoto Encyclopedia of Genes and Genomes (KEGG) catalog and collapsed to specified KEGG levels.

Statistics

Differences between biometrical parameters of both experimental dietary groups were analyzed through an unpaired *t*-test assuming data homoscedasticity (GraphPad PRISM 7.00; $p < 0.05$).

Raw data extracted from microarrays were imported and analyzed using GeneSpring version 14.5 GX software (Agilent Technologies). The 75th percentile normalization was used to standardize the arrays for comparisons, and data were filtered by expression. The DEGs were obtained from a gene-level differential expression analysis. An unpaired *t*-test was conducted without correction ($p < 0.05$) to identify DEGs between dietary treatments. The DEGs were grouped according to their fold-change value (FC, $p < 0.05$) and represented using the GraphPad PRISM software. The Principal Component Analysis (PCA) on conditions was carried out using GeneSpring software; four eigenvectors were calculated using a covariance matrix to describe the aggrupation of the control and EOs groups in a 3D plot. The gene expression values (log2-expression ratios) were represented by a hierarchical clustering heatmap analysis (MeV software v4.0), with Pearson distance and average linkage (9).

All data analysis of the intestinal microbiota was processed using Phyloseq and Vegan libraries in R statistical package. Readings were normalized based on rarefaction curves (46,331 reads) and singletons were removed. In addition, it was calculated the coverage using the Good's coverage coefficient, as well as the ecological indexes. Alpha diversity was estimated using the Chao1, Shannon, and Simpson indices, to assess taxonomic wealth, diversity, and dominance, respectively. For statistical analyses between diversity indices, the *t*-test ($p < 0.05$) was used; while the taxonomic comparison was carried out using the R package DESeq2 ($p < 0.01$). Differences in the functional prediction between diets were made using the ANOVA multiple comparison test with the Tukey-Kramer correction (corrected $p < 0.05$).

RESULTS

Growth Performance

At the end of the study, no significant differences were observed between fish fed the EOs-supplemented diet and the control diet in terms of somatic growth (BWf = 150.8 ± 14.9 vs. 157.8 ± 14.2 g; SLf = 17.1 ± 0.6 vs. 17.3 ± 0.6 mm), daily growth rates in terms of BW (SGR_{BW} = 2.03 ± 0.01 vs. 2.12 ± 0.07% BW/day) and Fulton's condition factor (K = 3.0 ± 0.1 vs. 3.1 ± 0.1), respectively (Unpaired *t*-test, $p > 0.05$). A survival rate of 96 and 92% was recorded for the EOs-supplemented and control diets, respectively.

Microarrays and Gut Transcripteractome

A total of 581 DEGs were found when comparing the transcriptomic profiling of the intestine from fish fed both diets ($p < 0.05$; **Supplementary Table 1**). The detailed analysis of gene FC revealed that genes were mostly upregulated in the fish fed the diet containing the functional additive (70.2% of DEGs), although its modulation was moderate in terms of FC intensity. In particular, 408 of the abovementioned DEGs were upregulated, with 404 of them within the $1.0 < FC < 1.5$ interval. The remaining four DEGs were grouped within the $2.0 \leq FC \leq 3.0$ interval. In addition, 173 DEGs were downregulated (29.8% of DEGs; $p < 0.05$) and all of them were grouped within the $-1.5 \leq FC \leq -1.0$ interval (**Figure 1A**). Common segregation among the pool samples within the same dietary treatment was observed in the hierarchical clustering of the intestine transcriptomic response based on correlation patterns from the DEGs response ($p < 0.05$) (**Figure 1B**). PCA analysis confirmed the differential transcriptomic profile among dietary treatments. The first component (Y-axis) accounted for 79.03% of variation; the second and third components (X-Axis and Z-axis, respectively) accounted for 6.26 and 6.03% of the variation; these three components show the perfect separation between the control diet and the fish fed with the additive (**Figure 1C**).

From the whole set of DEGs, a functional network analysis was performed. The transcripteractome showed 252 coding proteins (nodes) with 473 interactions (edges). The remaining 329 DEGs (annotated as unknown genes) were excluded from the analysis. Based on the 70 GO terms obtained from the enrichment analysis (**Supplementary Table 2**), 6 main representative groups for the biological processes were identified in the transcripteractome: (1) proteolysis; (2) immunity; (3) transport and secretion; (4) response to cyclic compounds; (5) symbiosis; and (6) gene expression (**Figure 2**).

The tested functional feed additive resulted in the positive regulation of biological processes related to the proteolysis category (32 upregulated genes and 16 downregulated genes; **Supplementary Figure 2**; **Supplementary Table 3**). Several biological processes were considered, namely, "proteolysis," "regulation of proteolysis," "regulation of peptidase activity," "regulation of endopeptidase activity," and "protein deubiquitination." In addition, biological processes associated with immunity showed a more balanced regulation in fish fed the EOs-supplemented diet (17 upregulated genes and 14 downregulated genes; **Supplementary Figure 3**; **Supplementary Table 4**). Several relevant GOs related to immunity were obtained, such as "cell activation," "leukocyte activation," "leukocyte activation involved in immune response," "neutrophil activation," "neutrophil degranulation," and "regulated exocytosis." The tested functional feed additive also favored biological processes associated with transport and secretion (50 upregulated genes and 26 downregulated genes; **Supplementary Figure 4**; **Supplementary Table 5**). Among them, "transport," "intracellular transport," "vesicle-mediated transport," and "secretion" processes were identified in the functional network. Moreover, some biological processes in the category of the response to cyclic compounds were positively affected by the dietary inclusion of EOs (25 upregulated genes and 11 downregulated genes; **Supplementary Figures 5, 6**; **Supplementary Table 6**). In particular, the following processes were evidenced, such as the "response to organic cyclic compound," "cellular response to organic cyclic compound,"

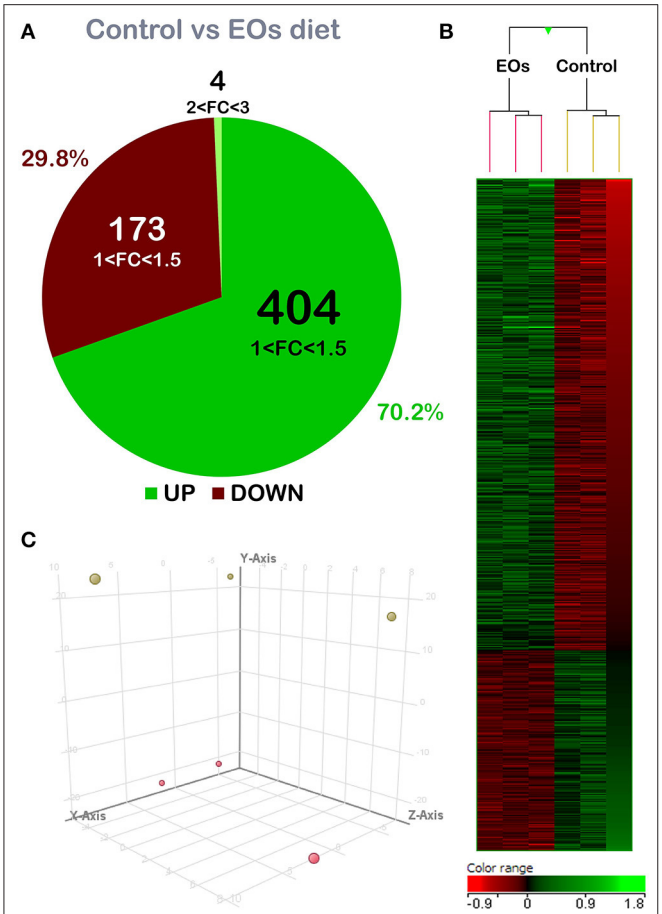

FIGURE 1 | Differential expression analysis of the gilthead seabream (*Sparus aurata*) mid-anterior intestine transcriptomic response to the garlic, carvacrol, and thymol essential oils (EOs)-supplemented diet. **(A)** Comparing both groups, 581 differentially expressed genes (DEGs) ($p < 0.05$) were found. From these, 408 genes were upregulated: 404 mainly concentrated in the 1.0–1.5-fold change (FC) interval; and 4 DEGs were grouped in the $2.0 \leq FC \leq 3.0$ interval. Additionally, 173 genes were downregulated ($p < 0.05$) and grouped in the range $-1.5 \leq FC \leq -1.0$. **(B)** Hierarchical clustering of the gilthead seabream mid-anterior intestine transcriptomic response for the control diet and EOs-supplemented diet, based on similitude patterns of the DEGs detected from three sample pools per dietary group. Data of the six microarrays are depicted, one for each represented pool. Both increased and decreased gene expression patterns are shown in green and red, respectively. All transcripts represented are statistically significant ($p < 0.05$). **(C)** Principal component analysis (PCA) of the DEGs of gilthead seabream intestine response to the control diet (yellow) and EOs-supplemented diet (red). PC1, PC2, and PC3 components loadings (Y-axis = component 1, 79.03% of variation; X-axis = component 2, 6.26% of variation; Z-axis = component 3, 6.03% variation). For DEGs details, please see also **Supplementary Table 1**.

"response to lipid," "cellular response to lipid," "response to hormone," "response to steroid hormone," "cellular response to hormone stimulus," "cellular response to steroid hormone stimulus," "response to alkaloid," "response to nitrogen compound," and "response to organonitrogen compound." Furthermore, symbiosis correlated biological processes, such as "symbiont process," "interspecies interaction between organisms," and "multi-organism process," were positively modulated (33 upregulated genes and 13 downregulated genes) in the intestine of fish fed the diet containing the functional feed additive (**Supplementary Figure 7**; **Supplementary Table 7**). Finally, the biological processes associated with gene expression and RNA processing (62 upregulated genes and 10 downregulated genes; **Supplementary Figure 8**; **Supplementary Table 8**), among them "gene expression," "RNA processing," "RNA splicing," "messenger RNA (mRNA) processing," "mRNA metabolic process," "mRNA export from nucleus," and "ribonucleoprotein complex export from nucleus" were observed to be much more upregulated in the intestine of fish fed the EOs-supplemented diet than in the control group.

A reasonable number of genes were observed to be shared among the immunity category and the other categories of gene expression/RNA processing (16%), proteolysis (29%), transport/secretion (77%), response to cyclic compounds (32%), and symbiosis (32%), suggesting a strong relationship between these biological processes that favors the host mucosal tissue immunity in response to the dietary EOs. Additionally, from the total DEGs obtained from the transcriptomic profile of the fish fed the EOs-supplemented diet, a set of genes was selected based on their expression and biological relevance (**Table 2**) in order to assess the participation of the intestine transcriptional regulation upon the observed microbiota modulation.

Intestine Microbiota Analysis

No variation was registered on the alpha diversity indices of the intestinal microbiota, regardless of the region of the intestine considered (**Table 3**; $p > 0.05$). However, the coefficient of variation (CV) for the Chao1 index was higher in the anterior (CV = 18.7 vs. 5.2%) and posterior (CV = 23.9 vs. 12.3%) intestinal segments of fish fed the diet containing the functional feed additive (**Supplementary Figure 9**). Similarly, the Shannon and Simpson diversity indexes were neither affected by the inclusion of the functional feed additive in the diet. Library coverage was calculated using Good's coverage index with a result of 99.98 ± 0.01.

The relative abundance of microbial taxa at the phylum level is shown in **Figure 3A**. Proteobacteria, Firmicutes, and Actinobacteria were commonly found in all samples regardless of the dietary condition and region of the intestine considered. However, only the phylum Spirochaetes showed significantly lower abundances in the posterior intestine in fish fed the diet supplemented with the functional feed additive ($p < 0.05$). At class level, *γ-Protebacteria* were the dominant group (60–73%; $p < 0.05$) in all samples assayed, whereas the abundance of *Clostridia* in the anterior intestine, and *Brevinematae* and *Bacteroidia* in the posterior intestine significantly decreased in fish fed the diet containing the blend of EOs (*t*-test, $p < 0.05$; **Figure 3B**).

At the genus taxonomic level, bacterial abundance (relative abundance > 1%) was significantly affected by the functional feed additive tested (*t*-test, $p < 0.05$). In particular, the anterior intestine of gilthead seabream fed the EOs-supplemented diet showed a significant increase (*t*-test, $p < 0.05$) in *Photobacterium* (γ-Proteobacteria, *Vibronaceae*) and *Corynebacterium*

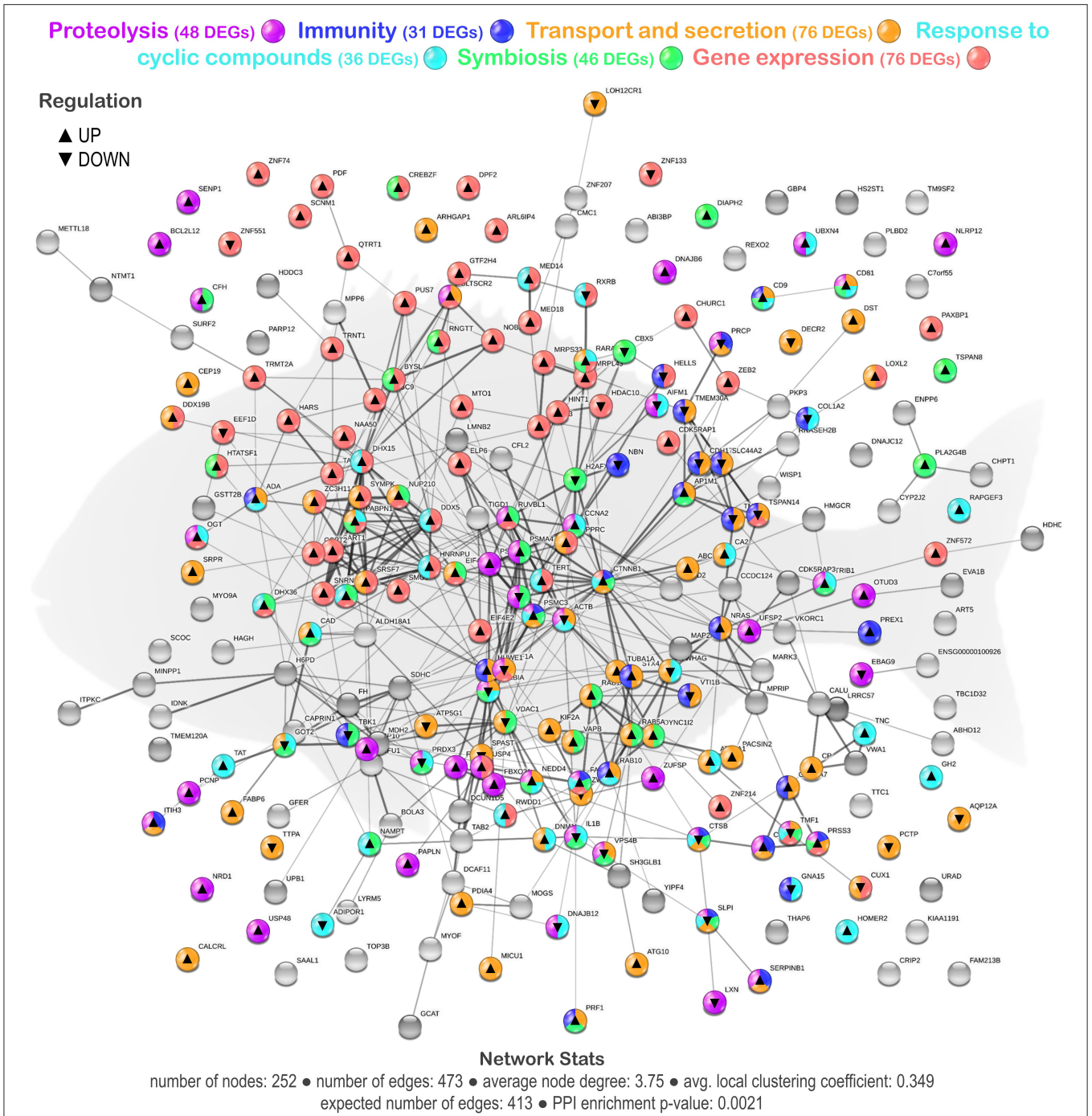

FIGURE 2 | Transcripteractome of the differentially expressed genes (DEGs) in the mid-anterior intestine of juvenile gilthead seabream (*S. aurata*) fed the garlic, carvacrol, and thymol essential oils (EOs)-supplemented diet (see also **Supplementary Tables** and **Supplementary Figures 2–8**). Protein–Protein Interactions Network (PPI) network nodes colors indicate the six representative processes identified from the functional enrichment analysis for each DEG represented—proteolysis, immunity, transport, and secretion, response to cyclic compounds, symbiosis, and gene expression. ▲ nodes represent upregulated genes and ▼ nodes represent downregulated genes. Graphic keys and network stats are indicated in the graphical figure legend.

(Actinobacteria, *Corynebacteriaceae*) abundance whereas a reduction in *Comamonas* (Proteobacteria, *Comamonadaceae*) was also found (*t*-test, $p < 0.05$; **Figure 4**). Regarding the posterior intestine, a significant decrease in the abundance of the genera *Paracoccus* (Proteobacteria, *Rhodobacteraceae*), *Prevotella* (Bacteroidetes, *Bacteroidaceae*), and *Rothia* (Actinobacteria, *Micrococcaceae*) was also detected in fish fed the functional feed additive (*t*-test, $p < 0.05$; **Figure 5**).

TABLE 2 | List of selected differentially expressed genes (DEGs) of the mid-anterior intestine of juvenile gilthead seabream (*Sparus aurata*) fed a diet supplemented with a blend of garlic, carvacrol, and thymol essential oils (EOs).

Gene name	Acronym	FC	*P*-value
PROTEOLYSIS AND DEUBIQUITINATION			
UFM1 Specific Peptidase 2	*ufsp2*	1.621	0.012
Proteasome 20S Subunit Alpha 6	*psma6*	1.491	0.014
Ubiquitin Specific Peptidase 10	*usp10*	1.490	0.026
Proteasome 26S Subunit, ATPase 3	*psmc3*	1.413	0.040
Ubiquitin Specific Peptidase 48	*usp48*	1.359	0.036
Proteasome 20S Subunit Alpha 4	*psma4*	1.289	0.027
OTU Deubiquitinase 3	*otud3*	1.256	0.035
Ubiquitin Specific Peptidase 4	*usp4*	1.103	0.007
Interleukin 1 Beta	*il-1β*	−1.167	0.025
NFKB Inhibitor Alpha	*nfkbia*	−1.327	0.047
Proteasome 20S Subunit Beta 6	*psmb6*	−1.495	0.048
IMMUNITY			
Leukocyte Elastase Inhibitor	*serpinb1*	1.561	0.024
Adenosine Deaminase	*ada*	1.517	0.025
Phosphatidylinositol-3,4,5-Trisphosphate Dependent Rac Exchange Factor 1	*prex1*	1.478	0.018
CD9 Molecule	*cd9*	1.283	0.033
CD81 Molecule	*cd81*	1.279	0.018
Perforin 1	*prf1*	1.181	0.034
Cathepsin B	*ctsb*	−1.340	0.031
TRANSPORT AND SECRETION			
Fatty Acid Binding Protein 6	*fabp6*	2.659	0.044
Serine Protease 3	*prss3*	1.824	0.002
RAB5A, Member RAS Oncogene Family	*rab5a*	1.668	0.023
RAB10, Member RAS Oncogene Family	*rab10*	1.456	0.030
Rho GTPase Activating Protein 1	*arhgap1*	1.363	0.048
NRAS Proto-Oncogene, GTPase	*nras*	1.257	0.010
RAB1A, Member RAS Oncogene Family	*rab1a*	1.238	0.025
Hypoxia Inducible Factor 1 Subunit Alpha	*hif1a*	−1.259	0.002
RESPONSE TO CYCLIC COMPOUNDS			
Carbonic Anhydrase 2	*ca2*	2.089	0.046
Tribbles Pseudokinase 1	*trib1*	1.740	0.011
Glutathione S-Transferase Theta 2B	*gstt2b*	1.456	0.018
Cytochrome P450 Family 2 Subfamily J Member 2	*cyp2j2*	1.284	0.045
Growth Hormone 2	*gh2*	1.283	0.032
ATPase Na+/K+ Transporting Subunit Alpha 1	*atp1a1*	1.271	0.022
Peroxiredoxin 3	*prdx3*	−1.220	0.009
Glutamic-Oxaloacetic Transaminase 2	*got2*	−1.254	0.008
Adiponectin Receptor 1	*adipor1*	−1.262	0.041
Cathepsin B	*ctsb*	−1.340	0.031
SYMBIOSIS			
Retinoic Acid Receptor Alpha	*rara*	1.164	0.003
Retinoid X Receptor Beta	*rxrb*	−1.172	0.030
GENE EXPRESSION			
Zinc Finger Protein 572	*znf572*	1.389	0.019
CDK5 Regulatory Subunit Associated Protein 3	*cdk5rap3*	1.341	0.014
Zinc Finger E-Box Binding Homeobox 2	*zeb2*	1.315	0.003
Heterogeneous Nuclear Ribonucleoprotein U	*hnrnpu*	1.284	0.012
Cellular Communication Network Factor 4	*wisp1*	1.280	0.040
NOP53 Ribosome Biogenesis Factor	*gltscr2*	1.263	0.034
Zinc Finger Protein 74	*znf74*	1.256	0.038
Pre-MRNA Processing Factor 8	*prpf8*	1.214	0.005
Zinc Finger CCCH-Type Containing 11A	*zc3h11a*	1.207	0.023
Zinc Finger Protein 214	*znf214*	1.201	0.008
Small Nuclear Ribonucleoprotein U5 Subunit 200	*snrnp200*	1.192	0.008
F-Box Protein 31	*fbxo31*	1.178	0.021
Spliceosome Associated Factor 1, Recruiter Of U4/U6.U5 Tri-SnRNP	*sart1*	1.155	0.005
Zinc Finger Protein 133	*znf133*	−1.127	0.006
Zinc Finger Protein 551	*znf551*	−1.168	0.001
Nibrin	*nbn*	−1.238	0.031

(Continued)

TABLE 2 | Continued

Genes were arranged according to six representative processes identified from the functional enrichment analysis. Gene description, respective acronym, fold-change intensity (FC), modulation (green: upregulation; red: downregulation), and p-value are described.

TABLE 3 | Alpha diversity of bacterial communities in the anterior and posterior intestinal tract sections of gilthead seabream (*Sparus aurata*) fed a control and the diet supplemented with a blend of garlic, carvacrol, and thymol essential oils (EOs).

			Chao1	Shannon	Simpson
Intestine	Anterior	Control	64.583 ± 3.357	2.513 ± 0.231	0.863 ± 0.046
		EOs diet	69.437 ± 13.013	2.288 ± 0.470	0.838 ± 0.093
	Posterior	Control	58.167 ± 7.182	2.401 ± 0.550	0.807 ± 0.164
		EOs diet	62.770 ± 14.983	2.363 ± 0.220	0.863 ± 0.039

The PICRUSt analysis enabled the prediction of the functional capacities of the microbial communities detected in the gilthead seabream intestine based on the treatment applied. The low Nearest Sequenced Taxon Index (NSTI) value (0.04 ± 0.02) from the PICRUSt analysis indicated a good prediction accuracy. The functional analysis of KEGG pathways revealed significant differences at second- and third-level classification KEGG pathways in both sections of the intestine (ANOVA, $p < 0.05$). Regarding the anterior intestine and considering the second-level classification of KEGG pathways, a reduction in carbohydrate metabolism in fish fed the diet supplemented with the functional feed additive was obtained (ANOVA, $p < 0.05$) (**Figure 6A**). When considering the third-level classification of KEGG pathways in the anterior intestine, a larger proportion

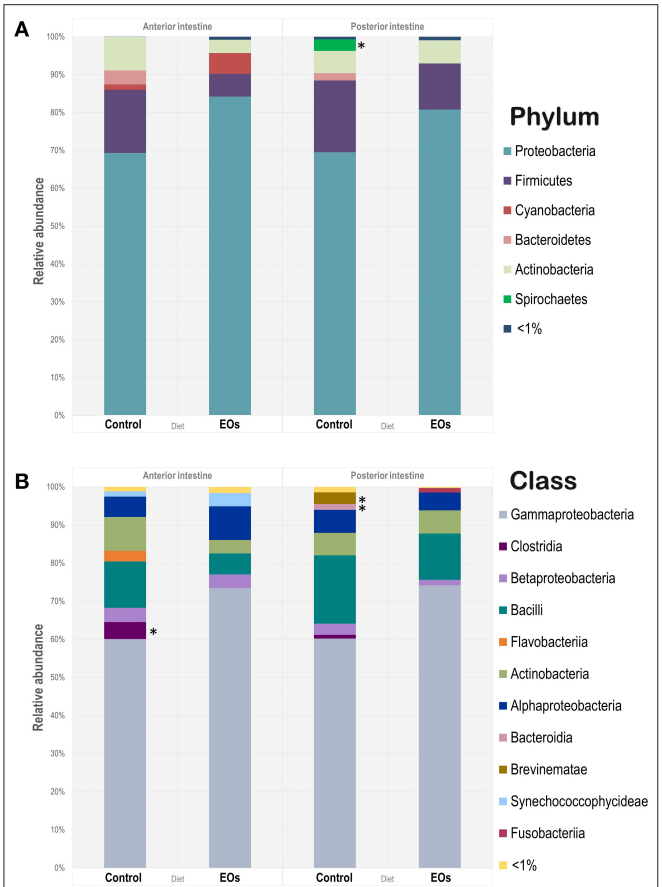

FIGURE 3 | Microbiota composition at phylum **(A)** and class **(B)** level of the anterior and posterior sections of the intestinal tract of gilthead seabream (*S. aurata*) fed control and garlic, carvacrol, and thymol essential oils (EOs)-supplemented diet. Asterisk (*) indicate significant differences among diets ($p > 0.05$).

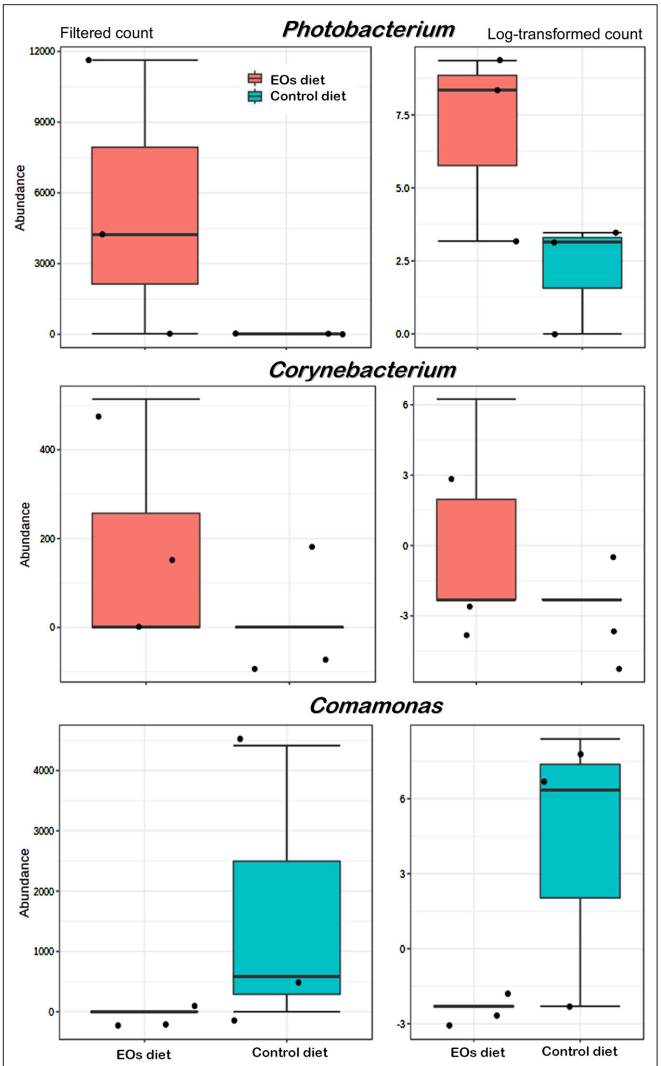

FIGURE 4 | Average abundances of genera showing significant differences ($p < 0.01$) in the anterior intestine of gilthead seabream (*S. aurata*) fed the garlic, carvacrol, and thymol essential oils (EOs)-supplemented diet in comparison with fish receiving the control diet.

of sequences associated with glutathione and lipid metabolism, and a reduction of sequences related to drug metabolism was found in fish fed the EOs-supplemented diet (**Figure 6B**). Regarding the posterior intestine, processes related to membrane transport at the second-level classification of KEGG pathways were significantly reduced in fish fed the EOs-supplemented diet (**Figure 6C**), while processes related to the sulfur relay system and naphthalene degradation at the third-level classification of KEGG pathways were significantly enhanced in fish fed the EOs-supplemented diet (**Figure 6D**).

DISCUSSION

The fish intestine is a complex multifunctional organ. In addition to diet digestion and nutrient absorption functions, this organ is critical for other key physiological mechanisms including water and electrolyte balance, endocrine regulation upon digestion and metabolism, and immunity (7), as well as for the establishment of commensal microbiota (2, 14). As one of the main portals of pathogens' entry into the organism, and due to its intricate immune system associated to a lymphoid tissue that allows microbial colonization, the intestine of farmed fish is a target tissue for dietary manipulations (2, 7). We aimed to describe the effect of the dietary combination of garlic, carvacrol, and thymol EOs in the intestinal mucosa of gilthead seabream at a transcriptional level and its impact on gut microbiota modulation.

Effect of Garlic, Carvacrol, and Thymol EOs Additive on Proteolysis, Protein Deubiquitination, and Inflammatory Regulation

The dietary supplementation of EOs affected the regulation of several genes associated with proteolytic pathways, peptidases activity, and protein deubiquitination. In particular, several genes coding for proteasomes (*psma6*, *psmc3*, *psma4*, and

psmb6) and ubiquitin peptidases (*usp4*, *usp10*, *usp48*, *otud3*, and *ufsp2*) were activated by the dietary supplementation of EOs. Protein ubiquitination and subsequent proteolysis and degradation by the proteasome are important mechanisms in the regulation of the cell cycle, cell growth and differentiation, gene transcription, signal transduction, and apoptosis, including tissue regeneration (15). As important factors for the maintenance of intestinal epithelial integrity and immune homeostasis, the ubiquitin-proteasome proteolytic system plays a pivotal role in the activation of the nuclear factor kB (NF-kB) pathway. The NF-kB pathway is involved in the transcriptional regulation of several proinflammatory genes, playing a critical role in regulating the survival, activation, and differentiation of innate and adaptive immune cells (16). As an important feedback regulatory mechanism following NF-kB activation, the NFKB inhibitor alpha (*nfkbia*), also known as *IkBα*, is one of the first genes to be activated (16). In our transcriptional analysis, *nfkbia* was downregulated. In regard to the NF-kB signaling pathway, we also registered the upregulation of several deubiquitination-related genes, such as the referred ubiquitin peptidases, that could be blocking the ubiquitination and degradation of the NF-kB inhibitors. This mechanism might be accompanied by commensal γ-*Protebacteria* strains, the dominant class in our study, that prevent or limit epithelial gut inflammation (17); thus, evidencing the close cooperation between gut and microbiota in the inflammatory regulation in response to dietary shifts. Accordingly, the proinflammatory cytokine interleukin-1 beta (*il-1β*) was downregulated in the fish fed the EOs-supplemented diet, corroborating the reduction of the transcription of proinflammatory genes mediated by the NF-kB pathway. Collectively, these data suggest a direct and selective regulation of the NF-kB and ubiquitin-proteasome pathways established through the interaction between the transcriptome response and their commensal bacteria in the gut of sea bream fed the EOs-supplemented diet.

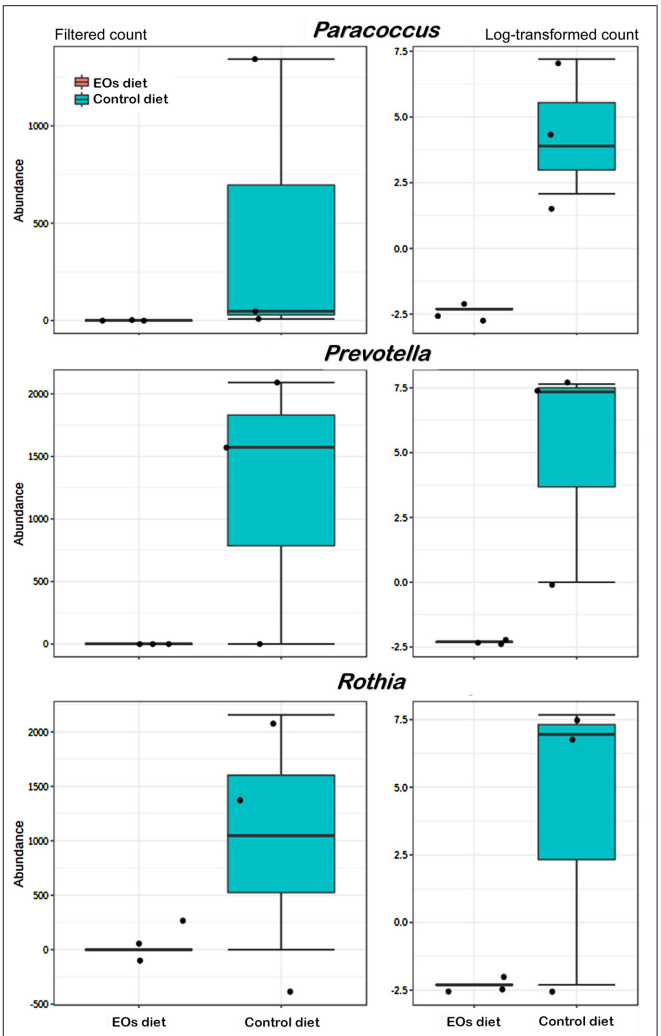

FIGURE 5 | Average abundance of genera showing significant differences ($p < 0.01$) in the posterior intestine of gilthead seabream (*S. aurata*) fed the garlic, carvacrol, and thymol essential oils (EOs)-supplemented diet in comparison with fish receiving the control diet.

Effect of Garlic, Carvacrol, and Thymol EOs Additive on Immune Effector Processes

The dietary administration of EOs showed the modulation of several biological processes related to innate immune effector cells, such as "leukocyte activation," "leukocyte activation involved in immune response," "neutrophil activation," and "neutrophil degranulation." In the case of neutrophils, their main function is the control of microorganisms that cross the epithelium barrier to invade the mucosa. Contrarily to mammals, fish neutrophils are not so abundantly present in the bloodstream, whereas they are stored in hematopoietic reservoirs instead, which could signify a disadvantage for rapid migration and effective resolution of infection and inflammation events (7). Thus, the results of our functional analysis regarding leukocyte activation, and granulocytes, in particular, might suggest an increased intestinal specific immune capacity promoted by the tested functional diet. In fact, the dietary supplementation of garlic or its bioactive compounds (18), carvacrol, and/or thymol (19) have been reported to increase the number of white blood cells and other immune parameters in several cultivated fish species. Similarly to our results, the activation of the degranulation transcriptional response of the neutrophils was previously observed in the gills of gilthead seabream fed the same EOs-supplemented diet and attributed to its increased defense capacity against a monogenean helminth parasite infection (9).

Further analyses on immune-related processes modulated by the tested EOs also showed an increase of the expression in *prex1*, a gene coding for the phosphatidylinositol 3,4,5-trisphosphate-dependent Rac exchanger 1 that regulates adhesion, migration, tissue recruitment, and reactive oxygen species (ROS) formation in the neutrophils (20). In addition, the leukocyte elastase inhibitor gene (*serpinb1*) was also upregulated in the intestine of fish fed the EOs-supplemented diet. This gene encodes a serine protease inhibitor that specifically inhibits neutrophil elastase, cathepsin G, and proteinase-3 present in the neutrophil granules;

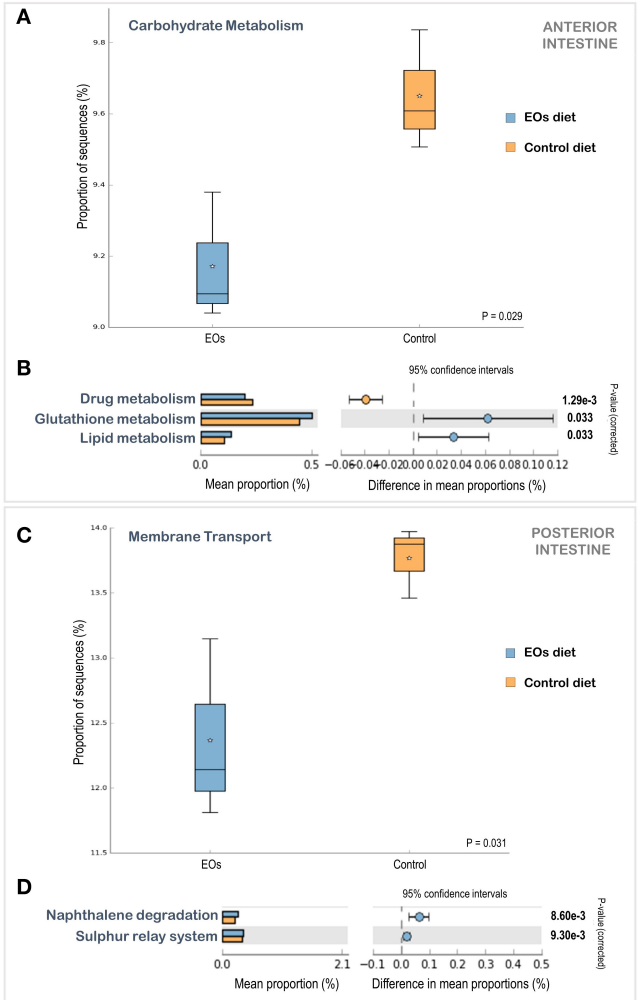

FIGURE 6 | Comparison of the relative abundance of PICRUSt generated functions profile in the anterior **(A,B)** and posterior **(C,D)** intestinal microbiota of gilthead seabream (*S. aurata*) fed the control and the garlic, carvacrol, and thymol essential oils (EOs)-supplemented diet. Box plots show the relative abundances of significant changes in level 2 Kyoto Encyclopedia of Genes and Genomes (KEGG) pathways in the anterior **(A)** and posterior **(C)** intestinal microbiota. Box plot central lines indicate the median and star symbols indicate the mean of the data. Significant KEGG pathways at level 3 pathways in the anterior **(B)** and posterior **(D)** intestinal microbiota, by ANOVA with a *post-hoc* Tukey–Kramer multiple-comparison test ($p < 0.05$).

thus, protecting not only tissues from damage at inflammatory sites during stress or infection, but also the neutrophil itself (21). SERPINB1 also limits the activity of inflammatory caspases during inflammation by suppressing their caspase-recruitment domain oligomerization and enzymatic activation, representing an important regulator of tissue inflammation (22). Under current experimental conditions, these results may indicate a well-balanced intestinal immunity, where both immune effector cells activation and an anti-inflammatory response were promoted.

The expression of several genes associated with adaptive immunity was modulated by the EOs-supplemented diet as well. For instance, perforin-1 (*prf1*) was upregulated in the intestine of fish fed the EOs-diet. Perforin is a pore-forming cytolytic protein found in the granules of cytotoxic T lymphocytes (CTLs) and natural killer (NK) cells, playing a key role in killing other cells that are recognized as non-self by the immune system (23). In fish, studies have reported the upregulation of *prf1* in response to viral stimulation (24). Furthermore, the upregulation of adenosine deaminase (*ada*) was also promoted by the tested EOs-supplemented diet. In particular, *ada* acts as a positive regulator of T-cell co-activation, participates in the regulation of lymphocyte-epithelial cell adhesion, and enhances dendritic cell immunogenicity (25, 26). Additionally, *cd9* and *cd81* were both upregulated in the fish fed the EOs-supplemented diet. These genes encode tetraspanins, key players in the processes of adhesion, extravasation, and recruitment of leukocytes into inflammation sites, regulating several steps of the immune response (27). CD9 and CD81 were found to be extensively present in Atlantic salmon (*Salmo salar*) IgM^+ B-cells (28). Last but not least, tetraspanins were considered to be required for bacteria adhesion to the epithelial cells (29); which may be in agreement with the presence of both DEGs in the symbiosis-related processes from our transcriptional analysis, as discussed below. Therefore, the regulation of genes involved in both B and T lymphocytes activity may suggest the stimulation of not only the innate, but also the adaptive immune response as well, although further research is needed to confirm this hypothesis.

The proportion of up to downregulated genes related to an immune response was not as marked as the observed for the remaining biological processes activated by the inclusion of EOs in diet, indicating an effective and balanced proinflammatory and anti-inflammatory regulation of the induced immune response, as previously suggested. Nonetheless, it is legitimate to assume that due to its immunostimulatory characteristics, the EOs-based functional feed might have an impact on the composition of the gilthead seabream intestinal microbiota, which in turn may also have played a critical role in mediating the abovementioned immune response. In fact, numerous studies have indicated that diet is an important factor in the modulation of the gut microbiome composition in vertebrates, dictating also the role of that microbiome in fish health status (2). Regarding the EOs tested, garlic (4), carvacrol, and/or thymol (5) were previously reported to modulate fish microbiota composition, exerting beneficial effects (30), and improving significantly its resistance to *Vibrio anguillarum* after intestinal infection and stress challenge (31). The administration of similar functional diets with immunostimulatory and/or antimicrobial properties have been also reported to reduce gut microbial diversity (30); however, in our study, alpha diversity was not significantly altered by the dietary EOs, which may be associated with the heterogeneity of analyzed samples, as observed in CV values for the Chao1 index. Under present experimental conditions, the only phylum that showed significant differences among dietary treatments was the Spirochaetes. This phylum contains important gut pathogenic species, such as *Brachyspira* species, for livestock and humans (32). Nonetheless, the impact of

this phylum modulation upon gilthead seabream intestine homeostasis is not clear yet, and further studies should be performed in order to assess which members of the phylum could be participating in the immune response observed.

Effect of Garlic, Carvacrol, and Thymol EOs Additive on Immune-Related Transport and Secretion Processes

The obtained immune-related biological processes were observed to share 77% of DEGs with the transport and secretion category, which genes were observed to be positively affected, in its majority, by the dietary EOs. The substantial amount of DEGs shared among the two categories clearly indicates a common role in the overall observed transcriptional response. In this sense, similar vesicle-mediated transport processes associated with active biogenesis and neutrophil-mediated immune response were observed in the gills of gilthead seabream fed the same EOs-supplemented diet (9), which seemed to indicate a similar action of this functional additive on different mucosal tissues. Epithelial cells are also directly involved in the initiation of the immune response, such as the one mediated by neutrophils. Accordingly, several genes encoding RAS-related GTPases (*nras*, *rab1a*, *rab5a*, *rab10*, and *arhgap1*), recognized as leading regulators of membrane trafficking directing immunity and inflammation cellular responses (33), were upregulated in the intestine of fish fed the functional feed additive. On the other hand, the hypoxia inducible factor 1 subunit alpha (*hif1a*) was downregulated in the fish fed the EOs-supplemented diet. HIF1a functions as a master transcriptional regulator of the adaptive response to hypoxia and it was observed to be transcriptionally induced by ROS through NF-kB (34), contributing in the intestinal mucosa to inflammatory resolution. The decrease in *hif1a* expression by the EOs dietary administration corroborated once again, that although neutrophil activation and vesicle-mediated transport processes were stimulated in the intestine of fish, inflammation derived from ROS release was probably not occurring.

Furthermore, the serine protease 3 (*prss3*) was another gene positively regulated in the intestine of fish fed the EOs-supplemented diet. This protease is involved in the synthesis of antibacterial substances (35); thus, we hypothesized that *prss3* may be involved in the regulation of intestinal immunity. PRSS3 is also a digestive protease specialized for the degradation of trypsin inhibitors (36). Trypsin inhibitors are anti-nutritional factors found in plant-protein sources that impair diet digestibility and generate digestive and metabolic disorders (37). Although the substitution of fishmeal by plant-derived protein sources was not in the scope of our study, *prss3* upregulation in the EOs-supplemented might indicate that the tested EOs could enhance diet digestibility.

Moreover, the expression of the gene coding for the fatty acid binding protein 6 (*fabp6*) was the most positively affected gene by the dietary EOs. Similarly, FABP6 was significantly increased in the intestine of gilthead seabream fed a combination of carvacrol, thymol, and a prebiotic (38), while this gene was downregulated in response to enteritis induced by a parasitic pathogen (39). Furthermore, FABP6 is involved in the transport of bile acids in ileal enterocytes (40). Besides, the influence of the intestinal microbiota on the activity of FABP6 was suggested in zebrafish, since *fabp6* expression decreased significantly after antibiotic treatment (41). Interestingly, in our study, the abundance of *Bacteroidia* class (Bacteroidetes) decreased significantly in the posterior intestine of fish fed the EOs-supplemented diet. Within the *Bacteroidia* class, *Bacteroides* genus bacterial metabolism of bile acids was observed to modulate gut T-cells homeostasis (42). Particularly, shifts toward the phylum Bacteroidetes including the *Bacteroidia* class coincides with mucosal $CD4^+$ T-cell depletion and enterocyte damage (43). Therefore, the upregulation of *fabp6* and the decrease of *Bacteroidia* class might indicate a modulation of the bile acids secretion by the tested EOs, potentially affecting lipids metabolism. Since bile acids are recognized as signaling molecules between the host microbiota and the innate immunity (44), alterations in its secretion could have a role in our observed immune-related transcriptional response previously discussed. Nevertheless, further studies need to be addressed in order to evaluate the impact of the EOs-based feed additive in the digestive secretions and metabolism of gilthead seabream.

Under the transport and secretion context, gut microbiota mediate the metabolism and transport of dietary xenobiotics through the modulation of metabolites of the host or through microbial secretion (45). Accordingly, our functional analysis of KEGG pathways of the posterior intestine microbiota of individuals fed the EOs-supplemented diet showed a decrease in bacterial sequences related to membrane transport. Considering that membrane transport in prokaryotes is associated with bacterial secretion, this decrease could indicate a lower export of enzymes and bacterial toxins, commonly present in the intestinal tract of different fish species (2), representing a potential beneficial effect of the EOs administration in the gut health.

Effect of Garlic, Carvacrol, and Thymol EOs Additive on the Response to Lipids and Hormones

Under a complex neuroendocrine regulation, the gut microbiota also regulate the metabolism of carbohydrates, lipids, and amino acids, whose composition, in turn, is susceptible to diet, health status, and drugs (46). Formerly, we suggested that the dietary administration of the EOs might affect the secretion of bile acids. If right, this could be inducing a response that could be affecting lipid metabolism and/or steroid hormone signaling. In accordance with this hypothesis, some biological processes related to responses to cyclic compounds, such as lipids and hormones, were positively affected by the inclusion of the EOs-based feed additive in the intestinal mucosa of gilthead seabream. For instance, the ATPase Na^+/K^+ transporting subunit alpha 1 (*atp1a1*) was significantly upregulated in the intestine of fish fed the EOs-supplemented diet. In other studies, diet-induced lipid alterations dramatically affected enterocytes lipid profile in gilthead seabream, reducing significantly Na^+/K^+ ATPase specific activity, suggesting a regulatory role of the lipid microenvironment on the enzyme activity (47). Additionally, tribbles pseudokinase 1 (*trib1*) gene expression was upregulated

in the gilthead seabream fed the EOs-supplemented diet. This gene is known to beneficially affect plasma lipid concentration, playing also major roles in myeloid cells, improving macrophage lipid metabolism, and counteracting inflammation (48). On the other hand, the glutamic-oxaloacetic transaminase 2 (*got2*) gene was downregulated in the fish fed the EOs-supplemented diet. A study in rats suggested that leptin downregulates *got2* in adipocytes (49). Likewise, the adiponectin receptor 1 (*adipor1*) was also downregulated in the fish fed the EOs diet. Adiponectin is an essential hormone predominantly secreted by adipocytes that regulates glucose and lipid metabolism, which along with leptin are considered to be potential proinflammatory adipocytokines (50). Under current experimental conditions, the regulation of genes involved in the cellular response to lipids might suggest the modulation of lipid-related intracellular signaling pathways in the fish fed the EOs-supplemented diet, with a potential role on the immune-inflammatory profile obtained.

Lipids affect the gut microbiota both as substrates for bacterial metabolic processes and by inhibiting bacterial growth by toxic influence (51). In turn, gut microbiota are also pointed as one of the key elements affecting inflammation associated with lipid metabolism dysfunction (2). In fish, the gut microbiota are also recognized to affect considerably the lipid metabolism of the host (41). In agreement to our transcriptional analysis and to the abovementioned findings, the PICRUSt analysis of the microbiota from the anterior intestine of fish fed the EOs-supplemented diet showed a higher abundance of sequences associated with lipid metabolism when compared to the control group. In fact, garlic and its derivatives are widely recognized for their hypolipidemic effect. For instance, one of the primary components of garlic, diallyl disulfide, was suggested to affect both lipid metabolism and gut microbiota in mice through the regulation of the expression of genes associated with lipogenesis and lipid metabolism (52). In other studies, the combined dietary administration of thymol and carvacrol have demonstrated to modulate the intestinal microbiota in piglets, changes that were correlated with an increase in lipid metabolism, among others metabolic effects (53). In this context, our taxonomical analysis at the genus level showed a significant increase in the abundance of *Corynebacterium* (Actinobacteria) in the anterior intestine of fish fed the EOs-supplemented diet. This genus has been reported as a predominant one along the whole digestive tract of gilthead seabream, while its abundance may be modulated by functional diets (54) and dietary lipid levels (55). These results are of special relevance since *Corynebacterium* species are reputed for contributing to manganese acquisition and producing superoxide dismutase and lipases to form organic fatty acids and thioalcohols (56). This genus also showed a higher presence in rainbow trout (*Oncorhynchus mykiss*) intestinal microbiota when the fish were fed high lipid diets (55), evidencing the impact of the tested EOs on the host and microbial lipid metabolism.

Furthermore, a decrease in the abundance of *Rothia* was also detected in the posterior intestine of fish fed the EOs-supplemented diet. *Rothia* abundance was observed to be affected by fish age and sex hormones in gilthead sea bream (14). In effect, the results from our transcriptional analysis revealed a positive regulation of processes related with a response to hormone stimulus. Changes in hormone secretion, such as cortisol, may interfere with the gut immune response (57) and microbiome (58), which could explain the obtained immunity activation and regulation of hormone-sensitive bacteria, such as those belonging to *Rothia* (14). Moreover, stress and stress-related hormones are known to affect carbohydrate, protein, and lipid metabolisms in fish (59), which in turn are also regulated in the host by the gut microbiota. In this sense, a similar feed additive containing garlic and labiatae plant EOs (0.02% inclusion) was demonstrated to reduce significantly plasma cortisol levels in European seabass (*Dicentrarchus labrax*) (60); thus, the potential regulation of stress-related hormones by the tested EOs could explain the response to steroid hormones processes obtained in our functional analysis.

In the present study, the administration of the garlic, carvacrol, and thymol EOs positively affected the expression of growth hormone 2 (*gh2*), although no significant differences in somatic growth were observed at the end of the 65 days of feeding trial. However, GH is not only involved in somatic growth; this hormone also directly stimulates several fish immune factors (61), and participates in the epithelial osmoregulation of euryhaline fish, interacting with cortisol to increase secretory chloride cells and ion transporters involved in salt secretion, such Na^+/K^+ ATPase (62). As a matter of fact, besides immunity and digestion, the gastrointestinal tract of marine teleost fish also plays an important role in osmoregulation. Under this context, the carbonic anhydrase 2 (*ca2*) was the second most positively affected gene by the EOs inclusion in the diet, playing an active role in acid–base regulation through bicarbonate secretion and facilitating epithelial water transport (63). In fact, osmoregulation has been linked to endocrine secretory factors with a significant impact on the fish immune system and microbiota (64).

As previously referred, the *Bacteroidia* class (Bacteroidetes) decreased significantly in the posterior intestine of fish fed the EOs diet. Kan et al. (65) demonstrated that within the *Bacteroidia* class, *Bacteroides* genus abundance increased in goldfish (*Carassius auratus*) when exposed to a toxic environment. Interestingly, our microbiota analysis showed a higher abundance of bacterial 16S rRNA sequences associated with the metabolism of glutathione in the anterior intestine. Glutathione is one of the most important intracellular antioxidant and antitoxin enzymes, whereas its metabolism is regulated by the gut microbiota through the modulation of the amino acid metabolism of the host (66) and tissue oxidative stress (67). Furthermore, glutathione plays important roles in nutrient metabolism and in the regulation of cellular events, such as gene expression, DNA and protein synthesis, cell proliferation and apoptosis, immune response, among others (67). Glutathione S-transferase is one of the key enzymes involved in the second phase of xenobiotics' metabolism and cellular detoxification, catalyzing the conjugation of reduced glutathione to various substances; thus, suggesting a key role in the host immune response modulation (68). Accordingly, in our transcriptional analysis, the glutathione S-transferase theta 2B (*gstt2b*) gene was observed to be upregulated in the intestine of gilthead seabream

following the administration of dietary EOs. The differences observed regarding both transcriptional and microbiota analysis between our experimental diets suggested an improvement of the enterocytes' lipid metabolism and detoxification potential promoted by the additive.

The microbiota analysis also showed a reduction in the proportion of bacterial sequences related to drug metabolism. Accordingly, the EOs-supplemented diet promoted the increase of the cytochrome P450 2J2 (*cyp2j2*) gene transcripts in the intestine of the gilthead seabream. In fish, the cytochrome P450 proteins, and CYP2 family members, in particular, participate in the metabolism of steroidal hormones and other lipids, besides their role in the metabolism of exogenous compounds like drugs and pharmaceuticals (69). Several garlic organosulfur compounds, as well as carvacrol, have been described to selectively modulate the levels of cytochrome P450 genes and proteins (70, 71). Moreover, the mitochondrial peroxiredoxin 3 (*prdx3*) and cathepsin B (*ctsb*) genes were downregulated. Both *prdx3* and *ctsb* are biomarkers of fish stressors (72), whose downregulation might indicate a decrease of the oxidative stress in the fish intestine and a positive impact of the tested additive on fish welfare. Overall, our results indicate that the administrated EOs promotes the enhancement of the antioxidative status in the fish intestine, supporting the gut homeostasis under an immune stimulation scenario.

Effect of Garlic, Carvacrol, and Thymol EOs Additive on the Response to Organic Nitrogen and Aromatic Compounds

In our transcriptional analysis, several genes comprising a response to nitrogenous compounds related processes were also observed to be positively regulated by the presence of garlic, carvacrol, and thymol EOs in the diet. Interestingly, the inclusion of the EOs in the gilthead seabream diet showed a significant decrease in the abundance of the genera *Paracoccus* (Proteobacteria), *Prevotella* (Bacteroidetes) in the posterior intestine, and *Comamonas* (Proteobacteria) in the anterior intestine of fish. All these bacteria are reputed for their capacity for nitrate reduction, as well as being potentially involved in the metabolism of nitrogenous compounds (73). In particular, *Prevotella*, are members of the anaerobic, hydrogen sulfide producing bacterial community (73) that have been previously detected in the intestine of gilthead seabream (54). In humans, an increase in *Pretovella* species at mucosal sites is often associated with chronic inflammation (74). In our study, the PICRUSt analysis showed a lower abundance of predicted carbohydrate degradation pathway in the anterior intestine of fish fed the EOs-supplemented diet, which may be associated with a reduction in *Prevotella* abundance. *Paracoccus* is a genus in the family *Rhodobacteraceae* previously reported in gilthead seabream gut and described as a potential probiotic for this species (75). The relevance of the decrease in the abundance of *Paracoccus* genus needs further investigations in terms of its impact on the condition of the host as no negative effects on gut conditions were observed under present nutritional conditions.

Furthermore, some *Comamonas* strains are also known to have genes for naphthalene degradation (76). The posterior intestine of fish fed the EOs-supplemented diet showed an increase in bacterial sequences related to naphthalene degradation. Naphthalene is an aromatic hydrocarbon present in many EOs with antibacterial, antioxidant, and antiparasitic properties (77). Although suggested to have a positive impact at low concentrations by decreasing DNA damage in some fish species (78), an enhancement in naphthalene and similar compounds degradation is crucial in order to avoid a potential toxicity of the EOs for the host.

The transcriptional analysis showed the positive regulation of the response to alkaloids biological process in the fish fed the EOs-supplemented diet. Alkaloids are versatile heterocyclic nitrogen compounds produced by plants, that along with EOs and phenolic compounds, provide antipathogenic and antioxidant protection (79). This response may not only be associated with the previously referred alteration in the metabolism of nitrogen and carbohydrates induced by the microbiota reshaping, but also with the direct response of the intestinal mucosa to the phenolic monoterpenes carvacrol and thymol (80) and other cyclic compounds derived from garlic (81) with recognized immunomodulatory properties. Moreover, allicin, the main antimicrobial compound in garlic, is also a sulfoxide that bacteria can use in the sulfur-relay system (82). This is in agreement with the observed increase in sequences associated with genes of the sulfur-relay system in the posterior intestine of fish fed the EOs-supplemented diet. Thereafter, considering the complexity of the EOs biochemistry, the transcriptional and bacterial response to those compounds is equally multifaceted. Further studies should be addressed in order to clarify the impact of these potential metabolic alterations in the gilthead seabream gut immune status.

Effect of Garlic, Carvacrol, and Thymol EOs Additive on Symbiosis Processes

The intricate host-microbiota symbiosis in the fish is still substantially unexplored when compared with mammals, and considering its complex challenges to define an "ideal" microbiome for each species since microbiota are strongly modulated by environmental and dietary factors (2). Even though both transcriptional and microbiota modulations by the EOs supplementation were observed, our results fit within the farmed gilthead seabream gut microbiome profile in terms of dominant phyla bacterial composition (14), discarding warnings of a diet-induced dysbiosis. The transcriptomic functional analysis was able to particularly detect such interactions through the expression of several genes related to symbiotic, multi-organism processes, and interspecies interaction between organisms.

For instance, the microbiota taxonomical analysis at the genus level showed an increase in the abundance of *Photobacterium* (Proteobacteria, Vibrionaceae) in the anterior intestine of fish fed the EOs diet. Although some members of this genus, such as *Photobacterium damselae* subsp *piscicida* and *P. damselae* subsp *damselae* have been reported as important pathogens for gilthead seabream (83), they are generally detected in the

intestine of healthy specimens (84, 85). Most species of the *Photobacterium* genus are non-pathogenic and are usually in a symbiotic relationship with marine organisms as enteric commensals. In fact, *Photobacterium* spp. have been even found to be beneficial as a member of the fish intestinal microbiota by its ability to aid with digestion of compounds, such as chitin (86), to produce polyunsaturated fatty acids or even antibacterial secondary metabolites that could inhibit the growth of other pathogenic bacteria (87). This genus has been reported as a member of the intestinal microbiota of marine farmed fish, including gilthead seabream (54, 85), and it has been demonstrated that this genus is one of the most modulated genera in the fish when applying functional diets (88). Regarding the antimicrobial effect of the EOs-supplemented diet, an *in vitro* study demonstrated that the ethanolic extracts of oregano leaves, predominantly composed of carvacrol and thymol, presented a strong bactericidal activity against several pathogens including *Photobacterium damselae,* besides its immunostimulatory effect on gilthead seabream head kidney leukocytes (89). Therefore, our results might suggest a selective antimicrobial effect of the compounds administrated, evidencing the importance of the host-microbiota symbiotic relationship in the modulation of the response to a dietary change.

Additionally, in our transcriptional analysis, the retinoic acid receptor alpha (*rara*) and the retinoic X receptor beta (*rxrb*) genes were both up and downregulated, respectively, in the gut of fish fed the EOs-supplemented diet. The retinoic acid (RA) is the most important transcriptionally active component of the vitamin A, an essential dietary nutrient for fish that plays a significant role in a range of physiological processes including the differentiation and maintenance of epithelial cells and immunity (90). Under this context, another case of symbiotic interaction between organisms is the relation between vitamin A metabolism of the host and its commensal microbiota. Remarkably, *Clostridia* (Firmicutes) abundance was significantly reduced in gilthead seabream fed the EOs diet, which could then be positively affecting the RA availability and the observed regulation of the nuclear receptors (90), potentially participating in the local immunity boost observed in our study. In fact, dietary garlic powder was demonstrated to have an antimicrobial effect on *Clostridium* human bacteria, being suggested to temporarily modulate the gut microbiota (91). In rainbow trout, different levels of garlic extract (1%, 1.5%, and 2%) positively affected the abundance of this genus (4). Curiously, a similar dietary additive composed of garlic and labiatae plants oils was observed to enrich the *Clostridia* class in European seabass fed a low fishmeal and fish oil diet (30). However, carvacrol and thymol, in particular, were numerously observed to exert an antimicrobial effect on *Clostridium* species, proving beneficial for the gut health of several organisms (92); thus, attributing to carvacrol and thymol the main role in the observed reduction of the genus. Given the significance of this symbiosis, the manipulation of RA signaling derived from dietary components acting directly on nuclear receptors and/or on the intestinal microbiota might represent a strategy to promote gut immunostimulation.

Effect of Garlic, Carvacrol, and Thymol EOs Additive on Gene Expression and RNA Processing

Dietary manipulations are widely recognized to directly or indirectly influence the regulation of the fish gut gene expression, in order to reshape its metabolic and physiological responses to different requirements. Indeed, the utmost upregulated biological processes in the intestine of fish fed the functional feed additive tested in our study, in terms of the number of DEGs, were those related to gene expression and processes involved in RNA processing, RNA splicing, mRNA metabolism, and mRNA and ribonucleoprotein export from nucleus. The regulation of gene expression comprises diverse cell mechanisms in order to increase or decrease the production of a specific gene product, either RNA or a protein. For instance, several zinc finger proteins were up (*znf572*, *zeb2*, *znf74*, *zc3h11a*, and *znf214*) and down (*znf133*, *znf551*) regulated in our transcriptional analysis. Besides the stimulation of the transcriptional machinery (93), several genes involved in the spliceosome-mediated splicing (*snrnp200*, *sart1*, *hnrnpu*, and *prpf8*) were also observed to be upregulated by dietary EOs. The spliceosome splicing complex removes intronic non-coding sequences from pre-mRNA to form mature mRNA that can be translated into protein (94).

In another hand, the intestine is *per se* a highly regenerative organ characterized by its continual cell renewal, allowing the epithelium to bear the constant exertion of food digestion, nutrient absorption, and waste elimination (6). Either tissue damage or microbial invasion promotes inflammation and possible DNA damage, so its repair plays a vital role in maintaining genomic integrity during the cell cycle. For instance, DNA damage responses may be induced by proinflammatory cytokines (95), in which transcriptional response appeared not to be promoted by the EOs in our study, as previously discussed. However, genes coding DNA damage checkpoint proteins were up (*fbxo31*, *gltscr2*, *wisp1*, *usp10*, and *cdk5rap3*) and down (*nbn*) regulated by the EOs-supplemented diet, evidencing a regulation of the cell turnover independent from inflammatory stimuli. This hypothesis is reinforced by the upregulation of *cdk5rap3*, the gene encoding CDK5 regulatory subunit associated protein 3, an interactor controlling cell proliferation that among other functions negatively regulates NF-kB mediated gene transcription (96), as initially suggested. Our results also evidence the tight functional connection and coordination between DNA damage responses and immunity, a link that is recognized by its involvement in the protection of the host from infectious microorganisms and surveillance against malignant diseases (97). Therefore, the upregulation of a substantial number of genes that modulates others' expression and that has an implication in transcriptional, translational and DNA repair processes validates the effect of the EOs-supplemented diet on the direct transcriptional regulation of several intestinal cellular processes, including the modulation of the inflammatory and immune response.

CONCLUSIONS

The present complementary analysis of the intestinal transcriptomic profiling and microbiota response to a diet supplemented with garlic, carvacrol, and thymol EOs aimed to take a further step in the evaluation of functional feeds in an attempt to understand how diet-induced shifts can affect the overall gut status of farmed fish from an integrative perspective. This kind of integrative analysis can lead to the "chicken or egg" causality dilemma, and exact mechanisms are still elusive. Nevertheless, the present work suggested that the dietary administration of garlic, carvacrol, and thymol EOs modulated the immune transcriptional response of the mid-anterior intestinal mucosa *per se*, but also its microbiota composition, resulting in complex interactions that resulted in the activation of significant biological processes. Taken together, the combined regulation of the referred pathways could suggest the promotion of an immune reinforcement by the EOs dietary administration *in situ*, most probably induced by host-microbial co-metabolism, which could further attenuate the processes of pathogenesis, putting in evidence the re-adaptation response of the intestinal mucosa to the changes observed in the microbiota composition, and *vice versa*. Moreover, no indications of an inflammation associated with the immunostimulation, which could compromise the intestine integrity, were observed. Since no interference with fish growth was observed, promoted changes in both the intestine mucosa and microbiota were assumed to not significantly affect the gut overall metabolism and nutritional status. Thus, the use of the tested EOs is suggested as a promising alternative to chemotherapeutics to be further evaluated in functional diets under the presence of biotic or abiotic stressors.

DATA AVAILABILITY STATEMENT

The datasets presented in this study can be found in online repositories. The names of the repository/repositories and accession number(s) can be found in the article/ **Supplementary Material**.

ETHICS STATEMENT

All animal experimental procedures were conducted in compliance with the research protocol approved by the IRTA's Committee of Ethics and Animal Experimentation and in accordance with the Guidelines of the European Union Council (86/609/EU) for the use of laboratory animals.

AUTHOR CONTRIBUTIONS

AE and EG designed and carried out the experiments. Biological samplings were performed by EG, AE, RS, and JF. The transcriptomic data analysis and interpretation were performed by JF, RS, EV-V, and FER-L. MB, IC, and MM carried out the microbiota analyses. YR-C reviewed and validated the methodology used in the study. The study was supervised by EG, FER-L, and LT. JF wrote the original draft. All the authors provided the critical feedback, read, and agreed to the published version of the manuscript.

FUNDING

This work has been supported by the project Nutritional strategies for the improvement of productive performance: the use of functional feeds and health diets in aquaculture (DIETAplus), funded by JACUMAR [Ministry of Agriculture, Fisheries and Environment of Spain, Ministerio de Agricultura y Pesca, Alimentación y Medio Ambiente (MAPAMA)] and Fondo Europeo Marítimo y de Pesca (FEMP, EU), as well as the project ADIPOQUIZ (RTI2018-095653-R-I00) funded by the Ministerio de Ciencia, Innovación y Universidades (Spain). FER-L was supported by Fondecyt Regular grant (Nb. 1211841; ANID; Goverment of Chile). JF has been subsidized by the Industrial Ph.D. program of Generalitat de Catalunya and TECNOVIT-FARMFAES S.L. (Nb. 2017 DI 017). EV-V was granted with DICYT-USACH post-doctoral fellowship (Nb.022043IB). RS was supported by a Ph.D. grant from the government of Paraguay (BECAL). Collaboration between Ibero-American researchers has been done under the framework of the network LARVAplus Strategies for the development and improvement of fish larvae production in Ibero-America (117RT0521) funded by the Ibero-American Program of Science and Technology for Development (CYTED, Spain).

SUPPLEMENTARY MATERIAL

The Supplementary Material for this article can be found online at: https://www.frontiersin.org/articles/10.3389/fimmu.2021.625297/full#supplementary-material

REFERENCES

1. Asif MB, Hai FI, Price WE, Nghiem LD. Impact of pharmaceutically active compounds in marine environment on aquaculture. In: Hai F, Visvanathan C, Boopathy R, editors. *Sustainable Aquaculture. Applied Environmental Science and Engineering for a Sustainable Future*. Cham: Springer (2018) p. 265–99.
2. Hoseinifar SH, Van Doan H, Dadar M, Ringø E, Harikrishnan R. Feed additives, gut microbiota, and health in finfish aquaculture. In: Derome N, editor. *Microbial Communities in Aquaculture Ecosystems: Improving Productivity and Sustainability*. Cham: Springer International Publishing (2019). p. 121–42.
3. Sutili FJ, Gatlin DM, Heinzmann BM, Baldisserotto B. Plant essential oils as fish diet additives: benefits on fish health and stability in feed. *Rev Aquac.* (2017) 10:716–26. doi: 10.1111/raq.12197
4. Büyükdeveci ME, Balcázar JL, Demirkale I, Dikel S. Effects of garlic-supplemented diet on growth performance and intestinal microbiota of rainbow trout (*Oncorhynchus mykiss*). *Aquaculture.* (2018) 486:170–4. doi: 10.1016/j.aquaculture.2017.12.022

5. Zhang R, Wang XW, Liu LL, Cao YC, Zhu H. Dietary oregano essential oil improved the immune response, activity of digestive enzymes, and intestinal microbiota of the koi carp, *Cyprinus carpio*. *Aquaculture.* (2020) 518:734781. doi: 10.1016/j.aquaculture.2019.734781
6. Celi P, Cowieson AJ, Fru-Nji F, Steinert RE, Kluenter AM, Verlhac V. Gastrointestinal functionality in animal nutrition and health: new opportunities for sustainable animal production. *Anim Feed Sci Technol.* (2017) 234:88–100. doi: 10.1016/j.anifeedsci.2017.09.012
7. Salinas I, Parra D. 6–fish mucosal immunity: intestine. In: Beck BH, Peatman E, editor. *Mucosal Health in Aquaculture*. San Diego, CA: Academic Press (2015). p. 135–70.
8. Nadal AL, Ikeda-Ohtsubo W, Sipkema D, Peggs D, McGurk C, Forlenza M, et al. Feed, microbiota, and gut immunity: using the zebrafish model to understand fish health. *Front Immunol.* (2020) 11:114. doi: 10.3389/fimmu.2020.00114
9. Firmino JP, Vallejos-Vidal E, Sarasquete C, Ortiz-Delgado JB, Balasch JC, Tort L, et al. Unveiling the effect of dietary essential oils supplementation in *Sparus aurata* gills and its efficiency against the infestation by *Sparicotyle chrysophrii*. *Sci Rep.* (2020) 10:17764. doi: 10.1038/s41598-020-74625-5
10. Dezfooli SM, Gutierrez-Maddox N, Alfaro A, Seyfoddin A. Encapsulation for delivering bioactives in aquaculture. *Rev Aquac.* (2019) 11:631–60. doi: 10.1111/raq.12250
11. Sutton SG, Bult TP, Haedrich RL. Relationships among fat weight, body weight, water weight, and condition factors in wild atlantic salmon parr. *Trans Am Fish Soc.* (2000) 129:527–38. doi: 10.1577/1548-8659(2000)129<0527:RAFWBW>2.0.CO;2
12. Calduch-Giner JA, Sitjà-Bobadilla A, Pérez-Sánchez J. Gene expression profiling reveals functional specialization along the intestinal tract of a carnivorous teleostean fish (*Dicentrarchus labrax*). *Front Physiol.* (2016) 7:359. doi: 10.3389/fphys.2016.00359
13. Tapia-Paniagua ST, Chabrillón M, Díaz-Rosales P, de la Banda IG, Lobo C, Balebona MC, et al. Intestinal microbiota diversity of the flat fish *Solea senegalensis* (Kaup, 1858) following probiotic administration. *Microb Ecol.* (2010) 60:310–9. doi: 10.1007/s00248-010-9680-z
14. Piazzon MC, Naya-Català F, Simó-Mirabet P, Picard-Sánchez A, Roig FJ, Calduch-Giner JA, et al. Sex, age, and bacteria: how the intestinal microbiota is modulated in a protandrous hermaphrodite fish. *Front Microbiol.* 10:2512. doi: 10.3389/fmicb.2019.02512
15. Glickman MH, Ciechanover A. The ubiquitin-proteasome proteolytic pathway: destruction for the sake of construction. *Physiol Rev.* (2002) 82:373–428. doi: 10.1152/physrev.00027.2001
16. Dorrington MG, Fraser IDC. NF-κB signaling in macrophages: dynamics, crosstalk, and signal integration. *Front Immunol.* (2019) 10:705. doi: 10.3389/fimmu.2019.00705
17. Neish AS, Gewirtz AT, Zeng H, Young AN, Hobert ME, Karmali V, et al. Prokaryotic regulation of epithelial responses by inhibition of IkappaB-alpha ubiquitination. *Science.* (2000) 289:1560–3. doi: 10.1126/science.289.5484.1560
18. Nya EJ, Dawood Z, Austin B. The garlic component, allicin, prevents disease caused by *Aeromonas hydrophila* in rainbow trout, *Oncorhynchus mykiss* (Walbaum). *J Fish Dis.* (2010) 33:293–300. doi: 10.1111/j.1365-2761.2009.01121.x
19. Ahmadifar E, Razeghi Mansour M, Keramat Amirkolaie A, Fadaii Rayeni M. Growth efficiency, survival and haematological changes in great sturgeon (*Huso huso* Linnaeus, 1758) juveniles fed diets supplemented with different levels of thymol–carvacrol. *Anim Feed Sci Technol.* (2014) 198:304–8. doi: 10.1016/j.anifeedsci.2014.08.012
20. Welch HC. Regulation and function of P-Rex family Rac-GEFs. *Small GTPases.* (2015) 6:49–70. doi: 10.4161/21541248.2014.973770
21. Baumann M, Pham CT, Benarafa C. SerpinB1 is critical for neutrophil survival through cell-autonomous inhibition of cathepsin G. *Blood.* (2013) 121:3900–7. doi: 10.1182/blood-2012-09-455022
22. Choi YJ, Kim S, Choi Y, Nielsen TB, Yan J, Lu A, et al. SERPINB1-mediated checkpoint of inflammatory caspase activation. *Nat Immunol.* (2019) 20:276–87. doi: 10.1038/s41590-018-0303-z
23. Spicer BA, Conroy PJ, Law RHP, Voskoboinik I, Whisstock JC. Perforin-A key (shaped) weapon in the immunological arsenal. *Semin Cell Dev Biol.* (2017) 72:117–23. doi: 10.1016/j.semcdb.2017.07.033
24. Leal E, Ordás MC, Soleto I, Zarza C, McGurk C, Tafalla C. Functional nutrition modulates the early immune response against viral haemorrhagic septicaemia virus (VHSV) in rainbow trout. *Fish Shellfish Immunol.* (2019) 94:769–79. doi: 10.1016/j.fsi.2019.09.070
25. Ginés S, Mariño M, Mallol J, Canela EI, Morimoto C, Callebaut C, et al. Regulation of epithelial and lymphocyte cell adhesion by adenosine deaminase-CD26 interaction. *Biochem J.* (2002) 361:203–9. doi: 10.1042/0264-6021:3610203
26. Casanova V, Naval-Macabuhay I, Massanella M, Rodríguez-García M, Blanco J, Gatell JM, et al. Adenosine deaminase enhances the immunogenicity of human dendritic cells from healthy and HIV-infected individuals. *PLoS ONE.* (2012) 7:e51287. doi: 10.1371/journal.pone.0051287
27. Saiz ML, Rocha-Perugini V, Sánchez-Madrid F. Tetraspanins as organizers of antigen-presenting cell function. *Front Immunol.* (2018) 9:1074. doi: 10.3389/fimmu.2018.01074
28. Peñaranda MMD, Jensen I, Tollersrud LG, Bruun JA, Jørgensen JB. Profiling the Atlantic salmon IgM^+ B cell surface proteome: novel information on teleost fish B cell protein repertoire and identification of potential B cell markers. *Front Immunol.* (2019) 10:37. doi: 10.3389/fimmu.2019.00037
29. Green LR, Monk PN, Partridge LJ, Morris P, Gorringe AR, Read RC. Cooperative role for tetraspanins in adhesin-mediated attachment of bacterial species to human epithelial cells. *Infect Immun.* (2011) 79:2241–9. doi: 10.1128/iai.01354-10
30. Rimoldi S, Torrecillas S, Montero D, Gini E, Makol A, Valdenegro VV, et al. Assessment of dietary supplementation with galactomannan oligosaccharides and phytogenics on gut microbiota of European sea bass (*Dicentrarchus Labrax*) fed low fishmeal and fish oil based diet. *PLoS ONE.* (2020) 15:e0231494. doi: 10.1371/journal.pone.0231494
31. Torrecillas S, Terova G, Makol A, Serradell A, Valdenegro V, Gini E, et al. Dietary phytogenics and galactomannan oligosaccharides in low fish meal and fish oil-based diets for European sea bass (*Dicentrarchus labrax*) juveniles: Effects on gut health and implications on *in vivo* gut bacterial translocation. *PLoS ONE.* (2019) 14:e0222063. doi: 10.1371/journal.pone.0222063
32. Hampson DJ, Ahmed N. Spirochaetes as intestinal pathogens: lessons from a *Brachyspira* genome. *Gut Pathogens.* (2009) 1:10. doi: 10.1186/1757-4749-1-10
33. Prashar A, Schnettger L, Bernard EM, Gutierrez MG. Rab GTPases in immunity and inflammation. *Front Cell Infect Microbiol.* (2017) 7:435. doi: 10.3389/fcimb.2017.00435
34. Bonello S, Zähringer C, BelAiba RS, Djordjevic T, Hess J, Michiels C, et al. Reactive oxygen species activate the HIF-1alpha promoter via a functional NFkappaB site. *Arterioscler Thromb Vasc Biol.* (2007) 27:755–61. doi: 10.1161/01.ATV.0000258979.92828.bc
35. Sveinbjornsson B, Olsen R, Paulsen S. Immunocytochemical localization of lysozyme in intestinal eosinophilic granule cells (EGCs) of Atlantic salmon, *Salmo salar* L. *J Fish Dis.* (1996) 19:349–55. doi: 10.1046/j.1365-2761.1996.d01-87.x
36. Szmola R, Kukor Z, Sahin-Tóth M. Human mesotrypsin is a unique digestive protease specialized for the degradation of trypsin inhibitors. *J Biol Chem.* (2003) 278:48580–9. doi: 10.1074/jbc.M310301200
37. Kokou F, Fountoulaki E. Aquaculture waste production associated with antinutrient presence in common fish feed plant ingredients. *Aquaculture.* (2018) 495:295–310. doi: 10.1016/j.aquaculture.2018.06.003
38. Perez-Sanchez J, Benedito-Palos L, Estensoro I, Petropoulos Y, Calduch-Giner JA, Browdy CL, et al. Effects of dietary NEXT ENHANCE®150 on growth performance and expression of immune and intestinal integrity related genes in gilthead sea bream (*Sparus aurata* L.). *Fish Shellfish Immunol.* (2015) 44:117–28. doi: 10.1016/j.fsi.2015.01.039
39. Calduch-Giner JA, Sitjà-Bobadilla A, Davey GC, Cairns MT, Kaushik S, Pérez-Sánchez J. Dietary vegetable oils do not alter the intestine transcriptome of gilthead sea bream (*Sparus aurata*), but modulate the transcriptomic response to infection with *Enteromyxum leei*. *BMC Genomics.* (2012) 13:470. doi: 10.1186/1471-2164-13-470
40. Dawson PA, Karpen SJ. Intestinal transport and metabolism of bile acids. *J Lipid Res.* (2015) 56:1085–99. doi: 10.1194/jlr.R054114
41. Sheng Y, Ren H, Limbu SM, Sun Y, Qiao F, Zhai W, et al. The presence or absence of intestinal microbiota affects lipid deposition and related genes expression in zebrafish (*Danio rerio*). *Front Microbiol.* (2018) 9:1124. doi: 10.3389/fmicb.2018.01124

42. Campbell C, McKenney PT, Konstantinovsky D, Isaeva O, Schizas M, Verter J, et al. Bacterial metabolism of bile acids promotes generation of peripheral regulatory T cells. *Nature.* (2020) 581:475–9. doi: 10.1038/s41586-020-2193-0
43. Allers K, Stahl-Hennig C, Fiedler T, Wibberg D, Hofmann J, Kunkel D, et al. The colonic mucosa-associated microbiome in SIV infection: shift towards bacteroidetes coincides with mucosal $CD4^+$ T cell depletion and enterocyte damage. *Sci Rep.* (2020) 10:10887. doi: 10.1038/s41598-020-67843-4
44. Fiorucci S, Biagioli M, Zampella A, Distrutti E. Bile acids activated receptors regulate innate immunity. *Front Immunol.* (2018) 9:1853. doi: 10.3389/fimmu.2018.01853
45. Spanogiannopoulos P, Bess EN, Carmody RN, Turnbaugh PJ. The microbial pharmacists within us: a metagenomic view of xenobiotic metabolism. *Nat Rev Microbiol.* (2016) 14:273–87. doi: 10.1038/nrmicro.2016.17
46. Wang S-Z, Yu Y-J, Adeli K. Role of gut microbiota in neuroendocrine regulation of carbohydrate and lipid metabolism via the microbiota-gut-brain-liver axis. *Microorganisms.* (2020) 8:527. doi: 10.3390/microorganisms8040527
47. Diaz M, Dopido R, Gomez T, Rodriguez C. Membrane lipid microenvironment modulates thermodynamic properties of the Na^+-K^+-ATPase in branchial and intestinal epithelia in euryhaline fish *in vivo*. *Front Physiol.* (2016) 7:589. doi: 10.3389/fphys.2016.00589
48. Niespolo C, Salamanca Viloria J, Deshmukh S, Villacanas Perez O, Sudbery I, Wilson H, et al. BS25 Investigating the MIR-101-3P/TRIB1 axis in macrophage immunometabolism. *Heart.* (2019) 105:A156. doi: 10.1136/heartjnl-2019-BCS.188
49. Berk PD, Zhou S, Kiang C, Stump DD, Fan X, Bradbury MW. Selective upregulation of fatty acid uptake by adipocytes characterizes both genetic and diet-induced obesity in rodents. *J Biol Chem.* (1999) 274:28626–31. doi: 10.1074/jbc.274.40.28626
50. Sanz Y., Moya-Pérez A. Microbiota, Inflammation and obesity. In: Lyte M., Cryan J. editors. *Microbial Endocrinology: The Microbiota-Gut-Brain Axis in Health and Disease. Advances in Experimental Medicine and Biology*, New York, NY: Springer (2014) 817. doi: 10.1007/978-1-4939-0897-4_14
51. Schoeler M, Caesar R. Dietary lipids, gut microbiota and lipid metabolism. *Rev Endocr Metab Disord.* (2019) 20:461–72. doi: 10.1007/s11154-019-09512-0
52. Yang Y, Yang F, Huang M, Wu H, Yang C, Zhang X, et al. Fatty liver and alteration of the gut microbiome induced by diallyl disulfide. *Int J Mol Med.* (2019) 44:1908–20. doi: 10.3892/ijmm.2019.4350
53. Li Y, Fu X, Ma X, Geng S, Jiang X, Huang Q, et al. Intestinal microbiome-metabolome responses to essential oils in piglets. *Front Microbiol.* (2018) 9:1988. doi: 10.3389/fmicb.2018.01988
54. Estruch G, Collado MC, Peñaranda DS, Tomás Vidal A, Jover Cerdá M, Pérez Martínez G, Martinez-Llorens S. Impact of fishmeal replacement in diets for gilthead sea bream (*Sparus aurata*) on the gastrointestinal microbiota determined by pyrosequencing the 16S rRNA gene. *PLoS ONE.* (2015) 10:e0136389. doi: 10.1371/journal.pone.0136389
55. Huyben D, Vidaković A, Werner Hallgren S, Langeland M. High-throughput sequencing of gut microbiota in rainbow trout (*Oncorhynchus mykiss*) fed larval and pre-pupae stages of black soldier fly (*Hermetia illucens*). *Aquaculture.* (2019) 500:485–91. doi: 10.1016/j.aquaculture.2018.10.034
56. Johnson DI. *Corynebacterium* spp. In: Johnson DI, editor. *Bacterial Pathogens and Their Virulence Factors*. Cham: Springer International Publishing (2018). p. 73–9.
57. Kvamme BO, Gadan K, Finne-Fridell F, Niklasson L, Sundh H, Sundell K, et al. Modulation of innate immune responses in Atlantic salmon by chronic hypoxia-induced stress. *Fish Shellfish Immunol.* (2013) 34:55–65. doi: 10.1016/j.fsi.2012.10.006
58. Webster TMU, Rodriguez-Barreto D, Consuegra S, Garcia de Leaniz C. Cortisol-induced signatures of stress in the fish microbiome. *bioRxiv.* (2019) 826503. doi: 10.1101/826503
59. Mommsen TP, Vijayan MM, Moon TW. Cortisol in teleosts: dynamics, mechanisms of action, and metabolic regulation. *Rev Fish Biol Fish.* (1999) 9:211–68. doi: 10.1023/A:1008924418720
60. Serradell A, Torrecillas S, Makol A, Valdenegro V, Fernández-Montero A, Acosta F, et al. Prebiotics and phytogenics functional additives in low fish meal and fish oil based diets for European sea bass (*Dicentrarchus labrax*): Effects on stress and immune responses. *Fish Shellfish Immunol.* (2020) 100:219–29. doi: 10.1016/j.fsi.2020.03.016
61. Yada T. Growth hormone and fish immune system. *Gen Compar Endocrinol.* (2007) 152:353–8. doi: 10.1016/j.ygcen.2007.01.045
62. McCormick SD. Endocrine control of osmoregulation in teleost fish. *Am Zool.* (2015) 41:781–94. doi: 10.1093/icb/41.4.781
63. Lin TY, Liao BK, Horng JL, Yan JJ, Hsiao CD, Hwang PP. Carbonic anhydrase 2-like a and 15a are involved in acid-base regulation and Na^+ uptake in zebrafish H^+-ATPase-rich cells. *Am J Physiol Cell Physiol.* (2008) 294:C1250–60. doi: 10.1152/ajpcell.00021.2008
64. Lin G, Zheng M, Li S, Xie J, Fang W, Gao D, et al. Response of gut microbiota and immune function to hypoosmotic stress in the yellowfin seabream (*Acanthopagrus latus*). *Sci Total Environ.* (2020) 745:140976. doi: 10.1016/j.scitotenv.2020.140976
65. Kan H, Zhao F, Zhang XX, Ren H, Gao S. Correlations of gut microbial community shift with hepatic damage and growth inhibition of *Carassius auratus* induced by pentachlorophenol exposure. *Environ Sci Technol.* (2015) 49:11894–902. doi: 10.1021/acs.est.5b02990
66. Mardinoglu A, Shoaie S, Bergentall M, Ghaffari P, Zhang C, Larsson E, et al. The gut microbiota modulates host amino acid and glutathione metabolism in mice. *Mol Syst Biol.* (2015) 11:834. doi: 10.15252/msb.20156487
67. Wu G, Fang YZ, Yang S, Lupton JR, Turner ND. Glutathione metabolism and its implications for health. *J Nutr.* (2004) 134:489–92. doi: 10.1093/jn/134.3.489
68. Vallejos-Vidal E, Reyes-Cerpa S, Rivas-Pardo JA, Maisey K, Yáñez JM, Valenzuela H, et al. Single-nucleotide polymorphisms (SNP) mining and their effect on the tridimensional protein structure prediction in a set of immunity-related expressed sequence tags (EST) in Atlantic salmon (*Salmo salar*). *Front Genet.* (2020) 10:1406. doi: 10.3389/fgene.2019.01406
69. Schlenk D, Celander M, Gallagher E, George S, James M, Kullman S, et al. Biotransformation in fishes. In: Di Giulio RT, Hinton DE, editors. *The Toxicology of Fishes*. Boca Raton, FL: CRC Press (2008). p. 153–234.
70. Gao C, Jiang X, Wang H, Zhao Z, Wang W. Drug metabolism and pharmacokinetics of organosulfur compounds from garlic. *J Drug Metab Toxicol.* (2013) 4:159. doi: 10.4172/2157-7609.1000159
71. Khan I, Bhardwaj M, Shukla S, Min SH, Choi DK, Bajpai VK, et al. Carvacrol inhibits cytochrome P450 and protects against binge alcohol-induced liver toxicity. *Food Chem Toxicol.* (2019) 131:110582. doi: 10.1016/j.fct.2019.110582
72. Espinosa C, Cuesta A, Esteban M. Effects of dietary polyvinylchloride microparticles on general health, immune status and expression of several genes related to stress in gilthead seabream (*Sparus aurata* L.). *Fish Shellfish Immunol.* (2017) 68:251–9. doi: 10.1016/j.fsi.2017.07.006
73. Purushe J, Fouts DE, Morrison M, White BA, Mackie RI, Coutinho PM, et al. Comparative genome analysis of *Prevotella ruminicola* and *Prevotella bryantii*: insights into their environmental niche. *Microb Ecol.* (2010) 60:721–9. doi: 10.1007/s00248-010-9692-8
74. Larsen JM. The immune response to *Prevotella* bacteria in chronic inflammatory disease. *Immunology.* (2017) 151:363–74. doi: 10.1111/imm.12760
75. Makridis P, Martins S, Vercauteren T, Van Driessche K, Decamp O, Dinis MT. Evaluation of candidate probiotic strains for gilthead sea bream larvae (*Sparus aurata*) using an *in vivo* approach. *Lett Appl Microbiol.* (2005) 40:274–7. doi: 10.1111/j.1472-765X.2005.01676.x
76. Goyal AK, Zylstra GJ. Genetics of naphthalene and phenanthrene degradation by *Comamonas testosteroni*. *J Ind Microbiol Biotechnol.* (1997) 19:401–7. doi: 10.1038/sj.jim.2900476
77. Igwaran A, Iweriebor BC, Ofuzim Okoh S, Nwodo UU, Obi LC, Okoh AI. Chemical constituents, antibacterial and antioxidant properties of the essential oil flower of *Tagetes minuta* grown in Cala community Eastern Cape, South Africa. *BMC Complement Altern Med.* (2017) 17:351. doi: 10.1186/s12906-017-1861-6
78. Disner GR, Calado SL, Assis CS, Cestari MM. Toxicity of naphthalene in the neotropical fish *Astyanax lacustris* (Characiformes: Characidae) and *Geophagus brasiliensis* (Perciformes: Cichlidae). *Evidência.* (2017) 17:e12976. doi: 10.18593/eba.v17i1.12976
79. Fialová SB, Rendekova K, Mucaji P, Slobodnikova L. Plant natural agents: polyphenols, alkaloids and essential oils as perspective solution of microbial resistance. *Curr Organ Chem.* (2017) 21:1875–84. doi: 10.2174/1385272821666170127161321

80. Daferera DJ, Tarantilis PA, Polissiou MG. Characterization of essential oils from *lamiaceae* species by fourier transform Raman spectroscopy. *J Agric Food Chem.* (2002) 50:5503–7. doi: 10.1021/jf0203489
81. Dziri S, Casabianca H, Hanchi B, Hosni K. Composition of garlic essential oil (*Allium sativum* L.) as influenced by drying method. *J Essent Oil Res.* (2014) 26:91–6. doi: 10.1080/10412905.2013.868329
82. Leimkühler S, Bühning M, Beilschmidt L. Shared sulfur mobilization routes for tRNA thiolation and molybdenum cofactor biosynthesis in prokaryotes and eukaryotes. *Biomolecules.* (2017) 7:5. doi: 10.3390/biom7010005
83. Magariños B, Romalde JL, Santos Y, Casal JF, Barja JL, Toranzo AE. Vaccination trials on gilthead seabream (*Sparus aurata*) against *Pasteurella piscicida*. *Aquaculture.* (1994) 120:201–8. doi: 10.1016/0044-8486(94)90078-7
84. Pujalte MJ, Sitjà-Bobadilla A, Álvarez-Pellitero P, Garay E. Carriage of potentially fish-pathogenic bacteria in *Sparus aurata* cultured in Mediterranean fish farms. *Dis Aquat Organ.* (2003) 54:119–26. doi: 10.3354/dao054119
85. Silva FC, Nicoli JR, Zambonino-Infante JL, Kaushik S, Gatesoupe FJ. Influence of the diet on the microbial diversity of faecal and gastrointestinal contents in gilthead sea bream (*Sparus aurata*) and intestinal contents in goldfish (*Carassius auratus*). *FEMS Microbiol Ecol.* (2011) 78:285–96. doi: 10.1111/j.1574-6941.2011.01155.x
86. Itoi S, Okamura T, Koyama Y, Sugita H. Chitinolytic bacteria in the intestinal tract of Japanese coastal fishes. *Can J Microbiol.* (2006) 52:1158–63. doi: 10.1139/w06-082
87. Moi IM, Roslan NN, Leow ATC, Ali MSM, Rahman RNZRA, Rahimpour A, et al. The biology and the importance of *Photobacterium* species. *Appl Microbiol Biotechnol.* (2017) 101:4371–85. doi: 10.1007/s00253-017-8300-y
88. Rico RM, Tejedor-Junco MT, Tapia-Paniagua ST, Alarcón FJ, Mancera JM, López-Figueroa F, et al. Influence of the dietary inclusion of *Gracilaria cornea* and *Ulva rigida* on the biodiversity of the intestinal microbiota of *Sparus aurata* juveniles. *Aquac Int.* (2016) 24:965–84. doi: 10.1007/s10499-015-9964-x
89. Beltrán JMG, Silvera DG, Ruiz CE, Campo V, Chupani L, Faggio C, et al. Effects of dietary *Origanum vulgare* on gilthead seabream (*Sparus aurata* L.) immune and antioxidant status. *Fish Shellfish Immunol.* (2020) 99:452–61. doi: 10.1016/j.fsi.2020.02.040
90. Hernandez LH, Hardy RW. Vitamin A functions and requirements in fish. *Aquac Res.* (2020) 51:3061–71. doi: 10.1111/are.14667
91. Filocamo A, Nueno-Palop C, Bisignano C, Mandalari G, Narbad A. Effect of garlic powder on the growth of commensal bacteria from the gastrointestinal tract. *Phytomedicine.* (2012) 19:707–11. doi: 10.1016/j.phymed.2012.02.018
92. Yin D, Du E, Yuan J, Gao J, Wang Y, Aggrey SE, et al. Supplemental thymol and carvacrol increases ileum *Lactobacillus* population and reduces effect of necrotic enteritis caused by *Clostridium perfringes* in chickens. *Sci Rep.* (2017) 7:7334. doi: 10.1038/s41598-017-07420-4
93. Laity J, Lee B, Wright P. Zinc finger proteins: new insights into structural and functional diversity. *Curr Opin Struct Biol.* (2001) 11:39–46. doi: 10.1016/S0959-440X(00)00167-6
94. Will CL, Lührmann R. Spliceosomal UsnRNP biogenesis, structure and function. *Curr Opin Cell Biol.* (2001) 13:290–301. doi: 10.1016/S0955-0674(00)00211-8
95. Zeng H, Nanayakkara GK, Shao Y, Fu H, Sun Y, Cueto R, et al. DNA checkpoint and repair factors are nuclear sensors for intracellular organelle stresses—inflammations and cancers can have high genomic risks. *Front Physiol.* (2018) 9:516. doi: 10.3389/fphys.2018.00516
96. Wang J, An H, Mayo MW, Baldwin AS, Yarbrough WG. LZAP, a putative tumor suppressor, selectively inhibits NF-kappaB. *Cancer Cell.* (2007) 12:239–51. doi: 10.1016/j.ccr.2007.07.002
97. Nakad R, Schumacher B. DNA damage response and immune defense: links and mechanisms. *Front Genet.* (2016) 7:147. doi: 10.3389/fgene.2016.00147

Conflict of Interest: JF is a current TECNOVIT-FARMFAES S.L. employee conducting an Industrial Ph.D.

The remaining authors declare that the research was conducted in the absence of any commercial or financial relationships that could be construed as a potential conflict of interest.

frontiers in Immunology

ORIGINAL RESEARCH
published: 12 March 2021
doi: 10.3389/fimmu.2021.633621

Carvacrol, Thymol, and Garlic Essential Oil Promote Skin Innate Immunity in Gilthead Seabream (*Sparus aurata*) Through the Multifactorial Modulation of the Secretory Pathway and Enhancement of Mucus Protective Capacity

Joana P. Firmino[1,2,3], Laura Fernández-Alacid[4], Eva Vallejos-Vidal[5], Ricardo Salomón[1,3], Ignasi Sanahuja[4], Lluis Tort[6], Antoni Ibarz[4], Felipe E. Reyes-López[6,7,8] and Enric Gisbert[1]**

[1] IRTA, Centre de Sant Carles de la Ràpita (IRTA-SCR), Aquaculture Program, Sant Carles de la Ràpita, Spain, [2] TECNOVIT–FARMFAES, S.L. Pol. Ind. Les Sorts, Alforja, Spain, [3] Ph.D. Program in Aquaculture, Universitat Autònoma de Barcelona, Bellaterra, Spain, [4] Department of Cell Biology, Physiology and Immunology, Faculty of Biology, University of Barcelona, Barcelona, Spain, [5] Departamento de Biología, Facultad de Química y Biología, Centro de Biotecnología Acuícola, Universidad de Santiago de Chile, Santiago, Chile, [6] Department of Cell Biology, Physiology and Immunology, Universitat Autònoma de Barcelona, Bellaterra, Spain, [7] Facultad de Medicina Veterinaria y Agronomía, Universidad de Las Américas, Santiago, Chile, [8] Consorcio Tecnológico de Sanidad Acuícola, Ictio Biotechnologies S.A., Santiago, Chile

One of the main targets for the use of phytogenics in aquafeeds is the mucosal tissues as they constitute a physical and biochemical shield against environmental and pathogenic threats, comprising elements from both the innate and acquired immunity. In the present study, the modulation of the skin transcriptional immune response, the bacterial growth capacity in skin mucus, and the overall health condition of gilthead seabream (*Sparus aurata*) juveniles fed a dietary supplementation of garlic essential oil, carvacrol, and thymol were assessed. The enrichment analysis of the skin transcriptional profile of fish fed the phytogenic-supplemented diet revealed the regulation of genes associated to cellular components involved in the secretory pathway, suggesting the stimulation, and recruitment of phagocytic cells. Genes recognized by their involvement in non-specific immune response were also identified in the analysis. The promotion of the secretion of non-specific immune molecules into the skin mucus was proposed to be involved in the *in vitro* decreased growth capacity of pathogenic bacteria in the mucus of fish fed the phytogenic-supplemented diet. Although the mucus antioxidant capacity was not affected by the phytogenics supplementation, the regulation of genes coding for oxidative stress enzymes suggested the reduction of the skin oxidative stress. Additionally, the decreased levels of cortisol in mucus indicated a reduction in the fish allostatic load due to the properties of the tested additive. Altogether, the dietary garlic, carvacrol, and thymol appear to promote the gilthead seabream skin innate immunity and the mucus protective capacity, decreasing its susceptibility to be colonized by pathogenic bacteria.

Keywords: SALT, innate immunity, stress, aquaculture, *Vibrio* infection, teleost fish skin mucus, phytogenic additive, interactome

OPEN ACCESS

Edited by:
Benjamin Costas, University of Porto, Portugal

Reviewed by:
Bernardo Baldisserotto, Federal University of Santa Maria, Brazil
Samuel A. M. Martin, University of Aberdeen, United Kingdom

***Correspondence:**
Enric Gisbert
Enric.Gisbert@irta.cat
Felipe E. Reyes-López
Felipe.Reyes@uab.cat

Specialty section:
This article was submitted to Nutritional Immunology, a section of the journal Frontiers in Immunology

Received: *25 November 2020*
Accepted: *11 February 2021*
Published: *12 March 2021*

Citation:
Firmino JP, Fernández-Alacid L, Vallejos-Vidal E, Salomón R, Sanahuja I, Tort L, Ibarz A, Reyes-López FE and Gisbert E (2021) Carvacrol, Thymol, and Garlic Essential Oil Promote Skin Innate Immunity in Gilthead Seabream (Sparus aurata) Through the Multifactorial Modulation of the Secretory Pathway and Enhancement of Mucus Protective Capacity. Front. Immunol. 12:633621. doi: 10.3389/fimmu.2021.633621

INTRODUCTION

Fish infectious diseases are one of the main constraints of the aquaculture sector, representing a serious economic, social, and environmental challenge for the industry (1). Since fish farmers depend on high survival rates and healthy animals, strategies to improve their performance, immune status, and welfare are highly demanded for supporting health management practices that positively impact in the final revenue of the fish farm. On this basis, the development of functional feed additives designed to physiologically support fish to cope with pathogenic and other external challenges intrinsic to aquaculture rearing conditions, represents a promising tool to be implemented in a sustainable and environmentally-responsible aquaculture industry (2).

Functional feeds containing essential oils, one of most commonly used group of phytogenics in aquafeeds, have received increased attention during these last years due to their antimicrobial, immunostimulant, antioxidant, anti-stress, and growth-promoting properties (3–5). Besides essential oils being repeatedly demonstrated to stimulate both humoral and cellular components of the fish innate immunity (6), numerous have been also shown to display a noteworthy antimicrobial activity against a wide range of fish pathogens (7, 8), putting them on the spotlight for the development of sustainable prophylactics. Particularly, phytogenics derived from garlic (*Allium sativum* L., Alliaceae, Liliaceae), oregano (*Oreganum vulgare*, Labiateae), and thyme (*Thymus vulgare*, Labiateae) are among the most studied and administrated, due to their recognized health-promoting properties for aquatic species (6).

One of the main targets for this type of nutritional strategies is the mucosal tissues, due to their importance in the protection against the immediate contact with the environment and potential pathogens. Besides acting as a physical barrier, the mucosal layer also offers a biochemical shield, in which elements from both the innate and acquired immunity are present (9). In particular, the fish skin mucus represents the largest mucosal barrier with its whole epidermis directly exposed to the environment. It is responsible for the first line of defense against external threats, determining pathogen adhesion to the epithelial surfaces (10, 11). Furthermore, skin mucus participates in important physiological processes like osmoregulation, swimming, sensory reception (12), and ecological intra and interspecific interactions (11). Additionally, the fish skin is also characterized by its active mucosal immunity, containing a skin-associated lymphoid tissue (SALT), which is able to respond in case of infection (12, 13). In fact, the immune response described in fish skin against antigen stimulation is similar to other mucosa (14). That immune response involves the secretion of innate immune molecules and the action of specialized cells [(15) and references therein].

Therefore, the improvement of both the epidermal mucus composition and the SALT response to environmental stressors including infective agents by means of dietary tools such as functional feed additives, represents a promising approach for preventing bacterial-induced pathologies in farmed fish. In this context, the aim of the present study was to evaluate the inclusion of a functional feed additive composed by a blend of garlic essential oil, carvacrol, and thymol (the main bioactive compounds of Labiateae plants essential oils) in a standard on-growing diet for gilthead seabream (*Sparus aurata*), assessing its effects on the skin transcriptional response, pathogenic bacterial growth capacity in skin mucus, and fish overall health condition. This species was chosen since it is the most important marine farmed fish species in the Mediterranean with an annual production of 85,385.1 t in 2018 and an economic value of 502,398,000 US$ (16); thus, improving health management strategies based on sustainable dietary approaches for this farmed species is of relevance for this growing industry.

MATERIALS AND METHODS

Diets and Fish Rearing

Juveniles of gilthead seabream were purchased from a Mediterranean fish farm (Piscicultura Marina Mediterránea S.L., Andromeda Group, Valencia, Spain) and on-grown at IRTA–Sant Carles de la Ràpita facilities for research purposes (17). Before the onset of the trial, fish were individually measured in body weight (BW) and standard length (SL) to the nearest 0.1 g and 1 mm, respectively (BW = 40.3 ± 0.1 g; SL = 12.0 ± 0.2 mm). Then, 150 juveniles were randomly distributed among six 450 L tanks (25 fish per tank; initial density = 2 kg m^{-3}; three replicate tanks per experimental group) connected to an IRTAmar® system working under an open-flow regime.

Fish were fed two experimental diets, one devoid of the functional feed additive (control diet) and a second one supplemented with 0.5% of a microencapsulated functional additive containing synthetic garlic essential oil, carvacrol, and thymol (AROTEC-G®, TECNOVIT-FARMFAES, S.L., Spain). Both diets were tested in triplicate tanks and administered for a period of 65 days. Fish were hand-fed two times per day at the daily rate of 3.0% of the stocked biomass, which approached apparent satiation. The control diet was formulated with high levels of marine-derived protein sources (30% fishmeal, 2.5% soluble protein concentrate—CPSP 90® and 2.5 krill meal), containing 46% crude protein, 18% crude fat, and 21.5 MJ/kg gross energy (**Table 1**). Both tested experimental diets were formulated to fulfill the nutritional requirements of juvenile gilthead seabream for summer conditions (18). Diets were manufactured by Sparos Lda. (Olhão, Portugal). In particular, main ingredients were ground (below 250 μm) in a micropulverizer hammer mill (SH1; Hosokawa Micron, B.V., Doetinchem, The Netherlands). Powder ingredients and oils were then mixed according to the target formulation in a paddle mixer (RM90; Mainca, S.L., Granollers, Spain). All diets were manufactured by temperature-controlled extrusion (pellet sizes: 2.0 mm) by means of a low-shear extruder (P55; Italplast, S.r.l., Parma, Italy). Upon extrusion, all feed batches were dried in a convection oven (OP 750-UF; LTE Scientifics, Oldham, UK) for 4 h at 45°C.

The nutritional assay was performed under natural photoperiod (August–September), with daily monitoring of the water temperature (25.1 ± 1.5°C, range: 22.6–28°C), oxygen (6.8 ± 1.7 mg/L; >80% saturation) (OXI330, Crison Instruments, Barcelona, Spain) and pH (7.5 ± 0.01) (pHmeter 507, Crison

TABLE 1 | Formulation of the control diet used during the nutritional assay.

Ingredients	Control diet (%)
Fishmeal 70 LT FF Skagen	20.0
Fishmeal CORPESCA Super Prime	10.0
CPSP 90	2.5
Squid meal	2.5
Soy protein concentrate (Soycomil)	5.0
Wheat Gluten	5.0
Corn gluten	8.0
Korfeed 60	4.5
Soybean meal 48	8.0
Rapeseed meal	4.0
Sunflower meal	3.0
Wheat meal	7.0
Whole peas	2.5
Fish oil–COPPENS	9.0
Soybean oil	1.5
Rapeseed oil	2.5
Vitamin and mineral Premix PV01	2.0
Soy lecithin–Powder	2.0
Antioxidant powder (Paramega)	0.4
Dicalcium phosphate	0.6
Proximate composition, % in dry basis	
Crude protein	46.2
Crude fat	18.4
Gross energy (MJ/kg)	21.5

Instruments). Salinity (35‰) (MASTER-20 T; ATAGO Co. Ltd, Tokyo, Japan), ammonia (0.13 ± 0.1 mg NH_4^+/L), and nitrite (0.18 ± 0.1 mg NO_2^-/L) levels (HACH DR9000 Colorimeter, Hach®, Spain) were weekly measured.

Sampling

At the end of the trial, all fish were anesthetized (buffered 150 mg/L MS-222, Sigma-Aldrich, Madrid, Spain) and measured for individual body weight and standard length ($BW_{control\ diet} = 157.8 \pm 14.2$ g and $SL_{control\ diet} = 17.3 \pm 0.6$ cm; $BW_{supplemented\ diet} = 150.8 \pm 14.9$ g and $SL_{supplemented\ diet} = 17.1 \pm 0.6$ cm) as published in (17). Then, eight fish from each tank ($n = 24$ per dietary treatment) were randomly selected and skin mucus sample collected following the method described in (19). In brief, skin mucus was collected from the over-lateral line of anesthetized fish in a front to caudal direction using sterile glass slides, and mucus was carefully pushed and collected in a sterile tube (2 mL), avoiding the contamination with blood and/or urine-genital and intestinal excretions. The above-mentioned procedure lasted <2 min in order to avoid the degradation of mucus metabolites. Mucus samples were homogenized using a sterile Teflon pestle to desegregate mucus mesh before centrifugation at 14,000 × g during 15 min at 4°C. The resultant mucus supernatants were collected, avoiding the surface lipid layer, aliquoted, and stored at −80°C for further analysis. For transcriptional analysis purposes, other four fish were randomly selected from each tank ($n = 12$ fish per dietary treatment) and euthanized with an anesthetic overdose. A ca. 1 cm^2 section of the skin from the mid region of the body over the lateral line of the right side from each fish was dissected, and the muscle tissue attached to it removed. Samples were immersed in RNAlater™ (Invitrogen, Thermo Fisher Scientific, Lithuania), incubated overnight (4°C) and stored at −80°C for further RNA extraction.

Skin Transcriptomic Analysis

RNA Isolation and Quality Control

Total RNA from the skin of twelve randomly selected fish per dietary treatment was extracted using the RNeasy® Mini Kit (Qiagen, Germany). Total RNA was eluted in a final volume of 35 μL nuclease-free water and treated with DNAse (DNA-free™ DNA Removal Kit; Invitrogen, Lithuania). Total RNA concentration and purity were measured using Nanodrop-2000® spectrophotometer (Thermo Scientific, USA) and stored at −80°C until analysis. Prior to hybridization with microarrays, RNA samples were diluted to 133.33 ng/μL concentration, checked for RNA integrity (Agilent 2100 Bioanalyzer; Agilent Technologies, Spain) and selected by the criteria of a RIN value >8.5. Three different pools of samples per dietary treatment were established ($n = 4$ fish each pool).

Microarray Hybridization and Analysis

Skin transcriptional analysis from both experimental groups was carried out using the Aquagenomics *Sparus aurata* oligonucleotide microarray v2.0 (4 × 44 K) (SAQ) platform. Detailed information and transcriptomic raw data are available at the Gene Expression Omnibus (GEO) public repository at the US National Center for Biotechnology Information (NCBI), accession numbers GPL13442, and GSE162504, respectively. The sampling labeling, hybridization, washes, and scanning was performed as described in (19). Briefly, a one-color RNA labeling was used (Agilent One-Color RNA Spike-In kit; Agilent Technologies, USA). RNA from each sample pool (200 ng) was reverse-transcribed with spike-in. Then, total RNA was used as template for Cyanine-3 (Cy3) labeled cRNA synthesis and amplified with the Quick Amp Labeling kit (Agilent Technologies). cRNA samples were purified using the RNeasy® micro kit (Qiagen). Dye incorporation and cRNA yield were checked (NanoDrop ND-2000® spectrophotometer). Then, Cy3-labeled cRNA (1.5 mg) with specific activity >6.0 pmol Cy3/mg cRNA was fragmented at 60°C for 30 min, and hybridized with the array in presence of hybridization buffer (Gene expression hybridization kit, Agilent Technologies) at 65°C for 17 h. For washes, microarrays were incubated with Gene expression wash buffers, and stabilization and drying solution according to manufacturer instructions (Agilent Technologies). Microarray slides were then scanned (Agilent G2505B Microarray Scanner System), and spot intensities and other quality control features extracted (Agilent Feature Extraction software version 10.4.0.0).

The Search Tool for the Retrieval of Interacting Genes (STRING) public repository version 11.0 (https://string-db.org) was used to generate the skin transcripteractome for the

fish fed the phytogenic-supplemented diet. A Protein-Protein interaction (PPI) Networks Functional Enrichment Analysis for all the differentially expressed genes (DEGs) was conducted with a high-confidence interaction score (0.9) using *Homo sapiens* as model organism (17, 20). Gene Ontology (GO) and Kyoto Encyclopedia of Genes and Genomes (KEGG) enrichment analysis of all the DEGs obtained were also assessed through STRING ($P < 0.05$). In order to confirm match of gene acronyms between both *Homo sapiens* and gilthead seabream species, human orthology identification based on gene/protein name was accessed through the Genecards (www.genecards.org) (21) and Uniprot (www.uniprot.org) databases. Additionally, protein-protein BLAST (BLASTp) were run ($E < 10^{-7}$; query cover > 95%).

Skin Mucus Parameters

Bacterial Growth Assessment in Skin Mucus

Two bacterial fish pathogens were used for the growth curve assay, *Vibrio anguillarum* (CECT number: 522T), and *Pseudomonas anguilliseptica* (CECT number: 899T) from the Spanish Type Culture Collection (CECT, University of Valencia, Valencia, Spain), and the non-pathogenic bacterium for fish, *Escherichia coli* (DSMZ number: 423) from the German Collection of Microorganisms and Cell Cultures (Leibniz Institute DSMZ, Germany). The two pathogenic bacteria were cultured at 30°C for 24 h in marine broth (MB-2216, Becton and Dickinson, USA) and the *E. coli* was cultured at 37°C for 24 h in trypticasein soy broth (TSB, Laboratorios Conda, Spain). For the culture in skin mucus, bacterial suspension with optical density (OD) of 0.2 were centrifuged and the pellet resuspended in sterile PBS, diluted in new growth medium and adjusted to 106 colony-forming units (CFU) mL^{-1}. Then, to study the bacterial growth capacity in the skin mucus, aliquots of 100 μL of the previously cultured bacteria were incubated in 100 μL of skin mucus (3 pools of 6 individual fish per dietary treatment). In parallel, 100 μL of the same cultured bacteria were also incubated in 100 μL of its respective culture media, as a positive control. Triplicates of 100 μL of each fish mucus samples added to 100 μL of culture media were used as negative control and values subtracted from the bacteria–mucus aliquot results. The bacterial growth was measured by absorbance at $\lambda = 400$ nm every 30 min for 14 h at 25°C in flat-bottomed 96-well plates using an Infinity Pro200^{TM} spectrophotometer. Similar temperature values for bacterial growth cultures (25°C) and fish rearing (25.1°C) were chosen in order to standardize mucus analyses with regard to fish rearing conditions used in the nutritional trial.

Skin Mucus Metabolites and Cortisol Analyses

Glucose concentration on fish skin mucus was determined by an enzymatic colorimetric test (LO-POD glucose, SPINREACT®, St. Esteve de Bas, Spain) as described in (19). The OD of the reaction was determined at $\lambda = 505$ nm with a microplate reader and glucose values expressed as μg glucose per mL of skin mucus. Lactate concentration was determined by an enzymatic colorimetric test (LO-POD lactate, SPINREACT®) following the manufacturer's instructions but with slight modifications for fish skin mucus (19). The OD was determined at $\lambda = 505$ nm and lactate values expressed as μg lactate per mL of skin mucus. Protein concentration of previously homogenized mucus samples was determined using the Bradford assay (22) using bovine serum albumin (Sigma Aldrich, Madrid, Spain) as standard. In particular, mucus samples or standard solutions (from 0 to 1.41 mg mL^{-1}) were mixed with 250 μL of Bradford reagent and incubated for 5 min at room temperature. The OD was determined at $\lambda = 596$ nm in a microplate reader. Protein values were expressed as mg protein per mL of skin mucus. Cortisol levels were measured using an ELISA kit (IBL International, Tecan Group, Switzerland) following the manufacturer's instructions for saliva determinations. Values of OD were determined at $\lambda = 450$ nm with a microplate reader. Cortisol values were expressed as ng cortisol per mL of skin mucus. All standards and samples were analyzed in triplicate (methodological replicates) and spectrophotometric measurements were conducted with an Infinity Pro200^{TM} spectrophotometer (Tecan, Männedorf, Switzerland).

Mucus ratios referred to protein (glucose/protein, lactate/protein and cortisol/protein) were calculated in order to avoid the putative dilution or concentration derived from mucus sampling. As an indicator of the metabolic aerobic response, the glucose/lactate ratio was also calculated (19).

Ferric Antioxidant Power (FRAP) was measured by means of an enzymatic colorimetric test (Ferric antioxidant status detection kit, Invitrogen, Thermo Fisher Scientific, Spain), following the manufacturer's instructions for plasma, with minor modifications. Briefly, 20 μL of mucus sample or standard solutions (from 0 to 1,000 μM μL^{-1} of $FeCl_2$) were mixed with 75 μL of FRAP color solution and incubated at room temperature for 30 min, in triplicate. The OD was measured at $\lambda = 560$ nm. Antioxidant values were expressed as nmol FRAP per mL of mucus, and nmol FRAP per mg of mucus protein. All measurements were performed with a microplate spectrophotometer reader (Infinity Pro200^{TM} spectrophotometer).

Statistical Analysis

Differences between growth performance parameters were analyzed through an unpaired *t*-test ($P < 0.05$) with GraphPad PRISM 7.00 assuming data homoscedasticity. Differences between skin mucus metabolites and cortisol, and differences in bacterial growth inhibition between the two dietary treatments were assessed with SPSS Statistics for Windows, Version 22.0 (IBM Corp, Armonk, NY, USA) through an unpaired *t*-test ($P < 0.05$). Microarrays extracted raw data were imported and analyzed with GeneSpring version 14.5 GX software (Agilent Technologies). The 75% percentile normalization was used to standardize arrays for comparisons and data were filtered by expression. An unpaired *t*-test was conducted without correction to identify those DEGs between both dietary treatments. A $P < 0.05$ was considered statistically significant. The representation for the principal component analysis (PCA) and the hierarchical heatmap were generated using GeneSpring version 14.5 GX software.

RESULTS

Skin Transcriptomic Profile

Under present experimental conditions, in order to determine the modulatory effect of the dietary supplementation of a blend of garlic essential oil, carvacrol, and thymol upon the skin transcriptome, a microarray-based transcriptomic analysis was conducted in gilthead seabream. In total, 534 differentially-expressed genes (DEGs) were found in the skin from both experimental groups ($P < 0.05$; **Supplementary Table 1**). Among these, 393 genes were up-regulated with 390 belonging to the 1.0–1.5-fold change (FC) interval. The other 3 DEGs were grouped in the $1.5 \leq FC \leq 2.0$ interval. On the other hand, 141 genes were down-regulated ($P < 0.05$) and grouped in the range of $-1.5 \geq FC \geq -1.0$. Although genes were observed to be mostly up-regulated in the group fed with the blend of phytogenics (73.6% of DEGs), gene modulation was moderated in terms of fold-change intensity (**Figure 1A**). Common segregation among the pool samples within the same dietary treatment was observed in the hierarchical clustering for the skin transcriptomic response based in similitude patterns of the DEGs response ($P < 0.05$) (**Figure 1B**). The observed differential profile among dietary treatments is supported by the PCA analysis for the analyzed samples (**Figure 1C**).

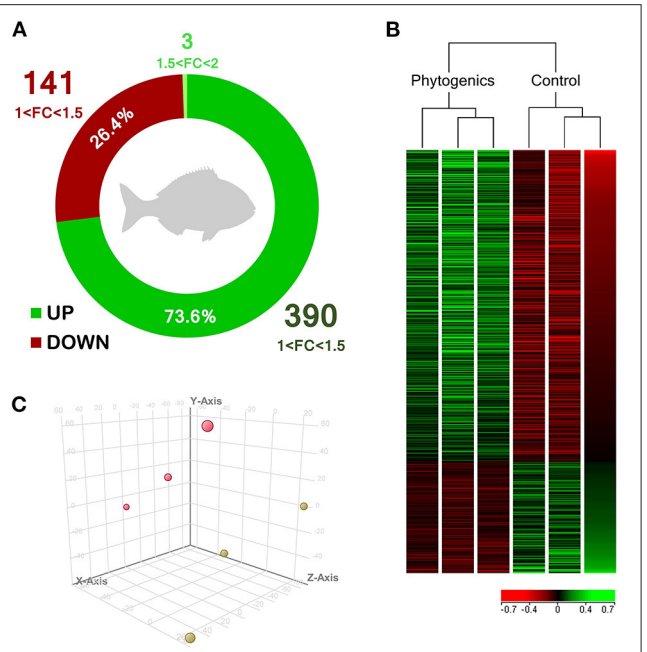

FIGURE 1 | Skin transcriptomic profile of gilthead seabream (*Sparus aurata*) fed a diet supplemented with a blend of garlic essential oil, carvacrol and thymol. **(A)** Differential expression analysis of the gilthead seabream skin transcriptomic response fed a diet supplemented with a blend of garlic, carvacrol and thymol. **(B)** Hierarchical clustering for the control and phytogenic-supplemented diets, based in similitude patterns of the differentially expressed genes (DEGs) detected from three sample pools per dietary group. Data of the six microarrays are depicted, one for each represented pool. Both increased and decreased gene expression pattern is shown in green and red, respectively. All transcripts represented are statistically significant ($P < 0.05$). **(C)** Principal component analysis (PCA) of the DEGs of gilthead seabream skin response to the control diet (yellow) and phytogenic-supplemented diet (pink). Please refers to **Supplementary Table 1** for details.

When considering the complete list of annotated DEGs, a functional network (transcripteractome) containing 203 nodes was generated (**Figures 2**, **3**), which resulted in 341 interactions (edges). The remaining 331 DEGs, annotated as unknown genes, were excluded from the analysis. The enrichment analysis identified in the transcripteractome two main representative processes that were considered to encompass the several Gene Ontology (GO) annotations obtained (**Supplementary Table 2**), denoted as (a) Transcription Regulation, and (b) Secretory Pathway.

The "RNA processing" biological process (GO:0006396; 12 up-regulated genes; 14 down-regulated genes) was the exclusive differentially regulated GO term for the skin of fish fed the diet supplemented with the additive (**Figure 2**). Molecular functions "protein binding" (GO:0005515) and "protein-containing complex binding" (GO:0044877) were also obtained.

In order to elucidate the location relative to the cellular structures in which the DEGs perform their function, several cellular components were identified in the functional network, representing the association between them (**Figure 3**). The analysis included the, "ribonucleoprotein complex" (GO:1990904; 10 up-regulated genes; 9 down-regulated genes), "vesicle" (GO:0031982; 20 up-regulated genes; 20 down-regulated genes), "transport vesicle membrane" (GO:0030658; 2 up-regulated genes; 5 down-regulated genes), "COPII-coated ER to Golgi transport vesicle" (GO:0030134; 2 up-regulated genes; 3 down-regulated genes), "Golgi-associated vesicle" (GO:000579810; 3 up-regulated genes; 4 down-regulated genes), "endosome" (GO:0005768; 10 up-regulated genes; 9 down-regulated genes), "vacuole" (GO:0005773; 9 up-regulated genes; 12 down-regulated genes), "lysosome" (GO:0005764; 7 up-regulated genes; 7 down-regulated genes), and "proton-transporting two-sector ATPase complex" (GO:0016469; 1 up-regulated genes; 3 down-regulated genes).

In order to identify the pathways significantly impacted by the total DEGs obtained, the functional analysis of KEGG pathways revealed also significant differences in the regulation of genes associated with "protein processing in endoplasmic reticulum" (hsa04141; 3 up-regulated genes; 5 down-regulated genes), "phagosome" pathway (hsa04145; 3 up-regulated genes; 5 down-regulated genes), and "*Vibrio cholerae* infection" pathway (hsa05110, belonging to the "infectious disease: bacterial" group; 1 up-regulated gene; 4 down-regulated genes) in the skin of the group fed with the blend of tested phytogenics (**Figure 4** and **Supplementary Table 3**).

Additionally, from the total DEGs obtained from the skin transcriptomic profile of fish fed the phytogenic-supplemented diet, a set of genes were selected by their involvement in the "immune system process" (GO:0002376; 12 up-regulated genes; 5 down-regulated genes). Among the processes related to immunity, "antigen processing and presentation of exogenous peptide antigen via MHC class I" (GO:0002479; 1 up-regulated genes; 2 down-regulated genes), "leukocyte activation"

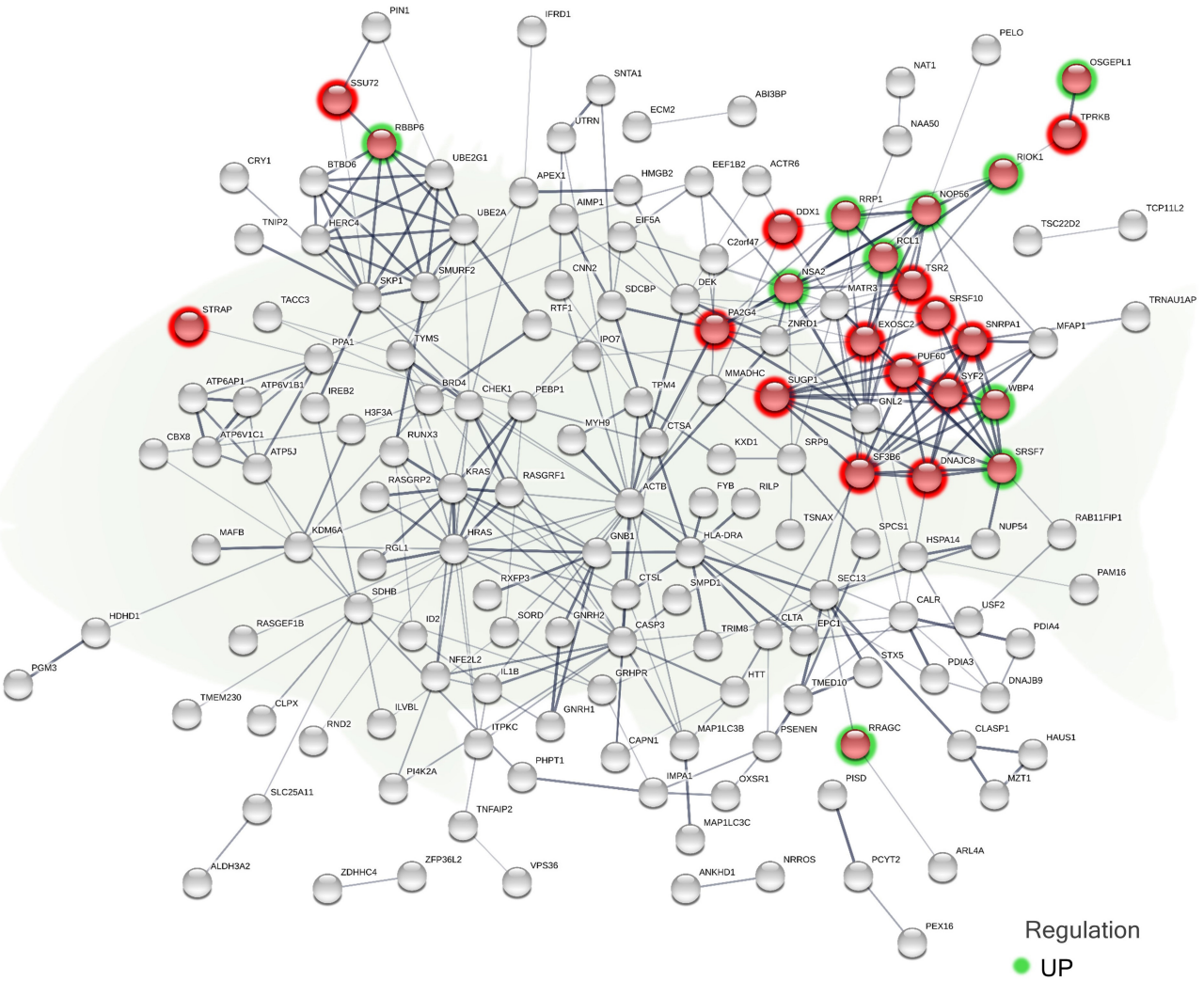

FIGURE 2 | Functional biological network of the differentially expressed genes (DEGs) in the skin of juvenile gilthead seabream (*Sparus aurata*) fed a diet supplemented with a blend of garlic essential oil, carvacrol, and thymol. Green-shaded nodes represent up-regulated genes and red-shaded nodes represent down-regulated genes. Graphic keys and network stats: number of nodes = 203; number of edges = 341; average node degree = 3.36; average local clustering coefficient = 0.4; expected number of edges = 286; PPI enrichment *p*-value = 0.000807. Gene Ontology (GO) definition, count of DEGs within the biological process and respective false discovery rate are described in the graphical figure legend (bottom). For details, please refers to **Supplementary Table 2**.

(GO:0045321; 6 up-regulated genes; 1 down-regulated genes), "regulation of NIK/NF-kappaB signaling" (GO:1901222; 2 up-regulated genes; 1 down-regulated genes), "positive regulation of T cell cytokine production" (GO:0002726; 2 up-regulated genes; 0 down-regulated genes), and "regulation of T cell proliferation" (GO:0042129; 2 up-regulated genes; 1 down-regulated genes) biological processes were highlighted (**Figure 5** and **Supplementary Table 4**).

Bacterial Growth Capacity on Skin Mucus

The transcriptome response arose the modulation of genes associated to immune processes involved in the response to infectious bacterial diseases. Thus, we evaluated whether such response implies a functional protective mechanism against pathogenic bacterial growth on skin mucus. Considering that our data registered a specific response to *Vibrio*, we included in our analysis the fish pathogen *V. anguillarum*. In addition, we also included as control *P. anguilliseptica* (another pathogenic marine fish bacteria) and *E. coli* as non-pathogenic fish bacterium.

When cultured with the skin mucus from fish fed the phytogenic-supplemented diet, a reduction on the growth of the pathogenic bacteria *V. anguillarum* was observed (*t*-test; $P < 0.05$; **Figures 6A,B**). Growth decrease was recorded between 4 and 14 h of bacterial culture; the most accentuated decrease in growth values compared with control diet (over 30%) were found between 8 and 12 h (**Figures 6A,B**). Regarding

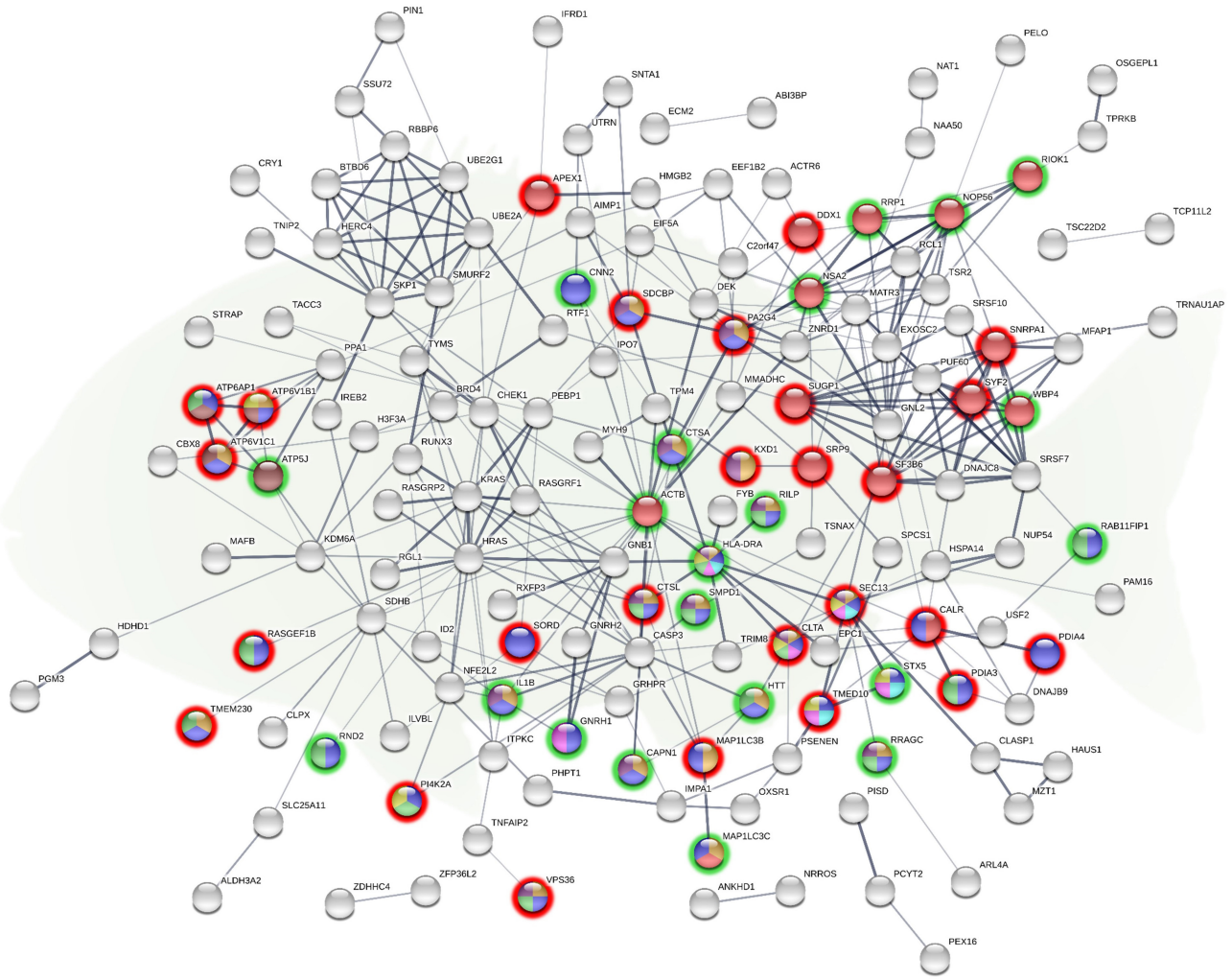

GO-term		Description	Count in gene set	False discovery rate
GO:1990904		Ribonucleoprotein complex	19 of 770	0.012
GO:0005773		Vacuole	21 of 682	0.001
GO:0031982		Vesicle	40 of 2318	0.017
GO:0030134		COPII-coated ER to Golgi transport vesicle	5 of 75	0.024
GO:0005798		Golgi-associated vesicle	7 of 155	0.024
GO:0030658		Transport vesicle membrane	7 of 181	0.044
GO:0005768		Endosome	19 of 876	0.033
GO:0005764		Lysosome	14 of 582	0.044
GO:0016469		Proton-transporting two-sector ATPase complex	4 of 49	0.032

Regulation
UP
DOWN

FIGURE 3 | Functional network representing cellular components related to secretory pathways of the differentially expressed genes (DEGs) in the skin of juvenile gilthead seabream (*Sparus aurata*) fed a diet supplemented with a blend of garlic essential oil, carvacrol and thymol. Node colors indicate the cellular component for each DEG represented. Green-shaded nodes represent up-regulated genes and red-shaded nodes represent down-regulated genes. Graphic keys and network stats: number of nodes = 203; number of edges = 341; average node degree = 3.36; average local clustering coefficient = 0.4; expected number of edges = 286; PPI enrichment *p*-value = 0.000807. Gene Ontology (GO) definition, count of DEGs within the biological process and respective false discovery rate are described in the graphical figure legend (bottom). For details, please refers to **Supplementary Table 2**.

P. anguilliseptica, a decline in bacterial growth was observed in both gilthead seabream skin mucus samples from fish fed the control and phytogenic-supplemented diets (**Figures 6C,D**). However, *P. anguilliseptica* growth decline was observed to be more accentuated in the mucus from fish fed the phytogenic-supplemented diet than in that of the control group at 12–14 h of culture (*t*-test; $P < 0.05$), with a maximum decrease in growth of 50.2 ± 1.6% at 14 h (**Figure 6D**).

Gilthead seabream mucus from both nutritional groups showed a decrease of *E. coli* growth during all the culture period (**Figures 6E,F**), though the most emphasized bacterial growth decrease was observed in the initial interval of 4–8 h

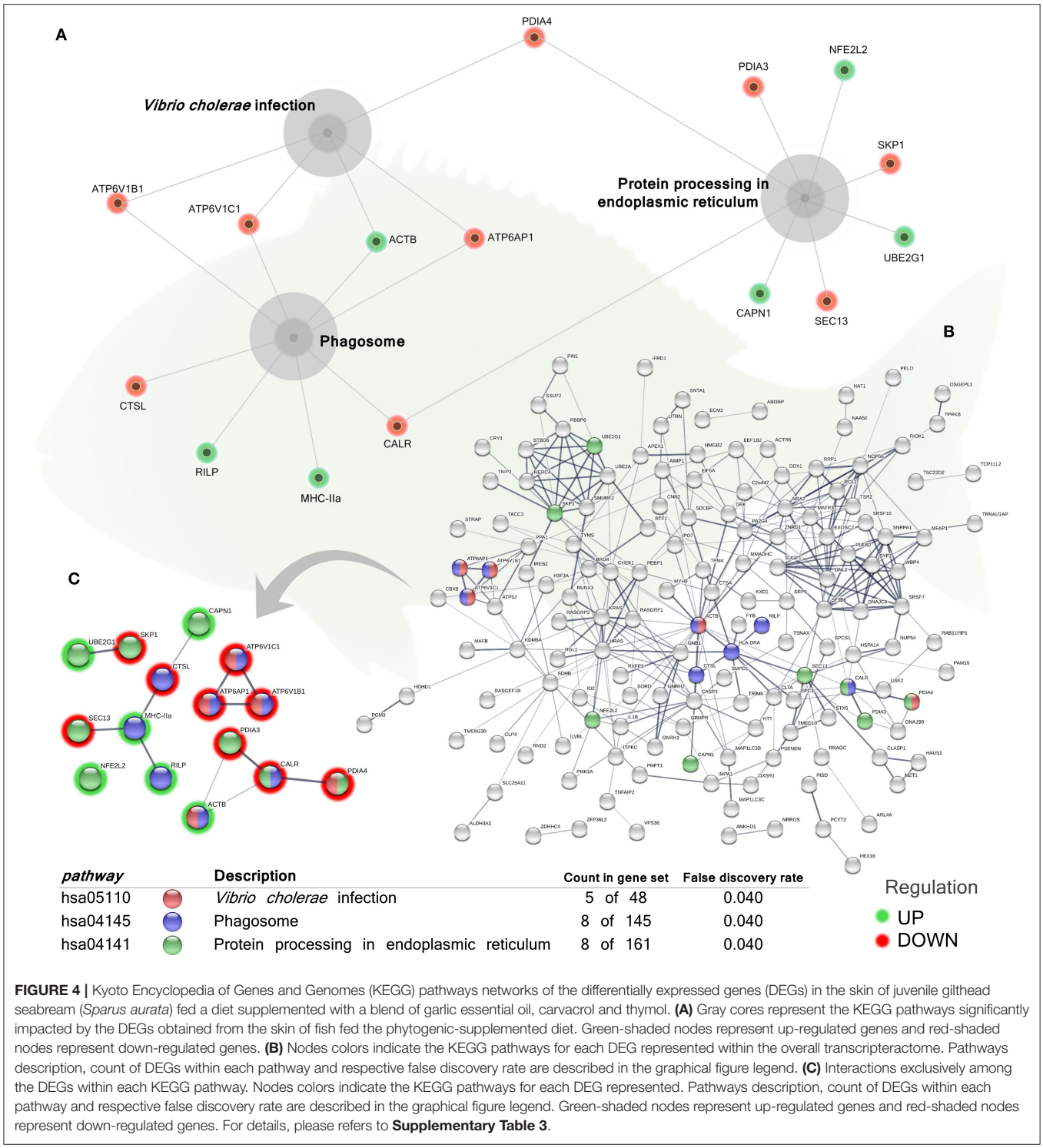

FIGURE 4 | Kyoto Encyclopedia of Genes and Genomes (KEGG) pathways networks of the differentially expressed genes (DEGs) in the skin of juvenile gilthead seabream (*Sparus aurata*) fed a diet supplemented with a blend of garlic essential oil, carvacrol and thymol. **(A)** Gray cores represent the KEGG pathways significantly impacted by the DEGs obtained from the skin of fish fed the phytogenic-supplemented diet. Green-shaded nodes represent up-regulated genes and red-shaded nodes represent down-regulated genes. **(B)** Nodes colors indicate the KEGG pathways for each DEG represented within the overall transcripteractome. Pathways description, count of DEGs within each pathway and respective false discovery rate are described in the graphical figure legend. **(C)** Interactions exclusively among the DEGs within each KEGG pathway. Nodes colors indicate the KEGG pathways for each DEG represented. Pathways description, count of DEGs within each pathway and respective false discovery rate are described in the graphical figure legend. Green-shaded nodes represent up-regulated genes and red-shaded nodes represent down-regulated genes. For details, please refers to **Supplementary Table 3**.

with decreased growth value of 60.3 ± 2.5%, reducing gradually (**Figure 6F**).

Mucus Stress Biomarkers

The skin mucus stress-related biomarkers and their ratios, as well as the ferric antioxidant power are summarized in **Table 2**. The content of soluble protein was not significantly affected by the functional feed additive (t-test, $P > 0.05$). However, glucose, lactate and cortisol levels were observed to be significantly lower in the mucus of gilthead seabream fed the phytogenic-supplemented diet (t-test, $P < 0.05$). No differences among dietary groups were observed in terms of the ferric skin mucus

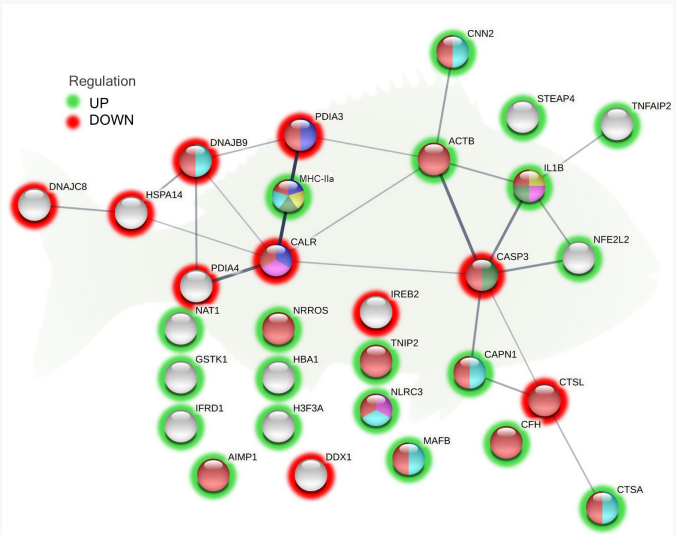

GO-term	Description	Count in gene set	False discovery rate
GO:0002376	Immune system process	17 of 2370	1.07e-05
GO:0002479	Antigen processing and presentation of exogenous peptide antigen via MHC class I, TAP-dependent	3 of 25	0.0037
GO:0045321	Leukocyte activation	7 of 894	0.024
GO:0002726	Positive regulation of T cell cytokine production	2 of 19	0.0265
GO:1901222	Regulation of NIK/NF-kappaB signaling	3 of 97	0.0265
GO:0042129	Regulation of T cell proliferation	3 of 151	0.0496

Gene description	Gene acronym	FC	P
Major Histocompatibility Complex, Class II, Alpha	*mhc-IIa*	1.493	0.029
STEAP4 Metalloreductase	*steap4*	1.39	0.0496
MAF BZIP Transcription Factor B	*mafb*	1.288	0.0042
Hemoglobin Subunit Alpha 1	*hba1*	1.276	0.0421
TNFAIP3 Interacting Protein 2	*tnip2*	1.265	0.0295
Interferon Related Developmental Regulator 1	*ifrd1*	1.226	0.0044
Small Inducible Cytokine Subfamily E Member 1	*aimp1*	1.223	0.001
NLR Family CARD Domain Containing 3	*nlrc3*	1.217	0.0258
TNF Alpha Induced Protein 2	*tnfaip2*	1.195	0.0206
Interleukin 1 Beta	*il1b*	1.192	0.0186
H3 Histone Family Member 3A	*h3f3a*	1.151	0.0182
Calponin 2	*cnn2*	1.138	0.0497
Negative Regulator of Reactive Oxygen Species	*nrros*	1.136	0.0425
Complement Factor H	*cfh*	1.119	0.0294
Nuclear Factor, Erythroid 2 Like 2	*nfe2l2*	1.116	0.0204
Calpain 1	*capn1*	1.105	0.0393
Glutathione S-Transferase Kappa 1	*gstk1*	1.097	0.0357
N-Acetyltransferase 1	*nat1*	1.091	0.0358
Cathepsin A	*ctsa*	1.061	0.049
Actin Beta	*actb*	1.048	0.0357
Protein Disulfide Isomerase Family A Member 3	*pdia3*	-1.09	0.0125
Protein Disulfide Isomerase Family A Member 4	*pdia4*	-1.1	0.0289
Iron-Responsive Element-Binding Protein 2	*ireb2*	-1.102	0.0153
Heat Shock Protein Family A (Hsp70) Member 14	*hspa14*	-1.103	0.0145
DEAD-Box Helicase 1	*ddx1*	-1.11	0.0302
DnaJ Heat Shock Protein Family (Hsp40) Member C8	*dnajc8*	-1.114	0.0024
Cathepsin L	*ctsl*	-1.158	0.0074
Caspase 3	*casp3*	-1.187	0.0137
Calreticulin	*calr*	-1.204	0.0138
DnaJ Heat Shock Protein Family (Hsp40) Member B9	*dnajb9*	-1.205	0.0105

FIGURE 5 | Functional biological network of differentially expressed genes (DEGs) recognized by their involvement in the immune response in the skin of juvenile gilthead seabream (*Sparus aurata*) fed a diet supplemented with a blend of garlic essential oil, carvacrol, and thymol. Green-shaded nodes represent up-regulated genes and red-shaded nodes represent down-regulated genes. Graphic keys and network stats: number of nodes = 30; number of edges = 24; average node degree = 1.6; average local clustering coefficient = 0.4; expected number of edges = 9; PPI enrichment *p*-value = 1.25e-05. Gene Ontology (GO) definition, count of DEGs within the biological process and respective false discovery rate are described in the graphical figure legend (bottom left). For details, please refers to **Supplementary Table 4**. Gene description, respective acronym, fold-change intensity (FC), modulation (color scale), and P-value are described (right).

antioxidant power (*t*-test, $P > 0.05$). When data on skin mucus biomarkers were normalized with the protein content of the sample, only cortisol levels (cortisol/protein) were observed to be significantly reduced in skin mucus from fish fed the phytogenic-supplemented diet when compared to the control diet (*t*-test, $P < 0.05$). Metabolic aerobic response, measured in mucus as glucose/lactate ratio, was neither significantly affected by the dietary treatment.

DISCUSSION

The fish skin mucosal surface is in direct contact with the aquatic environment and represents the first line of defense against external threats, determining pathogen adhesion to the epithelial surface (10, 12). As a mucosal tissue, the skin is characterized by its ability to produce mucus, which apart from being an intrinsic physical barrier, it contains glycosaminoglycans, lectins, antibacterial enzymes, immunoglobulins, and several structural, metabolic, stress-related, and signal transduction proteins [(23–25); among others]. In addition to mucus continuous secretion and replacement (26), its components provide an impermeable capacity against most bacteria and other pathogens, immobilizing them and inhibiting their proliferation before they can contact epithelial surfaces (10). Importantly, an intimate crosstalk between skin tissue and its exuded mucus in response to stimulus has been recently proposed (27), reinforcing the coordinated response capacity that takes place in this mucosal-associated lymphoid tissue.

In the present study, we evaluated the protective benefits of a blend of dietary garlic essential oil, carvacrol, and thymol on gilthead seabream in terms of skin transcriptome and skin mucus secretions. The potential increased skin mucus protective capacity observed in our gilthead seabream fed with phytogenic-supplemented diet could be attributed to the exudation of a variety of biologically active substances and several molecules of the innate and acquired immune system. In fact, many of them have an already reported biostatic and biocidal activities

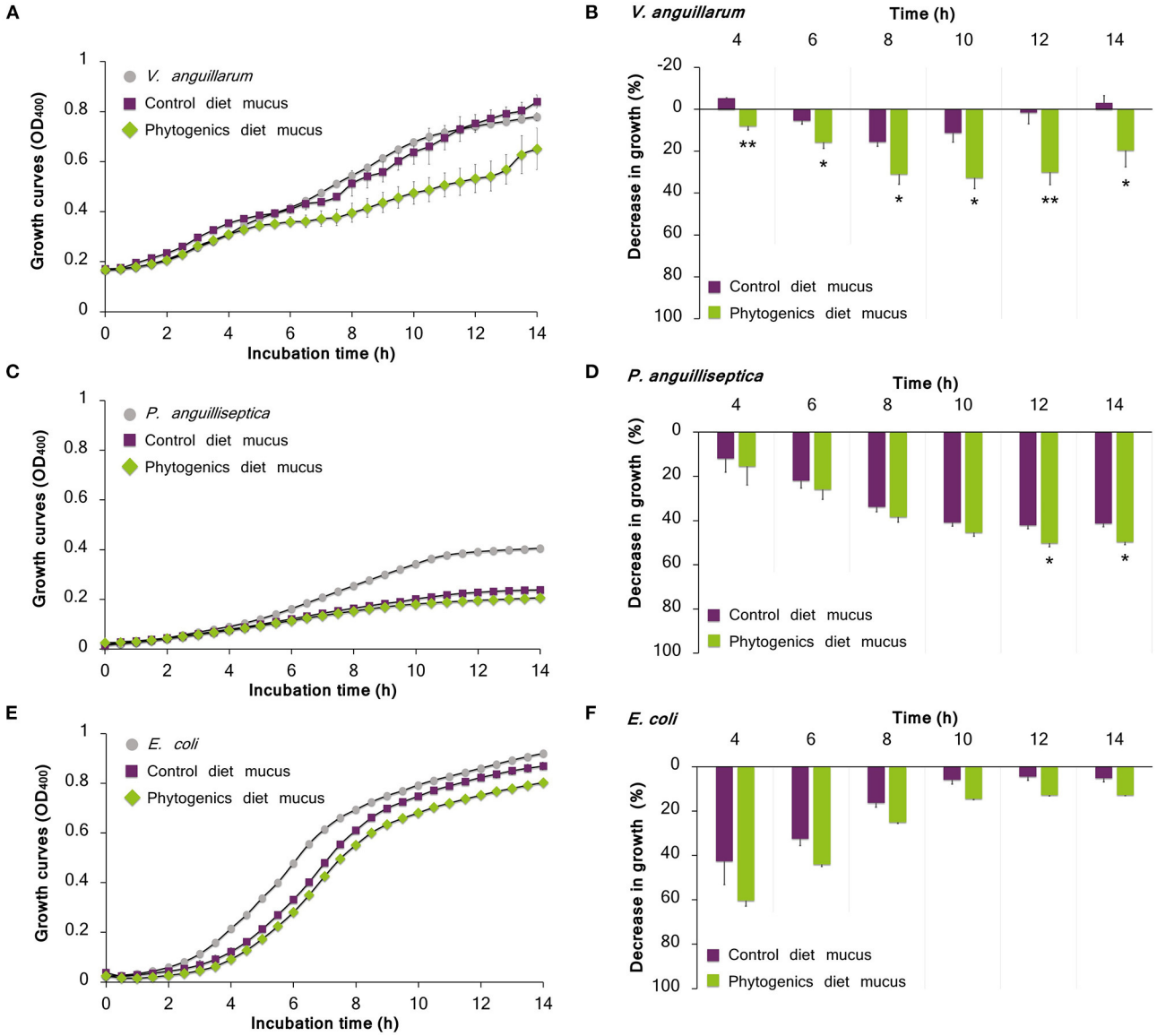

FIGURE 6 | Bacterial growth on skin mucus of juvenile gilthead seabream (*Sparus aurata*) fed a diet supplemented with a blend of garlic essential oil, carvacrol and thymol, and a control diet devoid of the feed additive. Mucus samples were obtained from 3 pools of 6 individual fish. Data correspond to the mean ± SEM of triplicate bacterial growth curves of *V. anguillarum* **(A)**, *P. anguilliseptica* **(C)** and *E. coli* **(E)**. Gray circles correspond to bacteria growth in medium devoid of mucus; purple squares correspond to bacteria growth in the mucus of fish fed the control diet; and green rhombus correspond to bacteria growth in the mucus of fish fed the phytogenic-supplemented diet. Details on the statistical differences in bacterial growth between the experimental dietary groups is provided by the percentage of decrease in growth of *V. anguillarum* **(B)**, *P. anguilliseptica* **(D)**, and *E. coli* **(F)**. Asterisks indicate significant differences in bacterial growth between dietary groups (*t*-test, $P < 0.05$).

(28). Under this context, our transcriptomic analysis for the skin revealed that several genes coding proteins potentially involved in an enhanced skin mucosal protective capacity. For instance, the H3 Histone Family Member 3A gene (*h3f3a*) was up-regulated in the skin of fish fed the phytogenic-supplemented diet. Histones, full-length proteins and/or fragments, are recognized antimicrobial molecules (29), which are found in the mucus of several fish species (30, 31), including gilthead seabream (32, 33). Calpain 1 (*capn1*), a non-lysosomal cysteine protease, was observed to be up-regulated by the functional additive as well. Several calpain proteins were mapped in gilthead seabream's epidermal mucus (34) while its presence in the skin mucus of cod (*Gadus morhua*) was suggested to be a key protective element against *V. anguillarum* infection (35).

Iron is an essential micronutrient required for most bacteria to grow; in the host, this metal is associated to iron-binding proteins, such as transferrin found in fish skin and mucus (23, 30, 32), limiting its availability to invading pathogenic bacteria

TABLE 2 | Skin mucus stress biomarkers of gilthead seabream fed an experimental diet supplemented with a blend of garlic essential oil, carvacrol and thymol, and the control diet devoid of the feed additive ($n = 24$ per dietary treatment).

	Diet	
	Control	**Phytogenics**
Skin mucus stress biomarkers		
Protein (mg/mL)	16.73 ± 2.22	12.86 ± 1.77
Glucose (μg/mL)	13.43 ± 3.95	6.88 ± 1.63*
Lactate (μg/mL)	9.80 ± 2.62	3.62 ± 1.09*
Cortisol (ng/mL)	3.47 ± 0.85	0.35 ± 0.05*
FRAP (μmol/mL)	1,923 ± 244	1,790 ± 315
Skin mucus stress biomarkers ratios		
Glucose/Protein (μg/mg)	0.74 ± 0.16	0.60 ± 0.17
Lactate/Protein (μg/mg)	0.46 ± 0.05	0.31 ± 0.12
Glucose/Lactate (mg/mg)	0.69 ± 0.14	0.77 ± 0.15
Cortisol/Protein (ng/g)	208 ± 48.80	31.85 ± 7.03**
FRAP/Protein (μmol/mg)	114 ± 16.9	139 ± 23.1

*Asterisks indicate significant differences between experimental diets (*P < 0.05, **P < 0.01; t-test).*

(36). For instance, *V. anguillarum* iron-uptake system is crucial for sequestering iron from these proteins and accomplishing skin colonization and penetration (37). Interestingly, some genes related with iron metabolism were observed to be down-regulated in the skin of fish fed the functional diet. In our transcriptional analysis, the Iron-Responsive Element-Binding Protein 2 (*ireb2*) gene was down-regulated in fish fed the phytogenic-supplemented diet. When cell's iron levels are low or depleted, this RNA-binding protein binds to iron-responsive elements, found for instance in transferrin mRNAs, regulating the translation and stability of those mRNAs and consequently regulating iron availability (38). In zebrafish, the increase of *ireb2* expression in spleen was proposed to be linked to an augmented iron uptake from *V. anguillarum* (39). Hence, the down-regulation of *ireb2* observed in the skin of fish fed the phytogenic-diet could be suggesting a decrease in the cellular iron uptake as a consequence of the reduction of pathogenic bacteria load in the mucosal tissue. This hypothesis is supported by the decreased growth capacity for pathogenic bacteria in skin mucus observed in the fish fed the tested functional diet.

On the other hand, iron plays an important role in hemoglobin production. The Hemoglobin Subunit Alpha (*hba1*) was up-regulated in the skin of fish fed the phytogenic-supplemented diet. Hemoglobin functionality is not restricted to oxygen transport, since it also binds to pathogen-associated molecular patterns (PAMPs), triggering an immune Toll-like receptor (TLR)-mediated signal transduction (40). In addition, the STEAP4 Metalloreductase (*steap4*) transcripts increased by the phytogenic-diet. This metalloreductase is involved in iron and copper homeostasis, playing also a role in the protection against inflammatory-mediated cellular damage (41). In Atlantic salmon (*Salmo salar*) skin, *steap4* was up-regulated by dietary phytogenics, which was associated to iron sequestration, inflammation and an increased protective capacity against lice infection (42). The *hba1* and *steap4* up-regulation in the skin observed in our study may be implicated in a reduction in iron availability in the skin surface and mucus of fish fed the phytogenics, hampering pathogenic bacteria growth as observed in the potential mucus antibacterial capacity observed in our study.

Fish SALT is characterized by both humoral and cellular components which intimately communicate to mount an immune response in which both innate and adaptive defense mechanisms are involved (15). For instance, the Interferon Related Developmental Regulator 1 (*ifrd1*) was up-regulated by the functional diet. *Ifrd1* gene encodes a protein related to interferon family. In fish is widely recognized by its involvement in the innate immune antiviral response (43), while it is also highly expressed in differentiating neutrophils, playing an important role in neutrophils effector function (44). An increase of *ifrd1* transcripts was observed in the skin of zebrafish (*Danio rerio*) infected by *Aeromonas hydrophila* (45), whereas its up-regulation was also related to its role in the immediate response of the fish immune system to stress (46). Moreover, transcripts of the Complement Factor H (*cfh*) increased in the skin of gilthead seabream fed the phytogenic-supplemented diet. CFH, a major regulator of the complement system, is essential for directing the complement system toward pathogen-related infections, since its transcription is induced by lipopolysaccharide (LPS) (47), whereas it increases the contact between neutrophils and pathogens, increasing cell's phagocytosis capacity and antimicrobial activity (48). CFH is also reputed for protecting host cells and tissues from the self-innate immunity (49). This occurs due to the interaction of the factor H with the C3 convertase and the C3b component (50). Although CFH is predominantly expressed in the liver compared to other tissues and organs like the muscle, intestine, fins, eyes, and gills (47), present data indicate that the skin may also play a relevant role in the regulation of the alternative pathway of complement in skin secretions. This data is in agreement with different studies that have identified several complement factors in fish skin mucus secretions for several species (30, 51), including gilthead seabream (23, 24).

Our study also revealed that Cathepsin A (*ctsa*) was up-regulated in the skin of fish fed the phytogenic-supplemented diet. An increase in turbot (*Scophthalmus maximus*) *ctsa* expression in skin was described in response to infection challenges, while *ctsa* genes microbial binding capacity was also observed, in which a high affinity to LPS, and a lower affinity to lipoteichoic acid (LTA) and peptidoglycan (PGN), was suggested to be implicated in the sensing and phagocytosis of bacterial pathogens (52). By contrast, in our study the expression of Cathepsin L (*ctsl*) was down-regulated. Different cathepsins have been detected in the mucus of several fish species, which were observed to exhibit high bacteriolytic activity against several fish pathogens (53, 54), evidencing their key role in fish mucosal innate immunity. Fish skin *ctsl* transcripts were observed to be significantly up-regulated after challenges with several bacterial pathogens, including *V. anguillarum* (54, 55). Moreover, as for *ctsa* genes, it was demonstrated that *ctsl* genes have strong

in vitro binding capacity to microbial ligands, suggesting an important role of *ctsl* in fish mucosal immunity (55). The different gene expression pattern observed for *ctsa* and *ctsl* could be related to a time-dependent response, as suggested previously for genes involved in the immune response in fish subjected to feeding trials (56). The differential expression between both cathepsins could be also attributed to the mucosal tissue response specificity. In this way, it has been reported that the same stimulus may differentially modulate the expression for the same genes depending of the mucosal tissue evaluated (57). However, if both genes are linked with the decrease in the bacterial growth observed at skin mucus deserves further investigations.

Fish professional phagocytes include macrophages, granulocytes, dendritic cells and B cells, and as for other vertebrates, phagocytosis in fish is recognized as a critical component of the innate and adaptive immune responses against pathogens, known to elicit several antimicrobial mechanisms. Under this context, the KEGG "Phagosome" pathway obtained from our functional analysis suggests the modulation of phagocytic events by the administered phytogenics. For instance, despite the extracellular roles of cathepsins (58), these proteins are mainly found in endolysosomal structures where they are crucial for protein degradation and Major Histocompatibility Complex (MHC) Class II mediated immune responses (59). Interestingly, the MHC Class II Alpha gene (*mhc-IIa*) was the second most up-regulated gene in the skin of fish fed the phytogenic-supplemented diet. While MHC-IIa protein was identified in gilthead seabream skin mucus proteome (34), the main function of fish MHC Class II molecules is to present the peptides generated in the endolysosomal structure on the cell surface of B cells and phagocytes for their recognition by the CD4+ T cells (60). In fact, the gilthead seabream acidophilic granulocytes, considered the main professional phagocytic cell type for this fish species, were demonstrated to show high *mhc-IIa* gene expression (61). Moreover, they have also proved to have phagocytic activity against bacterial pathogens such *V. anguillarum* (62), being able to release antimicrobial peptides into the phagosome of the ingested pathogenic bacteria (63). The "leukocyte activation", "regulation of T cell proliferation", and "antigen processing and presentation of exogenous peptide antigen via MHC class I" biological processes obtained from our enrichment analysis, might suggest the activity of acidophilic granulocytes and/or other immune cells in the skin of gilthead seabream fed the functional diet. Similarly, previous transcriptional results on the effect of the same functional feed additive in gilthead seabream mucosal tissues such gills (17) suggested the recruitment and activation of acidophilic granulocytes as a consequence of the immunostimulatory effect of this additive.

The functionality and modulation of genes related to the "endosome" and "lysosome" cellular components reinforce the hypothesis of an increased professional phagocytic activity in the skin of fish fed the phytogenic-supplemented diet. Among them, Rab-interacting proteins coding genes (*rilp*, *rab11fip1*) were up-regulated. These genes are involved in several processes like (i) endosomal recycling (64), (ii) endocytic transport to degradative compartments (65) and (iii) in the control of membrane trafficking along the phagocytic pathway (66). In addition, the Microtubule Associated Protein 1 Light Chain 3 Gamma (*map1lc3c*) was up-regulated. This autophagy-related protein is involved in the LC3-associated phagocytosis, in which LC3 is recruited to the phagosome membrane during phagocytosis of pathogens, enhancing the fusion between phagosome and lysosomes (67). In fact, fish epidermal macrophages are characterized by well-developed endoplasmic reticulum and Golgi areas and several lysosome-like vesicles and phagosomes (68). Remarkably, the up-regulation of the MAF BZIP Transcription Factor B (*mafb*), a myeloid lineage-specific transcription factor, which expression levels increase during macrophage differentiation and maturation (69), was also observed in the skin of fish fed the phytogenic-supplemented diet. Therefore, the regulation of LC3 proteins-coding genes and the up-regulation of *mafb* by the phytogenics might support the participation of phagocytic cells in the immune response from the skin observed in our study. The down-regulation of Microtubule Associated Protein 1 Light Chain 3 Beta (*map1lc3b*) opens the possibility to selective and differential mechanisms of activation aimed to the promotion of the phagocytic activity in response to phytogenic supplementation.

Garlic, carvacrol, and/or thymol have been several times described to improve immune cells phagocytic capacity. For instance, dietary garlic (0.5 and 1% inclusion) enhanced the activity of head kidney macrophages phagocytic in rainbow trout (*Oncorhynchus mykiss*) (70). Similar results were observed for blood leukocytes of juvenile hybrid tilapia (*Oreochromis niloticus* x *Oreochromis aureus*) fed a 0.5% garlic-supplemented diet (71). Likewise, carvacrol and thymol supplementation (0.2%) in juvenile hybrid tilapia's diet significantly enhanced phagocytosis of head kidney macrophages (72). The phagocytic activity of serum leukocytes from common carp (*Cyprinus carpio*) was increased due to dietary oregano's essential oil, which is rich in carvacrol and thymol, in a dose-dependent manner (73). A similar enhanced head kidney leukocytes' phagocytosis was also found in gilthead seabream fed a diet supplemented with oregano powder (0.5 and 1%) (74).

Phagocytic events are driven by rearrangements of the actin cytoskeleton (75). Calponin 2 (*cnn2*), an actin cytoskeleton-associated regulatory protein that restricts the pro-inflammatory activation of macrophages (76), was up-regulated in the skin by the phytogenics. Similarly, the Actin Beta (*actb*) gene was also up-regulated. Actin is commonly found in the mucus of several fish species, including gilthead seabream (23, 32), which has led to speculations on its immune function in fish defense. In fact, ACTB levels were observed to be significantly increased in sea lice challenged Atlantic salmon (30, 51). In gilthead seabream, *actb* expression in skin mucus was favored by a dietary probiotic administration (24). Furthermore, the extracellular cytoplasmic actin in insects was observed to bind to bacteria surface, mediating its phagocytosis and killing (77), suggesting that actin could be functionally active in fish skin mucus as well. However, this hypothesis needs further investigation. In summary, our transcriptional analysis could be indicating an enhanced phagocyte function in the skin of fish fed the

phytogenic-diet, which would suggest the promotion of the host's defense ability in resisting bacterial infections.

In order to prevent the stable colonization of potential pathogens, mucus is continuously synthesized, secreted and replaced (26). This continuous regulation of mucus secretions represents one of the first barriers against potential pathogens and toxins (10). Accordingly, our functional analysis determined the modulation of the KEGG "Protein processing in endoplasmic reticulum" pathway and several cellular components connected to the secretory pathway, such as transport vesicles, Golgi-associated vesicles and vacuoles. The regulation of the secretory machinery could be supporting the active biosynthesis and release of immune-related factors on the skin mucus that would mediate in the response observed in our study. The mucus secretion is a complex process that represents the endpoint of the interaction between the innate immune system, endocytosis and autophagy events, ROS generation and mucin secretion (78). From the immunological point of view, cytokines, and chemokines are molecules trafficked in secretory granules and vesicles through secretory pathways in immune cells (79) that could be also involved in the response observed. Under this context, transcripts of the pro-inflammatory cytokine Interleukin 1 Beta (*il-1β*) were observed to be increased in the skin of fish fed the phytogenic-supplemented diet. In fish, IL-1β is a recognized chemoattractant for leukocytes (80). Additionally, the Aminoacyl tRNA Synthetase Complex Interacting Multifunctional Protein 1 (*aimp1*) gene was also up-regulated. Secreted AIMP1 possesses inflammatory cytokine activity responsible for activating monocytes and inducing the production of pro-inflammatory cytokines, mainly the Tumor Necrosis Factor (TNF) (81). In accordance, genes that are activated in response to the pro-inflammatory cytokine TNF, such the TNF Alpha Induced Protein 2 (*tnfaip2*) and TNFAIP3-Interacting Protein 2 (*tnip2*) were also up-regulated by the phytogenics in our study. The last inhibits the NF-kB pathway activation (82), negatively regulating the transcription of other pro-inflammatory cytokines and, consequently, controlling the inflammatory response. Thus, such response could be intimately related with the role of AIMP1 in dermal fibroblast proliferation and wound repair (83).

Other mediators of the inflammatory response were also observed to be regulated in the skin of fish fed the phytogenic-diet. For instance, the Negative Regulator of Reactive Oxygen Species (*nrros*) gene expression was increased. The NRROS protein regulates ROS production by phagocytes during inflammatory response, allowing phagocytes to produce high amounts of ROS in case of infection, while minimizing host's tissue damage (84). NRROS is also suggested to play a role in the maintenance of the immune homeostasis through the inhibition of TLR-mediated MAPK and NF-kB activation (85). Another negative mediator of the inflammatory response, the NLR Family CARD Domain Containing 3 (*nlrc3*) was also observed to be up-regulated in fish fed the phytogenic-supplemented diet. NLRC3 is known to negatively regulate NLR-mediated inflammatory responses (86). In several fish species, the overexpression of *nlrc3* was observed to be systematically induced by bacterial and LPS challenges (87, 88), including in mucosal tissues (89), demonstrating its important role in the fish innate immune response and homeostasis maintenance. The DEAD-Box Helicase 1 (*ddx1*), reported to enhance NF-kB mediated transcriptional activation (90) and recently associated to antiviral responses in fish (91), was also down-regulated in the skin of fish fed the phytogenic-supplemented diet. Therefore, according to the overall response observed considering the transcriptomic profiling of *il-1β*, *aimp1*, *tnfaip2*, *tnip2*, *nrros*, *nlrc3*, and *ddx1*, the regulation of these pro- and anti-inflammatory genes suggests an active cytokine secretion, an immune cell-cell signaling, and the tight control of such response.

Regardless of its critical function protecting the host, the skin mucus also represents an important portal of entry for pathogens since it can provide a favorable microenvironment for some bacteria, the main disease agents for fish, which may induce the development of biofilms depending on the pathogen adhesion capacity (10). Interestingly, the down-regulation of genes of the KEGG "*Vibrio cholerae* infection" pathway was obtained from the analysis of the DEGs of fish fed the phytogenic-based additive. Although the analysis was performed using *Homo sapiens* as model organism, the down-regulation of several genes of the "*Vibrio cholerae* infection" KEGG pathway could also be applied, from a comparative point of view, to an infection process involving a *Vibrio* species in a mucosal tissue, such as *V. anguillarum*, as a consequence of the protective effect of the additive. For instance, the down-regulation of several coding genes for V-type H+ ATPase subunits (*atp6v1c1*, *atp6v1b1*, *atp6ap1*) in fish fed the phytogenic-supplemented diet was obtained. The V-type H+ ATPase complex in endosomes and lysosomes is responsible for the vesicle import of protons and maintenance of the internal acidic pH, crucial for degradative enzymes activity (92). Apart from the "proton-transporting two-sector ATPase complex" cellular component obtained from our enrichment analysis, the down-regulation of the above-mentioned genes also figured in the KEGG "Phagosome" pathway, which could be suggesting a decreased phagosomal activity at the sampling time evaluated (65 days of diet administration). Such gene modulation could be associated to a decrease in skin bacterial pathogens in our fish fed with phytogenic-supplemented diet. This hypothesis is in agreement with the results obtained from the bacterial growth assessment in the epidermal mucus *in vitro*.

Bacterial growth in gilthead seabream mucus was evaluated for both dietary groups, control and phytogenic-supplemented diets, using two pathogenic fish bacteria, *V. anguillarum* and *P. anguilliseptica*, as well as a non-pathogenic fish bacterium, *E. coli*. Our study revealed that the tested feed additive reduced bacteria growth capacity, suggesting an enhanced skin mucus inhibitory capacity against both *V. anguillarum* and *P. anguilliseptica*. The chosen pathogenic bacteria are widely recognized as disease causing agents in several fish species (93, 94), including gilthead seabream (95). The observed reduced growth capacity of *V. anguillarum* in the skin mucus of gilthead seabream fed the phytogenic-supplemented diet is especially relevant because of the evidence that *Vibrio* strains exhibit a chemotactic response to mucus (37). In the last years, disease records indicate that *Vibrio* spp. infections are the most common bacterial

infections in gilthead seabream, mostly reported during the hatchery phase (96). Besides, *P. anguilliseptica* is one of the main agents responsible for outbreaks associated with "winter disease" in gilthead seabream farming, being considered a more opportunistic pathogen whose infections in gilthead seabream usually occur when fish are under environmental stress (97). The different growth curves behavior of *V. anguillarum* and *P. anguilliseptica* in gilthead seabream mucus may be attributed to different virulence of pathogenic bacteria, differences in chemotaxis to skin mucus and adherence capacity.

Our results suggest that the phytogenic-supplemented diet may reduce the settlement of the studied bacteria in the skin surface, decreasing the risk of infection. Previous nutritional studies in which diets containing garlic, carvacrol, or thymol provided effective mucus antibacterial characteristics against fish pathogens. For instance, dietary garlic supplementation (5 and 10 g kg-1) was demonstrated to significantly increase skin mucus antimicrobial activity against several bacterial pathogens in the freshwater Caspian roach (*Rutilus rutilus*) (98). A similar increased bactericidal activity against *Photodamselae* subsp. *piscicida* was observed in the skin mucus of gilthead seabream juveniles fed diets supplemented with oregano powder (0.5 and 1% inclusion) for 15 and 30 days (74). In addition, an enhanced skin mucus bactericidal activity against *V. parahaemolyticus* and *Aeromonas hydrophila* was observed in Pacific red snapper (*Lutjanus peru*) fed a diet supplemented with a medicinal plant extract rich in carvacrol and thymol (0.5, 1, and 2% inclusion) (99). On the contrary, other studies incorporating *Oliveria decumbens*, which is rich in carvacrol (18.8 and 52.9% included in an essential oil and aromatic water fractions, respectively) and thymol (20.3 and 37.6% included in an essential oil and an aromatic water fractions, respectively), in Nile tilapia (*O. niloticus*) diets reported the absence of changes in mucus bactericidal activity against *Streptococcus iniae*. By contrast, the compounds showed high antibacterial capacity when evaluated *in vitro* (100). Similarly, Beltrán et al. (74) did not find an enhancement of antibacterial activity against *V. anguillarum* in the mucus of gilthead seabream fed a diet supplemented with *Origanum vulgare* at 0.5 and 1.0%, although a significant increased bactericidal activity against *Photobacterium damselae* subsp. *piscicida* was observed. The above-mentioned contradictory results could be a consequence of different factors, such as different phytogenics and their content in bioactive compounds, supplementation period of the functional diet, dietary compounds delivery and bioavailability, or an evidence of the synergy between the phytogenics tested that might improve such bactericidal capacity.

Moreover, the *E. coli*, a non-pathogenic bacterium for fish, was also used as an indicator of the potential antibacterial capacity of the skin mucus, neglecting a potentially acquired immunization. Although no significant differences were observed among the experimental diets, a decreasing trend in *E. coli* growth was observed due to the presence of mucus from both dietary groups in the culture medium. Interestingly, garlic-supplemented diets caused a significant increase in the Caspian roach fry skin mucus antibacterial activity against *E. coli* when compared to the control group (98). In addition, carvacrol and thymol were reported to have a bacteriostatic and bacteriolytic *in vitro* activity against most Gram positive and negative bacteria, including *E. coli* (101). Nevertheless, the absence of an inhibitory response against *E. coli* growth in our study could be suggesting the promotion of the skin innate immunity against fish pathogens (102).

From a physiological perspective, bacterial pathogens such *V. anguillarum* are able to elicit strong cortisol-mediated stress responses when they adhere to the mucosal surface (36). For this reason, in this current study we also measured classic skin mucus stress biomarkers in order to establish a correlation between the gene expression profile, antibacterial response and the fish physiological status. Therefore, only cortisol was observed to be significantly reduced in fish fed the phytogenic-supplemented diet. Although the exact mechanisms involved in cortisol exudation through fish mucus are still unclear, cortisol is the main glucocorticoid and the final product of the HPI axis response to stress, varying considerably among species and according to the duration and severity of the stressor (103). Cortisol decrease also favors the fish local mucosal immunity, promoting more effective defense responses against pathogens (104). Besides the hypothesized decrease in skin pathogenic bacteria and its potential impact on cortisol-induced responses, and *vice versa*, several phytogenic active substances have been reported to have sedative properties in fish (105). For instance, garlic powder inclusion in common carp diet (0.5, 1, and 1.5%) decreased plasma cortisol and glucose levels, mitigating ammonia stress-induced effects (106). Similar results were obtained in rainbow trout fed 3% garlic powder supplemented diets (107). Accordingly, the dietary supplementation of a similar additive containing garlic and Labiatae plant essential oils (0.02% inclusion) reduced significantly plasma cortisol levels in European seabass (*Dicentrarchus labrax*) challenged by confinement (108). Although the diet effect on fish stress response is usually evaluated in blood, a positive correlation between cortisol levels on plasma and fish mucus was demonstrated (109, 110) including for gilthead seabream (111). Therefore, the observed decrease in mucus cortisol may suggest a decrease in the allostatic load due to the properties of the phytogenics used in this current study and/or as a consequence of the promotion of the non-specific innate immunity, although these two hypotheses are not mutually excluding.

During stress adaptation, cortisol has been suggested as a signal factor that induces tissue specific molecular programming in fish (112). Cortisol is able to induce a skin local stress response in fish (57, 94, 109, 113), which is particularly characterized by the increase of the secretory activity, related vesicles, apoptosis (114), and transcriptional alterations (57). Under this context, the observed changes in mucus cortisol secretion might be contributing to the obtained secretory-related transcriptional response as well. Furthermore, since a correlation between cortisol secretion and skin mucus oxidative stress was demonstrated (115), a reduction of the skin oxidative stress in response of an increase in antioxidative power induced by the tested phytogenics would be also expected. In fact, in our current study genes coding for antioxidative enzymes were observed to be up-regulated in the skin of fish fed the phytogenic-supplemented diet, as for example the Glutathione S-Transferase Kappa 1 (*gstk1*). GSTK1 belongs to the as Glutathione S-Transferase (GST) superfamily of oxidative stress enzymes,

which are mainly known for their important role in cellular detoxification (116). GSTs have been used as markers for fish antioxidative capacity (117), including the evaluation of phytogenics in aquafeeds (118). Under stress-imposed conditions or injury, the transcription of skin *gst* is usually decreased and associated to immunosuppression in gilthead seabream (33). The Nuclear Factor Erythroid 2 Like 2 (*nfe2l2*), an important transcription factor that positively regulates the expression of cytoprotective genes (119), and the N-Acetyltransferase 1 (*nat1*), known for its participation in the detoxification of drugs and other xenobiotics (120), were also observed to be up-regulated by the functional diet. In addition, Heat Shock Protein family genes (*dnajc8*, *dnajb9*, and *hspa14*) were down-regulated in the fish fed the phytogenic-supplemented diet. In particular, HSPA14 is member of the Hsp70 family, which proteins levels have been described to increase in fish under stress or pathological conditions (121, 122). Therefore, the regulation of these genes is supporting the involvement of immune cells in the skin response observed, suggesting a reduction of the skin oxidative stress in response of the reduced mucus cortisol secretion and/or by the antioxidative characteristics of the tested phytogenics. In fact, the inclusion of garlic (106, 123), carvacrol, and thymol (73, 124) in aquafeeds have been continuously demonstrated to enhanced fish antioxidant status. In the present study, the epidermal mucus antioxidant capacity was also measured by mean of the FRAP analysis (102, 115). Although our transcriptional analysis revealed the regulation of several markers of oxidative stress, according to FRAP's analyses the mucus antioxidant power was not significantly changed by the tested additive. Our results are in agreement with some previous studies which reported that the dietary supplementation of carvacrol and/or thymol-rich compounds did not affect the skin mucus biochemical contents or mucus antioxidant status (74, 100).

Collectively, these data clearly suggest a relationship between the tested phytogenics, the increased skin innate immunity and a cortisol-mediated response, promoting the overall animal welfare. In fact, according to the only biological process significantly regulated among the experimental diets, the RNA processing biological process, several genes implicated in ribosomal proteins synthesis (*riok1*, *rcl1*, *rrp1*, *nop56*, *nsa2*, *tsr2*) were mainly up-regulated in fish fed the phytogenic-supplemented diet. Since ribosome biogenesis is the cell's most costly process in terms of energy expenditure, this process must be tightly regulated in order to avoid wasted energy (125). Consequently, the up-regulation of such genes could be suggesting less stressed cells able to direct their energy into this process. Since skin from the control group appear to be more susceptible to be colonized by pathogenic bacterial strains, it could be spending more energy in defense mechanisms and bacterial clearance than fish fed the phytogenic-supplemented diet.

In summary, our analysis of the skin transcriptional profiling as well as the skin mucus biomarkers and lower pathogenic bacterial growth capacity revealed a multifactorial response to the dietary administration of garlic essential oil, carvacrol, and thymol, mainly through the transcriptional regulation of factors of the innate immunity and the stimulation of the secretory pathway. Our results suggest that the phytogenic-supplemented diet induces the activation of the mucosal immune response that promotes the secretion of non-specific immune molecules into the skin mucus, resulting in the decrease of bacterial growth capacity in mucus. From our transcriptomic enrichment analysis, the regulation of genes related with the secretory pathway suggests that the tested phytogenics could be also stimulating the recruitment of phagocytic cells. The reduction in skin mucus cortisol is in line with the recognized properties of the phytogenics. Since the exact mechanisms promoted by the tested phytogenics were not yet demystified, further analysis should be made in order to assess the effect of the experimental diet on skin phagocytes and phagocytosis potential. More efforts are also needed for determining the impact of the functional additive on the skin defensive status against other pathogenic bacteria that threaten the success of aquaculture under intensive farming regime.

DATA AVAILABILITY STATEMENT

The datasets presented in this study can be found in online repositories. The names of the repository/repositories and accession number(s) can be found in the article/**Supplementary Material**.

ETHICS STATEMENT

IRTA facilities, where the trial was conducted, are certified and have the necessary authorization for the breeding and husbandry of animals for scientific purposes. All procedures involving the handling and treatment of the fish were approved as far as the care and use of experimental animals are concerned, by the European Union (86/609/EU), the Spanish Government (RD 1201/2005), and the University of Barcelona (Spain).

AUTHOR CONTRIBUTIONS

Biological samplings were performed by EG, JF, RS, LF-A, IS, and AI. The transcriptomic data analysis and interpretation was performed by JF, RS, EV-V, and FER-L. LF-A, IS, and AI carried out the skin mucus analyses. The study was supervised by EG, FER-L, and LT. JF wrote the original draft. Funding was obtained by EG and LT. All the authors provided critical feedback, read, and agreed to the published version of the manuscript.

FUNDING

This work has been supported by the project Nutritional strategies for the improvement of productive performance: the use of functional feeds and health diets in aquaculture (DIETAplus), funded by JACUMAR (Ministry of Agriculture, Fisheries and Environment of Spain, MAPAMA) and FEMP (EU). Collaboration between Ibero-American researchers has been done under the framework of the LARVAplus network Strategies for the development and improvement of fish larvae production in Ibero-America (117RT0521) funded by the Ibero-American Program of Science and Technology for Development (CYTED, Spain). The funder bodies were not involved in

the study design, collection, analysis, interpretation of data, the writing of this article or the decision to submit it for publication. FER-L thanks the support of Fondecyt regular grant (Nb. 1211841; ANID; Goverment of Chile). JF have been subsidized by the Industrial PhD program of Generalitat de Catalunya and TECNOVIT-FARMFAES S.L. (Nb. 2017 DI 017). EV-V was financially granted with DICYT-USACH Postdoctoral fellowship (Nb. 022043IB). Héctor R. Salomón Figueredo is supported by a Ph.D. grant from the government of Paraguay (BECAL).

ACKNOWLEDGMENTS

We thank Dr. Alicia Estevez who led and supervised the nutritional assay.

SUPPLEMENTARY MATERIAL

The Supplementary Material for this article can be found online at: https://www.frontiersin.org/articles/10.3389/fimmu.2021.633621/full#supplementary-material

REFERENCES

1. Assefa A, Abunna F. Maintenance of fish health in aquaculture: review of epidemiological approaches for prevention and control of infectious disease of fish. *Vet Med Int.* (2018) 10:5432497. doi: 10.1155/2018/5432497
2. Waagbø R, Remø SC. 7 - functional diets in fish health management. In: Kibenge FSB, Powell MD, editors. *Aquaculture Health Management*. Academic Press (2020). p. 187–234. doi: 10.1016/B978-0-12-813359-0.00007-5
3. Sutili FJ, Gatlin DM, Heinzmann BM, Baldisserotto B. Plant essential oils as fish diet additives: benefits on fish health and stability in feed. *Rev Aquacult.* (2017) 10:716–26. doi: 10.1111/raq.12197
4. Souza CF, Baldissera MD, Baldisserotto B, Heinzmann BM, Martos-Sitcha JA, Mancera JM. Essential oils as stress-reducing agents for fish aquaculture: a review. *Front Physiol.* (2019) 10:785. doi: 10.3389/fphys.2019.00785
5. Hernández-Contreras Á, Hernández MD. Chapter 14 - Application of aromatic plants and their extracts in aquaculture. In: Florou-Paneri P, Christaki E, Giannenas I, editors. *Feed Additives*. Academic Press (2020). p. 239–59. doi: 10.1016/B978-0-12-814700-9.00014-5
6. Elumalai P, Kurian A, Lakshmi S, Faggio C, Esteban MA, Ringø E. Herbal immunomodulators in aquaculture. *Rev Fish Sci Aquaculture*. (2020) 29, 33–57. doi: 10.1080/23308249.2020.1779651
7. Anastasiou TI, Mandalakis M, Krigas N, Vezignol T, Lazari D, Katharios P, et al. Comparative evaluation of essential oils from medicinal-aromatic plants of Greece: chemical composition, antioxidant capacity and antimicrobial activity against bacterial fish pathogens. *Molecules.* (2020) 25:148. doi: 10.3390/molecules25010148
8. Cunha JA, Heinzmann BM, Baldisserotto B. The effects of essential oils and their major compounds on fish bacterial pathogens - a review. *J Appl Microbiol.* (2018) 125:328–44. doi: 10.1111/jam.13911
9. Peterson TS. 3 - Overview of mucosal structure function in teleost fishes. In: *Beck BH, Peatman E*, editors. *Mucosal Health in Aquaculture*. San Diego: Academic Press (2015). p. 55–63. doi: 10.1016/B978-0-12-417186-2.00003-0
10. Benhamed S, Guardiola FA, Mars M, Esteban MÁ. Pathogen bacteria adhesion to skin mucus of fishes. *Vet Microbiol.* (2014) 171:1–12. doi: 10.1016/j.vetmic.2014.03.008
11. Reverter M, Tapissier-Bontemps N, Lecchini D, Banaigs B, Sasal P. Biological and ecological roles of external fish mucus: a review. *Fishes.* (2018) 3:41. doi: 10.3390/fishes3040041
12. Cabillon NAR, Lazado CC. Mucosal barrier functions of fish under changing environmental conditions. *Fishes.* (2019) 4:2. doi: 10.3390/fishes4010002
13. Salinas I. The mucosal immune system of teleost fish. *Biology.* (2015) 4:525–39. doi: 10.3390/biology4030525
14. Xu Z, Parra D, Gómez D, Salinas I, Zhang Y-A, Jørgensen, LG, et al. Teleost skin, an ancient mucosal surface that elicits gut-like immune responses. *Proc Natl Acad Sci USA.* (2013) 110:13097–102. doi: 10.1073/pnas.1304319110
15. Esteban MÁ, Cerezuela R. 4 - Fish mucosal immunity: skin. In: Beck BH. Peatman E, editors. *Mucosal Health in Aquaculture*. San Diego: Academic Press (2015). p. 67–92. doi: 10.1016/B978-0-12-417186-2.00004-2
16. FAO. Fishery and Aquaculture Statistics. Global aquaculture production 1950-2018 (FishstatJ). In: *FAO Fisheries and Aquaculture Department*. Rome (2020). Available online at: http://www.fao.org/3/cb1213t/CB1213T.pdf
17. Firmino JP, Vallejos-Vidal E, Sarasquete C, Ortiz-Delgado JB, Balasch JC, Tort L, et al. Unveiling the effect of dietary essential oils supplementation in *Sparus aurata* gills and its efficiency against the infestation by *Sparicotyle chrysophrii*. *Sci Rep.* (2020) 10:17764. doi: 10.1038/s41598-020-74625-5
18. Mongile F, Bonaldo A, Fontanillas R, Mariani L, Badiani A, Bonvini E, et al. Effects of dietary lipid level on growth and feed utilisation of gilthead seabream (*Sparus aurata* L.) at Mediterranean summer temperature. *Italian J Animal Sci.* (2014) 13:30–5. doi: 10.4081/ijas.2014.2999
19. Fernández-Alacid L, Sanahuja I, Ordóñez-Grande B, Sánchez-Nuño S, Viscor G, Gisbert E, et al. Skin mucus metabolites in response to physiological challenges: a valuable non-invasive method to study teleost marine species. *Sci Total Environ.* (2018) 644:1323–35. doi: 10.1016/j.scitotenv.2018.07.083
20. Szklarczyk D, Gable AL, Lyon D, Junge A, Wyder S, Huerta-Cepas J, et al. STRING v11: protein-protein association networks with increased coverage, supporting functional discovery in genome-wide experimental datasets. *Nucleic Acids Res.* (2019) 47:D607–613. doi: 10.1093/nar/gky1131
21. Stelzer G, Rosen N, Plaschkes I, Zimmerman S, Twik M, Fishilevich S, et al. The GeneCards suite: from gene data mining to disease genome sequence analyses. *Curr Protocols Bioinformat.* (2016) 54:1.30.31–31.30.33. doi: 10.1002/cpbi.5
22. Bradford MM. A rapid and sensitive method for the quantitation of microgram quantities of protein utilizing the principle of protein-dye binding. *Analyt Biochem.* (1976) 72:248–54. doi: 10.1016/0003-2697(76)90527-3
23. Sanahuja I, Ibarz A. Skin mucus proteome of gilthead sea bream: a non-invasive method to screen for welfare indicators. *Fish Shellf Immunol.* (2015) 46:426–35. doi: 10.1016/j.fsi.2015.05.056
24. Cordero H, Morcillo P, Cuesta A, Brinchmann MF, Esteban MA. Differential proteome profile of skin mucus of gilthead seabream (*Sparus aurata*) after probiotic intake and/or overcrowding stress. *J Proteom.* (2016) 132:41–50. doi: 10.1016/j.jprot.2015.11.017
25. Sanahuja I, Fernández-Alacid L, Sánchez-Nuño S, Ordóñez-Grande B, Ibarz A. Chronic cold stress alters the skin mucus interactome in a temperate fish model. *Front Physiol.* (2019) 9:1916. doi: 10.3389/fphys.2018.01916
26. Ibarz A, Ordóñez-Grande B, Sanahuja I, Sánchez-Nuño S, Fernández-Borràs J, Blasco J, et al. Using stable isotope analysis to study skin mucus exudation and renewal in fish. *J Exp Biol.* (2019) 222:jeb195925. doi: 10.1242/jeb.195925
27. Reyes-López FE, Ibarz A, Ordóñez-Grande B, Vallejos-Vidal E, Andree KB, Balasch JC, et al. Skin multi-omics-based interactome analysis: Integrating the tissue and mucus exuded layer for a comprehensive understanding of the teleost mucosa functionality as model of study. *Front Immunol.* (2021) 11:613824. doi: 10.3389/fimmu.2020.613824
28. Esteban MÁ. An overview of the immunological defenses in fish skin. *ISRN Immunol.* (2012) 2012:1–29. doi: 10.5402/2012/853470
29. Fernandes JMO, Kemp GD, Molle MG, Smith VJ. Anti-microbial properties of histone H2A from skin secretions of rainbow trout, *Oncorhynchus mykiss*. *Biochem J.* (2002) 368:611–20. doi: 10.1042/bj20020980
30. Provan F, Jensen LB, Uleberg KE, Larssen E, Rajalahti T, Mullins J, et al. Proteomic analysis of epidermal mucus from sea lice–infected Atlantic salmon, *Salmo salar* L. *J Fish Dis.* (2013) 36:311–21. doi: 10.1111/jfd.12064

31. Cordero H, Brinchmann MF, Cuesta A, Meseguer J, Esteban MA. Skin mucus proteome map of European sea bass (*Dicentrarchus labrax*). *Proteomics.* (2015) 15:4007–20. doi: 10.1002/pmic.201500120
32. Jurado J, Fuentes-Almagro CA, Guardiola FA, Cuesta A, Esteban MÁ, Prieto-Álamo, et al. Proteomic profile of the skin mucus of farmed gilthead seabream (*Sparus aurata*). *J Proteom.* (2015) 120:21–34. doi: 10.1016/j.jprot.2015.02.019
33. Cordero H, Brinchmann MF, Cuesta A, Esteban MA. Chronic wounds alter the proteome profile in skin mucus of farmed gilthead seabream. *BMC Genom.* (2017) 18:939. doi: 10.1186/s12864-017-4349-3
34. Pérez-Sánchez J, Terova G, Simó-Mirabet P, Rimoldi S, Folkedal O, Calduch-Giner JA, et al. Skin mucus of gilthead sea bream (*Sparus aurata* L.). Protein mapping and regulation in chronically stressed fish. *Front Physiol.* (2017) 8:34. doi: 10.3389/fphys.2017.00034
35. Rajan B, Lokesh J, Kiron V, Brinchmann MF. Differentially expressed proteins in the skin mucus of Atlantic cod (*Gadus morhua*) upon natural infection with *Vibrio anguillarum*. *BMC Vet Res.* (2013) 9:103. doi: 10.1186/1746-6148-9-103
36. Reyes-López FE, Aerts J, Vallejos-Vidal E, Ampe B, Dierckens K, Tort L, et al. Modulation of innate immune-related genes and glucocorticoid synthesis in gnotobiotic full-sibling European sea bass (*Dicentrarchus labrax*) larvae challenged with *Vibrio anguillarum*. *Front Immunol.* (2018) 9:914. doi: 10.3389/fimmu.2018.00914
37. Frans I, Michiels CW, Bossier P, Willems KA, Lievens B, Rediers H. *Vibrio anguillarum* as a fish pathogen: virulence factors, diagnosis and prevention. *J Fish Dis.* (2011) 34:643–61. doi: 10.1111/j.1365-2761.2011.01279.x
38. Muckenthaler MU, Galy B, Hentze MW. Systemic iron homeostasis and the iron-responsive element/iron-regulatory protein (IRE/IRP) regulatory network. *Annual Rev Nutrit.* (2008) 28:197–213. doi: 10.1146/annurev.nutr.28.061807.155521
39. Zhang H, Fei C, Wu H, Yang M, Liu Q, Wang Q, et al. Transcriptome profiling reveals Th17-like immune responses induced in zebrafish bath-vaccinated with a live attenuated *Vibrio anguillarum*. *PLoS ONE.* (2013) 8:e73871. doi: 10.1371/journal.pone.0073871
40. Lee SK, Ding JL. A perspective on the role of extracellular hemoglobin on the innate immune system. *DNA Cell Biol.* (2013) 32:36–40. doi: 10.1089/dna.2012.1897
41. Scarl RT, Lawrence CM, Gordon HM, Nunemaker CS. STEAP4: its emerging role in metabolism and homeostasis of cellular iron and copper. *J Endocrinol.* (2017) 234:R123–34. doi: 10.1530/JOE-16-0594
42. Holm HJ, Wadsworth S, Bjelland A-K, Krasnov A, Evensen Ø, Skugor, S. Dietary phytochemicals modulate skin gene expression profiles and result in reduced lice counts after experimental infection in Atlantic salmon. *Parasites Vectors.* (2016) 9:271. doi: 10.1186/s13071-016-1537-y
43. Zou J, Secombes CJ. Teleost fish interferons and their role in immunity. *Dev Comparat Immunol.* (2011) 35:1376–87. doi: 10.1016/j.dci.2011.07.001
44. Gu Y, Harley IT, Henderson LB, Aronow BJ, Vietor I, Huber LA, et al. Identification of IFRD1 as a modifier gene for cystic fibrosis lung disease. *Nature.* (2009) 458:1039–42. doi: 10.1038/nature07811
45. Lü AJ, Hu XC, Wang Y, Zhu AH, Shen LL, Tian J, et al. Skin immune response in the zebrafish, *Danio rerio* (Hamilton), to *Aeromonas hydrophila* infection: a transcriptional profiling approach. *J Fish Dis.* (2015) 38:137–50. doi: 10.1111/jfd.12214
46. Ferrari S, Rey S, Høglund E, Øverli Ø, Chatain B, MacKenzie S, et al. Physiological responses during acute stress recovery depend on stress coping style in European sea bass, *Dicentrarchus labrax*. *Physiol Behav.* (2020) 216:112801. doi: 10.1016/j.physbeh.2020.112801
47. Sun G, Li H, Wang Y, Zhang B, Zhang S. Zebrafish complement factor H and its related genes: identification, evolution, and expression. *Funct Integrat Genom.* (2010) 10:577–87. doi: 10.1007/s10142-010-0182-3
48. Avery VM, Gordon DL. Characterization of factor H binding to human polymorphonuclear leukocytes. *J Immunol.* (1993) 151:5545–53.
49. Parente R, Clark SJ, Inforzato A, Day AJ. Complement factor H in host defense and immune evasion. *Cell Mol Life Sci.* (2017) 74:1605–24. doi: 10.1007/s00018-016-2418-4
50. Ferreira VP, Pangburn MK, Cortés C. Complement control protein factor H: the good, the bad, the inadequate. *Mol Immunol.* (2010) 47:2187–97. doi: 10.1016/j.molimm.2010.05.007
51. Easy RH, Ross NW. Changes in Atlantic salmon (*Salmo salar*) epidermal mucus protein composition profiles following infection with sea lice (*Lepeophtheirus salmonis*). *Comparat Biochem Physiol.* (2009) 4:159–67. doi: 10.1016/j.cbd.2009.02.001
52. Fu Q, Yang N, Gao C, Tian M, Zhou S, Mu X, et al. Characterization, expression signatures and microbial binding analysis of cathepsin A in turbot, *Scophthalmus maximus* L. (SmCTSA). *Fish Shellf Immunol.* (2018) 81:21–8. doi: 10.1016/j.fsi.2018.07.002
53. Aranishi F. Lysis of pathogenic bacteria by epidermal cathepsins L and B in the Japanese eel. *Fish Physiol Biochem.* (1999) 20:37–41. doi: 10.1023/A:1007763711158
54. Wang R, Song L, Su B, Zhao H, Zhang D, Peatman E, et al. Mucosal expression signatures of two Cathepsin L in channel catfish (*Ictalurus punctatus*) following bacterial challenge. *Fish Shellf Immunol.* (2015) 47:582–9. doi: 10.1016/j.fsi.2015.09.047
55. Chen J, Zhang L, Yang N, Cao M, Tian M, Fu Q, et al. Characterization of the immune roles of cathepsin L in turbot (*Scophthalmus maximus* L.) mucosal immunity. *Fish Shellf Immunol.* (2020) 97:322–35. doi: 10.1016/j.fsi.2019.12.005
56. Reyes-Cerpa S, Vallejos-Vidal E, Gonzalez-Bown MJ, Morales-Reyes J, Pérez-Stuardo D, Vargas D, et al. Effect of yeast (*Xanthophyllomyces dendrorhous*) and plant (Saint John's wort, lemon balm, and rosemary) extract based functional diets on antioxidant and immune status of Atlantic salmon (*Salmo salar*) subjected to crowding stress. *Fish Shellf Immunol.* (2018) 74:250–9. doi: 10.1016/j.fsi.2017.12.061
57. Khansari AR, Balasch JC, Vallejos-Vidal E, Parra D, Reyes-López FE, Tort L. Comparative immune- and stress-related transcript response induced by air exposure and *Vibrio anguillarum* bacterin in rainbow trout (*Oncorhynchus mykiss*) and gilthead seabream (*Sparus aurata*) mucosal surfaces. *Front Immunol.* (2018) 9:856. doi: 10.3389/fimmu.2018.00856
58. Vidak E, Javoršek U, Vizovišek M, Turk B. Cysteine cathepsins and their extracellular roles: shaping the microenvironment. *Cells.* (2019) 8:3. doi: 10.3390/cells8030264
59. Kasteren SI, Overkleeft HS. Endo-lysosomal proteases in antigen presentation. *Curr Opin Chem Biol.* (2014) 23:8–15. doi: 10.1016/j.cbpa.2014.08.011
60. Wilson AB. MHC and adaptive immunity in teleost fishes. *Immunogenetics.* (2017) 69:521–8. doi: 10.1007/s00251-017-1009-3
61. Cuesta A, Ángeles Esteban M, Meseguer J. Cloning, distribution and up-regulation of the teleost fish MHC class II alpha suggests a role for granulocytes as antigen-presenting cells. *Mol Immunol.* (2006) 43:1275–85. doi: 10.1016/j.molimm.2005.07.004
62. Sepulcre M, Pelegrín P, Mulero V, Meseguer J. Characterisation of gilthead seabream acidophilic granulocytes by a monoclonal antibody unequivocally points to their involvement in fish phagocytic response. *Cell Tissue Res.* (2002) 308:97–102. doi: 10.1007/s00441-002-0531-1
63. Mulero I, Noga EJ, Meseguer J, García-Ayala A, Mulero V. The antimicrobial peptides piscidins are stored in the granules of professional phagocytic granulocytes of fish and are delivered to the bacteria-containing phagosome upon phagocytosis. *Dev Comparat Immunol.* (2008) 32:1531–8. doi: 10.1016/j.dci.2008.05.015
64. Schafer JC, McRae RE, Manning EH, Lapierre LA, Goldenring JR. Rab11-FIP1A regulates early trafficking into the recycling endosomes. *Exp Cell Res.* (2016) 340:259–73. doi: 10.1016/j.yexcr.2016.01.003
65. Cantalupo G, Alifano P, Roberti V, Bruni CB, Bucci C. Rab-interacting lysosomal protein (RILP): the Rab7 effector required for transport to lysosomes. *EMBO J.* (2001) 20:683–93. doi: 10.1093/emboj/20.4.683
66. Harrison RE, Bucci C, Vieira OV, Schroer TA, Grinstein S. Phagosomes fuse with late endosomes and/or lysosomes by extension of membrane protrusions along microtubules: role of Rab7 and RILP. *Mol Cell Biol.* (2003) 23:6494–506. doi: 10.1128/MCB.23.18.6494-6506.2003
67. Bah A, Vergne I. Macrophage autophagy and bacterial infections. *Front Immunol.* (2017) 8:1483. doi: 10.3389/fimmu.2017.01483
68. Iger Y, Balm PHM, Bonga SEW. Cellular responses of the skin and changes in plasma cortisol levels of trout (*Oncorhynchus mykiss*) exposed to acidified water. *Cell Tissue Res.* (1994) 278:535–42. doi: 10.1007/BF00331371

69. Barreda D, Hanington PC, Walsh C, Wong P, Belosevic M. Differentially expressed genes that encode potential markers of goldfish macrophage development *in vitro*. *Dev Comparat Immunol.* (2004) 28:727–46. doi: 10.1016/j.dci.2003.11.005
70. Nya EJ, Austin B. Use of garlic, *Allium sativum*, to control *Aeromonas hydrophila* infection in rainbow trout, *Oncorhynchus mykiss* (Walbaum). *J Fish Dis.* (2009) 32:963–70. doi: 10.1111/j.1365-2761.2009.01100.x
71. Ndong D, Fall J. The effect of garlic (*Allium sativum*) on growth and immune responses of hybrid tilapia (*Oreochromis niloticus* × *Oreochromis aureus*). *J Clin Immunol Immunopathol Res.* (2011) 3:1–9.
72. Ran C, Hu J, Liu W, Liu Z, He S, Dan BC, et al. Thymol and carvacrol affect hybrid tilapia through the combination of direct stimulation and an intestinal microbiota-mediated effect: insights from a germ-free zebrafish model. *J Nutr.* (2016) 146:1132–40. doi: 10.3945/jn.115.229377
73. Abdel-Latif HMR, Abdel-Tawwab M, Khafaga AF, Dawood MAO. Dietary origanum essential oil improved antioxidative status, immune-related genes, and resistance of common carp (*Cyprinus carpio* L.) to *Aeromonas hydrophila* infection. *Fish Shellf Immunol.* (2020) 104:1–7. doi: 10.1016/j.fsi.2020.05.056
74. Beltrán JMG, Silvera DG, Ruiz CE, Campo V, Chupani L, Faggio C, et al. Effects of dietary *Origanum vulgare* on gilthead seabream (*Sparus aurata* L.) immune and antioxidant status. *Fish Shellf Immunol.* (2020) 99:452–461. doi: 10.1016/j.fsi.2020.02.040
75. May RC, Machesky LM. Phagocytosis and the actin cytoskeleton. *J Cell Sci.* (2001) 114:1061–77.
76. Plazyo O, Sheng JJ, Jin JP. Downregulation of calponin 2 contributes to the quiescence of lung macrophages. *Am J Physiol Cell Physiol.* (2019) 317:C749–61. doi: 10.1152/ajpcell.00036.2019
77. Sandiford SL, Dong Y, Pike A, Blumberg BJ, Bahia AC, Dimopoulos G. Cytoplasmic actin is an extracellular insect immune factor which is secreted upon immune challenge and mediates phagocytosis and direct killing of bacteria, and is a Plasmodium antagonist. *PLoS Pathogens.* (2015) 11:e1004631. doi: 10.1371/journal.ppat.1004631
78. Birchenough GMH, Johansson ME, Gustafsson JK, Bergström JH, Hansson GC. New developments in goblet cell mucus secretion and function. *Mucosal Immunol.* (2015) 8:712–9. doi: 10.1038/mi.2015.32
79. Blank U, Madera-Salcedo IK, Danelli L, Claver J, Tiwari N, Sánchez-Miranda E, et al. Vesicular trafficking and signaling for cytokine and chemokine secretion in mast cells. *Front Immunol.* (2014) 5:453. doi: 10.3389/fimmu.2014.00453
80. Zou J, Secombes C. The function of fish cytokines. *Biology.* (2016) 5:23. doi: 10.3390/biology5020023
81. Park H, Park SG, Kim J, Ko YG, Kim S. Signaling pathways for TNF production induced by human aminoacyl-tRNA synthetase-associating factor, p43. *Cytokine.* (2002) 20:148–53. doi: 10.1006/cyto.2002.1992
82. Dai T, Zhao X, Li Y, Yu L, Li Y, Zhou X, et al. miR-423 promotes breast cancer invasion by activating NF-κB signaling. *OncoTargets Therapy.* (2020) 13:5467–78. doi: 10.2147/OTT.S236514
83. Park SG, Shin H, Shin YK, Lee Y, Choi EC, Park BJ, et al. The novel cytokine p43 stimulates dermal fibroblast proliferation and wound repair. *Am J Pathol.* (2005) 166:387–98. doi: 10.1016/S0002-9440(10)62262-6
84. Noubade R, Wong K, Ota N, Rutz S, Eidenschenk C, Valdez PA, et al. NRROS negatively regulates reactive oxygen species during host defence and autoimmunity. *Nature.* (2014) 509:235–9. doi: 10.1038/nature13152
85. Su X, Mei S, Liang X, Wang S, Liu J, Zhang Y, et al. Epigenetically modulated LRRC33 acts as a negative physiological regulator for multiple Toll-like receptors. *J Leukocyte Biol.* (2014) 96:17–26. doi: 10.1189/jlb.0813457
86. Gültekin Y, Eren E, Özören N. Overexpressed NLRC3 acts as an anti-inflammatory cytosolic protein. *J Innate Immun.* (2014) 7:25–36. doi: 10.1159/000363602
87. Álvarez CA, Ramírez-Cepeda F, Santana P, Torres E, Cortés J, Guzmán F, et al. Insights into the diversity of NOD-like receptors: Identification and expression analysis of NLRC3, NLRC5 and NLRX1 in rainbow trout. *Mol Immunol.* (2017) 87:102–13. doi: 10.1016/j.molimm.2017.03.010
88. Gao F-y, Pang J-c, Lu M-x, Yang X-l, Zhu H-p, Ke X-l. Molecular characterization, expression and functional analysis of NOD1, NOD2 and NLRC3 in Nile tilapia (*Oreochromis niloticus*). *Fish Shellf Immunol.* (2018) 73:207–19. doi: 10.1016/j.fsi.2017.12.012
89. Hou Z, Ye Z, Zhang D, Gao C, Su B, Song L, et al. Characterization and expression profiling of NOD-like receptor C3 (NLRC3) in mucosal tissues of turbot (*Scophthalmus maximus* L.) following bacterial challenge. *Fish Shellf Immunol.* (2017) 66:231–9. doi: 10.1016/j.fsi.2017.05.014
90. Ishaq M, Ma L, Wu X, Mu Y, Pan J, Hu J, et al. The DEAD-box RNA helicase DDX1 interacts with RelA and enhances nuclear factor kappaB-mediated transcription. *J Cell Biochem.* (2009) 106:296–305. doi: 10.1002/jcb.22004
91. Mojzesz M, Klak K, Wojtal P, Adamek M, Podlasz P, Chmielewska-Krzesinska M, et al. Viral infection-induced changes in the expression profile of non-RLR DExD/H-box RNA helicases (DDX1, DDX3, DHX9, DDX21 and DHX36) in zebrafish and common carp. *Fish Shellf Immunol.* (2020) 104:62–73. doi: 10.1016/j.fsi.2020.06.010
92. Saftig P, Klumperman J. Lysosome biogenesis and lysosomal membrane proteins: trafficking meets function. *Nat Rev Mol Cell Biol.* (2009) 10:623–35. doi: 10.1038/nrm2745
93. Austin B, Austin DA. Pseudomonads. In: *Bacterial Fish Pathogens: Disease of Farmed and Wild Fish*. Cham: Springer International Publishing (2016). p. 475–98. doi: 10.1007/978-3-319-32674-0_9
94. Austin B, Austin DA. Vibrios. In: *Bacterial Fish Pathogens: Disease of Farmed and Wild Fish*. Cham: Springer International Publishing (2016). p. 499–601. doi: 10.1007/978-3-319-32674-0_10
95. Borrego J, Labella A, Castro D, Ortiz-Delgado J, Sarasquete C. Updated of the pathologies affecting cultured gilthead seabream, *Sparus aurata*. *Annals Aquaculture Res.* (2017) 4:1033.
96. Muniesa A, Basurco B, Aguilera C, Furones D, Reverté C, Sanjuan-Vilaplana A, et al. Mapping the knowledge of the main diseases affecting sea bass and sea bream in Mediterranean. *Transboundary Emerg Dis.* (2020) 67:1089–1100. doi: 10.1111/tbed.13482
97. Ibarz A, Padrós F, Gallardo MÁ, Fernández-Borràs J, Blasco J, Tort L. Low-temperature challenges to gilthead sea bream culture: review of cold-induced alterations and 'Winter Syndrome'. *Rev Fish Biol Fish.* (2010) 20:539–56. doi: 10.1007/s11160-010-9159-5
98. Ghehdarijani MS, Hajimoradloo A, Ghorbani R, Roohi Z. The effects of garlic-supplemented diets on skin mucosal immune responses, stress resistance and growth performance of the Caspian roach (*Rutilus rutilus*) fry. *Fish Shellf Immunol.* (2016) 49:79–83. doi: 10.1016/j.fsi.2015.12.021
99. Maldonado-Garcia M, Angulo C, Vazquez-Martinez J, Sanchez V, Lopez MG, Reyes-Becerril M. Antioxidant and immunostimulant potentials of *Chenopodium ambrosioides* L. *in Pacific red snapper (Lutjanus peru)*. *Aquaculture.* (2019) 513:734414. doi: 10.1016/j.aquaculture.2019.734414
100. Vazirzadeh A, Jalali S, Farhadi A. Antibacterial activity of Oliveria decumbens against *Streptococcus iniae* in *Nile tilapia* (*Oreochromis niloticus*) and its effects on serum and mucosal immunity and antioxidant status. *Fish Shellf Immunol.* (2019) 94:407–16. doi: 10.1016/j.fsi.2019.09.025
101. Xu J, Zhou F, Ji BP, Pei RS. The antibacterial mechanism of carvacrol and thymol against *Escherichia coli*. *Lett Appl Microbiol.* (2008) 47:174–9. doi: 10.1111/j.1472-765X.2008.02407.x
102. Sanahuja I, Fernández-Alacid L, Ordóñez-Grande B, Sánchez-Nuño S, Ramos A, Araujo RM, et al. Comparison of several non-specific skin mucus immune defences in three piscine species of aquaculture interest. *Fish Shellf Immunol.* (2019) 89:428–36. doi: 10.1016/j.fsi.2019.04.008
103. Barton BA. Stress in fishes: a diversity of responses with particular reference to changes in circulating corticosteroids. *Integrat Comparat Biol.* (2002) 42:517–25. doi: 10.1093/icb/42.3.517
104. Parra D, Reyes-Lopez, Tort FE. L. Mucosal immunity and B cells in teleosts: effect of vaccination and stress. *Front Immunol.* (2015) 6:354. doi: 10.3389/fimmu.2015.00354
105. Aydin B, Barbas LAL. Sedative and anesthetic properties of essential oils and their active compounds in fish: a review. *Aquaculture.* (2020) 520:734999. doi: 10.1016/j.aquaculture.2020.734999
106. Yousefi M, Vatnikov YA, Kulikov EV, Plushikov VG, Drukovsky SG, Hoseinifar SH, et al. The protective effects of dietary garlic on common carp (*Cyprinus carpio*) exposed to ambient ammonia toxicity. *Aquaculture.* (2020) 526:735400. doi: 10.1016/j.aquaculture.2020.735400
107. Esmaeili M, Kenari AA, Rombenso A. Immunohematological status under acute ammonia stress of juvenile rainbow trout (*Oncorhynchus mykiss*

Walbaum, 1792) fed garlic (*Allium sativum*) powder-supplemented meat and bone meal-based feeds. *Comparat Clin Pathol.* (2017) 26:853–66. doi: 10.1007/s00580-017-2457-8

108. Serradell A, Torrecillas S, Makol A, Valdenegro V, Fernández-Montero A, Acosta F, et al. Prebiotics and phytogenics functional additives in low fish meal and fish oil based diets for European sea bass (*Dicentrarchus labrax*): effects on stress and immune responses. *Fish Shellf Immunol.* (2020) 100:219–29. doi: 10.1016/j.fsi.2020.03.016
109. Carbajal A, Reyes-López FE, Tallo-Parra O, Lopez-Bejar M, Tort L. Comparative assessment of cortisol in plasma, skin mucus and scales as a measure of the hypothalamic-pituitary-interrenal axis activity in fish. *Aquaculture.* (2019) 506:410–6. doi: 10.1016/j.aquaculture.2019.04.005
110. Fernández-Alacid L, Sanahuja I, Ordóñez-Grande B, Sánchez-Nuño S, Herrera M, Ibarz A. Skin mucus metabolites and cortisol in meagre fed acute stress-attenuating diets: correlations between plasma and mucus. *Aquaculture.* (2019) 499:185–194. doi: 10.1016/j.aquaculture.2018.09.039
111. Guardiola FA, Cuesta A, Esteban MÁ. (2016). Using skin mucus to evaluate stress in gilthead seabream (*Sparus aurata* L.), *Fish Shellf Immunol.* 59, 323–30. doi: 10.1016/j.fsi.2016.11.005
112. Aluru N, Vijayan MM. Stress transcriptomics in fish: a role for genomic cortisol signaling. *Gen. an Compar. Endocrinol.* (2009) 164:142–150. doi: 10.1016/j.ygcen.2009.03.020
113. Fernández-Alacid L, Sanahuja I, Ordóñez-Grande B, Sánchez-Nuño S, Herrera M, Ibarz A. Comparison between properties of dorsal and ventral skin mucus in Senegalese sole: response to an acute stress. *Aquaculture.* (2019) 513:734410. doi: 10.1016/j.aquaculture.2019.734410
114. Iger Y, Balm PH, Jenner HA, Wendelaar Bonga. S.E. Cortisol induces stress-related changes in the skin of rainbow trout (*Oncorhynchus mykiss*). *Gen. an Compar. Endocrinol.* (1995) 97:188–198. doi: 10.1006/gcen.1995.1018
115. De Mercado E, Larrán AM, Pinedo J, Tomás-Almenar C. Skin mucous: a new approach to assess stress in rainbow trout. *Aquaculture.* (2018) 484:90–97. doi: 10.1016/j.aquaculture.2017.10.031
116. Li J, Xia Z, Ding J. Thioredoxin-like domain of human κ class glutathione transferase reveals sequence homology and structure similarity to the θ class enzyme. *Protein Sci.* (2005) 14:2361–9. doi: 10.1110/ps.051463905
117. Vallejos-Vidal E, Reyes-Cerpa S, Rivas-Pardo JA, Maisey K, Yáñez JM, Valenzuela H, et al. Single-nucleotide polymorphisms (SNP) mining and their effect on the tridimensional protein structure prediction in a set of immunity-related expressed sequence tags (EST) in Atlantic salmon (*Salmo salar*). *Front Genet.* (2020) 10:1406. doi: 10.3389/fgene.2019.01406
118. Hoseinifar SH, Shakouri M, Yousefi S, Van Doan H, Shafiei S, Yousefi M, et al. Humoral and skin mucosal immune parameters, intestinal immune related genes expression and antioxidant defense in rainbow trout (*Oncorhynchus mykiss*) fed olive (*Olea europea* L.) waste. *Fish Shellf Immunol.* (2020) 100:171–8. doi: 10.1016/j.fsi.2020.02.067
119. Hayes JD, Dinkova-Kostova AT. The Nrf2 regulatory network provides an interface between redox and intermediary metabolism. *Trends Biochem Sci.* (2014) 39:199–218. doi: 10.1016/j.tibs.2014.02.002
120. Dupret JM, Rodrigues-Lima F. Structure and regulation of the drug-metabolizing enzymes arylamine N-acetyltransferases. *Curr Med Chem.* (2005) 12:311–8. doi: 10.2174/0929867053363289
121. Song L, Li C, Xie Y, Liu S, Zhang J, Yao J, et al. Genome-wide identification of Hsp70 genes in channel catfish and their regulated expression after bacterial infection. *Fish Shellf Immunol.* (2016) 49:154–62. doi: 10.1016/j.fsi.2015.12.009
122. Eissa N, Wang H-P, Yao H, Shen Z-G, Shaheen AA, Abou-ElGheit EN. Expression of Hsp70, Igf1, and three oxidative stress biomarkers in response to handling and salt treatment at different water temperatures in yellow perch, *Perca flavescens*. *Front Physiol.* (2017) 8:683. doi: 10.3389/fphys.2017.00683
123. Mosbah A, Guerbej H, Boussetta H, Bouraoui Z, Banni M. Protective effects of dietary garlic powder against cadmium-induced toxicity in sea bass liver: a chemical, biochemical, transcriptomic approach. *Biol Trace Element Res.* (2018) 183:370–8. doi: 10.1007/s12011-017-1146-4
124. Giannenas I, Triantafillou E, Stavrakakis S, Margaroni M, Mavridis S, Steiner T, et al. Assessment of dietary supplementation with carvacrol or thymol containing feed additives on performance, intestinal microbiota and antioxidant status of rainbow trout (*Oncorhynchus mykiss*). *Aquaculture.* (2012) 350–3. doi: 10.1016/j.aquaculture.2012.04.027
125. Piazzi M, Bavelloni A, Gallo A, Faenza I, Blalock WL. Signal transduction in ribosome biogenesis: a recipe to avoid disaster. *Int J Mol Sci.* (2019) 20:E2718. doi: 10.3390/ijms20112718

Conflict of Interest: JF is a current TECNOVIT-FARMFAES S.L employee conducting an Industrial Ph.D.

The remaining authors declare that the research was conducted in the absence of any commercial or financial relationships that could be construed as a potential conflict of interest.

frontiers in Immunology

ORIGINAL RESEARCH
published: 15 March 2021
doi: 10.3389/fimmu.2021.660448

Methionine and Tryptophan Play Different Modulatory Roles in the European Seabass (*Dicentrarchus labrax*) Innate Immune Response and Apoptosis Signaling—An *In Vitro* Study

Marina Machado[1,2,3,4*], *Cláudia R. Serra*[1], *Aires Oliva-Teles*[1,5] *and Benjamín Costas*[1,3*]

[1] Centro Interdisciplinar de Investigação Marinha e Ambiental (CIIMAR), Matosinhos, Portugal, [2] Instituto de Investigação e Inovação em Saúde (i3S), Universidade do Porto, Porto, Portugal, [3] Instituto de Ciências Biomédicas Abel Salazar (ICBAS-UP), Universidade do Porto, Porto, Portugal, [4] Instituto de Biologia Molecular e Celular, Universidade do Porto, Porto, Portugal, [5] Departamento de Biologia, Faculdade de Ciências da Universidade do Porto (FCUP), Porto, Portugal

OPEN ACCESS

Edited by:
Felipe E. Reyes-López, Universitat Autònoma de Barcelona, Spain

Reviewed by:
Chunxiao Zhang, Jimei University, China
Morgane Henry, Hellenic Centre for Marine Research (HCMR), Greece
Carlo C. Lazado, Fisheries and Aquaculture Research (Nofima), Norway
Elisabeth Holen, Norwegian Institute of Marine Research (IMR), Norway

***Correspondence:**
Marina Machado
mcasimiro@ciimar.up.pt
Benjamín Costas
bcostas@ciimar.up.pt

Specialty section:
This article was submitted to Nutritional Immunology, a section of the journal Frontiers in Immunology

Received: 29 January 2021
Accepted: 25 February 2021
Published: 15 March 2021

Citation:
Machado M, Serra CR, Oliva-Teles A and Costas B (2021) Methionine and Tryptophan Play Different Modulatory Roles in the European Seabass (Dicentrarchus labrax) Innate Immune Response and Apoptosis Signaling—An In Vitro Study. Front. Immunol. 12:660448. doi: 10.3389/fimmu.2021.660448

The range of metabolic pathways that are dependent on a proper supply of specific amino acids (AA) unveils their importance in the support of health. AA play central roles in key pathways vital for immune support and individual AA supplementation has shown to be able to modulate fish immunity. *In vitro* trials are important tools to evaluate the immunomodulatory role of AA, and the present study was conceived to evaluate methionine and tryptophan roles in immune-related mechanisms aiming to understand their effects in leucocyte functioning and AA pathways. For that purpose, head-kidney leucocytes were isolated and a primary cell culture established. The effect of methionine or tryptophan surplus on cell viability was assessed. Medium L-15 10% FBS without AA addition (0.5mM of L-methionine, 0.1 mM of L-tryptophan) was used as control. To that, L-methionine or L-tryptophan were supplemented at 1 and 2 times (M1x or M2x, and T1x or T2x). Nitric oxide, ATP, total antioxidant capacity, and immune-related genes were evaluated in response to lipopolysaccharides extracted from *Photobacterium damselae* subsp. *piscicida* or UV-inactivated bacteria). Moreover, caspase 3 activity and apoptosis-related genes were evaluated in response to the apoptosis-inducing protein, AIP56. Distinct roles in leucocytes' immune response were observed, with contrasting outcomes in the modulation of individual pathways. Methionine surplus improved cell viability, polyamine production, and methionine-related genes expression in response to an inflammatory agent. Also, methionine supplementation lowered signals of apoptosis by AIP56, presenting lower caspase 3 activity and higher *il1β* and *nf-κb* expression. Cells cultured in tryptophan supplemented medium presented signals of an attenuated inflammatory response, with decreased ATP and enhanced expression of anti-inflammatory and catabolism-related genes in macrophages. In response to AIP56, leucocytes cultured in a tryptophan-rich medium presented lower resilience to the toxin,

higher caspase 3 activity and expression of caspase 8, and lower expression of several genes, including *nf-κb* and *p65*. This study showed the ability of methionine surplus to improve leucocytes' response to an inflammatory agent and to lower signals of apoptosis by AIP56 induction, while tryptophan attenuated several cellular signals of the inflammatory response to UV-inactivated bacteria and lowered leucocyte resilience to AIP56.

Keywords: amino acids, inflammation, fish, AIP56, *Photobacterium damselae* subsp. *piscicida*

INTRODUCTION

Amino acids (AA) are key players for the biosynthesis of vital molecules for immune support (1) and their use as nutraceutical supplements in mammals (2) and poultry (3, 4) is a current strategy. The role of individual AA in the innate immune response is associated with their role in key pathways essential for cellular function and as precursors of hormones and enzymes. Likewise, following the presuppose that the requirement of specific AA increases in response to inflammation and infection (5), their dietary supplementation may allow the modulation of particular immune-related pathways with the final goal of enhancing host immunity. Having this in mind, *in vivo* studies were developed to achieve nutritional strategies that modulate the fish immune response through the increase of AA availability (6–14), while few *in vitro* studies (15, 16) aiming to collect information at the cellular level were performed.

Previous studies in fish contributed with some insights on the key role of methionine in the fish immune system. Dietary methionine supplementation was able to increase European seabass (*Dicentrarchus labrax*) peripheral neutrophil numbers and innate immune response to an inflammatory insult with UV-inactivated *Photobacterium damselae* subsp. *piscicida* (*Phdp*) (11, 13) and increase disease resistance to *Phdp* (14). Also, juvenile Jian carp (*Cyprinus carpio* var. Jian) fed with increased levels of methionine presented an increased peripheral leucocyte concentration and humoral response, in response to *Aeromonas hydrophila* (9). Additionally, methionine supplementation was shown to be key for European seabass immune support in an extreme feed formulation (0% fish meal) (17). Data from those studies are sustained by the recognized role of methionine as a methyl group donor for the methylation, transsulfuration, and aminopropylation routes, with coenzyme S-adenosylmethionine (SAM) as the leading factor. The increase of methionine input can increase DNA methylation ratio, known to be dependent on the supply of SAM (18). Through the aminopropylation route, methionine contributes to polyamine synthesis thus contributing to cell proliferation (19). Finally, by the transsulfuration pathway, methionine is the precursor of cysteine, an AA constituent of the powerful antioxidant molecule glutathione (GSH) (1). *In vitro* results on this matter are scarce. Nonetheless, Azeredo et al. (16) showed the ability of methionine supplementation to boost European seabass head-kidney (HK) leucocytes (HKL) nitric oxide (NO), superoxide anion, and ATP production in the absence of stimulus, and improved HKL NO production in response to UV-inactivated *Vibrio anguillarum*. These authors discussed that methionine potential for immune improvement seems to be directly related to the enhancement of cell response by the enhancement of the methionine-related pathways.

Tryptophan has been the target of *in vivo* studies in several animal models focusing its function as a precursor of compounds involved in stress modulation, antioxidant properties, and immune tolerance (20–22). Studies in fish showed that increasing dietary tryptophan levels did not significantly modulate European seabass (11) and Persian sturgeon (*Acipenser persicus*) (23) basal innate immune-related mechanisms activity, while a clear effect of tryptophan surplus was observed upon inflammation induction. For instance, in European seabass Azeredo et al. (12) observed an inhibitory action of tryptophan on HK inflammatory transcripts while Machado et al. (24) reported a compromised immune response and disease resistance to *Phdp*. In macrophages, tryptophan catabolism occurs through the kynurenine-niacin pathway, mediated by indoleamine 2, 3-dioxygenase (IDO) (25). In response to inflammation, IDO is induced, exerting anti-microbial effects by tryptophan extracellular depletion (26, 27), setting an antioxidant system by the consumption of superoxide radicals, and its metabolites regulate T-cell function (28). *In vitro* results pointed to the impairment of pro-inflammatory signals offsetting the inflammatory response caused by tryptophan higher availability (16).

The inflammatory response and the overall innate immune system is sustained by phagocytes (i.e. neutrophils and macrophages). These myeloid cells are responsible for the incorporation and digestion of other cells or cell components, as pathogens or apoptotic and necrotic host-cells. Moreover, fish phagocytes are responsible for the initiation and resolution of inflammation by the production and secretion of pro- and anti-inflammatory chemical messengers (autocrine signaling) and cell-to-cell signaling communication (paracrine signaling) (29). In fact, as widely described in mammals, monocytes can adapt their phenotypes according to the response stage and differentiated into three distinct groups formerly determined by the inductor of differentiation (30–33). Upon activation, circulating monocytes (M0 type) are differentiated into macrophages that under inflammatory settings and in the presence of pathogens and tumor cells, are described as M1 type. Whereas M2 macrophages are found in sterile conditions

or in the repair stage of the innate response (34). This has only been recently described in fish, particularly in the common carp (*Cyprinus carpio* L) (35). Additionally, cell inactivation and clearance through apoptosis takes part in the proper function of the immune system. As a defense mechanism, apoptosis is responsible for the clearance of damaged cells and can be initiated by a wide variety of stimuli, as infection and stress (36). Since macrophages present themselves as a useful tool for *in vitro* functional studies on the fish innate immune response, the present work focused on the study of the response of innate activated macrophages induced by microbial stimuli and with key roles in the phagocytosis of pathogens and the production of pro-inflammatory signals (37).

Phdp is a bacterial pathogen for many marine fish species that owns part its successful pathogenesis to the ability to produce and release the exotoxin AIP56 to the extracellular environment (38). AIP56 cleaves the transcription factor NF- κB, therefore inhibiting the transcription of key immune-related genes (39) and inducing extensive apoptosis of macrophages and neutrophils (38). Therefore, *Phdp* can act at distance, without direct contact with the host cells, and leads to the depletion of host primary cell defense mechanisms, the phagocytes.

The present study aimed to evaluate *in vitro*, at the leucocytes functional and transcriptional level, the modulatory effects of two supplementation levels of methionine and tryptophan on the response of HKL against UV- inactivated *Phdp* (*Phdp*UV) or *Phdp* lipopolysaccharides (LPS*Phdp*), and the apoptosis process in response to the AIP56 toxin.

MATERIAL AND METHODS

The experiments were approved by the CIIMAR Animal Welfare Committee, carried out in a registered installation (N16091.UDER), and performed by trained scientists in full compliance with national rules and following the European Directive 2010/63/EU of the European Parliament and the European Union Council on the protection of animals used for scientific purposes.

Photobacterium damselae subsp. piscicida Inactivation

Phdp strain PP3, isolated from yellowtail (*Seriola quinqueradiata*; Japan), was obtained from the Fish Immunology and Vaccinology group (i3S/IBMC, University of Porto). Bacteria were routinely cultured at 22°C in tryptic soy broth (TSB) or tryptic soy agar (TSA) (both from Difco Laboratories) supplemented with NaCl to a final concentration of 2% (w/v) (TSB-2 and TSA-2, respectively). Live bacteria were stored at −80°C in TSB-2 supplemented with 15% (v/v) glycerol.

To maintain the structural integrity of bacterial antigens but prevent bacterial growth, *Phdp* were killed by UV irradiation. For this, bacteria were grown in TSB-2 and, after reaching the exponential growth phase (OD_{600nm}= 0.523; 6.7 x 10^8 colony forming units (CFUs) ml^{-1}), were placed in a sterile tray (maximum inoculum height of 0.2 mm) at a distance of 10 centimeters of a UV lamp and inactivated by exposure to UV irradiation for 2 h. Bacteria were then recovered by centrifugation at 1500 × *g* for 30 min, the pellet resuspended in Hank's Balanced Salt Solution (HBSS, Gibco), and bacterial concentration adjusted to a virtual dose of 1 × 10^7 CFU ml^{-1} taking into account their concentration prior to inactivation. Lack of bacterial viability was confirmed by plating the inoculum on TSA-2.

Photobacterium damselae subsp. piscicida Lipopolysaccharides Extraction and Purification

Lipopolysaccharides (LPS) from *Phdp* (LPS*Phdp*) were extracted by hot phenol-water according to the method described by Rezania et al. (40) with modifications (16). Purified LPS*Phdp*, without any residual phenol, was lyophilized, resuspended in PBS to a final concentration of 2 mg ml^{-1}, and kept at −20°C until use. Visualization was achieved by SDS-PAGE (12%) electrophoretic resolution of 20 μg purified LPS*Phdp* and consequent staining following the improved silver stain protocol described by Zhu et al. (41).

Recombinant AIP56

Recombinant AIP56 (38) was obtained from the Fish Immunology and Vaccinology group (i3S/IBMC, University of Porto) and stored in 20 nM Tris-HCl, pH 8.0 at -80 °C until use.

Fish and Establishment of HKL Primary Cell Cultures

European seabass (*Dicentrarchus labrax*) juveniles (8 ± 0.5 g) were obtained from a certified hatchery (MARESA, Spain), acclimatized to laboratory conditions, and reared for 2 years in a recirculation water system to a final body weight of 700 ± 50 g. Water parameters were maintained as followed: O_2 saturation at 7.38 ± 0.01 mg/l, salinity at 35 ppt, temperature at 18°C, and 10 h dark: 14 h light photoperiod. Fish were daily fed a commercial diet (Sorgal, Portugal) and no clinical signs of disease and illness were observed.

European seabass were euthanized by an overdose of anesthetic (>1ml/l, 2-phenoxyethanol, Merck) and bled by collecting blood from the caudal vessels using a heparinized vacuum system and cut off the branchial arches. HKL were isolated and maintained following Secombes (42) with modifications. The head-kidney was aseptically removed and the tissue disrupted by passing through a 100 μl nylon mesh in 30 mL of Leibovitz L-15 medium (L-15, Gibco) supplemented with 2% fetal bovine serum (FBS, Gibco), 100 IU ml^{-1} penicillin and streptomycin (Gibco), and 30 U ml^{-1} heparin (Braun) (L-15 2% FBS). After centrifugation, a clear separation between leucocytes and erythrocytes was observed and the upper leucocyte layer was carefully collected and separated from the erythrocytes bottom layer and the resulting cell suspension was resuspended in fresh L-15 2% FBS and centrifuged at 600 × *g* at 4°C for 10 minutes. The collected leucocytes were washed two times at 600 × *g* at 4°C for 10 minutes and finally resuspended in L-15 medium with 0.1% FBS (L-15 0.1% FBS) and antibiotics. Leucocytes viability

was determined by the trypan blue exclusion method. Leucocytes were diluted four times in a 0.4% trypan blue solution and concentration adjusted to 1×10^7 viable cells ml^{-1} after counting in a hemocytometer. One hundred microliters of the leucocyte suspension were plated in 96-well plate for ATP, total antioxidants concentration (TAC), polyamines, nitric oxide (NO), and caspase 3-active assays. For gene expression, 500 µl of the leucocyte suspension was plated in 24-well plates.

Experimental Design

After primary cell culture isolation and plating, the leucocyte monolayer was maintained for 2 h in L-15 2% FBS for cell adhesion and subsequently washed with HBSS, removing non-adherent cells. Adherent cells, characterized mostly by the monocyte lineage (43) were then incubated with fresh L-15 10% FBS supplemented with methionine or tryptophan for 24 h at 18 °C and leucocyte viability was evaluated by the 3-(4,5-dimethylthiazol-2-yl)-2, 5-diphenyltetrazolium bromide (MTT) assay. Two supplementation levels of each AA were selected based in previous studies (16). Both AA were supplemented at 1 × or 2 × the basal concentration found in L-15 with the final concentration of L-methionine (M1x, 1mM or M2x, 1.5 mM) and L-tryptophan (T1x, 0.2 mM or T2x, 0.3 mM). As a control, L-15 10% FBS without AA addition was used (containing 0.5mM of L-methionine and 0.1 mM of L-tryptophan, Gibco).

Two trials, each comprising a total of six fish were performed (**Figure 1**). Cellular response (Trial 1) was assessed upon stimulation with *Phdp*UV (1×10^6 CFU ml^{-1} with an expected LPS concentration of 0.006 µg ml^{-1}), LPS*Phdp* (10 µg ml^{-1}), or the absence of a stimulus (Ø). Concentration of each stimulus was selected according to (16). Gene expression, ATP, and TAC were measured at the end of 4 and 24 h of stimulation since most innate immune mechanisms are activated upon acute stimulation. Polyamines production was evaluated in L-15, M1x, and M2x after 48 h of stimulation since methionine has a direct role in polyamine biosynthesis (19), but only in *Phdp*UV and Ø treatments due to technical limitations. Finally, NO production was evaluated at 72 and 96 h according to previous studies (16, 44). The apoptosis assays (Trial 2) consisted of evaluating caspase 3-active and gene expression in response to AIP56 protein (2 µg ml^{-1}) (45) or in Ø during a time-course study (i.e. 1, 3, and 6 h) with the cell culture media replaced by a fresh solution at each hour. Staurosporine (2.33 µg ml^{-1}, Sigma) was used in L-15 wells as a positive control for apoptosis (46).

All analyses were performed with triplicate analytic replicates in a total of six biological replicates.

MTT Assay

The leucocytes viability was assessed by the MTT reduction by the NAD(P)H-dependent cellular oxidoreductase enzymes produced under cell metabolic activity, reflecting the number of viable cells (47). After 24 h incubation at 18 °C in L-15 10% FBS supplemented with the desired AA, 20 µl of MTT (5 mg ml^{-1}) was added to each well and incubated for 4 h at 18 °C. After centrifugation at 110 × *g* for 5 min, the insoluble resultant formazan was dissolved in 100 µl

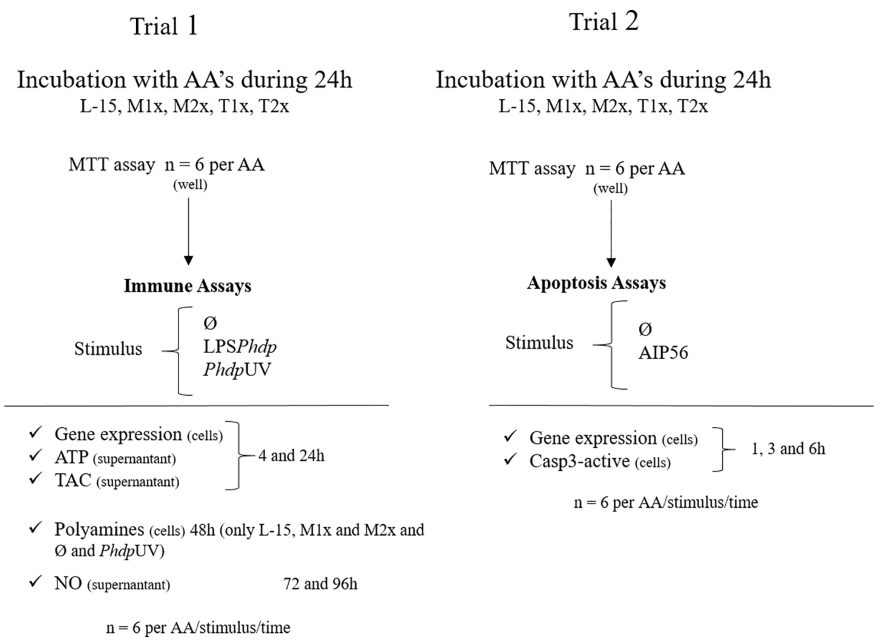

FIGURE 1 | Experimental design. L-15 (Leibowitz L-15 medium); M1x (Leibowitz L-15 medium supplemented with 1 mM of L-methionine); M2x (Leibowitz L-15 medium supplemented with 1.5 mM of L-methionine); T1x (Leibowitz L-15 medium supplemented 0.2 mM of L-tryptophan); T2x (Leibowitz L-15 medium supplemented 0.3 mM of L-tryptophan); MTT (3-(4,5-dimethylthiazol-2-yl)-2, 5-diphenyltetrazolium bromide assay); Ø (unstimulated cells); LPS*Phdp* (Lipopolysaccharides extracted from *Phdp*); *Phdp*UV (UV-inactivated *Phdp*); ATP (Adenosine triphosphate); TAC (total antioxidant capacity); NO (nitric oxide).

of dimethyl sulfoxide (DMSO) and the absorbance read at 550 nm (Synergy HT, Biotek). A total of twelve biological replicates were evaluated (6 biological replicates per trial).

Immune Assays

ATP Assay

ATP production by the leucocytes monolayers incubated with LPS*Phdp*, *Phdp*UV, or in the absence of stimuli for 4 and 24 h with each AA treatment was measured with an ATP Colorimetric Assay Kit (Sigma). From each well, 50 µl of the cell supernatant was transferred to a new 96-well plate and the protocol performed according to the manufacture's indications. The absorbance was read at 570 nm (Synergy HT, Biotek) and ATP concentration was calculated according to a standard ATP curve after subtraction of background absorbance values.

TAC Assay

The total antioxidants concentration (TAC), such us oxygen species and reactive nitrogen species, was determined in the supernatant of cells incubated with LPS*Phdp*, *Phdp*UV, or Ø during 4 and 24 h and previously incubated for 24 h with the different AA treatments. Cell supernatants were collected, diluted in Protein Mask in a 1:1 ratio according to manufacturer's indications (The Total Antioxidant Capacity Kit, Sigma), and 100 µl of the mixture was added to a 96-well plate and the protocol performed. The absorbance was read at 570 nm (Synergy HT, Biotek). Background absorbance values were subtracted and TAC concentration was calculated from a standard curve.

Polyamines Assay

The Total Polyamine Assay Kit (BioVision) was used for fluorometric assessment of polyamine content in cells either stimulated with *Phdp*UV or unstimulated for 48 h after incubation with L-15, M1x, or M2x for 24 h. According to the manufacturer's indications, a sample background wells fluorescence (Ex/Em= 535/587 nm) was subtracted to the standards and reaction wells and the concentration determined according to the standard curve previously prepared.

NO Assay

NO production was measured in the supernatant collected from leucocyte primary cell cultures formerly incubated with the different AA treatments for 24 h and stimulated with *Phdp*LPS, *Phdp*UV, or in the absence of stimuli for 72 or 96 h. At each time, 50 µl of supernatant was transferred to a new 96-well plate and total nitrite and nitrate concentrations in the sample were assessed using the Nitrite/Nitrate colorimetric method kit (Roche). Nitrite concentration was calculated by comparison with a sodium nitrite standard curve. Since nitrite and nitrate are endogenously produced as oxidative metabolites of the messenger molecule NO, these compounds are considered as indicative of NO production.

Apoptosis Assays

After incubation for 24 h with the different AA treatments, the cell culture media was replaced by a fresh solution without stimuli or containing AIP56. The medium was renewed at each hourly, for 6 h (45), and cells collected for caspase 3-active assay or for gene expression after 1, 3 and 6 hours. The inability of the AA, at the highest supplementation level, to inhibit AIP56 activity on the cleavage of the leucocytes p65 subunit was tested by SDS-PAGE and Western blotting.

SDS-PAGE and Western Blotting

Leucocytes from four fish were incubated with L-15, M2x or T2x during 24h and afterwards incubated the with Ø or 2 µg ml^{-1} of AIP56 for 2 h. Supernatant was removed and cells (5× 10^6 cells) were lysed and collected by adding 40 µl SDS-PAGE sample buffer (50mMTris-HCl [pH 8.8], 2% SDS, 0.05% bromophenol blue, 10% glycerol, 2mM EDTA, and 100 mM DTT) (48). Samples were then boiled for 5 min and 20 µl (2.5× 10^6 cells) were loaded For Western blotting, the proteins were transferred onto nitrocellulose membranes. The efficiency of transfer and the protein loading on the membranes was controlled by staining with Ponceau S. The membranes were blocked for 1 h at room temperature (RT) with 5% skim milk in Tris-buffered saline (TBS) containing 0.1% Tween 20 (T-TBS) followed by incubation for 1 h at RT with the anti-sea bass NF- κB p65 rabbit serum diluted in blocking buffer (1:500) (49). Immunoreactive bands were detected using alkaline phosphatase-conjugated secondary antibodies (1:0000) and nitrobluetetrazolium–5-bromo-4-chloro-3-indolylphosphate (NBT/BCIP) (Promega).

Caspase 3-Active

The caspase 3-active assay was performed for each AA treatment in cells stimulated for 1, 3, and 6 h with AIP56. Cells without stimuli were used as control. The assay kit (Abcam) quantifies the cleavage of a substrate by caspase 3 or related caspases. The fluorescence (Ex/Em= 400/505 nm) was read and the fold-increase in caspase 3 activity was determined by comparing with the level determined in unstimulated cells cultured with L-15.

Gene Expression

Total RNA was extracted from cells collected for innate immune response and apoptosis as following. After supernatant collection, wells were washed with HBSS and 50 µl of NZYol (NZYTech) reagent was added to each well, RNA was isolated following the manufacturer's indications (NZY Total RNA Isolation kit) and resuspended in free nuclease water (NZYTech). RNA was quantified using the DS-11 Spectrophotometer (DeNovix) and samples were treated with DNase using RQ1 RNase-free DNase kit (Promega) following the manufacturer's indications. First-strand cDNA was synthesized with NZY First-Strand cDNA Synthesis Kit (NZYTech). Quantitative PCR assays and primer design (**Table 1**) were performed as described by Machado et al. (24). The expression of the target gene was normalized using the average

TABLE 1 | Forward and reverse primers for real-time PCR.

Acronym	Gene	Gene Bank ID	Eff[1]	AT[2]	Product lenght[3]	Forward primer sequence (5'-3')	Reverse primer sequence (5´-3´)	Trial
ef1α	Elongation factor 1α	AJ866727.1	96.45	57	144	AACTTCAACGCCCAGGTCAT	CTTCTTGCCAGAACGACGGT	Housekeeping
40s	40S ribosomal protein	HE978789.1	93	55	79	TGATTGTGACAGACCCTCGTG	CACAGAGCAATGGTGGGGAT	Housekeeping
il1β	Interleukin 1 β	AJ311925	96.70	57	105	AGCGACATGGTGCGATTTCT	CTCCTCTGCTGTGCTGATGT	Both trials
mtor	Mechanistic target of rapamycin	DLAgn_00134190	127.25	55	848	CAGAACCAAGGACGTGACGA	TGGTAGTAGAGGTCCCAGGC	Both trials
il8	Interleukin 8	AM490063.1	102.87	55	140	CGCTGCATCCAAACAGAGAGCAAAC	TCGGGGTCCAGGCAAACCTCTT	Both trials
tnfα	Tumor necrosis factor α	DQ070246.1	108.81	55	112	AGCCACAGGATCTGGAGCTA	GTCCGCTTCTGTAGCTGTCC	Both trials
amd1	Adenosylmethionine Decarboxylase 1	KM225770	118.64	57	63	CTGACGGAACTTACTGGACCATC	CGAAGCTGACGTAGGAGAACTC	Both trials
sms	Spermine synthase	DLAgn_00042290	111.71	55	132	GCACCTTTGGTTTCTCCTGA	AACTCAGTCCCACAGGGTTG	Both trials
dnmt1	DNA methyltransferase 1	DLAgn_00191600	84.37	60	193	ATGGCTTCACAAATGGCTCT	GATGGCTGTTTCCCACTGTT	Both trials
dnmt3a	DNA methyltransferase 3a	DLAgn_00025050	79.08	60	126	AAGTGGAAGATGGAGGCAGA	AGGCGATGGGTGTTTGATTA	Both trials
dnmt3b	DNA methyltransferase 3b	DLAgn_00125770	79.08	60	172	AAGCCCAAAGAAGGAGAGGA	GCAGGTTTCCCCAGAAGTATC	Both trials
ido2	Indoleamine -dioxygenase 2	DLAgn_00014730	108.20	55	74	TGAAGGTGTGAGCAATGAGC	CAAAGCACTGAATGGCTGAA	Both trials
afmid	Arylformamidase-like	DLAgn_00177950	128.26	55	112	CGTTTCCACCTGTTTGACCT	CCTAGCCTGCTGAAGGACTG	Both trials
il6	Interleukin 6	AM490062.1	134.62	55	81	AGGCACAGAGAACACGTCAAA	AAAAGGGTCAGGGCTGTCG	Immune
il10	Interleukin 10	AM268529.1	116.00	55	164	ACCCCGTTCGCTTGCCA	CATCTGGTGACATCACTC	Immune
il13r	Interleukin 13 receptor	KT809426.1	100.6183	55	118	AGGAACCGATGGAGTGAGTG	CCATAGCCATACCGCTTCAT	Immune
cox2	Cyclooxygenase 2	AJ630649.1	81.30	61	160	CATTCTTTGCCCAGCACTTCACC	AGCTTGCCATCCTTGAAGAGTC	Immune
infγ	Interferon γ	FQ310507.3	118.3801	55	194	GTACAGACAGGCGTCCAAAGCATCA	CAAACAGGGCAGCCGTCTCATCAA	Immune
odc	Ornithine decarboxylase	KM225771	111.71	60	69	GGGCTGTAGTTATGACACTGGCATCC	GCTGAATCTCCATCTTGCTTGCACAGT	Immune
arg2	Arginase 2	KM225768.1	90.25	57	145	TTGGCGACCTCAACTTCCAC	CCCAGCATGACAAGGGTGTG	Immune
sod	Superoxide dismutase	CX660893.1	103.0254	55	71	GGAGAGTGATTCAGCCCCTG	GGAAACCATGCTCACCAGGA	Immune
nf-κb	Nuclear Factor Kappa B	DLAgn_00239840	113.28	55	136	GCTGCGAGAAGAGAGGAAGA	GGTGAACTTTAACCGGACGA	Apoptosis
p65	Nuclear factor NF-kappa-B p65 subunit	DLAgn_00141590	97.63	62	204	GTGTGGTTTGTGTTGCCTTG	CCCTGAACCCATCTCGACTA	Apoptosis
casp3	Caspase 3	DQ345773.1	130.10	55	235	CTGATTTGGATCCAGGCATT	CGGTCGTAGTGTTCCTCCAT	Apoptosis
casp8	Caspase 8	DLAgn_00001990	107.71	60	140	CCGATGTTCTGGTAGCCATT	GAGGATGGTGGTCATGTCGT	Apoptosis
casp9	Caspase 9	DLAgn_00133660	103.73	60	127	TCTTGAGGAAAATGCGGTTA	TTTGCGGAGGAAGTTAAAGG	Apoptosis
stat3	Signal transducer/activator of transcription 3	DLAgn_00192560	110.68	55	275	GACATCAGCGGAAAGACCCA	GGGGTGACGCAGATGAACTT	Apoptosis

[1]*The efficiency of PCR reactions was calculated from serial dilutions of tissue RT reactions in the validation procedure.*

[2]*Annealing temperature (°C).*

[3]*Amplicon (bp).*

expression of European seabass *elongation factor 1α* (ef1α) and the *40s ribosomal protein* (40s). The target genes were selected according to the goal of each trial, direct immune mechanisms or apoptosis signaling. PCR efficiency and relative expression ratio of target gene in experimental groups versus those in control groups were calculated according Pfaffl method (50).

Statistical Analysis

All results are expressed as mean ± standard deviation (mean ± SD). Data were analyzed for normality (Shapiro-Wilk's W test) and homogeneity of variance (Levene's test) and, when necessary, transformed before being treated statistically. Data were analyzed by one-way (MTT assay) or multifactorial ANOVA, with AA, time, and stimulus as factors, and followed by Tukey post-hoc test to identify differences between the experimental treatments. All statistical analyses were performed using the computer package STATISTICA 12 for WINDOWS. The level of significance used was $p \leq 0.05$ for all statistical tests.

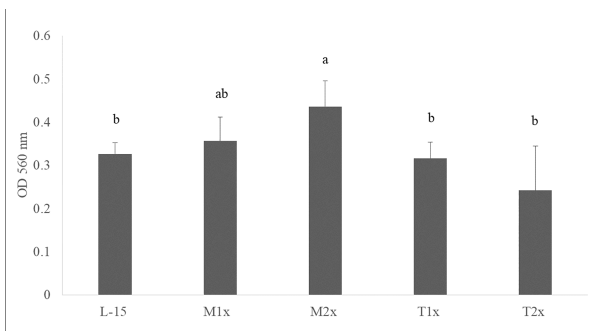

FIGURE 2 | Cell viability after 24 h incubation with the different AA treatments. Values are presented as means ± SD (n = 12). P-values from one-way ANOVA (*p-value* = 0.001). Tukey *post hoc* test was used to identify differences in the experimental treatments. Different letters indicate differences among AA treatments.

RESULTS

MTT Assay

After 24 h incubation of HKL with the different AA concentrations, the cell viability of the leucocytes cultured with M2x was increased compared to the control (L-15) as indicated by the different lower case letters in **Figure 2**. Tryptophan treatments (T1x and T2x) failed to alter HKL viability compared do L-15.

Immune Response

ATP Production

All AA treatments presented higher ATP concentrations in response to *Phdp*UV compared to Ø and LPS*Phdp* after 4 h while at 24 h of incubation, only L-15 cells displayed higher ATP when incubated with *Phdp*UV than those incubated with LPS*Phdp* (capital letters in **Figure 3**). Methionine-treated cells (M1x and M2x) failed to alter ATP production compared to the control medium (L-15). Nevertheless, and as previously described ATP concentration was significantly increased in both methionine doses (M1x and M2x) in response to *Phdp*UV compared to the remaining stimulus at 4 h, with this production significantly decreasing at 24 h for the M1x. Similarly to methionine treatments, both T1x and T2x failed to increase ATP production in response to LPS*Phdp* compared to Ø whereas an increase of its production in response to *Phdp*UV at 4 h was observed. In fact, the higher tryptophan dose (T2x) showed the same pattern (increase of ATP production in response to *Phdp*UV compared to Ø) after 24 h of incubation. Finally, as pointed by the different lower case letters, T1x and T2x incubated for 4 h with *Phdp*UV presented a lower ATP concentration than cell culture in L-15 at the same time and stimuli.

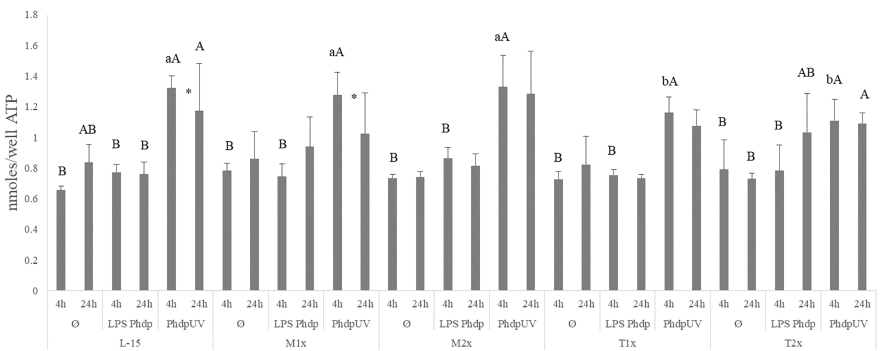

FIGURE 3 | Extracellular ATP concentration in the supernatant of HKL subjected to the experimental treatments. Values are presented as means ± SD (n = 6). P-values from multifactorial ANOVA (*p-value* < 0.001). Tukey *post hoc* test was used to identify differences between the experimental treatments. Different low case letters indicate differences among AA treatments at the same time and stimuli, while capital letters denote statistically significant differences between stimuli, within the same AA treatment, at the same time. An asterisk indicates differences between times with the same stimulus.

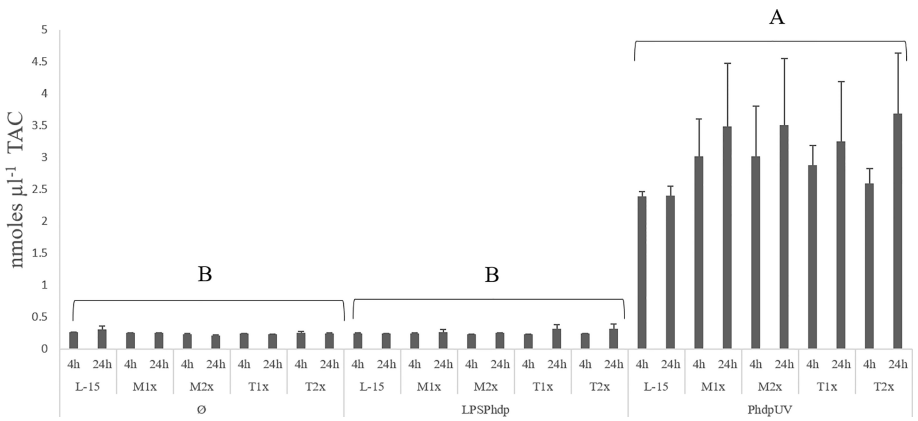

FIGURE 4 | Extracellular TAC (total antioxidants concentration) in the supernatant of HKL subjected to the experimental treatments. Values are presented as means ± SD (n = 6). P-values from multifactorial ANOVA (*p-value* < 0.001). Tukey *post hoc* test was used to identify differences in the experimental treatments. Capital letters denote statistically significant differences between stimuli, within the same AA treatment, at the same time.

TAC Concentration

Results on TAC, presented in the **Figure 4**, were organized by stimulus contrary to the previous figure in order to properly point to the observed difference. A single significant increase in the total antioxidants was observed in the supernatant of HKL subjected to *Phdp*UV, regardless of exposure time and AA treatment, compared to the remaining stimulus.

Polyamines Concentration

Since methionine has a recognized role in the polyamine biosynthesis pathway and no direct effect of tryptophan is expected, the assay was only performed in cells incubated with L-15, M1x, and M2x after 48 h stimulation with *Phdp*UV or unstimulated (Ø) (**Figure 5**). In the absence of an immune stimulus (Ø) cells cultured with M2x showed the ability to increased polyamine production compared to L-15, while M1x failed to do so (lower case letters). Besides that, upon immune stimulation by *Phdp*UV incubation for 48 h, both methionine doses, M1x and M2x, showed a higher polyamine production than those incubated in the standard medium, L-15.

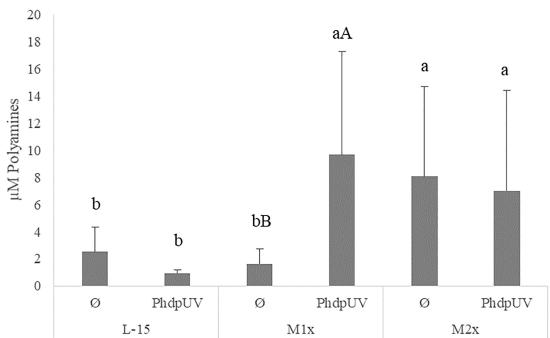

FIGURE 5 | Extracellular polyamines concentration in the supernatant of HKL subjected to the experimental treatments. Values are presented as means ± SD (n = 6). P-values from multifactorial ANOVA (*p-value* = 0.048). Tukey *post hoc* test was used to identify differences in the experimental treatments. Different low case letters indicate differences among AA treatments at the same stimuli, while capital letters denote statistically significant differences between stimuli within the same AA treatment.

NO Production

Nitric oxide production is presented in **Figure 6**. The NO production in response to the different stimuli was modulated in both methionine doses. Both methionine treatments, M1x and M2x, presented higher NO production in response to *Phdp*UV than L-15 treatment, regardless of incubation time, while tryptophan failed to show any alterations compared to L-15 (lower case letters). In fact, in response to *Phdp*UV and regardless time of exposure, M1x enhanced NO concentration compared to Ø, while M2x-treated cells and stimulated with *Phdp*UV showed increased NO production compared to both Ø and LPS*Phdp* (capital letters).

Gene Expression

Gene expression results are presented in **Supplementary Table 1**. In response to stimuli, the mRNA transcripts of *il1β* and *dnmt1* were up-regulated in HKL exposed to *Phdp*UV compared to the remaining stimulus, regardless of AA treatment and time

When looking to the methionine treatments, the highest medium supplementation (M2x) led to an increase of the overall expression of *dnmt1* when compared to the reaming AA treatments and disregarding stimuli or time of exposure (**Figure 7A**). Also, in response to *Phdp*UV, M2x treated-cells presented a significant up-regulation of *tnfα* (**Figure 7B**) and *odc* (**Figure 7C**) compared to both L-15 and M1x (lower case letters). In fact, this cells (M2x-cultured cells exposed to *Phdp*UV, regardless time) presented a significantly higher expression of *tnfα* and *odc* compared to LPS*Phdp* or Ø, respectively (capital letters). Methionine surplus (M1x and M2x) also increased *sms* (**Figure 7D**) mRNA expression when stimulated with LPS*Phdp*,

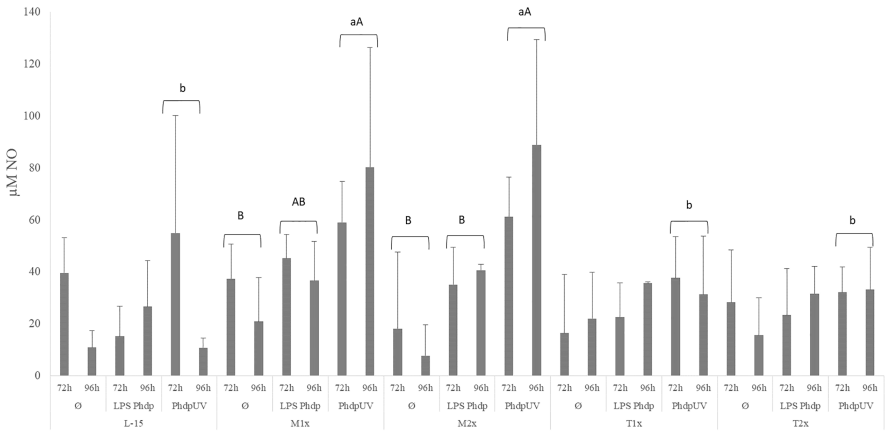

FIGURE 6 | Extracellular nitric oxide concentration in the supernatant of HKL subjected to the experimental treatments. Values are presented as means ± SD (n = 6). P-values from multifactorial ANOVA (*p-value* = 0.009). Tukey *post hoc* test was used to identify differences in the experimental treatments. Different low case letters indicate differences among AA treatments while capital letters denote differences between stimuli.

compared to L-15. Also, the same treatments (M1x and M2x LPS*Phdp*) presented an improved expression compared to both unstimulated (Ø) and *Phdp*UV (capital letters).

Regarding tryptophan medium supplementation, HKL showed an up-regulation of the anti-inflammatory gene *il10* (**Figure 7E**) with the higher tested dose (T2x) presenting increased expression compared to M1x and M2x. However, as perceived by the different capital letters in **Figure 7F**, the highest tryptophan dose, T2x, up-regulated *arg2* transcripts in response to *Phdp*UV compared to the remaining AA treatments, and its unstimulated and LPS*Phdp* counterparts (capital letters). Additionally, T2x-treated cells showed an increase in time of *ido2* (**Figure 7G**) expression in response to *Phdp*UV with a significantly higher expression compared to all the remaining AA treatments (lower case letters) and its equivalents stimulated with LPS*Phdp* and Ø after a 24 h incubation (capital letters).

Apoptotic Response

Amino Acids on AIP56 Cleaving Activity of the p65 Subunit

A total of four fish were used to test the activity of the AIP56 in the presence of the highest AA treatments by the evaluation of the p65 cleavage, as presented in **Figure 8**. Similarly to L-15, both M2x and T2x did not hampered AIP56 activity on p65 of HKL as seen by the lower detection in leucocytes incubated with the toxin. **Figure 8** presents the results of two biological replicate.

Caspase-3 Active

A fold-change of caspase 3 activity relative to the unstimulated cells cultured with L-15 at 1 h was performed and presented in **Figure 9**. The activity of caspase 3 was evaluated in cells cultured with the different AA concentrations after 1, 3, and 6 h of stimulation with AIP56 or in the absence of the stimulus. No statistical modulation of caspase 3-activity was observed by methionine supplementation compared to L-15 and, despite the clear tendency, the expected increase of caspase 3- activity in response to AIP56 was not observed when compared to Ø, which could be explained by the relative high activity in methionine unstimulated (Ø) treatments (**Figure 8**). In the case of tryptophan, higher activity of caspase 3 was observed in HKL incubated with both supplementation levels, T1x and T2x, relative to L-15 and regardless of time or stimulus (lower case letters). Moreover, indicated by the capital letters, cells cultured in L-15, T1x, and T2x presented an increase of caspase 3- activity in response to AIP56.

Gene Expression

Due to the amount of data resulted from the gene expression, all data regarding is presented in **Supplementary table 2** including the main effects of the tested factors and the possible interactions.

In response AIP56 stimuli, was observed a down-regulation of the *nf-κβ* regardless of AA treatment and time, while increasing the expression of *il1β* at 1h of exposure, regardless of AA (**Supplementary Table S2**). Additionally, L-15- incubated cells showed increased *casp3* expression at 3 h in response to AIP56 (**Figure 10A**), compared to Ø at the same time. L-15 cells showed increased *mtor*, *amd1*, and *dnmt3b* expression at 3 h compared to 1 and 6 h (**Supplementary Table S2**).

A general increase in the expression of pro-inflammatory genes, as *il1β*, *nf-κb*, and *il8* was found in response to methionine medium supplementation. Irrespective of stimuli, the expression of the pro-inflammatory signals *nf-κb* (**Figure 10B**) and *il8* (**Figure 10C**) *was* higher in M1x and M2x after 3 h, respectively, compared to L-15 and with both genes presenting a peak of expression at 3 h. M2x also showed higher *amd1* at 3 h, regardless of stimuli, and *mtor* was also found higher in M1x-treated cells at 3 h (**Figure 10D**). In response to AIP56, both methionine supplementation levels (M1x and M2x) allowed HKL to increase *il1β* (**Figure 10E**) transcripts compared to L-15 while decreasing the expression of *casp3* at 3 h (**Figure 10A**).

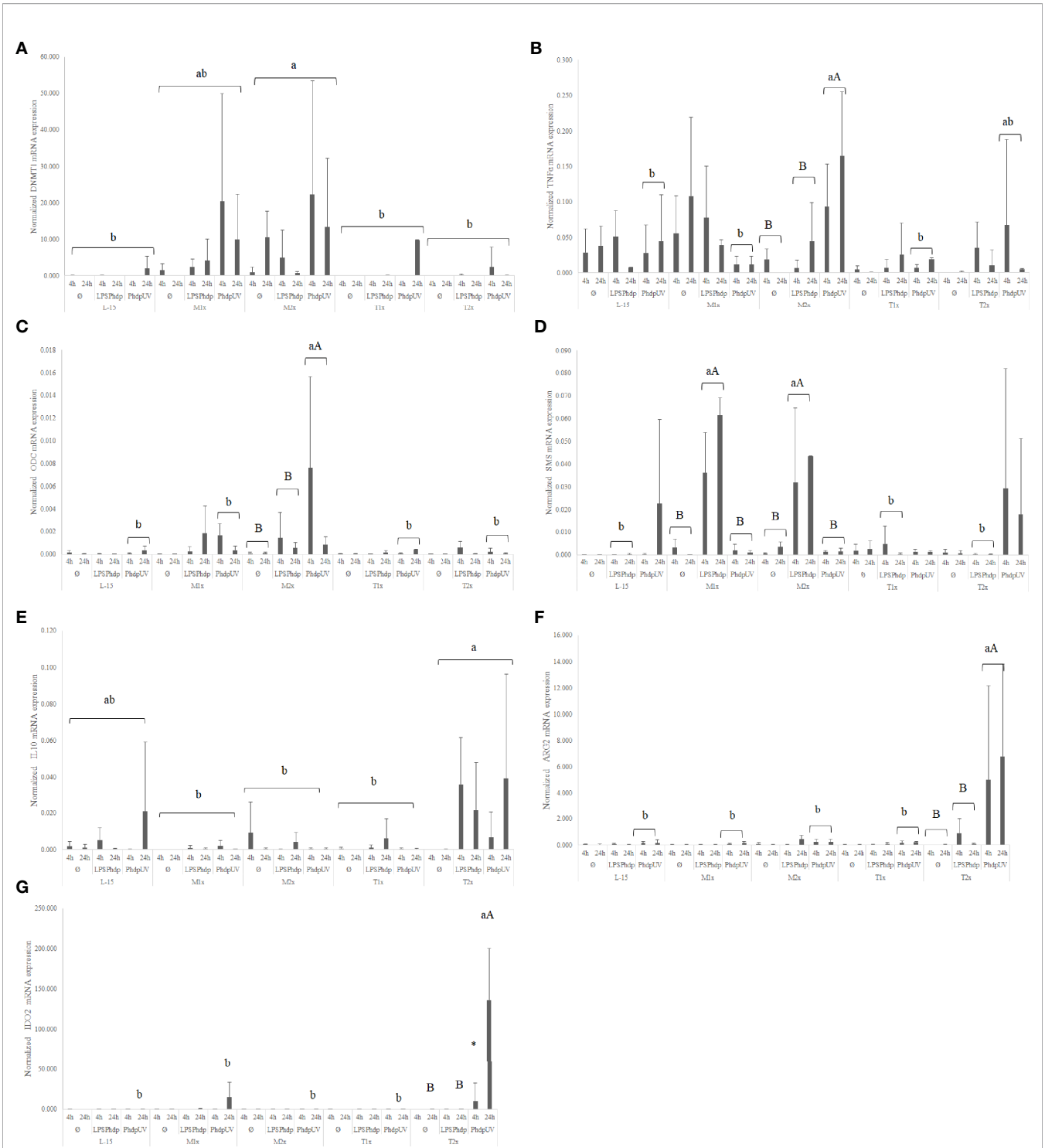

FIGURE 7 | Quantitative expression of **(A)** DNA methyltransferase 1 (*p-value = 0.003*), **(B)** tumor necrosis factor α (*p-value = 0.001*), **(C)** ornithine decarboxylase (*p-value = 0.028*), **(D)** spermine synthase (*p-value <0.*001), **(E)** interleukin 10 (*p-value= 0.037*), **(F)** arginase 2 (*p-value < 0.001*) and **(G)** indoleamine dioxygenase 2 (*p-value < 0.001*) in HKL subjected to the experimental treatments. Values are presented as means ± SD (n = 6). Multifactorial ANOVA was followed by Tukey *post hoc* test was used to identify differences in the experimental treatments. Different low case letters indicate differences among AA treatments while capital letters denote statistically significant differences between stimuli. An asterisk indicates differences between times.

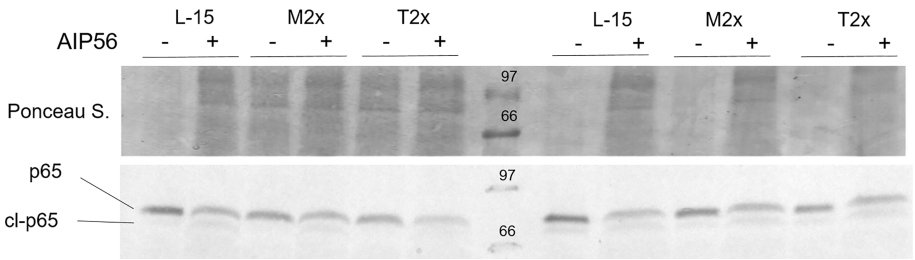

FIGURE 8 | Example of a western blot of p65 cleavage in HKL lysates subjected to the experimental treatments and incubated for 2 h with Ø (-) or 2 μg ml^{-1} of AIP56 (+).

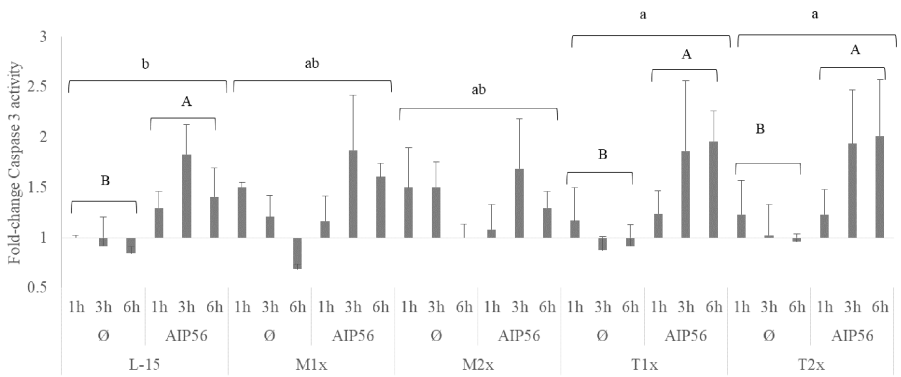

FIGURE 9 | Caspase 3 activity of HKL subjected to the experimental treatments. Values are presented as means ± SD (n = 6). P-values from multifactorial ANOVA (*p- value* < 0.001). Tukey *post hoc* test was used to identify differences in the experimental treatments. Different low case letters indicate differences among AA treatments while capital letters denote statistically significant differences between stimuli for the same AA treatment.

HKL incubated in a rich-tryptophan medium showed modulation of key apoptotic, catabolism, and nutrient sensing-related genes. Regardless of stimuli or incubation time, the expression of *p65* (**Figure 10F**) and *afmid* (**Figure 10G**) were down-regulated in both tryptophan levels and T1x, respectively, relative to L-15, while *dnmt3b* (**Figure 10H**) expression was down-regulated specifically at 3 h. Also, unstimulated (Ø) HKL cultured with T2x showed lower *sms* mRNA expression than HKL cultured with T1x and L-15 (**Supplementary Table S2**). Moreover, T2x showed decreased *amd1* expression at 3 h and increased *mtor* expression at 6 h, which presented a peak of expression at that time (**Supplementary Table S2**). In response to AIP56, *casp3* (**Figure 10A**) *transcripts* were down-regulated at 3 h in T1x and T2x compared to L-15, while *casp8* (**Figure 10I**), was found increased in T1x at 6 h incubation with AIP56 compared to all treatments.

DISCUSSION

The potential of methionine and tryptophan supplementation in the response of HKL upon immune stimulation with LPS-extracted and UV-inactivated *Phdp* was studied *in vitro*. Moreover, the HKL apoptosis instigated by AIP56 toxin was evaluated. The following discussion was assembled in order to individually debate each AA effect on the direct immune mechanism in response to the stimulus, on the AA-related pathways with close association with the innate mechanisms, and apoptotic signals.

The present study showed that, regardless of AA treatment, cell immune responses were not triggered following exposure to LPS*Phdp*. Most changes were observed in response to *Phdp*UV challenge, both at functional and transcriptional levels. Indeed, cultured cells exposed to LPS*Phdp* exhibited only one difference compared to the unstimulated cells in an AA surplus scenario (discussed later) while being generally surpassed by the *Phdp*UV effect. In response to *Phdp*UV, HKL increased *il1β* and *dnmt1* expressions, regardless AA treatment. *IL1β* is the key mediator of the inflammatory response produced by activated macrophages (51) and *DNMT1* is an enzyme that catalyzes the transfer of methyl groups derived from SAM to specific CpG structures of the DNA regulating gene expression (18). Together with *il1β* and *dnmt1* mRNA expressions, an increase of extracellular ATP and antioxidant concentrations (TAC) was observed in the HKL cultured in standard L-15 in response to *Phdp*UV comparatively to LPS*Phdp*. Increasing levels of extracellular

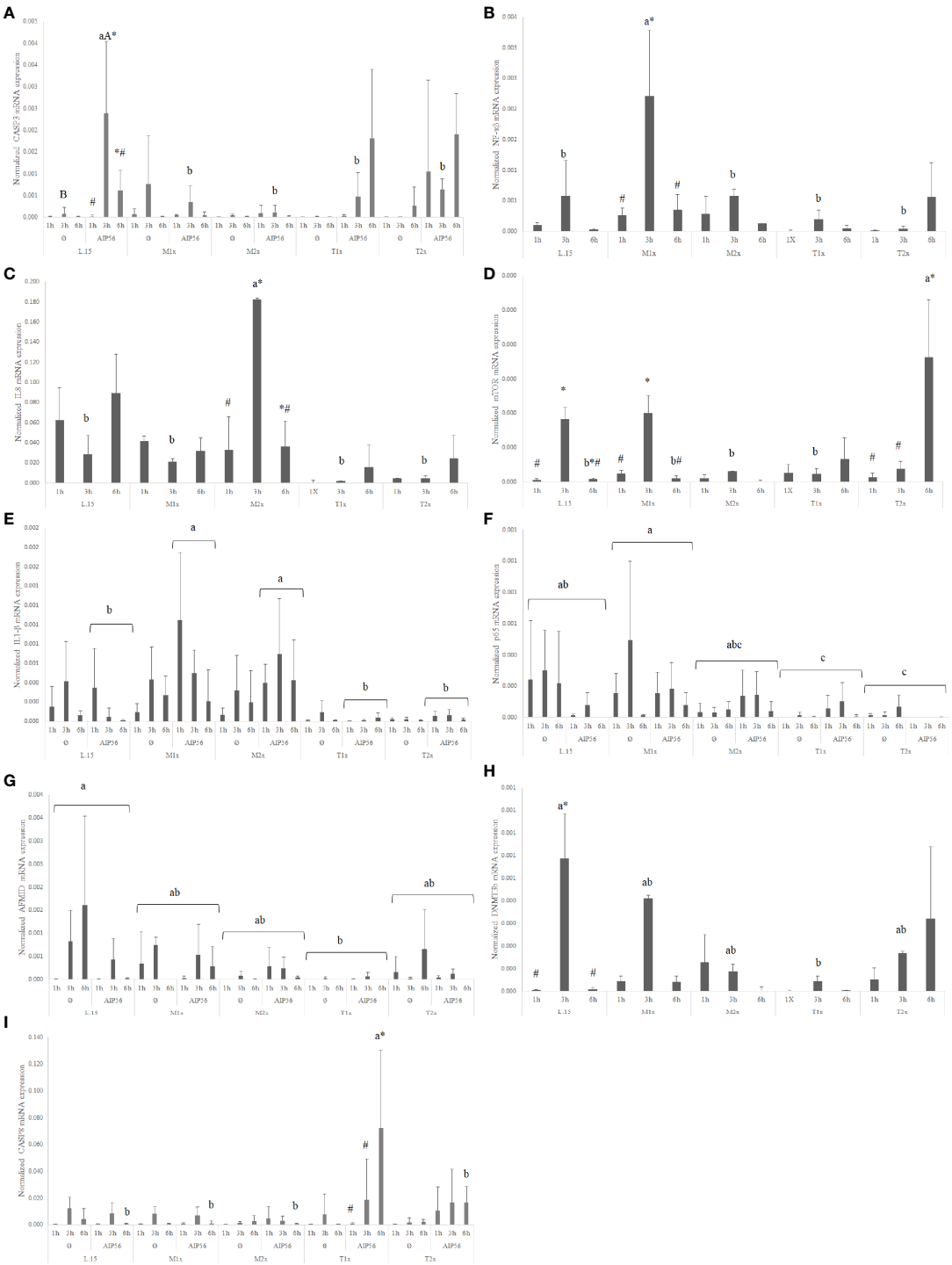

FIGURE 10 | Quantitative expression of **(A)** caspase 3 (*p-value = 0.011*), **(B)** nuclear factor kappa B (*p-value = 0.012*), **(C)** interleukin 8 (*p-value 0.015*), **(D)** mechanistic target of rapamycin (*p-value < 0.001*), **(E)** interleukin 1 β (*p-value = 0.032*), **(F)** transcription factor p65 (*p-value < 0.011*), **(G)** arylformamidase (*p-value < 0.025*), **(H)** DNA (cytosine-5-)-methyltransferase 3 beta (*p-value < 0.026*) and **(I)** caspase 8 (*p-value < 0.011*), in HKL subjected to the experimental treatments. Values are presented as means ± SD (n = 6). Multifactorial ANOVA was followed by Tukey *post hoc* test was used to identify differences in the experimental treatments. Different low case letters indicate differences among AA treatments while capital letters denote statistically significant differences between stimuli. Symbols indicate differences between times.

ATP and antioxidant production are expected during inflammatory conditions (52, 53) since ATP acts as an inflammatory mediator during inflammation in macrophages (53). Also, antioxidants production are increased in response to inflammatory stimuli as a direct response to the enhanced production and release of reactive oxygen species (52). Likewise, the absence of pro-inflammatory indicators increment in response to LPS*Phdp* compared to the *Phdp*UV may point to other bacterial components rather than LPS that may be responsible for the observed response. Actually, the expected level of LPS within the *Phdp*UV inoculum at a concentration of 1×10^6 CFU ml^{-1} was 0.006 μg ml^{-1}, a value significantly lower than the 10 μg ml^{-1} LPS inoculum in LPS*Phdp*. Additionally, LPS recognition mechanisms by most teleost fish are still unknown, and there seems to be a lack of membrane receptor (i.e. Toll-like receptor) able to recognize LPS and induce inflammation (54). Indeed, Bi et al. (55) proposed the use of other strategies, such as outer membrane vesicles produced by Gram-negative bacteria, to serve as vehicle for LPS introduction to the intracellular host environment. These authors observed that, similarly to mammals, fish cytoplasmic NOD1 receptor is able to recognize LPS activating the NF- κB signal pathway and concomitant expression of pro-inflammatory signals. Hence, the limited effects observed in the present work upon purified LPS cell-stimulation could be explained by the lack of an intermediary vehicle to deliver LPS into the cell cytosol (56).

AIP56 is an exotoxin secreted by virulent *Phdp* and induces apoptotic macrophages death (57), impairing the host's phagocytic capacity. Moreover, NF-κB, a key transcriptional factor in the initiation of inflammation (58), is the central target of cleavage by AIP56 (49). In the present work, the effectiveness of the toxin regardless AA treatment was confirmed by Western blot that displayed AIP56 ability to cleave the NF- κB- p65 subunit, together with a significant reduction of *nf-κb* expression.

Methionine

In the present study, cultured cell viability was improved after 24 h incubation with a medium containing two times more methionine than the L-15 medium. The role of methionine in polyamine biosynthesis (19) has been proven to enhance European seabass leucocyte proliferation and response to infection *in vivo* (11, 14). Nonetheless, since proliferation and differentiation capacity of the present HKL cultured cells is very limited or even absent, increased viability strictly point to a potential improvement of cell fitness. A noteworthy finding is that both methionine supplementation levels led to an increase of polyamines cellular content after 48 h incubation period in response to *Phdp*UV. Moreover, the highest methionine supplementation level (i.e. M2x) presented increased polyamine content even in the absence of stimulus, together with the up-regulation of *dnmt1*, an enzyme that has a key role in the regulation of gene expression (18). In fact, recent *in vivo* study performed in European seabass juveniles (14) point to methionine surplus ability to increase the concentration of circulating leucocytes and neutrophils after 15 days of feeding. This supports the methionine-availability aptitude to modulate both aminopropylation (18) and methylation pathways (19) in the absence of immune stimuli.

Nevertheless, in response to an immune challenge, as LPS*Phdp*, both methionine supplementation levels improved *sms* mRNA expression. Spermine synthase, coded by *sms*, is an enzyme responsible for the conversion of polyamine spermidine into spermine. Moreover, when the immune insult was *Phdp*UV, HKL cultured in methionine-rich medium (M2x) were able to increase *odc* expression. Ornithine decarboxylase, coded by *odc*, is responsible for decarboxylation of ornithine to putrescine in the polyamine pathway also in macrophages (59). Also, an increase of tumor necrosis factor, *tnfα*, was observed. TNFα presents critical cell functions in cell proliferation, survival, differentiation, and apoptosis, with macrophages as major producers (60). It is then hypothesized that, together with an improvement of immune functions, modulation of methionine-related pathways, more precisely the aminopropylation and methylation routes, were stimulated. This agrees with previous *in vivo* studies that demonstrated an improvement of cellular immune status and immune response following an inflammatory insult, with modulation of the methionine-related polyamine biosynthesis pathway (11, 14). Moreover, both methionine-supplementation levels led to an improvement of NO production in response to inactivated bacteria (*Phdp*UV) compared to the control medium. Also, M1x and M2x were the only treatments that increased NO production in response to both unstimulated and LPS*Phdp* groups. As previously observed by Azeredo et al. (16) in response to UV-inactivated *Vibrio anguillarum*, the increased NO production in response to *Phdp*UV could be related to methionine ability to indirectly modulate respiratory burst mechanisms. As cysteine precursor, and consequently precursor of the free radical scavenger glutathione, methionine could have an important role in redox potential modulation (9).

When the apoptotic mechanisms were induced by the bacterial exotoxin AIP56 (57), methionine supplementation led to a down-regulation of *casp3* compared to the control after 3 h of stimulus, in spite of overall high caspase 3- activity (non-significant). Despite that, the decreased expression of *casp3* was accompanied by the higher expression of *nf-κb* in M1x-cultured cells at 3 h, regardless of stimulus. Caspase 3 is an apoptotic executioner caspase, triggered by the resulting chain reaction of the formerly activated initiator caspases (e.g. caspases 8 and 9) (61). Also, as previously discussed, NF-κB cleavage by AIP56 action (49) and may impair key inflammatory mechanisms such as the transcription of DNA and cytokine production (58), leucocyte recruitment, and cell survival (62). Knowing that *in vitro* methionine deprivation induces apoptosis (63, 64), it was considered that by the improvement of overall cell fitness, sustained by the increase of cell viability, polyamine content, NO production and increased expression of TNFα as well as methionine metabolism-related genes in response to and

immune stimuli (LPS*Phdp* or *Phdp*UV), methionine supplementation may have contributed to the decrease of apoptotic signals, possibly alleviating AIP56-induced apoptosis signals. In fact, the expression of the cytokine IL1β, a pro-inflammatory cytokine induced by the NF-κB (39), was found increased in response to AIP56, showing signs of higher activity of the transcription factor.

Overall, present results point to an improvement of HKL immune response by methionine medium supplementation, mostly at the highest supplementation level (i.e. 1.5 mM). It is then proposed that the effects observed in recent *in vivo* works, where dietary methionine supplementation was able to enhance European seabass immune status and inflammatory machinery (11, 12, 65), rely on the amelioration of the pathways related to methionine catabolism, with a strict relationship with the leucocyte response, as the aminopropylation (18) and methylation pathways (19). Finally, the overall improved cell status in the methionine-supplemented medium seems to be in accordance with the protection against the apoptotic agent AIP56, and could be essential for the improvement of disease resistance against *Phdp*, as previously observed by Machado et al. (14).

Tryptophan

Despite the tendency to reduce, the culture-medium supplementation of tryptophan during 24 h did not affect cell viability. Tryptophan involvement in the immune system relies mostly on the suppressor role of its metabolites, and despite a reduction of NO production was expected (16, 66), only a reduction of the extracellular ATP was detected in response to *Phdp*UV. The ATP released by the inflammatory cells acts as a pro-inflammatory autocrine/paracrine purinergic signal (67) and, by tryptophan supplementation, this indicator was reduced. Macrophages can be differentiated into distinct groups according to not only the inductor of differentiation but also to the inflammation stage and perceived signals (30, 35). Commonly baptized as SHIP [Sample, Heal (M2), Inhibit (M1), and Present (antigen)] (33), macrophages present some plasticity regarding their state, and type 2 macrophages (M2) are associated with the healing and repair phase of the inflammation. In the present study, HKL cultured in tryptophan enriched environment expressed more M2/repair type genotype, as suggested by the increased expression of arginase 2 (*arg2)* in response *Phdp*UV. Also, despite non-significant, a tendency to increase the expression of the anti-inflammatory cytokine interleukin 10 (*il10)* in response to LPS*Phdp* of T2x-treatmed cells compared to L-15 was observed. Polarized M2 macrophages are known to produce large quantities of *il10* (35, 68) and ornithine generated from arginase is associated with M2 phenotype (31). Despite contradictory, the specific function of the IDO enzyme is believed to be anti-inflammatory, as reviewed by Yang and Ming (69). Accordingly, in the present study, changes in the expression of *ido2* were also perceived. The indoleamine dioxygenase 2 enzyme mediates tryptophan catabolism by the kynurenine pathway in macrophages and relies on both tryptophan availability (5) and induction by an inflammatory stimulus (25). Thus, as expected, *ido2* was up-regulated in the higher tryptophan medium (T2x) after 24 h exposure to *Phdp*UV while LPS*Phdp* failed to induce expression.

In response to AIP56, cells cultured in tryptophan-supplemented medium (both T1x and T2x) presented an increase of caspase 3 activity relative to the control cells (L-15 medium cultured HKL). Curiously, the expression of *casp3*, an executioner caspase, was down-regulated relative to L-15 at 3 h of stimulus, while expression of *mtor*, which is involved in cell proliferation, was induced at 6 h in T2x-culture cells. It can be speculated that the apoptotic mechanisms were empowered by tryptophan surplus since, together with caspase 3 activity, the initiator caspase 8 expression increased at 6 h in cells cultured with T1x. The immunosuppressive role of tryptophan surplus is further supported by the observed down-regulation of *amd1* (19), *sms*, and *dntm3b* (18), which are genes with key roles in the support of cell proliferation and differentiation. Moreover, the expression of the target of AIP56 cleavage associated protein, the *p65* subunit, which is involved in the translocation and activation of NF-κB, was also down-regulated by tryptophan supplementation. Despite most differences presented in this study included both unstimulated and AIP56-stimulated cells, results seem to point to some level of aggravation of cell capacity to respond to AIP56 by tryptophan surplus.

Tryptophan supplementation above the level present in the L-15 medium, points to an attenuated inflammatory response, mostly sustained in the heal/repair extend of the immune system. Despite the lack of changes in the modulation of genes related to AA pathways, it is hypothesized that those mechanisms could have been prompted to sustain the M2/healing type of response to both LPS*Phdp* and *Phdp*UV. Some recent *in vivo* evidence indicates that the dietary supplementation of tryptophan in European seabass compromises leucocytes' inflammatory response to UV-inactivated (11–13) and live *Phdp*, ultimately jeopardizing fish disease resistance to the pathogen (24). This is in agreement with the general increase of apoptotic indicators and compromised immune response to AIP56 in the cultured cells.

An Integrated View of the Different Roles of Methionine and Tryptophan

The range of metabolic pathways that are dependent on a proper supply of specific AA unveils their importance in the support of metabolism and health (70). Immune homeostasis, which comprises host capacity to recognize, properly respond, and repair, relies on the adequate supply of specific AA. All these mechanisms are highly controlled and each pathway is initiated or inhibited according to numerous perceived signals. Nonetheless, specific AA can have a lead role in the pro-inflammatory part of the event (e.g. methionine) while others seem to play a more important role in the resolution of inflammation (e.g. tryptophan), presenting both the same importance in the overall immune response.

On the one hand, this was evident in the present study with methionine improving cell viability and polyamine production necessary for cell proliferation (19). These observations were

accompanied by the increased expression of pro-inflammatory and methionine-related pathways indicators. With the increased expression of DNMT1 and up-regulation of *sms* and *odc*, the modulation of the methylation and aminopropylation pathways, respectively, are displayed. Finally, improved cell responses to an inflammatory agent were accompanied by lower signals of apoptosis by AIP56 with higher impression of pro-inflammatory indicators compared to the control treatment.

On the other hand, immune tolerance is of great importance, specifically in the limitation of self-damage and tryptophan seems to present a key role in such response. Most tryptophan-dependent pathways associated to the immune system are related to the assemblage of anti-inflammatory machinery. In macrophages, tryptophan consumption through the kynurenine pathway is catalyzed by IDO (71). In fact, IDO2 expression was found increased by tryptophan surplus and seemed to have induced signs of macrophages anti-inflammatory phenotype (i.e. high expression of arginase 2, *arg2*, in response to LPS*Phdp*) (68). Likewise, when submitted to AIP56 induced-apoptosis, cultured cells incubated with tryptophan presented increased signs of apoptosis and reduced expression of a critical regulator of immune and inflammatory responses (i.e. NF-κB P65), as well as proliferation and differentiation indicators (e.g. SMS, AMD1).

To conclude, in the present study it was specifically showed that methionine and tryptophan have their distinct roles in immune response, with different and contrasting outcomes by the modulation of individual key pathways. Methionine seems to positively contribute to the progress of inflammation, improving the underlying mechanisms activated in response to an inflammatory agent and lowering signals of apoptosis by AIP56, whereas tryptophan seems to presented a clear role in the tolerance process responsible for restriction of the pro-inflammatory cluster of the immune response. This is supported by the several signals of an attenuated inflammatory response to *Phdp*UV and lowered cell resilience to AIP56.

DATA AVAILABILITY STATEMENT

The datasets presented in this study can be found in online repositories. The names of the repository/repositories and accession number(s) can be found in the article/**Supplementary Material**.

ETHICS STATEMENT

The animal study was reviewed and approved by the CIIMAR Animal Welfare Committee, carried out in a registered installation (N16091.UDER).

AUTHOR CONTRIBUTIONS

MM and BC conceived the experiments and MM conducted the experimental trials. CS purified the LPS*Phdp*. MM wrote the manuscript under the supervision of AO-T, CS, and BC. All authors contributed to the article and approved the submitted version.

FUNDING

This work was partially supported by UIDB/04423/2020, UIDP/04423/2020 and INFLAMMAA (reference PTDC/CVT-CVT/32349/2017), financed by Portugal and the European Union through FEDER and COMPETE 2020, and national funds through Fundação para a Ciência e a Tecnologia (FCT, Portugal). MM and BC were supported by FCT, Portugal (SFRH/BD/108243/2015 and IF/00197/2015, respectively).

ACKNOWLEDGMENTS

The authors would like to acknowledge Dr[a]. Ana do Vale and Dr°. Nuno dos Santos (i3S/IBMC) for the kindly providing the AIP56 toxin and Dr°. Johnny Lisboa (i3S/IBMC) and Dr[a]. Cassilda Pereira (i3S/IBMC) for all the assistance in the Western blot protocol.

SUPPLEMENTARY MATERIAL

The Supplementary Material for this article can be found online at: https://www.frontiersin.org/articles/10.3389/fimmu.2021.660448/full#supplementary-material

REFERENCES

1. Grimble RF, Grimble GK. Immunonutrition: Role of sulfur amino acids, related amino acids, and polyamines. *Nutrition* (1998) 14(7-8):605–10. doi: 10.1016/S0899-9007(98)80041-5
2. Martinez Y, Li X, Liu G, Bin P, Yan W, Mas D, et al. The role of methionine on metabolism, oxidative stress, and diseases. *Amino Acids* (2017) 49(12):2091–8. doi: 10.1007/s00726-017-2494-2
3. Bunchasak C. Role of Dietary Methionine in Poultry Production. *J Poult Sci* (2009) 46(3):169–79. doi: 10.2141/jpsa.46.169
4. Jankowski J, Kubińska M, Zduńczyk Z. Nutritional and immunomodulatory function of methionine in poultry diets – a review. *Ann Anim Sci* (2014) 14 (1):17. doi: 10.2478/aoas-2013-0081
5. Le Floc'h N, Melchior D, Obled C. Modifications of protein and amino acid metabolism during inflammation and immune system activation. *Livestock Product Sci* (2004) 87(1):37–45. doi: 10.1016/j.livprodsci.2003.09.005
6. Adamidou S, Nengas I, Alexis M, Foundoulaki E, Nikolopoulou D, Campbell P, et al. Apparent nutrient digestibility and gastrointestinal evacuation time in European seabass (*Dicentrarchus labrax*) fed diets containing different levels of legumes. *Aquaculture* (2009) 289(1-2):106–12. doi: 10.1016/j.aquaculture.2009.01.015
7. Tang L, Wang GX, Jiang J, Feng L, Yang L, Li SH, et al. Effect of methionine on intestinal enzymes activities, microflora and humoral immune of juvenile Jian carp (*Cyprinus carpio* var. *Jian) Aquacult Nutr* (2009) 15(5):477–83. doi: 10.1111/j.1365-2095.2008.00613.x
8. Costas B, Conceicao LEC, Dias J, Novoa B, Figueras A, Afonso A. Dietary arginine and repeated handling increase disease resistance and modulate

innate immune mechanisms of Senegalese sole (*Solea senegalensis* Kaup, 1858). *Fish Shellfish Immunol* (2011) 31(6):838–47. doi: 10.1016/j.fsi.2011.07.024
9. Kuang SY, Xiao WW, Feng L, Liu Y, Jiang J, Jiang WD, et al. Effects of graded levels of dietary methionine hydroxy analogue on immune response and antioxidant status of immune organs in juvenile Jian carp (*Cyprinus carpio* var. Jian). *Fish Shellfish Immunol* (2012) 32(5):629–36. doi: 10.1016/j.fsi.2011.12.012
10. Azeredo R, Perez-Sanchez J, Sitja-Bobadilla A, Fouz B, Tort L, Aragao C, et al. European Sea Bass (*Dicentrarchus labrax*) Immune Status and Disease Resistance Are Impaired by Arginine Dietary Supplementation. *PloS One* (2015) 10(10):e0139967. doi: 10.1371/journal.pone.0139967
11. Machado M, Azeredo R, Diaz-Rosales P, Afonso A, Peres H, Oliva-Teles A, et al. Dietary tryptophan and methionine as modulators of European seabass (*Dicentrarchus labrax*) immune status and inflammatory response. *Fish Shellfish Immunol* (2015) 42(2):353–62. doi: 10.1016/j.fsi.2014.11.024
12. Azeredo R, Machado M, Afonso A, Fierro-Castro C, Reyes-Lopez FE, Tort L, et al. Neuroendocrine and Immune Responses Undertake Different Fates following Tryptophan or Methionine Dietary Treatment: Tales from a Teleost Model. *Front Immunol* (2017) 8:1226. doi: 10.3389/fimmu.2017.01226
13. Azeredo R, Machado M, Guardiola FA, Cerezuela R, Afonso A, Peres H, et al. Local immune response of two mucosal surfaces of the European seabass, *Dicentrarchus labrax*, fed tryptophan- or methionine-supplemented diets. *Fish Shellfish Immunol* (2017) 70:76–86. doi: 10.1016/j.fsi.2017.09.016
14. Machado M, Azeredo R, Fontinha F, Fernández-Boo S, Conceição LEC, Dias J, et al. Dietary Methionine Improves the European Seabass *(Dicentrarchus labrax)* Immune Status, Inflammatory Response, and Disease Resistance. *Front Immunol* (2018) 9:2672. doi: 10.3389/fimmu.2018.02672
15. Jiang J, Shi D, Zhou XQ, Hu Y, Feng L, Liu Y, et al. In vitro and in vivo protective effect of arginine against lipopolysaccharide induced inflammatory response in the intestine of juvenile Jian carp (*Cyprinus carpio* var. *Jian) Fish Shellfish Immunol* (2015) 42(2):457–64. doi: 10.1016/j.fsi.2014.11.030
16. Azeredo R, Serra CR, Oliva-Teles A, Costas B. Amino acids as modulators of the European seabass, *Dicentrarchus labrax*, innate immune response: an in vitro approach. *Sci Rep* (2017) 7(1):18009. doi: 10.1038/s41598-017-18345-3
17. Machado M, Engrola S, Colen R, Conceição LEC, Dias J, Costas B. Dietary methionine supplementation improves the European seabass (*Dicentrarchus labrax*) immune status following long-term feeding on fish meal free diets. *Br J Nutr* (2020) 124(9):890–902. doi: 10.1017/S0007114520001877
18. Waterland RA. Assessing the effects of high methionine intake on DNA methylation. *J Nutr* (2006) 136(6):1706S–10S. doi: 10.1093/jn/136.6.1706S
19. Igarashi K, Kashiwagi K. Polyamines: Mysterious modulators of cellular functions. *Biochem Biophys Res Commun* (2000) 271(3):559–64. doi: 10.1006/bbrc.2000.2601
20. Moffett JR, Namboodiri MA. Tryptophan and the immune response. *Immunol Cell Biol* (2003) 81(4):247–65. doi: 10.1046/j.1440-1711.2003.t01-1-01177.x
21. Le Floc'h N, Seve B. Biological roles of tryptophan and its metabolism: Potential implications for pig feeding. *Livestock Sci* (2007) 112(1-2):23–32. doi: 10.1016/j.livsci.2007.07.002
22. Wang B, Min Z, Yuan J, Zhang B, Guo Y. Effects of dietary tryptophan and stocking density on the performance, meat quality, and metabolic status of broilers. *J Anim Sci Biotechnol* (2014) 5(1):44. doi: 10.1186/2049-1891-5-44
23. Hoseini SM, Mirghaed AT, Mazandarani M, Zoheiri F. Serum cortisol, glucose, thyroid hormones' and non-specific immune responses of Persian sturgeon, *Acipenser persicus to* exogenous tryptophan and acute stress. *Aquaculture* (2016) 462:17–23. doi: 10.1016/j.aquaculture.2016.04.031
24. Machado M, Azeredo R, Domingues A, Fernandez-Boo S, Dias J, Conceição LEC, et al. Dietary tryptophan deficiency and its supplementation compromises inflammatory mechanisms and disease resistance in a teleost fish. *Sci Rep* (2019) 9(1):7689. doi: 10.1038/s41598-019-44205-3
25. Cortes J, Alvarez C, Santana P, Torres E, Mercado L. Indoleamine 2,3-dioxygenase: First evidence of expression in rainbow trout (*Oncorhynchus mykiss*). *Dev Comp Immunol* (2016) 65:73–8. doi: 10.1016/j.dci.2016.06.020
26. MacKenzie CR, Hadding U, Daubener W. Interferon-gamma-induced activation of indoleamine 2,3-dioxygenase in cord blood monocyte-derived macrophages inhibits the growth of group B streptococci. *J Infect Dis* (1998) 178(3):875–8. doi: 10.1086/515347
27. Daubener W, MacKenzie CR. IFN-gamma activated indoleamine 2,3-dioxygenase activity in human cells is an antiparasitic and an antibacterial effector mechanism. *Adv Exp Med Biol* (1999) 467:517–24. doi: 10.1007/978-1-4615-4709-9_64
28. Munn DH, Mellor AL. Indoleamine 2,3 dioxygenase and metabolic control of immune responses. *Trends Immunol* (2013) 34(3):137–43. doi: 10.1016/J.It.2012.10.001
29. Secombes CJ, Wang T, Hong S, Peddie S, Crampe M, Laing KJ, et al. Cytokines and innate immunity of fish. *Dev Comp Immunol* (2001) 25(8-9):713–23. doi: 10.1016/S0145-305x(01)00032-5
30. Forlenza M, Fink IR, Raes G, Wiegertjes GF. Heterogeneity of macrophage activation in fish. *Dev Comp Immunol* (2011) 35(12):1246–55. doi: 10.1016/j.dci.2011.03.008
31. Mills CD. M1 and M2 Macrophages: Oracles of Health and Disease. *Crit Rev Immunol* (2012) 32(6):463–88. doi: 10.1615/critrevimmunol.v32.i6.10
32. Mills CD, Ley K. M1 and M2 Macrophages: The Chicken and the Egg of Immunity. *J Innate Immun* (2014) 6(6):716–26. doi: 10.1159/000364945
33. Mills CD. Anatomy of a discovery: m1 and m2 macrophages. *Front Immunol* (2015) 6:212. doi: 10.3389/fimmu.2015.00212
34. Ley K. M1 Means Kill; M2 Means Heal. *J Immunol* (2017) 199(7):2191–3. doi: 10.4049/jimmunol.1701135
35. Wentzel AS, Janssen JJE, de Boer VCJ, van Veen WG, Forlenza M, Wiegertjes GF. Fish Macrophages Show Distinct Metabolic Signatures Upon Polarization. *Front Immunol* (2020) 11:152. doi: 10.1007/s10787-007-0013-x10.3389/fimmu.2020.00152
36. Elmore S. Apoptosis: a review of programmed cell death. *Toxicol Pathol* (2007) 35(4):495–516. doi: 10.1080/01926230701320337
37. Mosser DM. The many faces of macrophage activation. *J Leukoc Biol* (2003) 73(2):209–12. doi: 10.1189/jlb.0602325
38. do Vale A, Silva MT, dos Santos NMS, Nascimento DS, Reis-Rodrigues P, Costa-Ramos C, et al. AIP56, a novel plasmid-encoded virulence factor of Photobacterium damselae subsp. piscicida with apoptogenic activity against sea bass macrophages and neutrophils. *Mol Microbiol* (2005) 58(4):1025–38. doi: 10.1111/j.1365-2958.2005.04893.x
39. Liu T, Zhang L, Joo D, Sun S-C. NF-κB signaling in inflammation. *Signal Transduct Target Ther* (2017) 2:17023. doi: 10.1007/s10787-007-0013-x10.1038/sigtrans.2017.23
40. Rezania S, Amirmozaffari N, Tabarraei B, Jeddi-Tehrani M, Zarei O, Alizadeh R, et al. Extraction, Purification and Characterization of Lipopolysaccharide from *Escherichia coli* and *Salmonella typhi*. *Avicenna J Med Biotechnol* (2011) 3(1):3–9.
41. Zhu Z-X, Cong W-T, Ni M-W, Wang X, Ma W-D, Ye W-J, et al. An improved silver stain for the visualization of lipopolysaccharides on polyacrylamide gels. *ELECTROPHORESIS* (2012) 33(7):1220–3. doi: 10.1002/elps.201100492
42. Secombes C. Isolation of salmonid macrophages and analysis of their killing activity. In: J Stolen, editor. *Techniques in Fish Immunology*. Fair Haven, NJ: SOS Publications (1990). p. 137–54.
43. Sarmento A, Guilhermino L, Afonso A. Mercury chloride effects on the function and cellular integrity of sea bass (*Dicentrarchus labrax*) head kidney macrophages. *Fish Shellfish Immunol* (2004) 17(5):489–98. doi: 10.1016/j.fsi.2004.05.004
44. Tafalla C, Novoa B. Requirements for nitric oxide production by turbot (*Scophthalmus maximus*) head kidney macrophages. *Dev Comp Immunol* (2000) 24(6-7):623–31. doi: 10.1016/s0145-305x(99)00087-7
45. Costa-Ramos C, Vale AD, Ludovico P, dos Santos NMS, Silva MT. The bacterial exotoxin AIP56 induces fish macrophage and neutrophil apoptosis using mechanisms of the extrinsic and intrinsic pathways. *Fish Shellfish Immunol* (2011) 30(1):173–81. doi: 10.1016/j.fsi.2010.10.007
46. Pereira LMG, Pinto RD, Silva DS, Moreira AR, Beitzinger C, Oliveira P, et al. Intracellular Trafficking of AIP56, an NF-κB-Cleaving Toxin from *Photobacterium damselae* subsp. *piscicida Infect Immun* (2014) 82 (12):5270–85. doi: 10.1128/iai.02623-14
47. Mosmann T. Rapid colorimetric assay for cellular growth and survival: application to proliferation and cytotoxicity assays. *J Immunol Methods* (1983) 65(1-2):55–63. doi: 10.1016/0022-1759(83)90303-4
48. Laemmli UK. Cleavage of Structural Proteins during the Assembly of the Head of Bacteriophage T4. *Nature* (1970) 227(5259):680–5. doi: 10.1007/s10787-007-0013-x10.1038/227680a0

49. Silva DS, Pereira LMG, Moreira AR, Ferreira-da-Silva F, Brito RM, Faria TQ, et al. The apoptogenic toxin AIP56 is a metalloprotease A-B toxin that cleaves NF-κb P65. *PloS Pathog* (2013) 9(2):e1003128–e1003128. doi: 10.1371/journal.ppat.1003128
50. Pfaffl MW. A new mathematical model for relative quantification in real-time RT-PCR. *Nucleic Acids Res* (2001) 29(9):e45–5. doi: 10.1007/s10787-007-0013-x10.1093/nar/29.9.e45
51. Smirnova MG, Kiselev SL, Gnuchev NV, Birchall JP, Pearson JP. Role of the pro-inflammatory cytokines tumor necrosis factor-alpha, interleukin-1 beta, interleukin-6 and interleukin-8 in the pathogenesis of the otitis media with effusion. *Eur Cytokine Netw* (2002) 13(2):161–72.
52. Hussain SP, Hofseth LJ, Harris CC. Radical causes of cancer. *Nat Rev Cancer* (2003) 3(4):276–85. doi: 10.1038/nrc1046
53. Cruz CM, Rinna A, Forman HJ, Ventura ALM, Persechini PM, Ojcius DM. ATP Activates a Reactive Oxygen Species-dependent Oxidative Stress Response and Secretion of Proinflammatory Cytokines in Macrophages. *J Biol Chem* (2007) 282(5):2871–9. doi: 10.1074/jbc.M608083200
54. Palti Y. Toll-like receptors in bony fish: from genomics to function. *Dev Comp Immunol* (2011) 35(12):1263–72. doi: 10.1016/j.dci.2011.03.006
55. Bi D, Wang Y, Gao Y, Li X, Chu Q, Cui J, et al. Recognition of Lipopolysaccharide and Activation of NF-κB by Cytosolic Sensor NOD1 in Teleost Fish. *Front Immunol* (2018) 9:1413. doi: 10.3389/fimmu.2018.01413
56. Vanaja SK, Russo AJ, Behl B, Banerjee I, Yankova M, Deshmukh SD, et al. Bacterial Outer Membrane Vesicles Mediate Cytosolic Localization of LPS and Caspase-11 Activation. *Cell* (2016) 165(5):1106–19. doi: 10.1007/s10787-007-0013-x10.1016/j.cell.2016.04.015
57. do Vale A, Marques F, Silva MT. Apoptosis of sea bass *(Dicentrarchus labrax* L.) neutrophils and macrophages induced by experimental infection with Photobacterium damselae subsp. *piscicida Fish Shellfish Immunol* (2003) 15 (2):129–44. doi: 10.1016/S1050-4648(02)00144-4
58. Rahman MM, McFadden G. Modulation of NF-kappaB signalling by microbial pathogens. *Nat Rev Microbiol* (2011) 9(4):291–306. doi: 10.1038/nrmicro2539
59. Mills CD. Macrophage arginine metabolism to ornithine/urea or nitric oxide/citrulline: a life or death issue. *Crit Rev Immunol* (2001) 21(5):399–425. doi: 10.1615/CritRevImmunol.v21.i5.10
60. Parameswaran N, Patial S. Tumor necrosis factor-α signaling in macrophages. *Crit Rev Eukaryotic Gene Expression* (2010) 20(2):87–103. doi: 10.1007/s10787-007-0013-x10.1615/critreveukargeneexpr.v20.i2.10
61. Sun XM, Butterworth M, MacFarlane M, Dubiel W, Ciechanover A, Cohen GM. Caspase activation inhibits proteasome, function during apoptosis. *Mol Cell* (2004) 14(1):81–93. doi: 10.1016/S1097-2765(04)00156-X
62. Lawrence T. The nuclear factor NF-kappaB pathway in inflammation. *Cold Spring Harbor Perspect Biol* (2009) 1(6):a001651–a001651. doi: 10.1101/cshperspect.a001651
63. Yen C-LE, Mar M-H, Craciunescu CN, Edwards LJ, Zeisel SH. Deficiency in Methionine, Tryptophan, Isoleucine, or Choline Induces Apoptosis in Cultured Cells. *J Nutr* (2002) 132(7):1840–7. doi: 10.1093/jn/132.7.1840
64. Song B, Zeng Q, Liu Y, Wu B. Effect of methionine deficiency on the apoptosis and cell cycle of kidney in broilers. *Res Vet Sci* (2019). doi: 10.1016/j.rvsc.2019.09.013
65. Machado M, Azeredo R, Fontinha F, Fernandez-Boo S, Conceição LEC, Dias J, et al. Dietary methionine improves the European seabass (Dicentrarchus labrax) immune status, inflammatory response and disease resistance. *Front Immunol* (2018). doi: 10.3389/fimmu.2018.02672
66. Sharma JN, Al-Omran A, Parvathy SS. Role of nitric oxide in inflammatory diseases. *Inflammopharmacology* (2007) 15(6):252–9. doi: 10.1007/s10787-007-0013-x
67. Dosch M, Gerber J, Jebbawi F, Beldi G. Mechanisms of ATP Release by Inflammatory Cells. *Int J Mol Sci* (2018) 19(4):1222. doi: 10.3390/ijms19041222
68. Tan H-Y, Wang N, Li S, Hong M, Wang X, Feng Y. The Reactive Oxygen Species in Macrophage Polarization: Reflecting Its Dual Role in Progression and Treatment of Human Diseases. *Oxid Med Cell Longevity* (2016) 2016:1–16. doi: 10.1155/2016/2795090
69. Yang Z, Ming X-F. Functions of arginase isoforms in macrophage inflammatory responses: impact on cardiovascular diseases and metabolic disorders. *Front Immunol* (2014) 5:533. doi: 10.3389/fimmu.2014.00533
70. Li P, Yin YL, Li D, Kim SW, Wu GY. Amino acids and immune function. *Br J Nutr* (2007) 98(2):237–52. doi: 10.1017/S000711450769936X
71. Ball HJ, Yuasa HJ, Austin CJ, Weiser S, Hunt NH. Indoleamine 2,3-dioxygenase-2; a new enzyme in the kynurenine pathway. *Int J Biochem Cell Biol* (2009) 41(3):467–71. doi: 10.1016/j.biocel.2008.01.005

Conflict of Interest: The authors declare that the research was conducted in the absence of any commercial or financial relationships that could be construed as a potential conflict of interest.

frontiers in Immunology

ORIGINAL RESEARCH
published: 12 May 2021
doi: 10.3389/fimmu.2021.663106

Dietary Phytogenics and Galactomannan Oligosaccharides in Low Fish Meal and Fish Oil-Based Diets for European Sea Bass (*Dicentrarchus labrax*) Juveniles: Effects on Gill Structure and Health and Implications on Oxidative Stress Status

Silvia Torrecillas[1], Genciana Terova[2], Alex Makol[3], Antonio Serradell[1], Victoria Valdenegro-Vega[4], Marisol Izquierdo[1], Felix Acosta[1] and Daniel Montero[1]*

[1] Grupo de Investigación en Acuicultura (GIA), IU-ECOAQUA, Universidad de Las Palmas de Gran Canaria, Las Palmas, Spain, [2] Department of Biotechnology and Life Sciences, University of Insubria, Varese, Italy, [3] Delacon Biotechnik GmbH, Global Solution Aquaculture Unit, Engerwitzdorf, Austria, [4] Biomar A/S, Global RD Health. BioMar AS, Trondheim, Norway

OPEN ACCESS

Edited by:
Jorge Galindo-Villegas, Nord University, Norway

Reviewed by:
Prabhugouda Siriyappagouder, Nord University, Norway
Mingchun Ren, Chinese Academy of Fishery Sciences, China

***Correspondence:**
Silvia Torrecillas
silvia.torrecillas@giaqua.org

Specialty section:
This article was submitted to Nutritional Immunology, a section of the journal Frontiers in Immunology

Received: *02 February 2021*
Accepted: *15 April 2021*
Published: *12 May 2021*

Citation:
Torrecillas S, Terova G, Makol A, Serradell A, Valdenegro-Vega V, Izquierdo M, Acosta F and Montero D (2021) Dietary Phytogenics and Galactomannan Oligosaccharides in Low Fish Meal and Fish Oil-Based Diets for European Sea Bass (Dicentrarchus labrax) Juveniles: Effects on Gill Structure and Health and Implications on Oxidative Stress Status. Front. Immunol. 12:663106. doi: 10.3389/fimmu.2021.663106

An effective replacement for fish meal (FM) and fish oil (FO) based on plant-based raw materials in the feed of marine fish species is necessary for the sustainability of the aquaculture sector. However, the use of plant-based raw materials to replace FM and FO has been associated with several negative health effects, some of which are related to oxidative stress processes that can induce functional and morphological alterations in mucosal tissues. This study aimed to evaluate the effects of dietary oligosaccharides of plant origin (5,000 ppm; galactomannan oligosaccharides, GMOS) and a phytogenic feed additive (200 ppm; garlic oil and labiatae plant extract mixture, PHYTO) on the oxidative stress status and mucosal health of the gills of juvenile European sea bass (*Dicentrarchus labrax*). The experimental diets, low FM and FO diets (10%FM/6%FO) were supplemented with GMOS from plant origin and PHYTO for 63 days. GMOS and PHYTO did not significantly affect feed utilization, fish growth, and survival. GMOS and PHYTO downregulated the expression of *β-act*, *sod*, *gpx*, *cat*, and *gr* in the gills of the fish compared with that in fish fed the control diet. The expression of *hsp70* and *ocln* was upregulated and downregulated, respectively, in the GMOS group compared with that in the control group, whereas the expression of *zo-1 was* downregulated in the PHYTO group compared with that in the GMOS group. The morphological, histopathological, immunohistochemical, and biochemical parameters of the fish gills were mostly unaffected by GMOS and PHYTO. However, the PHYTO group had lower incidence of lamellar fusion than did the control group after 63 days. Although the tissular distribution of goblet cells

was unaffected by GMOS and PHYTO, goblet cell size showed a decreasing trend (–11%) in the GMOS group. GMOS and PHYTO significantly reduced the concentration of PCNA+ in the epithelium of the gills. The above findings indicated that GMOS and PHYTO in low FM/FO-based diets protected the gill epithelia of *D. labrax* from oxidative stress by modulating the expression of oxidative enzyme-related genes and reducing the density of PCNA+ cells in the gills of the fish.

Keywords: European sea bass, gill morphology, oxidative stress, functional diets, prebiotics, phytogenics, low FM/FO diets

INTRODUCTION

The interaction between gill mucosal epithelia and the external environment is complex and highlights the importance of this tissue as an organ of defense against a wide range of hazards, including stress and physicochemical and biological alterations (1, 2). Gill epithelia facilitate respiration by separating blood circulation from external media through an exceptionally thin epithelium, which is composed mainly of two cell types, pavement cells (PVCs) and mitochondria-rich cells (MRCs) (3). PVCs provide physical protection and are involved in gas and osmotic exchange, as well as in acid–base regulation (1, 4–6). MRCs are involved in active ion transport and regulation, gas exchange, and maintenance of blood acid–base balance (1). These cells are characterized by a mitochondria-rich cytoplasm and the presence of an extensive tubulovesicular system located in the apical region of the cell, where the Na^+/K^+-ATPase transporter enzyme is located (6, 7). When challenged, both types of cells can gain functionality with respect to their structural roles and anatomical localizations (3). Gill associated lymphoid tissue (GIALT) is composed mainly of B cells, T cells, eosinophilic granulocytes, macrophages, neutrophils, and goblet cells, and contains several humoral immune-related molecules (2, 8). Like other mucosal immune systems, the gill has an associated microbiota; however, because of the nature of this tissue, microbial colonization seems to be restricted to protected areas (gaps between pharyngeal arches and lamellae) (9).

Reared fish are exposed to several natural and induced stressors, some of which produce reactive oxygen species and nitrogen species (RONS), which can induce physiological and morphological alterations (10), especially in susceptible mucosal tissues, including fish gills. Histopathological gill lesions are considered a good indicator of oxidative stress-inducing factors such as xenobiotics (11–15).

Oxidative stress results from an imbalance between the levels of RONS and the capacity of the antioxidant defense system to cope with them (16). This imbalance triggers the oxidation of essential biomolecules and favors multiple disease conditions (17). Similar to higher vertebrates, the methods for fish antioxidant defenses include enzymatic mechanisms and non-enzymatic endogenous and exogenous compounds (18). Superoxide dismutase (SOD), catalase (CAT), and glutathione peroxidase (GPX) are the main antioxidant enzymes that constitute the first line of defense against oxidative stress and have been traditionally used as indicators of the antioxidant status of an organism (19). Moreover, proteins, such as heat shock proteins (HSPs), play a cytoprotective role against oxidative stress by initiating protein folding, repair, and degradation of irreparable proteins, as well as regulating the endogenous generation of reactive species *via* a modulation of the inflammatory cascade and intrinsic apoptosis processes (20, 21). However, an increase or inhibition of antioxidant activity can vary depending on the intensity and duration of the stressors, as well as on the susceptibility of the exposed fish species (19, 22).

Non-enzymatic endogenous antioxidants, such as uric acid, tripeptide glutathione, or melatonin (23), and exogenous antioxidants can be ingested through the diet or as dietary supplements. Additionally, some dietary compounds that do not directly neutralize reactive species, but rather enhance endogenous enzymatic activity, may also be classified as antioxidants (24).

Under some oxidative/nitrosative stress conditions, such as those attributed to intensive fish culture practices, dietary supplementation with exogenous antioxidants such as vitamins, flavonoids, carotenoids, plant polyphenols, allyl sulfides, curcumin, melatonin, or polyamines may offer a good functional strategy to maintain proper levels of RONS (23, 25, 26). Although most of the studies investigating fish oxidative stress are related to the effects of xenobiotics or pollutants, the use of functional additives, which are capable of triggering the fish antioxidant system, has gained attention during the last decade in aquaculture because of its potential benefit in preventing diseases and promoting health (17, 27–32).

Among these additives are phytogenic feed additives (PFA), consisting of highly active plant substances that encompass much more than essential oils because they include phytochemical compounds such as saponins, flavonoids, mucilages or tannins (33). A wide variety of products and extracts are available; garlic and labiate plant essential oils have been proven to have antioxidant properties (34) in higher vertebrates (35–38) and fish (39–43). These antioxidant capacities are not limited to functional PFA compounds, as several authors have observed antioxidant properties in other functional additives such as prebiotics, particularly glucomannans (19, 44).

However, little is known about how these dietary functional additives may affect the oxidative status of fish gills and their associated GIALT function, particularly when they are included in plant-based fish diets. Thus, the aim of the present study was to determine the effects of galactomannan oligosaccharides of

plant origin (GMOS) and a PFA (mixture of garlic oil and labiatae plant extracts) on the oxidative stress status and mucosal health of the gills of juvenile European sea bass when supplemented in low FM/FO diets. For this purpose, structural, cellular, and oxidative dietary-associated changes were evaluated using gene expression analyses and optical and electron microscopy studies.

MATERIALS AND METHODS

Diets

Three low fish meal (10%FM) and fish oil (6%FO)-based diets were formulated according to commercial standards. One of the experimental diets was void of the test ingredients (control diet), while the remaining two contained 5,000 ppm of galactomannan oligosaccharides (GMOS; Delacon, Austria) and 200 ppm of a blend of garlic and labiatae-plant oils (PHYTO; Delacon, Austria), respectively. The diets were formulated to meet the nutritional requirements of European sea bass. The specific composition of PHYTO and GMOS cannot be disclosed due to confidentiality issues because these functional additives are a prototype of potential commercial products (Delacon internal product code: SBPMH01 and SBPMH02, respectively).

The isoenergetic and isonitrogenous diets were industrially produced in the BioMar Tech-Centre (Brande, Denmark) using an extrusion process. To ensure product stability, GMOS was included in the mix during the pre-extrusion process, whereas PHYTO was homogenized with dietary oil and included by vacuum coating during the post-extrusion process. The stability of the functional products was checked before the production of the diet and at the beginning of the feeding trial. The ingredients used in the diets and their proximate composition are detailed in **Table 1**.

TABLE 1 | Main ingredients and analyzed proximate composition of the diets.

Ingredients (%)	DIETS		
	CONTROL	GMOS	PHYTO
Fish meal[1]	9.6	9.6	9.6
Soya protein concentrate	18.2	18.2	18.2
Soya Meal	11.6	11.6	11.6
Corn gluten meal	24.1	24.1	24.1
Wheat	8.5	8,0	8.5
Wheat gluten	1.9	1.9	1.9
Guar Meal	7.7	7.7	7.7
Rapeseed extracted	3.0	3.0	3.0
Fish oil[2]	6.5	6.5	6.5
Rapeseed oil[3]	5.2	5.2	5.2
Vitamin and mineral premix[4]	3.6	3.6	3.6
Antioxidant[5]	0.06	0.06	0.06
Galactomannan oligosaccharides[6]	0	0.5	0
Phytogenic[7]	0	0	0.02
Proximate composition (% of dry matter)			
Crude lipids	19.91	20.44	20.47
Crude protein	49.30	49.27	49.76
Moisture	5.10	5.01	5.06
Ash	7.02	6.41	6.49
Gross Energy (MJ/kg, as is)[8]	22.07	22.11	22.17

[1]South-American, Superprime 68% (63-68% protein; 8-9.5% lipids). [2]South American fish oil. [3]DLG AS, Denmark. [4]Vilomix, Denmark. [5]BAROX BECP, Ethoxyquin. [6]Delacon Biotechnik GmbH, Austria. [7]Delacon Biotechnik GmbH, Austria. [8]Determined using a calorimetric bomb (Eurofins Food & Feed testing, Norway, AS).

Experimental Conditions

The study was carried out at the facility of the Parque Científico-Tecnológico Marino (PCTM), University of Las Palmas de Gran Canaria (Telde, Canary Island, Spain). Healthy juvenile European sea bass were procured from a local farm (Aquanaria, Castillo del Romeral, Gran Canaria, Canary Islands, Spain). The fish were acclimatized for four weeks to the new environment (6.6–6.1 ppm dissolved O_2, 18.2–20.2°C). Thereafter, the fish (mean weight: 23.02 ± 0.67 g; mean length: 11.89 ± 0.15 cm) were randomly assigned to nine 500 L (75 fish/tank) fiberglass tanks at an initial density of 3.5 kg·m^3. The tanks were equipped with an open flow-through water system and the fish were exposed to natural photoperiod (12L:12D). The fish were fed three times a day to apparent satiation six days a week for 63 days. Before final sampling, each fish was anesthetized in accordance with the regulations of the European Union Directive (2010/63/EU) and Spanish legislation (RD 53/2013) for animal experiments. Fish handling was performed under natural clove oil anesthesia (0.2 ml/L; Guinama S.L; Spain, Ref. Mg83168), and discomfort, stress, and pain to the experimental animals were avoided as much as possible during the experiment. For sampling, fish were euthanized using an overdose of natural clove oil (5 ml/L; Guinama S.L; Spain, Ref. Mg83168).

The second and third holobranch from the right basket of the gill (n = 4 fish/tank) were stored in 4% paraformaldehyde at 4 °C for 48–72 h before being embedded in paraffin for morphological and immunohistochemical studies. Portions of the same holobranchs (central region) were fixed at 4°C in 2.5% glutaraldehyde and 0.15 M HEPES buffer (pH = 7.4) for structural studies (n = 3 fish/tank). Sections of the second and third holobranch from the right basket of the gill were sampled (n = 4 fish/tank) and stored at −80°C for gene expression analysis. The Bioethical Committee of the University of Las Palmas de Gran Canaria approved all the protocols used in the present study (approval no. 007/2012 CEBA ULPGC).

Proximate Compositions and Gross Energy of Diets

The proximate compositions of the feed were analyzed according to standard procedures (45). Dry matter content was determined after drying in an oven (110°C) to constant weight, and ash content was determined by combustion in a muffle furnace (600°C, 12 h). The crude lipids were extracted as described in Ref. (46) and crude protein content was determined (N × 6.25) using the Kjeldahl method. The gross energy content of diets was determined using a calorimetric bomb (Eurofins Food & Feed testing, Norway, AS).

RT-qPCR Analysis

Total RNA was extracted from the gill samples using TRI-Reagent (Sigma-Aldrich, Sant Louis, MO, USA) and RNeasy® mini-Kit (QIAGEN, Germany) according to the manufacturer's

instructions. The RNA was quantified by spectrophotometry (Nanodrop 1000, Thermo Fisher Scientific Inc., USA) and its integrity evaluated on a 1.4% agarose gel with Gel Red™ (Biotium Inc., Hayward, CA, USA).

Total RNA was reverse transcribed in a 20 µl reaction volume containing 2 µg total RNA, using a ThermoScript TM Reverse Transcriptase kit (Invitrogen, California, USA), until cDNA was obtained in a thermocycler (Mastercycle ® nexus GSX1, Eppendorf AG, Hamburg, Germany) run according to the manufacturer's instructions. The samples were then diluted to 1:10 in MiliQ water and stored at −20°C.

An aliquot of cDNA obtained by reverse transcription was then amplified by Real Time-qPCR using a designed primer set for each gene. The target genes were: *superoxide dismutase* (*sod*), *glutathione peroxidase (gpx), glutathione reductase (gr), catalase (cat), heat shock protein 70 kilodaltons (hsp70), zonula occludens 1 (zo-1)* and *occludin (ocln)*. Primers for the target genes and for the housekeeping gene (*α-tubulin*) were designed based on the cDNA sequences available in the GenBank database for *Dicentrarchus labrax*. The GenBank accession numbers and primer sequences are listed in **Table 2**.

The Real Time-qPCR was carried out in a final volume of 20 µl, containing 3 µl of cDNA (100 ng), 10 µl of iTaq Universal SYBR® Green Supermix (Bio-Rad, Milan, Italy), and 500 nM of each primer, using CFX96 real-time PCR instrument (Bio-Rad, Milan, Italy), according to the manufacturer's instructions. The reaction thermal conditions were as follows: 95°C for 1 min, then 40 cycles at 95°C for 10 s, and 60°C for 30 s. A blank sample containing nuclease-free water instead of the cDNA template was included in each assay as a negative control. Relative expression levels were calculated using the $2^{-\Delta\Delta Ct}$ method (47), and *α-tubulin* as housekeeping gene.

For the ΔΔCt calculation to be valid, the amplification efficiencies of the target and reference gene must be approximately equal. For this, The CFX Maestro™ Software (Biorad) was used to calculate the efficiency (E) of each primer set (**Supplementary Figure 1**). The same software allowed the selections of the appropriate reference gene based on the average M value and analyzes gene stability by means of the reference gene selection tool (CFX Maestro™ Software User Guide Version 1.1).

To calculate the expression data, we related the PCR signal of the target transcript in the treatment groups (GMOS and PHYTO) to that of samples of an untreated control (CTRL), which was considered as one.

TABLE 2 | Primers used for RT-qPCR.

Gene	Accession number	Primer	Nucleotide sequence (5'- 3')
sod	FJ860004.1	Forward	CATGTTGGAGACCTGGGAGA
		Reverse	TGAGCATCTTGTCCGTGATGT
gpx	FM013606.1	Forward	AGTTCGTGCAGTTAATCCGGA
		Reverse	GCTTAGCTGTCAGGTCGTAAAAC
gr	FM020412.1	Forward	CACTCGTCACCAAAGACCCA
		Reverse	GCAATGGCAACAGGTGTGAG
cat	FJ860003.1	Forward	TGGGACTTCTGGAGCCTGAG
		Reverse	GCAAACCTCGATCGCTGAAC
hsp70	AY423555.2	Forward	GGACATCAGCCAGAACAAGAGA
		Reverse	GCTGGAGGACAGGGTTCTC
zo-1	MH321323.1	Forward	CGGCCTGCAGATGTTCCTAA
		Reverse	GCTGAGGGAATTGGCTTTGA
ocln	MH321322.1	Forward	GGACGAAGACGACAACAACGA
		Reverse	CCATGGGAGAAAGCCTCTGA
α-tub (hk)	AY326429.1	Forward	AGGCTCATTGGCCAGATTGT
		Reverse	CAACATTCAGGGCTCCATCA

hk, housekeeping.

Morphological Studies

For morphological examinations, 4 µm transverse and sagittal gill sections were stained with hematoxylin and eosin (H&E) for optical examination, with Alcian Blue (pH = 2.5) for goblet cell differentiation, and with May–Gr̈nwald Giemsa (MGG) to study leukocyte distribution and presence (48). Digital images of the slides were obtained using Olympus VS120 digital scanner (Optic system BX61VS, Tokyo, Japan) equipped with VC50 and VS-XM10 cameras and were processed with Olympus VS software (VS-NIS-SQL-V2.6, Tokyo, Japan).

Histopathological Examination of Gill

Histopathological examination of the gills was performed on H&E-/MGG-stained sections (n = 12 fish per diet). The effects of GMOS and PHYTO on the incidence of fish lamellar fusion or branching, lamellar telangiectasis/aneurysms, chloride cell hyperplasia, as well as on the inflammation status and leukocyte-infiltrated populations of the gills were evaluated. The examiners were unaware of the experimental treatments, and assessments were based on a previously established semiquantitative scoring system as follows: 1 (weak), 2 (moderate), and 3 (high).

Gill Mucus Production Studies

Digitalized images of gill transverse sections (Alcian Blue pH = 2.5) were used to determine the morphological characteristics of gill goblet cells. For that purpose, CellSens Dimension Desktop 1.16 (Olympus Iberia, Spain) was calibrated to determine the area (μm^2), minimum diameter, and minimum perimeter (µm) of the goblet cell for each transverse section of the gill. Sagittal sections stained with Alcian Blue (pH = 2.5) were used to determine the location of the goblet cells along the primary lamellae and interlamellar spaces.

Gill Immunohistochemistry

Gill sagittal and transverse sections were routinely dewaxed and rehydrated. After antigen retrieval (High pH (Dako, Denmark) endogenous peroxidase activity was blocked with peroxidase blocking solution (Dako, Denmark). The sections were incubated in a humid chamber overnight at 4°C with primary rabbit antibody anti-iNOS-2 (diluted 1:200; Santa Cruz Biotechnology, CA, USA), and anti-PCNA (diluted 1:200; Thermo Fisher Scientific, CA, USA). Immunohistochemical staining was performed using a horseradish peroxidase (HRP) anti-rabbit EnVision System (Dako, Denmark) with diaminobenzidine (Dako, Denmark) or with 3-amino-9-ethylcarbazole (AEC+) chromogenic substrate system (Dako, Denmark). Negative controls were processed by replacing primary antibodies with a primary antibody diluent. Immunopositivity for anti-iNOS-2 was evaluated semi-qualitatively according to a previously established immunohistochemical scoring system with

immunolabeling intensity grades as follows: 1 (weak), 2 (moderate), and 3 (strong) for each area/cell evaluated. All slides, except for the negative controls, showed immunoreactivity to the antibodies assayed. Immunopositivity evaluation for PCNA-positive cells was carried out using the CellSens Dimension Desktop 1.16 software (Olympus Iberia, Spain), which was calibrated to determine the percentage of gill area covered by positive PCNA cells for each transverse section. None of the negative controls showed any immunoreactivity.

Gill Ultrastructure Examination

Gill transverse primary lamellar samples were post-fixed at 4°C in 2% osmium tetroxide and 2% uranyl acetate, dehydrated, and embedded individually in an Embed 812 (Electron Microscopy Sciences (EMS), PA, USA) resin block. Semi-thin serial transverse sections (n = 3–5 per individual fish) were contrasted with toluidine blue and examined under a light microscope (49). Ultrathin (50 nm) sections were qualitatively evaluated using a JEOL JEM-1011 transmission electron microscope (TEM; JEOL USA, Inc., USA) equipped with a digital camera MegaView III soft imaging system CCD camera (EMSIS GmbH, Germany). Cellular membrane lining appearance, primary and secondary lamellar structure, cellular morphology, TJ structure, microridge structure, mitochondria-rich cells (chloride cells) microvilli, and the number of infiltrated leukocytes were the main parameters evaluated.

Statistical Analyses

Statistical analyses were performed following the methods described in Ref. (50). All data were tested for normality and homogeneity of variance. Differences were considered significant at $p \leq 0.05$. Differences between dietary treatments were determined using one-way ANOVA. When F values were significant, individual means were compared using *post hoc* Tukey or Games–Howell tests for multiple means comparison. When required, data arcsine square root transformation was performed, particularly for data expressed in percentage (51). Morphological and immunohistochemical findings, which were based on a range scale evaluation, were analyzed by paired comparisons (Mann–Whitney U test). Analyses were performed using the SPSS Statistical Software System v21.0 (SPSS, Chicago, IL, USA) and GraphPad Prism 8 software (GraphPad Software, Inc., La Jolla, CA, USA).

RESULTS

Growth Parameters

At the end of the feeding trial, dietary supplementation with the additives did not affect ($p > 0.05$) fish growth and diet utilization, as described previously in Ref. (52). Mortality was negligible (<1%) and not associated with a specific diet.

RT-qPCR Analyses

The RT-qPCR showed that the expression of the target genes was significantly different in the different diet groups (**Figure 1**). The expression of *sod*, *gpx*, and *gr* decreased by half in fish fed the GMOS and PHYTO supplemented diets compared with the expression level in fish fed the control diet. Similarly, the expression of *cat* in the gills of fish fed the supplemented diets were significantly lower compared with that in fish fed the control diet, with the GMOS group recording the lowest expression. Contrarily, the expression of *hsp70* was significantly higher in fish fed the GMOS supplemented diet compared with

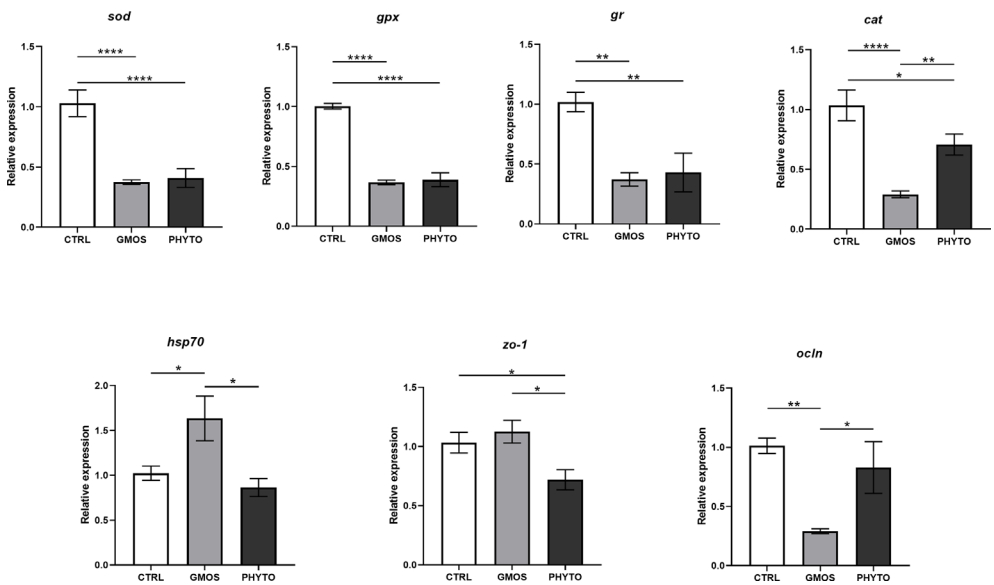

FIGURE 1 | Expression levels of genes of interest in gills of *Dicentrarchus labrax* samples. Diets: CTRL (control diet), GMOS (5,000 ppm galactomannan oligosaccharides), PHYTO (200 ppm phytogenic). (****p-value < 0.001, **p-value < 0.01, *p-value < 0.05; one-way ANOVA; Tukey).

that in fish fed the control and PHYTO supplemented diets. Fish fed PHYTO supplemented diet recorded significantly lower expression level of *zo-1* compared with that in fish fed the control and GMOS diets, whereas the expression of *ocln* was significantly downregulated in the gills of sea bass fed GMOS supplemented diet compared with that in fish fed the control and PHYTO supplemented diets.

Morphological Studies

Histopathological Examination of Gill

Histopathological evaluation of H&E-/MGG-stained sagittal and transverse gill sections of segments corresponding to the second and third right holobranch revealed a well-organized secondary and primary lamellar pattern and an intact epithelial barrier in fish fed the different experimental diets (**Figure 2**). However, some morphological changes were found at the end of the experimental period, such as telangiectasis, lamellar thrombosis (**Figures 3A**, **B**), and focal lamellar fusion, characterized by filling of the interlamellar space with proliferating PVCs (**Figure 3C**). The incidence of lamellar fusion was significantly ($p < 0.05$) lower in fish fed the PHYTO supplemented diet than that in fish fed the control diet. However, the MRC size and density and the inflammation status of the gills were not significantly ($p > 0.05$) affected by GMOS and PHYTO, as the gills exhibited similar lymphocyte and granulocyte infiltration levels (**Table 3** and **Figures 4C–E**).

Transverse sections of the epithelial basal area of the gill arch showed clear variations in the disposition of epithelial cell nuclei in relation to the basement membrane (**Figures 4A–C**); the basal epithelial cells presented elongated cells with a central and perpendicular nuclei disposition, whereas mid epithelial cells presented a round shape with the nucleus situated parallel to the basement membrane. The surface epithelial cells presented a flat morphology with nuclei parallel to the basement membrane. Goblet cells were dispersed among the surface epithelial cells (**Figures 4B, C**). GMOS and PHYTO did not significantly affect the morphology and number of interbranchial lymphoid tissue (ITL), lymphocytes, granulocytes, and rodlet cells (**Figures 4D–F** and **Table 3**).

Gill Mucus Production

GMOS and PHYTO did not significantly affect goblet cell count and distribution. An examination of the longitudinal holobranch sections showed that goblet cells along the primary lamella were located at high density in the interlamellar spaces (between secondary lamellae) (**Figure 5A**), surrounding and protecting the top region of the primary lamella (**Figure 5B**), as well as protecting the lymphoid tissue located at the base of the primary lamellae (**Figures 5C, D**). Although the morphometric characteristics of the goblet cell was not significantly ($p > 0.05$) affected by the supplements, the goblet cell area in the gills of fish fed the GMOS and PHYTO diets reduced by 11 and 5%, respectively, compared to the goblet cell area of the gills of fish fed the control diet (**Table 4**).

Gill Immunohistochemistry

Immunoreactivity to anti-PCNA and anti-iNOS-2 was detected in all fish gill sections studied (**Figure 6**). The presence of PCNA+ cells in the gill epithelium of fish fed the GMOS and PHYTO diets was lower than that in the gill epithelium of fish fed the control diet (**Figure 7**). The presence of anti-iNOS-2 in the gills was not significantly affected by the supplements (**Figures 6C, D**). Gill goblet cells, several leukocytes, and MCRs were immunopositive for anti-iNOS (**Figures 6C, D**).

Gill Ultrastructure

The results of the qualitative TEM analysis showed that the ultrastructure of the gills was not affected by the dietary

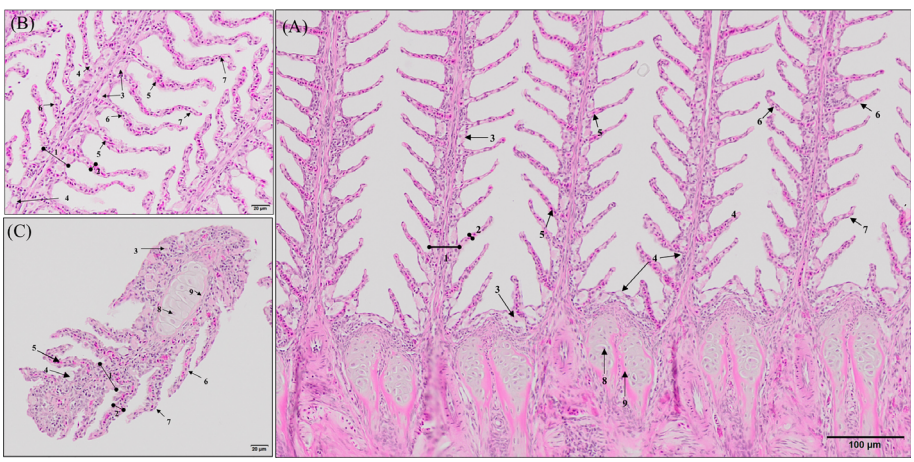

FIGURE 2 | General morphology of European sea bass (*Dicentrarchus labrax*) gill. **(A, B)** Representative micrograph of a longitudinal section of the central segment corresponding to the second right holobranch. (Hematoxilin–Eosin; Bar = 100 & 20 µm). **(C)** Representative micrograph of a transversal section in the middle part of the second right holobranch. (Hematoxilin–Eosin; Bar = 20 µm). (1) Primary lamella, (2) Secondary lamella, (3) Chloride cell, (4) Goblet cell, (5) Erythrocytes, (6) Pilar cell, (7) Epithelial cell, (8) Chondrocytes, (9) Extracellular cartilaginous matrix.

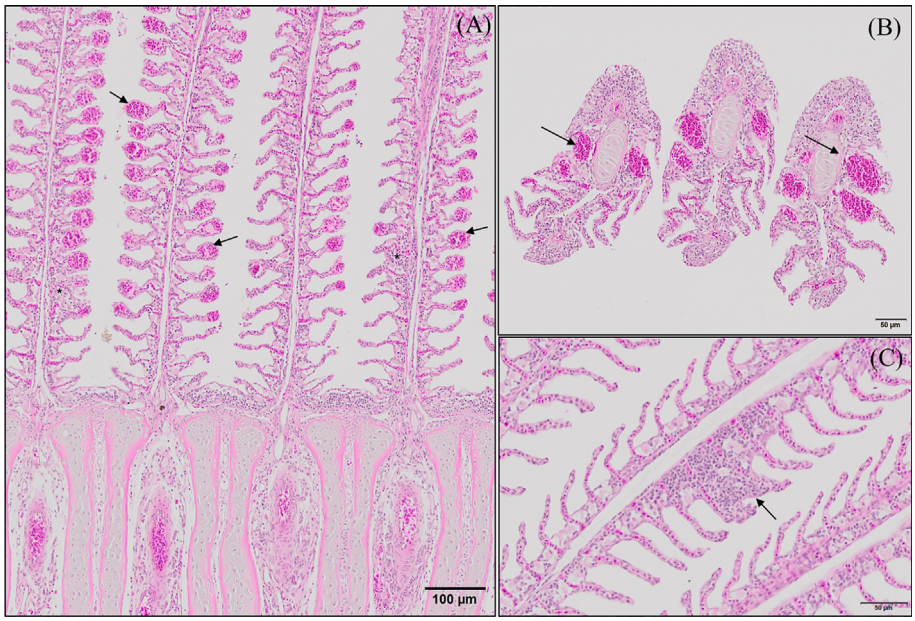

FIGURE 3 | Representative micrographs of the main morphological alterations found at the end of the experimental period on European sea bass (*Dicentrarchus labrax*) gills. **(A, B)** Longitudinal and transversal sections of the primary lamellae where severe telangiectasis and/or lamellar thrombosis are indicated with arrows (Hematoxilin–Eosin; Bar = 100 & 50 µm). Focal lamellar fusion is indicated with symbols (*). **(C)** Detail of primary lamella focal lamellar fusion. Observe the filling of interlamellar space with proliferating pavement cells. (Hematoxilin–Eosin; Bar = 50 µm). Fish fed PHYTO diet presented reduced incidence ($p < 0.05$) of lamellar fusion compared to fish fed the rest of the dietary treatments.

TABLE 3 | Semi quantitative evaluation of the main histopathological alterations found in the gills of juvenile European sea bass (*Dicentrachus labrax*) at the end of the feeding trial (63 days).

	Dietary treatments		
	C	GMOS	PHYTO
Lamellar fusion	1-2^{a}	1-2^{ab}	0-1^{b}
Lamellar telangiectasis/aneurysms	0-1	0-1	0
MRCs cell hyperplasia	1-2	1-2	1
General gill inflammation	1-2	1-2	1-2
ILT infiltrated leucocytes	1-2	1-2	1-2
ILT infiltrated granulocytes	1-2	1-2	1-2

*1 (weak), 2 (moderate) and 3 (strong) for each parameter evaluated. Diets: C (control diet), GMOS (5000 ppm galactomannan oligosaccharides), PHYTO (200ppm phytogenic). Gill main histopathological alteration detailed in **Figure 2**. Different letters within a row denote significant differences among dietary treatments ($p \leq 0.05$; Kruskal-Wallis for independent samples; U Mann-Whitney tests).*

functional additives, as the gills were healthy. The gills exhibited normal appearance of secondary and primary lamellar membrane linings; normal junctional unions between cells; and normal leukocytes, pilar cells, PVCs, MRCs, and goblet cell structure and distribution. Additionally, the structure of the microridges was unaffected (**Figure 8**). Goblet cells containing secretory granules of variable electron density were in the primary lamellae, particularly in the interlamellar space between secondary lamellae (**Figure 8D**). Pilar cells were characterized by a polymorphic nucleus with condensed heterochromatin at the nuclear periphery (**Figure 8B**), and red blood cells were localized within the blood space, both being enveloped by the collagen bundle (**Figures 8A–C**) and surrounded by PVCs. Surface PVC microridges were clearly observed (**Figure 8F**). TEM analysis showed the presence of leukocytes and granulocytes in the lamellae and interbranchial lymphoid tissue (**Figure 8E**). Like the result of the histopathological examination, GMOS and PHYTO did not significantly affect the leukocyte infiltration level and distribution of the gills. **Figure 8** shows the typical structure of the MRCs, where its crypt surrounded by PVCs can be observed. MRC morphology was normal in the fish, with electron dense microvilli in the upper region and a mitochondria-rich region in the basal region. GMOS and PHYTO did not significantly affect the morphology of the tubulovesicular system of the MRCs, the intercellular union, and the appearance of the membrane lining of the evaluated cells (**Figure 9**).

DISCUSSION

In the present study, GMOS and PHYTO induced a significant downregulation of the expression of several genes associated with the antioxidant defense system in gills, such as *sod*, *cat*, *gpx*, and *gr*, and this may be due to an improved scavenging of excess free radicals in the gills. Previous studies have demonstrated that some prebiotics of plant origin and PFAs, such as those derived from garlic and labiate plant extracts have a potent antioxidant activity

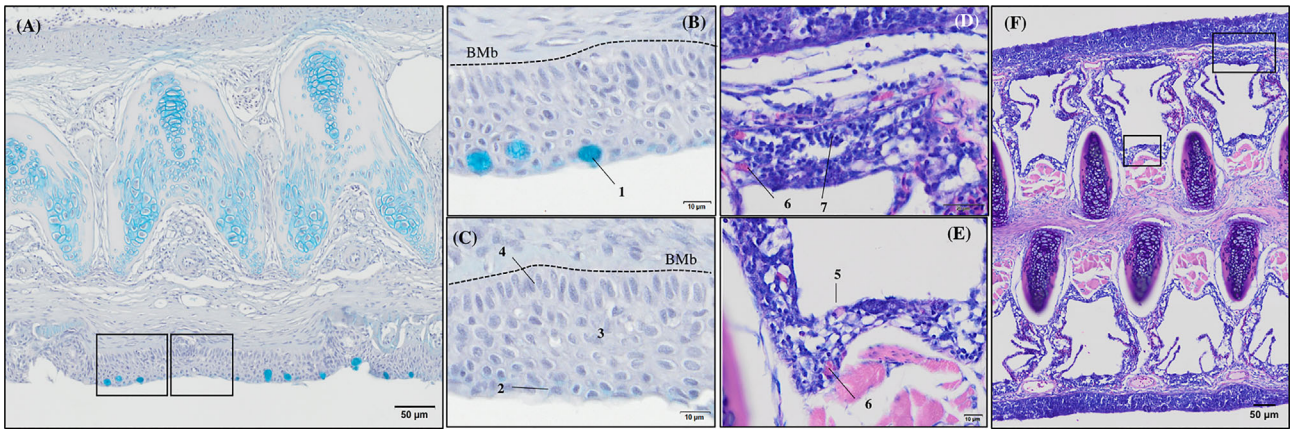

FIGURE 4 | General morphology of European sea bass (*Dicentrarchus labrax*) gill base section and gill associated lymphoid tissue leucocytes populations' distribution. **(A-C)** Representative micrograph of a transversal section of the gill base the second/third right holobranch (Alcian-Blue PAS, pH = 2.5; Bar = 50 & 10 µm). Observe the variations on the epithelial cells' nuclei orientation. **(D-F)** Representative transversal micrograph of the interbranchial lymphoid tissue (ILT) located at the gill base the second/third right holobranch (MGG; Bar = 50 & 10 µm). (1) Goblet cell, (2) surface epithelial cells, (3) mid epithelial cells, (4) basal epithelial cells, (5) rodlet cells, (6) granulocytes, (7) lymphocytes. BMb, basement membrane.

in fish (10, 40, 41, 43, 53–57). In this regard, dietary functional additives with systemic and local antioxidant capacity have been reported to act in both dose-dependent and time-dependent manner. Dietary PFAs increased fish antioxidant enzyme activity in plasma and target tissues in a dose-dependent manner, and reduced malondialdehyde (MDA) formation and tissue TBARS levels in some freshwater species, such as Nile tilapia (*Oreochromis niloticus*), rainbow trout (*Oncorhynchus mykiss*), and channel catfish (*Ictalurus punctatus*) (40, 42, 43, 58–60). Although rainbow trout juveniles fed a mixture of labiatae essential oils presented increased SOD, G6PD, and GPX activities after 30 days of feeding, the activities of CAT, GST, and GR were reduced after 60 days of dietary supplementation, while MDA concentration remained unaffected (42). A time-dependent regulation of an organism's antioxidant capacity may be associated with self-regulation of its antioxidant system activity after reducing ROS levels. Some studies on gills have shown a discrepancy between enzymatic activity and gene expression levels (61), supporting the notion of a time-dependent self-modulation of a tissue's antioxidant capacity, which does not always result in a positive correlation between enzymatic activity and gene expression levels.

Among the dietary supplements considered to be exogenous antioxidants or endogenous enzymatic activity enhancers of plant origin are flavonoids, plant polyphenols, allyl sulfides, and curcumin (23), some of which are present in plant extracts, garlic oil, and rich fiber extracts originating from plants and seeds. Flavonoids are phenolic substances with potent *in vitro* antioxidant properties because of their ability to reduce the formation of free radicals and scavenge free radicals. However, information available on their pharmacokinetics is limited and thus, the antioxidant activity of these compounds and their mode of action *in vivo* is poorly understood (62). Based on low plasma and tissue flavonoid concentration detected after their dietary supplementation, their significance as scavengers of free radicals was examined in higher vertebrates (63). The mode of action of flavonoids might be based on their ability to interact with several protein kinases, including mitogen-activated protein kinases (MAPKs), which is mediated *via* oxidative stress signaling cascades by several cellular reactions to vastly different stressors (63). MAPKs control the expression of endogenous antioxidant enzymes and regulate cell proliferation in several disease-associated processes, thus exerting a chemoprotective effect as modulators of oxidative stress-MAPK signaling pathways and complementing their antioxidant role scavengers of free radicals (63–66). Therefore, the observed downregulation of the expression levels of *sod, gpx, gr*, and *cat* in the gills of fish fed the supplemented diets may be partly due to the actions of GMOS and PHYTO, which regulated the endogenous antioxidant system and reduced the production of free radicals, through the MAPK signaling pathway. Furthermore, garlic derivatives, such as allyl sulfides are recognized as potent antioxidants, mainly because of their high capacity for the scavenging of free radicals (23), inhibition of leucocyte ROS production (67), control of lipid peroxidation (68, 69), and triggering of endogenous antioxidant activity (69, 70).

Protection of the gill against oxidative damage is important, as it is the site for gas exchange, osmoregulation, nitrogenous waste excretion, and pH regulation (71, 72). Furthermore, conserving the functional structure of the gill epithelium is essential for maintaining fish health, as it is continuously challenged by foreign substances and infectious agents (72). Authors of Ref. (61) examined oxidative stress in Atlantic salmon suffering from amoebic gill disease (AGD) reported reduced expression of *sod*, *cat*, and *gr* in non-affected gill areas compared with that in the affected areas (gill areas with lesion), indicating the negative effect of oxidative stress. Similarly, in the present study, we observed lower PCNA+ counts in the gills of

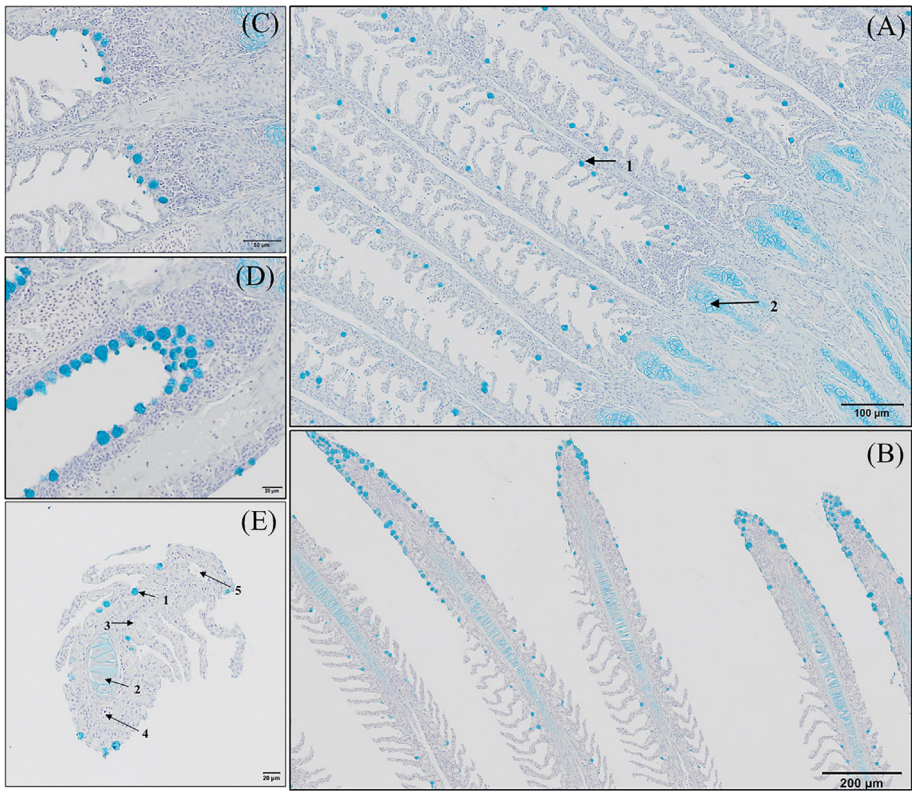

FIGURE 5 | Goblet cells distribution along the gill of European sea bass (*Dicentrarchus labrax*). **(A-D)** Longitudinal section corresponding to the central segment of the second right holobranch goblet cells distribution along the primary lamella (Alcian Blue pH = 2.5). Observe how primary lamella goblet cells are mainly located between secondary lamellae (**A**; Bar = 100 µm) and in higher density surrounding the top region of the primary lamella (**B**; Bar = 300 µm). Observe the increased density of goblet cells between basal regions of the primary lamellae in contact with the interbranchial gill associated lymphoid tissue (**C**, **D**; Bar = 50 & 20 µm). **(E)** Transversal section corresponding to the central segment of the second right holobranch goblet cells

TABLE 4 | Gill goblet cells morphometry of juvenile European sea bass (*Dicentrarchus labrax*) at the end of the feeding trial (63 days).

	Dietary treatments		
	C	**GMOS**	**PHYTO**
Area (µm²)	59.68 ± 4.91	53.10 ± 2.30	56.34 ± 2.94
Perimeter (µm)	38.90 ± 5.89	31.71 ± 0.72	34.47 ± 0.59
Mean radius (µm)	4.12 ± 0.20	3.93 ± 0.06	4.02 ± 0.13
Minimum diameter (µm)	6.29 ± 0.45	6.12 ± 0.09	6.11 ± 0.33

Diets: C (control diet), GMOS (5000 ppm galactomannan oligosaccharides), PHYTO (200ppm phytogenic). Morphometric studies carried out on transversal sections. Different letters within a row denote significant differences among dietary treatments ($p \leq 0.05$; one-way ANOVA; Tukey).

fish fed PHYTO and GMOS supplemented diets compared with that in the gills of fish fed the control diet. Changes in the production of PCNA in the mucosal epithelium could be an early symptom of alterations in tissue homeostasis. The upregulation of the expression of gene regulating PCNA is commonly used as a marker of proliferation associated with the development of neoplastic tissue (73–76), which may be induced by exposure to external or internal stressors. Authors of Ref. (77) detected strong immunopositivity for PCNA, iNOS, HSP70, and Bax in the gills of *Hypostomus francisci* exposed to prolonged anthropogenic influences. Therefore, the reduction in PCNA counts in the gills of the fish fed PHYTO and GMOS supplemented diets might be associated with reduced levels of oxidative species *via* a modulation of the endogenous antioxidant capacity. Garlic extract, such as flavonoids, ameliorated oxidative stress in rat cardiomyocytes by reducing the production of NO and H_2S (78, 79). Although GMOS and PHYTO did not significantly affect the iNOS concentration and inflammation status of the gills in the present study, in a parallel study (79), reported that GMOS and PHYTO at the same dose and test duration with that of the present study mitigated leucocytic apoptotic processes associated with stress in European sea bass at the genetic level. Fish fed the PHYTO supplemented diet had lower level of lamellar fusion and a tendency to reduce the incidence of lamellar telangiectasis and MRC hyperplasia. Although the distribution of goblet cells in the primary lamellae was unaffected by the supplements, fish fed GMOS supplemented diet presented a smaller goblet cell area compared with that in the control group, and this agrees with the

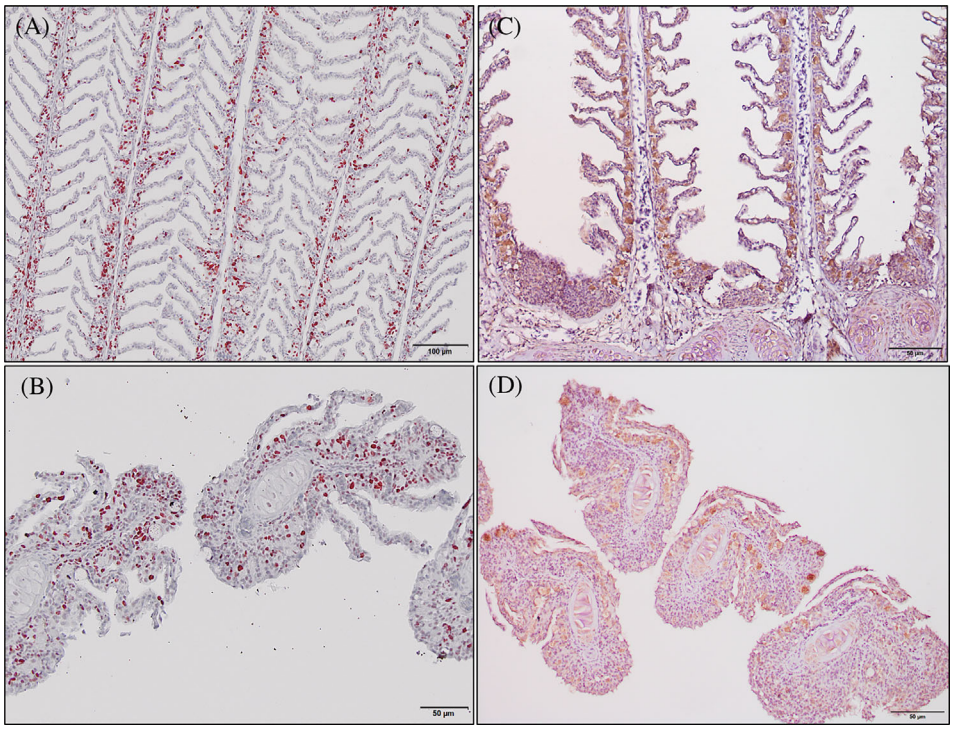

FIGURE 6 | Photomicrographs of the gill immunoreactivity with the antihuman anti-PCNA and anti-iNOS-2 antibodies at the end of the feeding trial. Immunoreactivity to anti-PCNA and anti-iNOS-2 was detected in all fish gills sections studied. European sea bass gill immunoreactivity to anti-PNCA antibody (**A**, **B**; Bars = 100 and 50 µm) and to anti-INOS-2 antibody (**C**, **D**; Bar = 50 µm).

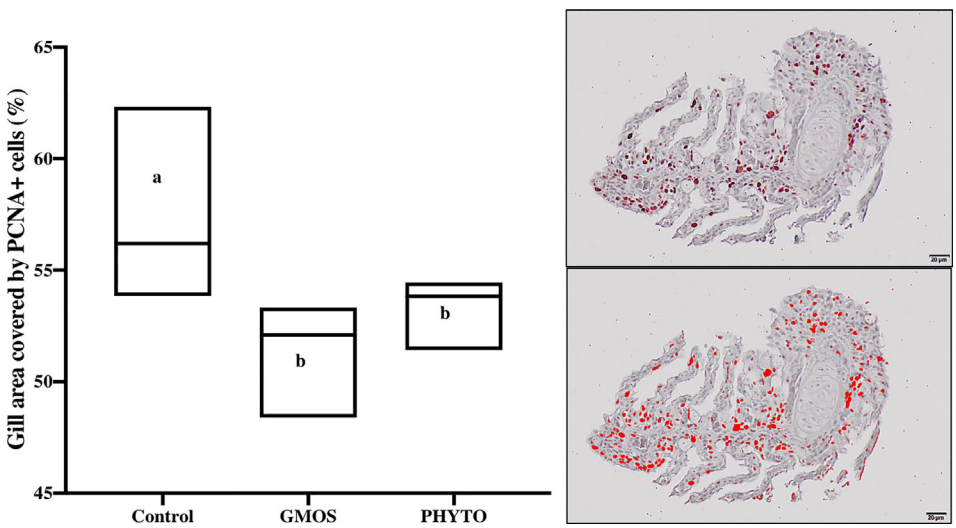

FIGURE 7 | Total gill epithelium covered by PCNA+ cells on transversal sections at the end of the feeding trial (63 days). Observe as fish fed GMOS and PHYTO diets presented lower coverage of PCNA+ cells compared to fish fed control diet. Boxes in boxplot represent mean ± SD. Different letters denote significant differences among dietary treatments ($p \leq 0.05$; oneway ANOVA; Tukey). Observe the automatically detected immunopositivity (marked in red) comparing the graph accompanying images.

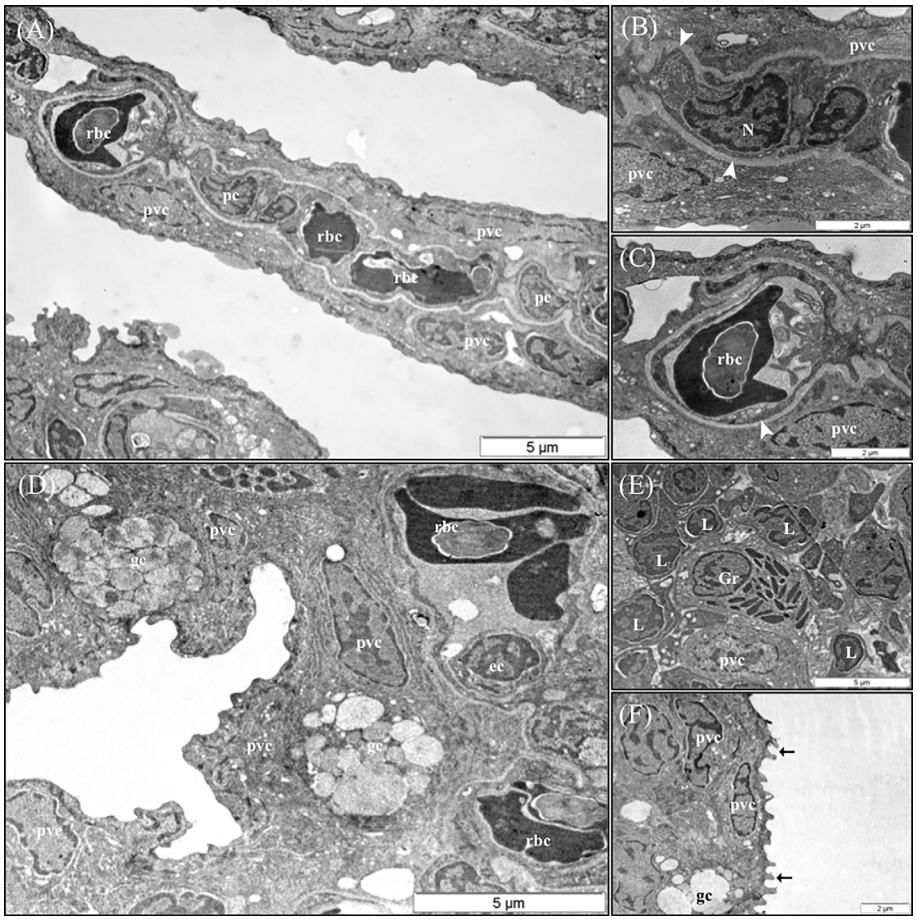

FIGURE 8 | Representative TEM micrographs of the gill of European sea bass (*Dicentrarchus labrax*) fed the different dietary treatments. No significant alterations on the structural pattern of healthy gills were observed among fish fed the different dietary treatments. **(A)** Cross-section through the secondary lamellae. Observe the polymorphic nucleus of pilar cells, the electron dense red blood cells within the blood spaces and pavement cells surrounding the collagen bundle. Scale bar 5 µm. Detailed micrograph pilar cell **(B)** and blood space **(C)**, observe the collagen bundle embracing both structures (arrowhead). Scale bars 2 µm. **(D)** Pattern of the space between two secondary lamellae, where goblet cells (gc) are located and surrounded by pavement cells. Epithelial cell visible inside the blood space. Scale bar 5 µm. **(E)** Detailed micrograph of interbranchial lymphoid tissue leucocytes population. Scale bar 5 µm. **(F)** Detail of pavement cells microridges. Scale bar 2 µm. pc, Pilar cells; rbc,red blood cells; pvc, pavement cells; gc, goblet cells; ec, ephitelial cell; Gr, granulocyte; L, Lymphocyte.

results of previous studies. Authors of Ref. (52) reported reduced intestinal goblet cell hyperplasia in European sea bass fed low FM/FO diets supplemented with GMOS and PHYTO. The change in goblet cell area may be because of an induced dysbiosis, which was produced by low dietary FM/FO diets (80). However, direct changes in the composition and consistency of gill mucus after functional diet supplementation, which may protect individual secondary lamellae from adhesion, should not be discarded because any potential change in the composition of gill mucus may affect the dynamics of pathogen invasion and persistence in the host (81).

In this regard, cell junctions play an important role in protecting the host's mucosal health (81, 82); however, as in other cultured fish species, the regulation of the functions of gill junctional complexes in European sea bass, particularly the roles of functional additives, is not well understood. Among the regulators of tight junctions are *zo-1* and *ocln*. In the present study, the expression of *ocln* was downregulated by GMOS, whereas *zo-1* showed an increasing trend; however, the opposite tendency was observed in fish fed PHYTO diet. The expression of certain genes related to the tight junction complex is involved in the response to environmental stressors, such as hypoxic stress (83–85) or pathogen exposure (82). In the present study, the gills of fish fed the functional diets had higher *zo-1* and *hsp70* expression levels and lower expression of *ocln*. In a similar study, we observed a downregulation of the expression of hypoxia inducible factor *(hif-1)*, lower cortisol levels, and a reduction in apoptosis in head kidney leucocytes after 2 h of stress by confinement in fish fed GMOS and PHYTO diets (79). An increase in the deposition of *ocln* and specific *claudins* was observed in the tight junctions of single-seeded insert cultures of PVCs from puffer fish (*Tetraodon nigroviridis*) in response to cortisol (86), thus, conditioning the permeability of the paracellular pathway. Variations in the expression of genes

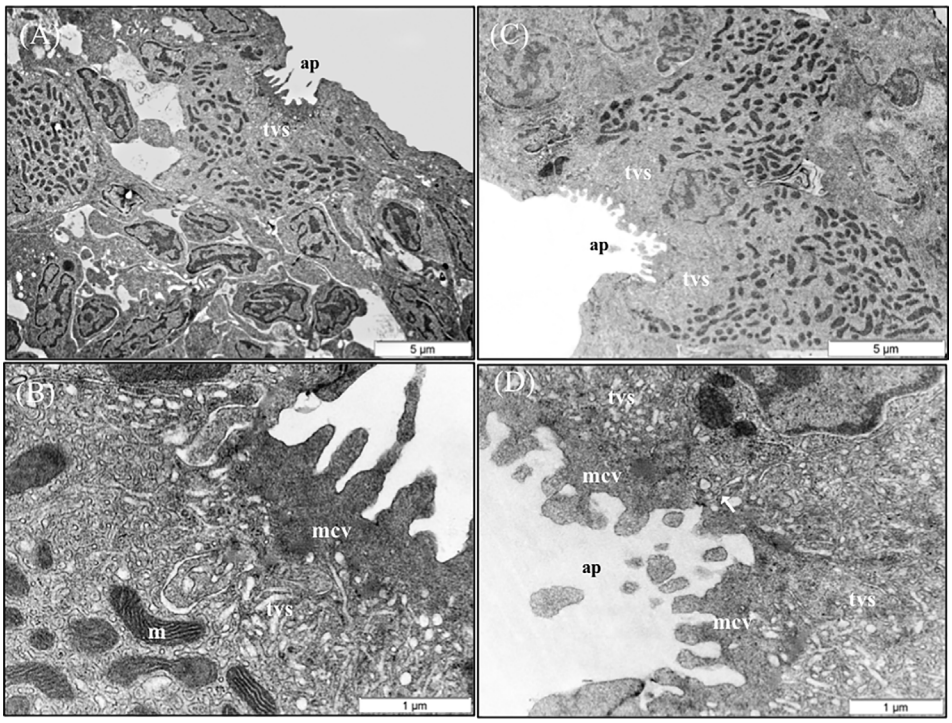

FIGURE 9 | TEM micrographs of mitochondria rich cells (MRCs) present in European sea bass primary lamellae. **(A)** The crypt of MRC is usually bordered by pavement cells. Scale bar 5 µm. **(B)** Detail of the apical region of MRC, observe the electron dense microvilli, the tubulovesicular system located just below the microvilli and the mitochondria rich region in the lower region. Scale bar 1 µm. **(C)** Two MRCs sharing one apical pit. Scale bar 5 µm. **(D)** Detail of two chloride cells sharing the same apical pit. Juctional unions are indicated by arrows. tvs, Tubulovesicular system; mvc, microvilli; ap, apical pit; m, mitochondria.

related to tight junction complexes might affect both the cellular reorganization of the cytoskeleton and bacterial binding (85).

GMOS and PHYTO dietary supplementation did not exert a clear effect on the morphology and density of the ITL-infiltrated leucocytes on a qualitative basis, the anti-inflammatory role of PFAs and GMOS and their effects on the ITL cytokine microenvironment and possible mechanisms involved on cytoskeleton rearrangement should be considered in future studies.

In conclusion, our findings indicated that dietary GMOS (5,000 ppm) and PHYTO (200 ppm) in 10%FM/6%FO-based diets protected the gill epithelia of European sea bass from oxidative stress by modulating the expression patterns of oxidative enzyme-related genes and lowering PCNA+ cell count. Moreover, PHYTO supplementation reduced lamellar fusion, whereas GMOS supplementation reduced goblet cell count by 11%, but did not affect the distribution goblet cells along the primary lamellae. These protective effects should be considered in future prevention strategies against gill mucosal diseases in fish species, especially those sensitive to gill-associated pathogens. Further studies should be conducted to establish the modes of action that are affected by each functional product under different scenarios of oxidative stress.

DATA AVAILABILITY STATEMENT

The datasets presented in this study can be found in online repositories. The names of the repository/repositories and accession number(s) can be found in the article/**Supplementary Material**.

ETHICS STATEMENT

The Bioethical Committee of the University of Las Palmas de Gran Canaria approved all the protocols used in the present study (approval no. 007/2012 CEBA ULPGC).

AUTHOR CONTRIBUTIONS

ST, MI, FA, and DM contributed to the conception and design of the study. ST performed formal analysis. ST, AS, and GT performed the statistical analyses. ST wrote the first draft of this manuscript. ST, MI, FA, and DM acquired funding. Resources were provided by ST, DM, VV-V, GT, and AM. All authors contributed to the article and approved the submitted version.

FUNDING

This work was funded by the Spanish Ministry of Economy, Industry and Competitiveness ("Subprograma Estatal de Generación de Conocimiento, en el marco del Plan Estatal de Investigación Científica y Técnica y de Innovación 2013-2016") by the PROINMUNOIL PLUS (AGL2016-79725-P) project: "Functional diets for marine raw materials replacement: boosting the fish disease resistance through epithelial barriers reinforcement and immunization tools," in which DM, ST, FA, MI and AS were involved. GT was responsible for the gene expression analyses, which were funded by the EU Horizon 2020 AquaIMPACT (Genomic and nutritional innovations for genetically superior farmed fish to improve efficiency in European aquaculture), number: 818367. Besides, the Spanish Ministry of Economy, Industry, and Competitiveness funded ST research though the "Subprograma Juan de la Cierva-Incorporación, Convocatoria 2015, IJCI2015-25748.

ACKNOWLEDGMENTS

Special thanks to Delacon Biotechnik GmbH and BioMar A/S, which provided the functional products and diets.

SUPPLEMENTARY MATERIAL

The Supplementary Material for this article can be found online at: https://www.frontiersin.org/articles/10.3389/fimmu.2021.663106/full#supplementary-material

REFERENCES

1. Carmona R, García-Gallego M, Sanz A, Domezaín A, Ostos-Garrido MV. Chloride Cells and Pavement Cells in Gill Epithelia of *Acipenser naccarii*: Ultrastructural Modifications in Seawater-Acclimated Specimens. *J Fish Biol* (2004) 64:553–66. doi: 10.1046/j.1095-8649.2003.00321.x
2. Lazado CC, Caipang CMA. Mucosal Immunity and Probiotics in Fish. *Fish Shellfish Immunol* (2014) 39:78–89. doi: 10.1016/j.fsi.2014.04.015
3. Lai KP, Li J-W, Gu J, Chan T-F, Tse WFK, Wong CKC. Transcriptomic Analysis Reveals Specific Osmoregulatory Adaptive Responses in Gill Mitochondria-Rich Cells and Pavement Cells of the Japanese Eel. *BMC Genomics* (2015) 16:1072. doi: 10.1186/s12864-015-2271-0
4. Perry SF. The Chloride Cell: Structure and Function in the Gills of Freshwater Fishes. *Annu Rev Physiol* (1997) 59:325–47. doi: 10.1146/annurev.physiol.59.1.325
5. Goss GG, Perr SF, Fryer JN, Laurent P. Gill Morphology and Acid–Base Regulation in Freshwater Fishes. *Comp Biochem Physiol* (1998) 119A:107–15. doi: 10.1046/j.1095-8649.2003.00321
6. Wilson JM, Laurent P, Tufts BL, Bemos DJ, Donowitz M, Vogl AW, et al. NaCl Uptake by the Branchial Epithelium in Freshwater Teleost Fish. An Immunological Approach to Ion-Transport Protein Localization. *J Exp Biol* (2000) 203:2279–96. doi: 10.1242/jeb.203.15.2279
7. Karnaky K, Kinter LB, Kinter WB, Stirling CE. Teleost Chloride Cell. II: Autoradiographic Localization of Gill Nafl, Kfl-ATPase in Killifish *Fundulus heteroclitus* Adapted to Low and High Salinity Environment. *J Cell Biol* (1976) 70:157–77. doi: 10.1083/jcb.70.1.157
8. Gomez D, Sunyer JO, Salinas I. The Mucosal Immune System of Fish: The Evolution of Tolerating Commensals While Fighting Pathogens. *Fish Shellfish Immunol* (2013) 35:1729–39. doi: 10.1016/j.fsi.2013.09.032
9. Merrifield DL, Rodiles A. *The Fish Microbiome and its Interactions With Mucosal Tissues*. BH Beck, E Peatman, editors. Mucosal Health in Aquaculture, Academic Press (2015) p. 273–29pp. doi: 10.1016/B978-0-12-417186-2.00010-8
10. Tovar-Ramírez D, Mazurais D, Gatesoupe J, Quazuguel P, Cahu C, Zambonino-Infante J. Dietary Probiotic Live Yeast Modulates Antioxidant Enzyme Activities Andgene Expression of Sea Bass (Dicentrarchus labrax) Larvae. *Aquaculture* (2010) 300:142–7. doi: 10.1016/j.aquaculture.2009.12.015
11. Rosety-Rodriguez M, Ordoñez FJ, Rosety M, Rosety JM, Ribelles A, Carrasco C. Morpho-Histochemical Changes in the Gills of Turbot, Scophthalmus maximus L., induced by sodium dodecyl sulfate. *Ecotoxicol Environ Saf* (2002) 51:223–8. doi: 10.1006/eesa.2001.2148
12. Oropesa-Jiménez AL, García-Cambero JP, Gómez-Gordo L, Roncero-Cordero V, Soler-Rodríguez F. Gill Modifications in the Freshwater Fish Cyprinus Carpio After Subchronic Exposure to Simazine. *Bull Environ Contam Toxicol* (2005) 74:785–92. doi: 10.1007/s00128-005-0650-y
13. Ballesteros ML, Bianchi GE, Carranza M, Bistoni MA. Endosulfan Acute Toxicity and Histomorphological Alterations in *Jenynsia multidentate* (Anablepidae, Cyprinodontiformes). *J Environ Sci Heal B* (2007) 42:351–7. doi: 10.1080/03601230701309577
14. Korkmaz N, Cengiz EI, Unlu E, Uysal E, Yanar M. Cypermethrin-Induced Histopathological and Biochemical Changes in Nile Tilapia (*Oreochromis niloticus*), and the Protective and Recuperative Effect of Ascorbic Acid. *Environ Toxicol Pharmacol* (2009) 28:198–205. doi: 10.1016/j.etap.2009.04.004
15. Abdel-Moneim AM, Abu El-Saad HMA, Hussein KH, Dekinesh SI. Gill Oxidative Stress and Histopathological Biomarkers of Pollution Impacts in Nile Tilapia From Lake Mariut and Lake Edku, Egypt. *J Aquat Anim Health* (2012) 24:148–60. doi: 10.1080/08997659.2012.675924
16. Almeida JA, Barreto RE, Novelli ELB, Castro FJ, Moron SE. Oxidative Stress Biomarkers and Aggressive Behavior in Fish Exposed to Aquatic Cadmium Contamination. *Neotrop Ichthyol* (2009) 7:103–8. doi: 10.1590/S1679-62252009000100013
17. Ighodaro OM, Akinloye OA. First Line Defence Antioxidants-Superoxide Dismutase (SOD), Catalase (CAT) and Glutathione Peroxidase (GPX): Their Fundamental Role in the Entire Antioxidant Defence Grid. *Alexandria Med J* (2018) 54:287–93. doi: 10.1016/j.ajme.2017.09.001
18. Di Giulio RT, Meyer JN. Reactive Oxygen Species and Oxidative Stress. In: RT Di Giulio, DE Hinton, editors. *The Toxicology of Fishes*. Boca Raton: CRC Press, Taylor and Francis Group (2008). p. 273–324.
19. Slaninova A, Smutna M, Modra H, Svobodova Z. A Review: Oxidative Stress in Fish Induced by Pesticides. *Neuro Endocrinol Lett* (2009) 30 Suppl 1:2–12.
20. Oksala NKJ, Ek,mekçi FG, Özsoy E, Kirankaya S, Kokkola T, Emecen G, et al. Natural Thermal Adaptation Increases Heat Shock Protein Levels and Decreases Oxidative Stress. *Redox Biol* (2014) 3:25–8. doi: 10.1016/j.redox.2014.10.003
21. Ikwegbue PC, Masamba P, Oyinloye BE, Kappo AP. Roles of Heat Shock Proteins in Apoptosis, Oxidative Stress, Human Inflammatory Diseases, and Cancer. *Pharmaceuticals (Basel)* (2017) 11(1):2. doi: 10.3390/ph11010002
22. Oruç EO, Usta D. Evaluation of Oxidative Stress Responses and Neurotoxicity Potential of Diazinon in Different Tissues of Cyprinus carpio. *Environ Toxicol Pharmacol* (2007) 23:48–55. doi: 10.1016/j.etap.2006.06.005
23. Moussa Z, Zaher MAJ, Saleh AA. Nonenzymatic Exogenous and Endogenous Antioxidants. *Intechopen* (2019). doi: 10.5772/intechopen.87778
24. Kurtutas EB. The Importance of Antioxidants Which Play the Role in Cellular Response Against Oxidative/Nitrosative Stress: Current State. *Nutr J* (2015) 15:71. doi: 10.1186/s12937-016-0186-5
25. Mirończuk-Chodakowska I, Witkowska AM, Zujko ME. Endogenous non-Enzymatic Antioxidants in the Human Body. *Adv Med Sci* (2018) 63:68–78. doi: 10.1016/j.advms.2017.05.005
26. Nimse SB, Palb D. Free Radicals, Natural Antioxidants, and Their Reaction Mechanisms. *RSC Adv* (2015) 5:27986. doi: 10.1039/C4RA13315C
27. Belló ARR, Fortes E, Belló-Klein A, Bello AA, Llesuy SF, Robaldo RB, et al. Lipid Peroxidation Induced by *Clinostomum truncatum* in Muscle of the Freshwater fish Rhamdia Quelen. *Dis Aquat Org* (2000) 42:233–6. doi: 10.3354/dao042233

28. Dautremepuits C, Betoulle S, Vernet G. Stimulation of Antioxidant Enzymes Levels in Carp (Cyprinus carpio L.) Infected by *Ptychobothrium sp.* (Cestoda). *Fish Shellfish Immunol* (2003) 15:467–71. doi: 10.1016/S1050-4648(03)00007-X
29. Marcogliese DJ, Brambilla LG, Gagné F, Gendron AD. Joint Effects of Parasitism and Pollution on Oxidative Stress Biomarkers in Yellow Perch Perca flavescens. *Dis Aquat Organ* (2005) 63:77–84. doi: 10.3354/dao063077
30. Stumbo AD, Goater CP, Hontela A. Parasite-Induced Oxidative Stress in Liver Tissue of Fathead Minnows Exposed to Trematode Cercariae. *Parasitol* (2012) 139:1666–71. doi: 10.1017/S0031182012001023
31. Mozhdeganloo Z, Heidarpour M. Oxidative Stress in the Gill Tissues of Goldfishes (Carassius auratus) Parasitized by Dactylogyrus spp. *J Parast Dis* (2014) 38:269–72. doi: 10.1007/s12639-013-0239-z
32. Mehjbeen J, Ahmad I, Usmani N, Ahmad M. Multiple Biomarjer Responses (Serum Biochesmistry, Oxidative Stress, Genotoxicity and Histopathology) in Channa Punctatus Exposed to Heavy Metal Loaded Wastewater. *Sci Rep* (2017) 7:1675. doi: 10.1038/s41598-017-01749-6
33. Edris AE. Pharmaceutical and Therapeutic Potentials of Essential Oils and Their Individual Volatile Constituents: A Review. *Phytother Res* (2007) 21:308–23. doi: 10.1002/ptr.2072
34. Bozin B, Mimica-Dukic N, Samojlik I, Jovin E. Antimicrobial and Antioxidant Properties of Rosemary and Sage (*Rosmarinus officinalis* L. and *Salvia officinalis* L., Lamiaceae) Essential Oils. *J Agric Food Chem* (2007) 55:7879–85. doi: 10.1021/jf0715323
35. Llana-Ruiz-Cabello M, Gutiérrez-Praena D, Puerto M, Pichardo S, Jos Á, Cameán AM. In Vitro Pro-Oxidant/Antioxidant Role of Carvacrol, Thymol and Their Mixture in the Intestinal Caco-2 Cell Line. *Toxicol In Vitro* (2015) 29:647–56. doi: 10.1016/j.tiv.2015.02.006
36. Khatua TN, Borkar RM, Mohammed SA, Dinda AK, Srinivas R, Banerjee SK. Novel Sulfur Metabolites of Garlic Attenuate Cardiac Hypertrophy and Remodeling Through Induction of Na+/K+-ATPase Expression. *Front Pharmacol* (2017) 8:18. doi: 10.3389/fphar.2017.00018
37. Wei HK, Xue HX, Zhou ZX, Peng J. A Carvacrol-Thymol Blend Decreased Intestinal Oxidative Stress and Influenced Selected Microbes Without Changing the Messenger RNA Levels of Tight Junction Proteins in Jejunal Mucosa of Weaning Piglets. *Animal* (2017) 11:193–201. doi: 10.1017/S1751731116001397
38. Gomaa AMS, Abdelhafez AT, Aamer HA. Garlic (*Allium sativum*) Exhibits a Cardioprotective Effect in Experimental Chronic Renal Failure Rat Model by Reducing Oxidative Stress and Controlling Cardiac Na+/K+-ATPase Activity and Ca2+ Levels. *Cell Stress Chaperones* (2018) 23:913–20. doi: 10.1007/s12192-018-0898-x
39. Kykkidou S, Giatrakou V, Papavergou A, Kontominas MG, Savvaidis IN. Effect of Thyme Essential Oil and Packaging Treatments on Fresh Mediterranean Swordfish Fillets During Storage At 4°C. *Food Chem* (2009) 115:169–75. doi: 10.1016/j.foodchem.2008
40. Giannenas I, Triantafillou EL, Stavrakakis S, Margaroni M, Mavridis S, Steiner T, et al. Assessment of Dietary Supplementation With Carvacrol or Thymol Containing Feed Additives on Performance, Intestinal Microbiota and Antioxidant Status of Rainbow Trout (Oncorhynchus mykiss). *Aquaculture* (2012) 350–353:26–32. doi: 10.1016/j.aquaculture.2012.04.027
41. Nya EJ, Austin B. Development of Immunity in Rainbow Trout (Oncorhynchus mykiss, Walbaum) to Aeromonas Hydrophila After the Dietary Application of Garlic. *Fish Shellfish Immunol* (2011) 30:845–50. doi: 10.1016/j.fsi.2011.01.008
42. Sönmez Y, Bilen S, Alk G, Hisar I, Yanik T, Biswas G. Growth Performance and Antioxidant Enzyme Activities in Rainbow Trout (Oncorhynchus mykiss) Juveniles Fed Diets Supplemented With Sage, Mint and Thyme Oils. *Fish Physiol Biochem* (2015) 41:165–75. doi: 10.1007/s10695-014-0014-9
43. Amer AA, Metwally AE, Ahmed SAA. The Influence of Dietary Supplementation of Cinnamaldehyde and Thymol on the Growth Performance, Immunity and Antioxidant Status of Monosex Nile Tilapia Fingerlings *(Oreochromis niloticus). Egypt J Aquat Res* (2018) 44:251–6. doi: 10.1016/j.ejar.2018.07.004
44. Bauerova K, Ponist S, Navarova J, Dubnickova M, Paulovicova E, Pajtinka M, et al. Glucomannan in Prevention of Oxidative Stress and Inflammation Occurring in Adjuvant Arthritis. *Neuro Endocrinol Lett* (2008) 29:691–6. doi: 10.2478/v10102-011-007-9
45. AOAC. *Official Methods of Analysis*. Washington, DC: Association of Official Analytical Chemists (2000).
46. Folch J, Lees M, Sloane-Stanley GH. A Simple Method for the Isolation and Purification of Total Lipids From Animal Tissues. *J Biol Chem* (1957) 226:497–509. doi: 10.1016/S0021-9258(18)64849-5
47. Livak KJ, Schmittgen TD. Analysis of Relative Gene Expression Data Using Real-Time Quantitative PCR and the 2(-Delta Delta C(T)) Method. *Methods* (2001) Dec25(4):402–8. doi: 10.1006/meth.2001.1262
48. Martoja R, Martoja-Pierson M. *Técnicas De Histología Animal*. Barcelona: Toray-Masson S.A (1970).
49. Hoffman EO, Flores TR, Coover J, Garret HB. Polychrome Stains for High Resolution Light Microscopy. *Lab Med* (1983) 14:779–81. doi: 10.1093/labmed/14.12.779
50. Sokal RR, Rolf SJ. *Biometry. The Principles and Practice of Statistics in Biological Research. 3rd Ed*. New York: Freeman (1995).
51. Fowler J, Cohen L, Jarvis P. *Practical Statistics for Field Biology*. NewYork: Wiley (1998).
52. Torrecillas S, Terova G, Makol A, Serradell A, Valdenegro V, Gini E, et al. Dietary Phytogenics and Galactomannan Oligosaccharides in Low Fish Meal and Fish Oil-Based Diets for European Sea Bass (Dicentrarchus labrax) Juveniles: Effects on Gut Health and Implications on In Vivo Gut Bacterial Translocation. *PloS One* (2019) 14(9):e0222063. doi: 10.1371/journal.pone.0222063
53. Volpatti D, Bulfon C, Tulli F, Galeotti M. Growth Parameters, Innate Immune Response and Resistance to *Listonella* (*vibrio*) *anguillarum* of *Dicentrarchus labrax* Fed Carvacrol Supplemented Diets. *Aquac Res* (2013) 45(1):31–44. doi: 10.1111/j.1365-2109.2012.03202.x
54. Awad E, Awaad AS, Esteban MA. Effects of Dihydroquercetin Obtained From Deodar (Cedrus Deodara) on Immune Status of Gilthead Seabream (Sparus aurata L.) *Fish Shellfish Immunol* (2015) 43:43–50. doi: 10.1016/j.fsi.2014.12.009
55. Guardiola FA, Bahu A, Bakhrouf A, Esteban MA. Effects of Dietary Supplementation With Fenugreek Seeds, Alone or in Combination With Probiotics, on Gilthead Seabream (Sparus aurata L.) Skin Mucosal Immunity. *Fish Shellfish Immunol* (2017) 65:169–78. doi: 10.1016/j.fsi.2017.04.014
56. Lillehoj H, Liu Y, Calsamiglia S, Fernández-Miyakawa ME, Chi F, Cravens RL, et al. Phytochemicals as Antibiotic Alternatives to Promote Growth and Enhance Host Health. *Vet Res* (2018) 49:76. doi: 10.1186/s13567-018-0562-6
57. Hoseinifar SH, Sun YZ, Zhou Z, Van Doan H, Davies JR, Harikrishnan R. Boosting Immune Function and Disease Biocontrol Through Environment-Friendly and Sustainable Approaches in Finfish Aquaculture: Herbal Therapy Scenarios. *Rev Fisheries Sci Aquaculture* (2020) 28:303–27. doi: 10.1080/23308249.2020.1731420
58. Zheng ZL, Tan JYW, Liu HY, Zhou XH, Xiang X, Wang KY. Evaluation of Oregano Essential Oil (*Origanum heracleoticum* L.) on Growth, Antioxidant Effect and Resistance Against *Aeromonas hydrophila* in Channel Catfish (*Ictalurus punctatus*). *Aquaculture* (2009) 292:214–8. doi: 10.1016/j.aquaculture.2009.04.025
59. Al-Sagheer AA, Mahmoud HK, Reda FM, Mahgoub SA, Ayyat MS. Supplementation of Diets for Oreochromis Niloticus With Essential Oil Extracts From Lemongrass (Cymbopogon citratus) and Geranium (Pelargonium graveolens) and Effects on Growth, Intestinal Microbiota, Antioxidant and Immune Activities. *Aquacult Nutr* (2018) 24:1006–14. doi: 10.1111/anu.12637
60. Mohebbi A, Nematollahi A, Dorcheh EE, Asad FG. Influence of Dietary Garlic (*Allium sativum*) on the Antioxidative Status of Rainbow Trout (*Oncorhynchus mykiss*). *Aquacult Res* (2012) 43:1184–93. doi: 10.1111/j.1365-2109.2011.02922.x
61. Marcos-López M, Espinosa Ruiz C, Rodger HD, O´Connor I, MacCarthy E, Esteban MA. Local and Systemic Humoaral Immune Response in Farmed Atlantic Salmon (Salmo salar L.) Under a Natural Amoebic Gill Disease Outbreak. *Fish Shellfish Immunol* (2017) 66:207–16. doi: 10.1016/j.fsi.2017.05.029
62. Pietta PG. Flavonoids as Antioxidants. *J Nat Prod* (2000) 63:1035–42. doi: 10.1021/np9904509
63. Brunetti C, Di Ferdinando M, Fini A, Pollastri S, Tattini M. Flavonoids as Antioxidants and Developmental Regulators: Relative Significance in Plants and Humans. *Int J Mol Sci* (2013) 14:3540–55. doi: 10.3390/ijms14023540
64. Surth YJ. Cancer Chemoprevention With Dietary Phytochemicals. *Nat Rev Cancer* (2003) 3:768–80. doi: 10.1038/nrc1189

65. Hu R, Kong AN. Activation of MAP Kinases, Apoptosis and Nutrigenomics of Gene Expression Elicited by Dietary Cancer-Prevention Compounds. *Nutrition* (2004) 20:83–8. doi: 10.1016/j.nut.2003.09.015
66. Chen C, Kong AN. Dietary Cancer-Chemopreventive Compounds: From Signaling and Gene Expression to Pharmacological Effects. *Trends Pharmacol Sci* (2005) 26:318–26. doi: 10.1016/j.tips.2005.04.004
67. Schepetkin IA, Kirpotina LN, Khlebnikov AI, Balasubramanian N, Quinn MT. Neutrophil Immunomodulatory Activity of Natural Organosulfur Compounds. *Molecules* (2019) 24:1809. doi: 10.3390/molecules24091809
68. Augusti KT, Sheela CG. Antiperoxide Effect of S-allyl Cysteine Sulfoxide, an Insulin Secretagogue, in Diabetic Rats. *Experientia* (1996) 52:115–20. doi: 10.1007/BF01923354
69. Metwally MAA. Effects of Garlic (Allium Sativum) on Some Antioxidant Activities in Tilapia Nilotica (Oreochromis Niloticus). *WJFMS* (2009) 1:56–64.
70. Mosbah A, Guerbej H, Boussetta H, Bouraoui Z, Banni M. Protective Effects of Dietary Garlic Powder Against Cadmium-Induced Toxicity in Sea Bass Liver: A Chemical, Biochemical, and Transcriptomic Approach. *Biol Trace Elm Res* (2018) 183:370–8. doi: 10.1007/s12011-017-1146-4
71. Evans DH, Piermarini PM, Choe KP. The Multifunctional Fish Gill: Dominant Site of Gas Exchange, Osmoregulation, Acid-Base Regulation, and Excretion of Nitrogenous Waste. *Physiol Rev* (2005) 85:97–177. doi: 10.1152/physrev.00050.2003
72. Koppang EO, Kvelelstad, Fisher U. *Fish Mucosal Immunity: Gill*. BH Beck, E Peatman, editors. Mucosal Health in Aquaculture, Academic Press (2015) p. 93–133. doi: https://doi.org/10.1016/B978-0-12-417186-2.00005-4
73. Manera M, Biavati S. An Immuno-Histochemical Technique Used to Demonstrate the Transition Form of a Squamous Cell Carcinoma in a Mirror Carp, Cyprinus carpio L. *J Fish Dis* (1994) 17:93–6. doi: 10.1111/j.1365-2761.1994.tb00349.x
74. Bunton TE. Brown Bullhead (Ameiurus Nebulosus) Skin Carcinogenesis. *Exp Toxic Pathol* (2000) 52:209–20. doi: 10.1016/S0940-2993(00)80031-7
75. Haramis APG, Hurlstone A, van der Velden Y, Begthel H, van den Born M, Offerhaus GJA, et al. Adenomatous Polyposis Coli-Deficient Zebrafish are Susceptible to Digestive Tract Neoplasia. *EMBO Rep* (2006) 7:444–9. doi: 10.1038/sj.embor.7400638
76. Dezfuli BS, Giari L, Lui A, Squerzanti S, Cataldelli G, Shinn AP. Proliferative Cell Nuclear Antigen (PCNA) Expression in the Intestine of *Salmo trutta trutta* Naturally Infected With an Acanthocephalan. *Parasites Vectors* (2012) 5:198. doi: 10.1186/1756-3305-5-198
77. Ferreira Sales C, Enes dos Santos P, Rizzo E, Maciel de Azambuja Ribeiro RI, dos Santos HB, Thomé RG. Proliferation, Survival and Cell Death in Fish Gills Remodeling: From Injury to Recovery. *Fish Shellfish Immunol* (2017) 68:10–8. doi: 10.1016/j.fsi.2017.07.001
78. Louis XL, Murphy R, Thandapilly SJ, Yu L, Netticadan T. Garlic Extracts Prevent Oxidative Stress, Hypertrophy and Apoptosis in Cardiomyocytes: A Role for Nitric Oxide and Hydrogen Sulfide, BMC Complement. *Altern Med* (2012) 12:110. doi: 10.1186/1472-6882-12-140
79. Serradell A, Torrecillas S, Makol A, Valdenegro V, Fernández-Montero A, Acosta F, et al. Prebiotics and Phytogenics Functional Additives in Low Fish Meal and Fish Oil Based Diets for European Sea Bass (Dicentrarchus labrax): Effects on Stress and Immune Responses. *Fish Shellfish Immunol* (2020) 100:219–29. doi: 10.1016/j.fsi.2020.03.016
80. Rimoldi S, Torrecillas S, Montero D, Gini E, Makol A, Valdenegro VV, et al. Assessment of Dietary Supplementation With Galactomannan Oligosaccharides and Phytogenics on Gut Microbiota of European Sea Bass (Dicentrarchus labrax) Fed Low Fishmeal and Fish Oil-Based Diet. *PloS One* (2020) 15:e0231494. doi: 10.1371/journal.pone.0231494
81. Peatman E, Lange M, Zhao H, Beck BH. Physiologu and Immunology of Mucosal Barriers in Catfish (Ictalurus Spp.). *Tissue Barriers* (2015) 3:4, e1068907. doi: 10.1080/21688370.2015.1068907
82. Li C, Zhang Y, Wang R, Lu J, Nandi S, Mohanty S, et al. RNA-Seq Analysis of Mucosal Immune Responses Reveals Signatures of Intestinal Barrier Disruption and Pathogen Entry Following Edwardsiella Ictaluri Infection in Channel Catfish, Ictalurus Punctatus. *Fish Shellfish Immunol* (2012) 32:816–27. doi: 10.1016/j.dci.2011.03.006
83. Zhang J, Liss M, Wolburg H, Blasig IE, Abdelilah-Seyfried S. Involvement of Claudins in Zebrafish Brain Ventricle Morphogenesis. *Ann N Y Acad Sci* (2012) 1257:193–8. doi: 10.1111/j.1749-6632.2012.06507.x
84. Kolosov D, Chasiotis H, Kelly SP. Tight Junction Protein Gene Expression Patternsand Changes in Transcript Abundance During Development of Modelfish Gill Epithelia. *J Exp Biol* (2014) 15:217:1667–81. doi: 10.1242/jeb.098731
85. Sun L, Liu S, Bao L, Li Y, Feng J, Liu Z. Claudin Multigene Family in Channel Catfish and Their Expression Profiles in Response to Bacterial Infection and Hypoxia as Revealed by Meta-Analysis of RNA-Seq Datasets. *Comp Biochem Physiol Part D Genomics Proteomics* (2015) 13:60–9. doi: 10.1016/j.cbd.2015.01.002
86. Bui P, Bagherie-lachidan M, Kelly SP. Cortisol Differentially Alters Claudin Isoforms in Cultured Puffer Fish Gill Epithelia. *Mol Cell Endocrinol* (2010) 317:120–6.

Conflict of Interest: Author AM and VV-V were employed by company Delacon Biotechnik GmbH and Biomar A/S, respectively.

The remaining authors declare that the research was conducted in the absence of any commercial or financial relationships that could be construed as a potential conflict of interest.

frontiers in Immunology

ORIGINAL RESEARCH
published: 25 June 2021
doi: 10.3389/fimmu.2021.696803

Oral Administration of *Lactococcus lactis* Producing Interferon Type II, Enhances the Immune Response Against Bacterial Pathogens in Rainbow Trout

*Alvaro Santibañez[1,2], Diego Paine[1,2], Mick Parra[1,2], Carlos Muñoz[1,2], Natalia Valdes[1,2], Claudia Zapata[1,2], Rodrigo Vargas[1], Alex Gonzalez[3] and Mario Tello[1,2,4]**

[1] Departamento de Biología, Laboratorio de Metagenómica Bacteriana, Facultad de Química y Biología, Universidad de Santiago de Chile, Santiago, Chile, [2] Consorcio Tecnológico de Sanidad Acuícola, Ictio Biotechnologies S.A., Santiago, Chile, [3] Laboratorio de Microbiología Ambiental y Extremófilos, Departamento de Ciencias Biológicas, Universidad de los Lagos, Osorno, Chile, [4] IctioBiotic SpA, Santiago, Chile

OPEN ACCESS

Edited by:
Peter Bossier,
Ghent University, Belgium

Reviewed by:
Kerry Lynne Bartie,
University of Stirling, United Kingdom
Patricia Diaz-Rosales,
Centro de Investigación en Sanidad Animal (CISA), Spain

***Correspondence:**
Mario Tello
mario.tello@usach.cl

Specialty section:
This article was submitted to Comparative Immunology, a section of the journal Frontiers in Immunology

Received: 17 April 2021
Accepted: 08 June 2021
Published: 25 June 2021

Citation:
Santibañez A, Paine D, Parra M, Muñoz C, Valdes N, Zapata C, Vargas R, Gonzalez A and Tello M (2021) Oral Administration of Lactococcus lactis Producing Interferon Type II, Enhances the Immune Response Against Bacterial Pathogens in Rainbow Trout. Front. Immunol. 12:696803. doi: 10.3389/fimmu.2021.696803

Lactic acid bacteria are a powerful vehicle for releasing of cytokines and immunostimulant peptides at the gastrointestinal level after oral administration. However, its therapeutic application against pathogens that affect rainbow trout and Atlantic salmon has been little explored. Type II interferon in Atlantic salmon activates the antiviral response, protecting against viral infection, but its role against bacterial infection has not been tested *in vivo.* In this work, through the design of a recombinant lactic acid bacterium capable of producing Interferon gamma from Atlantic salmon, we explore its role against bacterial infection and the ability to stimulate systemic immune response after oral administration of the recombinant probiotic. Recombinant interferon was active *in vitro*, mainly stimulating IL-6 expression in SHK-1 cells. *In vivo*, oral administration of the recombinant probiotic produced an increase in IL-6, IFNγ and IL-12 in the spleen and kidney, in addition to stimulating the activity of lysozyme in serum. The challenge trials indicated that the administration of the IFNγ-producing probiotic doubled the survival in fish infected with *F. psychrophilum*. In conclusion, our results showed that the oral administration of lactic acid bacteria producing IFNγ managed to stimulate the immune response at a systemic level, conferring protection against pathogens, showing a biotechnological potential for its application in aquaculture.

Keywords: *Lactococcus lactis*, interferon type II, *Flavobacterium psychrophilum*, salmonids, oral administration

INTRODUCTION

Interferons are a group of cytokines originally discovered by its antiviral properties (1). In mammals, these cytokines can be classified in three families according their homology, receptors, structure and function (2). Interferon types I and III are multi-gene families (17 type I and four type III) strongly induced by viruses, playing a major role controlling viral infection (3–5). Interferon

type I also show a strong pro-apoptotic and anti-proliferative activity, being currently applied in anticancer and antiviral therapies (6).

In contrast, interferon type II or gamma Interferon (IFNγ) is a single gene encoded immunoregulatory cytokine, produced mainly by activated Natural Killer (NK) and T lymphocytes (T cells), although also can be secreted by B lymphocytes (B cells) and professional antigen-presenting cells (APCs) (7–9). Besides its antiviral properties, IFNγ also allows the activation of macrophages, improves the antigen presentation and induction of Major Histocompatibility Complex (MHC)-peptides complexes, regulates the T cell polarization, regulates the CD8 T cell homeostasis, stimulates apoptosis and improves the antimicrobial mechanism against intracellular bacteria or parasites (8, 10–12). IFNγ is clinically used against infection in patients with Chronic Granulomatous Disease, although it is also effective against *Mycobacterium tuberculosis*, Salmonella and fungal infection (13–16).

Teleost and mammalian immune systems show several parallels in innate and acquired immunity. Bioactivity assays using recombinant IFNγ from *Salmo salar* or *Oncorhynchus mykiss* have shown this cytokine is able to induce the expression of MHC-I, MHC-II and proteins related to the processing of the antigens and increase the respiratory burst of phagocytic cells (17–20). *In vitro*, IFNγ from *S. salar* also has antiviral properties against Salmonid Alphavirus (SAV) and Infectious Pancreatic Necrosis Virus (IPNV) (21). Moreover, in *O. mykiss* cells, IFNγ is able to reduce *in vitro* the load of *Piscirickettsia salmonis*, suggesting that in salmonids, as in mammals, IFNγ also has antibacterial properties (22).

IFNγ has the potential to be used as a therapeutic or prophylactic treatment against bacterial and viral pathogens from salmonid aquaculture. However, the application of these cytokines has been limited due to the lack of a feasible vehicle of delivery compatible with the fish physiology.

In the last decades, Lactic Acid Bacteria (LAB) have risen as a feasible vehicle for the *in situ* delivery of cytokines and bioactive peptides inside of the gastrointestinal tract of mammalians (23, 24). Alpha Interferon (IFNα) (25–27), beta Interferon (IFNβ) (28), IFNγ (29, 30), and IL-10 (31) have been successfully expressed in LAB under its biologically functional form, producing local and systemic effects after administration to animals.

In *S. salar* and *O. mykiss* the use of LAB for *in situ* delivery of bioactive proteins has been poorly explored, being used only for delivery of antigenic peptides (32, 33). In this work we use *Lactococcus lactis* for the expression of a functional IFNγ from *S. salar*. The oral administration of this modified LAB reduces the susceptibility of treated fish against *F. psychrophilum* infection, an important bacterium that affects the salmonid industry.

MATERIALS AND METHODS

Construction of MT009 Strain

The gene encoding for the recombinant IFNγ from *S. salar* (rIFNγ) was designed *in silico* using the protein sequence of type II interferon from *S. salar* (FJ263446.1), the Usp45 Signal peptide (SP), the tag GGGHHHHHH, and the promotor P1 of *L. lactis*. The Usp45 SP, type II interferon and tag sequence, were arranged in frame downstream of the P1 promoter. The sequence was synthesized in GenScript and codogenically optimized according to the codon usage of *L. lactis*. This sequence was cloned in the pNZ8149 plasmid (MoBiTec GmbH, Germany) between the sites NcoI and XbaI. The ligation product was electroporated into *L. lactis* NZ3900. The identity of the new construct, prIFNγ, was corroborated by sequencing. The *L. lactis* strain NZ3900 containing the plasmid prIFNγ, was named MT009.

The preparation of electrocompetent *L. lactis* NZ3900 cells was performed based on the protocol suggested by Mobitec GmbH (34). A colony of *L. lactis* NZ3900 was inoculated in 5 ml of SG-GM17 medium (M17 medium containing 0.5 M sucrose, 2.5% glycine, and 0.5% glucose) and cultured overnight at 30°C without agitation. The culture was inoculated in 40 ml of SG-GM17 medium and grown for 16 h at 30°C without shaking. The next day, this culture was inoculated in 400 ml of SG-GM17 medium and grown to an OD600 between 0.2 and 0.3. Subsequently, the culture was centrifuged at 6,000×*g* for 20 min at 4°C and the collected pellet was washed three times in cold wash buffer (0.5 M sucrose, 10% glycerol, 4°C). In each step, the pellet was collected by centrifugation at 6,000×*g* for 20 min at 4°C and was resuspended by vortex in the corresponding buffer. After the final wash, the pellet was resuspended in 3 ml of wash buffer, aliquoted into 200 µl fractions, and then stored at −80°C.

MT009 Culture Conditions for Hybridization and Biological Activity Assays

From an isolated colony of MT009 a pre-culture was prepared in 0.5% M17-Lactose medium, after incubating overnight, this culture was used to inoculate (2%) 40 ml of M17-Lactose 0.5% medium. After reaching an optical density at 600 nm between 0.4 and 0.6, the culture was induced with nisin 10 ng/ml for 2 h. Bacteria were separated from the supernatant by centrifugation at 6,000×*g* for 20 min at 4°C. The obtained pellet was used in western blot and biological functionality tests, while the supernatant was used in dot blot assays. The MT009 cultures were carried out at 30°C without shaking.

Preparation of Cytoplasmic Extracts

From the MT009 culture, the bacterial pellet was resuspended in 1 ml of 1× PBS supplemented with 1 mM protease inhibitor Phenylmethylsulfonyl fluoride (PMSF). For their rupture, the resuspended cells were kept on ice and sonicated (ultrasonic processor, Sonic Vibracell) for 2 min divided into EIGHT pulses (130 W, 20 kHz, 100%, 2 mm Cv188 stem) of 15 s with intervals of 1 min. After treatment, the cellular debris was separated by centrifugation (13,000×*g*, for 10 min at 4°C). The supernatant containing the cytoplasmic proteins was removed and stored at −20°C. Total protein concentration was determined by the Bradford method.

SDS-PAGE and Western Blot

For the detection of rIFNγ in cytoplasmic extracts, proteins were separated according to their mass by SDS-PAGE (Stacking gel: 8% Acrylamide/Bisacrylamide 29: 1, pH 6.8; Resolving gel: 10% Acrylamide/Bisacrylamide 29: 1, pH 8.8). Ten µg of total protein extracts from MT009 and control strains MT005 (*L. lactis* NZ3900 with pNZ8149) were loaded, together with the BenchMark ™ His-tagged Protein Standard. The samples were subjected to electrophoresis for 90 min at 100 V. After electrophoresis the proteins were electrotransferred (300 mA for 2 h at 16°C) to a nitrocellulose membrane. Subsequently, the membrane was blocked for 1 h in a 2% BSA solution and washed three times with 1× PBS-Tween 20 (0.5%). The membrane was incubated with Rabbit polyclonal anti-His antibody (Abcam) (dilution 1/5,000) for 1 h at 37°C and then washed three times with PBS-Tween 20 (0.5%). Subsequently, the membrane was incubated with the polyclonal anti-rabbit IgG antibody conjugated to Horseradish Peroxidase (HRP) (1/5,000 dilution) for 1 h at 37°C. Then the membrane was washed three times with PBS-Tween 20 (0.5%). The membrane was incubated with 10 ml chemiluminescent developer solution (Pierce™ ECL Western Blotting Substrate) and exposed to photographic film. For the detection of rIFNγ in the extracellular protein concentrate, a dot blot was performed. The nitrocellulose membrane was loaded with 10 µl of extracts to give 1 µg of total protein per sample. Once air-dried, the membrane was hybridized and developed following the same protocol described for the western blot.

Culture Cells

Cultures of the Atlantic salmon head kidney cell line (SHK-1) (Sigma-Aldrich) were prepared up to 80% confluence in L15 medium supplemented with 4 mM glutamine and 5% fetal bovine serum. These cultures were incubated for 8 h at 16°C with 0 to 200 ng/ml of *L. lactis* cytoplasmic extracts containing rIFNγ (MT009). The total protein concentration was adjusted to the same value with cytoplasmic protein extract of the control strain MT005. After the treatment with cytoplasmic extracts, SHK-1 cell cultures were processed to extract total RNA.

RT-qPCR

Total RNA from cell cultures was extracted using total RNA kit (Omega Bio-tek), while the total RNA from spleen and kidney was extracted with TRIZOL using approximately 30 mg of each organ. In both cases total RNA integrity was evaluated using agarose gels (1%, TAE 1X) and quantified by absorbance at 260 nm, using the Tecan Infinite 200 PRO equipment or a Synergy™ 2.0 multi-well reader (Biotek). The RNA (2 µg) was treated with 1 U of RQ1 RNase-Free DNase (Promega, USA) for 30 min at 37°C in a 10 µl volume. The RNase-Free DNase was inactivated adding 1 µl of 25 mM EDTA and incubating at 65°C during 10 min. The RT reaction was performed with 1 µg of total RNA previously treated with RNase-Free DNase, 200 Units of M-MLV reverse transcriptase (Promega, USA) and 100 pmol of oligo-dT 18-mer, in a 25 µl volume. The RT reaction was performed at 42°C for 1 h and stopped by denaturation at 70°C for 15 min. The qPCR reaction was set up using the SYBR Fast Universal qPCR kit (Kapa Biosystem USA), in a 20 µl volume, using 2 µl of the RT reaction, and 10 pmol of each primer. To detect and quantify expression of Stat-1, gamma IP10, IFNγ, IL-1β, TNFα, TGFβ, IL-12, IL-6, Mx and eF1α, the thermal program consisted of 40 cycles of 15 s at 95°C, 15 s at the annealing temperature, and 30 s at 72°C. The qPCR reactions were performed in duplicate on a Stratagene Mx3000P qPCR cycler. The expression of the genes was normalized with respect to the control condition and the expression of the eF1α gene using the ΔΔCt method described by Pfaffl (35). The primers used together the annealing temperature are listed in **Table 1**.

Oral Administration of MT009 and Challenge Trials

To analyze the expression of genes that respond to IFNγ during oral administration of MT009, *O. mykiss* of approximately 25 g were placed in two experimental groups of 12 fish into 27 l tanks. After 7 d of acclimatation, one group was fed with food supplemented with MT009 and the other group continued with a normal diet. Samples of three fish were taken from each group at the beginning of the experiment (T0) and at 2, 4 and 6 d during the treatment with MT009. Each sampled fish was euthanized (see section *Fish Maintenance and Euthanize Protocols*) and processed to extract blood, spleen and kidney.

To analyze the effect of MT009 on the expression of genes that respond to IFNγ after oral administration, we followed a similar design as above, with fish placed into three experimental groups of 12 fish into 27 l tanks. After one week of acclimatation, one group was fed 7 d with feed supplemented with MT009, the second group was fed with feed supplemented with the control strain (MT005) and the third group continued with a normal diet. After administration of MT005 and MT009 fish were fed with normal feed. Samples of three fish were taken from each group at 1, 3, 5 and 7 d after the end of the treatment with the test strain. The fish were euthanized and processed to extract blood, spleen and kidney tissues.

TABLE 1 | Primers used in qPCR experiments.

Gene	Sequence	Ta	Ref
EF1a	F: 5'-GGGTGAGTTTGAGGCTGGTA-3' R: 5'-TTCTGGATCTCCTCAAACCG-3'	60°C	(36)
IL-12	F: 5'-TGACGCTTTTTCTCACCGGTTGT-3' R: 5'-ACGCTTTGCAGCATGAGCTTGA-3'	60°C	(37)
IFN-γ	F: 5'-CCGTACACCGATTGAGGACT-3' R: 5'-GCGGCATTACTCCATCCTAA-3'	60°C	(36)
TGF-β	F: 5'-AGCTCTCGGAAGAAACGACA-3' R: 5'-AGTAGCCAGTGGGTTCATGG-3'	60°C	(36)
IL-1β	F: 5'-CCCCATTGAGACTAAAGCCA-3' R: 5'-GCAACCTCCTCTAGGTGCAG-3'	60°C	(36)
IL-6	F: 5'- CCTTGCGGAACCAACAGTTTG-3' R: 5'- CCTCAGCAACCTTCATCTGGTC- 3'	60°C	(38)
STAT-1	F: 5'- GACCAGCGAACCCAAGAACCTGAA-3' R: 5'-CACAAAGCCCAGGATGCAACCAT-3'	60°C	(38)
Gamma IP-10	F: 5'-GTGTCTGAATCCAGAGGCTCCA-3' R: 5'-TCTCATGGTGCTCTCTGTTCCA-3'	60°C	This work
rpoC	F: 5'-AGG GAG ACT GCC GGT GAT A-3' R: 5'-ACTACGAGGCGCTTTCTCA-3'	55°C	(39)

For the challenge assay with *Flavobacterium psychrophilum* strain 10094 (ETECMA) (40), six tanks of 27 l with 12 specimens of *O. mykiss* of approximately 25 g were arranged in three experimental groups as for the feed trials above. The 6th day post treatment, the groups fed with MT005 (one tank) and MT009 (two tanks), and the untreated fish (two tanks) were challenges by intraperitoneal injection with 10^8 CFU of *F. psychrophilum* suspended in 100 µl of sterile PBS. As control, one tank of untreated fish was injected with 100 µl of sterile PBS.

The RPS of the MT009 treatment was calculated according to the following formula:

$$RPS = \left(1 - \frac{\%M^{MT009}}{\%M^{NF}}\right) \times 100$$

Where $\%M^{MT009}$ is the percentage of mortality of the group fed with MT009 and $\%M^{NF}$ is the percentage of mortality of the group fed with normal feed.

The *F. psychrophilum* load in surviving fish was determined by qPCR using absolute quantification of *rpoC* gene with a standard curve. Approximately 30 mg of spleen were processed to extract total DNA using Wizard® Genomic DNA Purification Kit (Promega). The DNA was quantified with an Infinite® 200 PRO NanoQuant (TECAN) and adjusted to 50 ng/µl. The qPCR was set up using the SensiFAST™ SYBR® No-ROX Kit (Bioline), in a 10 µl volume, using 50 ng of DNA from spleen, 2.5 pmol of rpoC-Fp forward primer, and 2.5 pmol of rpoC-Fp reverse primer (**Table 1**) (39). The thermal program consisted of one initial denaturation of 3 min at 95°C followed by 35 cycles of 30 s at 95°C, 15 s at 55°C, and 20 s at 72°C. The standard curve was set up using a plasmid that contain cloned the *rpoC* gene of *F. psychrophilum* (the plasmid was donated by Ictio Biotechnologies S.A). The plasmid was diluted in a range between 10^1 and 10^9 copies/µl.

Lysozyme Activity

The lysozyme activity in serum was evaluated using the *Micrococcus lysodeikticus* assay. Samples of blood were coagulated at room temperature and centrifugated at 6,000×*g* for 15 min at 4°C. The serum was separated in a clean tube and stored at −80°C. Lysozyme activity was measured according to the protocol described by Shugar (41) adapted in a microtiter plate. Briefly, 20 µl of serum was mixed with 180 µl of 0.015% [w/v] *M. lysodeikticus* cell suspension in 50 mM Potassium Phosphate Buffer, pH 6.24. The changes in the A_{450} of samples (S) and blank (B) were measured for 5 min. The slopes (Δ450/min) of sample and blank were used to calculate the lysozyme activity according to the following formula:

$$\text{Lysozyme activity } \left[\frac{U}{ml}\right] = \frac{\left(\frac{\Delta A^S_{450}}{min} - \frac{\Delta A^B_{450}}{min}\right) \times Df}{2 \times 10^{-5}\,[ml]}$$

Preparation of the Pathogen Inoculum for Challenge Assays

For the challenge assay with *F. psychrophilum* strain 10094, the bacteria were grown in 10 ml of Tryptone Yeast Extract Salts (TYES) medium pH 7.2 at 15°C with constant agitation (200 rpm) for 72 h. Five milliliters of this pre-inoculum were used to inoculate 95 ml of sterile TYES broth pH 7.2, then the bacteria were cultured for 4 d at 15°C with constant agitation (200 rpm). At the end of the culture final density was adjusted with TYES to 10^9 CFU/ml and 100 µl of this culture was used to infect the fish intraperitoneally. *F. psychrophilum* strain 10094 was isolated on November 6th, 2015 from a specimen of *O. mykiss* in Chiloé, Chile.

Fish Maintenance and Euthanize Protocols

Fish were acclimated for one week before treatment at 12°C in freshwater aquariums with a biomass not higher than 14 g/l, with continuous aeration, and fed with commercial pellets (EWOS MICRO™ 2 mm) at 1% of body weight. The fish were maintained in freshwater with a pH between 6.6 and 7, the salinity was adjusted to 6 PSU with NaCl to prevent fungal infection, and total ammonia was maintained in a range below 0.02 mg/l. Seventy percent of the water in all the aquaria were changed every day after feeding. Water parameters were monitored daily prior to and after changing the water. Feeding, changing the water, and measuring water parameters were all done manually. The *L. lactis* strains (MT009 or MT005) were administered to the fish together with feed. The bacterial pellet of the cultures was washed with 1 ml of M17 medium, collected by centrifugation at 6,000×*g* for 10 min at 4° C and resuspended in M17 medium in a volume equivalent to 1/10 of the volume of the original culture. The bacteria suspension was mixed with edible oil in a 2:1 ratio and emulsified by vortexing. The emulsion obtained was mixed with the feed, homogenized by shaking in a plastic container and incubated for 1 h at 30°C to allow absorption and drying on feed pellets.

To avoid unnecessary suffering of fish during the challenge and sampling, fish were anesthetized with benzocaine 40 mg/l no longer than 2 min before the intraperitoneal injection, while fish sampled were euthanized with an overdose of anesthesia with benzocaine 40 mg/l for 5–10 min. The fish were maintained in accordance with the ethical standards of the Institutional Ethics Committee of the Universidad de Santiago de Chile and the relevant legislation in force.

RESULTS

Expression of rIFNγ in *L. lactis* NZ3900

The interferon type II encoded in the *S. salar* genome is a 21.2 kDa protein in its immature form. The modification introduced to allow its expression and secretion in *L. lactis*, included the replacement of the eukaryotic signal peptide (SP) by the prokaryotic SP of Usp45 protein, the introduction of a GGGHHHHHH tag in the C-terminal, the codon optimization to the codon usage of *L. lactis* and the inclusion of a P1 promoter to allow a basal expression. This *in silico* design produces a theoretical protein (rIFNγ) of 22.2 kDa. This sequence was synthesized and cloned into pNZ8149 using *L. lactis* NZ3900 as host. The plasmid containing the rIFNγ gene in pNZ8149 was

named prIFNγ and the strain of the *L. lactis* containing this plasmid was named MT009.

The expression of rIFNγ was evaluated in the cytoplasmic and in extracellular extracts of the MT009 strain. The expression was evaluated in the presence of different concentration of nisin (1, 5, and 10 ng/ml), which is the inducer of the pNIS promoter present in the plasmid pNZ8149. We also analyzed the expression of rIFNγ in cultures of MT009 without nisin. As a negative control, we used the cytoplasmic or extracellular extract prepared from cultures of the MT005 strain (*L. lactis* NZ3900). We identified a protein of approximately 23–24 kDa close to the theoretical 22.2 kDa. This protein was present in the cytoplasmic extract from MT009 with and without presence of the inducer, suggesting that promoter P1 acts constitutively and is able to quench the pNIS promoter (**Figure 1**). When the supernatant was analyzed, no band was identified, so the supernatant was concentrated and, after this, a thin band at 21 kDa was identified (data not shown), suggesting poor extracellular secretion.

Bioactivity of rIFNγ

In order to test if the rIFNγ present in the cytoplasmic extracts was functional, we designed a test using SHK-1 cell cultures. These cells were exposed to several concentrations (0 to 200 ng/ml) of cytoplasmic protein extracted from MT009 cultures. To control the effect on the cells of different concentrations of bacterial proteins from cytoplasm of *L. lactis* NZ3900, the total concentration of cytoplasmic bacterial proteins was adjusted to 200 ng/ml using cytoplasmic protein extracts from MT005 cultures grown under the same condition. We evaluated the effect over the expression of genes under the activation pathway of IFNγ, STAT1, gamma IP10, IL-6 and IFNγ. We also evaluated the effect on the expression of general anti-inflammatory and inflammatory cytokines TGF-β and IL-1β, respectively. We observed a dose dependent tendency in the expression of all the genes that were downstream in the pathway of genes activated by IFNγ, particularly in the expression of IFNγ and IL-6. We also observed that the cytoplasmic extracts of MT009 showed no effects on the expression of anti-inflammatory cytokine TGF-β, and in the increase of the expression of IL-1β suggesting that cells respond to other bacterial components present in the MT009 protein extract (**Figure 2**).

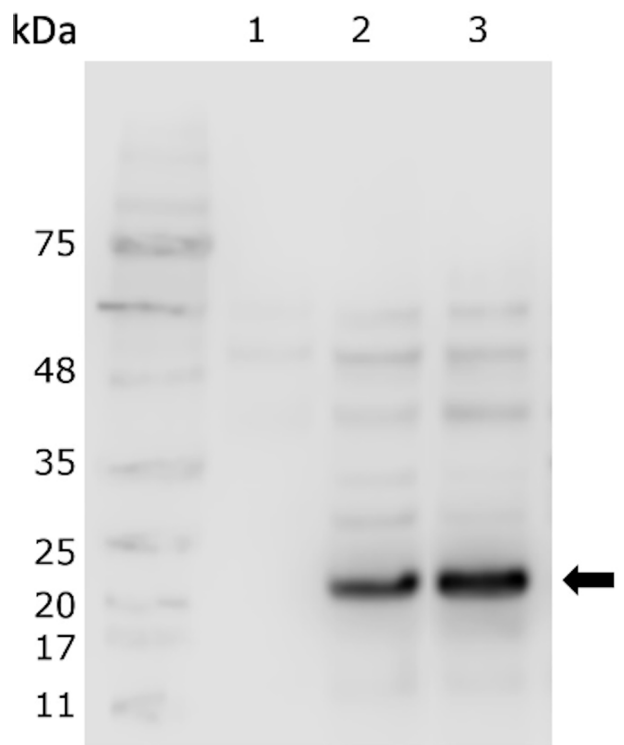

FIGURE 1 | Presence of rIFNγ in the cytoplasmic extract of MT009. The figure shows a western blot using anti-histag and the cytoplasmic extract from cultures of MT005 (1), MT009 without induction (2) and induced with nisin 5 ng/ml (3). The arrow indicates the band of ∼23 kDa corresponding to the rIFNγ. The effects of the nisin from 1 ng/ml and 10 ng/ml are shown in the **Supplementary Figure 1**.

In vivo Effects During the Oral Administration of MT009 on the Expression of IFNγ Related Genes

Our initial results showed that rIFNγ was biologically active *in vitro* stimulating the genes related with the IFNγ response. To determine if the MT009 strain stimulate the interferon γ pathway when administered orally to rainbow trout, we designed an experiment where fish were fed with 10^7 CFU of MT009 per day for one week. Tissues from fish were taken every 2 d during the feeding. The expression of IFNγ, STAT-1, gamma IP-10, and IL-6 was evaluated in the spleen and kidney. We observed an increase in the expression of IFNγ in kidney between days 2 and 4 after MT009 feeding began, returning to the initial values on day 6. In the spleen, the increase in the expression of IFNγ began later, on day 4 and remained high until day 6. A similar pattern was observed with gamma IP10 which increased its expression in the kidney between days 2 and 4, and returned to values close to those observed in the control fish on day 6. In the spleen, we observed an increase in the expression of gamma IP10 only on day 2. STAT-1 also increased its expression mainly in kidney after day 4. IL-6 only increased its expression in kidney, such as is observed in SHK-1 cells (**Figure 3**). MT009 also increased the expression of IL-12, a cytokine secreted by macrophages in response to IFNγ, in the spleen and in a lower extent in kidney (**Supplementary Figure 2B**). Interestingly, the expression on IL-1β showed a slight increase in the spleen throughout the time analyzed, but in the kidney showed a strong increase after day 2 (**Supplementary Figure 2A**). Our results show that the kidney and spleen responded differentially to MT009, with the kidney an organ with a more robust and complex response than the spleen.

In Vivo Effects Post Oral Administration of MT009 on the Expression of IFNγ Related Genes

The previous results show that MT009 was able to induce the expression of genes related to the IFNγ pathway. These effects could be due to the bacterial host or the associated rIFNγ. In

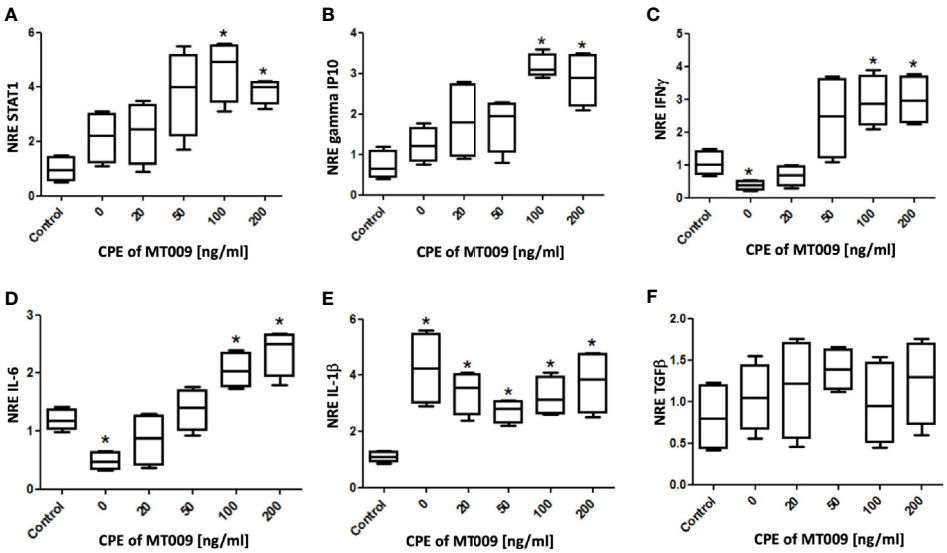

FIGURE 2 | Effect of MT009 protein extract on the expression of IFNγ related genes in SHK-1 cells. The figure shows the relative expression of genes related with the downstream IFNγ-response pathway Stat-1 **(A)**, gamma IP10 **(B)**, IFNγ **(C)** and IL-6 **(D)** after exposure to the cytoplasmic extract of MT009 (*L. lactis* NZ3900 prIFNγ). The figure also shows the effects of these extracts on the expression of **(E)** inflammatory (IL-1β) and **(F)** anti-inflammatory (TGF-β) cytokines. The expression was normalized with respect to the expression of eF1α (NRE). The concentration of bacterial cytoplasmic proteins extracts (CPE) was adjusted with extracts of MT005 (*L. lactis* pNZ8149) to 200 ng/ml. The NRE of each gene was compared against the NRE of the control (cells without treatment). The assays were performed using biological and technical replicates. The significance was analyzed using the Mann–Whitney test (*$p < 0.05$).

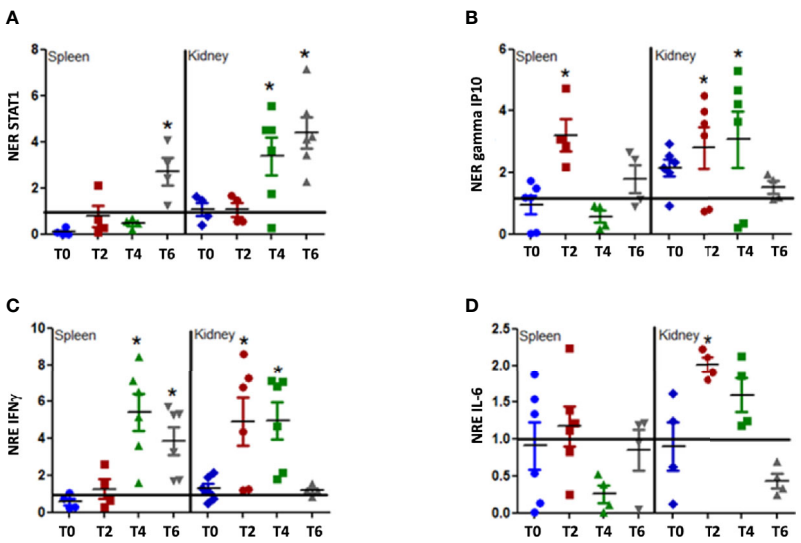

FIGURE 3 | Expression of IFNγ related genes during feeding with MT009. The figure shows the relative expression of STAT1 **(A)**, gamma IP10 **(B)**, IFNγ **(C)** and IL-6 **(D)**. The expression was evaluated in the spleen and kidney at the beginning of the treatment (T0) and every two days during treatment (T2, T4, T6). The expression was normalized with respect to the expression of eF1α gene and by the expression of the genes in the control condition at the same time point. The expression values were compared with the expression at T0. The significance was analyzed using the Mann–Whitney test (*$p < 0.05$).

order to determine whether MT009 influenced the immune system due to prIFNγ and if these effects are present post feed with MT009, we evaluated the expression of IFNγ, STAT-1, IL-6 and gamma IP10 in the spleen and kidney of fish fed with feed supplemented with MT009, MT005 (*L. lactis* NZ3900 with pNZ8149) and without any bacterial supplementation. Samples were taken every 2 d for a week, starting the first day after feeding with MT005 or MT009. Our results showed that *L. lactis* was also

able to induce the expression of IFNγ after feeding, but in the fish fed with *L. lactis* expressing rIFNγ, the induction of IFNγ remained high on day 7 post feeding compared to MT005 (∼4 fold in spleen and ∼1.2 fold in kidney). A similar pattern was observed with the expression of gamma IP10. A more prominent effect was observed in the expression of STAT-1 and IL-6 where maximum expression was observed on days 3 and 5 post treatment, respectively. This effect was observed in spleen and kidney and in both the expression decreased drastically on day 7 post treatment (**Figure 4**). Interestingly, both MT005 and MT009 were able to induce the expression of TGF-β, suggesting that the *L. lactis* possesses anti-inflammatory properties, besides the increase in the expression of IL-6 (**Supplementary Figure 3**).

Effect of MT009 on the Lysozyme Activity in Serum After Treatment

The previous finding indicated that IL-6 was strongly induced after treatment with MT009 and this effect was not present in the parental strain MT005, suggesting that is an effect related to the production of IFNγ by MT009. Taken into account that IFNγ and IL-6 induce the expression of lysozyme in mammals, we evaluated lysozyme activity in serum after treatment with MT009 and MT005. Our results showed a strong induction of the lysozyme activity in serum after treatment with MT009, but not with MT005, indicating that the induction of lysozyme activity is related to the presence of the prIFNγ in the strain MT009 (**Figure 5**). This induction was not observed in serum during the initial administration of MT009 (**Supplementary Figure 4**), suggesting that induction of lysozyme activity is consequence of a complex cascade and is probably achieved by the constant accumulation in serum due to the stimulation of the immune system.

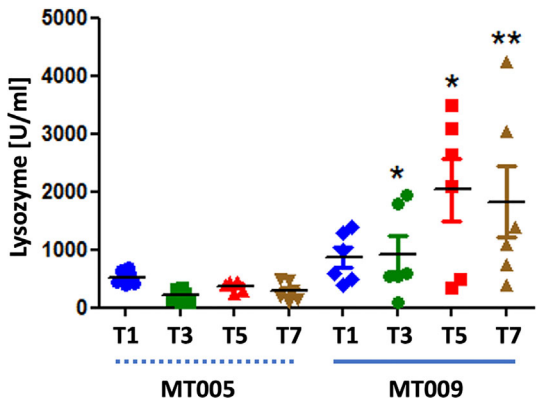

FIGURE 5 | Lysozyme activity in serum post treatment. The figure shows the lysozyme activity in serum of fish treated during seven days with MT009 (solid blue line) and MT005 (dashed blue line). Samples were taken at 1, 3, 5 and 7-days post treatment (PT). The assay was performed using three fish per day and the lysozyme activity was measure in triplicated. The significance was analyzed using the Mann–Whitney test (*p < 0.05, **p < 0.01).

Protective Activity of MT009 Against Bacterial Infection

In order to test if the immunostimulation produced by MT009 is able to confer protection against bacterial pathogens, we challenged *O. mykiss* with *F. psychrophilum*. After

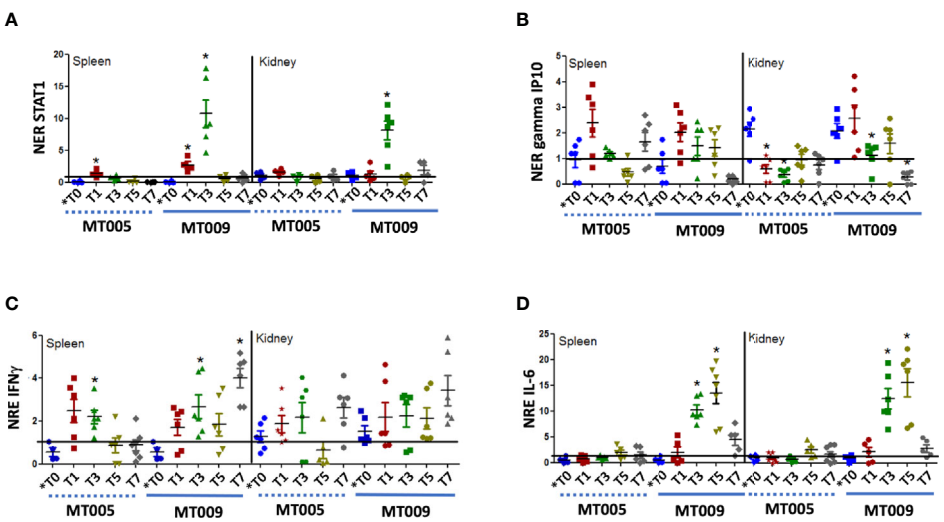

FIGURE 4 | Expression of IFNγ related genes after oral administration of MT009 and MT005. The figure shows the relative expression of STAT1 **(A)**, gamma IP10 **(B)**, IFNγ **(C)**, and IL-6 **(D)** in fish treated with MT009 (solid blue line) and fish treated with the *L. lactis* strain containing the plasmid pNZ8149 (MT005) (dashed blue line). Gene expression was evaluated in the spleen and kidney at the beginning of the treatment (*T0) and every two days after treatment (T1, T3, T5, T7). The expression was normalized with respect to the expression of eF1α gene and by the expression of the genes in the control condition at the same time point. The expression values were compared with the expression at T0. The significance was analyzed using the Mann–Whitney test (*p < 0.05).

intraperitoneal injection of *F. psychrophilum* strain 10094, the mortality started at day 6 in all groups challenged with the pathogen and remained similar up to day 10 when survival in the treated group with MT009 stabilized reaching an average of 73.3% at day 17 post-challenge, while the fish treated with MT005 and without treatment reached a 26.6 and 36.6% of survival, respectively. Kaplan–Meier analyses (42) of the survival of fish treated with MT009 showed a statistical difference with the survival curve of fish treated with MT005 ($p = 0.0052$, Log-rank (Mantel–Cox) Test; $p = 0.0169$, Gehan–Breslow–Wilcoxon Test) and without treatment ($p = 0.0077$, Log-rank (Mantel–Cox) Test; $p = 0.0180$, Gehan–Breslow–Wilcoxon Test). We were unable to identify statistically significant differences in the survival curve of fish treated with MT005 and without treatment. Thus, the Relative Percentage Survival (RPS) of fish treated with MT009 corresponded to 57.8% with respect to fish without treatment (**Figure 6**). The quantification by qPCR of the *F. psychrophilum* (39) in the spleen of survivors and in moribund fish indicated that the former had a bacterial load at least 10 times lower than the moribund fish. The surviving fish without treatment showed a bacterial load that was at least three orders lower than the bacterial load of moribund fish, while surviving fish treated with MT009 showed bacterial loads at least two orders lower than moribund fish (**Supplementary Figure 5**).

Comparison With Interferon Type II From Salmonids

The results above implies that rIFNγ from *S. salar* can also has biological effect on *O. mykiss*, a salmonid closely related to *S. salar*. Previous studies using IFNγ from *O. mykiss* have indicated that this interferon has a biological effect on *S. salar* kidney cell lines SHK-1, ASK, and TO (17, 21). These findings allow us to hypothesize that the MT009 strain may also have biological effects on other salmonids depending on the degree of relatedness among the type II interferon present in the species. To evaluate this possible range of action, a BLASTP search was performed using the IFNγ sequence of *S. salar* (NP_001117030.1) as query, and a subsequent phylogenetic reconstruction of these results was applied. BLAST analysis indicated that the closest type II interferons were found in *Salmo trutta* with 98.3% (XP_029599439.1) and 97.8% (XP_029599441.1) identity, followed by interferon present in *Salvelinus namaycush* with 94.3% (XP_038851623.1) and *O. mykiss* with 93.3% (CAR95729.1) identity. These results suggest that MT009 could also stimulate the response to type II interferon in *S. trutta* and *S. namaycush* (**Figure 7**).

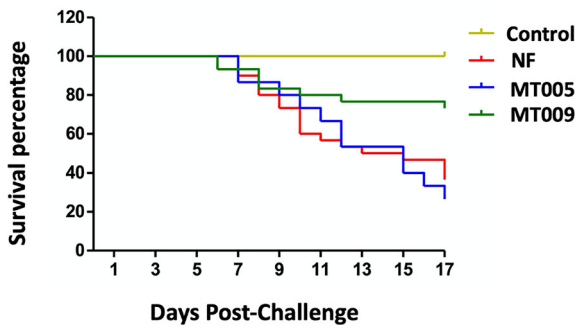

FIGURE 6 | Challenge assay with *Flavobacterium psychrophilum* strain 10094. The figure shows the Kaplan–Meier survival plot of *Oncorhynchus mykiss* specimens challenged intraperitoneally with 10^8 CFU of *F. psychrophilum* strain 10094. A total of three diets were analyzed, (1) fish fed with *L. lactis* NZ3900 producer of rIFNγ (MT009), (2) fish fed with *L. lactis* NZ3900 containing the plasmid pNZ3900 (MT005), and (3) fish fed with normal feed (NF, and Control). All conditions were challenged with *F. psychrophilum* 10094, with exception of the control. The challenge of fish treated with MT009 and NF was performed in duplicate.

DISCUSSION

The current work explores the hypothesis that probiotic microorganisms modified to express type II interferon are able to modify the immune status of the fish and confer protection against pathogens when orally administrated to fish. This protection would result from stimulation of the innate immunity, improving the serological or cellular components. These kind of probiotics, that stimulate the mucosa and beneficially regulate the immune system improving performance against microbial pathogens are termed immunobiotics (47). Some immunobiotics mainly belonging to *Lactobacillus* and *Bifidobacterium* genus, stimulate the expression of interferons (Types I and II) (48, 49) triggering a cascade that confers protection against viral pathogens, such as influenza (50), rotavirus (51) and respiratory syncytial virus (52), and also intracellular parasites like Toxoplasma (53). A common characteristic of these immunobiotics is their capacity to stimulate the cellular immune response mediated by Th1 lymphocytes (48), NK (54, 55) and macrophages (52, 53) which is initiated and amplified by the production of type II interferon.

The type II interferon is a pleotropic cytokine produced mainly by Th1 lymphocytes and NK cells in response to the secretion of IL-12, IL-18, and IL-1β produced by the APC (56). Type II interferon stimulates its own expression on Th1 cells polarizing the Th1/Th2 balance toward a Th1 response (57). Type II interferon also produces a polarization of macrophages M1/M2 balance, favoring the M1 cells phenotype (58). The polarization toward a Th1 and M1 response produces metabolic changes in these cells favoring a glycolytic metabolism, with increased expression of enzymes related to the production of Reactive Oxygen Species (ROS) and Reactive Nitrogen Species (RNS), and the expression of autophagy mediators, especially in M1 macrophages (59–61). These metabolic changes enhance the microbicidal capacity of the cells, improving cell-autonomous immunity against intracellular microorganisms (62). The M1 phenotype of macrophages also secretes IL-6 and TNF-α (63, 64), which in turn induces the expression of serum lysozyme, improving the antimicrobial activity in serum against extracellular pathogens (65, 66).

In teleost, although type II interferon has been much less studied, increasing evidence shows that type II interferon plays a similar role as in mammals sharing activation pathways and functions that are

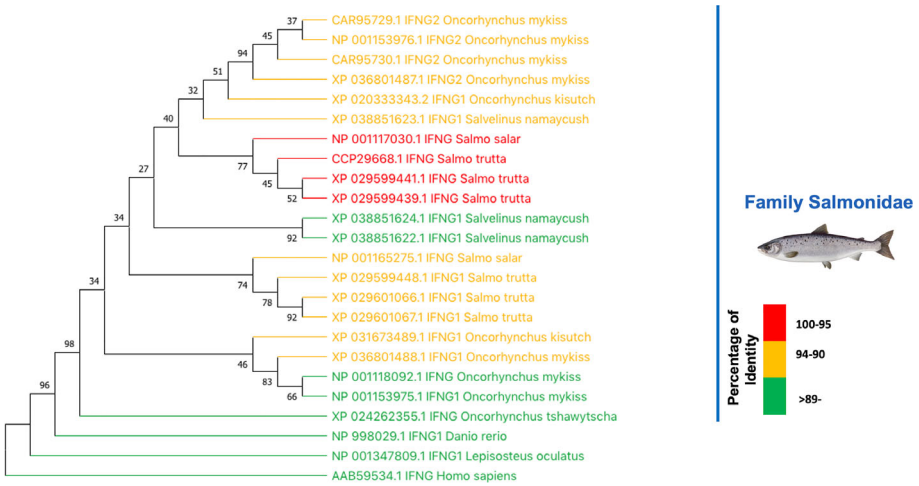

FIGURE 7 | Relationship between type II interferon in salmonids. The figure shows the phylogenetic relationship between the type II interferons of salmonids. The evolutionary history was inferred by using the Maximum Likelihood method and JTT matrix-based model (43). The bootstrap consensus tree inferred from 1,000 replicates (44) is taken to represent the evolutionary history of the taxa analyzed (44). Branches corresponding to partitions reproduced in less than 50% bootstrap replicates are collapsed. The percentage of replicate trees in which the associated taxa clustered together in the bootstrap test (1,000 replicates) is shown next to the branches (44). Initial tree for the heuristic search were obtained automatically by applying Neighbor-Join and BioNJ algorithms to a matrix of pairwise distances estimated using the JTT model, and then by selecting the topology with superior log likelihood value. This analysis involved 24 amino acid sequences. There were a total of 452 positions in the final datasets. Evolutionary analyses were conducted in MEGA X (45, 46). The colors represent the degree of identity of each type II interferon with the IFNγ of *S. salar*.

conserved and complexed with paralogous genes of non-redundant function (IFNrel) and diverse receptors (67).

Our work used a Gram-positive bacterial model to express IFNγ, an eukaryotic protein, which is predicted to be glycosylated, as its mammalian counterpart (20). In mammals and teleost specimens like rainbow trout, recombinant IFNγ has been produced in *Escherichia coli* (20). This recombinant IFNγ, has shown to be functional, indicating that glycosylation is not necessary for the activity, although glycosylation increases human interferon half-life protecting against proteolytic degradation (68).

In this work, we detected the rIFNγ mainly in the cytoplasmic fraction of MT009 cultures, despite our original design incorporating an Usp45 signal peptide to allow secretion of the rIFNγ. Low levels of secretion have been also detected in the recombinant production of human (25) and Atlantic salmon type I Interferons (unpublished data) using the Usp45 signal peptide. In human type I IFN this problem was resolved by introducing a spacer sequence between the Usp45 signal peptide and the rest of the interferon protein (25). It remains to determine whether this spacer sequence improves the secretion of rIFNγ by MT009 or not.

Others work have used recombinant overexpression of type II interferon in *E. coli* with further purification to study its function in fish (20). However, *L. lactis*, as an alternative recombinant protein system, may not offer as efficient a protein producer as *E. coli*, and purification of recombinant protein from *L. lactis* cultures may be limited (in yields). To overcome this, in this study we decided to evaluate the ability of different amounts of cytoplasmic extracts of the MT009 strain to stimulate the expression of genes that respond to type II interferon, but taking care to maintain the total amount of bacterial protein constant to evaluate if the effect was caused by the presence of rIFNγ or by some other bacterial component present in the extract.

This approach showed that the genes previously described in rainbow trout and mammalians that respond to type II interferon (Stat1, gamma IP10, IFNγ, and IL-6) (20, 63, 67) are also induced in SHK-1, dose-dependent of the MT009 extract, unlike the gene expression pattern of IL-1β that appeared to respond to the presence of a common component of *L. lactis*.

An interesting point is that *L. lactis* as a Gram-positive bacterium lacks LPS, an inducer of IFNγ expression, that supports that the activation of these genes is due to the presence of rIFNγ in the cytoplasmic extracts of MT009. Although it is not possible to rule out that the overall response is the product of the simultaneous interaction of rIFNγ and some other component of the bacterium. In mammals, type II interferon has been reported to improve the response of keratinocytes and macrophages after stimulation of Toll-Like Receptors (TLR) with microorganisms or agonist, respectively (69, 70).

Once the effect of Type II interferon was tested *in vitro*, we evaluated whether the administration of strain MT009 could induce the expression of genes markers from the response to interferon in the central immune organs of rainbow trout, the spleen and kidney. Although the first encounter of the MT009 strain with the fish immune system is through the digestive mucosa, we hypothesized that the immune cells (lymphocytes and macrophages) present in the GALT respond to type II

interferon and stimulate the central immune response, similar to how oral vaccines stimulate the immune response at the local and systemic level (71).

However, the mechanism of how GALT stimulation produces changes at the level of the central immune organs remains poorly understood in teleost. In the case of MT009, this could involve a) stimulation by rIFNγ of the immune cells of the GALT, which in turn responds by secreting cytokines that stimulate the spleen and kidney, b) diffusion of rIFNγ from the intestine to the central immune organs, or both. An interesting point is that during the administration of MT009, we identified an early response in the kidney of the IFNγ response genes, STAT-1, gamma IP10, and IFNγ which was out of phase with the later response observed in spleen. This difference could be the consequence of the presence of a population of immune cells with different activation thresholds by IFNγ or by another cytokine secreted in response to IFNγ. The transient increase in the expression of IFNγ in the spleen and kidney during feeding suggests an initial polarization of lymphocytes to a Th1 phenotype.

After feeding with MT009, changes were also observed in the expression of the genes in response to IFNγ, in particular, an increase in the expression of STAT-1 at 3 days post treatment with MT009. This change in expression could be a consequence of additive effect of rIFNγ and endogenous interferon produced during the administration of MT009. An experiment carried out in our laboratory indicated that *L. lactis* remains in the gut up to 4 days after oral administration has ended (data not shown), a situation that supports the proposal of a combined effect of rIFNγ and endogenous IFNγ.

An interesting point to note is that we also observed a slight increase in IFNγ expression in fish fed with *L. lactis* NZ3900 (MT005), but that it was not associated with a significant increase in other IFNγ response markers. This could be a result of the stimulating effect of *L. lactis*, as occurs in the case of some immunobiotics or lactic acid bacteria in finfish (47, 72). However, in fish fed with MT009, the effect on IFNγ expression was sustained until day 7, which suggests that the effect of rIFNγ administration initiates a cascade that is maintained even after feeding has ended. This is also reflected in the increased expression of IL-6, a cytokine that is secreted by the M1 phenotype of macrophages in mammals and teleosts (73) and also in the increased activity of serum lysozyme, which is induced specifically by strain MT009 and not by MT005.

Taking into consideration that M1 macrophages are producers of IL-6 (73) and lysozyme (65, 66), and that IL-6 also promotes differentiation of monocyte to macrophages in mammals (74), the results suggest that the administration of MT009 promotes macrophages with the phenotype M1 increasing the microbicidal activity at the cellular and humoral level.

This interpretation is consistent with the increase in resistance to extracellular infection such as that produced by *F. psychrophilum*, and potentially could aid the treatment or prevention of infection by intracellular pathogens such as *P. salmonis*. Taking into consideration that the challenge test was carried out by intraperitoneal injection, bypassing the mucosal barriers, the stimulation at the mucosal level by the MT009 strain would improve the ability of the fish to resolve the infection, increasing the fish survival.

The biological functionality of rIFNγ from *S. salar* was tested in *S. salar* cells and in *O. mykiss*, based that the IFNγ of both species presents 93% identity and 96% similarity. It therefore plausible that the MT009 strain could present activity in other salmonids whose type II interferon are closer to that of *S. salar*, such as the IFNγ of *S. trutta*, and *S. namaycush*. It however, remains to be determined whether MT009 actually has a stimulating effect on salmonids other than *O. mykiss* and *S. salar*.

CONCLUSIONS

Our results indicate that in *O. mykiss*, the oral administration of rIFNγ-producing *L. lactis* (MT009) stimulates the expression of genes that participate in the IFNγ-mediated response at the systemic level, producing a state of protection against infection of extracellular bacterial pathogens. This protection could be mediated by polarization towards the Th1 and M1 phenotypes. The process by which stimulation at the mucosal level with MT009 is connected to a change at the systemic level that provides protection remains to be elucidated. Further characterization of the IFNγ response genes and immune cell populations in GALT could help clarify this mechanism.

DATA AVAILABILITY STATEMENT

The raw data supporting the conclusions of this article will be made available by the authors, without undue reservation.

ETHICS STATEMENT

Ethical review and approval were not required for the animal study because the applied projects financed by CORFO do not require the approval of an ethics committee for their execution.

AUTHOR CONTRIBUTIONS

Conceptualization, MT. Methodology, AS, DP, MP, CM, NV, CZ and RV. Investigation, AS, DP, MP, CM, NV, CZ and RV. Resources, MT. Writing—original draft preparation, MT. Writing, review and editing, MT, RV, MP and AG. All authors contributed to the article and approved the submitted version.

FUNDING

This research was funded by CORFO-INNOVA, grant number 13CTI21257. The APC was funded by USACH. AS was supported by National Doctorate scholarship no. 21180465 (ANID; Government of Chile).

ACKNOWLEDGMENTS

We would like to thank the administrative team of Consorcio Tecnológico de Sanidad Acuícola S.A for its support in the execution of this research.

SUPPLEMENTARY MATERIAL

The Supplementary Material for this article can be found online at: https://www.frontiersin.org/articles/10.3389/fimmu.2021.696803/full#supplementary-material

REFERENCES

1. Isaacs A, Lindenmann J. Virus Interference. I. The Interferon. *Proc R Soc Lond B Biol Sci* (1957) 147:258–67. doi: 10.1098/rspb.1957.0048
2. Pestka S, Krause CD, Walter MR. Interferons, Interferon-Like Cytokines, and Their Receptors. *Immunol Rev* (2004) 202:8–32. doi: 10.1111/j.0105-2896.2004.00204.x
3. Lazear HM, Schoggins JW, Diamond MS. Shared and Distinct Functions of Type I and Type III Interferons. *Immunity* (2019) 50:907–23. doi: 10.1016/j.immuni.2019.03.025
4. McNab F, Mayer-Barber K, Sher A, Wack A, O'Garra A. Type I Interferons in Infectious Disease. *Nat Rev Immunol* (2015) 15:87–103. doi: 10.1038/nri3787
5. Teijaro JR. Type I Interferons in Viral Control and Immune Regulation. *Curr Opin Virol* (2016) 16:31–40. doi: 10.1016/j.coviro.2016.01.001
6. Antonelli G, Scagnolari C, Moschella F, Proietti E. Twenty-Five Years of Type I Interferon-Based Treatment: A Critical Analysis of its Therapeutic Use. *Cytokine Growth Factor Rev* (2015) 26:121–31. doi: 10.1016/j.cytogfr.2014.12.006
7. Zimonjic DB, Rezanka LJ, Evans CH, Polymeropoulos MH, Trent JM, Popescu NC. Mapping of the Immune Interferon Gamma Gene (IFNG) to Chromosome Band 12q14 by Fluorescence in Situ Hybridization. *Cytogenet Cell Genet* (1995) 71:247–8. doi: 10.1159/000134119
8. Kearney S, Delgado C, Lenz LL. Differential Effects of Type I and II Interferons on Myeloid Cells and Resistance to Intracellular Bacterial Infections. *Immunol Res* (2013) 55:187–200. doi: 10.1007/s12026-012-8362-y
9. Frucht DM, Fukao T, Bogdan C, Schindler H, O'Shea JJ, Koyasu S. IFN-Gamma Production by Antigen-Presenting Cells: Mechanisms Emerge. *Trends Immunol* (2001) 22:556–60. doi: 10.1016/s1471-4906(01)02005-1
10. Tewari K, Nakayama Y, Suresh M. Role of Direct Effects of IFN-Gamma on T Cells in the Regulation of CD8 T Cell Homeostasis. *J Immunol* (2007) 179:2115–25. doi: 10.4049/jimmunol.179.4.2115
11. Boehm U, Klamp T, Groot M, Howard JC. Cellular Responses to Interferon-γ. *Annu Rev Immunol* (1997) 15:749–95. doi: 10.1146/annurev.immunol.15.1.749
12. Xu H, Wipasa J, Yan H, Zeng M, Makobongo MO, Finkelman FD, et al. The Mechanism and Significance of Deletion of Parasite-Specific CD4(+) T Cells in Malaria Infection. *J Exp Med* (2002) 195:881–92. doi: 10.1084/jem.20011174
13. Ingram JP, Brodsky IE, Balachandran S. Interferon-γ in Salmonella Pathogenesis: New Tricks for an Old Dog. *Cytokine* (2017) 98:27–32. doi: 10.1016/j.cyto.2016.10.009
14. Miller CHT, Maher SG, Young HA. Clinical Use of Interferon-γ. *Ann N Y Acad Sci* (2009) 1182:69–79. doi: 10.1111/j.1749-6632.2009.05069.x
15. Armstrong-James D, Teo IA, Shrivastava S, Petrou MA, Taube D, Dorling A, et al. Exogenous Interferon-Gamma Immunotherapy for Invasive Fungal Infections in Kidney Transplant Patients. *Am J Transplant* (2010) 10:1796–803. doi: 10.1111/j.1600-6143.2010.03094.x
16. Razaghi A, Owens L, Heimann K. Review of the Recombinant Human Interferon Gamma as an Immunotherapeutic: Impacts of Production Platforms and Glycosylation. *J Biotechnol* (2016) 240:48–60. doi: 10.1016/j.jbiotec.2016.10.022
17. Martin SAM, Taggart JB, Seear P, Bron JE, Talbot R, Teale AJ, et al. Interferon Type I and Type II Responses in an Atlantic Salmon (Salmo Salar) SHK-1 Cell Line by the Salmon TRAITS/SGP Microarray. *Physiol Genomics* (2007) 32:33–44. doi: 10.1152/physiolgenomics.00064.2007
18. Martin SAM, Zou J, Houlihan DF, Secombes CJ. Directional Responses Following Recombinant Cytokine Stimulation of Rainbow Trout (Oncorhynchus Mykiss) RTS-11 Macrophage Cells as Revealed by Transcriptome Profiling. *BMC Genomics* (2007) 8:150. doi: 10.1186/1471-2164-8-150
19. Martin SAM, Mohanty BP, Cash P, Houlihan DF, Secombes CJ. Proteome Analysis of the Atlantic Salmon (Salmo Salar) Cell Line SHK-1 Following Recombinant IFN-Gamma Stimulation. *Proteomics* (2007) 7:2275–86. doi: 10.1002/pmic.200700020
20. Zou J, Carrington A, Collet B, Dijkstra JM, Yoshiura Y, Bols N, et al. Identification and Bioactivities of IFN-γ in Rainbow Trout Oncorhynchus Mykiss : The First Th1-Type Cytokine Characterized Functionally in Fish. *J Immunol* (2005) 175:2484–94. doi: 10.4049/jimmunol.175.4.2484
21. Sun B, Skjaeveland I, Svingerud T, Zou J, Jorgensen J, Robertsen B. Antiviral Activity of Salmonid Gamma Interferon Against Infectious Pancreatic Necrosis Virus and Salmonid Alphavirus and Its Dependency on Type I Interferon. *J Virol* (2011) 85:9188–98. doi: 10.1128/JVI.00319-11
22. Álvarez C, Marshall S, Mercado L. IFN-Gamma-Mediated Control of Piscirickettsia Salmonis Survival in Trout Macrophages. *Fish Shellfish Immunol* (2016) 53:112. doi: 10.1016/j.fsi.2016.04.084
23. Steidler L, Rottiers P, Coulie B. Actobiotics™ as a Novel Method for Cytokine Delivery. *Ann N Y Acad Sci* (2009) 1182:135–45. doi: 10.1111/j.1749-6632.2009.05067.x
24. Bahey-El-Din M, Gahan CGM, Griffin BT. Lactococcus Lactis as a Cell Factory for Delivery of Therapeutic Proteins. *Curr Gene Ther* (2010) 10:34–45. doi: 10.2174/156652310790945557
25. Zhang Q, Zhong J, Liang X, Liu W, Huan L. Improvement of Human Interferon Alpha Secretion by Lactococcus Lactis. *Biotechnol Lett* (2010) 32:1271–7. doi: 10.1007/s10529-010-0285-x
26. Bayat O, Baradaran A, Ariff A, Mohamad R, Rahim RA. Intracellular Production of IFN-alpha 2b in Lactococcus Lactis. *Biotechnol Lett* (2014) 36:581–5. doi: 10.1007/s10529-013-1390-4
27. Ma S, Li K, Li X-S, Guo X-Q, Fu P-F, Yang M-F, et al. Expression of Bioactive Porcine Interferon-Alpha in Lactobacillus Casei. *World J Microbiol Biotechnol* (2014) 30:2379–86. doi: 10.1007/s11274-014-1663-7
28. Zhuang Z, Wu Z-G, Chen M, Wang PG. Secretion of Human Interferon-Beta 1b by Recombinant Lactococcus Lactis. *Biotechnol Lett* (2008) 30:1819–23. doi: 10.1007/s10529-008-9761-y
29. Rupa P, Monedero V, Wilkie BN. Expression of Bioactive Porcine Interferon-Gamma by Recombinant Lactococcus Lactis. *Vet Microbiol* (2008) 129:197–202. doi: 10.1016/j.vetmic.2007.11.010
30. Bermúdez-Humarán LG, Cortes-Perez NG, L'Haridon R, Langella P. Production of Biological Active Murine IFN-gamma by Recombinant Lactococcus Lactis. *FEMS Microbiol Lett* (2008) 280:144–9. doi: 10.1111/j.1574-6968.2007.01038.x
31. Steidler L, Hans W, Schotte L, Neirynck S, Obermeier F, Falk W, et al. Treatment of Murine Colitis by Lactococcus Lactis Secreting Interleukin-10. *Science* (2000) 289:1352–5. doi: 10.1126/science.289.5483.1352
32. Min L, Li-Li Z, Jun-Wei G, Xin-Yuan Q, Yi-Jing L, Di-Qiu L. Immunogenicity of Lactobacillus-expressing VP2 and VP3 of the Infectious Pancreatic Necrosis Virus (IPNV) in Rainbow Trout. *Fish Shellfish Immunol* (2012) 32:196–203. doi: 10.1016/j.fsi.2011.11.015
33. Li-Li Z, Min L, Jun-Wei G, Xin-Yuan Q, Yi-Jing L, Di-Qiu L. Expression of Infectious Pancreatic Necrosis Virus (IPNV) VP2–VP3 Fusion Protein in Lactobacillus Casei and Immunogenicity in Rainbow Trouts. *Vaccine* (2012) 30:1823–9. doi: 10.1016/j.vaccine.2011.12.132
34. Mobitec GmbH. *Nice ® Expression System for Lactococcus Lactis The Effective & Easy-to-Operate NIsin Controlled Gene Expression System* (2015). Available at: www.mobitec.com (Accessed March 20, 2021).
35. Pfaffl MW. A New Mathematical Model for Relative Quantification in Real-Time RT-PCR. *Nucleic Acids Res* (2001) 29:e45. doi: 10.1093/nar/29.9.e45
36. Reyes-Cerpa S, Reyes-López F, Toro-Ascuy D, Montero R, Maisey K, Acuña-Castillo C, et al. Induction of Anti-Inflammatory Cytokine Expression by IPNV in Persistent Infection. *Fish Shellfish Immunol* (2014) 41:172–82. doi: 10.1016/j.fsi.2014.08.029
37. Parra M, Espinoza D, Valdes N, Vargas R, Gonzalez A, Modak B, et al. Microbiota Modulates the Immunomodulatory Effects of Filifolinone on Atlantic Salmon. *Microorganisms* (2020) 8:1320. doi: 10.3390/microorganisms8091320
38. Maisey K, Montero R, Corripio-Miyar Y, Toro-Ascuy D, Valenzuela B, Reyes-Cerpa S, et al. Isolation and Characterization of Salmonid

CD4+ T Cells. *J Immunol* (2016) 196:4150–63. doi: 10.4049/jimmunol.1500439
39. Strepparava N, Wahli T, Segner H, Petrini O. Detection and Quantification of Flavobacterium Psychrophilum in Water and Fish Tissue Samples by Quantitative Real Time PCR. *BMC Microbiol* (2014) 14:105. doi: 10.1186/1471-2180-14-105
40. Valdés N, Gonzalez A, Garcia V, Tello M. Analysis of the Microbiome of Rainbow Trout (Oncorhynchus Mykiss) Exposed to the Pathogen Flavobacterium Psychrophilum 10094. *Microbiol Resour Announc* (2020) 9:e01562–19. doi: 10.1128/mra.01562-19
41. Shugar D. The Measurement of Lysozyme Activity and the Ultra-Violet Inactivation of Lysozyme. *Biochim Biophys Acta* (1952) 8:302–9. doi: 10.1016/0006-3002(52)90045-0
42. Kaplan EL, Meier P. Nonparametric Estimation From Incomplete Observations. *J Am Stat Assoc* (1958) 53:457. doi: 10.2307/2281868
43. Jones DT, Taylor WR, Thornton JM. The Rapid Generation of Mutation Data Matrices From Protein Sequences. *Bioinformatics* (1992) 8:275–82. doi: 10.1093/bioinformatics/8.3.275
44. Felsenstein J. Confidence Limits on Phylogenies: An Approach Using the Bootstrap. *Evolution (N Y)* (1985) 39:783. doi: 10.2307/2408678
45. Kumar S, Stecher G, Li M, Knyaz C, Tamura K. Mega X: Molecular Evolutionary Genetics Analysis Across Computing Platforms. *Mol Biol Evol* (2018) 35:1547–9. doi: 10.1093/molbev/msy096
46. Stecher G, Tamura K, Kumar S. Molecular Evolutionary Genetics Analysis (MEGA) for Macos. *Mol Biol Evol* (2020) 37:1237–9. doi: 10.1093/molbev/msz312
47. Villena J, Kitazawa H. Editorial: Immunobiotics-interactions of Beneficial Microbes With the Immune System. *Front Immunol* (2017) 8:1580. doi: 10.3389/fimmu.2017.01580
48. Villena J, Chiba E, Vizoso-Pinto MG, Tomosada Y, Takahashi T, Ishizuka T, et al. Immunobiotic Lactobacillus Rhamnosus Strains Differentially Modulate Antiviral Immune Response in Porcine Intestinal Epithelial and Antigen Presenting Cells. *BMC Microbiol* (2014) 14:126. doi: 10.1186/1471-2180-14-126
49. Abt MC, Osborne LC, Monticelli LA, Doering TA, Alenghat T, Sonnenberg GF, et al. Commensal Bacteria Calibrate the Activation Threshold of Innate Antiviral Immunity. *Immunity* (2012) 37:158–70. doi: 10.1016/j.immuni.2012.04.011
50. Zelaya H, Alvarez S, Kitazawa H, Villena J. Respiratory Antiviral Immunity and Immunobiotics: Beneficial Effects on Inflammation-Coagulation Interaction During Influenza Virus Infection. *Front Immunol* (2016) 7:633. doi: 10.3389/fimmu.2016.00633
51. Villena J, Vizoso-Pinto MG, Kitazawa H. Intestinal Innate Antiviral Immunity and Immunobiotics: Beneficial Effects Against Rotavirus Infection. *Front Immunol* (2016) 7:563. doi: 10.3389/fimmu.2016.00563
52. Garcia-Castillo V, Tomokiyo M, Raya Tonetti F, Islam MA, Takahashi H, Kitazawa H, et al. Alveolar Macrophages are Key Players in the Modulation of the Respiratory Antiviral Immunity Induced by Orally Administered Lacticaseibacillus Rhamnosus CRL1505. *Front Immunol* (2020) 11:568636. doi: 10.3389/fimmu.2020.568636
53. Salas-Lais AG, Robles-Contreras A, Balderas-López JA, Bautista-de Lucio VM. Immunobiotic and Paraprobiotic Potential Effect of Lactobacillus Casei in a Systemic Toxoplasmosis Murine Model. *Microorganisms* (2020) 8:113. doi: 10.3390/microorganisms8010113
54. de Vrese M, Winkler P, Rautenberg P, Harder T, Noah C, Laue C, et al. Effect of Lactobacillus Gasseri PA 16/8, Bifidobacterium Longum SP 07/3, B. Bifidum MF 20/5 on Common Cold Episodes: A Double Blind, Randomized, Controlled Trial. *Clin Nutr* (2005) 24:481–91. doi: 10.1016/j.clnu.2005.02.006
55. Namba K, Hatano M, Yaeshima T, Takase M, Suzuki K. Effects of Bifidobacterium Longum BB536 Administration on Influenza Infection, Influenza Vaccine Antibody Titer, and Cell-Mediated Immunity in the Elderly. *Biosci Biotechnol Biochem* (2010) 74:939–45. doi: 10.1271/bbb.90749
56. Schoenborn JR, Wilson CB. Regulation of Interferon-γ During Innate and Adaptive Immune Responses. *Adv Immunol* (2007) 96:41–101. doi: 10.1016/S0065-2776(07)96002-2
57. Schulz EG, Mariani L, Radbruch A, Höfer T. Sequential Polarization and Imprinting of Type 1 T Helper Lymphocytes by Interferon-γ and Interleukin-12. *Immunity* (2009) 30:673–83. doi: 10.1016/j.immuni.2009.03.013
58. Martinez FO, Gordon S. The M1 and M2 Paradigm of Macrophage Activation: Time for Reassessment. *F1000Prime Rep* (2014) 6:13. doi: 10.12703/P6-13
59. Su X, Yu Y, Zhong Y, Giannopoulou EG, Hu X, Liu H, et al. Interferon-γ Regulates Cellular Metabolism and mRNA Translation to Potentiate Macrophage Activation. *Nat Immunol* (2015) 16:838–49. doi: 10.1038/ni.3205
60. Palmer CS, Ostrowski M, Balderson B, Christian N, Crowe SM. Glucose Metabolism Regulates T Cell Activation, Differentiation, and Functions. *Front Immunol* (2015) 6:1. doi: 10.3389/fimmu.2015.00001
61. Almeida L, Lochner M, Berod L, Sparwasser T. Metabolic Pathways in T Cell Activation and Lineage Differentiation. *Semin Immunol* (2016) 28:514–24. doi: 10.1016/j.smim.2016.10.009
62. MacMicking JD. Interferon-Inducible Effector Mechanisms in Cell-Autonomous Immunity. *Nat Rev Immunol* (2012) 12:367–82. doi: 10.1038/nri3210
63. Delneste Y, Charbonnier P, Herbault N, Magistrelli G, Caron G, Bonnefoy JY, et al. Interferon-γ Switches Monocyte Differentiation From Dendritic Cells to Macrophages. *Blood* (2003) 101:143–50. doi: 10.1182/blood-2002-04-1164
64. Beyer M, Mallmann MR, Xue J, Staratschek-Jox A, Vorholt D, Krebs W, et al. High-Resolution Transcriptome of Human Macrophages. *PloS One* (2012) 7:e45466. doi: 10.1371/journal.pone.0045466
65. Krishnaraju K, Hoffman B, Liebermann DA. The Zinc Finger Transcription Factor Egr-1 Activates Macrophage Differentiation in M1 Myeloblastic Leukemia Cells. *Blood* (1998) 92:1957–66. doi: 10.1182/blood.v92.6.1957
66. Lewis CE, McCarthy SP, Lorenzen J, McGee JO. Differential Effects of LPS, IFN-Gamma and TNF Alpha on the Secretion of Lysozyme by Individual Human Mononuclear Phagocytes: Relationship to Cell Maturity. *Immunology* (1990) 69:402–8.
67. Pereiro P, Figueras A, Novoa B. Insights Into Teleost Interferon-Gamma Biology: An Update. *Fish Shellfish Immunol* (2019) 90:150–64. doi: 10.1016/j.fsi.2019.04.002
68. Sareneva T, Pirhonen J, Cantell K, Julkunen I. N-Glycosylation of Human Interferon-γ: Glycans at Asn-25 are Critical for Protease Resistance. *Biochem J* (1995) 308:9–14. doi: 10.1042/bj3080009
69. Kajita A, Morizane S, Takiguchi T, Yamamoto T, Yamada M, Iwatsuki K. Interferon-Gamma Enhances Tlr3 Expression and Anti-Viral Activity in Keratinocytes. *J Invest Dermatol* (2015) 135:2005–11. doi: 10.1038/jid.2015.125
70. Müller E, Christopoulos PF, Halder S, Lunde A, Beraki K, Speth M, et al. Toll-Like Receptor Ligands and Interferon-γ Synergize for Induction of Antitumor M1 Macrophages. *Front Immunol* (2017) 8:1383. doi: 10.3389/fimmu.2017.01383
71. Muñoz-Atienza E, Diaz-Rosales P, Tafalla C. Systemic and Mucosal B and T Cell Responses Upon Mucosal Vaccination of Teleost Fish. *Front Immunol* (2021) 11:622377. doi: 10.3389/fimmu.2020.622377
72. Ringø E, Hoseinifar SH, Ghosh K, Van Doan H, Beck BR, Song SK. Lactic Acid Bacteria in finfish-An Update. *Front Microbiol* (2018) 9:1818. doi: 10.3389/fmicb.2018.01818
73. Wentzel AS, Petit J, van Veen WG, Fink IR, Scheer MH, Piazzon MC, et al. Transcriptome Sequencing Supports a Conservation of Macrophage Polarization in Fish. *Sci Rep* (2020) 10:13470. doi: 10.1038/s41598-020-70248-y
74. Chomarat P, Banchereau J, Davoust J, Palucka AK. IL-6 Switches the Differentiation of Monocytes From Dendritic Cells to Macrophages. *Nat Immunol* (2000) 1:510–4. doi: 10.1038/82763

Conflict of Interest: Author MT was employed by company Ictio Biotechnologies SA. The authors declare that the research carried out as well as the results present in this work have been in common agreement with Ictio Biotechnologies SA and the licensee Ictiobiotic SpA. Part of these results have been included in the patent application number 2897-2017 requested in the Chilean industrial property registry (INAPI).

The remaining authors declare that the research was conducted in the absence of any commercial or financial relationships that could be construed as a potential conflict of interest.

frontiers in Immunology

ORIGINAL RESEARCH
published: 06 July 2021
doi: 10.3389/fimmu.2021.693613

GAS1: A New β-Glucan Immunostimulant Candidate to Increase Rainbow Trout (*Oncorhynchus mykiss*) Resistance to Bacterial Infections With *Aeromonas salmonicida achromogenes*

Valérie Cornet[1‡], *Trinh Dinh Khuyen*[1†‡], *Syaghalirwa. N. M. Mandiki*[1], *Stéphane Betoulle*[2], *Peter Bossier*[3], *Felipe E. Reyes-López*[4,5,6], *Lluis Tort*[4] *and Patrick Kestemont*[1*]

[1] Research Unit in Environmental and Evolutionary Biology (URBE), Research Institute of Life, Earth & Environment, University of Namur (UNamur), Namur, Belgium, [2] UMR-INERIS 02 SEBIO StressEnvironnementaux et Biosurveillance des milieux aquatiques, Plateau technique mobile en cytométrie environnementale MOBICYTE, UFR Sciences Exactes et Naturelles, Université de Reims Champagne-Ardenne, Reims, France, [3] Laboratory of Aquaculture & Artemia Reference Center, Faculty of Bioscience Engineering, Ghent University, Ghent, Belgium, [4] Department of Cell Biology, Physiology and Immunology, Universitat Autònoma de Barcelona, Bellaterra, Spain, [5] Consorcio Tecnológico de Sanidad Acuícola, Ictio Biotechnologies S.A., Santiago, Chile, [6] Facultad de Medicina Veterinaria y Agronomía, Universidad de Las Américas, Providencia, Chile

β-glucans are prebiotic and/or food additives used by the aquaculture industry to enhance the immune response of fish. Their efficiency may vary according to their origin and structure. In this study, the immunostimulant effects of two β-glucan types extracted from wild-type baker's yeast (*Saccharomyces cerevisiae*) and its null-mutant Gas1 were investigated. Gas1 has a beta-1,3-glucanosyltransferase activity necessary for cell wall assembly. Using a positive (commercial product MacroGard®) and a negative control (a diet without glucans), we evaluated the immune responses and disease resistance of rainbow trout juveniles (mean weight, ~44 g) fed control, low (0.2%) and high (0.5%) doses of Macrogard®, Gas1, and Wild type-β-glucan after a short-term (15 days, D15) or mid-term (36 days, D36) feeding periods. We found that β-glucan supplemented diets did not affect growth performance, mortality, splenic index, or leukocyte respiratory burst activity on D15 nor D36. However, each β-glucan triggered different immune effectors, depending of the doses or length of exposure compared to others and/or the negative control. Indeed, high dose of MacroGard® significantly increased lysozyme activities at D15 compared with the control and other diets ($p<0.05$). At D36, MacroGard β-glucan enhanced the production of lymphocytes in comparison with the control diet ($p<0.05$). Regarding WT β-glucan, at D36, WT-β-glucan, especially the high dose, provided the highest enzymatic activities (lysozyme and ACH50) and Ig level ($p<0.01$). Furthermore, on D36, Gas1 also increased lysozyme activity, Ig proportion, and some immune genes (*mcsfra*, *hepcidin*) compared with MacroGard® ($p<0.05$). Besides, both doses of Gas1-β-

OPEN ACCESS

Edited by:
Brian Dixon, University of Waterloo, Canada

Reviewed by:
Seyed Hossein Hoseinifar, Gorgan University of Agricultural Sciences and Natural Resources, Iran
David Huyben, University of Guelph, Canada

***Correspondence:**
Patrick Kestemont
patrick.kestemont@unamur.be

†Present address:
Trinh Dinh Khuyen, Aquatic Genetic and Selective Breeding Unit, Department of Aquaculture, Faculty of Fisheries, Vietnam National University of Agriculture, Hanoi, Vietnam

‡*These authors have contributed equally to this work and share first authorship*

Specialty section:
This article was submitted to Comparative Immunology, a section of the journal Frontiers in Immunology

Received: *11 April 2021*
Accepted: *18 June 2021*
Published: *06 July 2021*

Citation:
Cornet V, Khuyen TD, Mandiki SNM, Betoulle S, Bossier P, Reyes-López FE, Tort L and Kestemont P (2021) GAS1: A New β-Glucan Immunostimulant Candidate to Increase Rainbow Trout (Oncorhynchus mykiss) Resistance to Bacterial Infections With Aeromonas salmonicida achromogenes. Front. Immunol. 12:693613. doi: 10.3389/fimmu.2021.693613

glucans increased the resistance of juveniles to bacterial infection highlighted by a higher survival rate at 14 days post-challenge compared with the control and other types and doses of β-glucans ($p<0.05$). In conclusion, our results suggest that Gas1-β-glucan could represent a promising immunostimulant that would help to prevent diseases in aquaculture even more efficiently than other β-glucans already in use. Mode of action and particular efficiency of this new Gas1 mutant are debated.

Keywords: immune gene expression, immunostimulant, rainbow trout, bacterial challenge, beta-glucan

INTRODUCTION

Diseases are major constraints to sustainable aquaculture production, especially for intensive aquaculture systems (1–3). Indeed, fish might often be exposed to stressful conditions, eventually becoming more susceptible to microbial infections (4). For the past few decades, the traditional strategy for fish disease control in aquaculture relied on the use of antibiotics and chemical disinfectants. However, application of antibiotics can lead to the development of antibiotic-resistant bacterial strains and cause many other problems, such as environmental hazards, food safety problems, and increasing resistance of pathogens (5). The use of antibiotics can also adversely affect the health status of the fish (6, 7). Further, sub-therapeutic doses of antibiotic have been often added to aquatic feeds to promote growth, and this has further contributed to drug resistance (8). Therefore, the prophylactic use of antibiotic treatments in aquaculture has resulted in a very limited use or a ban of most compounds in top aquaculture production countries and stringent regulations on the application of antibiotics worldwide (9). This situation and recent restrictions on the use of antibiotics have promoted the use of prebiotics, probiotics (or a combination of both named synbiotics), and immunostimulant compounds (such as glucans) as preventive strategies to limit and control fish diseases (10–13).

β-glucan is a heterogeneous group of glucose polysaccharides consisting of a backbone of β(1,3)-link β-D-glucopyranosyl units with β-(1,6)-link side chains of varying length and distribution (14) and are a major structural component of fungi, bacteria, plants, algae, yeast, and mushroom cell walls. Although the cell wall β-glucans of yeast and fungi is mostly composed of 1,3-β linked glycopyranosyl residues with small numbers of 1,6 β-linked branches, oat and barley cell walls are formed of unbranched β-glucans with 1,3 and 1,4 β-linked glycopyranosyl residues, bacteria have unbranched 1,3 β-linked glycopyranosyl residues (15). Because of some similar structure with fungal or bacterial gram-negative polysaccharides, the recognition of β-glucan by host's cell pattern recognition receptors can trigger inflammatory cascade, leading to the enhancement of the immune system (16).

Particularly, it has been reported that β-glucans bind to specific cell surface receptors of macrophages and neutrophilic granulocytes that promote the enhancement of an organism's protective activity against infection through the activation of leukocytes, phagocytic activity, inflammatory cytokines, chemokines, reactive oxygen free radicals, increase the activity of antioxidant enzymes, and initiate the development of adaptive immunity and elimination and killing of microorganisms (11, 17–19). A wide range of studies described numerous immunostimulant effects of β-glucans in several fish species with different levels of immune stimulation, depending on fish species, β-glucans structure, dose, and duration of administration (5, 20–23).

In the rainbow trout, the potential immunomodulatory of β-glucans has been reported in several publications. Djordjevic et al. (24) showed that dietary β-1,3/1,6-glucans (level 0.2% and 0.4% diets for 37 days) decreased the expression of genes involved in acute inflammatory reactions to the inflammatory agent, whereas major parts of the immune response remained un-changed. Also, Lauridsen & Buchmann (25) reported that dietary β-1,3/1,6-glucans (0.2% diets, for 46 days) fed rainbow trout increased resistance against challenge with *Ichthyophthirius multifiliis* (white spot disease). Moreover, Skov et al. (26) reported that dietary β-1,3-glucans from *Euglena gracilis* at 1% diets, 1% biomass day^{-1} for 84 consecutive days down-regulated the expression of pro-inflammatory genes, whereas no effect of β-1,3-glucans diets on survival after *Yersinia ruckeri* challenge.

However, the effects of β-glucans on fish immune system functions can be variable, depending on the frequency, location, and length of the side-chains, which may play a role in immunomodulation. Differences in molecular weight, shape, and structure of β-glucans explain not only the differences in biological activity (15) but also fish species and administration route. Indeed, diets supplemented by a commercial β-glucans (MacroGard®) administrated to channel catfish (*Ictalurus punctatus*) for 4 weeks did not significantly affect several immune parameters, such as plasma lysozyme, bactericidal and hemolytic complement activities, respiratory burst of phagocytes, and the number of lymphocytes found, survival rate in fish infected with *Edwardsiella ictaluri* (27). Positive dose-related effects of β-1,3-glucans extracted from by *Saccharomyces cerevisiae* have been reported on some immune functions in rainbow trout (28). Besides, Douxfils et al. (29) found that overdoses of β-glucans (MacroGard®) and/or prolonged medication can lead to a non-reactive physiological status and, consequently, to a poor immune response in rainbow trout. In a previous study, Han et al. (30) demonstrated that Gas1, a β-1,3-glucans produced by the null-mutant yeasts Gas1 of *Saccharomyces cerevisiae* provided the best protection to *A. franciscana* against *Vibrio harveyi* in comparison with wild-type (WT) *Saccharomyces cerevisiae* and commercial β-1,3-glucans. The authors partly explained this observation by a

different structure of the Gas1 β-1,3-glucans that has a lower degree of branching and a shorter side chain length in comparison with the two others.

In our study, we aimed to evaluate if Gas1 β-1,3-glucans could also improve fish resistance in comparison with the WT β-1,3-glucans of *Saccharomyces cerevisiae* and to a commercial one, MacroGard® that effects are already well described in literature. In that purpose, we conducted a comprehensive evaluation of short- and mid-term (D15 and D36) and dose effects (low dose at 0.2% diet vs high dose at 0.5% diet) of dietary administration of different types β-glucans extracted from yeast wild or cell-wall mutants Gas1 with different particle size and chemical structure (WT- and Gas1-β-glucan) extracted by the laboratory of Aquaculture and Artemia Reference Centre (ARC, UGent) compared to a commercial β-glucan (MacroGard®) on the immune functions and resistance to pathogens of rainbow trout juveniles. In that purpose, blood leukocyte cells, humoral immune parameters, and immune-related gene expression in relevant immune organs, such as spleen and kidneys, will be evaluated. Moreover, the disease resistance of trout juveniles was tested by applying a bacterial challenge test based on the intraperitoneal injection of *Aeromonas salmonicida achromogenes*.

MATERIALS AND METHODS

Experimental Fish

Feeding trial and bacterial challenge were carried out in agreement with the European and Belgian national legislation on animal welfare (Protocol number: 13197 KE). Rainbow trout juveniles (n = 315) were transported from a local fish farm (Hatrival, Belgium) to the University of Namur (in facilities of the research unit of environmental and evolutive biology) and distributed into nine fiberglass tanks of 100 L (35 fish/100 L/tank) in a recirculation system. Fish were allowed to acclimate to the new environment for 21 days.

During this period, water temperature was maintained at 13.9 ± 1.2°C by a cooling system, oxygen level averaged 11.6 ± 0.7 mg/L (aeration applied), constant photoperiod (light/dark ratio = 12:12), and fish were fed 1.5% of fish biomass, twice daily (at 9:00 AM and 5:00 PM) with a specific trout diet (Coppens TROCO SUPREME-16, The Netherlands, crude protein = 48%, crude fat = 15%).

Fish Diet and Experimental Design

After acclimation, fish (mean body weight, 44.5 ± 3.0 g) were fed by hand either a control diet (no β-glucans) or diets containing three types of β-glucans: a commercial mixture of β-glucans, MO (MacroGard®, Biorigin, Brazil), and two yeast β-glucan products, namely GAS1-β-glucans (GAS1) and wild type β-glucans (WT) extracted by the Laboratory of Aquaculture & Artemia Reference Center (ARC) of Ghent University, Belgium as described in Han et al. (30). For each type of β-glucans, two doses were tested (0.2% or 0.5% of the diet) for 36 days at 1% of fish biomass/day that are called further in the text: G0.2%, G0.5% for Gas1 glucan, M0.2%, M0.5% for MacroGard® glucan, W0.2%, W0.5% for wild-type glucan. All diets were formulated and pelleted in the laboratory of the University of Namur (**Table 1**). Three replicate tanks were used for each experimental diet. After 15 days (short-term nutrient test, D15) and 36 days (mid-term nutrient test, D36) of feeding, six fish per tank (18 fish per experimental diet) were anesthetized in buffered (pH 7) ethyl 3-aminobenzoate methane sulfonic acid salt (98% purity, MS-222, Sigma) solution (120 mg/L). Blood was obtained by caudal vein puncture using a heparinized syringe and stored on ice in heparinized tubes. Fish were then euthanized by overdose of buffered MS-222 (240 mg/L) before decapitation. Spleen and head kidney were dissected; a part of spleen was immediately homogenized after dissection to prepare for spleen respiratory burst activity analysis. The remaining spleen and kidney samples were immediately snap-frozen in liquid nitrogen and finally stored at −80°C until analysis (RT-qPCR immune-related genes). Heparinized blood was immediately analyzed for

TABLE 1 | Ingredients and proximate composition of the experimental pelleted diet.

Ingredients	Diet* (g/kg)				
Cod fish meal[a]	350.0				
Blood meal[b]	70.0				
Wheat gluten[c]	134.0				
Cod fish oil[d]	128.0				
Starch[e]	223.6				
Carboxylmethylcellulose[e]	20.0				
α- cellulose[e]	42.4				
Mineral mix[f]	10.0				
Vitamin mix[g]	10.0				
Betaine[e]	10.0				
BHA	1.0				
BHT	1.0				
Analyzed diet composition	Crude protein (%)	Crude fat (%)	Dry matter (%)	Ash (%)	Energy (MJ/kg)
	48.00	14.75	92.16	14.30	19.8

**b-glucan doses were added in respective % of the diet reducing the levels of a-cellulose. [a]Cod fish meal (CP-crude protein = 89%, CF-crude fat = 4.0%) provided by SNICK euroingredient NV, Ruddervoorde (Belgium). [b]Blood meal (CP = 87.6%, CF = 0.0) as Actipro Hemoglobin, Zwevezele (Belgium). [c]Wheat Gluten (CP = 80.0, CF = 6.0%), Roquette Freres, Lestrem (France). [d]Sigma-Aldrich, Saint-Louis, MO, (USA). [e]Mosselman SA, Chlin (Belgium). [f]Mineral mix (g kg^{-1} of mix) was prepared in the lab, from (CaHPO4)2H2O, 727.77; (MgSO4)7H2O, 127.50; NaCl, 60.00; KCl, 50.00; (FeSO4)7H2O, 25.00; (ZnSO4)7H2O, 5.50; (MnSO4)4H2O, 2.54; (CuSO4)5H2O, 0.78; (CoSO4)7H2O, 0.48; (CaIO3)6H2O, 0.29; (CrCl3)6H2O, 0.13 g. [g]Vitamin mix was provided by INVE Aquaculture Company. BHA (butylated hydroxyanisole) and BHT (butylated hydroxyl toluene) were provided by Sigma-Aldrich-Belgium.*

leukocyte populations by flow cytometry, and the remaining volume of blood was then centrifuged at 7,500*g* for 10 min to collect plasma stored at −80°C until subsequent analyses (lysozyme activity, alternative complement activity, total immunoglobulin content).

Bacterial Challenge

To evaluate whether β-glucan has a beneficial effect on disease resistance, rainbow trout juveniles were experimentally infected with a virulent strain of *Aeromonas salmonicida achromogenes* provided by the CER group (Centre d'Economie Rurale, Laboratoire de Pathologie des Poissons, Belgium). Bacteria were cultured in sterile Brain Heart Infusion (BHI; Sigma Aldrich, Saint-Louis, MO, USA) and incubated at 28°C for 24 h. A preliminary test infection, including various bacterial doses was performed to determine the LD50 CFU of the targeted rainbow trout population (LD50 = 3.1×10^7 CFU/100 g fish body weight).

On D37, a total of 30 fish from each dietary condition (10 fish × 3 replicate tanks) were anesthetized. Then, the fish were intraperitoneally injected with a weight-adjusted dose (3.1×10^7 CFU/100 g of fish body weight) of the freshly prepared *A. salmonicida achromogenes* culture and equally distributed into three 50-L tanks. The fish were confined at the animal facility (Biosafety level 2) along the infection assay. They were starved 1 day ahead of infection as well as the day of bacterial injection, and then fed the respective experimental diets until the end of the challenge test. At 35 h post-injection (D39), a total of nine fish from each dietary condition (3 fish × 3 replicate tanks) were anesthetized, and blood was sampled for subsequent immunological assays (lysozyme and alternative complement pathway activity). Levels of plasma total Ig content and spleen RBA were not determined because of limitations in this experiment. Fish were then euthanized, and spleen and kidney were sampled and immediately snap-frozen until immune gene expression analysis (RT-qPCR).

Blood Leukocyte Populations

Blood cell populations were analyzed at D15 and D36 of dietary treatment by flow cytometry (Flow Activated Cell Sorter Calibur; Flow Cytometry System) according to Inoue et al. (31), later adapted by Mathieu et al. (32). Briefly, 10 µl of fresh heparinized blood were mixed with 1950 µl of Hanks Balanced Salt Solution (HBSS, Sigma) and 40 µl of fluorochrome DiOC6 (3,3-dihexyloxacarbocyanine, Molecular Probes, Eugene) diluted 1:10 in ethanol. The tube was mixed gently and incubated at room temperature (RT) for 10 min. The FACS was calibrated with True Count Beads diluted in HBSS, Sigma-Aldrich, Steinheim, Germany). Each blood cell population was identified by its typical location in an FL-1 v. SSC (FITC filter *versus* Side-scattered light) and FSC *vs.* SSC (Forward Scatter *versus* Side-scattered light) according to Inoue et al. (31) and Pierrard et al. (33). Four clusters were identified, thrombocyte and lymphocyte cells were gathered in the same cluster according to Pierrard et al. (33).

Plasma Lysozyme Activity

Lysozyme activity assay was performed by the turbidimetric method of Siwicki and Studnicka (34), later adapted by Mathieu et al. (35). Briefly, 7 µl of plasma were added to 130 µl of freshly prepared *Micrococcus luteus* (Sigma-Aldrich, Saint-Louis, USA) solution (0.6 mg/ml of Na_2HPO_4 0.05 M, pH 6.2) in triplicate. Absorbance corresponding to *Micrococcus luteus* lysis was measured at 450 nm for 60 min at regular intervals (5 min). One unit (U) of lysozyme was determined as an absorbance decrease of 0.001 per min.

Plasma Hemolytic Activity of Alternative Complement Activity

Plasma hemolytic activity of alternative complement activity (ACH50) was assayed following Oriol Sunyer and Tort (36), later modified by Milla et al. (37). Briefly, 10 µl of rabbit red blood cell suspension (RRBC, Biomerieux, Mary-l'Etoile, France) suspended at 3% in veronal buffer was mixed with serial dilutions of plasma (70 µl of total volume). Hemolysis (100%) was obtained by adding 60 µl of distillate water to 10 µl of RRBC. Negative control (fresh water) was obtained by adding 60 µl of veronal buffer to 10 µl of RRBC. Samples were incubated 100 min at 27°C and centrifuged (3,000*g*, 5 min, 4°C). Then, 35 µl of supernatant was transferred to a new microplate to measure the absorbance at 405 nm. The ACH50 value was defined as the reciprocal of the plasma dilution that induced the hemolysis of 50% RRBC.

Plasma Total Immunoglobulin Assay

Analysis of total plasma immunoglobulin content (Ig) was based on a spectrophotometric technique described by Siwicki and Anderson and later adapted by Milla et al. (37) with some modifications. Immunoglobulin was precipitated using 10,000 kDa polyethylene glycol (PEG, Sigma). Plasma was mixed with an equal volume of 12% PEG solution and shake 150 rpm for 2 h at room temperature. After centrifugation at 1,000*g* for 10 min, the supernatant was collected and assayed for its protein concentration by the method of Bradford (38). Plasma total immunoglobulin content was calculated by subtracting this value from the total protein concentration in the plasma before precipitation with PEG.

Spleen Leukocyte Respiratory Burst Activity

Just after collection, spleen samples were conditioned in L15 medium (Sigma-Aldrich) at 4°C, and gently pressed through sterilized nylon mesh (40 µm, Dutscher) to obtain leukocyte suspensions. Then, the L15 medium-diluted samples were loaded onto Ficoll gradient (Healthcare, GE). After centrifugation (2500 rpm, 20 min, at 4°C), leukocyte suspensions were collected and washed twice in L15 medium and again centrifuged (1200 rpm, 5 min, 4°C). They were re-suspended in L15 medium and viable leukocytes were adjusted at 10^6 cells/ml before classification of leukocyte populations (lymphocyte, macrophage, and granulocyte) by flow cytometry. RBA analysis was performed using the flow cytometry method as previously described by Chilmonczyk and Monge (39) with some modifications of Jolly et al. (40). The RBA test corresponded to an evaluation of intracellular hydrogen peroxide production following cell activation or not with phorbol 12-myristate 13-acetate (PMA). The fluorescence levels of unstimulated and PMA-stimulated

cells were determined after 30 min of cell incubation (18°C in the dark) with 2′-7′dichlorofluorescin diacetate (DCFH-DA (5 μM) and DCFH-DA plus PMA (2 μg ml^{-1}), respectively. The spleen respiratory burst activities were expressed in a stimulation index as the ratio between the mean fluorescence measured in stimulated cells (DCFH-DA + PMA) and the basal mean fluorescence of control (DCFH-DA only).

RNA Precipitation and Complementary DNA Synthesis

Three pools of each experimental condition and time-point were collected to compare their gene expression profiles. Total RNA was extracted individually from the spleen and head kidney) by grounding 100 mg of the organ with a pestle until full homogenization in TriReagent (Sigma-Aldrich, St. Louis, MO). The next steps were performed according to the manufacturer's instructions. The pellet was dried and resuspended in 200 μl of RNase-free water. Total RNA concentration was determined by Nano Drop-2000 spectrophotometer (Thermo Scientific), and the integrity was checked by Experion RNA Std Sens analysis (Bio-Rad Laboratories, Hercules, CA). Total RNA (1 μg) was used to synthesize cDNA with iScript cDNA synthesis kit (Bio-Rad Laboratories) following this protocol: priming for 5 min at 25°C, reverse transcription for 20 min at 46°C, RT inactivation for 1 min at 95°C as recommended by the manufacturer.

Gene Expression Analysis

Real-time PCR assay was carried out to analyze the expression pattern of different genes of immunological relevance in spleen and kidney from rainbow trout stimulated with β-glucan. Samples were taken randomly from three fish of three different tanks for each treatment (n = 9) at D15 and D36 days of feeding with different doses and types of β-glucan. Samples of three randomly selected fish from each tank were pooled for each treatment (n = 3 fish per each pool). On day 37 of feeding, fish were challenged against *A. salmonicida achromogenes* and 35 h post-challenge (D39 of treatment) three fish of three different tanks for each treatment (n = 9 fish) were also collected. Samples were also taken using the same strategy from fish fed with basal diet and from non-infected fish (n = 3 fish per each pool). As a housekeeping gene, elongation factor 1 alpha (*ef-1α*) that exhibited the most stable expression (compared to *β-actin* and *18S* genes) between samples was amplified from all the evaluated samples. The gene expression of pro-inflammatory (*il-1*), macrophages (*mcsfra*), antibacterial (*Lysozyme, Hepcidin*), humoral (*mIgM*), membrane protein (TLR_2), neutrophils (*mpo*), Cathelicidin (*CATH1*), T-helper (*cd4-2β*), and anti-inflammatory responses (*il-10*, *tgf-β1*) were evaluated. The list of specific primers used for gene expression analysis is given in **Table 2**, and those were designed according to Cornet et al. (41) and Khuyen et al. (42). Real-time PCR reactions were carried out with iTaq Universal SYBR Green Supermix (Bio-Rad Laboratories) using a 1:40 dilution of the cDNA for target genes or 1:1000 dilutions for *ef-1α*.

Primers for target genes were used at 500 nM. The thermal conditions used were 3 min at 95°C of pre-incubation, followed by 40 cycles at 95°C for 30 s, and 60°C for 30 s. All reactions were performed using ABIprism 7300 (Applied Biosystem), and quantification was done according to the Pfaffl method (43) corrected for efficiency of each primer set. Values for each sample were expressed as normalized relative expression (NRE), calculated in relation to values of the control group, and normalized against those of the housekeeping gene *ef-1α*. The results are expressed as an average of values obtained in all pools from D15 and D36 of feeding, and D39 (after bacterial challenge test).

Statistical Analysis

Results are presented as box plot representing the quartile distribution of the data. Statistical analyses were performed using

TABLE 2 | Primers used for each gene expression analysis by real-time RT.

Genes	Primer sequence (5'-3')	Accession number	Amplicon size	Efficiency
ef-1α	Fw: 5'-ATGCCCCCAAGTTCCTGAAG-3' Rv: 5'-AACAGCAACAGTCTGCCTCA-3'	NM_001124339.1	140	1.95
il-1	Fw: 5'-TGAGAACAAGTGCTGGGTCC-3' Rv: 5'-GGCTACAGGTCTGGCTTCAG-3'	NM_001124347.2	148	2.02
lysozyme	Fw: 5'-TGCCTGTCAAAATGGGAGTC-3' Rv: 5'-CAGCGGATACCACAGACGTT-3'	NM_001124716.1	152	1.89
mIgM	Fw: 5'-AAAGCCTACAAGAGGGAGACCGAT-3' Rv: 5'-AGAGTTATGAGGAAGAGTATGATGAAGGTG-3'	X65263.1	128	2
mcsf-ra	Fw: 5'-ATCTCCACTCATGGCGACACA-3' Rv: 5'-CATCGCACTGGGTTTCTGGTA-3'	AB091826	177	2
mpo	Fw: 5'-GCAGAGTCACCAATGACACCA-3' Rv: 5'-ATCCACACGGGCATCACCTG-3'	GBTD01119227	68	2
il-10	Fw: 5'-CCGCCATGAACAACAGAACA-3' Rv: 5'-TCCTGCATTGGACGATCTCT-3'	NM_001245099.1	105	1.98
tgf-β1	Fw: 5'-GCCAAGGAGGTCCACAAGTT-3' Rv: 5'-GTGGTTTTGATGAGCAGGCG-3'	NM_001281366.1	146	2.06
cd4-2β	Fw: 5'-AAGCCCCTCTTGCCGAGGAA-3' Rv: 5'-CTCAACGCCTTTGGTACAGTGA-3'	AY899932	108	2
vapA	Fw: 5'-ATTAGCCCGAACGACAACAC-3' Rv: 5'-CCAACACAATGAAACCGTTG-3'	KP184543.1	148	2.02

Primers were designed according to Cornet et al. (41) and Khuyen et al. (42).

Rstudio software (R version 4.0.3). For each timepoint, which was treated independently, the effects of the concentration, type of glucan, and their interaction were analyzed using a generalized linear model with the following code: glm (variable ~ type of glucan × concentration, family = Gaussian, data = timepoint). Post hoc comparisons (Tukey's test) at a 5% significant level were performed on the factor (type of glucan or concentration) or their interaction (type of glucan × concentration) with general linear hypotheses and multiple comparisons for parametric models (multcomp R package) and Benjamin-Hochberg (BH) correction was applied. When two groups (from either the concentration, type of glucans or their interaction depending on the results of the glm) do not differ from each other, they will share the same letter annotation (for example "a"), and when two groups are significantly different, they will be identified by different letters ("a" and "b"). As in this study, the interaction of two factors is considered and that seven groups (control, 3 types β-glucans × 2 concentrations) are compared, it is possible that a group is annotated with more than one letter (for example "ab").

RESULTS

Specific Growth Rate, Mortality, and Splenic Index

Fish fed different β-glucan types showed no significant differences of SGR in comparison with the control diet either on day 15 (D15) or day 36 (D36) (**Table 3**). Mortality rate did not differ between controls and β-glucan treatments (**Table 3**). Furthermore, no significant changes in SI values were observed on D15 and D36 in all β-glucan diets compared with control diet (**Table 3**).

Humoral Immune Variables

On D36, the high dose of wild type β-glucan (W0.5%) significantly stimulated ACH50 level in comparison with M0.5% and G0.2%, whereas G0.2% significantly reduced it compared to the M0.2% ($p<0.01$, **Figure 1A**). At D15 and 2 days after bacterial injection (D39), there was no significant difference of plasma ACH50 level between treatment and control groups.

On D36, G0.2%, W0.2%, and W0.5% significantly elevated the levels of plasma total Ig ($p < 0.001$) compared to the control diet (**Figure 1B**) and M0.2%.

Concerning lysozyme parameters, on D15, M0.5% significantly improved its activity compared to the control diet and M0.2%. On the contrary, for GAS1 and wild type β-glucan, the lowest doses G0.2% and W0.2% were better to improve lysozyme activity in comparison with the control ($p<0.0001$) and their respective high dose (**Figure 1C**). At D36, we only observed a type of glucan effect, where WT exhibited a significant highest lysozyme activity, followed by Gas1 and then MacroGard ($p<0.0001$). After the bacterial infection, an effect of the concentration of β-glucan was highlighted, with a higher activity with 0.2% in comparison with 0.5% of β-glucan ($p<0.05$).

Eventually, levels of respiratory burst activity (RBA) of spleen lymphocytes (as for macrophage cells) did not significantly differ whatever the β-glucan administration doses and types on D15, and an effect of the concentration of β-glucan was highlighted, with a higher RBA in 0.2% compared to 0.5% ($p<0.05$) (**Figure 1D**).

Blood Leukocyte Cell Proportions

Blood leukocytes were composed of high percentages of lymphocytes followed by those of neutrophils, monocytes, and basophils (**Figures 2A–D**). Lymphocyte proportion was not modified at D15; however, on D36, lymphocyte proportions were higher with MacroGard β-glucan in comparison with the control ($p<0.01$).

On D15, the type of β-glucan significantly influenced the proportion of basophils with the highest quantity in fish fed MacroGard and control diets in comparison with Gas1 ($p<0.05$).

Finally, the type of β-glucan also significantly affected neutrophils proportion of fish as MacroGard diet reduced it in comparison of WT and the control diet.

Immune Gene Expression

Pro- and Anti-Inflammatory Gene Expressions

Expression levels of both pro-inflammatory (*il-1β*) and anti-inflammatory (*tgf-β1*, *il-10*) genes were evaluated in spleen and kidney organs of fish sampled after short-term (D15) or mid-term β-glucan administration, also the expression of some immune genes was recorded on D39 after bacterial challenge (**Figures 3A–F**).

In the spleen, no significant effect was observed at D15, whereas only the type of β-glucan affected the expression of *il-10*, with a significant decrease in MacroGard and WT diets in comparison of the control diet ($p < 0.05$, **Figure 3E**).

TABLE 3 | Mean (± SD) values for specific growth rate (SGR), mortality and splenic index (SI) of trout juveniles fed with low (0.2%) and high (0.5%) doses of different beta glucan types on day 15 and day 36 of the feeding trial.

Times (Days)	Variables	Control	Macrogard		GAS1		Wild type		$F_{-values}$	$P_{-values}$
			M0.2%	M0.5%	G0.2%	G0.5%	W0.2%	W0.5%		
15	SGR (%/day)	1.53 ± 0.33	1.46 ± 0.26	1.72 ± 0.32	1.56 ± 0.32	1.32 ± 0.37	1.80 ± 0.01	1.60 ± 0.18	1.497	0.254
	Mortality (%)	3.8 ± 6.6	4.8 ± 8.2	2.9 ± 4.9	4.8 ± 5.9	1.0 ± 1.6	4.8 ± 5.9	1.0 ± 1.6	0.233	0.958
	Splenic index (%)	0.11± 0.02	0.11 ± 0.02	0.13 ± 0.04	0.12 ± 0.03	0.12 ± 0.02	0.11 ± 0.01	0.11 ± 0.03	0.214	0.966
36	SGR (%/day)	1.58 ± 0.06	1.54 ± 0.10	1.73 ± 0.35	1.51 ± 0.08	1.75 ± 0.34	1.36 ± 0.34	1.54 ± 0.06	0.224	0.965
	Mortality (%)	3.3 ± 5.8	0.0 ± 0.0	1.1 ± 1.9	1.3 ± 2.2	1.1 ± 1.9	3.6 ± 3.5	1.1 ± 2.0	0.586	0.736
	Splenic index (%)	0.16 ± 0.03	0.16 ± 0.04	0.18 ± 0.03	0.18 ± 0.02	0.17 ± 0.01	0.16 ± 0.04	0.17 ± 0.00	0.438	0.841

Statistical differences between dietary treatments are indicated by different lower-case letters ($p < 0.05$). Splenic index = weight of spleen (g)/weight of body(g). (n= 3 for SGR and mortality and n=9 for SI).

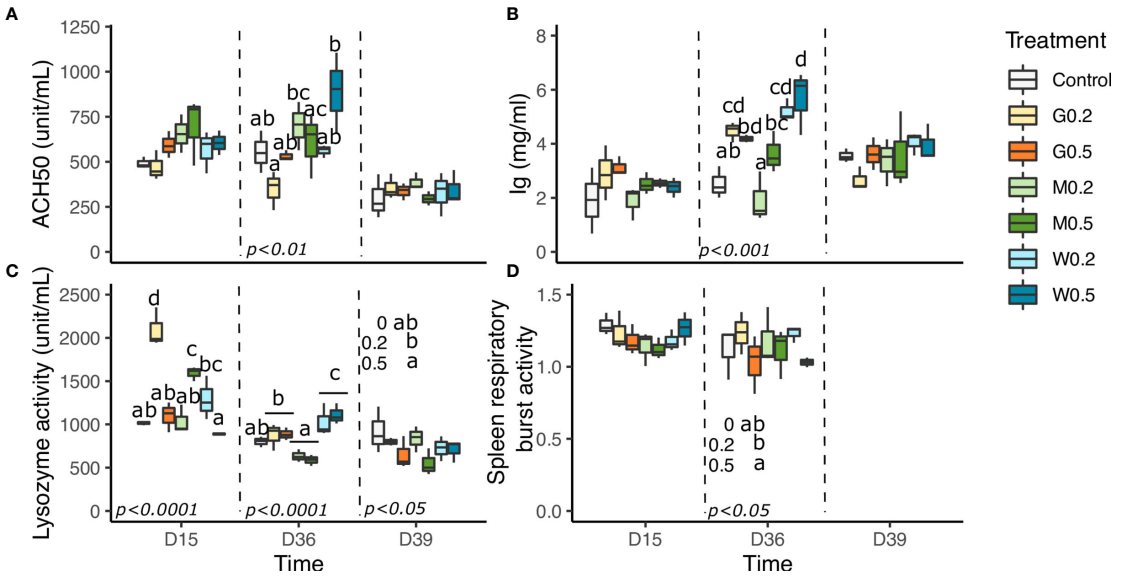

FIGURE 1 | Effects of dietary beta glucan administration on humoral parameters of fish sampled during the nutrient test on D15 and D36, or 2 days after bacterial infection (D39). **(A)** Plasma hemolytic alternative complement activity. **(B)** Plasma total immunoglobulin's content. **(C)** Plasma lysozyme activity. **(D)** Respiratory burst activity (RBA) of spleen macrophage cells. Values are expressed as mean ± SD of 18 fish/diet/day on D15, D36 and 9 fish/diet on D39. For spleen respiratory burst activity (RBA), plasma hemolytic alternative complement activity (ACH50) data are expressed as mean ± SD of 9 fish/diet/day on D15, D36. Statistical differences between groups are indicated by different letters Statistical differences, highlighted by letters, are indicated for glucan concentrations in front of 0, 0.2, and 0.5% next to the corresponding plot, for glucan type by letter above the horizontal bar grouping the two doses of the same glucan, for glucan type × concentrations interactions above each box. P values are shown at the bottom of each graph at a given timepoint (D15, D36, or D39).

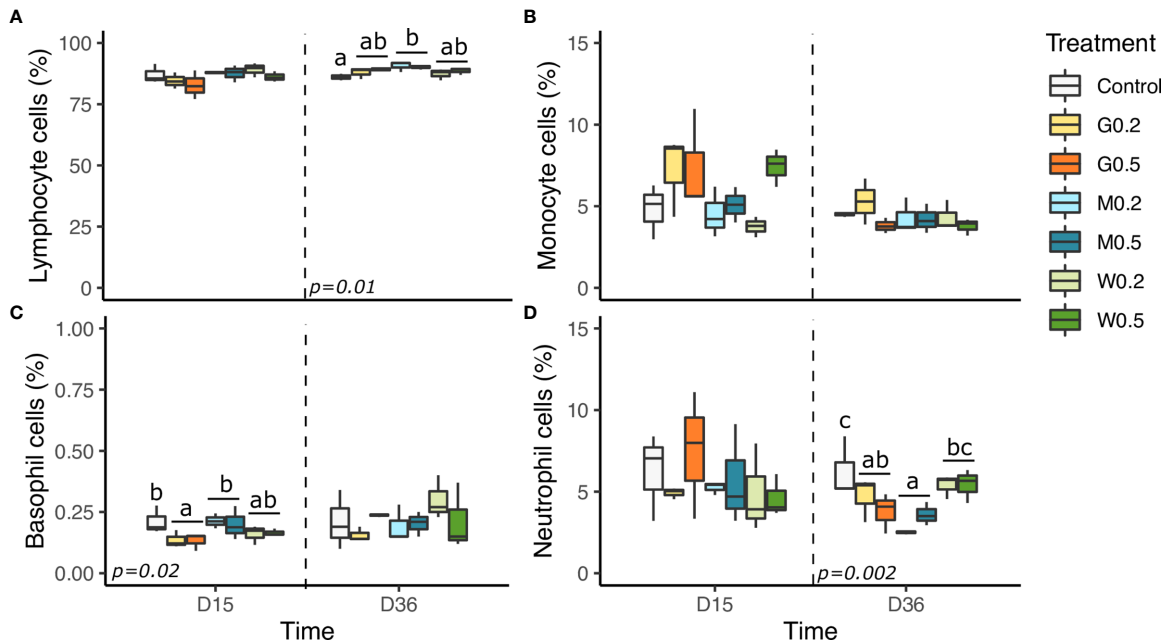

FIGURE 2 | Effects of dietary beta glucan administration on blood leukocyte cell proportions of fish sampled during the nutrient test on D15 and D36. **(A)** Lymphocyte + thrombocyte cells proportions. **(B)** Monocyte cells proportion. **(C)** Neutrophil cells proportion and **(D)** Basophil cells proportion in total blood leukocyte cells population. Values are expressed as mean ± SD of 18 fish/diet/day on D15, D36. Statistical differences, highlighted by letters, are indicated for glucan concentrations in front of 0, 0.2, and 0.5% next to the corresponding plot, for glucan type by letter above the horizontal bar grouping the two doses of the same glucan, for glucan type × concentrations interactions above each box. P values are shown at the bottom of each graph at a given time point (D15, D36, or D39).

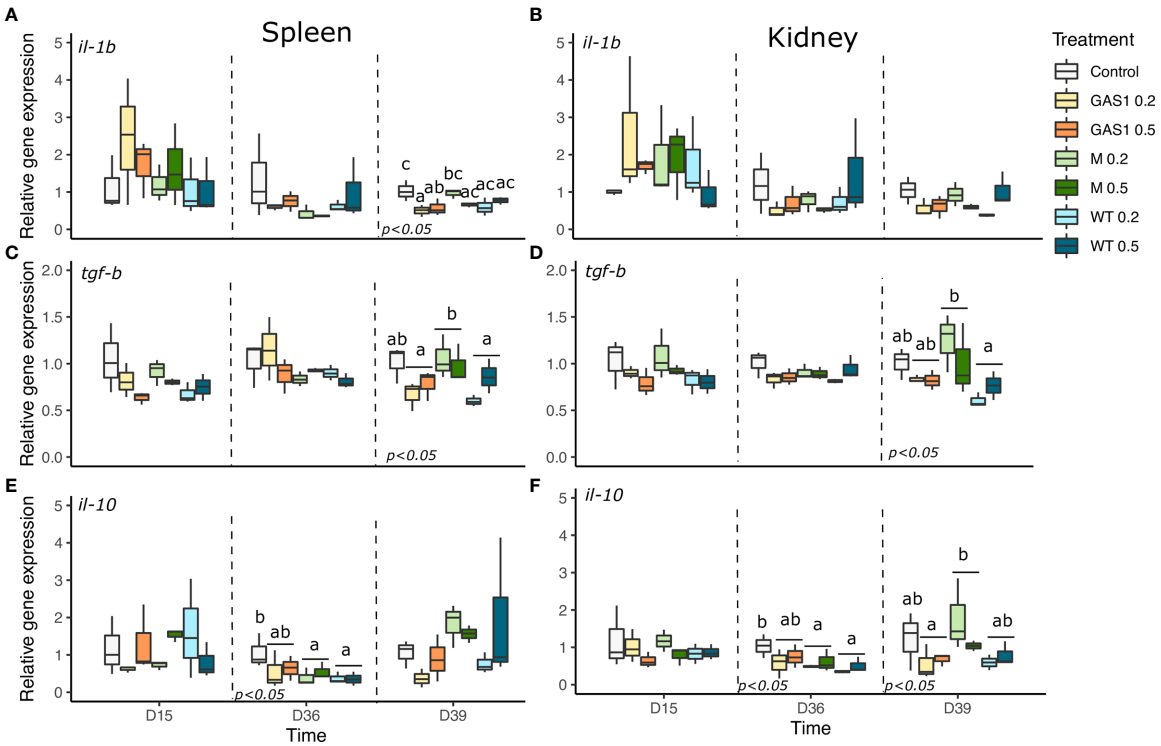

FIGURE 3 | Effects of dietary β-glucan on pro-inflammatory gene expressions in spleen and kidney of fish sampled during the nutrient test on D15 and D36, or 2 days after the bacterial challenge (D39). **(A–F)** are expression levels of *il-1β*, *tgf-β1*, and *il-10* in spleen and kidney, respectively. Relative transcript (mRNA) levels were determined by real-time RT-PCR and normalized by the arithmetic mean of *ef-1α* expression. Values are expressed as mean ± SD of three pool samples per experimental condition (3 fish per pool sample). Statistical differences, highlighted by letters, are indicated for glucan concentrations in front of 0%, 0.2%, and 0.5% next to the corresponding plot, for glucan type by letter above the horizontal bar grouping the two doses of the same glucan, for glucan type × concentrations interactions above each box. P values are shown at the bottom of each graph at a given time point (D15, D36, or D39).

On D39, after bacterial challenged, G0.2% and G0.5% diets significantly reduced *il-1β* gene expression compared to the control (p<0.05, **Figure 3A**). Meanwhile, MacroGard diet up-regulated *tgf-β1* gene expression in comparison with the Gas1 and WT diet (p<0.05, **Figure 3C**).

In kidneys, MacroGard and WT diets significantly reduced *il-10* gene expression in comparison of the control diet on D36 (p<0.05; **Figure 3F**). After bacterial challenge, only the type of β-glucan affected *tgf-β1* and *il-10* gene expression compared to the control (p<0.05, **Figures 3D, F**). Indeed, MacroGard diet significantly enhanced the expression of *tgf-β1* and *il-10* compared, respectively, to WT and Gas1 diets.

Expression of T-Helper, mIgM, Complements C_3, mcsfra, and TLR_2 Genes

The expression levels of T-helper genes (*cd4*-2β), membrane immunoglobulin M (mIgM), *complement C3*, *macrophage colony-stimulating factor receptor a (mcsfra)*, and *Toll like receptor* (*tlr2*) genes were determined in spleen and kidney samples (**Figure 4**).

In spleen, after 15 days, *cd4-2β* and *tlr2* gene expressions were modified by the type of β-glucan with a repression observed in fish-fed Gas1 and WT diets compared with the control group (p<0.05, **Figures 4A, E**). Similarly, Gas1 and Macrogard diets enhanced the expression of *mIgM* in comparison to WT diet at D15. In addition, Gas 1 diet also significantly raised the expression of *C3a* in comparison with MG and WT diets (**Figure 5A**). On D36, only *mcsfra* was modulated by the type of β-glucan with an increase of its expression with Gas1 and WT diets ($p < 0.05$, **Figure 5C**). After bacterial injection (D39), only *tlr2* was affected by the type of β-glucan as fish-fed Gas1 diet had a significant higher expression level compared with MacroGard and WT diets (p<0.05, **Figure 4E**).

In kidneys, WT diet significantly repressed *cd4-2β* gene expression compared with the control on D15 ($p < 0.05$; **Figure 4B**) on D15. On D36, no gene expression was modulated by the diets, while after bacterial infection, only *igm* and *mcsfra* expression was changed by the type of β-glucan in the diet. Indeed, WT diet significantly increase *igm* expression compared with the control ($p < 0.05$, **Figure 4D**), whereas it repressed *mcsfra* expression in comparison of control and MG diets ($p < 0.05$, **Figure 5D**). There was no change of *tlr2* and *C3a* gene expression in kidneys on D15, D36, and D39 after β-glucan treatments (**Figure 5B**).

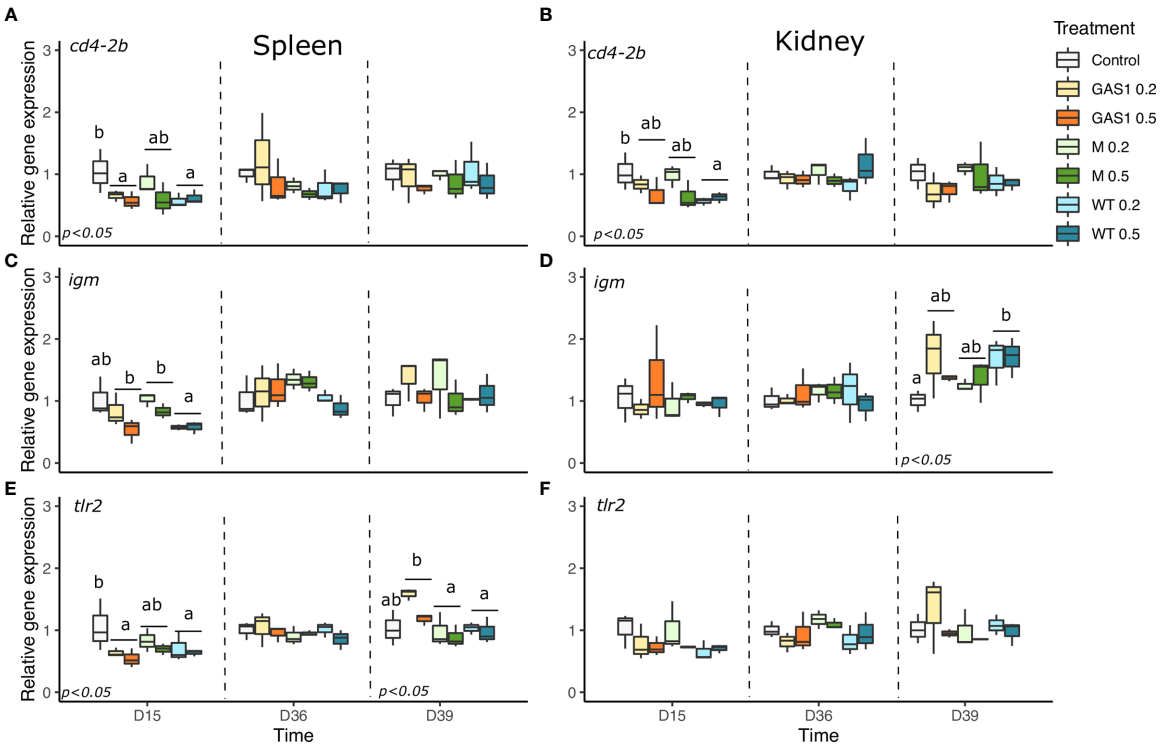

FIGURE 4 | Effects of dietary beta glucan on T-helper (*cd4-2β*), humoral (*mIgM*) and membrane protein (TLR_2) genes expressions in the spleen and kidney of fish sampled during the nutrient test on D15 and D36, or 2 days after the bacterial challenge (D39). **(A–F)** are expression levels of *cd4-2β*, *mIgM*, $TLR_{2\ in}$ spleen and kidney, respectively. Relative transcript (mRNA) levels were determined by real-time RT-PCR and normalized by the arithmetic mean of *ef-1α* expression. Values are expressed as mean ± SD of 3 pool samples per experimental condition (3 fish per pool sample). Statistical differences, highlighted by letters, are indicated for glucan concentrations in front of 0, 0.2, and 0.5% next to the corresponding plot, for glucan type by letter above the horizontal bar grouping the two doses of the same glucan, for glucan type × concentrations interactions above each box. P values are shown at the bottom of each graph at a given time point (D15, D36, or D39).

Antibacterial Gene Expressions

Expression of antibacterial genes (*C-type lysozyme, Hepcidin, Cathelicidin*, and *Myeloperoxidase*) were evaluated in the kidneys and spleen on D15, D36, and D39 (**Figures 6A–D** and **7A–D**).

In spleen at D15, Gas1 and WT diets caused a significant decrease of *Hepcidin* gene expression compared with the control diet (p=0.015, **Figure 6C**). On the contrary, at D36, *hepcidin* expression was higher in Gas1 and WT diet in comparison with the respective levels of fish fed MG diet (p<0.05, **Figure 6C**). After the bacterial infection, only *lysozyme* and *mpo* genes were affected by the type of β-glucan with an increase of their expression with Gas1 in comparison with MG diet ($p < 0.05$; **Figures 6A** and **7C**).

In kidneys, there was no change of *lysozyme* and *cathelicidin* gene expression on D15, D36, and D39 after β-glucan treatments (**Figures 6B** and **7B**). Regarding *hepcidin* gene expression, it was only modulated on D15 by the concentration of the compound with a higher expression of the gene with the lowest dose ($p < 0.05$; **Figure 6D**).

Survival Rate

The mortality rate increased earlier and more rapidly in trout fed with the control and most of β-glucan diets during the first week of infection, except for fish fed with low dose of GAS1 β-glucan (G0.2%) (**Figure 8**). The mortality of fish fed with G0.2% was reduced from day 5 and stopped on the 10th day after bacterial injections, whereas other β-glucan diets were stopped later between the 10th and 12th day post-infection. The survival rates were significantly higher in fish fed G0.2% (43.3%) and G0.5% (30.0%) than in controls (16.7%) 14 days after bacterial injection ($F = 6.5$, $p = 0.0019$; **Figure 8**), followed by M0.5% (26.7%). The higher mortality rates were observed in M0.2% and W0.5%.

DISCUSSION

In this study, rainbow trout juveniles were fed with a control diet or enriched diets with Macrogard-β-glucan, GAS1- β-glucan, and WT-β-glucan at low (0.2% diet) and high doses (0.5% diet), and fish were sampled after short-term (15 days) and mid-term (36 days) feedings. After 15 and 36 days of treatment, β-glucan diets did not significantly modify specific growth rate (SGR), mortality, or splenic index of treated fish in comparison with the control group. This result may be due to the duration of the experiment that was not long enough to induce a significant modification of growth

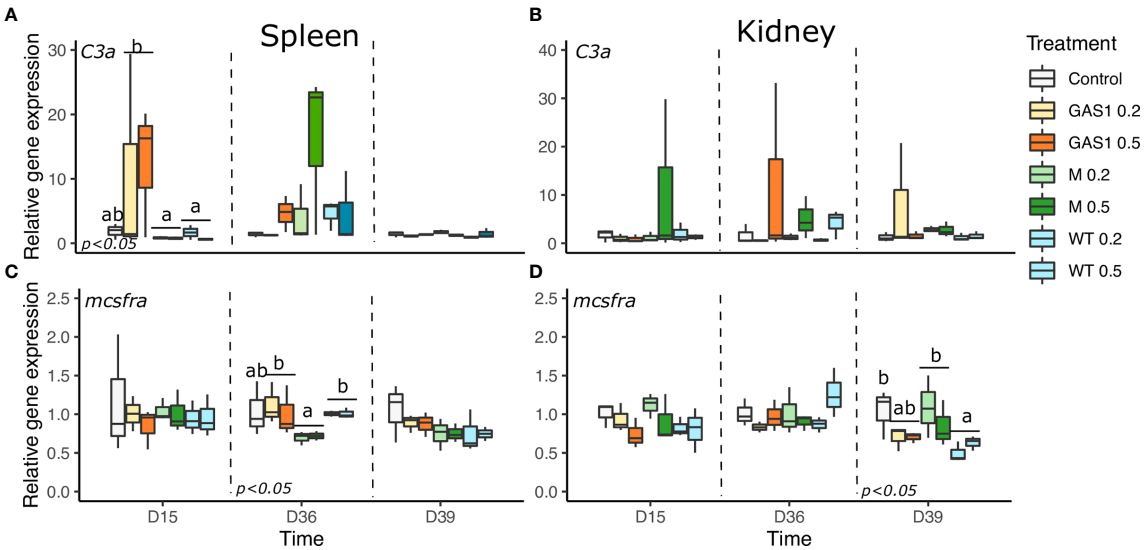

FIGURE 5 | Effects of dietary beta glucan on C3a complement (*c3a*) and macrophage colony-stimulating factor receptor a (*mcsfra*) genes expressions in the spleen and kidney of fish sampled during the nutrient test on D15 and D36, or 2 days after the bacterial challenge (D39). **(A–D)** are expression levels of *c3a* and *mcsfra* $_{in}$ spleen and kidney, respectively. Relative transcript (mRNA) levels were determined by real-time RT-PCR and normalized by the arithmetic mean of *ef-1α* expression. Values are expressed as mean ± SD of three pool samples per experimental condition (3 fish per pool sample). Statistical differences, highlighted by letters, are indicated for glucan concentrations in front of 0, 0.2, and 0.5% next to the corresponding plot, for glucan type by letter above the horizontal bar grouping the two doses of the same glucan, for glucan type × concentrations interactions above each box. P values are shown at the bottom of each graph at a given time point (D15, D36, or D39).

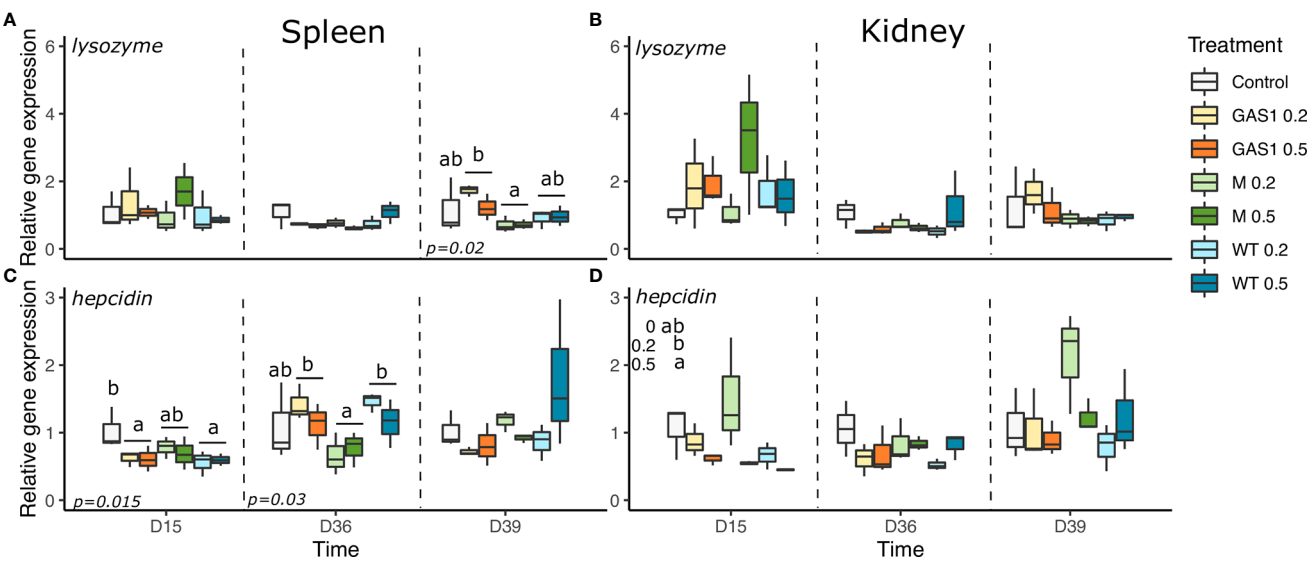

FIGURE 6 | Effects of dietary beta glucans on *C-type lysozyme* and *Hepcidin* genes expression in the spleen or kidney of fish sampled during the nutrient test on D15 and D36, or 2 days after the bacterial challenge (D39). **(A)** *lysozyme* gene expression in spleen. **(B)** *lysozyme* gene expression in kidney. **(C)** *Hepcidin* gene expression in spleen. **(D)** *Hepcidin* gene expression in kidney. Relative transcript (mRNA) levels were determined by real-time RT-PCR and normalized by the arithmetic mean of *ef-1α* gene expressions. Values are expressed as mean ± SD of three pool samples per experimental condition (3 fish per pool sample). Statistical differences, highlighted by letters, are indicated for glucan concentrations in front of 0%, 0.2%, and 0.5% next to the corresponding plot, for glucan type by letter above the horizontal bar grouping the two doses of the same glucan, for glucan type × concentrations interactions above each box. P values are shown at the bottom of each graph at a given time point (D15, D36, or D39).

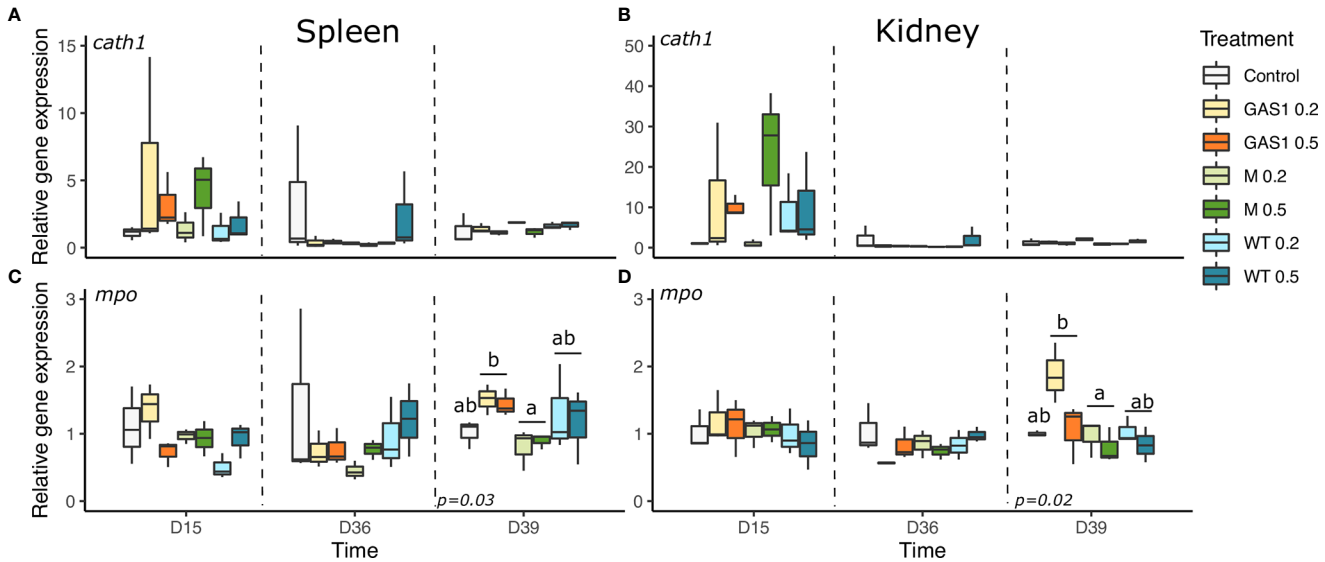

FIGURE 7 | Effects of dietary beta glucans on *Cathelicidin* and *Myeloperoxidase* (*MPO*) genes expression in spleen or kidney of fish sampled during the nutrient test on D15 and D36, or 2 days after the bacterial challenge (D39). **(A)** *CATH1* gene expression in spleen. **(B)** *CATH1* gene expression in kidney. **(C)** *MPO* gene expression in spleen. **(D)** *MPO* gene expression in kidney. Relative transcript (mRNA) levels were determined by real-time RT-PCR and normalized by the arithmetic mean of *ef-1α* gene expressions. Values are expressed as mean ± SD of 3 pool samples per experimental condition (3 fish per pool sample). Statistical differences, highlighted by letters, are indicated for glucan concentrations in front of 0%, 0.2%, and 0.5% next to the corresponding plot, for glucan type by letter above the horizontal bar grouping the two doses of the same glucan, for glucan type × concentrations interactions above each box. P values are shown at the bottom of each graph at a given time point (D15, D36, or D39).

performances. However, this was not the targeted effect in this study as apart from the effects on growth performance, β-glucans are mainly used for their immunostimulant capacities and previous studies highlighted the importance of the quality and structures of glucans in the activation of immune cells (22, 23, 44, 45).

In a previous paper, Han et al. (30) already demonstrated that Gas1 glucan, which was produced in their laboratory, could induce a higher survival of *Artemia franciscana* against *Vibrio harveyi* infection. The authors hypothesize that the structural features of β-glucans could be responsible for this protection, as Gas1 had lower degree of branching and shorter side chain length than WT glucan. In the present study, the capacity to trigger different immune responses of the two extracted β-glucans in the Ghent's laboratory (GAS1 and WT) and the commercial control (MacroGard®) was demonstrated.

MacroGard: The Well-Known Commercial β-Glucans

MacroGard is a well-known commercial β-glucan that was already proven to exert several immune stimulation in fish (29, 46, 47). In the present study, we showed that the high dose (0.5%) of Macrogard β-glucan (M0.5%) was better than the lower dose (M0.2%) to protect fish against bacterial infection but also to induce some effectors of the innate immune system. Indeed, on D15, M0.5% significantly stimulated plasma lysozyme activity. Lysozyme is an enzyme that possesses a lytic activity against both Gram-positive bacteria and Gram-negative bacteria and is known to activate the complement system and phagocytes and its activity reflects the activation of innate immunity of fish (48). Several studies have shown that Macrogard β-glucan could stimulate lysozyme activity. Particularly, dietary with this β-glucan at 0.2% and 0.3% increased lysozyme activity on Persian sturgeon juvenile (47) or sea bass-fed Macrogard (0.1%) diet for 30 days had a significant increase of serum lysozyme activity (46).

However, most of significant immune modulations induced by this β-glucan were observed on D36 and D39 (after bacterial infection) and were independent of the doses, except for M0.2% that significantly increased plasma alternative complement activity (ACH50) on D36 compared with G0.2%. This alternative complement activity plays a major role in the innate immune response by destroying the cell surface membranes of pathogens by creating pores and opsonizing the pathogens for destruction by increased phagocyte uptake, through ligand-receptor interactions between the two cell surfaces (49). In addition, on D36, MacroGard β-glucan enhanced the production of lymphocytes in comparison with the control diet. Siwicki et al. (50) already demonstrated the proliferative response of pronephros lymphocytes that was shown to be stimulated by mitogens.

Adversely, on D36, some immune parameters, such as lysozyme activity, immunoglobulin production, neutrophils proliferation, and genes involved in macrophage production (*mcsfra*) or in antibacterial activity (*hepcidin*) were down-regulated by the supplementation with MacroGard in comparison with Gas1/WT β-glucans or the control. Falco et al. (51) reported that treatment with dietary MacroGard β-glucan administered daily to carp for 14 days prior to infection in generally down-regulated the expression of several measured genes when compared to their corresponding control. In our study, the decreased were observed mostly in

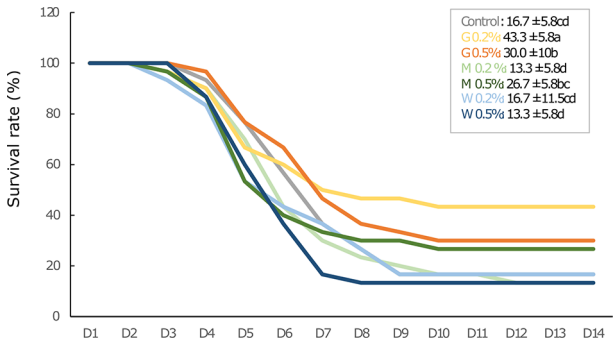

FIGURE 8 | Survival rate profile in rainbow trout juveniles fed with different types of beta glucan at low (0.2% diets) or high doses (0.5% diets) and challenged with Aeromonas salmonicida achromogenes (3.1 × 107 CFU/100g fish body weight) for 14 days. Statistical differences, highlighted by letters, are indicated for glucan concentrations in front of 0, 0.2, and 0.5% next to the corresponding plot, for glucan type by letter above the horizontal bar grouping the two doses of the same glucan, for glucan type x concentrations interactions above each box. P values are shown at the bottom of each graph at a given time point (D15, D36, or D39).

comparison with Gas1 and WT β-glucans potentially suggesting that MacroGard could induced a weakening of the immune system after a shorter period of supplementation. Nevertheless, a bacterial challenge was essential to validate this hypothesis.

After bacterial infection on D39, M0.5% diet slightly but not significantly improved fish survival after the infection to the pathogen *A. salmonicida achromogenes* in comparison to the control (26% vs 16%) while the survival in fish fed M0.2% was worse than the control diet. Although some immune genes involved in anti-inflammatory responses (i.e., *Tgfb* and *il-10*) were enhanced in comparison with Gas1 and/or WT β-glucans, several other essential in antibacterial activity (*lysozyme, mpo*) and Toll-NFkb pathway (*tlr2*) were repressed. Altogether, those results could support the hypothesis of a weakening of the innate immune system when the organism is exposed to such a high dose of β-glucan for a long period. Indeed, it has been reported that overdoses of β-glucan and/or prolonged medication can lead to non-reaction physiological status of rainbow trout (29). The decrease of several immune genes expression in this study may be explained by the high doses of β-glucan used in this experiment leading to high levels of butyric acid production in the guts by the fermentation of *bifidobacterium* and lactic acid producing bacteria. On the other hand, butyric acid is also a histone deacetylase (HDAC) inhibitor, such as HDAC1, HDAC2, HDAC3, and HDAC8, which inhibits the function of histone deacetylase enzymes leading to deacetylase (52). The decrease of HDCA causes the loss of structures of chromatin due to the decrease of electrostatic attraction between histone and DNA (52).

Therefore, our results suggest that MacroGard β-glucan supplementation in trout should be at least 0.5% of the diet and should be restricted to 15 days to avoid immune weakening and improve fish survival in case of bacterial infection.

GAS1: The Best β-Glucan to Improve Resistance to *A. salmonicida achromogenes*

As described by Han et al. (30), Gas1 is a β-glucan produced by the null-mutant yeasts Gas1 of *Saccharomyces cerevisiae* (isogenic deletion strains derived from baker's yeast strain BY 4741). This β-glucan possesses a lower degree of branching and shorter side chain length and exerted the most prominent *V. harveyi*-protective effects in *A. franciscana* (30). Similarly, in our study, low and high doses of Gas1-β-glucan (G0.2% and G0.5% diet) significantly increase trout immune system with different cellular or molecular immune effectors stimulated at the three timepoints (*i.e.*, D15, D36, and D39).

On D15, Gas1 β-glucan significantly decreased basophils proportions after a short-term exposure compared to control and MacroGard diets. In previous studies, the modulation capacity of the leukocyte production by β-glucans was already observed (53–55). In mammals, basophils are immune cells known to be involved in allergic process and antiparasitic immunity, and release inflammatory mediators, such as histamine, by degranulation and induce inflammation (56). In Teleost, although their function remains poorly described, basophils were proved to be activated in an antibody-dependent manner (bounding with IgM induced degranulation) and the released granules exhibited the capacity to induce the migration of various leukocytes (57). Furthermore, the expression of *cd4* coding for a co-receptor of the T cell receptor (TCR) that assists in the communication with antigen-presenting cells and *tlr2* were also repressed in fish fed Gas1. This repression of basophils proliferation and *cd4* with Gas1 could alter inflammatory processes, but further investigation would be necessary to evaluate to which extent. Nevertheless, Gas1 diet stimulated the activity of lysozyme and the expression of C3a involved in the alternative complement pathways in comparison to MacroGard and WT β-glucan potentially indicating a better response of innate immune system on D15.

On D36, Gas1 also increased lysozyme activity, Ig proportion and some immune genes involved in macrophage production (*mcsfra*) and antibacterial activity (*hepcidin*) in comparison with MacroGard β-glucans. As already described for MacroGard β-glucan, those results suggest the induction of some effectors of the immune system but triggered by different molecular pathways. Surprisingly, in another study, brood rainbow trout fed 0.2% MacroGard β-glucan diet for two months also exhibited

a significant increase of lysozyme activity and total Ig (54). Here, only Gas1 modified those immune parameters but this could be explained by the duration of feeding or the age of the fish at the moment of the experiment. Besides, the increase of plasma total Ig was also observed with both low and high doses of Gas1 β-glucan on D36. Immunoglobulins are complex glycoproteins that play critical functions in innate and adaptive immunity thanks to their capacity of recognition, binding, and fixation of cells (58).

In the context of a bacterial intrusion, those Ig could help to cope with the infection, and could be one of the immune effectors responsible for the results obtained on rainbow trout juvenile resistance to *A. salmonicida* pathogens at D39. Indeed, as already observed in Han et al. (30), low and high doses of Gas1-β-glucan (G0.2% and G0.5% diet) exhibited the best protective effect against the pathogen. Regarding the cumulative survival rate 10 days after bacterial challenge, fish fed with G0.2% displayed the highest survival rate with 43.3%, followed by G0.5% with 30% and fish fed control diet at 16.7%. Meanwhile, there was no difference in survival rate for fish fed low and high doses of Macrogard β-glucan, Wild type (WT)-β-glucan diets in comparison to those of the control. Numerous studies have reported the immunomodulation potential of β-glucan in fish disease resistance and the available results vary greatly depending on the fish species, doses, and administration modes (14, 28, 59–61). In the present study, in addition to higher amount of Ig, the immune protection of fish fed G0.2% and G0.5% may be related to a differential expression of several innate immune genes (*lysozyme, tlr2*). Particularly, on D39, myeloperoxidase gene was still enhanced after 35 h post-infection. This enzyme present in neutrophils was shown to exert a bactericidal activity by producing hypochlorous acid (HOCl) that oxidizes key components of the invading pathogens (62). Therefore, the higher *mpo* gene expression could have induced a higher production of the enzyme leading to a higher oxidant capacity to deal with the bacterial infection in fish fed Gas1 diet. Surprisingly, we also observed that several genes related to inflammatory process (*il1b*, *il10*, *tgfb*) were repressed after 35 h of infection with the low dose of Gas1, and could be explained by a modified dynamic of gene expression over time. Indeed, in a previous study, we have shown that infection of zebrafish by *A. salmonicida achromongenes* stimulated the expression of il6 at 6 h post-infection (hpi) but was already repressed after 24 hpi, and this decrease depended on the previous infections applied on the zebrafish (63). Altogether, our results suggest that Gas1 is an efficient β-glucan that should be used at a dose of 0.2% of the diet and can be given for a month although it could have provided an even better protection against pathogen after 15 days of feeding. The high dose at 0.5% can also be used but it exhibited some immune weakening as the survival was reduced compared to the low dose at 0.2%.

WT-β-Glucans: Similar Immune Stimulation Than Gas1, but Worst Resistance to Pathogens

This last β-glucans produced from wild-type yeast *S. cerevisiae* differs from Gas1 by its longer size and higher degree of branching. Our results of measured parameters highlighted substantial differences in the modulation of the immune systems at the three timepoints. First, on D15, W0.5% exhibited the lowest lysozyme activity compared with other diets. In addition, this β-glucan significantly reduced the expression of *cd4* and *hepcidin* in comparison with the control diet. On D36, W0.5% increased ACH50 and lysozyme activities, Ig production, and repressed one immune gene (*il-10*). Surprisingly, although the stimulation of these immune features appeared even more enhanced in WT-β-glucan than in Gas1, W0.2% and W0.5% provided no protection against *A. salmonicida achromogenes* in comparison with the control or MacroGard β-glucan at both doses. Other studies already reported that dietary β-glucans (0.1%, 0.2%, and 0.3% in diets) had no significant effect on survival of juvenile Persian sturgeon (47) or that the administration of dietary β-1,3-glucan from *Eulena gracilis* (1% in diet) had no effect on the survival rate of unvaccinated or vaccinated rainbow trout with *Y. ruckeri* after 70 or 84 days of treatments (26). In the present experiment, the results might indicate that the stimulation of ACH50 and lysozyme activities, Ig and monocyte production was not in itself sufficient in this case to protect the fish against bacterial infection. This lack of protection could be due, as already suggested for Macrogard β-glucan, to an overstimulation of the immune system, that would be too weak after 36 days of feeding trial to respond properly to an infection. Nevertheless, it could also be due to *mpo* in neutrophils or other bactericidal enzymes that activities would be more efficient in fish fed Gas1 diet than fish fed other β-glucan diets. Further studies should be performed to exclude the influence of the doses and duration on the absence of protection by testing lower and higher doses (for example 0.1 and 1%) with a bacterial challenge at 15 days of feeding. However, as previously suggested by Han et al. (30), one explanation to this huge difference in fish protection could be because of the size and degree of branching. Bohn et al. (45) indicate that the activation of the immune cells needs the presence of some structural features, such as β-1,3-linkages in the main chain and β-1,6 or β-1,4 branch of the glucan. Finally, it is possible that their structure influences their absorption in the intestine and the binding to the receptor, and this should be further investigated to understand why Gas1 is such more efficient to protect fish against pathogen infection.

CONCLUSIONS

In this study, the diet supplemented with 0.2% of GAS1-β-glucans was the most effective to protect rainbow trout juveniles against a bacterial infection with *A. salmonicida achromogenes*. After short-term β-glucan feeding (D15), the immune system of rainbow trout juveniles differentially responded to the two β-glucan doses tested depending on the type of β-glucans. Regarding lysozyme enzyme, low doses of Gas1 and WT (G0.2% and W0.2%) were better to stimulates its activity, while M0.5% exhibited the highest activity in comparison with M0.2%. On D36, independently of the doses, MacroGard supplementation resulted in the down-regulation of

several immune parameters such as lysozyme activity, immunoglobulin production, neutrophils proliferation, and immune genes (*mcsfra*, *hepcidin*) in comparison with Gas1 diet potentially suggesting a weakening of the immune system after a shorter period of supplementation confirmed by the low survival rates of fish fed with this diet. Besides, considering the difference of survival rate between Gas1 and WT fed fish, our results suggest that the structure of the β-glucan with a lower degree of branching and shorter side chain length could potentially play a substantial role in the efficiency of the immuno-stimulation. To conclude, in the context of a mid-term feeding (36 days), it appeared that Gas1 β-glucan represents the best immunostimulant as MacroGard already exhibited some immune weakening.

DATA AVAILABILITY STATEMENT

The raw data supporting the conclusions of this article will be made available by the authors, without undue reservation.

ETHICS STATEMENT

The animal study was reviewed and approved by Ethical commitee of Namur University, Protocol number: 13197 KE.

AUTHOR CONTRIBUTIONS

Ideas: SM, PB, LT, and PK. In vivo experiment: VC, TK, SM, SB, and FR-L. Data generation: TK, VC, FR-L, and SB. Data analysis: VC and TK. Manuscript preparation: VC, TK, SM, SB, PB, FR-L, LT, and PK. All authors contributed to the article and approved the submitted version.

FUNDING

The authors thank to Belgian Science Policy Office (Belspo) for financial supporting through the Inter-University Attraction Poles (IAP) "AquaStress" project. TK thanks Vietnamese Government for financial supporting through Vietnamese Students Postgraduate in Foreign Countries Programme (VIED). FR-L thanks Fondecyt regular grant (project number 1211841; ANID; Government of Chile).

ACKNOWLEDGMENTS

The authors thank Enora Flamion, Dr. David Parra, and Sébastien Baekelandt for their help in this experiment.

REFERENCES

1. Soltanian S, François JM, Dhont J, Arnouts S, Sorgeloos P, Bossier P. Enhanced Disease Resistance in Artemia by Application of Commercial β-Glucans Sources and Chitin in a Gnotobiotic Artemia Challenge Test. *Fish Shellfish Immunol* (2007) 23:1304–14. doi: 10.1016/j.fsi.2007.07.004
2. Marques A, Dhont J, Sorgeloos P, Bossier P. Immunostimulatory Nature of β-Glucans and Baker's Yeast in Gnotobiotic Artemia Challenge Tests. *Fish Shellfish Immunol* (2006) 20:682–92. doi: 10.1016/j.fsi.2005.08.008
3. Lieke T, Meinelt T, Hoseinifar SH, Pan B, Straus DL, Steinberg CEW. Sustainable Aquaculture Requires Environmental-Friendly Treatment Strategies for Fish Diseases. *Rev Aquac* (2020) 12:943–65. doi: 10.1111/raq.12365
4. Smith VJ, Brown JH, Haut C. Immunostimulation in Crustaceans: Does it Really Protect\Ragainst Infection? *Fish Shellfish Immunol* (2003) 15:12833917. doi: 10.1016/S1050-4648(02)00140-7
5. Rodrigues MV, Zanuzzo FS, Koch JFA, de Oliveira CAF, Sima P, Vetvicka V. Development of Fish Immunity and the Role of β-Glucan in Immune Responses. *Molecules* (2020) 25:5378. doi: 10.3390/molecules25225378
6. Cerezuela R, Guardiola FA, Meseguer J, Esteban MÁ. Increases in Immune Parameters by Inulin and Bacillus Subtilis Dietary Administration to Gilthead Seabream (Sparus Aurata L.) did Not Correlate With Disease Resistance to Photobacterium Damselae. *Fish Shellfish Immunol* (2012) 32:1032–40. doi: 10.1016/j.fsi.2012.02.025
7. Bojarski B, Kot B, Witeska M. Antibacterials in Aquatic Environment and Their Toxicity to Fish. *Pharmaceuticals* (2020) 13:189. doi: 10.3390/ph13080189
8. Serrano PH. Responsible Use of Antibiotics in Aquaculture. *FAO Fish Tech Pap n°469* (2005) 469:1–97. doi: 10.13140/RG.2.2.31012.94088
9. Carbone D, Faggio C. Importance of Prebiotics in Aquaculture as Immunostimulants. Effects on Immune System of Sparus Aurata and Dicentrarchus Labrax. *Fish Shellfish Immunol* (2016) 54:172–8. doi: 10.1016/j.fsi.2016.04.011
10. Dimitroglou A, Merrifield DL, Carnevali O, Picchietti S, Avella M, Daniels C, et al. Microbial Manipulations to Improve Fish Health and Production - a Mediterranean Perspective. *Fish Shellfish Immunol* (2011) 30:1–16. doi: 10.1016/j.fsi.2010.08.009
11. Ringø E, Erik Olsen R, Gonzalez Vecino JL, Wadsworth S. Use of Immunostimulants and Nucleotides in Aquaculture: A Review. *J Mar Sci Res Dev* (2011) 02:1–22. doi: 10.4172/2155-9910.1000104
12. Vallejos-Vidal E, Reyes-Lopez F, Teles M, MacKenzie S. The Response of Fish to Immunostimulant Diets. *Fish Shellfish Immunol* (2016) 56:34–69. doi: 10.1016/j.fsi.2016.06.028
13. Hasan MT, Je Jang W, Lee JM, Lee B-J, Hur SW, Gu Lim S, et al. Effects of Immunostimulants, Prebiotics, Probiotics, Synbiotics, and Potentially Immunoreactive Feed Additives on Olive Flounder (Paralichthys Olivaceus): A Review. *Rev Fish Sci Aquac* (2019) 27:417–37. doi: 10.1080/23308249.2019.1622510
14. Rodríguez I, Chamorro R, Novoa B, Figueras A. β-Glucan Administration Enhances Disease Resistance and Some Innate Immune Responses in Zebrafish (Danio Rerio). *Fish Shellfish Immunol* (2009) 27:369–73. doi: 10.1016/j.fsi.2009.02.007
15. Volman JJ, Ramakers JD, Plat J. Dietary Modulation of Immune Function by β-Glucans. *Physiol Behav* (2008) 94:276–84. doi: 10.1016/j.physbeh.2007.11.045
16. Dalmo RA, Bøgwald J. ß-Glucans as Conductors of Immune Symphonies. *Fish Shellfish Immunol* (2008) 25:384–96. doi: 10.1016/j.fsi.2008.04.008
17. Brown GD, Gordon S. Fungal Beta-Glucans and Mammalian Immunity. *Immunity* (2003) 19:311–5. doi: 10.1016/S1074-7613(03)00233-4
18. Glencross BD, Huyben D, Schrama JW. The Application of Single-Cell Ingredients in Aquaculture Feeds—A Review. *Fishes* (2020) 5:22. doi: 10.3390/fishes5030022
19. Meena DK, Das P, Kumar S, Mandal SC, Prusty AK, Singh SK, et al. Beta-Glucan: An Ideal Immunostimulant in Aquaculture (a Review). *Fish Physiol Biochem* (2013) 39:431–57. doi: 10.1007/s10695-012-9710-5
20. Fry BG, Roelants K, Champagne DE, Scheib H, Tyndall JDA, King GF, et al. The Toxicogenomic Multiverse: Convergent Recruitment of Proteins Into Animal Venoms. *Annu Rev Genomics Hum Genet* (2009) 10:483–511. doi: 10.1146/annurev.genom.9.081307.164356
21. Kim YS, Ke F, Zhang QY. Effect of β-Glucan on Activity of Antioxidant Enzymes and Mx Gene Expression in Virus Infected Grass Carp. *Fish Shellfish Immunol* (2009) 27:336–40. doi: 10.1016/j.fsi.2009.06.006
22. Koch JFA, de Oliveira CAF, Zanuzzo FS. Dietary β-Glucan (Macrogard®) Improves Innate Immune Responses and Disease Resistance in Nile Tilapia

Regardless of the Administration Period. *Fish Shellfish Immunol* (2021) 112:56–63. doi: 10.1016/j.fsi.2021.02.014
23. Kazuń B, Małaczewska J, Kazuń K, Kamiński R, Żylińska-Urban J. Dietary Supplementation With Lactobacillus Plantarum and β-Glucan Affects Immune Parameters in the Tench (Tinca Tinca) Fry. *Pol J Vet Sci* (2020) 23:611–8. doi: 10.24425/pjvs.2020.135808
24. Djordjevic B, Skugor S, Jørgensen SM, Overland M, Mydland LT, Krasnov A. Modulation of Splenic Immune Responses to Bacterial Lipopolysaccharide in Rainbow Trout (Oncorhynchus Mykiss) Fed Lentinan, a Beta-Glucan From Mushroom Lentinula Edodes. *Fish Shellfish Immunol* (2009) 26:201–9. doi: 10.1016/j.fsi.2008.10.012
25. Lauridsen JH, Buchmann K. Effects of Short- and Long-Term Glucan Feeding of Rainbow Trout (Salmonidae) on the Susceptibility to *Ichthyophthirius Multifiliis* Infections. *Acta Ichthyol Piscat* (2010) 40:61–6. doi: 10.3750/AIP2010.40.1.08
26. Skov J, Kania PW, Holten-Andersen L, Fouz B, Buchmann K. Immunomodulatory Effects of Dietary β-1,3-Glucan From Euglena Gracilis in Rainbow Trout (Oncorhynchus Mykiss) Immersion Vaccinated Against Yersinia Ruckeri. *Fish Shellfish Immunol* (2012) 33:111–20. doi: 10.1016/j.fsi.2012.04.009
27. Welker TL, Lim C, Yildirim-Aksoy M, Shelby R, Klesius PH. Immune Response and Resistance to Stress and Edwardsiella Ictaluri Challenge in Channel Catfish, Ictalurus Punctatus, Fed Diets Containing Commercial Whole-Cell Yeast or Yeast Subcomponents. *J World Aquac Soc* (2007) 38:24–35. doi: 10.1111/j.1749-7345.2006.00070.x
28. Ji L, Sun G, Li J, Wang Y, Du Y, Li X, et al. Effect of Dietary β-Glucan on Growth, Survival and Regulation of Immune Processes in Rainbow Trout (*Oncorhynchus Mykiss*) Infected by Aeromonas Salmonicida. *Fish Shellfish Immunol* (2017) 64:56–67. doi: 10.1016/j.fsi.2017.03.015
29. Douxfils J, Fierro-Castro C, Mandiki SNM, Emile W, Tort L, Kestemont P. Dietary β-Glucans Differentially Modulate Immune and Stress-Related Gene Expression in Lymphoid Organs From Healthy and Aeromonas Hydrophila -Infected Rainbow Trout (Oncorhynchus Mykiss). *Fish Shellfish Immunol* (2017) 63:285–96. doi: 10.1016/j.fsi.2017.02.027
30. Han B, Baruah K, Nguyen DV, Williams DL, Devriendt B, Cox E, et al. Beta-Glucan's Varying Structure Characteristics Modulate Survival and Immune-Related Genes Expression From Vibrio Harveyi-Infected Artemia Franciscana in Gnotobiotic Conditions. *Fish Shellfish Immunol* (2020) 102:307–15. doi: 10.1016/j.fsi.2020.04.062
31. Inoue T, Moritomo T, Tamura Y, Mamiya S, Fujino H, Nakanishi T. A New Method for Fish Leucocyte Counting and Partial Differentiation by Flow Cytometry. *Fish Shellfish Immunol* (2002) 13:379–90. doi: 10.1006/fsim.2002.0413
32. Mathieu C, Milla S, Mandiki SNM, Douxfils J, Douny C, Scippo ML, et al. First Evidence of the Possible Implication of the 11-Deoxycorticosterone (DOC) in Immune Activity of Eurasian Perch (Perca Fluviatilis, L.): Comparison With Cortisol. *Comp Biochem Physiol - A Mol Integr Physiol* (2013) 165:149–58. doi: 10.1016/j.cbpa.2013.02.025
33. Pierrard MA, Roland K, Kestemont P, Dieu M, Raes M, Silvestre F. Fish Peripheral Blood Mononuclear Cells Preparation for Future Monitoring Applications. *Anal Biochem* (2012) 426:153–65. doi: 10.1016/j.ab.2012.04.009
34. Siwicki A, Studnicka M. The Phagocytic Ability of Neutrophils and Serum Lysozyme Activity in Experimentally Infected Carp, Cyprinus Carpio L. *Fish Biol* (1987) 31:57–60. doi: 10.1111/j.1095-8649.1987.tb05293.x
35. Mathieu C, Milla S, Mandiki SNM, Douxfils J, Kestemont P. In Vivo Response of Some Immune and Endocrine Variables to LPS in Eurasian Perch (Perca Fluviatilis, L.) and Modulation of This Response by Two Corticosteroids, Cortisol and 11-Deoxycorticosterone. *Comp Biochem Physiol A Mol Integr Physiol* (2014) 167:25–34. doi: 10.1016/j.cbpa.2013.09.006
36. Oriol Sunyer J, Tort L. Natural Hemolytic and Bactericidal Activities of Sea Bream Sparus Aurata Serum Are Effected by the Alternative Complement Pathway. *Vet Immunol Immunopathol* (1995) 45:333–45. doi: 10.1016/0165-2427(94)05430-Z
37. Milla S, Mathieu C, Wang N, Lambert S, Nadzialek S, Massart S, et al. Spleen Immune Status is Affected After Acute Handling Stress But Not Regulated by Cortisol in Eurasian Perch, Perca Fluviatilis. *Fish Shellfish Immunol* (2010) 28:931–41. doi: 10.1016/j.fsi.2010.02.012
38. Bradford MM. A Rapid and Sensitive Method for the Quantitation of Microgram Quantities of Protein Utilizing the Principle of Protein-Dye Binding. *Anal Biochem* (1976) 72:248–54. doi: 10.1016/0003-2697(76)90527-3
39. Chilmonczyk S, Monge D. Flow Cytometry as a Tool for Assessment of the Fish Cellular Immune Response to Pathogens. *Fish Shellfish Immunol* (1999) 9:319–33. doi: 10.1006/fsim.1998.0188
40. Jolly S, Jaffal A, Delahaut L, Palluel O, Porcher JM, Geffard A, et al. Effects of Aluminium and Bacterial Lipopolysaccharide on Oxidative Stress and Immune Parameters in Roach, Rutilus Rutilus L. *Environ Sci Pollut Res* (2014) 21:13103–17. doi: 10.1007/s11356-014-3227-7
41. Cornet V, Ouaach A, Mandiki SNM, Flamion E, Ferain A, Van Larebeke M, et al. Environmentally-Realistic Concentration of Cadmium Combined With Polyunsaturated Fatty Acids Enriched Diets Modulated Non-Specific Immunity in Rainbow Trout. *Aquat Toxicol* (2018) 196:104–16. doi: 10.1016/j.aquatox.2018.01.012
42. Khuyen TD, Mandiki SNM, Cornet V, Douxfils J, Betoulle S, Bossier P, et al. Physiological and Immune Response of Juvenile Rainbow Trout to Dietary Bovine Lactoferrin. *Fish Shellfish Immunol* (2017) 71:359–71. doi: 10.1016/j.fsi.2017.10.027
43. Pfaffl MW. A New Mathematical Model for Relative Quantification in Real-Time RT-PCR. *Nucleic Acids Res* (2001) 29:e45. doi: 10.1093/nar/29.9.e45
44. Soltanian S, Dhont J, Sorgeloos P, Bossier P. Influence of Different Yeast Cell-Wall Mutants on Performance and Protection Against Pathogenic Bacteria (Vibrio Campbellii) in Gnotobiotically-Grown Artemia. *Fish Shellfish Immunol* (2007) 23:141–53. doi: 10.1016/j.fsi.2006.09.013
45. Bohn JA, BeMiller JN. (1→3)-β-D-Glucans as Biological Response Modifiers: A Review of Structure-Functional Activity Relationships. *Carbohydr Polym* (1995) 28:3–14. doi: 10.1016/0144-8617(95)00076-3
46. Bagni M, Romano N, Finoia MG, Abelli L, Scapigliati G, Tiscar PG, et al. Short- and Long-Term Effects of a Dietary Yeast β-Glucan (Macrogard) and Alginic Acid (Ergosan) Preparation on Immune Response in Sea Bass (Dicentrarchus Labrax). *Fish Shellfish Immunol* (2005) 18:311–25. doi: 10.1016/j.fsi.2004.08.003
47. Aramli MS, Kamangar B, Nazari RM. Effects of Dietary β-Glucan on the Growth and Innate Immune Response of Juvenile Persian Sturgeon, Acipenser Persicus. *Fish Shellfish Immunol* (2015) 47:606–10. doi: 10.1016/j.fsi.2015.10.004
48. Saurabh S, Sahoo PK. Lysozyme: An Important Defence Molecule of Fish Innate Immune System. *Aquac Res* (2008) 39:223–39. doi: 10.1111/j.1365-2109.2007.01883.x
49. Holland MCH, Lambris JD. The Complement System in Teleosts. *Fish Shellfish Immunol* (2002) 12:399–420. doi: 10.1006/fsim.2001.0408
50. Siwicki AK, Zakęś Z, Terech-Majewska E, Kowalska A, Małaczewska J. Supplementing the Feed of Pikeperch [Sander Lucioperca (L.)] Juveniles With Macrogard and its Influence on Nonspecific Cellular and Humoral Defense Mechanisms. *Aquac Res* (2009) 40:405–11. doi: 10.1111/j.1365-2109.2008.02107.x
51. Falco A, Frost P, Miest J, Pionnier N, Irnazarow I, Hoole D. Reduced Inflammatory Response to Aeromonas Salmonicida Infection in Common Carp (Cyprinus Carpio L.) Fed With β-Glucan Supplements. *Fish Shellfish Immunol* (2012) 32:1051–7. doi: 10.1016/j.fsi.2012.02.028
52. Bourassa MW, Alim I, Bultman SJ, Ratan RR. Butyrate, Neuroepigenetics and the Gut Microbiome: Can a High Fiber Diet Improve Brain Health? *Neurosci Lett* (2016) 625:56–63. doi: 10.1016/j.neulet.2016.02.009
53. Selvaraj V, Sampath K, Sekar V. Adjuvant and Immunostimulatory Effects of β-Glucan Administration in Combination With Lipopolysaccharide Enhances Survival and Some Immune Parameters in Carp Challenged With Aeromonas Hydrophila. *Vet Immunol Immunopathol* (2006) 114:15–24. doi: 10.1016/j.vetimm.2006.06.011
54. Ghaedi G, Keyvanshokooh S, Mohammadi Azarm H, Akhlaghi M. Effects of Dietary β-Glucan on Maternal Immunity and Fry Quality of Rainbow Trout (Oncorhynchus Mykiss). *Aquaculture* (2015) 441:78–83. doi: 10.1016/j.aquaculture.2015.02.023
55. Do Huu H, Sang HM, Thanh Thuy NT. Dietary β-Glucan Improved Growth Performance, Vibrio Counts, Haematological Parameters and Stress Resistance of Pompano Fish, Trachinotus Ovatus Linnaeu. *Fish Shellfish Immunol* (2016) 54:402–10. doi: 10.1016/j.fsi.2016.03.161
56. Karasuyama H, Mukai K, Obata K, Tsujimura Y, Wada T. Nonredundant Roles of Basophils in Immunity. *Annu Rev Immunol* (2011) 29:45–69. doi: 10.1146/annurev-immunol-031210-101257
57. Odaka T, Suetake H, Maeda T, Miyadai T. Teleost Basophils Have Igm-Dependent and Dual Ig-Independent Degranulation Systems. *J Immunol* (2018) 200:2767–76. doi: 10.4049/jimmunol.1701051

58. Salinas I, Fernández-Montero Á, Ding Y, Sunyer JO. Mucosal Immunoglobulins of Teleost Fish: A Decade of Advances. *Dev Comp Immunol* (2021) 4:525–39. doi: 10.1016/j.dci.2021.104079
59. Ji L, Sun G, Li X, Liu Y. Comparative Transcriptome Analysis Reveals the Mechanism of β-Glucan in Protecting Rainbow Trout (Oncorhynchus Mykiss) From Aeromonas Salmonicida Infection. *Fish Shellfish Immunol* (2020) 98:87–99. doi: 10.1016/j.fsi.2019.12.022
60. Tukmechi A, Rahmati Andani HR, Manaffar R, Sheikhzadeh N. Dietary Administration of Beta-Mercapto-Ethanol Treated Saccharomyces Cerevisiae Enhanced the Growth, Innate Immune Response and Disease Resistance of the Rainbow Trout, Oncorhynchus Mykiss. *Fish Shellfish Immunol* (2011) 30:923–8. doi: 10.1016/j.fsi.2011.01.016
61. Lin S, Pan Y, Luo L, Luo L. Effects of Dietary β-1,3-Glucan, Chitosan or Raffinose on the Growth, Innate Immunity and Resistance of Koi (Cyprinus Carpio Koi). *Fish Shellfish Immunol* (2011) 31:788–94. doi: 10.1016/j.fsi.2011.07.013
62. Klebanoff SJ, Kettle AJ, Rosen H, Winterbourn CC, Nauseef WM. Myeloperoxidase: A Front-Line Defender Against Phagocytosed Microorganisms. *J Leukoc Biol* (2013) 93:185–98. doi: 10.1189/jlb.0712349
63. Cornet V, Douxfils J, Mandiki SNM, Kestemont P. Early-Life Infection With a Bacterial Pathogen Increases Expression Levels of Innate Immunity Related Genes During Adulthood in Zebrafish. *Dev Comp Immunol* (2020) 108:103672. doi: 10.1016/j.dci.2020.103672

Conflict of Interest: FER-L is Senior Research Associate for Ictio Biotechnologies S.A.

The remaining authors declare that the research was conducted in the absence of any commercial or financial relationships that could be construed as a potential conflict of interest.

frontiers in Immunology

ORIGINAL RESEARCH
published: 12 August 2021
doi: 10.3389/fimmu.2021.696781

Lactococcus lactis Expressing Type I Interferon From Atlantic Salmon Enhances the Innate Antiviral Immune Response *In Vivo* and *In Vitro*

Carlos Muñoz[1], Josue González-Lorca[1], Mick Parra[1], Sarita Soto[1], Natalia Valdes[1], Ana María Sandino[2,3], Rodrigo Vargas[1], Alex González[4] and Mario Tello[1,5]**

[1] Laboratorio de Metagenómica Bacteriana, Centro de Biotecnología Acuícola, Departamento de Biología, Facultad de Química y Biología, Universidad de Santiago de Chile, Santiago, Chile, [2] Laboratorio de Virología, Centro de Biotecnología Acuícola, Departamento de Biología, Facultad de Química y Biología, Universidad de Santiago de Chile, Santiago, Chile, [3] ActivaQ S.A., Santiago, Chile, [4] Laboratorio de Microbiología Ambiental y Extremófilos, Departamento de Ciencias Biológicas y Biodiversidad, Universidad de los Lagos, Osorno, Chile, [5] IctioBiotic SpA, Santiago, Chile

In salmon farming, viruses are responsible for outbreaks that produce significant economic losses for which there is a lack of control tools other than vaccines. Type I interferon has been successfully used for treating some chronic viral infections in humans. However, its application in salmonids depends on the proper design of a vehicle that allows its massive administration, ideally orally. In mammals, administration of recombinant probiotics capable of expressing cytokines has shown local and systemic therapeutic effects. In this work, we evaluate the use of *Lactococcus lactis* as a type I Interferon expression system in Atlantic salmon, and we analyze its ability to stimulate the antiviral immune response against IPNV, *in vivo* and *in vitro*. The interferon expressed in *L. lactis*, even though it was located mainly in the bacterial cytoplasm, was functional, stimulating Mx and PKR expression in CHSE-214 cells, and reducing the IPNV viral load in SHK-1 cells. *In vivo*, the oral administration of this *L. lactis* producer of Interferon I increases Mx and PKR expression, mainly in the spleen, and to a lesser extent, in the head kidney. The oral administration of this strain also reduces the IPNV viral load in Atlantic salmon specimens challenged with this pathogen. Our results show that oral administration of *L. lactis* producing Interferon I induces systemic effects in Atlantic salmon, allowing to stimulate the antiviral immune response. This probiotic could have effects against a wide variety of viruses that infect Atlantic salmon and also be effective in other salmonids due to the high identity among their type I interferons.

Keywords: interferon Ia, *Lactococcus lactis*, antiviral, IPNV, Atlantic salmon

OPEN ACCESS

Edited by:
Jorge Galindo-Villegas, Nord University, Norway

Reviewed by:
Jaime A. Tobar, Virbac-Centrovet, Chile
Luis Perez, Miguel Hernández University of Elche, Spain
Jean-Pierre Levraud, Institut Pasteur, France

***Correspondence:**
Mario Tello
mario.tello@usach.cl
Alex González
alex.gonzalez@ulagos.cl

Specialty section:
This article was submitted to Nutritional Immunology, a section of the journal Frontiers in Immunology

Received: *17 April 2021*
Accepted: *22 July 2021*
Published: *12 August 2021*

Citation:
Muñoz C, González-Lorca J, Parra M, Soto S, Valdes N, Sandino AM, Vargas R, González A and Tello M (2021) Lactococcus lactis Expressing Type I Interferon From Atlantic Salmon Enhances the Innate Antiviral Immune Response In Vivo and In Vitro. Front. Immunol. 12:696781. doi: 10.3389/fimmu.2021.696781

INTRODUCTION

In aquaculture, the implementation of immunotherapies based on interferon administration to combat viral infections has been poorly studied. Aquaculture is one of the fastest-growing industries in the world. According to FAO estimates, in 2050 this industry is expected to be the main source of protein for human consumption (1). The main cultivated species include shrimp, tilapia, carp, rainbow trout, and Atlantic salmon, which due to high-intensity cultivation conditions, experience health problems caused by bacterial and viral pathogens, which reduce their productivity (2, 3). Among the main viral pathogens, we can find White Spot Syndrome Virus (WSSV) in shrimp (4), Tilapia lake Virus (TiLV) in Tilapia (5), and Koi Herpesvirus in Carps (6). In salmonids, several viral pathogens have been identified. In Atlantic salmon, the main viral pathogens are IPNV (7) and ISAV (8), which have shown devastating effects on the Chilean salmon farming industry (9). In rainbow trout, Atlantic salmon, and other salmonids, several emerging viruses have been identified; namely, VHSV, IHNV, SAV, and PRV, which show a lower impact on production (2). The main strategy used to date by salmon farming to prevent viral infections has been the use of vaccines; however, it has not been shown that they confer the same protection as that observed in mammals, requiring successive re-stimulations (boosters) to achieve efficient protection (10, 11).

In Atlantic salmon and other teleosts, the main response of the innate immune system against viral infections consists in the expression and secretion of Type I interferons (12), whose expression is induced as a consequence of the recognition of viral RNA by the cytoplasmic receptors RIG-I and MDA5, or by the membrane-associated receptors TLR3, TLR22 and TLR7 (13, 14). The interaction of type I Interferon with its membrane receptors stimulates the induction of a set of genes called Interferon Stimulated Genes (ISG), among which Mx and PKR are well known effectors (15–17). Mx is a GTPase structurally related to dynamin, which forms oligomers around the nucleoprotein, preventing virus transcription and replication (18). PKR is a kinase that inactivates translation initiation factor 2 by phosphorylation, preventing translation (19). In Atlantic salmon, 6 groups of type I Interferon have been identified, named from a to f (omitting g, to avoid confusion with gamma interferon) (20). Some of the first type I interferons from Atlantic salmon to be characterized were SasaIFN- α1 and SasaIFN-α2, both belonging to the current group Ia (IFN-Ia) (21). *In vitro*, recombinant SasaIFN-α1 exhibits strong antiviral activity against IPNV (14, 21), but has no effect on ISAV infections (22, 23). *In vivo*, administering recombinant SasaIFN-α2 increases resistance to IHNV infections (24), while administering intramuscular plasmids expressing IFN-Ia locally stimulates the expression of antiviral genes (25), and enhances the protective effect of DNA vaccines that express the HE proteins of ISAV (26). On the other hand, administering plasmids that allow the expression of IFN-Ic in fish confers protection against ISAV (25) and SAV (27). This background shows that the use of interferon I could be an effective and broad-spectrum tool to prevent mortalities caused by viral infections. However, its implementation involves developing an efficient administration system that avoids the need to inject each fish.

In mammals, lactic acid bacteria have been used successfully to synthesis and release immunoactive molecules such as interferons, antigens, or peptide hormones (28). The oral administration of these improved probiotics produces systemic effects, conferring protection against virus (29), bacterial pathogens (30, 31), and parasites (32). In salmonids, oral administration of *Lactobacillus casei* species expressing IPNV epitopes has shown to confer protection against the virus (33–37), while *Lactococcus lactis* strains have been used to orally immunize against Hirame novirhabdovirus in flounder (38), Carp spring viremia in common carps (39), the protozoa *Ichthyophthirius multifiliis* in Goldfish (40), and against the viral hemorrhagic septicemia in rainbow trout (41). Oral administration of recombinant *Lactobacillus casei* expressing epitopes of *Aeromona veronii* confers protection against this pathogen in *Cyprinus carpio* (42, 43), and *Carassius carassius* (44), while *Lactobacillus plantarum* expressing G protein of spring viremia of carp virus (SVCV) (45) and the ORF81 protein of koi herpesvirus (KHV) has shown confers protection against both viruses with high titers of IgM after its oral administration to *Cyprinus carpio* (46). Altogether, these results have shown that lactic acid bacteria are an efficient vehicle for the release of immunostimulant peptides in fish.

In this work, we explore the use of *L. lactis* to produce IFN-Ia from Atlantic salmon. Recombinant interferon was shown to have *in vitro* activity on CHSE-214 and SHK-1 cell cultures, increasing the expression of Mx and PKR, and reducing the production of viral particles in IPNV infection assays. *In vivo*, the administration of this probiotic was able to stimulate the expression of Mx and PKR in the spleen and head kidney, in addition to reducing the viral load.

MATERIALS AND METHODS

Design and Synthesis of the P1-Usp45-IFNIa Module

To generate a module that allows the expression and export of Interferon I in *Lactococcus lactis*, a cDNA encoding for the IFN-Ia from *Salmo salar* (NM_001123710.1) between amino acid 24 and 175 was designed *in silico*, by *in frame* insertion of the sequence that encodes the peptide *Lactococcus lactis* Usp45 signal (GenBank: M35374), and incorporating the sequence of the constitutive promoter P1 from *Lactococcus lactis* (CP004884.1 1775802-1775887). The module was designed to be flanked by the NcoI and XbaI sites. The synthesis, codogenic optimization and cloning of this module (P1-Usp45-IFNIa) in the vector pUC57 was carried out by the company Genscript (http://www.genscript.com/).

By electroporation, plasmid pUC57/P1-Usp45-IFNIa was transformed into *E. coli* MC1061. Plasmid DNA was prepared from the transformants (FavorPrep ™ Plasmid DNA Extraction Mini Kit) and ~3 μg were digested sequentially, first with the XbaI enzyme (10 U), and then with the NcoI enzyme (10 U) in a

final volume of 20 µl at 37°C for 1 hour. The released fragment was separated by agarose gel electrophoresis (Agarose 1%, TAE buffer), purified (FavorPrep ™ GEL/PCR Purification Kit) and used for its cloning in the vector pNZ8149 (Mobitec GmbH).

Cloning of P1-Usp45-IFNIa in pNZ8149

Plasmid pNZ8149 was prepared in a similar manner to the P1-Usp45-IFNIa segment, ~ 3 µg of pNZ8149 DNA was treated first with XbaI (10 U), and then with NcoI (10 U) for 1 hour. The linearized plasmid was separated by agarose gel electrophoresis and purified using the FavorPrep ™ Plasmid DNA Extraction Mini Kit.

Purified P1-Usp45-IFNIa module and plasmid pNZ8149 from digestion with XbaI and NcoI were ligated with 400 U of T4 ligase (New England Biolabs) overnight at 4°C. The ligation was performed in an insert: vector ratio of 3: 1. Subsequently, the ligation was dialyzed against distilled H_2O using a 0.02 µm dialysis membrane (Millipore), and electrotransformed into *L. lactis* NZ3900. The bacteria were subsequently plated in Elliker medium, supplemented with 0.5% lactose and cultured for 48 hours at 30°C. In this medium, positive transformants forms yellow colonies, since pNZ8149 contains as selectable marker the *lacF* gene which allows to *L. Lactis* NZ3900 grows using lactose as sole carbon source. The yellow colonies were separated, seeded on new Elliker plates, and analyzed by colony PCR, using primers pNICEF and pNICER (**Table 1**) to detect the presence of the insert. The PCR positive clones were again separated on Elliker plates, and the identity of the insert was corroborated by sequencing, after isolation of plasmid DNA from the recombinant *L. lactis* clones. This construction was named pNZ8149/P1-Usp45-IFNIa.

Insertion of the Spacer and Histidine Tail at the COOH end of IFN-Ia

To detect the recombinant expression of IFN-Ia (rIFN-Ia), the plasmid pNZ8149/P1-Usp45-IFNIa was modified by adding at the 3' end of the IFN-Ia gene a sequence that codes for the GGGHHHHHH peptide. This sequence was incorporated by reverse PCR using the primers pNZIFN-HisF and pNZIFN-HisR (**Table 1**). The primer pNZINF-HisR hybridizes to the 3' end of the interferon I gene (codogenically optimized), and replaces the stop codon with a sequence encoding the GGGHHHHHH peptide. After this sequence, the primer incorporates a stop codon and a site for the restriction enzyme EcoRI. On the other hand, the primer pNZINF-HisF hybridizes in the plasmid pNZ8149 in the region corresponding to the XbaI site and incorporates an EcoRI site at its 5' end. After amplification, the PCR product was digested with the EcoRI enzyme, purified (FavorPrep ™ Plasmid DNA Extraction Mini Kit), and ligated with the T4-ligase enzyme. Subsequently, the ligation product was electroporated in *Lactococcus lactis* NZ3900. The identity of the new construct, prIFN-Ia, was corroborated by sequencing. The *Lactococcus lactis* strain NZ3900 containing the plasmid prIFN-Ia was named MT006.

TABLE 1 | Primers used for PCR and RT-qPCR.

Primer	Sequence
Mx-Fw	5' TGT AAC ACG ATG CCC TCT CG 3'
Mx-Rv	5' GAC GTC AGG GGA GCC AAT C 3'
PKR-Fw	5' CAA TGA CCG ATT CCA GCT CC 3'
PKR-Rv	5' CCC TTA TTT ATG CTAA TCC AG 3'
18S-Fw	5' CCT TAG ATG TCC GGG GCT 3'
18S-Rv	5' CTC GGC GAA GGG TAG ACA 3'
VP2F	5' GAA GTC TTT CTG AGG TGG AGA G 3'
VP2R	5' ATT CCT TTG GTC ACT AGT TGG T 3'
pNICEF	5´ TTA GAT ACA ATG ATT TCG TTC GAA GG 3´
pNICER	5´ CAA GCC TTG GTT TTC TAA TTT TGG 3´
pNZIFN-HisF	5´ TCT TAA TAA AGA ATT CAT AGT CTA GAG AGC TCA AGC 3´
pNZIFN-HisR	5´ TTA TTA AGA CGA ATT CTT AAT GAT GAT GAT GAT GAT GTC CAC CTC CAT ACA TTT GTG CAG CAA GAA T 3

Preparation of *Lactococcus lactis* Electrocompetent Cells

The electrocompetent *Lactococcus lactis* NZ3900 cells was prepared based on the protocol suggested by Mobitec GmbH (47). A colony of *Lactococcus lactis* NZ3900 was inoculated in 5 ml of SG-GM17 medium (M17 medium containing 0.5 M sucrose, 2.5% Glycine, and 0.5% glucose) and cultured overnight at 30°C without agitation. The culture was inoculated in 40 ml of SG-GM17 medium and grown for 16 hours at 30°C, without shaking. The next day, this culture was inoculated in 400 ml of SG-GM17 medium and grown to an OD_{600} between 0.2 and 0.3. Subsequently, the culture was centrifuged at 6,000 x g for 20 min at 4°C and the collected pellet was washed three times with a cold wash buffer (0.5 M sucrose, 10% glycerol, 4°C). In each step, the pellet was collected by centrifugation at 6,000 x g for 20 min at 4°C and was resuspended by vortex in the corresponding buffer. After the last wash, the pellet was resuspended in 3 ml of wash buffer, aliquoted into 200 µl fractions, and stored at -80°C.

MT006 Culture Conditions for Hybridization and Biological Activity Assays

From an isolated colony of MT006 (*Lactococcus lactis* NZ3900 prIFN-Ia), a pre-inoculum was prepared in 0.5% M17-Lactose medium; after incubating overnight, the culture was used to inoculate (2%) 40 ml of M17-Lactose 0.5% medium. After reaching an optical density at 600 nm between 0.6 and 0.8, the culture was induced with nisin 10 ηg/ml for 2 h. Bacteria were separated from the supernatant by centrifugation at 6,000 x g for 20 min at 4°C. The pellet obtained was used in western blot and biological functionality tests, while the supernatant was used in dot blot assays. The MT006 cultures were carried out at 30°C without shaking.

Preparation of Cytoplasmic Extracts of MT006

From the MT006 culture, the bacterial pellet was resuspended in 1 ml of 1X PBS supplemented with 1 mM protease inhibitor PMSF. For their rupture, the resuspended cells were kept on ice and sonicated (ultrasonic processor, Sonic Vibracell) for 2 minutes, divided into 8 pulses (130 watts, 20KHz, 100%, 2 mm

Cv188 stem) of 15 seconds with intervals of 1 minute. After treatment, the cellular debris was separated by centrifugation (13,000 x g, for 10 min at 4°C). The supernatant containing the cytoplasmatic proteins was removed and stored at -20°C. The total protein concentration was determined by the Bradford method.

Preparation of Extracellular Protein Extracts From MT006 Cultures

The MT006 culture supernatant was treated with TCA (10% final), incubated on ice for 30 min, and then the proteins were precipitated by centrifugation at 9,000 x g for 30 min at 4°C. The obtained pellet was washed twice with acetone and dried at room temperature for 30 min. The pellet was resuspended in 1 ml of 1X PBS, supplemented with 1 mM PMSF. The total protein concentration was determined by the Bradford method.

rIFN-Ia Detection in Cytoplasmic and Extracellular Protein Extracts From MT006 Culture

To detect rIFN-Ia in cytoplasmic extracts, the proteins were separated by mass using SDS-PAGE (Gel concentrator: 8% Acrylamide/Bisacrylamide 29:1, pH 6.8; resolutive gel: 10% Acrylamide/Bisacrylamide 29: 1, pH 8.8). 10 µg of total protein extracts from MT006 and MT005 (*Lactococcus lactis* NZ3900 pNZ8149) (control) were loaded together with the BenchMark ™ His-tagged Protein Standard. The samples were subjected to electrophoresis for 90 min at 100 V. After electrophoresis, proteins were electrotransferred (300 mA for 2 h at 16°C) to a nitrocellulose membrane. Subsequently, the membrane was blocked for 1 hour with a 2% BSA solution and washed 3 times with 1X PBS-Tween 20 (0.5%). The membrane was incubated with Rabbit polyclonal anti-His antibody (Abcam) (dilution 1/5000) for 1 hour at 37°C and washed three times with 1X PBS-Tween 20 (0.5%). It was then incubated with the polyclonal anti-rabbit IgG antibody conjugated to HRP (1/5000 dilution) for 1 hour at 37°C, followed by 3 washes with 1X PBS-Tween 20 (0.5%). The membrane was then incubated with 10 ml chemiluminescent developer solution (Pierce ™ ECL Western Blotting Substrate) and exposed to photographic film.

A dot blot was performed to detect rIFN-Ia in the extracellular protein concentrate. The nitrocellulose membrane was loaded with 10 µl of extracts to complete 1 µg of total protein per sample. Once air-dried, the membrane was hybridized and developed following the same protocol as described for the western blot.

Quantification of the Amount of rIFN-Ia Produced by MT006

rIFN-Ia in cytoplasmic extracts was quantified by means of an ELISA test using 1 µg of protein extract. The plates were activated overnight at 4°C using 1X PBS buffer in the presence of the cytoplasmic extract. The wells were blocked with 2% BSA in 1X PBS buffer for 1 hour at 25°C. The first antibody, rabbit polyclonal anti-His Tag antibody (AbCam) dilution 1/5,000 in 1X PBS Tween 20 0.5%, was incubated at 37°C for 1 hour. The second antibody, goat polyclonal Anti Rabbit IgG conjugated to HRP (dilution 1/5000 in 1X PBS Tween 20 0.5%), was incubated for 1 hour at 37°C. Between each step, the wells were washed 3 times with 200 µl 1X PBS-0.5% Tween 20. The presence of bound antibody was determined by development with 100 µl of commercial TMB one-solution developer solution (Promega). After 15 minutes of incubation at 37°C, the reaction was stopped by adding 100 µl of 1N HCl. The product obtained was quantified by absorbance measurement at 450 nm. To quantify the concentration of Interferon present in the cytoplasmic extract, the following formula was used: rIFN-Ia (nM) = (OD450-0.0685)/0.0035, where IFN-Ia is the Interferon concentration in nM, and OD450 is the absorbance at 450 nm of the ELISA assay for rIFN-Ia.

In Vitro Evaluation of the Immunostimulatory Activity of Recombinant Interferon

The determination of the immunostimulatory activity of the recombinant interferon was evaluated by the ability to induce the expression of the Mx and PKR genes. Both genes are part of the antiviral system activated by Interferon I and act as markers for this response.

Cultures of the CHSE-214 salmon embryo cell line were grown to 80% confluence in MEM supplemented with Fetal Bovine serum 2%, before treating them for 24 hours with different doses of recombinant interferon (10, 100 and 500 ηg/ml) from cytoplasmic extracts of MT006. The concentration of total proteins in each dose was equal to the protein concentration in the condition with the highest amount of rIFN-Ia (500 ηg/ml). Adjustment was achieved adding extracts of total protein from the *Lactococcus lactis* strain containing an empty pNZ8149 plasmid (strain MT005). PBS and cytoplasmic extracts of strains MT004 (*L. lactis* NZ3900) and MT005 were used as negative controls. As a positive control, cells were transfected with poly I:C (1 µg/ml), using 3 µl of FuGENE transfection reagent (Promega) following the instructions established by the manufacturer. After stimulation, cells were harvested, then total RNA was extracted using the E.Z.N.A. total RNA kit (Omega biotek), and quantification of the expression of Mx and PKR was performed using RT-qPCR. Each condition was assessed in triplicated (three independent experiments).

Quantification of Mx and PKR Expression in Cell Cultures

Changes in the expression of Mx and PKR were quantified and evaluated by RT-qPCR. Once the RNA was extracted, its integrity was evaluated using agarose gels (1%, TAE 1X) and its amount determined by absorbance at 260 nm, using the Tecan Infinite 200 PRO equipment or a Synergy ™ 2.0 multi-well reader (Biotek). For each extraction the RT reaction was performed using 1 µg of total RNA and 100 Units of M-MLV reverse transcriptase (Invitrogen, USA) and 4 pmol of oligo-dT 18 mer. The RT reaction was performed first at 25°C for 10 minutes, then at 42°C for 1 hour, and finally stopped by denaturation at 65°C for 10 minutes. The qPCR reaction was developed using the SYBR Fast Universal qPCR kit (Kapa

Biosystem USA), in 20 µl, using 2 µl of the RT reaction. To detect and quantify Mx, the primers Mx-Fw and Mx-Rv were used. The thermal program used consisted of 40 cycles of 15 seconds at 95°C, 15 seconds at 60°C, and 30 seconds at 72°C. PKR expression was quantified using the PKR-Fw and PKR-Rv primers (**Table 1**). A program similar to the one used with Mx was used for PKR, varying the melting temperature to 54°C. The 18S ribosomal RNA (18S-Fw and 18S-Rv primers, **Table 1**) was used to normalize the expression. The amplification program that was used consisted of 40 cycles of 15 seconds at 95°C, 15 seconds at 58°C and 30 seconds at 72°C. The qPCR reactions were performed in duplicate on a Stratagene Mx3000P kit. Each qPCR was performed in duplicated (technical replicates). The expression of the genes was normalized with regard to the control condition and the expression of the 18S gene using the ΔΔCt method described by Pfaffl (48).

Evaluation of the *In Vitro* Antiviral Activity of Recombinant Interferon

To determine the effect of the recombinant interferon produced by *Lactococcus lactis* on the viral load of IPNV, cultures of the SHK-1 cell line (Sigma-Aldrich) were grown up to 80% confluence in L15 medium supplemented with 4 mM glutamine and 5% fetal bovine serum. These cultures were incubated with *Lactococcus lactis* cytoplasmic extracts containing 10, 100 and 500 ηg/ml of rIFN for 24 h. The total protein concentration was also equal to the condition where there is a greater amount of rIFN-Ia using protein extract of the control strain MT005. Poly I:C 1 µg/ml (final concentration) was used as a positive control, which was transfected according to the protocol indicated above. At the end of the incubation time, the infection was carried out at an M.O.I of 0.1 plaque-forming units per cell (PFU/cell). After 1 h of adsorption, cells were washed with MEM medium and placed again in MEM medium supplemented with 2% fetal bovine serum. The culture supernatant was extracted at 0, 6, 24, 48, 72, 120, and 168 hours post-infection for quantification of the viral load. Each condition was assessed in triplicated. The virus used in the assay correspond to an isolated belonging to the serotype Sp-2, genogroup 5.

Quantification of Viral Load in Culture Supernatants

The viral load present in the culture supernatants of each well was determined under the following methodology. Total RNA was extracted from the supernatants using the EZNA total RNA kit (Omega Biotek). The RT and qPCR reaction was performed using the SYBR Fast One-Step qRT-PCR system (Kapa Biosystems), using 1 µg of total RNA, and the primers VP2F and VP2R (**Table 1**). To express the results in viral gene copy number, a calibration curve was established, based on the VP2 gene cloned in a pGEM-T vector. A range between 1×10^2 to 1×10^8 copies of the construct was used for the calibration curve.

Preparation of IPN Virus for Challenge Tests

Infectious pancreatic necrosis virus (IPNV Sp-2) was propagated in monolayers of CHSE-214 cells grown in MEM medium supplemented with 2% fetal bovine serum. The infection was carried out at an M.O.I of 0.1 plaque-forming units per cell (PFU/cell). After 1 h of adsorption, cells were washed with MEM medium and placed again in MEM medium supplemented with 2% fetal bovine serum. Subsequently, it was incubated again at 16°C until the presence of a visible cytopathic effect was observed, approximately 48 to 72 hours post-infection.

The viral titer present in the culture supernatant was determined by the lysis plate method. Starting with the supernatant from the infected wells, serial dilutions were prepared with MEM medium, starting at from 10^{-1} upto 10^{-11}. Subsequently, the dilutions of the supernatants were used to infect CHSE-214 cells. After 1 h of adsorption, cells were washed twice with PBS and kept for 72 hours in a semi-solid medium containing supplemented MEM and 0.5% w/v of agarose with low melting point. To fix the cells, 1 mL of formamide 37% v/v was added and incubated for another 30 minutes. To reveal the presence of lysis plaques, the agarose was removed, and 1 mL of crystal violet (1% crystal violet, 20% ethanol) was added to each well. After 30 minutes of incubation, excess crystal violet was removed, and the lysis plaques were quantified.

Mixing *L. lactis* Strains with Fish Feed

The *L. lactis* strains (MT006 or MT005) were administered to the fish together with feed. The bacterial pellet of the cultures was washed with 1 ml of M17 medium, collected by centrifugation at 6,000 x g for 10 minutes at 4°C and resuspended in M17 medium in a volume equivalent to 1/10 of the volume of the original culture. The bacterial suspension was mixed with edible oil in a 2: 1 ratio and emulsified using a vortex. The emulsion obtained was mixed with the food and homogenized by shaking it in a plastic container.

Evaluation of Immunostimulatory Activity *In Vivo*

The immunostimulatory activity *in vivo* was evaluated by determining the effect of the administration of the interferon-producing bacteria on the induction of the genes that express Mx and PKR in the main immunological organs of salmonids: spleen and head kidney. In the experiment, three groups of 15 fish (*Salmo salar* specimens of approximately 10 g each) were fed at 1% for 5 days. The first group was fed with food supplemented with 10^7 CFU/(fish x day) of MT006, the second, with 10^7 CFU/(fish x day) of MT005, and the third group received unsupplemented food.

Five fish of each group were sacrificed on days 1, 3, and 10 post-treatment. The spleen and anterior kidney immunological organs were extracted, collected in cryogenic tubes, and stored in liquid nitrogen. Total RNA was extracted from each immune organ, using TRISURE (Bioline) or the E.Z.N.A Total RNA kit (Omega Biotek) and the total RNA of each extraction was subsequently quantified by absorbance at 260 nm. RNA integrity was evaluated by agarose gel electrophoresis.

The RT-qPCR reaction was developed using the same procedure as that used to evaluate Mx and PKR expression in cell culture. The expression of Mx and PKR was analyzed in each

organ of each fish sampled (five per condition). Each qPCR was performed in duplicated (technical replicates). Gene expression was normalized to the control diet consisting in food supplemented with MT005 and the expression of the 18S gene using the ΔΔCt method described by Pfaffl (48).

In Vivo Effect of MT006 Administration on IPN Viral Load

Three groups of 10 fish (*Salmo salar*, 10 *gr*) were used to evaluate the effect of oral administration of strain MT006 on the *in vivo* viral load of IPNV. One group was fed for 5 days at 1% of their weight, with food supplemented with 10^7 CFU/(fish x day) of MT006. The other two groups functioned as controls and were fed at 1% with food supplemented with 10^7 CFU of MT005 (group 2) and with food without supplementation (group 3). Once the treatment was finished, on day 6 the fish were infected intraperitoneally with 10^8 PFU of IPN virus. Afterwards, the fish were sacrificed at 6, 25, and 60 days post-infection, and their immune organs, spleen, and head kidney were used to extract total RNA and perform RT-qPCR to quantify IPNV. Total RNA was extracted using TRISURE (Bioline) or the E.Z.N.A Total RNA kit (Omega Biotek). The integrity of the RNA was evaluated by agarose gels and its concentration was determined by absorbance at 260 nm. The RT-qPCR reaction was performed using 1 μg of total RNA and the SensiMix SYBR Hi-ROX One-Step kit (Bioline), under the same protocol described for the determination of viral load in cell culture.

Fish Maintenance and Euthanize Protocols

The fish were acclimated for one week before treatment at 12°C in freshwater aquariums with a biomass not higher than 14 g/L, with continuous aeration, and fed with commercial pellets (EWOS MICRO™ 2 mm) at 1% of body weight. Water was maintained with a pH between 6.6 and 7, the salinity was adjusted to 6 PSU with NaCl to prevent fungal infection, and total ammonia was maintained in a range below 0.02 mg/L. Seventy percent of the water in all the aquariums was changed every day after feeding. Water parameters were monitored daily prior to and after changing the water. Feeding, changing the water, and measuring water parameters were all performed manually. The *L. lactis* strains (MT006 or MT005) were administered to the fish together with food.

To avoid unnecessary suffering of fish during the challenge and sampling, fish were anesthetized with benzocaine 40 mg/L for no longer than 2 min prior to the intraperitoneal injection, while sampled fish were euthanized with an overdose of benzocaine 40 mg/L, exposing fish during 5 to 10 minutes. Finally, fish were maintained in accordance with the ethical standards of the Institutional Ethics Committee of the Universidad de Santiago de Chile (approved in internal report n°350) and the relevant legislation in force.

Phylogenetic Reconstruction and Bioinformatic Analysis

Evolutionary relationships between interferons encoded in the *Salmo salar* genome and that reported for SasaIFN-α1 was inferred using the Neighbor-Joining method (49) and the bootstrap test (1000 replicates) (50). The evolutionary distances were computed using the Poisson correction method (51) and are in the units of the number of amino acid substitutions per site. The rate variation among sites was modeled with a gamma distribution (shape parameter = 1). The ambiguous positions were removed for each sequence pair (pairwise deletion option). Evolutionary analyses were conducted in MEGA X (52). The amino acid sequences used are in the **Supplementary Table 1**.

The orthologous and paralogous sequences of Interferon Ia present in *Salmo salar* and other commercial salmonids species were identified using BLASTp against the genome of *Salmo trutta, Salvelinus alpinus, Oncorhynchus nekra, Oncorhynchus mykiss, Oncorhynchus kisutch*, and *Oncorhynchus keta.* As external groups we search also against the genome of *Esox lucius* and *Anguilla anguilla.* The minimum coverage cut-off was a 70%.

RESULTS

Identification of Interferon Ia Sequence With Antiviral Activity Against IPNV

The strategy outlined to evaluate the use of *L. lactis* as a release vehicle consisted of synthesizing *in vitro* a DNA segment that allows the constitutive expression of a gene that in its coding region allows in *L. lactis* the synthesis of recombinant interferon. On its amino-terminal end, this gene has the signal peptide of the protein Usp45, in its central region it encodes for interferon I from Atlantic salmon, and at its carboxyl end it encodes a tag for histidine that can be used for the detection of recombinant interferon (**Figure 1**). Once this synthetic DNA segment was obtained, it was cloned into the plasmid pNZ8149 and the production of the protein was evaluated *in vitro.* The antiviral activity *in vivo* and *in vitro* would be tested using IPNV for infection or challenge tests. As the Interferon I system of Atlantic salmon is constituted by six groups of genes, which show different degrees of antiviral activity, interest is focused on identifying a group with antiviral activity both *in vitro* and *in vivo*, which show functionality in its recombinant form produced in bacterial systems. Group Ia met these characteristics and, based on the work of Svingerud and collaborators (14), the sequence coding for Interferon Ia (SasaIFN-α1, NM_001123710.1, NP_001117182.1) was identified. Its classification as Interferon Ia was analyzed by phylogenetic reconstruction using interferon sequences from Atlantic salmon analyzed in the works by Liu and collaborators (20). The interferon encoded by NM_001123710.1 effectively clustered together with the IFN-Ia sequences encoded in the *Salmo salar* genome, indicating that the chosen sequence effectively encodes an IFN-Ia (**Figure 1**).

Expression of Recombinant Interferon in *Lactococcus lactis* NZ3900

To determine if the designed interferon Ia gene would allow the expression of rIFN-Ia in *L. lactis*, the gene was cloned in

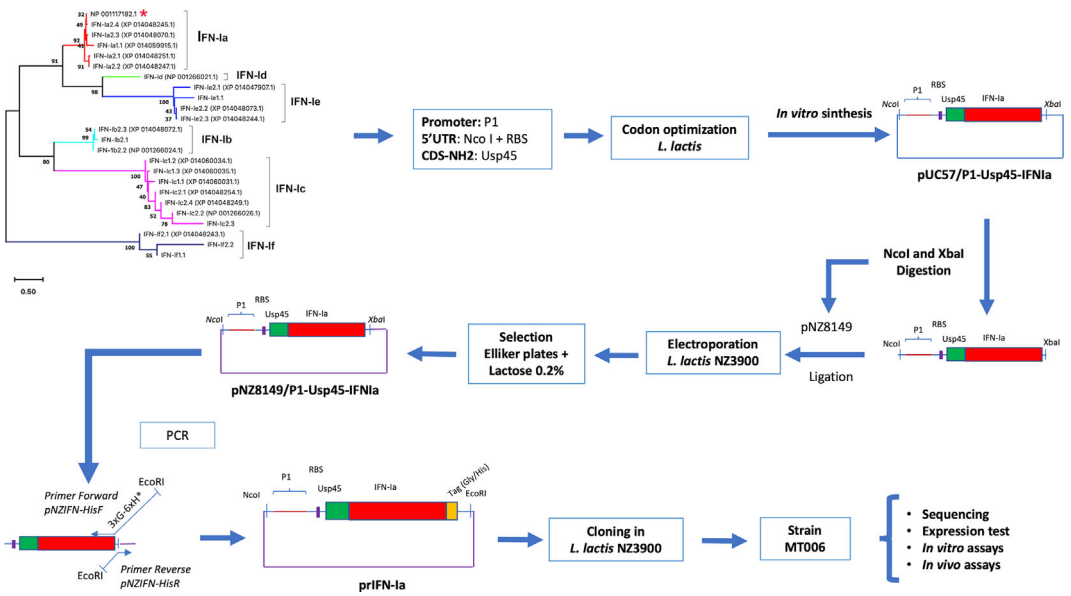

FIGURE 1 | Experimental design to evaluate the use of *L. lactis* as an oral administration system in Atlantic salmon. The figure shows the experimental scheme to evaluate *L. lactis* as an Interferon oral administration system. The chosen Interferon Ia (red asterisk) was modified by incorporating a promoter (P1), the signal peptide of the Usp45 protein. The sequence was codogenically optimized and cloned into pUC57 (pUC57/P1-Usp45-IFNIa). This segment was cloned in pNZ8149, electroporated in *L. lactis* NZ3900 and selected on Elliker medium supplemented with 0.2% lactose. A tag (Gly/His) was added to the terminal COOH end of Interferon Ia by reverse PCR. The plasmid generated prIFN-Ia was cloned in *L. lactis* NZ3900 giving rise to the strain MT006. The recombinant constructs were sequenced and the functionality of rIFN-Ia was analyzed *in vitro* and *in vivo*.

the vector pNZ8149 and transformed into *L. lactis* NZ3900. The chosen clones were sequenced to corroborate the identity of the gene, and then their expression was evaluated by western blot from cytoplasmic extracts and the culture supernatant. The cytoplasmic extract of the MT006 culture induced with nisin showed a band of approximately 22 KDa, close to the 21.9 KDa theoretically estimated for its cytoplasmic form. This band is not present in cytoplasmic extracts of the MT005 strain, which corresponds to the wild type strain transformed with plasmid pNZ8149. When the western blot was repeated using protein extracts from the MT006 culture supernatant, a signal of the expected size was not observed (data not shown), which may be due to low concentration of the extracellular interferon. Proteins of the supernatant were then precipitated with TCA and a dot blot was performed loading approximately 1 μg of total protein. Four different clones were tested. The results show a positive signal in all four MT006 clones. No signal was observed in the culture supernatant of *L. lactis* strain NZ3900 containing plasmid pNZ8149 (MT005). As in the western blot, protein extracts of the LMB030 strain were used as a positive control, which expresses a 40 KDa protein that presents a histidine tag (**Figure 2**).

Antiviral Activity of Cytoplasmic Extracts From *L. lactis* Expressing rIFN-Ia in Cell Cultures

To determine if the recombinant interferon produced by the MT006 strain shows bioactivity, CHSE-214 cell cultures were exposed to different amounts of rIFN-Ia (10, 100 and 500 ng/ml) for 24 hours. To keep constant the amount of total protein added to the CHSE-214 cell cultures in all conditions, the total amount of proteins was adjusted to the same concentration using cytoplasmic extracts of the MT005 control strain, which lacks the rIFN-Ia producing gene. The expression of Mx, and PKR was evaluated and also the effect of these extracts on the replication of IPNV in CHSE-214 cells. The results show that PKR expression increased in a dose-dependent manner (**Figure 3A**), while Mx reached its maximum induction (~1000 times) when cells were exposed to 100 ng/ml of extract from MT006 (**Figure 3B**). The induction of Mx and PKR at high concentrations of the MT006 extract exceeded the effect achieved by the Poly I:C transfection, indicating a specific effect achieved by the rIFN-Ia present in the MT006 extract.

Although several studies where the function of IFN-Ia from Atlantic salmon against IPNV has been tested in CHSE214 (14, 21), this cell line corresponds to an isolated from Chinook Salmon embryonic tissues. Thus, to properly test a more complex process such as resistance to IPNV infection in Atlantic salmon we change our cellular model to SHK-1 because is a cell line from Atlantic salmon. The SHK-1 was isolated from the head kidney of Atlantic salmon, and can be both infected and propagate IPNV Sp-2 (genogroup 5) (53, 54) in a mechanism dependent on macropinocytosis. However, to our knowledge, there is no direct evidence that Interferon Ia confers an antiviral state against IPNV infection, although several findings suggest it. SHK-1 increases the expression of Mx in response to Interferon Type I from rainbow trout (55),

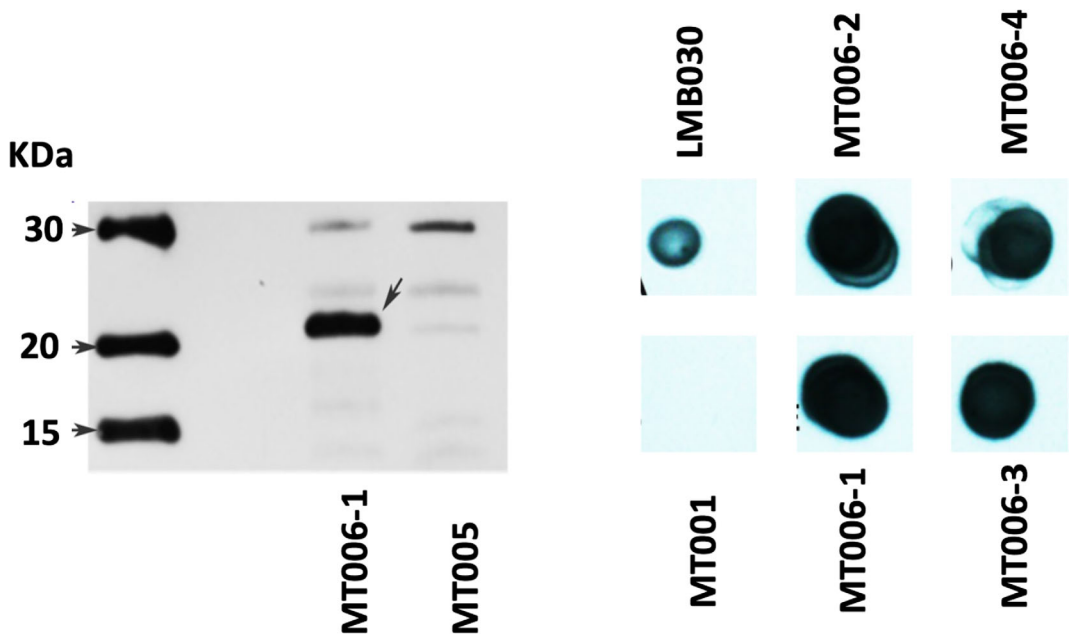

FIGURE 2 | Expression of recombinant IFN-Ia in *L. lactis* NZ3900. On the left panel, the figure shows a western blot using cytoplasmic extracts of cultures of the strain MT006 (*L. lactis* NZ3900 + prIFNIa), and MT005 (*L. lactis* NZ3900 + pNZ8149). The arrow points to the recombinant interferon Ia (rIFN-Ia) in lane of MT006. The right panel shows a dot blot of protein extracts of the supernatants of the used cultures obtained by precipitation with TCA and levosucranase in the dot loaded with the extracts obtained from strain LMB030.

Poly I:C, and supernatant of Atlantic salmon macrophages stimulated with Poly I:C (56). In SHK-1, Poly I:C also induces the expression of Interferon Ia (57). To validate the use of SHK-1 to test the antiviral activity of extracts containing rIFN-Ia we first evaluated the effect of its transfection with Poly I:C on the expression of Mx, PKR, IFN-Ia, and the viral load of IPNV. Transfection with Poly I:C induced the expression of Mx, PKR and IFN-Ia between 10 to 30-fold in the first 24 hours and reduced the viral load two orders after 7 d post-infection (data not shown), indicating that the activation of the interferon type I pathway was effective to control the infection of IPNV in SHK-1. Based on these results we proceeded with the experiments.

When the effect on the replication of the IPN virus was analyzed in SHK-1 cells, it was observed that cells exposed to the extracts of MT006 present a lower viral load, reducing the number of copies of the VP2 gene by up to 2 orders of magnitude at the maximum amount of extracts of MT006. The exposure of SHK-1 cells to extracts of *L. lactis* strains that do not express rIFN-Ia had no effect on the number of copies of the VP2 gene, suggesting that the normal components of *L. lactis* do not induce an antiviral state. The effects achieved by the MT006 extracts on the viral load showed a dose-dependent behavior, reaching the maximum reduction at 500 ng/ml of rIFN-Ia. These antiviral effects were also greater than those observed when cells were transfected with poly I:C prior to infection with IPNV, suggesting that the rIFN-Ia present in the extract of MT006 has a highly specific antiviral effect on IPNV (**Figure 3C**).

In Vivo Effect of the Oral Administration of MT006 on the Expression of Mx, PKR, and the Viral Load of IPNV

The results shown above indicate that extracts *L. lactis* expressing rIFN-Ia (strain MT006) stimulate the expression of antiviral genes (Mx and PKR) in CHSE-214 and reduce the viral load in the supernatant in SHK-1 cell cultures, suggesting that this strain could help control infections by IPNV or other viruses sensitive to IFN-Ia. To evaluate the functionality *in vivo*, the effect of the administration of MT006 for 5 days (10^7 CFU/(fish×day)) on the expression of Mx and PKR, and on the viral load in fish challenged with IPNV, was evaluated on 1, 3 and 10 days after the end of the treatment (fed) with MT006. The results show that the effect of administering MT006 is mainly on the spleen, where Mx reaches a maximum induction of 85,000 times the first day after the end of treatment with MT006 (**Figure 4A**), while PKR reaches an increase of around 8 to 9 times on days 1 and 3 post-treatment (**Figure 4B**). In the case of the head kidney, an inverse behavior to that observed in the spleen was noted, where a reduction of the expression is observed in the head kidney on the days of maximum induction (**Figures 4D, E**). To our knowledge, this striking behavior has not been previously described in salmonids, however the stimulation of fish with Poly I:C and R848 induce the expression of IFN-Ia mainly in the spleen, suggesting that this cytokine is related with the immune function of this organ (14). These data were normalized with respect to the fish fed with MT005, analyzing only the changes in

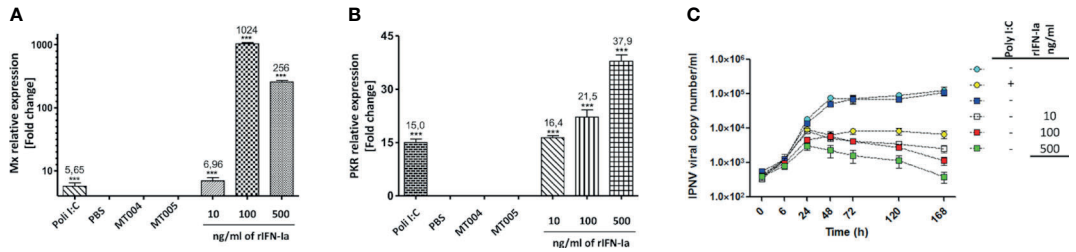

FIGURE 3 | Antiviral effect of cytoplasmic extracts containing rIFN-Ia. The figure shows the effect of 10, 100 and 500 ng/ml of rIFN-Ia on the gene expression of Mx **(A)** and PKR **(B)** in cultures of CHSE-214. The CHSE-214 cultures were exposed to a constant concentration of total protein which was achieved by mixing the MT006 extracts with the MT005 extracts. As a control, the extract of the *L. lactis* NZ3900 (MT005) and *L. lactis* NZ3900 (MT004) strains were used. The expression of Mx and PKR was evaluated by RT-qPCR and expressed as normalized change times with regard to the expression of 18S rRNA and with respect to the cultures exposed only to MT005. The effect of rIFN-Ia on the viral replication kinetic **(C)** was evaluated by qPCR on the culture media of SHK-1 cultures exposed to 10 ηg/ml (open squares), 100 ηg/ml (red squares), and 500 ηg/ml (green squares) of rIFN-Ia, during the first 168 h post infection with IPNV. The SHK-1 cultures were exposed to a constant concentration of bacterial protein which was achieved by mixing the MT006 and MT005 extracts. As control SHK-1 cells were exposed to extract of MT005 (blue squares), transfected with Poly I:C (yellow circles), or remains without treatment (light blue circles). The existence of statistically significant differences was determined using a one-way ANOVA analysis (***$p < 0.001$).

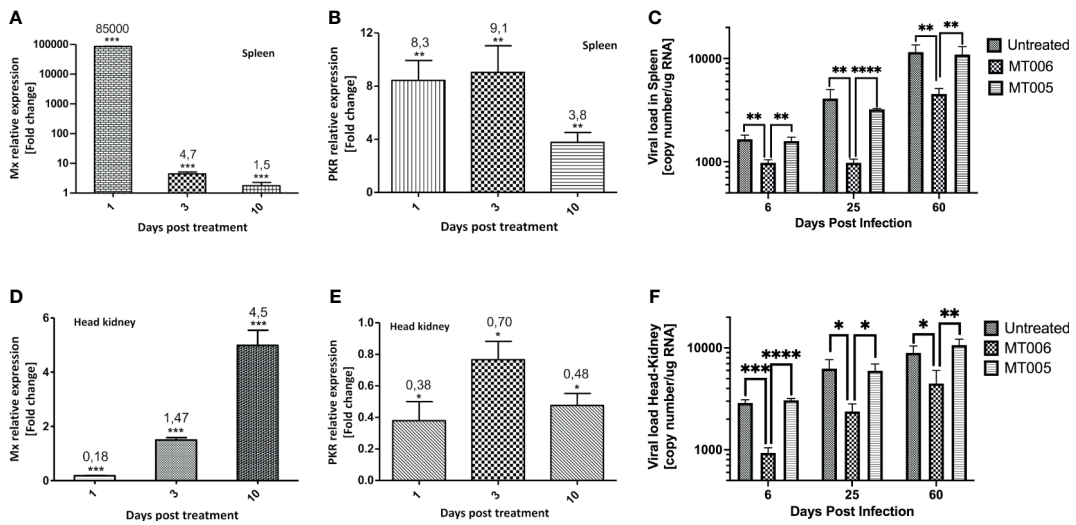

FIGURE 4 | *In vivo* effect of the administration of MT006. The figure shows the effect of the administration of MT006 for 5 days [10^7 CFU/(fish * day)] on the gene expression of Mx **(A, D)** and PKR **(B, E)** in spleen **(A, B)** and head kidney **(D, E)**. The effect on expression is shown as fold changes normalized to the expression of the gene encoding for 18S rRNA, and on expression in fish fed *L. lactis* NZ3900 containing plasmid pNZ8149 (MT005). The figure also shows the effect of MT006 administration on viral load in fish infected intraperitoneally with IPNV **(C, F)**. Viral load was normalized by the amount of RNA used in the RT-qPCR assay. The statistical analyzed was performed using a parametric t-test *$p < 0.05$, **$p < 0.01$, ***$p < 0.001$, ****$p < 0.0001$.

expression consequence of the rIFN-Ia expression. When we analyze if *L. lactis* perse could increase the expression of Mx and PKR in the spleen or kidney, we also observed a different pattern of stimulation in both organs. While in the spleen MT005 increased the expression of Mx (25-fold) and PKR (11-fold) only at 10 days post-treatment (**Supplementary Figures 1A, C**), a faster response was identified in the kidney that increased the expression of Mx (7.7 fold) and PKR (5 fold) only on the first day post feed with MT005 (**Supplementary Figures 1B, D**). Altogether these results showed that the spleen was the main target of the rIFN-Ia produced by MT006, showing a faster and strong response than the kidney. While the bacterial host (*L. lactis* NZ3900) induced an antiviral response weaker and later to that induced by MT006, targeting first to the kidney and later to the spleen.

When the effect of the administration of the probiotic expressing rIFN-Ia (MT006) was analyzed in challenge assays with IPNV, it was observed that fish treated with MT006 showed a lower viral load than fish treated with *L. lactis* NZ9000 or without treatment both in spleen as in head kidney (**Figures 4C, F**).

This effect was observed in the 3 timepoints analyzed (6, 25 and 60 days post-infection), although the magnitude of this effect decreased towards the end of the experiment, suggesting a long-term effect in increasing the antiviral capacity induced by MT006. Mortality was not detected in the fish challenged with the pathogen, in agreement with the current presence of QTL IPNV-resistant fish in Chilean salmon farming centers that results in a high prevalence of the infection with a lower mortality.

Potential Antiviral Effect of MT006 on Other Salmonids

Our results show that the rIFN-Ia produced by MT006 has *in vitro* and *in vivo* effects on the antiviral activity of *Salmo salar*, where the administration of the strain MT006 suffices to confer an antiviral state that reduces the load of IPNV. The application of MT006 in other salmonids will partially depend on the degree to which rIFN-Ia from *Salmo salar* can stimulate IFN-I receptors. To evaluate the potential effect of MT006 on other salmonids, it the protein sequence of rIFN-Ia was compared with the sequence of interferons previously identified in other salmonids. We identified genes that encode for proteins with over 90% identity to rIFN-Ia in Salmo trutta, *Salvelinus alpinus*, *Oncorhynchus nekra*, *Oncorhynchus mykiss*, *Oncorhynchus kisutch*, and *Oncorhynchus keta*, with higher identity in Interferons I of *Salmo trutta* and *Salvelinus alpinus* (**Figure 5**). These results suggest that oral administration of MT006 to other salmonids could help reduce the impact of viral infections in these species.

DISCUSSION

The microorganisms that conform the microbiota play an important role in the adequate stimulation of the immune system (58). Although this interaction has mainly been characterized in mammals, the common characteristics shared by the immune system of mammals and teleost fish, in addition to the similarities in the complexity of the microbiota that is established in the intestines and mucosa in both groups, suggest that the mechanisms of communication are conserved (59). Experiments using zebrafish as models have established the role of the microbiota in the maturation of the immune system (60), protection against pathogens (61), nutrient uptake (62), behavior (63), and in the formation of bones (64). In salmonids, although progress has been made in characterizing the composition of the microbiota in various environments and how it is affected by the culture and feeding conditions, there are few studies that show a direct relationship with the immune system (65–69). Indirect evidence has been obtained regarding the effect of probiotics on the immune system of salmonids, where in *Salmo salar* and *Oncorhynchus mykiss*, have been shown to stimulate the innate immune response against bacterial and viral pathogens (70). The mechanisms that allow the interaction between the immune system and the microbiota have not been fully clarified. The evidence obtained so far indicates that its communication is mediated by the interaction of structural components of microorganisms with PRR or host antibodies, and by molecules secreted by microorganisms that are detected by the immune system, in a mechanism similar to that used by the endocrine system (58, 71). The presence of these molecules in the microbiota of fish and mammals, as well as their receptors in their respective hosts (59), suggest that the communication mechanism arose early in evolution and has been conserved and improved in the various species (72).

The present work exploits this communication capacity of the host with its commensal microorganisms using a probiotic bacterium *L. lactis* as a vehicle for the production and release of rIFN-Ia in *Salmo salar* to stimulate the antiviral response of the fish. Moreover, *L. lactis* have been identified as normal components of the microbiota of mammals and salmonids (73, 74). Similar strategies have been used in mammals, allowing to stimulate the anticancer response through the secretion of IL-17A (75), stimulating the adaptive immune response by secreting IL-12 (76), or reducing the intestinal inflammation by secreting IL-10 (77), or IL-35 (78). The expression of functional proteins from animals using bacterial systems lacking the post-translational modification machinery is not always feasible when these modifications are necessary for the proper folding of the protein or for recognition by its receptor. In the case of cytokines, some of them, such as type I and II interferons in humans, are glycosylated or have glycosylation motifs (uniprot.org). The functionality of human type I interferon expressed in *E. coli* (79) and *L. lactis* (80) suggests that glycosylations are not related to the interaction with its receptor. However, they participate by increasing the half-life of the protein, stabilizing the 3D structure, or protecting it from the action of proteases (81, 82). In the case of Interferon Ia from *Salmo salar*, its glycosylated isoforms have not been described despite the fact that it also presents glycosylation motifs in its primary sequence. As in the case of Interferon I of humans, the expression of recombinant interferon Ia from *Salmo salar* in its biologically active form has also been successfully achieved using *E. coli* as a recombinant protein expression system (83), supporting our observation that Interferon Ia from *Salmo salar* is also biologically active in its non-glycosylated form.

Our original design involves modifying the primary sequence of *Salmo salar* IFN-Ia by introducing the signal peptide of the USP45 protein. This peptide has been widely used in order for *L. lactis* to secrete proteins to the extracellular medium (84). However, the efficiency of this signal appears to depend on the recombinant protein. In the case of human interferons, the signal peptide of the USP45 protein produces an inefficient secretion, just as we observed in the case of salmon rIFN-Ia presented in this work. This efficiency has been improved by incorporating additional signals to the USP45 protein peptide (85). It remains to be determined whether these signals could also increase the export efficiency of rIFN-Ia. However, according to our results, this inefficient secretion is sufficient to produce biological effects *in vivo*. This is consistent with the low concentrations of IFN-Ia in serum (100-1000 pg/mL) that are observed *in vivo* in response

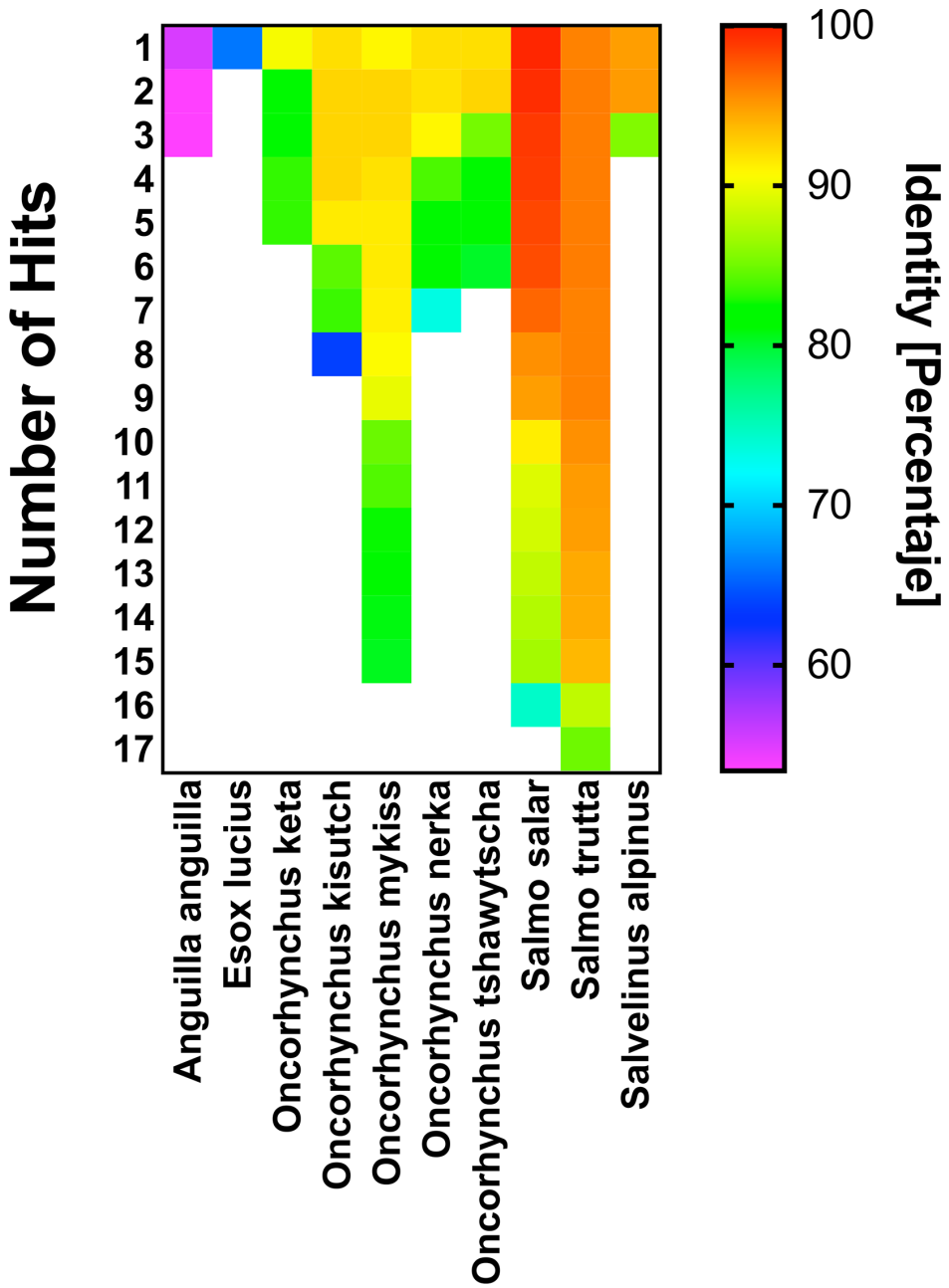

FIGURE 5 | Comparison of rIFN-Ia with interferons present in other Salmonids. The figure shows the percentage of identity of rIFN-Ia with interferons present in the salmonid species *Salmo trutta*, *Salvelinus alpinus*, *Oncorhynchus nekra*, *Oncorhynchus mykiss*, *Oncorhynchus kisutch*, *Oncorhynchus keta*, and in other fish (Eagle eel and Esox lucius). The figure shows the number of hits identified in each species and the percentage of identity. Both data were obtained by BLASTP alignment against database nr. The identity percentage is shown in a color scale and was constructed with the Prism 9.0 program.

to viral infections (86) or during the administration of interferon in hepatitis C treatments (87).

The mechanism by which the *in situ* release of these cytokines at the mucosal level produces local and systemic effects is not fully understood, but it is estimated that the release of these cytokines would stimulate the immune cells associated with the mucosa, and these, in turn, would amplify the effect when translocated into lymph nodes. An important difference in the organization of the immune system of fish and mammals is that the former have diffuse mucosal-associated immune tissue, without the presence of lymphoid nodes (88). Therefore, if the first suggested mechanism operates, it would imply that rIFN-Ia could stimulate the immune cells present in the intestinal mucosa or be phagocytosed by them, producing the migration

of these immune cells to the spleen or kidney. There, the immune cells could stimulate other cells either by endogenous release of interferon or by the release of interferon produced by MT006, in a mechanism similar to that observed when dendritic cells interact with commensal bacteria in the mammalian intestine and transport them to the lymph nodes (89). This mechanism could explain the immunizing properties of orally administered recombinant Lactic Acid Bacteria that express epitopes from microbial pathogens of fish (33–44). The dosages used in these experiments are between 10^7 to $2x10^8$ CFU per fish gram, around 30 to 600 times the used dosage of MT006. This high dosage allows reduce the spleen viral load of IPNV 32 times (37), far more than our results that show a reduction of 3 -4 times, in the first days after the challenge. It remains to determine whether longer treatment with MT006 has the potential to reduce the viral load to levels similar or lowers at the observed with the immunizing *Lactobacillus casei* expressing the epitopes of VP2 of IPNV (37). The characterization of the immune response at the gut level during and after the administration of MT006 should help to clarify if this proposed mechanism plays a role in the immune stimulation produced by the *Lactococcus lactis* strain expressing rIFN-Ia.

An alternative mechanism that could explain the systemic effects of orally administered probiotics could be the spread of these bacteria to different tissues. The translocation of bacteria from the gastrointestinal tract to other organs has been observed mainly under pathological conditions where inflammatory processes increase the permeability of the epithelial barrier. However, this has also been observed under physiological conditions (90). The translocation of *L. lactis* from the intestine to internal organs such as the mammary glands has been identified in pregnant female mice shortly before giving birth (91). Interestingly, IFN-I promotes the integrity of the gastrointestinal barrier mediated by a reduction in apoptosis of epithelial cells (92). Thus, if IFN-Ia has the same effect in fish, it is unlikely that rIFN-Ia secretion promotes the translocation of MT006. However, it cannot be discarded as a mechanism since there are several examples of symbiotic relationships between fish and bacteria based on the colonization of internal and external organs (93–96). On the other hand, the presence of bacteria in the liver and head kidney has also been detected in healthy wild fish (97), a situation that indicates that the relationship that fish have with their commensal bacteria is more complex than that observed in mammals.

The *in vivo* stimulation with MT006 also showed that the spleen and kidney have an opposite kinetics of Mx, being the spleen, the organ/tissue preferentially stimulated at a short time after treatment with MT006. To our knowledge, this behavior has not previously described, probably because most of the studies that analyze *in vivo* the effects of IFN-I have been conducted analyzing the expression in one organ at different times or comparing both organs at the same time. The preferential stimulation of the spleen could be explained if these organs express receptors specific for IFN-Ia which expression should be regulated at the translational level, since both organs show no differences in the transcription of IFN-Ia receptors (98). By other hand, the reason why the spleen is more sensitive to INF-Ia could be related to its function as a secondary immune organ related to the antibody production by B-cells, which is improved in Atlantic salmon by IFN-I (26). In relation to the opposite kinetics of Mx expression observed in the spleen and kidney, the reduction of Mx expression in the spleen cloud be the result of the lost MT006 in the intestine, while the increased expression of Mx in the kidney could be explained if the kidney responds to a secondary signal emitted by the spleen. Since interferon type I can stimulate its own expression, the rIFN-Ia could induce the expression of Interferon Ic or Ib which are able to produce systemic effects. It remains to determine whether Interferons type I shows a cross-stimulation pattern among them.

Our results showed that administration of MT006 before the infection with IPNV reduced the replication of the virus but was not able to help at resolves completely the infection, which continued achieving after 60 days a viral load like those observed on day 6. Continuous treatment with MT006 higher than five days could be useful to improve the capacity of fish to completely resolve the infections of IPNV, especially in fish with QTL resistant to the mortality but not to the infection, such as the fish cultured in Chilean salmon farming centers. Since IPNV has shown an immunosuppressive effect on fish (99), a reduction in viral load mediated by the oral administration of MT006 should help to improve the robustness of fish against co-infection with pathogens either bacterial or viral (100).

Interferon Ia has shown antiviral effects against IHNV (24), IPNV (83), SAV (101) and an adjuvant effect in vaccines against ISAV (26), a situation that allows us to suppose that the administration of MT006 could also have antiviral effects against SAV or act as adjuvant of ISAV vaccines in *Salmo salar* or other salmonids infected by these viruses, which possess a system of Interferons with a high percentage of identity (>90%) with the rIFN-Ia produced by MT006. For example, IPNV, and SAV can also infect *Salmo trutta*, and *Oncorhynchus mykiss* (7, 102–104); therefore, they could constitute species in which to evaluate the antiviral effect of the administration of MT006. This implies that MT006 could be used as a broad spectrum biotherapeutic agent in salmonid aquaculture, either to induce an antiviral state, or to enhance the effect of vaccines against various bacterial or viral pathogens that affect salmon farming.

CONCLUSIONS

The results obtained in this work indicate that *L. lactis* is a suitable vehicle to produce Interferon Ia from *Salmo salar* in its biologically active form and that oral administration of this rIFN-Ia producing bacterium stimulates the systemic antiviral response in fish, enabling a reduction in the viral load in immune organs.

Our work supports the use of *L. lactis* as a vehicle to specifically stimulate the immune response in teleost fish through the production and/or secretion of immunostimulating peptides.

DATA AVAILABILITY STATEMENT

The raw data supporting the conclusions of this article will be made available by the authors, without undue reservation.

ETHICS STATEMENT

Experiments with fish were designed and done in accordance with the ethical standards of the Institutional Ethics Committee of the Universidad de Santiago de Chile (approved in internal report n°350) and the relevant legislation in force.

AUTHOR CONTRIBUTIONS

Conceptualization, MT, CM and JG. Methodology, CM, MP, and JG. Investigation, CM, SS Resources, AS. Writing—original draft preparation, AG, R.V, NV. Funding acquisition, MT. All authors contributed to the article and approved the submitted version.

FUNDING

This research was funded by Fundacion Innovación Agraria (FIA), grant number PYT 2012-0056 to MT. The funder was not involved in the study design, collection, analysis, and interpretation of data, the writing of this article or the decision to submit it for publication.

SUPPLEMENTARY MATERIAL

The Supplementary Material for this article can be found online at: https://www.frontiersin.org/articles/10.3389/fimmu.2021.696781/full#supplementary-material

REFERENCES

1. FAO. *SOFIA 2018 - State of Fisheries and Aquaculture in the World 2018* (2018). Available at: http://www.fao.org/state-of-fisheries-aquaculture (Accessed September 25, 2018).
2. Kibenge FS. Emerging Viruses in Aquaculture. *Curr Opin Virol* (2019) 34:97–103. doi: 10.1016/j.coviro.2018.12.008
3. Kibenge FSB. Determinants of Emergence of Viral Diseases in Aquaculture. In: *Aquaculture Virology*. Elsevier Inc (2016). p. 35–48. doi: 10.1016/B978-0-12-801573-5.00006-1
4. Verma AK, Gupta S, Singh SP, Nagpure NS. An Update on Mechanism of Entry of White Spot Syndrome Virus Into Shrimps. *Fish Shellfish Immunol* (2017) 67:141–6. doi: 10.1016/j.fsi.2017.06.007
5. Surachetpong W, Roy SRK, Nicholson P. Tilapia Lake Virus: The Story So Far. *J Fish Dis* (2020) 43:1115–32. doi: 10.1111/jfd.13237
6. Bergmann SM, Jin Y, Franzke K, Grunow B, Wang Q, Klafack S. Koi Herpesvirus (KHV) and KHV Disease (KHVD) – a Recently Updated Overview. *J Appl Microbiol* (2020) 129:98–103. doi: 10.1111/jam.14616
7. Eriksson-Kallio A, Holopainen R, Koski P, Nousiainen A, Koskinen H, Kause A, et al. Susceptibility of Rainbow Trout to Three Different Genogroups of Infectious Pancreatic Necrosis Virus. *Dis Aquat Organ* (2020) 141:103–16. doi: 10.3354/dao03512
8. Rimstad E, Markussen T. Infectious Salmon Anaemia Virus—Molecular Biology and Pathogenesis of the Infection. *J Appl Microbiol* (2020) 129:85–97. doi: 10.1111/jam.14567
9. Kibenge FSB, Godoy MG, Fast M, Workenhe S, Kibenge MJT. Countermeasures Against Viral Diseases of Farmed Fish. *Antiviral Res* (2012) 95:257–81. doi: 10.1016/j.antiviral.2012.06.003
10. Flores-Kossack C, Montero R, Köllner B, Maisey K. Chilean Aquaculture and the New Challenges: Pathogens, Immune Response, Vaccination and Fish Diversification. *Fish Shellfish Immunol* (2020) 98:52–67. doi: 10.1016/j.fsi.2019.12.093
11. Evensen Ø, Leong JAC. DNA Vaccines Against Viral Diseases of Farmed Fish. *Fish Shellfish Immunol* (2013) 35:1751–8. doi: 10.1016/j.fsi.2013.10.021
12. Langevin C, Boudinot P, Collet B. IFN Signaling in Inflammation and Viral Infections: New Insights From Fish Models. *Viruses* (2019) 11:302–18. doi: 10.3390/v11030302
13. Kileng Ø, Albuquerque A, Robertsen B. Induction of Interferon System Genes in Atlantic Salmon by the Imidazoquinoline S-27609, a Ligand for Toll-Like Receptor 7. *Fish Shellfish Immunol* (2008) 24:514–22. doi: 10.1016/j.fsi.2007.10.005
14. Svingerud T, Solstad T, Sun B, Nyrud MLJ, Kileng Ø, Greiner-Tollersrud L, et al. Atlantic Salmon Type I IFN Subtypes Show Differences in Antiviral Activity and Cell-Dependent Expression: Evidence for High IFNb/IFNc–Producing Cells in Fish Lymphoid Tissues. *J Immunol* (2012) 189:5912–23. doi: 10.4049/jimmunol.1201188
15. Xu C, Evensen Ø, Munang'andu HM. De Novo Assembly and Transcriptome Analysis of Atlantic Salmon Macrophage/Dendritic-Like TO Cells Following Type I IFN Treatment and Salmonid Alphavirus Subtype-3 Infection. *BMC Genomics* (2015) 16:96–111. doi: 10.1186/s12864-015-1302-1
16. Schoggins JW, Rice CM. Interferon-Stimulated Genes and Their Antiviral Effector Functions. *Curr Opin Virol* (2011) 1:519–25. doi: 10.1016/j.coviro.2011.10.008
17. Das BK, Ellis AE, Collet B. Induction and Persistence of Mx Protein in Tissues, Blood and Plasma of Atlantic Salmon Parr, Salmo Salar, Injected With Poly I:C. *Fish Shellfish Immunol* (2009) 26:40–8. doi: 10.1016/j.fsi.2008.03.009
18. Dick A, Graf L, Olal D, Von Der Malsburg A, Gao S, Kochs G, et al. Role of Nucleotide Binding and GTPase Domain Dimerization in Dynamin-Like Myxovirus Resistance Protein a for GTPase Activation and Antiviral Activity. *J Biol Chem* (2015) 290:12779–92. doi: 10.1074/jbc.M115.650325
19. Dar AC, Dever TE, Sicheri F. Higher-Order Substrate Recognition of Eif2α by the RNA-Dependent Protein Kinase PKR. *Cell* (2005) 122:887–900. doi: 10.1016/j.cell.2005.06.044
20. Liu F, Wang T, Petit J, Forlenza M, Chen X, Chen L, et al. Evolution of IFN Subgroups in Bony Fish - 2. Analysis of Subgroup Appearance and Expansion in Teleost Fish With a Focus on Salmonids. *Fish Shellfish Immunol* (2020) 98:564–73. doi: 10.1016/j.fsi.2020.01.039
21. Robertsen B, Bergan V, Røkenes T, Larsen R, Albuquerque A. Atlantic Salmon Interferon Genes: Cloning, Sequence Analysis, Expression, and Biological Activity. *J Interf Cytokine Res* (2003) 23:601–12. doi: 10.1089/107999003322485107
22. Kileng Ø, Brundtland MI, Robertsen B. Infectious Salmon Anemia Virus is a Powerful Inducer of Key Genes of the Type I Interferon System of Atlantic Salmon, But Is Not Inhibited by Interferon. *Fish Shellfish Immunol* (2007) 23:378–89. doi: 10.1016/j.fsi.2006.11.011
23. Svingerud T, Holand JK, Robertsen B. Infectious Salmon Anemia Virus (ISAV) Replication Is Transiently Inhibited by Atlantic Salmon Type I Interferon in Cell Culture. *Virus Res* (2013) 177:163–70. doi: 10.1016/j.virusres.2013.08.004
24. Ooi EL, Verjan N, Haraguchi I, Oshima T, Kondo H, Hirono I, et al. Innate Immunomodulation With Recombinant Interferon-Alpha Enhances Resistance of Rainbow Trout (Oncorhynchus Mykiss) to Infectious Hematopoietic Necrosis Virus. *Dev Comp Immunol* (2008) 32:1211–20. doi: 10.1016/j.dci.2008.03.010

25. Chang C-J, Robertsen C, Sun B, Robertsen B. Protection of Atlantic Salmon Against Virus Infection by Intramuscular Injection of IFNc Expression Plasmid. *Vaccine* (2014) 32:4695–702. doi: 10.1016/j.vaccine.2014.05.059
26. Chang CJ, Sun B, Robertsen B. Adjuvant Activity of Fish Type I Interferon Shown in a Virus DNA Vaccination Model. *Vaccine* (2015) 33:2442–8. doi: 10.1016/j.vaccine.2015.03.093
27. Chang C-J, Jenssen I, Robertsen B. Protection of Atlantic Salmon Against Salmonid Alphavirus Infection by Type I Interferons IFNa, IFNb and IFNc. *Fish Shellfish Immunol* (2016) 57:35–40. doi: 10.1016/j.fsi.2016.08.020
28. Bermúdez-Humarán LG, Aubry C, Motta JP, Deraison C, Steidler L, Vergnolle N, et al. Engineering Lactococci and Lactobacilli for Human Health. *Curr Opin Microbiol* (2013) 16:278–83. doi: 10.1016/j.mib.2013.06.002
29. Taghinezhad-S S, Mohseni AH, Keyvani H, Razavi MR. Phase 1 Safety and Immunogenicity Trial of Recombinant Lactococcus Lactis Expressing Human Papillomavirus Type 16 E6 Oncoprotein Vaccine. *Mol Ther - Methods Clin Dev* (2019) 15:40–51. doi: 10.1016/j.omtm.2019.08.005
30. Peng X, Zhang R, Duan G, Wang C, Sun N, Zhang L, et al. Production and Delivery of Helicobacter Pylori NapA in Lactococcus Lactis and its Protective Efficacy and Immune Modulatory Activity. *Sci Rep* (2018) 8:6435–46. doi: 10.1038/s41598-018-24879-x
31. Gorain C, Singh A, Bhattacharyya S, Kundu A, Lahiri A, Gupta S, et al. Mucosal Delivery of Live Lactococcus Lactis Expressing Functionally Active JlpA Antigen Induces Potent Local Immune Response and Prevent Enteric Colonization of Campylobacter Jejuni in Chickens. *Vaccine* (2020) 38:1630–42. doi: 10.1016/j.vaccine.2019.12.064
32. Davarpanah E, Seyed N, Bahrami F, Rafati S, Safaralizadeh R, Taheri T. Lactococcus Lactis Expressing Sand Fly Ppsp15 Salivary Protein Confers Long-Term Protection Against Leishmania Major in Balb/C Mice. *PloS Negl Trop Dis* (2020) 14:1–18. doi: 10.1371/journal.pntd.0007939
33. Min L, Li-Li Z, Jun-Wei G, Xin-Yuan Q, Yi-Jing L, Di-Qiu L. Immunogenicity of Lactobacillus-Expressing VP2 and VP3 of the Infectious Pancreatic Necrosis Virus (IPNV) in Rainbow Trout. *Fish Shellfish Immunol* (2012) 32:196–203. doi: 10.1016/j.fsi.2011.11.015
34. Li-Li Z, Min L, Jun-Wei G, Xin-Yuan Q, Yi-Jing L, Di-Qiu L. Expression of Infectious Pancreatic Necrosis Virus (IPNV) VP2-VP3 Fusion Protein in Lactobacillus Casei and Immunogenicity in Rainbow Trouts. *Vaccine* (2012) 30:1823–9. doi: 10.1016/j.vaccine.2011.12.132
35. Duan K, Hua X, Wang Y, Wang Y, Chen Y, Shi W, et al. Oral Immunization With a Recombinant Lactobacillus Expressing CK6 Fused With VP2 Protein Against IPNV in Rainbow Trout (Oncorhynchus Mykiss). *Fish Shellfish Immunol* (2018) 83:223–31. doi: 10.1016/j.fsi.2018.09.034
36. Chen Y, Hua X, Ren X, Duan K, Gao S, Sun J, et al. Oral Immunization With Recombinant Lactobacillus Casei Displayed AHA1-CK6 and VP2 Induces Protection Against Infectious Pancreatic Necrosis in Rainbow Trout (Oncorhynchus Mykiss). *Fish Shellfish Immunol* (2020) 100:18–26. doi: 10.1016/j.fsi.2020.03.001
37. Hua X, Zhou Y, Feng Y, Duan K, Ren X, Sun J, et al. Oral Vaccine Against IPNV Based on Antibiotic-Free Resistance Recombinant Lactobacillus Casei Expressing CK6-VP2 Fusion Protein. *Aquaculture* (2021) 535:736425. doi: 10.1016/j.aquaculture.2021.736425
38. Zhao L, Tang X, Sheng X, Xing J, Zhan W. Surface Display of Hirame Novirhabdovirus (HIRRV) G Protein in Lactococcus Lactis and its Immune Protection in Flounder (Paralichthys Olivaceus). *Microb Cell Fact* (2019) 18:142–54. doi: 10.1186/s12934-019-1195-9
39. Zhang C, Guo S, Zhao Z, Guo ZR, Ma R, Wang GX, et al. Surface Display of Spring Viremia of Carp Virus Glycoprotein on Lactococcus Lactis and Its Protection Efficacy in Common Carp (Cyprinus Carpio L.). *Fish Shellfish Immunol* (2020) 104:262–8. doi: 10.1016/j.fsi.2020.06.021
40. Yao JY, Yuan XM, Xu Y, Yin WL, Lin LY, Pan XY, et al. Live Recombinant Lactococcus Lactis Vaccine Expressing Immobilization Antigen (I-Ag) for Protection Against Ichthyophthirius Multifiliis in Goldfish. *Fish Shellfish Immunol* (2016) 58:302–8. doi: 10.1016/j.fsi.2016.09.037
41. Naderi-Samani M, Soltani M, Dadar M, Taheri-Mirghaed A, Zargar A, Ahmadivand S, et al. Oral Immunization of Trout Fry With Recombinant Lactococcus Lactis NZ3900 Expressing G Gene of Viral Hemorrhagic Septicaemia Virus (VHSV). *Fish Shellfish Immunol* (2020) 105:62–70. doi: 10.1016/j.fsi.2020.07.007
42. Zhang L, Li Z, Li Y, Tian J, Jia K, Zhang D, et al. OmpW Expressed by Recombinant Lactobacillus Casei Elicits Protective Immunity Against Aeromonas Veronii in Common Carp. *Microb Pathog* (2019) 133:103552–59. doi: 10.1016/j.micpath.2019.103552
43. Zhang DX, Kang YH, Chen L, Siddiqui SA, Wang CF, Qian AD, et al. Oral Immunization With Recombinant Lactobacillus Casei Expressing OmpAI Confers Protection Against Aeromonas Veronii Challenge in Common Carp, Cyprinus Carpio. *Fish Shellfish Immunol* (2018) 72:552–63. doi: 10.1016/j.fsi.2017.10.043
44. Lin-Zhao Z, Tong-Yang B, Yi-Xuan Y, Ning-Guo S, Xing-Zhang D, Nan-Ji S, et al. Construction and Immune Efficacy of Recombinant Lactobacillus Casei Expressing OmpAI of Aeromonas Veronii C5–I as Molecular Adjuvant. *Microb Pathog* (2021) 156:104827. doi: 10.1016/j.micpath.2021.104827
45. Jia S, Zhou K, Pan R, Wei J, Liu Z, Xu Y. Oral Immunization of Carps With Chitosan–Alginate Microcapsule Containing Probiotic Expressing Spring Viremia of Carp Virus (SVCV) G Protein Provides Effective Protection Against SVCV Infection. *Fish Shellfish Immunol* (2020) 105:327–9. doi: 10.1016/j.fsi.2020.07.052
46. Cui LC, Guan XT, Liu ZM, Tian CY , Xu YG. Recombinant Lactobacillus Expressing G Protein of Spring Viremia of Carp Virus (SVCV) Combined With ORF81 Protein of Koi Herpesvirus (KHV): A Promising Way to Induce Protective Immunity Against SVCV and KHV Infection in Cyprinid Fish *via* Oral Vaccination. *Vaccine* (2015) 33:3092–9. doi: 10.1016/j.vaccine.2015.05.002
47. Mobitec GmbH. *NICE ® Expression System for Lactococcus Lactis The Effective & Easy-to-Operate NIsin Controlled Gene Expression System* (2015). Available at: www.mobitec.com (Accessed March 20, 2021).
48. Pfaffl MW. A New Mathematical Model for Relative Quantification in Real-Time RT-PCR. *Nucleic Acids Res* (2001) 29:e45. doi: 10.1093/nar/29.9.e45
49. Saitou N, Nei M. The Neighbor-Joining Method: A New Method for Reconstructing Phylogenetic Trees. *Mol Biol Evol* (1987) 4:406–25. doi: 10.1093/oxfordjournals.molbev.a040454
50. Felsenstein J. Confidence Limits on Phylogenies: An Approach Using the Bootstrap. *Evol (N Y)* (1985) 39:783. doi: 10.2307/2408678
51. Zuckerkandl E, Pauling L. Evolutionary Divergence and Convergence in Proteins. In: *Evolving Genes and Proteins* (1965). p. 97–166. doi: 10.1016/B978-1-4832-2734-4.50017-6
52. Stecher G, Tamura K, Kumar S. Molecular Evolutionary Genetics Analysis (MEGA) for macOS. *Mol Biol Evol* (2020) 37:1237–9. doi: 10.1093/molbev/msz312
53. Levican J, Miranda-Cárdenas C, Soto-Rifo R, Aguayo F, Gaggero A, León O. Infectious Pancreatic Necrosis Virus Enters CHSE-214 Cells *via* Macropinocytosis. *Sci Rep* (2017) 7:1–12. doi: 10.1038/s41598-017-03036-w
54. Levicán-Asenjo J, Soto-Rifo R, Aguayo F, Gaggero A, Leon O. Salmon Cells SHK-1 Internalize Infectious Pancreatic Necrosis Virus by Macropinocytosis. *J Fish Dis* (2019) 42:1035–46. doi: 10.1111/jfd.13009
55. Martin SAM, Taggart JB, Seear P, Bron JE, Talbot R, Teale AJ, et al. Interferon Type I and Type II Responses in an Atlantic Salmon (Salmo Salar) SHK-1 Cell Line by the Salmon TRAITS/SGP Microarray. *Physiol Genomics* (2007) 32:33–44. doi: 10.1152/physiolgenomics.00064.2007
56. Jensen I, Robertsen B. Effect of Double-Stranded RNA and Interferon on the Antiviral Activity of Atlantic Salmon Cells Against Infectious Salmon Anemia Virus and Infectious Pancreatic Necrosis Virus. *Fish Shellfish Immunol* (2002) 13:221–41. doi: 10.1006/fsim.2001.0397
57. Reyes-Cerpa S, Reyes-López FE, Toro-Ascuy D, Ibañez J, Maisey K, Sandino AM, et al. IPNV Modulation of Pro and Anti-Inflammatory Cytokine Expression in Atlantic Salmon Might Help the Establishment of Infection and Persistence. *Fish Shellfish Immunol* (2012) 32:291–300. doi: 10.1016/j.fsi.2011.11.018
58. Zheng D, Liwinski T, Elinav E. Interaction Between Microbiota and Immunity in Health and Disease. *Cell Res* (2020) 30:492–506. doi: 10.1038/s41422-020-0332-7
59. Kelly C, Salinas I. Under Pressure: Interactions Between Commensal Microbiota and the Teleost Immune System. *Front Immunol* (2017) 8:559–67. doi: 10.3389/fimmu.2017.00559
60. Rawls JF, Samuel BS, Gordon JI. Gnotobiotic Zebrafish Reveal Evolutionarily Conserved Responses to the Gut Microbiota. *Proc Natl Acad Sci USA* (2004) 101:4596–601. doi: 10.1073/pnas.0400706101

61. Stressmann FA, Bernal-Bayard J, Perez-Pascual D, Audrain B, Rendueles O, Briolat V, et al. Mining Zebrafish Microbiota Reveals Key Community-Level Resistance Against Fish Pathogen Infection. *ISME J* (2020) 15:702–19. doi: 10.1038/s41396-020-00807-8
62. Semova I, Carten JD, Stombaugh J, Mackey LC, Knight R, Farber SA, et al. Microbiota Regulate Intestinal Absorption and Metabolism of Fatty Acids in the Zebrafish. *Cell Host Microbe* (2012) 12:277–88. doi: 10.1016/j.chom.2012.08.003
63. Phelps D, Brinkman NE, Keely SP, Anneken EM, Catron TR, Betancourt D, et al. Microbial Colonization is Required for Normal Neurobehavioral Development in Zebrafish. *Sci Rep* (2017) 7:11244–56. doi: 10.1038/s41598-017-10517-5
64. Maradonna F, Gioacchini G, Falcinelli S, Bertotto D, Radaelli G, Olivotto I, et al. Probiotic Supplementation Promotes Calcification in Danio Rerio Larvae: A Molecular Study. *PloS One* (2013) 8:e83155. doi: 10.1371/journal.pone.0083155
65. Parra M, Espinoza D, Valdes N, Vargas R, Gonzalez A, Modak B, et al. Microbiota Modulates the Immunomodulatory Effects of Filifolinone on Atlantic Salmon. *Microorganisms* (2020) 8:1–21. doi: 10.3390/microorganisms8091320
66. Wang J, Jaramillo-Torres A, Li Y, Kortner TM, Gajardo K, Brevik ØJ, et al. Microbiota in Intestinal Digesta of Atlantic Salmon (Salmo Salar), Observed From Late Freshwater Stage Until One Year in Seawater, and Effects of Functional Ingredients: A Case Study From a Commercial Sized Research Site in the Arctic Region. *Anim Microbiome* (2021) 3:14–29. doi: 10.1186/s42523-021-00075-7
67. Li Y, Bruni L, Jaramillo-Torres A, Gajardo K, Kortner TM, Krogdahl Å. Differential Response of Digesta- and Mucosa-Associated Intestinal Microbiota to Dietary Insect Meal During the Seawater Phase of Atlantic Salmon. *Anim Microbiome* (2021) 3:8–25. doi: 10.1186/s42523-020-00071-3
68. Abid A, Davies SJ, Waines P, Emery M, Castex M, Gioacchini G, et al. Dietary Synbiotic Application Modulates Atlantic Salmon (Salmo Salar) Intestinal Microbial Communities and Intestinal Immunity. *Fish Shellfish Immunol* (2013) 35:1948–56. doi: 10.1016/j.fsi.2013.09.039
69. Perdiguero P, Martín-Martín A, Benedicenti O, Díaz-Rosales P, Morel E, Muñoz-Atienza E, et al. Teleost IgD+IgM– B Cells Mount Clonally Expanded and Mildly Mutated Intestinal IgD Responses in the Absence of Lymphoid Follicles. *Cell Rep* (2019) 29:4223–35.e5. doi: 10.1016/j.celrep.2019.11.101
70. Zorriehzahra MJ, Delshad ST, Adel M, Tiwari R, Karthik K, Dhama K, et al. Probiotics as Beneficial Microbes in Aquaculture: An Update on Their Multiple Modes of Action: A Review. *Vet Q* (2016) 36:228–41. doi: 10.1080/01652176.2016.1172132
71. Nicolas GR, Chang PV. Deciphering the Chemical Lexicon of Host–Gut Microbiota Interactions. *Trends Pharmacol Sci* (2019) 40:430–45. doi: 10.1016/j.tips.2019.04.006
72. Xu Z, Takizawa F, Casadei E, Shibasaki Y, Ding Y, Sauters TJC, et al. Specialization of Mucosal Immunoglobulins in Pathogen Control and Microbiota Homeostasis Occurred Early in Vertebrate Evolution. *Sci Immunol* (2020) 5:3254–71. doi: 10.1126/sciimmunol.aay3254
73. Opazo R, Gajardo F, Ruiz M, Romero J. Genome Sequence of a Lactococcus Lactis Strain Isolated From Salmonid Intestinal Microbiota. *Genome Announc* (2016) 4:e00881–16. doi: 10.1128/genomeA.00881-16
74. Pasolli E, De Filippis F, Mauriello IE, Cumbo F, Walsh AM, Leech J, et al. Large-Scale Genome-Wide Analysis Links Lactic Acid Bacteria From Food With the Gut Microbiome. *Nat Commun* (2020) 11:2610–21. doi: 10.1038/s41467-020-16438-8
75. Jacouton E, Maravilla ET, Boucard AS, Pouderous N, Vilela APP, Naas I, et al. Anti-Tumoral Effects of Recombinant Lactococcus lactis strain Secreting IL-17A Cytokine. *Front Microbiol* (2019) 10:3355–61. doi: 10.3389/fmicb.2018.03355
76. Bermúdez-Humarán LG, Langella P, Cortes-Perez NG, Gruss A, Tamez-Guerra RS, Oliveira SC, et al. Intranasal Immunization With Recombinant Lactococcus Lactis Secreting Murine Interleukin-12 Enhances Antigen-Specific Th1 Cytokine Production. *Infect Immun* (2003) 71:1887–96. doi: 10.1128/IAI.71.4.1887-1896.2003
77. Steidler L, Hans W, Schotte L, Neirynck S, Obermeier F, Falk W, et al. Treatment of Murine Colitis by Lactococcus Lactis Secreting Interleukin-10 (2000) (Accessed February 9, 2017).
78. Wang J, Tian M, Li W, Hao F. Preventative Delivery of IL-35 by Lactococcus Lactis Ameliorates DSS-Induced Colitis in Mice. *Appl Microbiol Biotechnol* (2019) 103:7931–41. doi: 10.1007/s00253-019-10094-9
79. Srivastava P, Bhattacharaya P, Pandey G, Mukherjee KJ. Overexpression and Purification of Recombinant Human Interferon Alpha2b in Escherichia Coli. *Protein Expr Purif* (2005) 41:313–22. doi: 10.1016/j.pep.2004.12.018
80. Bayat O, Baradaran A, Ariff A, Mohamad R, Rahim RA. Intracellular Production of IFN-Alpha 2b in Lactococcus Lactis. *Biotechnol Lett* (2014) 36:581–5. doi: 10.1007/s10529-013-1390-4
81. Katla S, Yoganand KNR, Hingane S, Ranjith Kumar CT, Anand B, Sivaprakasam S. Novel Glycosylated Human Interferon Alpha 2b Expressed in Glycoengineered Pichia Pastoris and its Biological Activity: N-Linked Glycoengineering Approach. *Enzyme Microb Technol* (2019) 128:49–58. doi: 10.1016/j.enzmictec.2019.05.007
82. Lilkova E, Petkov P, Ilieva N, Krachmarova E, Nacheva G, Litov L. Molecular Modeling of the Effects of Glycosylation on the Structure and Dynamics of Human Interferon-Gamma. *J Mol Model* (2019) 25:127–39. doi: 10.1007/s00894-019-4013-8
83. Ooi EL, Verjan N, Hirono I, Nochi T, Kondo H, Aoki T, et al. Biological Characterisation of a Recombinant Atlantic Salmon Type I Interferon Synthesized in Escherichia Coli. *Fish Shellfish Immunol* (2008) 24:506–13. doi: 10.1016/j.fsi.2007.10.004
84. Song AAL, In LLA, Lim SHE. Rahim RA. A Review on Lactococcus Lactis: From Food to Factory. *Microb Cell Fact* (2017) 16:55. doi: 10.1186/s12934-017-0669-x
85. Zhang Q, Zhong J, Liang X, Liu W, Huan L. Improvement of Human Interferon Alpha Secretion by Lactococcus Lactis. *Biotechnol Lett* (2010) 32:1271–7. doi: 10.1007/s10529-010-0285-x
86. François C, Bernard I, Castelain S, Charleston B, Fray MD, Capiod JC, et al. Quantification of Different Human Alpha Interferon Subtypes and Pegylated Interferon Activities by Measuring MxA Promoter Activation. *Antimicrob Agents Chemother* (2005) 49:3770–5. doi: 10.1128/AAC.49.9.3770-3775.2005
87. Smirne C, Minisini R, Burlone ME, Ceriani E, Corlianò F, Occhino G, et al. Interferon Alpha Concentrations in Blood and Peritoneal Fluid During Treatment for Hepatitis C. *Perit Dial Int* (2012) 32:664–6. doi: 10.3747/pdi.2011.00307
88. Bjørgen H, Koppang EO. Anatomy of Teleost Fish Immune Structures and Organs. *Immunogenetics* (2021) 73:53–63. doi: 10.1007/s00251-020-01196-0
89. Rescigno M, Urbano M, Valzasina B, Francolini M, Rotta G, Bonasio R, et al. Dendritic Cells Express Tight Junction Proteins and Penetrate Gut Epithelial Monolayers to Sample Bacteria. *Nat Immunol* (2001) 2:361–7. doi: 10.1038/86373
90. McPherson AC, Pandey SP, Bender MJ, Meisel M. Systemic Immunoregulatory Consequences of Gut Commensal Translocation. *Trends Immunol* (2021) 42:137–50. doi: 10.1016/j.it.2020.12.005
91. de Andrés J, Jiménez E, Chico-Calero I, Fresno M, Fernández L, Rodríguez JM. Physiological Translocation of Lactic Acid Bacteria During Pregnancy Contributes to the Composition of the Milk Microbiota in Mice. *Nutrients* (2018) 10:14–26. doi: 10.3390/nu10010014
92. Mirpuri J, Brazil JC, Berardinelli AJ, Nasr TR, Cooper K, Schnoor M, et al. Commensal Escherichia Coli Reduces Epithelial Apoptosis Through IFN-αa–Mediated Induction of Guanylate Binding Protein-1 in Human and Murine Models of Developing Intestine. *J Immunol* (2010) 184:7186–95. doi: 10.4049/jimmunol.0903116
93. Freed LL, Easson C, Baker LJ, Fenolio D, Sutton TT, Khan Y, et al. Characterization of the Microbiome and Bioluminescent Symbionts Across Life Stages of Ceratioid Anglerfishes of the Gulf of Mexico. *FEMS Microbiol Ecol* (2019) 95:146–56. doi: 10.1093/femsec/fiz146
94. Hinzke T, Kleiner M, Breusing C, Felbeck H, Häsler R, Sievert SM, et al. Host-Microbe Interactions in the Chemosynthetic Riftia Pachyptila Symbiosis. *MBio* (2019) 10:e02243–19. doi: 10.1128/mBio.02243-19
95. Belcaid M, Casaburi G, McAnulty SJ, Schmidbaur H, Suria AM, Moriano-Gutierrez S, et al. Symbiotic Organs Shaped by Distinct Modes of Genome Evolution in Cephalopods. *Proc Natl Acad Sci USA* (2019) 116:3030–5. doi: 10.1073/pnas.1817322116
96. Wu Z, Yang Y, Xie L, Xia G, Hu J, Wang S, et al. Toxicity and Distribution of Tetrodotoxin-Producing Bacteria in Puffer Fish Fugu Rubripes Collected From the Bohai Sea of China. *Toxicon* (2005) 46:471–6. doi: 10.1016/j.toxicon.2005.06.002

97. Meron D, Davidovich N, Ofek-Lalzar M, Berzak R, Scheinin A, Regev Y, et al. Specific Pathogens and Microbial Abundance Within Liver and Kidney Tissues of Wild Marine Fish From the Eastern Mediterranean Sea. *Microb Biotechnol* (2020) 13:770–80. doi: 10.1111/1751-7915.13537
98. Sun B, Greiner-Tollersrud L, Koop BF, Robertsen B. Atlantic Salmon Possesses Two Clusters of Type I Interferon Receptor Genes on Different Chromosomes, Which Allows for a Larger Repertoire of Interferon Receptors Than in Zebrafish and Mammals. *Dev Comp Immunol* (2014) 47:275–86. doi: 10.1016/j.dci.2014.08.007
99. Reyes-Cerpa S, Reyes-López F, Toro-Ascuy D, Montero R, Maisey K, Acuña-Castillo C, et al. Induction of Anti-Inflammatory Cytokine Expression by IPNV in Persistent Infection. *Fish Shellfish Immunol* (2014) 41:172–82. doi: 10.1016/j.fsi.2014.08.029
100. Kotob MH, Menanteau-Ledouble S, Kumar G, Abdelzaher M, El-Matbouli M. The Impact of Co-Infections on Fish: A Review. *Vet Res* (2016) 47:1–12. doi: 10.1186/s13567-016-0383-4
101. Xu C, Guo T-C, Mutoloki S, Haugland Ø, Marjara IS, Evensen Ø. Alpha Interferon and Not Gamma Interferon Inhibits Salmonid Alphavirus Subtype 3 Replication *In Vitro*. *J Virol* (2010) 84:8903–12. doi: 10.1128/JVI.00851-10
102. Bain N, Gregory A, Raynard RS. Genetic Analysis of Infectious Pancreatic Necrosis Virus From Scotland. *J Fish Dis* (2008) 31:37–47. doi: 10.1111/j.1365-2761.2007.00864.x
103. Deperasinska I, Schulz P, Siwicki AK. Salmonid Alphavirus (SAV). *J Vet Res* (2018) 62:1–6. doi: 10.2478/jvetres-2018-0001
104. Madhun AS, Isachsen CH, Omdal LM, Einen ACB, Bjørn PA, Nilsen R, et al. Occurrence of Salmonid Alphavirus (SAV) and Piscine Orthoreovirus (PRV) Infections in Wild Sea Trout Salmo Trutta in Norway. *Dis Aquat Organ* (2016) 120:109–13. doi: 10.3354/dao03009

Conflict of Interest: Authors MT and AS were employed by the company IctioBiotic SpA and ActivaQ S.A., respectively.

The remaining authors declare that the research was conducted in the absence of any commercial or financial relationships that could be construed as a potential conflict of interest.

Publisher's Note: All claims expressed in this article are solely those of the authors and do not necessarily represent those of their affiliated organizations, or those of the publisher, the editors and the reviewers. Any product that may be evaluated in this article, or claim that may be made by its manufacturer, is not guaranteed or endorsed by the publisher.

frontiers in Immunology

ORIGINAL RESEARCH
published: 20 August 2021
doi: 10.3389/fimmu.2021.708747

The Spleen as a Target to Characterize Immunomodulatory Effects of Down-Stream Processed *Cyberlindnera jadinii* Yeasts in Atlantic Salmon Exposed to a Dietary Soybean Meal Challenge

Byron Morales-Lange[1†], Jeleel Opeyemi Agboola[1†], Jon Øvrum Hansen[1], Leidy Lagos[1], Ove Øyås[1,2], Luis Mercado[3], Liv Torunn Mydland[1] and Margareth Øverland[1*]*

[1] Department of Animal and Aquaculture Sciences, Faculty of Biosciences, Norwegian University of Life Sciences, Ås, Norway, [2] Faculty of Chemistry, Biotechnology and Food Science, Norwegian University of Life Sciences, Ås, Norway, [3] Grupo de Marcadores Inmunológicos en Organismos Acuáticos, Pontificia Universidad Católica de Valparaíso, Valparaíso, Chile

OPEN ACCESS

Edited by:
Felipe E. Reyes-López, Universitat Autònoma de Barcelona, Spain

Reviewed by:
Shuyan Chi, Guangdong Ocean University, China
Patrick Kestemont, University of Namur, Belgium

***Correspondence:**
Byron Morales-Lange byron.maximiliano.morales.lange@nmbu.no
Margareth Øverland margareth.overland@nmbu.no

†These authors have contributed equally to this work

Specialty section:
This article was submitted to Comparative Immunology, a section of the journal Frontiers in Immunology

Received: *12 May 2021*
Accepted: *03 August 2021*
Published: *20 August 2021*

Citation:
Morales-Lange B, Agboola JO, Hansen JØ, Lagos L, Øyås O, Mercado L, Mydland LT and Øverland M (2021) The Spleen as a Target to Characterize Immunomodulatory Effects of Down-Stream Processed Cyberlindnera jadinii Yeasts in Atlantic Salmon Exposed to a Dietary Soybean Meal Challenge. Front. Immunol. 12:708747. doi: 10.3389/fimmu.2021.708747

Aquaculture feeds have changed dramatically from being largely based on fishmeal (FM) towards increased use of plant protein sources, which could impact the fish's immune response. In order to characterize immunomodulatory properties of novel functional ingredients, this study used four diets, one based on FM, a challenging diet with 40% soybean meal (SBM), and two diets containing 40% SBM with 5% of *Cyberlindnera jadinii* yeast exposed to different down-stream processing conditions: heat-inactivated (ICJ) or autolysation (ACJ). The immunomodulatory effects of the diets were analyzed in the spleen of Atlantic salmon after 37 days of feeding, using a transcriptomic evaluation by RNA sequencing (RNA-seq) and the detection of specific immunological markers at the protein level through indirect Enzyme-linked Immunosorbent Assay (indirect ELISA). The results showed that SBM (compared to FM) induced a down-regulation of pathways related to ion binding and transport, along with an increase at the protein level of pro-inflammatory cytokines such as tumor necrosis factor alpha (TNFα) and interferon gamma (IFNγ). On the other hand, while ICJ (compared to FM-group) maintain the inflammatory response associated with SBM, with higher levels of TNFα and IFNγ, and with an upregulation of creatine kinase activity and phosphagen metabolic process, the inclusion of ACJ was able to modulate the response of Atlantic salmon compared to fish fed the SBM-diet by the activation of biological pathways related to endocytosis, Pattern recognition receptor (PPRs)-signal transduction and transporter activity. In addition, ACJ was also able to control the pro-inflammatory profile of SBM, increasing Interleukin 10 (IL-10) levels and decreasing TNFα production, triggering an immune response similar to that of fish fed an FM-based diet. Finally, we suggest that the spleen is a good candidate to characterize the immunomodulatory effects of functional ingredients in Atlantic salmon. Moreover, the inclusion of ACJ in fish diets, with the ability to control inflammatory processes, could be considered in the formulation of sustainable salmon feed.

Keywords: *Salmo salar*, transcriptomics, ELISA, secondary lymphoid organ, inactivated yeast, autolysed yeast

INTRODUCTION

In aquaculture, the relationship between nutrition and immune system has been recognized as an important part of the fish production process, due to the maintenance of high production densities continuously faces challenges related to multi-stressor conditions such as infectious diseases and suboptimal nutrition (1). In addition, energy and nutrients provided by the feed are essential to maintain an optimal immune function (2). Future growth in aquaculture depends on feed ingredients that are capable of meeting nutritional needs and of improving the overall health of the fish (3).

The dietary composition of the salmon feed has shifted from marine ingredients such as fishmeal towards increased use of plant ingredients (4, 5). However, high inclusion of plant ingredients such as soybean meal, pea proteins and faba bean in diets for Atlantic salmon (*Salmo salar*) can have adverse effects on growth performance and fish health (6–9). In fish, it has already been described that these plant ingredients, due to an imbalanced nutritional composition, content of fiber and antinutritional factors (ANFs) (10, 11), can induce significant changes in gut-microbiome that affect the mucosal immunity, reducing its protective capacity or causing its overreaction, by increasing the secretion of antimicrobial peptides, immunoglobulins and muc-like proteins (3, 12–14). Considering this, solvent extracted soybean meal (SBM) has been used as a dietary challenge to study the impact of alternative ingredients and functional feed components on gut health. SBM has high level of ANFs, which can disrupt intestinal homeostasis and induce inflammation in the distal intestine, commonly referred to as SBM-induced enteritis (SBMIE) (6, 11, 15).

In recent years, novel microbial ingredients (MI), including bacteria and yeast, are gaining increasing interest as replacement for plant-based diets for salmonids (16, 17). Moreover, these ingredients have other properties beyond their nutritional values such as modulators of fish's immune response (3, 18–22) through components that can be detected as microbial-associated molecular patterns (MAMPs) by pattern recognition receptors (PRRs) in the fish (3, 23, 24).

Furthermore, Grammes et al. (19) reported that the use of MI in feeds could counteract intestinal inflammation in Atlantic salmon. Nevertheless, feeding is a long-term process and its modulation capacity may not only occur locally in the intestine, but also systemically in active immune organs such as the spleen, since immunity has a wide range of cellular and molecular components that can act in an integrated and systemic way. In fish, the spleen has been considered the primordial secondary lymphoid organ with a key role in the antigen presentation processes and lymphocyte activation, promoting humoral immunity, by the cellular coordination of dendritic cells (DC) and with the specific induction of T cell proliferation (25, 26). In addition, in salmonids such as rainbow trout (*Oncorhynchus mykiss*), it has already been described that fish fed functional diets (with the inclusion of *Lentinula edodes*) were able to regulate the acute inflammatory profile in the spleen, reducing possible harmful responses after a LPS-challenge (27). This could be because splenic antigen-presenting cells (APC) would polarize T cells towards regulatory phenotypes, which are important to control the immune responses and in the maintenance of fish homeostasis (28).

Based on this background, the present study proposes the evaluation of the spleen response, as a target organ for the characterization of immunomodulatory effects of down-stream processed *Cyberlindnera Jadinii* in Atlantic salmon exposed to a dietary SBM challenge. To meet this goal, our methodology combines a transcriptomic evaluation by RNA sequencing (RNA-seq) with the specific detection of immunological markers at the protein level by indirect Enzyme-linked Immunosorbent Assay (indirect ELISA). This is in order to increase the knowledge about the modulation of the immune response in Atlantic salmon fed MI.

MATERIALS AND METHODS

Experimental Design

Atlantic salmon with an average starting weight of 5.71 ± 0.06 g were sorted (at an initial stocking density of 3.21 kg/m^3) into 100 L replicated tanks exposed to a 24 h-light regime and recirculated fresh water (15°C). Oxygen content of the water was measured throughout the experiment and was maintained at an average of 9.5 ± 0.5 mg L^{-1}. Moreover, ammonia nitrogen in the recirculating system was kept below the toxic level for the fish, and no mortality or abnormal behavior in any of the fish was recorded in the experimental period.

In each tank, fish were fed for 37 days using one of the four experimental diets: fishmeal diet as a control diet (FM), 40% soybean meal diet as a challenging diet (SBM), and two diets with 40% SBM and 5% inclusion of *C. jadinii* after different downstream processes: heat-inactivated (ICJ) or autolysed (ACJ). *C. jadinii* yeast used in this experiment was produced by fed-batch fermentation using wood sugars as carbon source according to Lapeña et al. (29).

The diet composition was described in **Table 1** and each diet was formulated to meet the nutrient requirement of salmon and contain similar ratio of digestible protein to digestible energy (30). All diets were fed in 20% of excess based on the feed consumption of fish in each tank.

After the 37-day feeding period, six fish were randomly selected, anesthetized using metacaine at 50 mg L^{-1} and killed with a sharp blow to the head per tank. The individual body weight of each fish was recorded. The final weight per dietary group was 26.01 g ± 0.30 (FM), 24.50 g ± 1.11 (SBM), 24.33 g ± 0.66 (ICJ), 23.53g ± 1.46 (ACJ). No significant differences were detected in the final weight of the fish among dietary groups.

For this study, the spleen of 40 fish was obtained (10 fish per dietary group from duplicated tanks). Then, for each dietary group, six spleen samples were stored frozen in liquid nitrogen (-80°C) until protein extraction and four spleen samples were immediately suspended in RNAlater and stored overnight in the refrigerator, and then kept at -80 °C until total RNA extraction.

The fish experiment was carried out in the Fish Laboratory of Norwegian University of Life Sciences (Ås, Norway) in

TABLE 1 | Formulation and nutritional composition of experimental diets according to Agboola et al. (3).

	FM	SBM	ICJ	ACJ
Fishmeal[a]	433.4	161.4	158.4	158.4
Soybean meal[b]	0	400	400	400
Wheat gluten meal[c]	170	136	111	111
Yeast	–	–	50	50
Potato starch[d]	120	90	68	68
Fish oil[e]	130	130	130	130
Gelatin[f]	60	60	60	60
Cellulose	80	–	–	–
MCP[g]	0	10.0	10.0	10.0
Premix[h]	5.0	5.0	5.0	5.0
L-lysine[i]	–	3.0	3.0	3.0
DL-Methionine[j]	–	3.0	3.0	3.0
Choline chloride[k]	1.5	1.5	1.5	1.5
Yttrium oxide[l]	0.1	0.1	0.1	0.1
Diet composition (analyzed)				
Dry matter	924.3	906.5	899.8	914.3
Crude protein	496.6	477.8	474.1	479.4
Crude lipids	191.5	166.5	162.5	171.0
Ash	71.5	60.0	63.5	64.9
Gross Energy (MJ kg^{-1})	21.6	20.9	20.9	21.2
DP : DE[m]	23.0	22.9	22.7	22.6

[a]LT fishmeal, Norsildmel, Egersund, Norway; [b]Soybean meal, Denofa AS, Fredrikstad, Norway; [c]Wheat gluten, Amilina AB, Panevezys, Lithuania; [d]Lygel F 60, Lyckeby Culinar, Fjälkinge, Sweden; [e]NorSalmOil, Norsildmel, Egersund, Norway; [f]Rousselot 250 PS, Rousselot SAS, Courbevoie, France; [g]Monocalcium phosphate, Bolifor MCP-F, Oslo, Norway Yara; [h]Premix fish, Norsk Mineralnæring AS, Hønefoss, Norway. Per kg feed; Retinol 3150.0 IU, Cholecalciferol 1890.0 IU, α-tocopherol SD 250 mg, Menadione 12.6 mg, Thiamin 18.9 mg, Riboflavin 31.5 mg, d-Ca-Pantothenate 37.8 mg, Niacin 94.5 mg, Biotin 0.315 mg, Cyanocobalamin 0.025 mg, Folic acid 6.3 mg, Pyridoxine 37.8 mg, Ascorbate monophosphate 157.5 g, Cu: CuSulfate $5H_2O$ 6.3 mg, Zn: ZnSulfate 151.2 mg, Mn: Mn(II)Sulfate 18.9 mg, I: K-Iodide 3.78 mg, Ca 1.4 g; [i]L-Lysine CJ Biotech CO., Shenyang, China; [j]Rhodimet NP99, Adisseo ASA, Antony, France; [k]Choline chloride, 70% Vegetable, Indukern SA., Spain; [l]Y_2O_3. Metal Rare Earth Limited, Shenzhen, China. [m]DP : DE, digestible protein: digestible energy ratio. Calculated using internal digestibility values of various ingredients.

FM, fishmeal-based; SBM, Soybean meal-based, ICJ, 40% SBM and 5% of inactivated C. jadinii; ACJ, 40% SBM and 5% of autolyzed C. jadinii (ACJ). Diet formulation and composition are expressed in g kg^{-1} unless otherwise stated.

accordance with the institutional (Permit No. 174) and national regulations for control of live animal experiments in Norway (Norwegian Animal Welfare Law and Norwegian Animal Experimentation Regulations derived from Directive 2010/63/EU).

RNA-Seq

Total RNA was extracted from sixteen spleen samples (four per dietary group from duplicated tanks), using the RNeasy Mini Kit (Qiagen) following the supplier's instructions. Then, each RNA sample was quantified using a NanoDrop TM 8000 spectrophotometer (Nanodrop Technologies). Later, RNA integrity was determined using Agilent Bioanalyzer 2100. All samples showed a RNA integrity number (RIN) ≥ 8. Library preparation and RNA-seq were performed by the Norwegian Sequencing Center (UiO, Norway), using TruSeq Stranded mRNA library prep and Illumina HiSeq 4000 System (150 bp paired-end RNA sequencing).

RNA-seq data analysis was performed according to Håkenåsen et al. (31). Raw reads were cleaned by BBDuk (v34.56) to trim/remove low quality reads, adapter sequences and PhiX (Illumina spike-in) using: ktrim = r, k = 23, mink = 11, hdist = 1, tbo, tpe, qtrim = r, trimq = 15, maq = 15, minlen = 36, forcetrimright = 149. Thereafter, cleaned reads were aligned to *Salmo salar* genome ICSASG_v2 (RefSeq assembly accession: GCF_000233375.1) by HISAT (v2.1.0). Fragments mapping were counted using featureCounts (v1.4.6-p1) and differentially expressed genes (DEGs) were estimated between diets using SARTools R package (v1.7.3). Significant DEGs were determined when the adjusted p value (padj) was < 0.05.

To characterize differentially expressed genes, functional classification was performed using Gene Ontology (GO) analysis by g:Profiler (32). To achieve this, *Salmo salar* genome database (Ensembl) and gene IDs (Entrezgene_ACC) from significant DEGs list were used. GO categories (g:SCS threshold 0.05) were displayed in $-\log_2(p)$. In addition, EnrichmentMap v3.3 (33) in Cytoscape v3.81 (34) was used with default settings to visualize all diet comparisons in a single network of GO terms.

To further understand gene biological functions, significant DEGs and their expression values were used for Kyoto Encyclopedia of Genes and Genomes (KEGG) Pathway Enrichment Analysis among dietary groups (by clusterProfiler v3.16.1 package in R). Enriched pathways were selected (pvalueCutoff = 0.05) and displayed as $-\log_2(p)$. Enrichment maps were obtained using emapplot (Enrichplot package v.1.8.1 in R).

Detection of Immunological Markers

For the characterization of the immune response in the spleen of Atlantic salmon after a dietary challenge, biomarkers at the protein level were evaluated in six fish samples per dietary group (from duplicated tanks). Each sample was homogenized using metal beads and RIPA lysis buffer with protease inhibitor cocktail (1x). Then, the samples were centrifuged and total proteins were quantified from the supernatants using the Bicinchoninic acid protein assay kit (Pierce). Thereafter, indirect ELISA was performed following Morales-Lange et al. (35). Briefly, each sample was diluted in carbonate buffer (60 mM $NaHCO_3$ pH 9.6) and seeded by duplicate in a 96-well plate (Nunc) at 50 ng μL^{-1} (100 µL) for overnight incubation (4°C). Next day, the plates were washed three times with PBS-Tween20 (PBST 0.2%) and incubated with 200 µL of blocking solution (per well) for 2 h at 37°C (Pierce Clear Milk Blocking Buffer 1x). After successive washes with PBST 0.2%, 100 µL of the primary antibody (**Table 2**) was incubated for 90 min at 37°C and later, a secondary antibody diluted 1:5000 (goat anti mouse IgG-HRP or mouse anti rabbit IgG-HRP) was incubated per well during 60 min at 37°C. Chromagen substrate 3,3′,5,5′-tetramethylbenzidine single solution (TMB, Thermofisher) was added (100 µL) and incubated for 20 min at room temperature (in dark). All reactions were stopped with 50 µL of 1 N sulfuric acid and finally the plates were read at 450 nm in a SpectraMax microplate reader. (Molecular Devices).

Results from indirect ELISA were expressed in fold change relative to SBM. GraphPad Prism 8 was used to display the data and calculate means, standard deviations, one-way ANOVA and Tukey's test for multiple comparisons between diets.

Furthermore, Corrplot package in R (41) was used to make correlations among diets. All significant differences were determined when p value was <0.05.

RESULTS

Transcriptomics

DEGs number per diet comparison showed different patterns among groups (**Table 3**). The highest differentiated gene expression occurred when fish fed FM were compared to those fed SBM (313 down-regulated, 448 up-regulated). A lower number of DEGs were observed in ACJ-group compared with both FM (230 DEGs down-regulated, 163 DEGs up-regulated) and SBM (95 DEGs down-regulated, 51 DEGs up-regulated). Moreover, in ICJ-fed fish, few numbers of DEGs relative to both FM (seven down-regulated, 21 up-regulated) and SBM (21 down-regulated and four up-regulated) were detected.

The comparison between the two diets with *C. jadinii* (ACJ and ICJ) only showed four down-regulated and three up-regulated DEGs. Complete list of significant DEGs along with the name of each gene is attached in Supplementary File 2. In addition, RNA-seq raw data is available in Gene Expression Omnibus database (GEO-NCBI: GSE174262).

Gene Ontology

DEG classification by Gene Ontology using three categories (molecular function, biological processes and cellular components) showed 26 overrepresented GO terms (18 upregulated and 8 downregulated) in FM compared to SBM (FM|SBM, **Figure 1**). The analysis showed that the up-regulated terms in FM were mainly associated with ion binding, transporter and metabolic activity, while down-regulated GO terms were related to semaphorin activity, biological adhesion and cell adhesion. The same analysis comparing ICJ with both control diets showed only overrepresented GO terms (up-regulated) for ICJ compared to FM (ICJ|FM, **Figure 2A**). In this case, ICJ showed seven significant GO terms related to phosphagen metabolic and biosynthetic process. In addition, when comparing ACJ with FM (ACJ|FM, **Figure 2B**), the results showed one GO term up-regulated in ACJ (carbon-carbon lyase activity). On the other hand, the comparison between ACJ and SBM (ACJ|SBM, **Figure 2C**) showed two down-regulated terms (associated to intrinsic apoptotic signaling pathway) and 11 up-regulated terms in ACJ. Interestingly, the up-regulated terms observed in ACJ compared to SBM were similar to when FM was compared to SBM (molecular binding and gas transporter activity). The analysis between ACJ and ICJ did not show differentially significant GO terms.

By grouping the GO terms detected (from different diet comparisons) in a network (**Figure 3**), we observed that FM and ACJ (compared to SBM) share similarities associated with the up-regulation of tetrapyrrole binding, oxygen transport, oxygen carrier activity, hemoglobin complex, heme binding, gas transport, molecular carrier activity, oxygen binding and cytosol. Furthermore, it was possible to determine that FM compared to SBM (FM|SBM) was related to ICJ compared to FM (ICJ|FM) through ion binding.

TABLE 2 | Primary antibodies for indirect ELISA.

Marker	Source	Type	Dilution	Reference
CD3	Mouse	Monoclonal	1:400	(36)
CD4	Rabbit	Polyclonal	1:500	(37)
CD83	Rabbit	Polyclonal	1:200	(38)
IFNγ	Mouse	Polyclonal	1:400	(3)
IgD	Mouse	Monoclonal	1:400	(39)
IgM	Mouse	Monoclonal	1:400	(39)
IL-10	Mouse	Polyclonal	1:400	(40)
MHC II	Mouse	Polyclonal	1:400	(38)
TNFα	Mouse	Polyclonal	1:400	(3)
ZBTB46	Mouse	Polyclonal	1:400	**Supplementary Figure 1**

TABLE 3 | Significant differentially expressed genes (DEGs) per diet-comparison.

Diet-comparison	Downregulated	Upregulated
FM|SBM	313	448
ICJ|FM	7	21
ICJ|SBM	21	4
ACJ|FM	230	163
ACJ|SBM	95	51
ACJ|ICJ	4	3

KEGG Pathway Analysis

Pathway analyses according to KEGG showed that DEGs from FM compared with SBM (FM|SBM, **Figure 4A**) were related to five activated KEGG terms: biosynthesis of cofactors, peroxisome, herpes simplex virus 1 infection, carbon metabolism and metabolic pathways. Using these data, the association network showed that four of the five KEGG terms (except herpes simplex virus 1 infection) were related (**Figure 4B**). Moreover, DEGs from ICJ, compared to FM (ICJ|FM, **Figure 4C**), showed only a significant activation of metabolic pathways. The comparison between ICJ and SBM did not show any significant KEGG terms.

In **Figure 5A**, DEGs from ACJ compared to FM (ACJ|FM) showed the activation of 3 KEGG terms: arginine and proline metabolism, ECM-receptor interaction and phagosome, and the suppression of salmonella infection-pathway. However, the analysis of interactions from these pathways did not show close relationships (**Figure 5B**).

DEGs comparison between ACJ and SBM (ACJ|SBM) showed six KEGG terms significantly overrepresented in ACJ: herpes simplex virus 1 infection, endocytosis, cellular senescence, Toll-like receptor signalling pathway, C-type lectin receptor signalling pathway and salmonella infection (**Figure 5C**). Enrichment maps using these KEGG terms showed that all pathways were associated in a cluster (**Figure 5D**). Regarding the comparison between ACJ and ICJ, no significant KEGG terms were determined.

Immunological Markers

The detection of immunological markers by indirect ELISA showed lower levels of Cluster of differentiation 83 (CD83) in fish fed FM compared to SBM (0.88-fold, **Figure 6A**). Moreover,

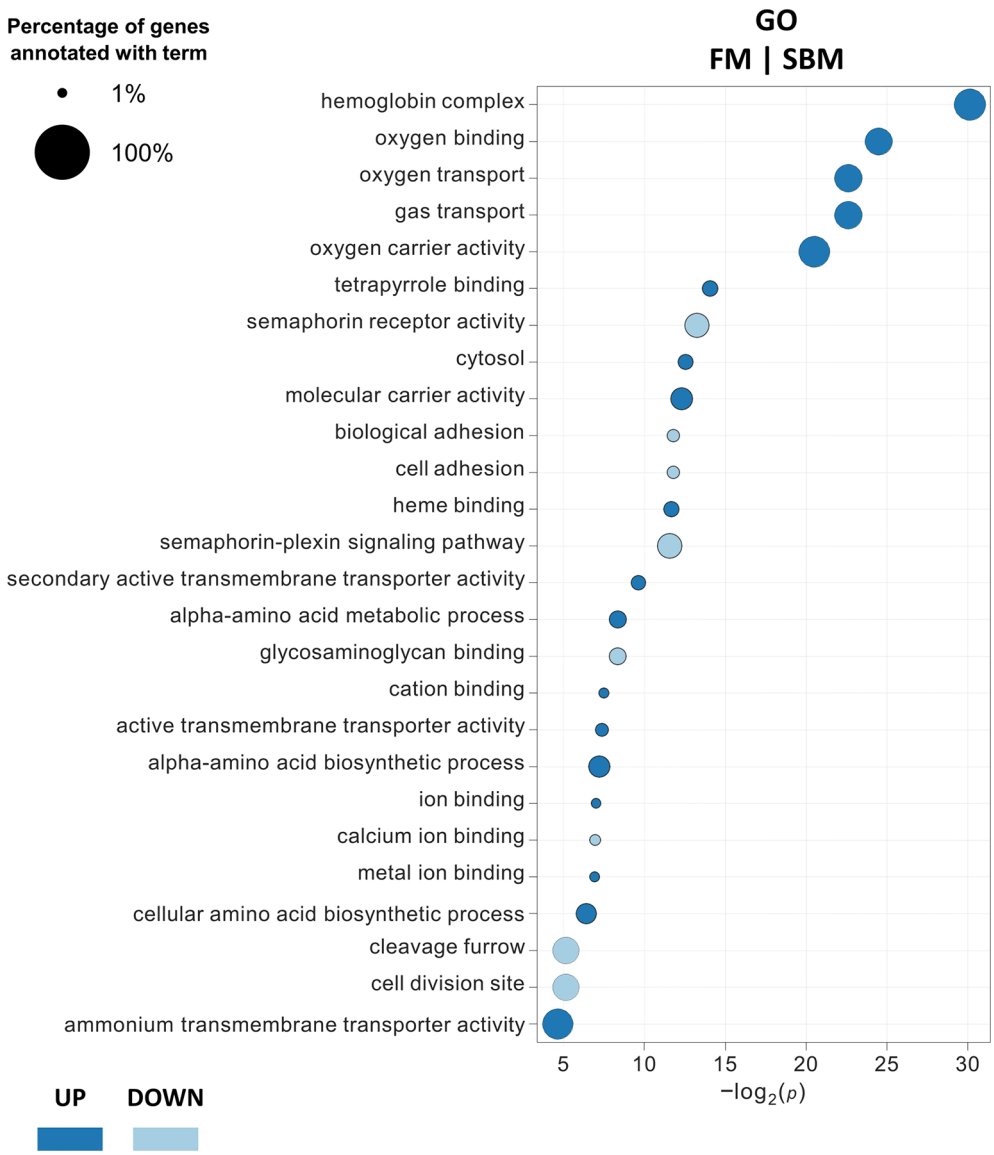

FIGURE 1 | Significantly enriched gene ontology (GO) terms (minGSSize = 3) in spleen of fish fed FM diet compared to SBM. The list is ordered by -$\log_2(p)$. Up, up-regulated (in blue); Down, down-regulated (in light blue).

an increased production of major histocompatibility complex class II (MHC II) was detected in fish fed both diets with *C. jadinii* inclusion (ICJ= 1.16-fold and ACJ= 1.10-fold, respectively) compared to FM (0.78-fold). In addition, the level of ZBTB46 (Zinc finger and BTB domain-containing protein 46) decreased in fish fed ICJ (0.64-fold) and ACJ (0.62-fold) diets, compared to both FM (1.00-fold) and SBM-fed fish (1.00-fold).

Also in **Figure 6**, only Cluster of differentiation 4 (CD4) was significantly different among diets (**Figure 6B**). It was higher in fish fed ACJ-diet (1.19-fold) compared to FM diet (0.66-fold). Cluster of differentiation 3 (CD3), Immunoglobulin D (IgD) and Immunoglobulin M (IgM) did not show significant differences between groups.

The level of cytokines in SBM-diet group (**Figure 6C**) showed a higher level of interferon gamma (IFNγ: 1.00-fold) and tumor necrosis factor alpha (TNFα: 1.00-fold) compared to FM (0.46-fold and 0.40-fold, respectively). A similar behavior to SBM-fed fish was detected in ICJ-diet group, where both pro-inflammatory cytokines showed an increase in their protein levels (IFNγ= 1.42-fold, TNFα= 1.33-fold) compared to FM. On the other hand, the cytokine values from ACJ-diet group, compared with SBM (**Figure 6C**), showed a reduction of TNFα levels (0.37-fold) and an increase in the availability of interleukin 10 (IL-10: 1.88-fold).

Finally, the correlation of all these immunological markers between the different diets (**Figure 6D**) showed a significant

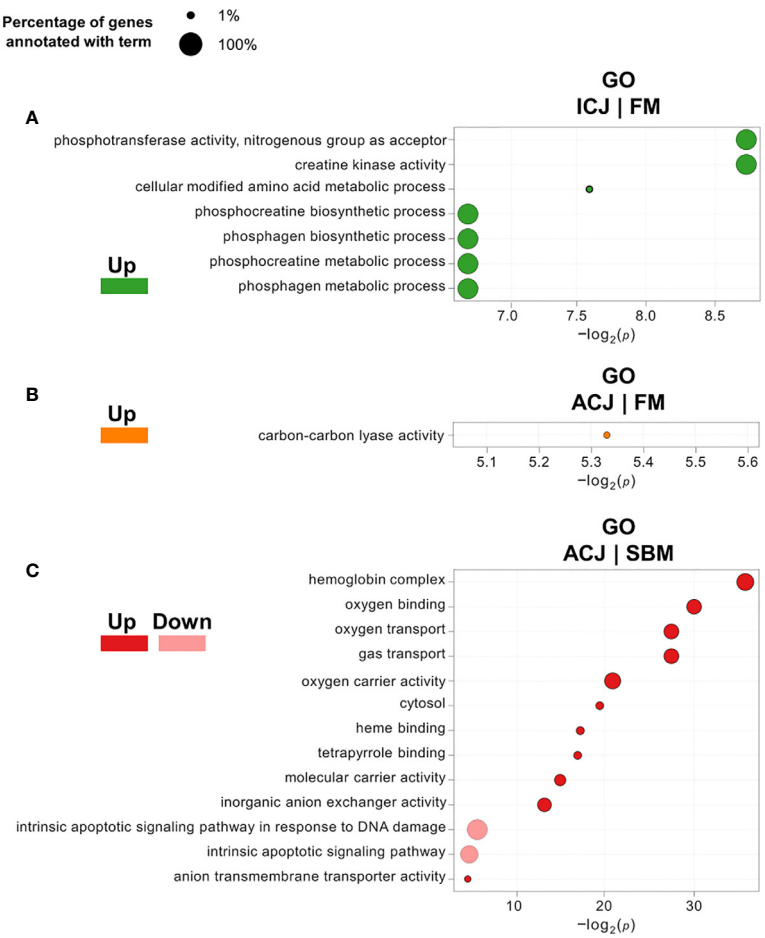

FIGURE 2 | Significantly enriched gene ontology (GO) terms (minGSSize = 3) in spleen of fish fed *C. jadinii* diets compared to control diets (FM and SBM). The list is ordered by -$\log_2(p)$. **(A)** GO terms in ICJ compared to FM. Up, up-regulated (in green). **(B)** GO terms in ACJ compared to FM. Up, up-regulated (in orange). **(C)** GO terms in ACJ compared to SBM. Up, up-regulated (in red); Down, down-regulated (in pink).

positive correlation among FM and ACJ diets (0.64). Correlations between other diets did not show significant results.

DISCUSSION

The proposal to consider the spleen as a target candidate for the characterization of immunomodulatory effects of down-stream processed *C. jadinii* in Atlantic salmon has been based on the fact that in fish the spleen has already been considered as the primordial secondary lymphoid organ and it has a central role in the systemic immune response through the coordination of the innate and adaptive immunity by the antigen presentation process (26). In Atlantic salmon, our results at the transcriptional level have shown that this organ also coordinates aspects related to molecular binding, transporter activity, receptor signalling pathways, cellular and metabolic processes, among others, which have already been described as important functions of the spleen in another salmonid specie such as rainbow trout (42).

On the other hand, from the use of different diets, we were able to detect that fish fed SBM diets, compared to FM, showed a down-regulation of GO and KEGG terms linked to ion binding, peroxisome, metabolic and transport-associated pathways. These results are also similar to those reported in intestine of salmon fed SBM diets. In intestine, in addition to inducing an inflammatory profile, SBM decreases barrier functions through the down-regulation of genes associated with iron-binding proteins, detoxification, transport and metabolic processes (43, 44).

The data also showed that the inclusion of SBM in the diets could induced systemic effects in Atlantic salmon that can be detected in the spleen after 37 days of feeding. Furthermore, the results at the protein level showed that SBM also elicits inflammatory responses in the spleen by increasing the production of cytokines such as TNFα and IFNγ, and inducing the availability of CD83. In higher vertebrates, CD83 is a molecule expressed mainly by mature dendritic cells and acts as an immuno-regulator protein by delivering co-stimulatory signals, which can trigger T helper cell-mediated responses that increase TNFα and IFNγ (45, 46). In fish,

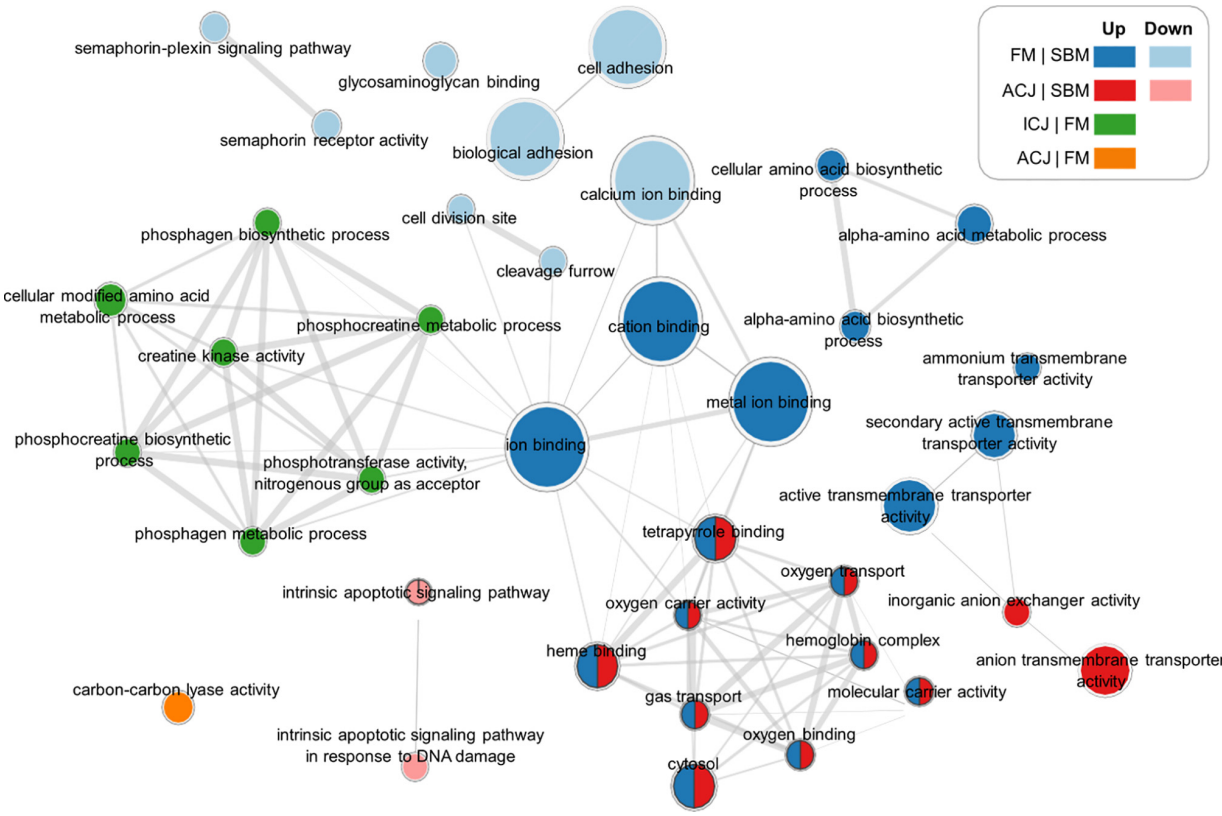

FIGURE 3 | Significant networks of enriched GO terms related to comparisons between different diets. FM|SBM: Up (up-regulated in blue), Down (down-regulated in light blue). ICJ|FM: Up (up-regulated in green). ACJ|FM: Up (up-regulated in orange). ACJ|SBM: Up (up-regulated in red), Down (down-regulated in pink).

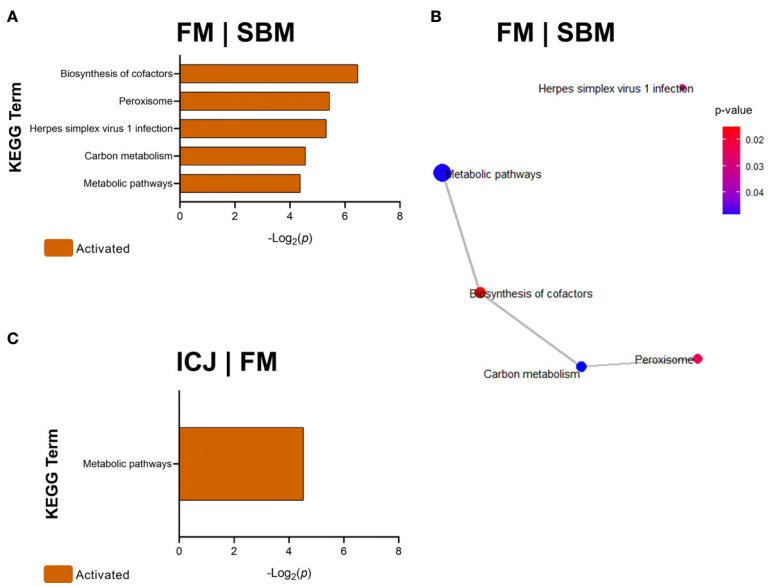

FIGURE 4 | KEGG Pathway Enrichment Analysis of DEGs (minGSSize = 3) from spleen in fish fed FM compared to SBM (FM|SBM) and ICJ compared to FM (ICJ|FM). List ordered by -$Log_2(p)$. **(A)** Significant KEGG terms in FM compared to SBM. **(B)** KEGG network analysis between FM and SBM. **(C)** Significant KEGG terms in ICJ compared to FM.

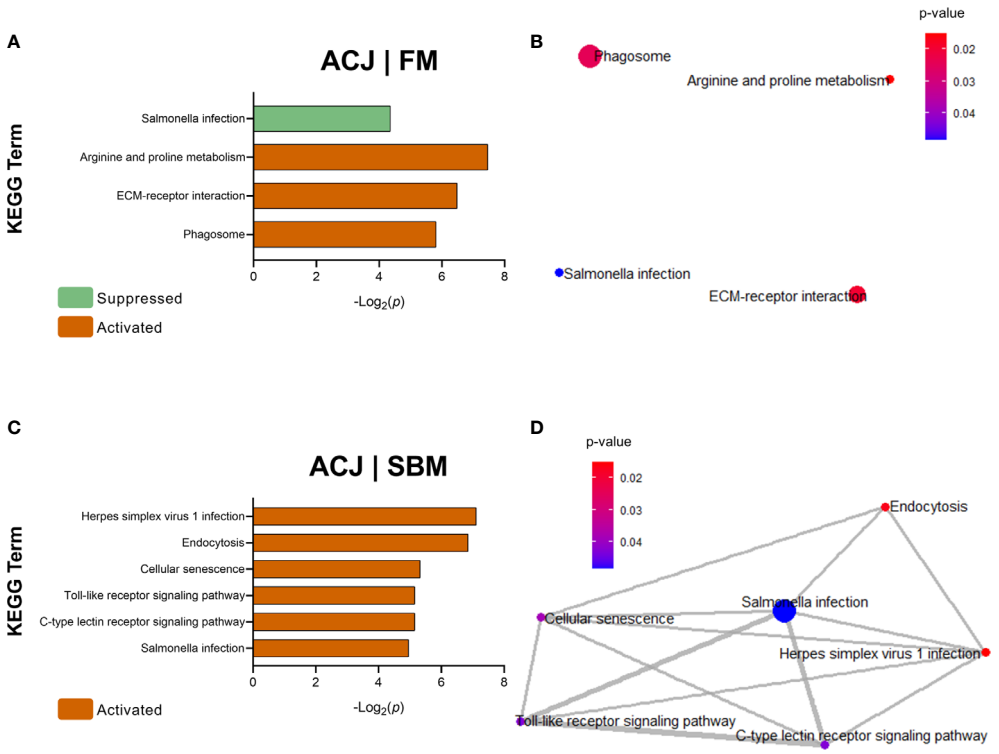

FIGURE 5 | KEGG Pathway Enrichment Analysis of DEGs (minGSSize = 3) from spleen in fish fed ACJ compared to control diets (FM and SBM). In orange: activated pathways, in light green: suppressed pathways. List ordered by -$Log_2(p)$. **(A)** Significant KEGG terms in ACJ compared to FM (ACJ|FM). **(B)** KEGG network analysis between ACJ and FM. **(C)** Significant KEGG terms in ACJ compared to SBM (ACJ|SBM). **(D)** KEGG network analysis between ACJ and SBM.

both cytokines have a key role in the inflammatory process by activating macrophages/phagocytes, thereby enhancing their phagocytic and antimicrobial activity (47).

Regarding the differences between ICJ and ACJ compared to control diets, we hypothesize that the down-stream processing of *C. jadinii* yeasts by autolysis before feed manufacture might explain the observed differences in responses. Different down-stream processes after the yeast is harvested may influence its nutritional value and the accessibility of its cell wall components (16). This could modulate the immune response of Atlantic salmon by exposing fish to different types or amount of MAMP's from *C. jadinii*, such as β-glucan, mannans, chitin and nucleic acids. Inactivated yeasts have already been described as having smooth surfaces without wrinkles, while autolysed yeasts are partially broken and wrinkled, releasing their intracellular content, exposing bioactive components (3, 22), which can be detected by PRRs from the fish, triggering a different immune response (23, 24).

The autolysis process has been reported to modify the nanomechanical properties of the yeast cell wall (without altering its chemical composition), increasing branching and availability of reactive molecules (48). Furthermore, previous works have described the effect of autolysis on the digestibility of yeast in Atlantic salmon, highlighting the importance of down-stream processing when using MI as protein source in feed production (3, 22).

When comparing ACJ with FM, the data showed activated KEGG terms such as phagosome and arginine and proline metabolism. These pathways are connected to the immune response through processes linked to the ability of cells to engulf solid particles to form internal vesicles (49) and with the maintenance of homeostasis, regulating the antioxidant activity in fish (50, 51). On the other hand, the inclusion of inactivated *C. jadinii* in SBM diets did not show marked differences compared to SBM diets. In fact, it seems to maintain a similar inflammatory profile of SBM compared to FM, with increased levels of TNFα and IFNγ. Regarding TNFα, this trend had already been reported in the intestine of Atlantic salmon fed ICJ (3). It is interesting to note that in fish both molecules (TNFα and IFNγ) would be capable of activating M1 macrophages, due to these cytokines can stimulate phagocytosis and the pro-oxidative process to destroy the potential aggressor (52), which would increase the inflammatory pattern of SBM.

On the contrary, the use of ACJ seems to control and regulate the inflammation caused by SBM. When comparing ACJ to SBM, we observed a similar pattern with the one observed among the comparison of FM with SBM. Both showed GO terms associated with molecular binding and transport. Moreover, ACJ was also able to up-regulate KEGG terms associated to endocytosis and signalling pathways of PRRs. We propose that the increase of IL-10 in ACJ contributed to the reduction of the

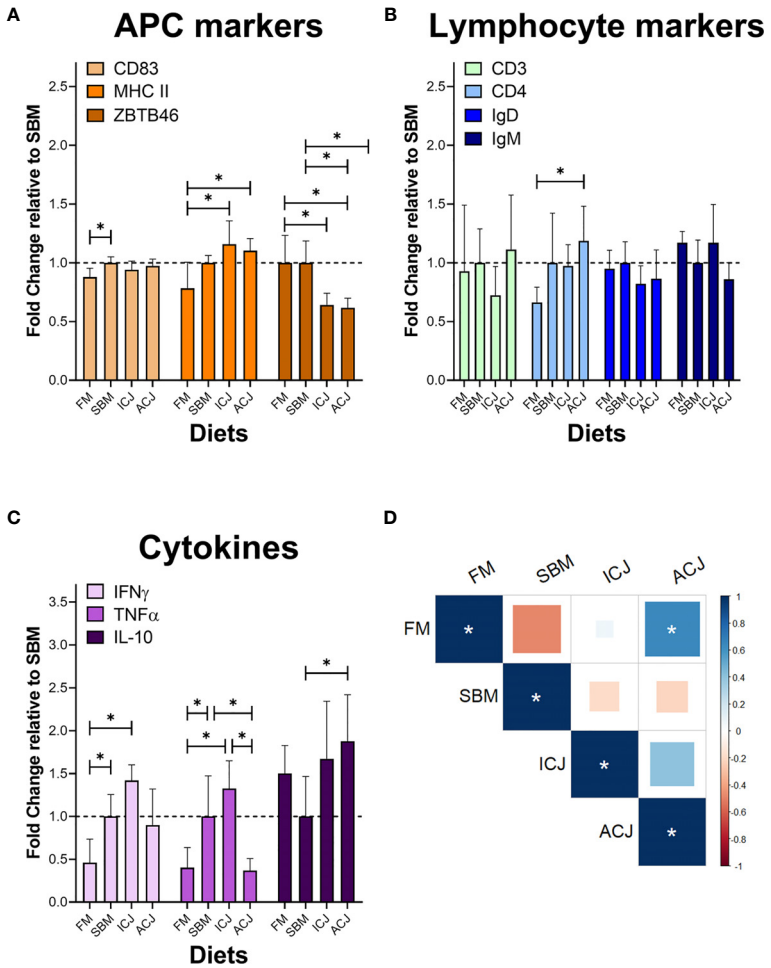

FIGURE 6 | Protein detection of immunological markers in spleen by indirect ELISA. **(A)** Antigen-presenting cell (APC) markers. **(B)** Lymphocyte markers. **(C)** Cytokines. **(D)** Correlation between diets using the data from different immunological markers (Degrees of freedom = 8). In **(A–C)** * shows significant differences among dietary groups ($p < 0.05$). In **(D)** * significant correlation ($p < 0.05$).

inflammatory profile associated with SBM, controlling the production of TNFα. In fish, IL-10 is a cytokine that acts as a suppressor and exerts a conserved role in dampening inflammatory responses (47). Furthermore, the cytokine profile in ACJ suggests a modulation of M1/M2 response, which has been reported as conserved in fish (53). While M1 macrophages increases the robustness of the immune response, M2 macrophages act as repair cells, capable of controlling tissue damage caused by both pathogens and the action of the immune system itself, through a phenotype regulated by molecules such as Transforming growth factor beta (TGFβ) and IL-10 (52, 54).

Additionally, Piazzon et al. (55) have reported that the regulatory activities of IL-10 would not only be associated with immunosuppression and M2 phenotype, but could also be related to the maintenance of memory cells over time. However, further studies must be conducted to better understand this relationship. In our work, ACJ was also able to increase CD4 levels compared to FM, nevertheless, its mechanism of action is not possible to explain with the present results. CD4 is the most characterized marker for T lymphocytes, which govern immune responses through specific antigen recognition and subsequent secretion of effector and regulatory cytokines (37). In rainbow trout, it has been described that cross-talk between activated splenocytes can induce an increase in Forkhead box P3 (FOXP3) (28), which is the transcriptional factor associated with polarization of naive T cells to Treg (56).

The positive correlation observed between FM and ACJ suggest a proportional immune response in these diets, which has also been described in the gut of Atlantic salmon (3). Moreover, in rainbow trout, the inclusion of β-glucans derived from fungi (*Lentinula edodes*) was able to control the acute inflammatory response in the spleen, reducing potential harmful responses for the fish (27).

It is also interesting that fish fed diets with *C. jadinii* showed higher levels of MHC II compared to the FM diet, in addition to a

lower level of ZBTB46 when compare to the FM and SBM diets. MHC II is a protein involved in the antigen-presentation of peptides derived from exogenous proteins to $CD4^+$ T-cells (57). On the other hand, ZBTB46 is a transcriptional factor that inhibits the maturation of APCs in higher vertebrates (58). In salmonids, this molecule has been described in rainbow trout (59). Furthermore, in Atlantic salmon, the modulation of ZBTB46 has been reported in spleen-APCs induced with IFNγ (38). Considering this background, the results in this study suggest an activation of APCs. However, in fish, APCs are still poorly described, and their detection and characterization should be studied deeper in future works to understand their role in the modulation of the immune response by functional diets. Despite this, we propose that the differential activation of APCs in diets with *C. jadinii* compared to SBM (with higher level of CD83, but without other modulated APC markers) would be due to leukocytes from which APCs progress are not a homogeneous subpopulation (38). Moreover, in mammals, APCs could be functional at different stages of maturity, depending on the cytokine environment in which they are found (60, 61).

In summary, we recommend the spleen as a target organ for characterization of immunomodulatory effects of down-stream processed *C. jadinii* in Atlantic salmon exposed to a dietary SBM challenge. Furthermore, our findings contribute to establish a baseline for the study of other novel ingredients that are capable of regulating the immune system of fish, without compromising nutritional parameters. The results from this study suggest that autolysis should be considered when formulating salmon feeds with *C. jadinii* as a functional ingredient with the ability to regulate inflammatory processes.

DATA AVAILABILITY STATEMENT

The datasets presented in this study can be found in online repositories. The names of the repository/repositories and accession number(s) can be found in the article/**Supplementary Material**.

ETHICS STATEMENT

The animal study was reviewed and approved by Norwegian University of Life Sciences in accordance with the institutional and national regulations for control of live animal experiments in Norway.

AUTHOR CONTRIBUTIONS

The study was conceived by BM-L and JOA with key inputs from JØH, LL, and MØ. The experiments and data analysis were performed by BM-L, JOA, and OØ. LM, and LL were in charge of the production and obtaining of antibodies used in this study. The funds for this investigation were acquired by LL, LTM and MØ. BM-L drafted the manuscript with substantial contributions from all other authors. All authors contributed to the article and approved the submitted version.

FUNDING

This study was funded by Foods of Norway a Centre for Research-based Innovation (237841/030) and Trained immunity and nutritional programming for resilient salmon (RCN 294821).

ACKNOWLEDGMENTS

The authors would like to thank Ricardo Tavares Benicio for his skillful help during the feeding experiment. BM-L thanks to the Postdoctoral program from the National Research and Development Agency of Chile (ANID-Chile 74200139).

SUPPLEMENTARY MATERIAL

The Supplementary Material for this article can be found online at: https://www.frontiersin.org/articles/10.3389/fimmu.2021.708747/full#supplementary-material

REFERENCES

1. FAO. *The State of World Fisheries and Aquaculture 2020-Sustainability in Action. Rome* (2020). Available at: http://www.fao.org/3/ca9229en/CA9229EN.pdf (Accessed on 30th of June).
2. Martin SAM, Król E. Nutrigenomics and Immune Function in Fish: New Insights From Omics Technologies. *Dev Comp Immunol* (2017) 75:86–98. doi: 10.1016/j.dci.2017.02.024
3. Agboola JO, Schiavone M, Øverland M, Morales-Lange B, Lagos L, Arntzen MØ, et al. Impact of Down-Stream Processing on Functional Properties of Yeasts and the Implications on Gut Health of Atlantic Salmon (*Salmo Salar*). *Sci Rep* (2021) 11:4496. doi: 10.1038/s41598-021-83764-2
4. Ytrestøyl T, Aas TS, Åsgård T. Utilisation of Feed Resources in Production of Atlantic Salmon *(Salmo Salar*) in Norway. *Aquaculture* (2015) 448:365–74. doi: 10.1016/j.aquaculture.2015.06.023
5. Aas TS, Ytrestøyl T, Åsgård T. Utilization of Feed Resources in the Production of Atlantic Salmon (*Salmo Salar*) in Norway: An Update for 2016. *Aquaculture Rep* (2018) 15:100216. doi: 10.1016/j.aqrep.2019.100216
6. Baeverfjord G, Krogdahl A. Development and Regression of Soybean Meal Induced Enteritis in Atlantic Salmon, *Salmo Salar* L., Distal Intestine: A Comparison With the Intestines of Fasted Fish. *J Fish Dis* (1996) 19:375–87. doi: 10.1046/j.1365-2761.1996.d01-92.x
7. Øverland M, Sørensen M, Storebakken T, Penn M, Krogdahl Å, Skrede A. Pea Protein Concentrate Substituting Fish Meal or Soybean Meal in Diets for Atlantic Salmon (*Salmo Salar*) - Effect on Growth Performance, Nutrient Digestibility, Carcass Composition, Gut Health, and Physical Feed Quality. *Aquaculture* (2009) 288(3-4):305–11. doi: 10.1016/j.aquaculture.2008.12.012
8. Penn MH, Bendiksen EÅ, Campbell P, Krogdahl Å. High Level of Dietary Pea Protein Concentrate Induces Enteropathy in Atlantic Salmon (*Salmo Salar* L.). *Aquaculture* (2011) 310(3-4):267–73. doi: 10.1016/j.aquaculture.2010.10.040
9. De Santis C, Crampton VO, Bicskei B, Tocher DR. Replacement of Dietary Soy- With Air Classified Faba Bean Protein Concentrate Alters the Hepatic Transcriptome in Atlantic Salmon (*Salmo Salar*) Parr. *Comp Biochem Physiol - Part D: Genomics Proteomics* (2015) 16:48–58. doi: 10.1016/j.cbd.2015.07.005
10. Gatlin DM III, Barrows FT, Brown P, Dabrowski K, Gaylord TG, Hardy RW, et al. Expanding the Utilization of Sustainable Plant Products in Aquafeeds: A Review. *Aquaculture Res* (2007) 38:551–79. doi: 10.1111/j.1365-2109.2007.01704.x
11. Booman M, Forster I, Vederas JC, Groman DB, Jones SRM. Soybean Meal-Induced Enteritis in Atlantic Salmon (*Salmo Salar*) and Chinook Salmon

(*Oncorhynchus Tshawytscha*) But Not in Pink Salmon (O. Gorbuscha). *Aquaculture* (2018) 483:238–43. doi: 10.1016/j.aquaculture.2017.10.025
12. Egerton S, Wan A, Murphy K, Collins F, Ahern G, Sugrue I, et al. Replacing Fishmeal With Plant Protein in Atlantic Salmon (*Salmo Salar*) Diets by Supplementation With Fish Protein Hydrolysate. *Sci Rep* (2020) 10:4194. doi: 10.1038/s41598-020-60325-7
13. Djordjevic B, Morales-Lange B, Øverland M, Mercado L, Lagos L. Immune and Proteomic Responses to the Soybean Meal Diet in Skin and Intestine Mucus of Atlantic Salmon (*Salmo Salar* L.). *Aquaculture Nutr* (2021) 27:929–40. doi: 10.1111/anu.13248
14. Sørensen SL, Park Y, Gong Y, Vasanth GK, Dahle D, Korsnes K, et al. Nutrient Digestibility, Growth, Mucosal Barrier Status, and Activity of Leucocytes From Head Kidney of Atlantic Salmon Fed Marine- or Plant-Derived Protein and Lipid Sources. *Front Immunol* (2021) 11:623726. doi: 10.3389/fimmu.2020.623726
15. Van den Ingh TSGAM, Krogdahl Å, Olli JJ, Hendriks HGCJM, Koninkx JGJF. Effects of Soybean-Containing Diets on the Proximal and Distal Intestine in Atlantic Salmon (*Salmo Salar*): A Morphological Study. *Aquaculture* (1991) 94(4):297–305. doi: 10.1016/0044-8486(91)90174-6
16. Øverland M, Skrede A. Yeast Derived From Lignocellulosic Biomass as a Sustainable Feed Resource for Use in Aquaculture. *J Sci Food Agric* (2017) 97 (3):733–42. doi: 10.1002/jsfa.8007
17. Glencross BD, Baily J, Berntssen MH, Hardy R, MacKenzie S, Tocher DR. Risk Assessment of the Use of Alternative Animal and Plant Raw Material Resources in Aquaculture Feeds. *Rev Aquaculture* (2020) 12:703–58. doi: 10.1111/raq.12347
18. Øverland M, Karlsson A, Mydland LT, Romarheim OH, Skrede A. Evaluation of *Candida Utilis*, *Kluyveromyces Marxianus* and *Saccharomyces Cerevisiae* Yeasts as Protein Sources in Diets for Atlantic Salmon (*Salmo Salar*). *Aquaculture* (2013) 402-403:1–7. doi: 10.1016/j.aquaculture.2013.03.016
19. Grammes F, Reveco FE, Romarheim OH, Landsverk T, Mydland LT, Øverland M. *Candida Utilis* and *Chlorella Vulgaris* Counteract Intestinal Inflammation in Atlantic Salmon (*Salmo Salar* L.). *PloS One* (2013) 8(12): e83213. doi: 10.1371/journal.pone.0083213
20. Vidakovic A, Langeland M, Sundh H, Sundell K, Olstorpe M, Vielma J, et al. Evaluation of Growth Performance and Intestinal Barrier Function in Arctic Charr (*Salvelinus Alpinus*) Fed Yeast (*Saccharomyces Cerevisiae*), Fungi (*Rhizopus Oryzae*) and Blue Mussel (*Mytilus Edulis*). *Aquaculture Nutr* (2016) 22:1348–60. doi: 10.1111/anu.12344
21. Sahlmann C, Djordjevic B, Lagos L, Mydland LT, Morales-Lange B, Hansen JØ, et al. Yeast as a Protein Source During Smoltification of Atlantic Salmon (*Salmo Salar* L.), Enhances Performance and Modulates Health. *Aquaculture* (2019) 513:734396. doi: 10.1016/j.aquaculture.2019.734396
22. Hansen JØ, Lagos L, Lei P, Reveco-Urzua FE, Morales-Lange B, Hansen LD, et al. Down-Stream Processing of Baker's Yeast (*Saccharomyces Cerevisiae*): Effect on Nutrient Digestibility and Immune Response in Atlantic Salmon (*Salmo Salar*). *Aquaculture* (2021) 530:1–10. doi: 10.1016/j.aquaculture.2020.735707
23. Gomez D, Sunyer JO, Salinas I. The Mucosal Immune System of Fish: The Evolution of Tolerating Commensals While Fighting Pathogens. *Fish Shellfish Immunol* (2013) 35(6):1729–39. doi: 10.1016/j.fsi.2013.09.032
24. Li Y, Li Y, Cao X, Jin X, Jin T. Pattern Recognition Receptors in Zebrafish Provide Functional and Evolutionary Insight Into Innate Immune Signaling Pathways. *Cell Mol Immunol* (2017) 14(1):80–9. doi: 10.1038/cmi.2016.50
25. Lugo-Villarino G, Balla KM, Stachura DL, Banuelos K, Werneck MB, Traver D. Identification of Dendritic Antigen-Presenting Cells in the Zebrafish. *Proc Natl Acad Sci* (2010) 107:15850–55. doi: 10.1073/pnas.1000494107
26. Neely HR, Flajnik MF. Emergence and Evolution of Secondary Lymphoid Organs. *Annu Rev Cell Dev Biol* (2016) 32:693–711. doi: 10.1146/annurev-cellbio-111315-125306
27. Djordjevic B, Skugor S, Jørgensen SM, Overland M, Mydland LT, Krasnov A. Modulation of Splenic Immune Responses to Bacterial Lipopolysaccharide in Rainbow Trout (*Oncorhynchus Mykiss*) Fed Lentinan, a Beta-Glucan From Mushroom Lentinula Edodes. *Fish Shellfish Immunol* (2009) 26(2):201–9. doi: 10.1016/j.fsi.2008.10.012
28. Morales-Lange B, Nombela I, Ortega-Villaizán MDM, Imarai M, Schmitt P, Mercado L. Induction of Foxp3 During the Crosstalk Between Antigen Presenting Like-Cells MHCII^{+}CD83^{+} and Splenocytes CD4^{+}IgM^{-} in Rainbow Trout. *Biology* (2021) 10:324. doi: 10.3390/biology10040324
29. Lapeña D, Olsen PM, Arntzen MØ, Kosa G, Passoth V, Eijsink VGH, et al. Spruce Sugars and Poultry Hydrolysate as Growth Medium in Repeated Fed-Batch Fermentation Processes for Production of Yeast Biomass. *Bioprocess Biosyst Eng* (2020) 43(4):723–36. doi: 10.1007/s00449-019-02271-x
30. National Research Council NRC. *Nutrient Requirements of Fish and Shrimp*. Washington, DC: The National Academies Press (2011). doi: 10.17226/13039
31. Håkenåsen IM, Øverland M, Ånestad R, Åkesson CP, Sundaram AYM, McLean Press C, et al. Gene Expression and Gastrointestinal Function Is Altered in Piglet Small Intestine by Weaning and Inclusion of *Cyberlindnera Jadinii* Yeast as a Protein Source. *J Funct Foods* (2020) 73:104118. doi: 10.1016/j.jff.2020.104118
32. Raudvere U, Kolberg L, Kuzmin I, Arak T, Adler P, Peterson H, et al. G: Profiler: A Web Server for Functional Enrichment Analysis and Conversions of Gene Lists (2019 Update). *Nucleic Acids Res* (2019) 47(W1):W191–8. doi: 10.1093/nar/gkz369
33. Merico D, Isserlin R, Stueker O, Emili A, Bader GD. Enrichment Map: A Network-Based Method for Gene-Set Enrichment Visualization and Interpretation. *PloS One* (2010) 5(11):e13984. doi: 10.1371/journal.pone.0013984
34. Shannon P, Markiel A, Ozier O, Baliga NS, Wang JT, Ramage D, et al. Cytoscape: A Software Environment for Integrated Models of Biomolecular Interaction Networks. *Genome Res* (2003) 13(11):2498–504. doi: 10.1101/gr.1239303
35. Morales-Lange B, González-Aravena M, Font A, Guzmán F, Mercado L. Detection of Peroxiredoxin-Like Protein in Antarctic Sea Urchin (*Sterechinus Neumayeri*) Under Heat Stress and Induced With Pathogen-Associated Molecular Pattern From Vibrio Anguillarum. *Polar Biol* (2018) 41:2065–73. doi: 10.1007/s00300-018-2346-x
36. Boardman T, Warner C, Ramirez-Gomez F, Matrisciano J, Bromage E. Characterization of an Anti-Rainbow Trout (*Oncorhynchus Mykiss*) CD3ε Monoclonal Antibody. *Veterinary Immunol Immunopathol* (2012) 145(1-2):511–5. doi: 10.1016/j.vetimm.2011.11.017
37. Maisey K, Montero R, Corripio-Miyar Y, Toro-Ascuy D, Valenzuela B, Reyes-Cerpa S, et al. Isolation and Characterization of Salmonid CD4^{+} T Cells. *J Immunol* (2016) 196(10):4150–63. doi: 10.4049/jimmunol.1500439
38. Morales-Lange B, Ramírez F, Schmitt P, Guzmán F, Lagos L, Øverland M, et al. Interferon Gamma Induces the Increase of Cell-Surface Markers (CD80/86, CD83 and MHC-II) in Splenocytes From Atlantic Salmon. *Front Immunol* (2021) 12:666356. doi: 10.3389/fimmu.2021.666356
39. Weththasinghe P, Lagos L, Cortés M, Hansen JØ, Øverland M. Dietary Inclusion of Black Soldier Fly (*Hermetia Illucens*) Larvae Meal and Paste Improved Gut Health But Had Minor Effects on Skin Mucus Proteome and Immune Response in Atlantic Salmon (*Salmo Salar*). *Front Immunol* (2021) 12:599530. doi: 10.3389/fimmu.2021.599530
40. Djordjevic B, Morales-Lange B, McLean Press C, Olson J, Lagos L, Mercado L, et al. Comparison of Circulating Markers and Mucosal Immune Parameters From Skin and Distal Intestine of Atlantic Salmon in Two Models of Acute Stress. *Int J Mol Sci* (2021) 22(3):1028. doi: 10.3390/ijms22031028
41. Wei T, Simko V. *R Package "Corrplot": Visualization of a Correlation Matrix (Version 0.84)* (2017). Available at: https://github.com/taiyun/corrplot.
42. Ali A, Rexroad CE, Thorgaard GH, Yao J, Salem M. Characterization of the Rainbow Trout Spleen Transcriptome and Identification of Immune-Related Genes. *Front Genet* (2014) 5:348. doi: 10.3389/fgene.2014.00348
43. Martin SAM, Dehler CE, Król E. Transcriptomic Responses in the Fish Intestine. *Dev Comp Immunol* (2016) 64:103–17. doi: 10.1016/j.dci.2016.03.014
44. Kiron V, Park Y, Siriyappagouder P, Dahle D, Vasanth GK, Dias J, et al. Intestinal Transcriptome Analysis Reveals Soy Derivative-Linked Changes in Atlantic Salmon. *Front Immunol* (2020) 11:596514. doi: 10.3389/fimmu.2020.596514
45. Aerts-Toegaert C, Heirman C, Tuyaerts S, Corthals J, Aerts JL, Bonehill A, et al. CD83 Expression on Dendritic Cells and T Cells: Correlation With Effective Immune Responses. *Eur J Immunol* (2007) 37:686–95. doi: 10.1002/eji.200636535
46. Chong SZ, Wong KL, Lin G, Yang CM, Wong SC, Angeli V, et al. Human CD8^{+} T Cells Drive Th1 Responses Through the Differentiation of TNF/iNOS-Producing Dendritic Cells. *Eur J Immunol* (2011) 41(6):1639–51. doi: 10.1002/eji.201041022
47. Zou J, Secombes CJ. The Function of Fish Cytokines. *Biology* (2016) 5(2):23. doi: 10.3390/biology5020023
48. Schiavone M, Sieczkowski N, Castex M, Dague E, Marie François J. Effects of the Strain Background and Autolysis Process on the Composition and Biophysical Properties of the Cell Wall From Two Different Industrial Yeasts. *FEMS Yeast Res* (2015) 15(2):fou012. doi: 10.1093/femsyr/fou012

49. Esteban MÁ, Cuesta A, Chaves-Pozo E, Meseguer J. Phagocytosis in Teleosts. Implications of the New Cells Involved. *Biology* (2015) 4(4):907–22. doi: 10.3390/biology4040907
50. Li HT, Feng L, Jiang WD, Liu Y, Jiang J, Li SH, et al. Oxidative Stress Parameters and Anti-Apoptotic Response to Hydroxyl Radicals in Fish Erythrocytes: Protective Effects of Glutamine, Alanine, Citrulline and Proline. *Aquat Toxicol* (2013) 126:169–79. doi: 10.1016/j.aquatox.2012.11.005
51. Hoseini SM, Ahmad Khan M, Yousefi M. Costas B. Roles of Arginine in Fish Nutrition and Health: Insights for Future Researches. *Rev Aquaculture* (2020) 12:2091–108. doi: 10.1111/raq.12424
52. Grayfer L, Kerimoglu B, Yaparla A, Hodgkinson JW, Xie J, Belosevic M. Mechanisms of Fish Macrophage Antimicrobial Immunity. *Front Immunol* (2018) 9:110. doi: 10.3389/fimmu.2018.0110
53. Wiegertjes GF, Wentzel AS, Spaink HP, Elks PM, Fink IR. Polarization of Immune Responses in Fish: The "Macrophages First" Point of View. *Mol Immunol* (2016) 69:146–56. doi: 10.1016/j.molimm.2015.09.026
54. Wentzel AS, Petit J, van Veen WG, Fink IR, Scheer MH, Piazzon MC, et al. Transcriptome Sequencing Supports a Conservation of Macrophage Polarization in Fish. *Sci Rep* (2020) 10:13470. doi: 10.1038/s41598-020-70248-y
55. Piazzon MC, Savelkoul HS, Pietretti D, Wiegertjes GF, Forlenza M. Carp Il10 Has Anti-Inflammatory Activities on Phagocytes, Promotes Proliferation of Memory T Cells, and Regulates B Cell Differentiation and Antibody Secretion. *J Immunol* (2015) 194(1):187–99. doi: 10.4049/jimmunol.1402093
56. Wang T, Secombes CJ. The Cytokine Networks of Adaptive Immunity in Fish. *Fish Shellfish Immunol* (2013) 35(6):1703–18. doi: 10.1016/j.fsi.2013.08.030
57. Grimholt U. MHC and Evolution in Teleosts. *Biology* (2016) 5(1):6. doi: 10.3390/biology5010006
58. Wang J, Wang T, Benedicenti O, Collins C, Wang K, Secombes CJ, et al. Characterisation of ZBTB46 and DC-SCRIPT/ZNF366 in Rainbow Trout, Transcription Factors Potentially Involved in Dendritic Cell Maturation and Activation in Fish. *Dev Comp Immunol* (2018) 80:2–14. doi: 10.1016/j.dci.2016.11.007
59. Wang Y, Sun HY, Kumar S, Puerta MDM, Jo H, Rezvan A. ZBTB46 Is a Shear-Sensitive Transcription Factor Inhibiting Endothelial Cell Proliferation *via* Gene Expression Regulation of Cell Cycle Proteins. *Lab Invest* (2019) 99:305–18. doi: 10.1038/s41374-018-0060-5
60. Crespo HJ, Lau JTY, Videira PA. Dendritic Cells: A Spot on Sialic Acid. *Front Immunol* (2013) 4:491. doi: 10.3389/fimmu.2013.00491
61. Kim MK, Kim J. Properties of Immature and Mature Dendritic Cells: Phenotype, Morphology, Phagocytosis, and Migration. *RSC Adv* (2019) 9 (20):11230–8. doi: 10.1039/c9ra00818g

Conflict of Interest: The authors declare that the research was conducted in the absence of any commercial or financial relationships that could be construed as a potential conflict of interest.

Publisher's Note: All claims expressed in this article are solely those of the authors and do not necessarily represent those of their affiliated organizations, or those of the publisher, the editors and the reviewers. Any product that may be evaluated in this article, or claim that may be made by its manufacturer, is not guaranteed or endorsed by the publisher.

frontiers in Immunology

ORIGINAL RESEARCH
published: 14 October 2021
doi: 10.3389/fimmu.2021.742827

Vaccination of Gilthead Seabream After Continuous Xenoestrogen Oral Exposure Enhances the Gut Endobolome and Immune Status *via* GPER1

Pablo Castejón[1†], Isabel Cabas[1†], Victoria Gómez[1], Elena Chaves-Pozo[2], Isabel Cerezo-Ortega[3], Miguel Ángel Moriñigo[3], Eduardo Martínez-Manzanares[3], Jorge Galindo-Villegas[4‡] and Alfonsa García-Ayala[1‡]*

[1] Department of Cell Biology and Histology, Regional Campus of International Excellence "Campus Mare Nostrum", University of Murcia, Instituto Murciano de Investigacion Biosanitaria (IMIB), Centro de Investigacion Biomedica en Red Enfermedades Raras (CIBERER), Murcia, Spain, [2] Aquaculture Department, Oceanographic Center of Murcia, Spanish Institute of Oceanography (IEO-CSIC), Murcia, Spain, [3] Department of Microbiology, Faculty of Sciences, University of Malaga, Málaga, Spain, [4] Faculty of Biosciences and Aquaculture, Nord University, Bodø, Norway

OPEN ACCESS

Edited by:
Uwe Fischer, Friedrich-Loeffler-Institute, Germany

Reviewed by:
Magdalena Chadzińska, Jagiellonian University, Poland
Lluis Tort, Universitat Autònoma de Barcelona, Spain

***Correspondence:**
Jorge Galindo-Villegas
jorge.galindo-villegas@nord.no

[†]These authors have contributed equally to this work

[‡]These authors have contributed equally to this work

Specialty section:
This article was submitted to Comparative Immunology, a section of the journal Frontiers in Immunology

Received: *16 July 2021*
Accepted: *15 September 2021*
Published: *14 October 2021*

Citation:
Castejón P, Cabas I, Gómez V, Chaves-Pozo E, Cerezo-Ortega I, Moriñigo MÁ, Martínez-Manzanares E, Galindo-Villegas J and García-Ayala A (2021) Vaccination of Gilthead Seabream After Continuous Xenoestrogen Oral Exposure Enhances the Gut Endobolome and Immune Status via GPER1. Front. Immunol. 12:742827. doi: 10.3389/fimmu.2021.742827

In fish culture settings, the exogenous input of steroids is a matter of concern. Recently, we unveiled that in the gilthead seabream (*Sparus aurata*), the G protein-coupled estrogen receptor agonist G-1 (G1) and the endocrine disruptor 17α-ethinylestradiol (EE_2) are potent modulators in polyreactive antibody production. However, the integral role of the microbiota upon immunity and antibody processing in response to the effect of EE_2 remains largely unexplored. Here, juvenile seabreams continuously exposed for 84 days to oral G1 or EE_2 mixed in the fish food were intraperitoneally (i.p.) immune primed on day 42 with the model antigen keyhole limpet hemocyanin (KLH). A critical panel of systemic and mucosal immune markers, serum VTG, and humoral, enzymatic, and bacteriolytic activities were recorded and correlated with gut bacterial metagenomic analysis 1 day post-priming (dpp). Besides, at 15 dpp, animals received a boost to investigate the possible generation of specific anti-KLH antibodies at the systemic and mucosal interphases by the end of the trial. On day 43, EE_2 but not G1 induced a significant shift in the serum VTG level of naive fish. Simultaneously, significant changes in some immune enzymatic activities in the serum and gut mucus of the EE_2-treated group were recorded. In comparison, the vaccine priming immunization resulted in an attenuated profile of most enzymatic activities in the same group. The gut genes qPCR analysis exhibited a related pattern, only emphasized by a significant shift in the EE_2 group's *il1b* expression. The gut bacterial microbiome status underwent 16S rRNA dynamic changes in alpha diversity indices, only with the exposure to oral G1, supporting functional alterations on cellular processes, signaling, and lipid metabolism in the microbiota. By the same token, the immunization elevated the relative abundance of *Fusobacteria* only in the control group, while this phylum was depleted in both the treated groups. Remarkably, the immunization also promoted changes in the bacterial class

Betaproteobacteria and the estrogen-associated genus *Novosphingobium*. Furthermore, systemic and mucosal KLH-specific immunoglobulin (Ig)M and IgT levels in the fully vaccinated fish showed only slight changes 84 days post-estrogenic oral administration. In summary, our results highlight the intrinsic relationship among estrogens, their associated receptors, and immunization in the ubiquitous fish immune regulation and the subtle but significant crosstalk with the gut endobolome.

Keywords: 16S rRNA, endocrine disruptors (EDCs), endobolome, estrogens, fish, G protein-coupled receptor 1, vaccination, vitellogenin (VTG)

INTRODUCTION

The endocrine system of multicellular organisms comprises secretory glands that release hormones that can regulate signal transduction pathways with exquisite specificity upon paracrine engagement with a specific cognate receptor in the target cells. These interactions lead to the modulation of a vast set of functions, including but not limited to energy balance metabolism, body weight regulation, growth development, reproduction, and immunity (1, 2). Alterations of the natural endocrine hormonal homeostatic balance eventually occur through the exposure to environmental single or mixed synthetic chemical pollutants exhibiting hormone-mimetic activities, collectively regarded as endocrine disruptor compounds (EDCs) (3, 4). However, endocrine disruption is not considered a toxicological endpoint *per se* but a functional change that may lead to adverse effects in the organism.

Estrogen plays an essential role in regulating immune responses through innate immune signaling modulation and the impairment of B-cell functions (5, 6). The natural estrogenic steroid 17β-estradiol (E_2) and the xenoestrogen, the synthetic oral contraceptive 17α-ethinylestradiol (EE_2), are two EDCs generally present in wastewaters that adversely affect aquatic organism and human health (7). The estrogenic ligands or compounds exert their canonical biological processes *via* the intracellular nuclear estrogen receptors (ERs) acting as the ligand-activated transcription factor, which binds to the estrogen-responsive element located within the promoter region of target genes (8). However, they can also rapidly activate transduction pathways *via* non-genomic mechanisms mediated by a membrane-anchored receptor called the G protein-coupled estrogen receptor 1 (GPER1) (9). Accumulating evidence indicates that both ERs and GPER1 mediates feedback loops or crosstalk among several complex signaling axes like the insulin-like growth factor-1 receptor/phosphatidylinositol 3-kinase–threonine protein kinase B–mammalian target of rapamycin (IGF-1R/PI_3K–Akt–mTOR) (10), epidermal growth factor receptor/extracellular signal-regulated kinase 1/2 (EGFR/ERK1/2) (11), cyclic adenosine monophosphate/protein kinase A (cAMP/PKA) (12), reactive oxygen species/calcium-apoptosis signal-regulating kinase 1-c-Jun N-terminal kinase (ROS/Ca_2^+ – ASK1 – JNK) (13), interferon (IFN), or the apoptotic pathway (14). Therefore, to examine the influences of particular EDCs and distinguish GPER1-mediated estrogen action from the classic ER activation, a nonsteroidal, high-affinity, and selective GPER1 agonist G-1 (G1) was developed (15, 16).

As most vertebrates, teleost fish are subjected to developmental immunologic programming triggered by the action of diverse microbiota inhabiting the surrounding environment (17–19). Particularly, growing evidence sheds light on the profound impact that some bacteria have in the gut and *vice versa* on the modulation of many long-lasting biological processes and functions, such as metabolism, inflammation, immune, and stress responses (20–25). Besides, it has been acknowledged that endogenous steroid hormones and EDCs interact with the gut microbiota through different pathways (26). By combining a myriad of previous findings, two novel concepts were recently coined. Estrobolome refers to the enteric bacterial species possessing β-glucuronidase and β-glucosidase enzymes involved in the deconjugation of endogenous estrogen at the gut level (27, 28). Furthermore, the expanded term endobolome includes the gut microbiota that can metabolize also the synthetic EE_2 (29).

Our former studies on the role of sex steroids in teleost fish immunity revealed that gilthead seabream (*Sparus aurata*) leukocytes express nuclear ERs and GPER1. GPER1 modulates leukocyte functions through a cAMP/protein kinase A/CREB signaling pathway (30, 31). We also provided evidence that EDCs altered the immune response by promoting long-lasting effects even when their disruptive estrogenic effects were not present (32, 33). Moreover, EE_2 bath-exposed specimens have an altered capacity to respond to an immune challenge, even though the compound does not behave as an immunosuppressor. Simultaneously, the oral intake of the same compound may stimulate antibody response and promote the extended production of natural neutralizing antibodies mediated through GPER1 (34). In addition, efforts on understanding the effect of keyhole limpet hemocyanin (KLH) as an immunogenic protein antigen model in gilthead seabream under diverse scenarios have been extensively conducted (32, 35, 36). Nevertheless, the impact of oral EE_2 exposure following a vaccination scheme targeting the adaptive immunity and relying on the generation of better and stronger responses after a primary immunization on the gilthead seabream-associated microbiome has never been explored before.

Therefore, this study aimed to investigate, *in vivo*, the effects resulting from supplementing the diet with exogenous EE_2 and the agonist G1 in the gilthead seabream. Specifically, changes in

the innate immune response were determined by quantifying the activity of humoral lytic and oxidative stress mediators. This study measured essential mucosal inflammatory marker genes, observed how goblet cells contribute to immunity at the gut mucosal surface, explored the microbiome landscape on the immune repertoire following priming immunization with KLH, and assessed the specific long-term systemic and mucosal antibody production under the proposed scheme. In summary, the results highlighted the intrinsic relationship between xenoestrogens and their associated receptors in the ubiquitous fish immune regulation, and the subtle but significant crosstalk with the fish gut endobolome is described here for the first time.

MATERIALS AND METHODS

Fish and Trial Setup

Ninety-six healthy juvenile European gilthead seabreams (*S. aurata*) were obtained from the Oceanographic Center of Murcia (Mazarrón, Spain). The fish were randomly divided into three treatment groups (n = 32 fish/treatment), and subsequently, each group was redistributed into a replicate tank. The animals were stocked in fiber-reinforced plastic tanks of 200 L at the same facility where they were obtained and provided with running seawater (dissolved oxygen 6 ppm) with continuous water renewal (flow rate 20% aquarium vol/h) and under natural temperature (21.0°C ± 3.0°C) and photoperiod. Before the start of the trial, the fish underwent a period of acclimatization of 2 weeks. The fish were fed thrice daily with a commercial pellet diet (44% protein and 22% lipids: Skretting) until apparent satiation. The environmental parameters, mortality, and behavioral changes were recorded daily.

Experimental Design

Following the acclimatization period, the fish were maintained by feeding on the basal (control) or supplemented diets (G1 or EE_2) for 3 months continuously. Briefly, 98% pure EE_2 (Sigma-Aldrich) or G1 (Tocris) was supplemented on the commercial feed at a single dose of 5 µg/g food using the ethanol evaporation method (0.3 L EtOH/kg of food), as described elsewhere (38). To evaluate the effect of G1 and EE_2 under an immunization program, specimens were intraperitoneally (i.p.) primed and 15 days later boosted with a model vaccine containing KLH (100 µg/fish; Sigma-Aldrich) and Imject Alum adjuvant (4 mg/fish; Thermo Scientific) (vaccinated/immunized fish) or phosphate-buffered saline (PBS) (unvaccinated fish) at 42 and 56 days of treatment. Please note that we have previously reported that Imject alum enhances the specific antibody levels to the model antigen KLH in gilthead seabream (35, 39). Strikingly, however, Imject alone fails to promote mature *il1b* release or enhance specific antibody levels compared to the complete KLH model vaccine. Therefore, the KLH- or alum-only groups were omitted to optimize economic resources on sequencing in the present experimental setting.

Sample Collection

As described in **Figure 1**, complete sets of samples were obtained 1 day post-priming (dpp) and 28 days post-booster coincident with the end of the trial on day 84. Prior to the sample collection, the fish were fasted for 24 h. Briefly, six specimens per treatment (three fish from each duplicated tank) and sampling point were sacrificed in less than 1 min through anesthetic (clove oil) overdose, and blood was collected from the caudal vein with 25- G needles attached to 2-ml syringe (40). The blood samples were allowed to clot for 1 h at room temperature, centrifuged (10,000g for 10 min), and the sera were collected and stored at -80°C until analysis. Meanwhile, the total gut mucus samples were collected using a sterile cell scraper and centrifuged at 3,000 for 1 min at 4°C to remove cells and debris. To separate bacteria from mucus, the cell-free supernatant was thereafter centrifuged at 10,000g for 10 min. The resulting supernatants were filtered through a 0.45-µm filter in order to detect the antibodies unbound to bacteria as explained elsewhere (41). In addition, the head-kidney and gut tissue samples free of fecal contents were also collected following standard aseptic procedures. Half of each sample obtained was immediately stabilized and protected from degradation by immersing it in 1.5-ml Eppendorf tubes prefilled with 1 ml of RNAlater solution (Thermo Fisher), while the other half was subjected to histological procedures as detailed further.

Determination of Serum Vitellogenin Levels

The serum vitellogenin (VTG) levels were quantified by an enzyme-linked immunosorbent assay (ELISA) using a commercial kit (Cayman Chemical), following the manufacturer's instructions, as previously described (34). In brief, an aliquot of 1:500 diluted serum from both the control and EE_2- or G1-treated fish (n = 6 fish/treatment) was added to a flat-bottomed 96-well plate, followed by a commercial polyclonal antibody against gilthead seabream VTG and an anti-rabbit immunoglobulin (Ig)G peroxidase (Sigma-Aldrich), both diluted at 1:1,000 and incubated at 25°C for 1 h. Finally, the chromogen tetramethylbenzidine (TMB) was added, and the absorbance was read at 450 nm using a SPECTROstart nano (BGM; LabTechnologies).

Detection of Serum and Gut Mucus Humoral Immune Parameters

Peroxidase activity was determined according to a previously described and adapted protocol for fish (42). One unit was defined as the amount of activity producing an absorbance change of 1, and the data were expressed as a fold increase relative to the mean of untreated and unvaccinated fish.

Antiprotease activity was determined by serum or gut mucus ability to inhibit the hydrolysis of azocasein by proteinase K activity (2 mg/ml) as previously suggested (43). The percentage of inhibition of proteinase K activity for each sample was calculated as [100- (% of protease activity)]. Results were expressed as a fold increase relative to the mean of untreated and unvaccinated fish.

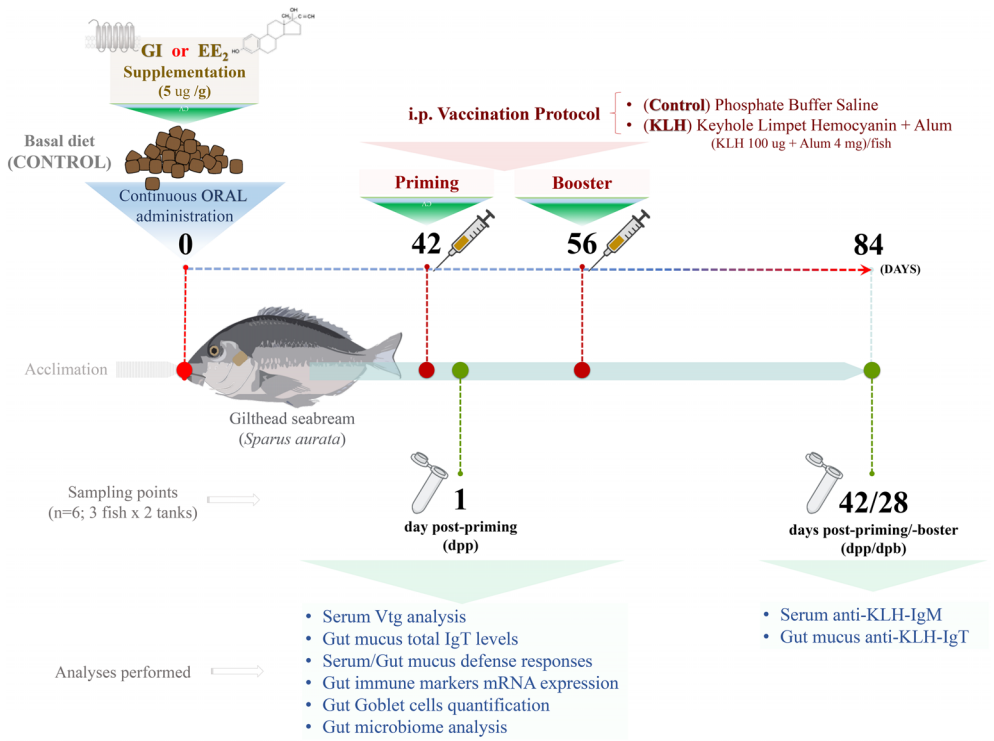

FIGURE 1 | Experimental setup. From day 0, control or supplemented diet with G1 or EE2, orally administered daily within 84 days (12 weeks) to gilthead seabream. After 6 weeks, on day 42, half of the animals from each group were immune primed and boosted 15 days later (8 weeks) by intraperitoneal injections (i.p.) with repeated doses of the model vaccine containing KLH as antigen. The analyses in the list were conducted at 1 and 42 days after receiving the priming immunization (6 and 12 weeks, respectively). N=6; three fish from each duplicated tank per treatment.

Lysozyme activity was measured using a previously described protocol (35). Briefly, the enzyme activity was quantified according to a turbidimetric method that uses the lysis of *Micrococcus lysodeiticus* ATCC No. 4698 (Sigma-Aldrich) with hen egg-white lysozyme as the standard. One unit of lysozyme activity was defined as a reduction in absorbance at 450 nm of 0.001/min. Results were expressed as the fold increase relative to the mean of untreated and unvaccinated fish.

Bactericidal activity was assessed by evaluating their effects on the bacterial growth of *Vibrio harveyi* curves as described elsewhere (44). The pathogenic marine bacteria *V. harveyi* (strain Lg 16/100) was grown and cultured as previously described (45). Results were corrected with the absorbance measured in each sample at the initial time point and expressed as a fold increase relative to the mean of untreated and unvaccinated fish.

Determination of IgM-Specific Antibody Levels

The hemocyanin-specific IgM level was determined by an ELISA kit (Aquatic Diagnostic, Ltd.) as previously described (35). Briefly, PBS as blank or fish sera from naive, hemocyanin-immunized, or pre-immune animals as control diluted 1:100 were added to the hemocyanin precoated 96-well ELISA plates, followed by the monoclonal antibody anti-seabream IgM at 1:1,000. Then, an anti-mouse IgG peroxidase antibody produced in goat (Sigma-Aldrich) diluted 1:1,000 was included as a reporter. Finally, the chromogen TMB (Sigma-Aldrich) was added, and the plates were incubated at 22°C. The reaction was stopped with the addition of 50 µl/well of 2 M H_2SO_4, and the absorbance was read at 450 nm on a SPECTROstart nano (BGM; LabTechnologies). The plotted values resulted from subtracting the absorbance from the control wells.

Determination of IgT Total and Specific Antibody Levels

Direct and indirect ELISAs were performed to analyze the total and hemocyanin-specific gut mucus IgT levels, respectively, as previously described (46). The specificity of the customized polyclonal anti-GSBIgT antibody used in this study has been previously validated by Western blot and ELISA (46). Briefly, to assess the total IgT here, 96-well plates were coated with fish gut mucus diluted 1:6 in carbonate/bicarbonate solution and incubated overnight at 4°C. Similarly, to measure the hemocyanin-specific IgT level, 1:5 dilutions of fish gut mucus from the naive, hemocyanin-immunized, or pre-immune animals as control were added to a hemocyanin precoated flat-bottomed ELISA plates. Then, each assay was followed by the

addition of a customized polyclonal anti-seabream IgT (GeneScript) and an anti-rabbit IgG peroxidase antibody produced in goat (Sigma-Aldrich, Spain), both diluted at 1:1,000. Finally, the chromogen TMB (Sigma-Aldrich) was added, and the plates were incubated at 22°C. The reaction was stopped with the addition of 50 µl/well of 2 M H_2SO_4, and the absorbance was read at 450 nm on a SPECTROstart nano (BGM; LabTechnologies). The plotted values resulted from subtracting the absorbance from the control wells.

RNA Extraction and Gene Expression Analysis

Total RNA was extracted from the hindgut of control or treated (vaccinated or not) fish (n = 6 fish/treatment) with TRIzol reagent (Invitrogen) following the manufacturer's instructions and quantified with a spectrophotometer (NanoDrop, ND-1000). The RNA was treated with DNase I, amplification grade (1 U/mg RNA; Invitrogen), to remove genomic DNA traces that might interfere with the PCRs. Subsequently, the SuperScript IV RNase H reverse transcriptase (Invitrogen, USA) was used to synthesize first-strand cDNA with oligo-dT18 primer from 1 µg total RNA, incubated at 50°C for 10 min. The b-actin (*actb*) gene was analyzed for sample content standardization using a semiquantitative PCR with an Eppendorf Mastercycle Gradient Instrument (Eppendorf). Briefly, the reaction mixtures were incubated for 2 min at 95°C, followed by 35 cycles of 45 s at 95°C, 45 s at the specific annealing temperature, 1 min at 72°C, and finally 10 min at 72°C. In the same samples, the expression levels of the genes coding for the pro-inflammatory cytokines *il1b* and *cox2* or the mucosal markers *imuc*, *muc13*, and *ight* were analyzed by real-time PCR performed with a QuantStudioTM 5 Flex instrument (Applied Biosystems) using SYBR Green PCR core reagents (Applied Biosystems). The reaction mixtures were incubated for 10 min at 95°C, followed by 40 cycles of 15 s at 95°C, 1 min at 60°C, and finally, 15 s at 95°C, 1 min at 60°C, and 15 s at 95°C. After verifying each primer pair amplification efficiency and single peak melting curve presence, the appropriate references were selected based on the average M value. Thereafter, the relative expression of each target gene was corrected by the content of two reference genes, the 40S ribosomal protein subunit 18 (*rps18*) and the subunit 11 (*rps11*) in each sample using the comparative cycle threshold method ($2^{-\Delta\Delta Ct}$) (47). The gilthead seabream-specific primers used as targets and housekeeping genes are listed in **Table 1**. In all cases, each PCR was performed in duplicate with three technical replicates each.

Intestine Histological Analysis

Hindgut samples (n = 6) from each experimental group were fixed in 10% buffered formalin solution and processed using routine methods. Subsequently, they were embedded in paraffin at 60°C to obtain a microtome cross-section with a thickness of 5 µm that was stained with periodic acid shift-alcian blue (PAS-A). The slides were mounted using approved substitute chemicals and subjected to optical microscopic evaluation. The abundance of goblet cells and intraepithelial lymphocytes was assessed.

DNA Extraction, PCR Amplification, Amplicon Library Construct and Sequencing

Genomic DNA was extracted from pooled intestine samples (n = 6 fish/treatment) using the TriSure method (Bioline). The quality and integrity of the extracted DNA were checked on 1% (w/v) agarose gel stained with GelRed Nucleic Acid Stain 20,000x (InTRON Biotechnology, Seoul). The DNA concentration and purity were quantified fluorometrically using the Qubit™ dsDNA HS assay kit (Thermo Scientific). The DNA samples were stored at -20°C, and 30 ng were used for subsequent analyses. Libraries were constructed with 2 × 300 bp paired-end sequencing in the Ultrasequencing Service of the Bioinnovation Center of the University of Málaga, Spain, on an Illumina MiSeq platform (Illumina). Briefly, Illumina paired-end sequencing was carried out using the sense forward (341F) 5′-CCTACGGGNGGCWGCAG-3′ and (805R) 5′-GACTACHVG GGTATCTAATCC-3′ reverse primers targeting the variable regions V3–V4 regions of the 16S rRNA gene. After removing the Illumina barcodes and demultiplexing, the readings were combined using the Mothur software package (1.39.5 version). In addition, the assembled readings were filtered, excluding readings lower or higher than 80–2,000 bp long. Besides, non-specific PCR amplicons and singleton sequences were excluded in the subsequent analyses. All processing was done using the Mothur pipeline. The Mothur script was used to detect and remove chimera against the reference database, and the remaining representative non-chimeric sequences were then subjected to taxonomic assignment against the Greengenes 16S database (48), with 97% 16S similarity as the cutoff and clustered into operational taxonomic units (OTUs). The sequencing depth level was determined by the rarefaction curves obtained by plotting the number of observed OTUs against the number of sequences and Good's coverage coefficient. The alpha diversity was estimated based on Shannon–Wiener, Chao1, and Simpson indices to determine taxonomic and phylogenetic structure diversity.

Functional Metagenome Prediction and Analysis

PICRUSt (version 1.1.3) was used to predict the putative metagenome functional profiles of intestines from vaccinated vs. naive fish using the previously obtained 16S rRNA sequencing reads (49). The resulting metagenome inferences were entered into the Greengenes database (version 13.5), and the metagenome prediction of bacterial communities was conducted using the calculated data set after normalizing the 16S rRNA copy number. Nearest Sequenced Taxon Index (NSTI) scores for evaluating the accuracy of predicted metagenomes were categorized with the Kyoto Encyclopedia of Genes and Genomes (KEGG) pathways database (50) and bacterial functional profiles until KEGG modules level 3 were compared.

Statistical Analysis

The microbiome data were analyzed by Good's coverage, rarefaction curves, and alpha diversity indices, including Chao1

TABLE 1 | List and GeneBank accession number of primers used for qPCR analysis of seabream samples.

Gene	Name	Sequence (5'-3')	Accesion number
il1b	F2	GGGTCTGAACAACAGCACTCTC	**AJ277166**
	R3	TTAACACTCTCCACCCTCCA	
cox-2	F2	CATCTTTGGGGAAACAATGG	**AM296029**
	R2	AGGCAGTGTTGATGATGTCG	
imuc	F	GTGTGACCTCTTCCGTTA	**JQ27712**
	R	GCAATGACAGCAATGACA	
muc13	F	TTCAAACCCGTGTGGTCCAG	**JQ27713**
	R	GCACAAGCAGACATAGTTCGGATAT	
ight	F	TGGCAAATTGATGGACAAAA	**FM145138**
	R	CCATCTCCCTTGTGGACAGT	
rps18	F	AGGGTGTTGGCAGACGTTAC	**AM490061**
	R	CTTCTGCCTGTTGAGGAACC	
rps11	F1	GGCGTCAACGTGTCAGAGTA	**NM_213377**
	R1	GCCTCTTCTCAAAACGGTTG	

richness estimation and community diversity (Shannon index and Simpson) with Microbiome eAnalyst web platform (51). Normality (Shapiro–Wilk) and homogeneity of variance (Levene's test) were performed, and the statistical significance of growth data and alpha diversity paired comparisons were determined by Student's t-test ($p < 0.05$). All tests were performed with XLSTAT software. DESeq2 software was used to test for differential representation of OTUs by treatment ($p < 0.01$). The STAMP (Statistical Analysis of Metagenomics Profiles) was used to analyze the differential abundance of modules based on the gut sections and diet using ANOVA multiple-comparison test with *post hoc* Tukey–Kramer test ($p < 0.05$). The results from the gene expression, Ig levels, goblet cell count, and antimicrobial humoral activities were analyzed by two-way ANOVA and *post hoc* Tukey's to determine the differences among groups. Note that in some figures, the number of individuals was lower than the established ($n = 6$) due to technical issues. Then, we ran again each data set using weighted and unweighted means, and the robustness of our data was not affected. The critical value for statistical significance was established at $p \leq 0.05$. All statistical analyses were carried out using the GraphPad Prism 8.04 software.

RESULTS

Oral EE_2 Exposure Strongly Disrupts the Seabream Hepatic Function Without Mirroring It in the Gut Cellular Immune Function

Following our established estrogen-feeding model, the diet was supplemented with the G1 agonist or a strong xenoestrogen (EE_2) and fed continuously for 84 days as described in detail (**Figure 1**). The continuous action of both treatments did not produce any fish mortality or abnormal behavior during the whole experimental period. However, after 42 days of constant EE_2 oral intake, a significant ($p < 0.001$) estrogenic-mediated endocrine disruption was found after evaluating the VTG level from the blood serum (**Figure 2A**). On the contrary, the continuous administration of the G1 receptor agonist within the same period did not affect the VTG production supporting the notion that the action of EE_2 triggers specific disruption. At the same time, the hindgut's local adaptive immune response was not affected by any dietary supplementation, as demonstrated by the invariant yet modest levels of total mucus IgT recorded in both treated groups and the control fish (**Figure 2B**).

Immunological Priming Reduces the Excessive Enzymatic Activity Triggered by EE_2 in the Fish Systemic Response

The magnitude of some major biochemical indicators known for impacting the cellular and defense functions in seabreams was assessed. After 1 day post-immunization, at 43 days of continuously treating the fish with the G1- or EE_2-supplemented feed at naive or immunized conditions, a selected panel of proteolytic and bacteriolytic assays such as peroxidase, antiprotease, lysozyme, and bactericidal activities in the serum was collected as indicators. Interestingly, the naive fish treated with EE_2 showed a markedly significant ($p < 0.001$) increase in the peroxidase activity relative to the control fish (**Figure 3A**). Unexpectedly, we observed that the priming immunization of the vaccine resulted in a significant ($p < 0.01$) decrease of the peroxidase activity in the EE_2 group, even though the response remains significantly ($p < 0.05$) higher than that in the immunized controls. For the antiprotease response, a similar significant ($p < 0.05$) effect was also recorded at the EE_2-treated group between the naive and immunized conditions, while the G1 treatment of the naive condition produced an opposite response by producing a significant ($p < 0.001$) inhibition (**Figure 3B**). At the same time, the lysozyme and bactericidal activities did not show any significant variations at any stage (**Figures 3C, D**).

G1 and EE_2 Exposures Hardly Alter the Antimicrobial Activities in the Gut Mucus Interphase

Furthermore, to explore the constitutive gut mucus interphase as influenced by continuously feeding the seabreams with G1 or EE_2, the biochemical assays previously described in the serum were conducted. We observed that the intestinal mucus of the

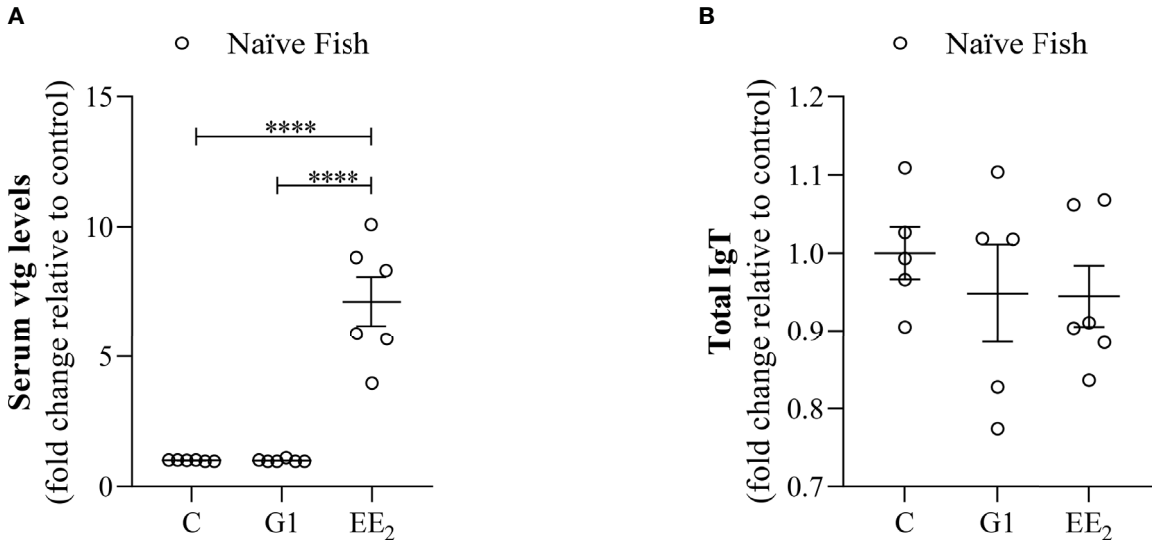

FIGURE 2 | Dietary addition of xenoestrogen impairs vitellogenin but not total IgT production. Serum or intestinal mucus from gilthead seabream which had been treated with G1 or EE2 (5 μg/g food) for 43 days were assayed for: **(A)** serum vitellogenin (Vtg) level. **(B)** Intestinal mucus total immunoglobulin T (IgT). Both parameters were assessed with a double specific antibody procedure by ELISA. Representative ± SEM are shown (n = 6). The asterisks denote statistically significant differences after Student's t-test between each treated and the untreated groups. ****(p<0.001).

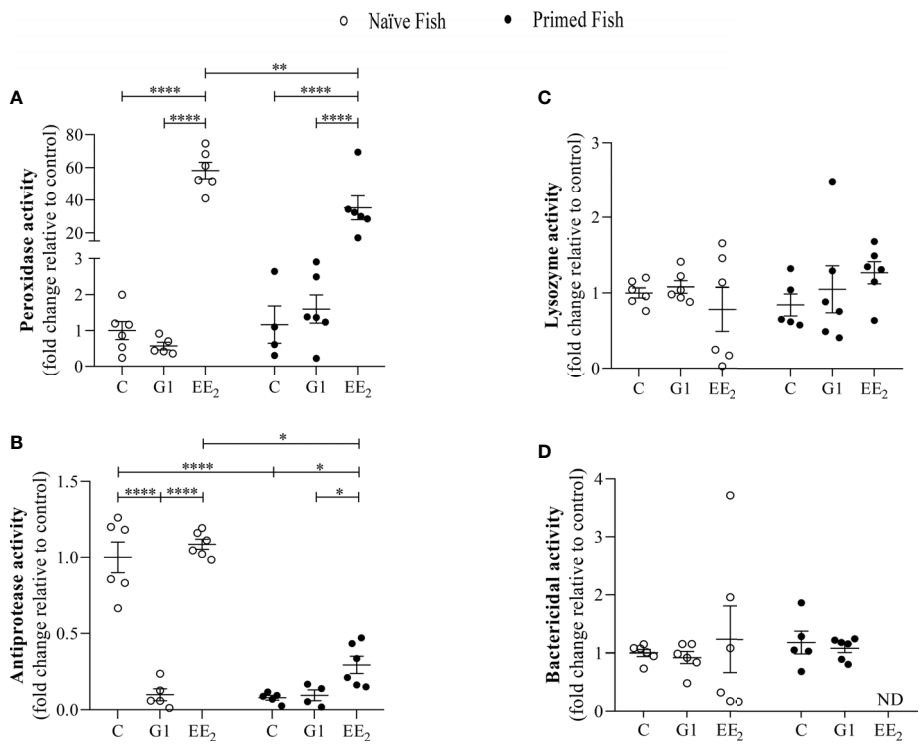

FIGURE 3 | 17α-ethinylestradiol (EE2) exposure and further immune priming modulates the antimicrobial humoral activities in the serum of gilthead seabream. The fish had been orally treated with G1 or EE2 (5 μg/g food) for 43 days and either immune primed with KLH or not (naive) on the sampling day. **(A)** Peroxidase, **(B)** Lysozyme, **(C)** Antiprotease **(D)** Bactericidal activity. Data represents means ± standard error (n = 6). Asterisks denote statistically significant differences between the groups. *(p<0.05) **(p<0.01) ****(p<0.001).

animals exposed to either G1 or EE_2 hardly showed any significant changes in either the peroxidase activity or the bactericidal capacity among the exposed groups and between the two conditions *per se* (**Figures 4A, D**). Although the gut mucus lysozyme present in the naive fish dietary administered with EE_2 showed a dual effect by significantly ($p < 0.05$) increasing its activity level within the naive initial stage but resulting in a significant ($p < 0.05$) decrease after priming (**Figure 4C**). The antiprotease activity showed a significant variation resulting from treating the fish orally with the G1 agonist and comparing the response between the naive and the immunized conditions (**Figure 4B**).

The Intestinal Level of Inflammatory Mediators Was Affected by the Oral Administration of EE_2 and Can Be Reversed Through Vaccination

An accurate understanding of how the oral administration of G1 and EE_2 reconfigures the immune system in the seabream is crucial to comprehend its disruptive effect. To address this, on day 43 of the trial, we profiled and quantified five critical inflammatory mediators, *cox2*, *imuc*, *muc13*, *ight*, and *il1b* at the transcriptional level. Differences in the expression pattern of the different mediators were assessed by quantitative-PCR (qPCR) following a naive scheme and after receiving the vaccine priming immunization. The mRNA transcriptional levels of the inducible inflammatory mediators *cox2* and *imuc* and the constitutive *muc13* and *ight* genes revealed subtle, yet not significant, changes in their expression at the naive condition (**Figures 5A–D**). At the same time, naive animals fed with EE_2 showed a significant ($p < 0.05$) increase in the transcription level of *il1b* when compared to the G1-treated group. Furthermore, as seen in the previously analyzed parameters, the effect of priming immunization on the naive EE_2 enhanced the expression of *il1b* significantly ($p < 0.05$) but eventually reverted to similar basal levels as those recorded in the untreated group (**Figure 5E**).

Extended Oral Administration of EE_2 Alters the Actively Secreting Mucus Cells

To further validate the positive effect of the immunization as previously observed on seabream expressing toxic effects after receiving a continuous oral dose of EE_2, we analyzed the gut of the treated animals histologically under naive and immunized conditions. After 43 days of trial under naive conditions, we noted an increase in the volume and number of interepithelial lymphocytes (IELs) at the lamina propria and the PAS-A-stained (light blue) cells throughout the mucosal fold height architecture of EE_2-treated fish. Likewise, this is morphologically consistent with neutral and acidic staining goblet cells, a specialized epithelial cell type that produces the main component of the

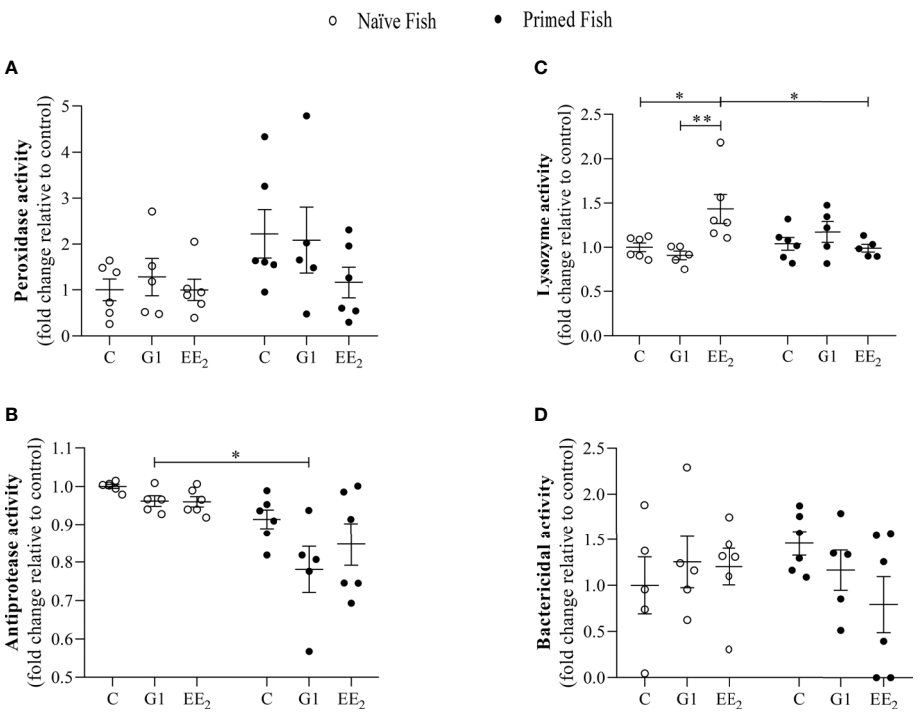

FIGURE 4 | The gut mucus antimicrobial humoral activity is seldom affected by the presence of 17α-ethinylestradiol (EE2) or KLH-immune priming in gilthead seabream. The fish had been orally treated with G1 or EE2 (5 μg/g food) for 43 days and either immune primed with KLH or not (naive) on the previous day. **(A)** Peroxidase, **(B)** Lysozyme, **(C)** Antiprotease **(D)** Bactericidal activity. Data represent means ± standard error (n=6). Asterisks denote statistically significant differences between the groups. *(p<0.05) **(p<0.01).

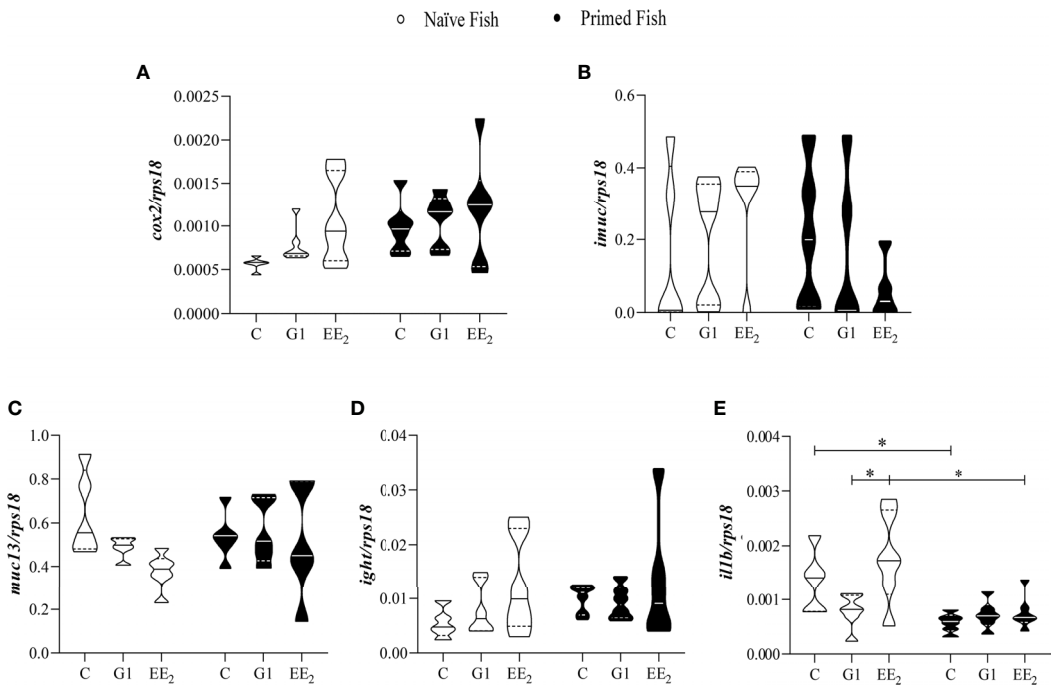

FIGURE 5 | The relative immune gene expression in the gut of gilthead seabream in response to the exposure in either G1 or EE2 under naive or immune primed condition minimally change. The fish had been orally treated with G1 or EE2 (5 μg/g food) for 43 days and either primed with KLH or not (naive) on the previous day. Gene expression levels **(A)** cyclooxygenase-2; **(B)** intestinal mucin; **(C)** mucin-13; **(D)** immunoglobulin T heavy chain; **(E)** interleukin-1beta are related to the expression of the 40S ribosomal protein subunit 18 (rps18). The violin graphs visualize quantitative and qualitative attributes of the samples comprised in each group. The mean is represented by the central solid line on each plot (n=6). Asterisks denote statistically significant differences between the groups. *($p<0.05$).

mucus barrier. Unexpectedly, 24 h after the fish received the priming immunization of the vaccine, the previously altered goblet cells reverted to the basal state (**Figure 6A**). However, after quantifying the number of stained goblet cells on each treatment at either the naive or immunized stage using light microscopy, it was shown that the shift was not statistically supported. Yet, a decreasing trend can be observed (**Figure 6B**).

Treating the Naive Seabream Orally With G1 and EE_2, Together With the Vaccine Priming Immunization, Modulates the Gut Microbiota Communities

The analysis of the different taxonomic levels in the three groups of naive fish revealed three dominant bacterial groups. The Proteobacteria showed the highest relative abundance (>75%) across all samples. It was followed by the phyla Firmicutes (6%–16%) and Bacteroidetes (4%–7%). Interestingly, the naive fish exposed to the action of the agonist G1 showed a significant abundance reduction of Actinobacteria and Firmicutes compared to the untreated or EE_2-exposed animals (**Figure 7A**). At the class level, in naive fish, the dominant groups were the α- and γ-Proteobacteria in the naive fish, with the last class particularly more pronounced in the G1-treated fish (**Figure 7B**). Regarding the individual OTUs at the genus level, the three naive groups shared a high proportion of *Pseudomonas* with relative abundance ranging from 48% to 59%. Among the remaining genera, the most predominant genera in the three groups were *Vibrio*, *Streptococcus*, *Sphingomonas*, *Phenylobacterium*, *Nevskia*, *Methylobacterium*, and *Acinetobacter*, showing abundances between 1% and 9% but without any significant differences (**Figure 7C**). Unexpectedly, while the presence of *Shewanella* was recorded in the control and G1 naive groups, the EE_2 treatment fully abrogated its presence causing a significant ($p < 0.01$) difference between groups. On the other hand, the results in immunized fish at the phyla, class, and genus levels (**Figures 7D–F**) mostly mirrored those previously reported for naive fish. However, significant differences in some OTUs were detected. At the phylum level, *Fusobacteria* was present only in the control group (**Figure 7D**), while the OTUs in the class β-Proteobacteria remarkably shifted in the gut microbiota abundance between the G1- and EE_2-treated and immunized conditions (**Figure 7E**). The taxonomic analysis at the genus level revealed the largest variations in OTUs when comparing the core microbiota of untreated fish with the G1- and EE_2-treated and priming immunized fish. *Brochothrix* in the G1-treated and *Staphylococcus* and *Novosphingobium* in the EE_2-treated specimens were the most highly abundant genera between the naive and the vaccinated conditions (**Figure 7F**). Note that those sequences not assigned to any known microbial taxonomical classification were designated as ETC, which represented less than 1% of the entire individual data sets presented.

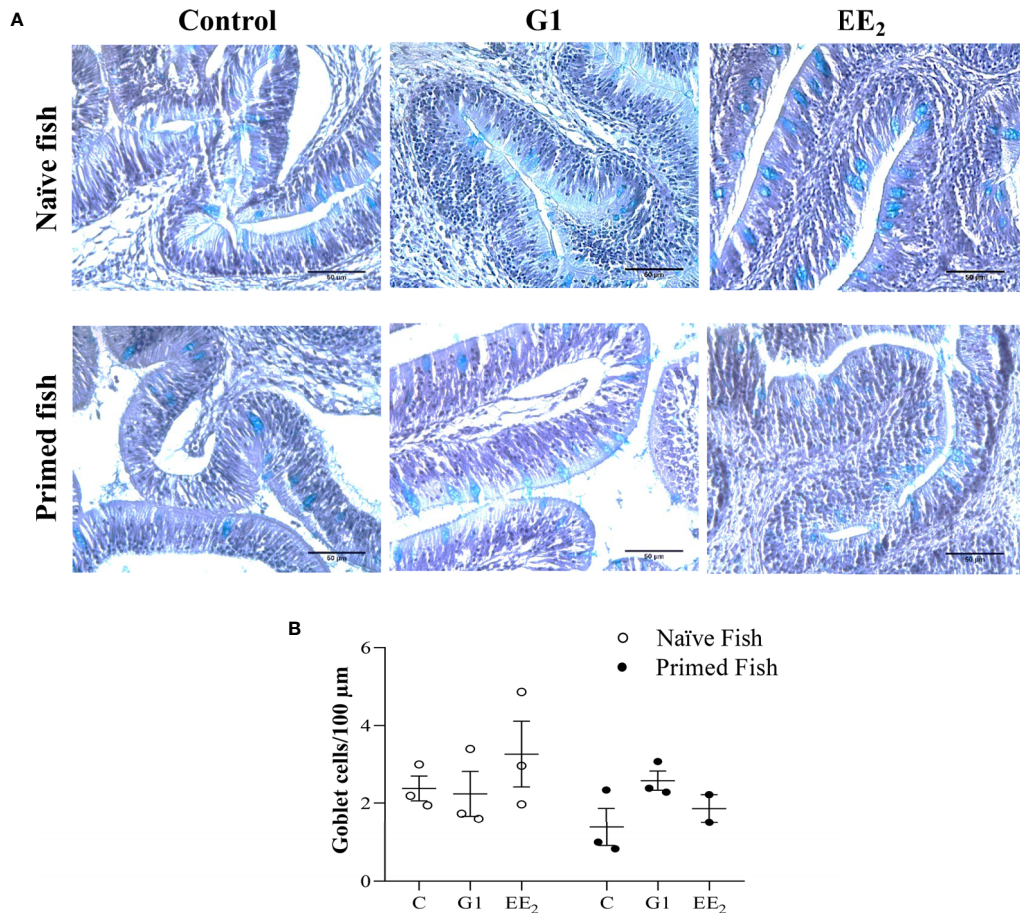

FIGURE 6 | Oral exposure of G1, EE2 and immune priming induce structural changes along the hindgut of gilthead seabream. The fish had been orally treated with G1 or EE2 (5 µg/g food) for 43 days and either immune primed with KLH or not (naive) on the previous day. **(A)** Representative histomorphology image of PAS-A-stained hindgut longitudinal sections with neutral and acid staining goblet cells highlighted in light blue. Besides, note the high number of IEC infiltrates present in the lamina propria on both G1 and EE2 conditions. (n = 6; Scale bar = 50µm). **(B)** Representative average histological quantification of the mean number of PAS-positive goblet cells on three randomly selected slides per treatment and condition in duplication.

Activation of the GPER1 Receptor Significantly Modulates the Gut Microbiome Structure

An average of 76,282.75 ± 12,605.17 reads was obtained from the samples analyzed. Furthermore, these sequences were successfully clustered in OTUs with 97% identity. The Good's coverage estimations ranked between 99.98% and 99.99%, indicating an adequate sequencing depth. A random subsampling was conducted to normalize the data size to 42,494 reads that were assigned to 87 genera distributed among 14 phyla. The alpha diversity of the gut microbial community concerning its richness, diversity, and average evenness indices in every single sample within a treatment group, obtained from the next-generation sequencing (NGS) data, is summarized in **Table 2**. Oral treatment with G1 under naive conditions significantly ($p < 0.05$) decreased the Chao1 species richness and the Shannon diversity estimator indices for the gut mucosa-associated microbiota compartments. Interestingly, the Simpson index of diversity was decreased in the same G1-treated group, but this variation was not statistically supported. However, following the priming immunization variations on any of the three indices among groups, or changes between the control and the two experimental oral treatments were not observed.

The Activation of the GPER1-Mediated Estrogen Action Modulates the Gut-Associated Microbiota Functional Activity

The changes in the presumptive functions of the gut microbiota of fish showing significant differences in their microbiotas in comparison with non-immunized untreated fish were examined by predicting the metagenomes using PICRUSt. The accuracy of the prediction was evaluated by computing the NSTI, and the mean of the samples was 0.048 ± 0.005, indicating a relatively good match to reference genomes [ideal NSTI ≤0.03 (52)]. The KEGG ortholog functional predictions showed a significant difference ($p < 0.015$) only between the unvaccinated control fish and those treated with G1. The increased abundances of the

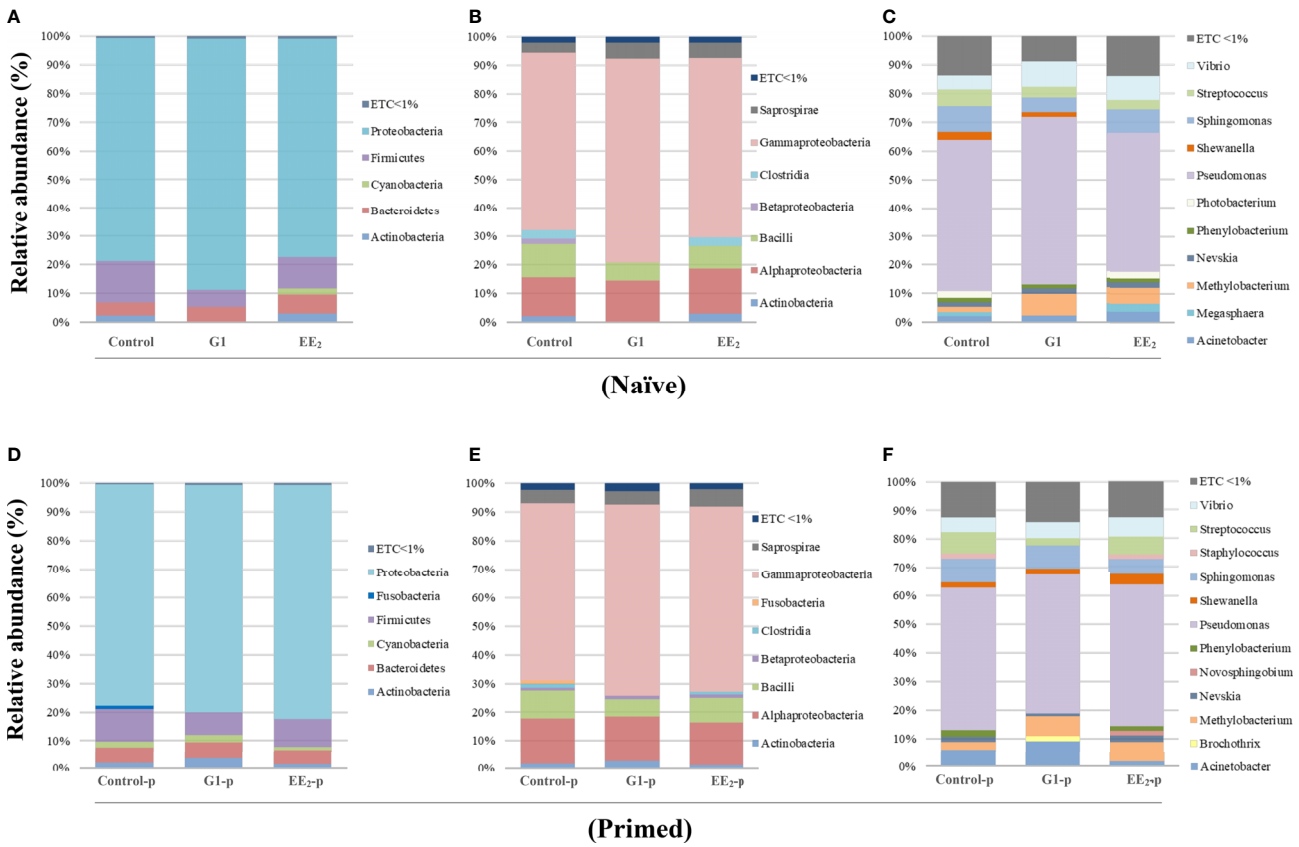

FIGURE 7 | Relative abundance of the intestinal bacteria communities of gilthead seabream, at different taxonomic levels is affected by the oral G1 and EE2 exposure and further potentiated by immune priming. Phyla **(A, D)**. Class **(B, E)**. Genera **(C, F)**. *Left to right*, representing the received dietary treatment received (Control, G1, or EE2). *Up to down*; immune status (Naive or immune primed with KLH). ETC: average relative abundance < 1%, (n = 6).

specific functional category associated with cellular processes and signaling of inorganic ion transport and metabolism, pore ion channels, and membrane and intracellular structural molecules are predicted with significant changes on the G1-fed group, with the latter category presenting the highest significance ($p < 0.009$) value (**Figure 8A**). For the control and G1 groups, the level 2 KEGG annotations revealed seven functional associations related to metabolic, replication and repair, and genetic information categories. By applying the more detailed annotation type, the KEGG level 3, 12 significantly different functional pathways were revealed between the two analyzed groups. Specifically, categories associated with phenylalanine metabolism, lipopolysaccharide (LPS) biosynthesis proteins, arachidonic acid metabolism, biosynthesis of unsaturated fatty acids, and glutathione metabolism were significantly more abundant in fish exposed to G1, whereas categories such as cysteine and methionine metabolism showed lower abundance in this same group (**Figure 8B**).

TABLE 2 | Alpha-diversity indices expressed as the richness, diversity, and average evenness (Chao1, Shannon and Simpson) of bacterial communities present in the hindgut of gilthead seabream (n=6 fish per condition) treated with G1 or EE_2 (5 µg/g food) for 43 days either immune primed or not with KLH on the previous day's (24 h) sampling.

Treatments	Immune Status	Chao1	Shannon	Simpson
Control (C)	Naïve	64.50 ± 7.59	2.53 ± 0.29	0.80 ± 0.06
G1		**50.87 ± 8.51***	**2.14 ± 0.20***	0.74 ± 0.07
EE_2		60.25 ± 8.17	2.57 ± 0.17	0.83 ± 0.04
Control-Vac	Vaccinated	61.69 ± 5.98	2.56 ± 0.13	0.81 ± 0.02
G1-Vac		61.62 ± 9.96	2.65 ± 0.12	0.83 ± 0.02
EE_2-Vac		66.12 ± 5.36	2.56 ± 0.22	0.81 ± 0.04

(*) denotes significant differences ($p<0.05$). For details refer to the statistics section.

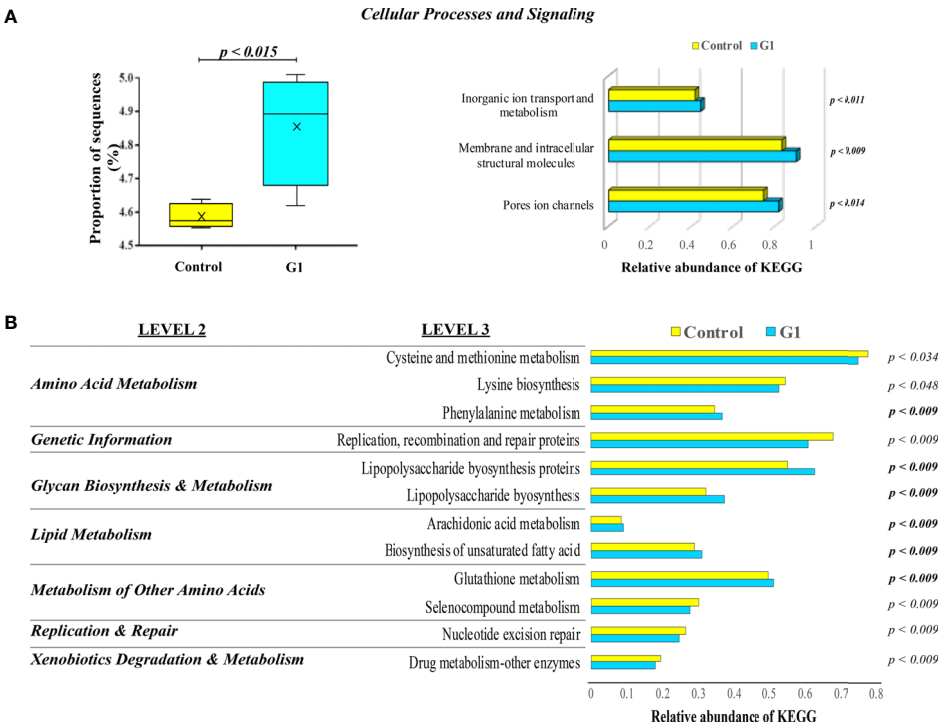

FIGURE 8 | KEGG pathways and functional annotation analysis of gut mucosa-associated microbiota compartments in unvaccinated seabream. **(A)** Box plots representing the significant proportion of the relevant abundance of PICRUSt generated functions profile in the hindgut microbiota of gilthead seabream. The box represents the values between the 25th and 75th percentiles. The maximum and minimum values are represented by up and low caps. Treatment with the G1 containing diet led to a significant increase in the relative abundance of gene sequences influencing critical cellular processes and signaling terms. **(B)** Significant Kyoto Encyclopedia of Genes and Genomes (KEEG) pathways level 2 and 3 enriched by predicted genomes of microbiota from control fish vs. G1-orally treated animals for 43 days. The significant overexpression of each KEGG term in G1 compared to control fish fractions are indicated by the resulting p-value in bold analyzed by ANOVA with a *post-hoc* Tukey-Kramer multiple comparison test ($p<0.05$).

Vaccination Does Not Alter the Production of Systemic and Mucosal-Specific Antibodies in G1- and EE_2-Treated Fish

The KLH-specific IgM and IgT levels in the serum and intestinal mucus were evaluated by ELISA on day 84 (end of the trial). The samples were collected from control, G1-treated, and EE_2-treated seabreams, both naive and fully immunized after receiving the vaccine priming and booster doses on days 42 and 56, respectively. As expected, in naive animals, EE_2 altered the production of natural antibodies that should have been overlapping with some epitopes of the specific IgM and IgT levels measured. However, the response followed a differentially expressed pattern between both targets. The IgM level in the naive EE_2-fed animals produced a significantly ($p < 0.001$) elevated response compared to the control or G1-treated groups (**Figure 9A**). On the contrary, the specific IgT production in the gut mucosal secretion of naive fish at the same time point was significantly ($p < 0.05$) lower in both orally treated groups, suggesting an inhibitory effect on this parameter (**Figure 9B**). The specific systemic or mucosal anti-KLH was inversely differentiated from the naive condition. Although the vaccine did not trigger any significant enhancement in any group, it displayed a more stable effect in the control group when compared to the naive condition. Furthermore, no effect was observed at the end of the trial in the vaccinated and orally treated specimens with either the G1 agonist or the strong disruptor EE_2.

DISCUSSION

In farmed teleost fish, the proper crosstalk between the commensal bacteria residing in the mucosa and the immune cells within the mucosal interphase is essential for controlling and preventing major immune disorders (53, 54). This link highlights the critical importance of cautiously monitoring the immune interventions in the presence of exogenous elements from either a spontaneous or planned artificial origin (e.g., environmentally generated EDCs or vaccination) that may alter such delicate crosstalks. Yet, in fish, the underpinning mechanisms and the key actors that govern the host–microbe intercommunication following the effect of combining the EDC and vaccination in a single setting are poorly understood.

Using our proven estrogen-feeding model and a two-step vaccination program, we found that the systematic oral intake of

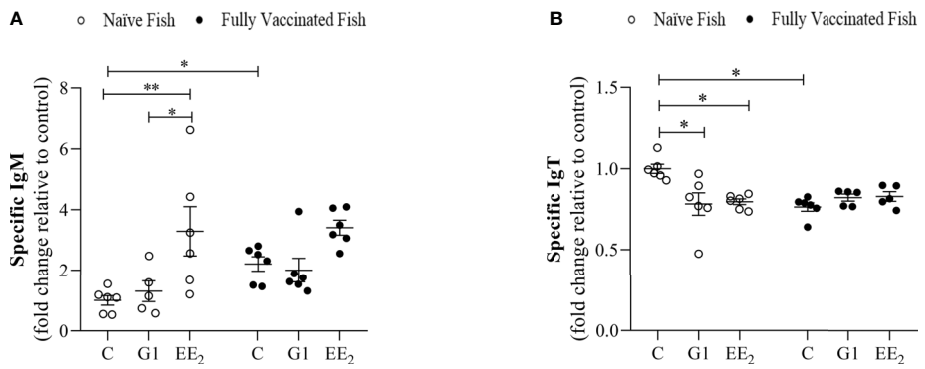

FIGURE 9 | Vaccination differentially regulates the activity induced by the oral exposure to xenoestrogens on the systemic and mucosal antibody production in the gilthead seabream. The anti-KLH IgM and IgT levels (**A** and **B**, respectively) in fish dietary treated with G1 or EE2 (5 μg/g food) for 84 days and either vaccinated following priming and boosted doses of KLH or not (naive) are shown. Data were obtained in duplication by ELISA using independent biological samples and represent means ± standard error (n=6). Asterisks denote statistically significant differences between the groups. Data were analyzed by ANOVA with a *post hoc* Tukey-Kramer multiple comparison test, *($p<0.05$) **($p<0.01$).

a moderate dose of G1 or EE_2 promotes diverse physiological alterations that can potentially contribute to developing pathological profiles that are detrimental to exposed individuals. The fact that estrogens generate reactive oxygen species (ROS), induce peroxidation, and play a key modulatory role in mammals and fish immune systems is not new (34, 55). In our model, the observed endocrine disruption is attributed to the upregulation of hepatic signaling saturation by EE_2 that resulted in excessive VTG production. However, parallel mechanisms equally linked with EE_2 involving divergent pathways associated with the estrogenic, antiandrogenic, thyroid, peroxisome proliferator-activated receptor γ, retinoid, and actions mediated through other nuclear receptors; steroidogenic enzymes; neurotransmitter receptors and systems could not be ruled out from participating in the response. Consequently, altering the systemic and local immune transduction pathways *via* non-genomic mechanisms is mediated by GPER1, as previously suggested (56). Indeed, evidence for host–microbe interactions in mammals supports GPER1 as one of the host factors responsible for crosstalk with microbiota (57). However, the role of the GPER1 agonist, the G1, in modulating the alpha diversity indices and generating a microbial dysbiosis highlighted by the shift of *Shewanella* and *Photobacterium* proportions in the gut of naive fish is reported here for the first time. Thus, we anticipate that after longer exposures to EDCs, dysbiotic events must be monitored to prevent possible metabolic dysregulation and changes to gut barrier function that can lead to diseases in exposed fish.

Cumulative evidence emphasizes the influence of the gut microbiota on humoral and cellular vaccine responses (58, 59). Therefore, several studies have attempted to identify the core microbiota of gilthead seabream (60–62). Despite being not completely established, most studies have agreed with our findings on putting forward Proteobacteria, Firmicutes, Bacteroidetes, and Actinobacteria as the dominant microbial phyla present in the gut. However, these results are not surprising. From the trillions of commensal microorganisms that constitute the intestinal microbiota of most vertebrates, Firmicutes and Bacteroidetes predominate and represent ~90% of the total (63). However, the subtle but significant shifts observed in the relative abundance of Actinobacteria and Fusobacteria under the naive condition in response to the vaccination regardless of the treatment prompted our attention.

In our study, the endocrine disruption generated by EE_2 altered (at least to some extent) most of the humoral and cellular parameters screened in the treated naive fish, although this did not trigger a distinct inflammatory pattern as determined by the lack of significant upregulation of inflammatory mediators at the intestinal mRNA or the cellular resolution. Nevertheless, the EE_2 treatment generated an increase in size and number of goblet cells, promoted the IEL infiltration to the lamina propria, and perhaps also contributed to a general redistribution of leukocytes among the entire system. Furthermore, it is accepted that EE_2 can interact with other components of the endocrine pathway, e.g., ER corepressors or coactivators, and modulate the activity of the enzymes involved in steroid conversion, e.g., aromatase CYP19 converts testosterone to E_2 (64). This conversion leads to stimulation or inhibition of endogenous hormone biosynthesis. Besides, EDCs like the EE_2 can bind to circulating hormone-binding proteins and disrupt the local endogenous hormonal balance expressing cortisol that ultimately regulates neuroimmunoendocrine circuitries, elicits stress-induced immunosuppression, and contributes to allostatic imbalances (65). In any case, in our study, vaccination significantly contributes to the immune restoration and cellular and biochemical homeostasis in fish 24 h post priming immunization on day 42 of the trial. Presumably, the positive effect of the vaccine has over the estrogenic disruption by EE_2 was mediated through the rapid release of specific commensal microbial factors after a single priming immunization dose. Previously, we have demonstrated that damage-associated molecular patterns released from dying cells mediate alum adjuvant activity when combined with KLH (39). However,

in this study, the role of alum as adjuvant remains elusive, and future studies are required to understand its associated mechanisms. In mammals, it has been demonstrated that estrogen generates changes in the gut microbiota and might promote the enrichment of bacteria associated with immune regulation (66). In addition, the diversity of the gut microbiota has been shown to influence systemic estrogen levels through enzymatic and immune pathways (67). Although, in the present study, an increased modulation of the adaptive immunity expressed as specific IgM and IgT levels by the end of the trial in any group was unsupported.

The alpha diversity indices (richness, diversity, and average evenness) of the gut microbial community in every pooled sample within a treatment group only showed significant differences in fish from the G1 naive treatment. This indicates that the bacterial diversity in these communities was mostly covered regardless of the diet. In the gut microbiota of fish, including the gilthead seabream, Actinobacteria is a predominant low-represented phylum (60, 68). In the present study, Actinobacteria was completely abrogated at the phyla and class levels in the G1-treated naive fish when compared to the control or EE_2 treatments. However, in the same group of the vaccinated fish, Actinobacteria was always present among the bacterial OTU repertoires. Previous studies have suggested that mice treated with G1 and subjected to a mucosal bacterial infection have reduced bacterial burden (69). Moreover, the low bacterial burden generated local levels of the neutrophil-recruiting chemokine *cxcl1* and the inflammatory cytokine *il1b*, like our results. Therefore, we hypothesize that, in our study, G1 also promoted a diversity reduction through the enhancement of the endothelial and epithelial gut–blood barrier integrity and increased permeability through the reorganization of dynamic structures like the tight junctions in a way that the paracellular permeability can adapt to the required characteristics of diffusion restriction mediated by the external stimuli. On this basis, we speculate that G1 has a strong potential utility as a viable solution to enhance specific bacteria releasing variated lytic compounds (70), as probiotic (71) or by producing secondary metabolites that have critical functions in the physiological, biochemical, or defensive role within their host (72).

With respect to the vaccine response, our results indicate that at the genus level, *Staphylococcus*, *Brochothrix*, and *Novosphingobium* may have driven many of the differences observed in the response to vaccines. In particular, *Novosphingobium* is well known for its capacity to degrade a wide range of environmental pollutants, with a particular emphasis on the removal of estrogen (73). These experimental findings support the hypothesis that differences in estrogen metabolism are associated with variability in the gut microbial diversity. *Novosphingobium* also assists in the metabolism of nitrogenous compounds and sulfanilic acid, so its ability to metabolize several xenobiotics has also been described (74, 75). Besides, the relationships between gut microbial richness, systemic and fecal estrogens, and beta-glucuronidase activity have been demonstrated (67). Based on these concepts, the term estrobolome was coined to define the gene repertoire of the gut microbiota capable of metabolizing estrogens (28, 76). However, just recently, the wider term endobolome was also suggested to address the group of gut microbiota, genes, and pathways involved in the metabolism of any EDC, including the target of this study, the EE_2 (29). Together, these concepts explain why a balanced bacterial composition is a key player in eliciting downstream gene activation and triggering intracellular signaling cascades to maintain intestinal and distal mucosal sites immunity and homeostasis.

Meanwhile, the PICRUSt analysis of our study showed that seabream fed with the G1-containing diet acquired a significant increase in the relative abundance of gene sequences influencing critical cellular processes and signaling terms. Specifically, the categories associated were related to ion channels, membrane, intracellular molecules, inorganic ion transport, and metabolism. At the immune level, ion exchange between intracellular and extracellular spaces is the primary mechanism for controlling cell metabolism and signal transduction (77). This process is mediated by the predicted overexpressed ion channels and transporters on the plasma membrane or intracellular membranes that surround various organelles in response to environmental stimuli like the one generated by the presence of EE_2. In fish, we have already demonstrated the importance of the ion channels in mucosal tissues on the transportation of calcium between the extracellular and intracellular environment to initiate inflammatory processes mediated through the transient receptor potential vanilloid 4 (TRPV4) (78). EE_2 potentiates TRPV1 as an activated ionotropic membrane receptor coupling with mitochondrial function and cell survival in injured immunocytes following an oxidative manner (79). G1-treated fish also showed predicted functions associated with LPS biosynthesis and arachidonic acid (ARA) metabolism. ARA is an n-6 essential fatty acid present in the membrane phospholipid released by phospholipase A2 that further is used to produce eicosanoids. Recent studies have elucidated that ARA influences innate immunity *via* regulating the development and differentiation of innate immune cells and the function of the intestinal barrier (80). Therefore, in our study, ARA generation in the intestine of seabream may directly affect the gut immune environment by enhancing the crosstalk between the intestinal epithelial barrier and the professional immune cells inhabiting the same. In addition, it has been observed that the proliferation of Firmicutes inhibits the proliferation of LPS-producing bacteria, reducing the transfer of potential bacterial inflammatory products to the liver (81), thus exacerbating the hepatic toxicity generated by the presence of the EDC. Similarly, the microbiota of G1-treated fish in our study showed a reduction in Firmicutes. Perhaps, this effect was related to the increased abundance of LPS biosynthesis. Also, the changes observed in the gut microbiota of fish from the G1 treatment are associated with ARA metabolism. This opens the possibility that the microbiota in the gut exerts a potential exogenous effect in promoting ARA release since fish lack the ability to synthesize polyunsaturated fatty acid (PUFA) and require preformed dietary PUFA from linolenic and linoleic acids such as ARA for their normal growth and development (82).

In summary, we have provided evidence of the beneficial effects of the gut bacteria, which overall appear capable of processing endogenous estrogens or xenoestrogens such as EE_2 through the endobolome. Moreover, these bacteria, together with a vaccination scheme, seem to provide robust supplementary support on the health management of the cultured seabream subjected to the action of EDCs, despite lacking a significant enhanced specific antibody production. However, this knowledge requires extensive further studies to validate the proposed concepts functionally.

DATA AVAILABILITY STATEMENT

The original contributions presented in the study are publicly available. These data can be found here: National Center for Biotechnology Information (NCBI) BioProject database under accession number PRJNA749661. The BioProject is permanently accessible through the following link: https://www.ncbi.nlm.nih.gov/bioproject/?term=PRJNA749661.

ETHICS STATEMENT

This study was carried out in strict accordance with the recommendations under the Guide for Care and Use of Laboratory Animals of the European Union Council (2010/63/UE). The number of animals used was determined following a highly restricted *f* size *a priori* effect established at the 0.05 a-error probability on the power analysis, determined as previously suggested (37). The Bioethical Committee approved the experimental protocol of the IEO (reference REGA ES300261040017) and the "Consejería de Agua, Agricultura y Medio Ambiente" of the "Región de Murcia", Spain (approval number A13160508). Written informed consent was obtained from the owners for the participation of their animals in this study.

AUTHOR CONTRIBUTIONS

AG-A conceived and designed the experiments. PC, IC, VG, EC-P, and IC-O performed the experiments. EC-P, MM, EM-M, JG-V, and AG-A analyzed the data. PC original draft preparation, and JG-V reviewed and editing. All authors contributed to the article and approved the submitted version.

FUNDING

This study was funded by the Ministerio de Ciencia e Innovación and FEDER (AGL2017-85978-C2-1-R). The Fundación Séneca (CARM) (19883/GERM/15). Nord University Access Fund covers the OA publication cost.

ACKNOWLEDGMENTS

We thank I. Fuentes for her excellent technical assistance and "Servicio de Apoyo a la Investigación" at Murcia University for variated technical assistance. To A. Nedoluzhko and J. L. Superio at Nord University for proofreading and providing suggestions to improve the article.

REFERENCES

1. La Merrill MA, Vandenberg LN, Smith MT, Goodson W, Browne P, Patisaul HB, et al. Consensus on the Key Characteristics of Endocrine-Disrupting Chemicals as a Basis for Hazard Identification. *Nat Rev Endocrinol* (2020) 16:45–57. doi: 10.1038/s41574-019-0273-8
2. Shen H-H, Zhang T, Yang H-L, Lai Z-Z, Zhou W-J, Mei J, et al. Ovarian Hormones-Autophagy-Immunity Axis in Menstruation and Endometriosis. *Theranostics* (2021) 11:3512–26. doi: 10.7150/thno.55241
3. Mhaouty-Kodja S, Naulé L, Capela D. Sexual Behavior: From Hormonal Regulation to Endocrine Disruption. *Neuroendocrinology* (2018) 107:400–16. doi: 10.1159/000494558
4. Combarnous Y, Nguyen TMD. Comparative Overview of the Mechanisms of Action of Hormones and Endocrine Disruptor Compounds. *Toxics* (2019) 7 (1):5. doi: 10.3390/toxics7010005
5. Taneja V. Sex Hormones Determine Immune Response. *Front Immunol* (2018) 9:1931. doi: 10.3389/fimmu.2018.01931
6. Khan D, Ansar Ahmed S. The Immune System Is a Natural Target for Estrogen Action: Opposing Effects of Estrogen in Two Prototypical Autoimmune Diseases. *Front Immunol* (2015) 6:635. doi: 10.3389/fimmu.2015.00635
7. Maurício R, Dias R, Ribeiro V, Fernandes S, Vicente AC, Pinto MI, et al. 17α-Ethinylestradiol and 17β-Estradiol Removal From a Secondary Urban Wastewater Using an RBC Treatment System. *Environ Monit Assess* (2018) 190:320. doi: 10.1007/s10661-018-6701-8
8. Jin J, Wu P, Zhang X, Li D, Wong W-L, Lu Y-J, et al. Understanding the Interaction of Estrogenic Ligands With Estrogen Receptors: A Survey of the Functional and Binding Kinetic Studies. *J Environ Sci Health C Toxicol Carcinog* (2020) 38:142–68. doi: 10.1080/26896583.2020.1761204
9. DeLeon C, Wang DQ-H. Arnatt CK. G Protein-Coupled Estrogen Receptor, GPER1, Offers a Novel Target for the Treatment of Digestive Diseases. *Front Endocrinol (Lausanne)* (2020) 11:578536. doi: 10.3389/fendo.2020.578536
10. Wang X-W, Yuan L-J, Yang Y, Zhang M, Chen W-F. IGF-1 Inhibits MPTP/MPP+-Induced Autophagy on Dopaminergic Neurons Through the IGF-1r/PI3K-Akt-mTOR Pathway and GPER. *Am J Physiol Endocrinol Metab* (2020) 319:E734–43. doi: 10.1152/ajpendo.00071.2020
11. Zhang K-S, Chen H-Q, Chen Y-S, Qiu K-F, Zheng X-B, Li G-C, et al. Bisphenol A Stimulates Human Lung Cancer Cell Migration *via* Upregulation of Matrix Metalloproteinases by GPER/EGFR/ERK1/2 Signal Pathway. *BioMed Pharmacother* (2014) 68:1037–43. doi: 10.1016/j.biopha.2014.09.003
12. Yu X, Li F, Klussmann E, Stallone JN. Han G. G Protein-Coupled Estrogen Receptor 1 Mediates Relaxation of Coronary Arteries *via* cAMP/PKA-Dependent Activation of MLCP. *Am J Physiol Endocrinol Metab* (2014) 307:E398–407. doi: 10.1152/ajpendo.00534.2013
13. Huang M, Huang M, Li X, Liu S, Fu L, Jiang X, et al. Bisphenol A Induces Apoptosis Through GPER-Dependent Activation of the ROS/Ca2+-ASK1-JNK Pathway in Human Granulosa Cell Line KGN. *Ecotoxicol Environ Saf* (2021) 208:111429. doi: 10.1016/j.ecoenv.2020.111429
14. Schüler-Toprak S, Skrzypczak M, Ignatov T, Ignatov A, Ortmann O. Treeck O. G Protein-Coupled Estrogen Receptor 1 (GPER-1) and Agonist G-1 Inhibit Growth of Ovarian Cancer Cells by Activation of Anti-Tumoral Transcriptome Responses: Impact of GPER-1 mRNA on Survival. *J Cancer Res Clin Oncol* (2020) 146:3175–88. doi: 10.1007/s00432-020-03333-4

15. Brescia S. Thresholds of Adversity and Their Applicability to Endocrine Disrupting Chemicals. *Crit Rev Toxicol* (2020) 50:213–8. doi: 10.1080/10408444.2020.1740973
16. Wang C, Lv X, He C, Hua G, Tsai MY, Davis JS. The G-Protein-Coupled Estrogen Receptor Agonist G-1 Suppresses Proliferation of Ovarian Cancer Cells by Blocking Tubulin Polymerization. *Cell Death Dis* (2013) 4:e869. doi: 10.1038/cddis.2013.397
17. Galindo-Villegas J, García-Moreno D, de Oliveira S, Meseguer J, Mulero V. Regulation of Immunity and Disease Resistance by Commensal Microbes and Chromatin Modifications During Zebrafish Development. *Proc Natl Acad Sci USA* (2012) 109:E2605–14. doi: 10.1073/pnas.1209920109
18. Siriyappagouder P, Galindo-Villegas J, Dhanasiri AKS, Zhang Q, Mulero V, Kiron V, et al. Pseudozyma Priming Influences Expression of Genes Involved in Metabolic Pathways and Immunity in Zebrafish Larvae. *Front Immunol* (2020) 11:978. doi: 10.3389/fimmu.2020.00978
19. Pirr S, Viemann D. Host Factors of Favorable Intestinal Microbial Colonization. *Front Immunol* (2020) 11:584288. doi: 10.3389/fimmu.2020.584288
20. Siriyappagouder P, Galindo-Villegas J, Lokesh J, Mulero V, Fernandes JMO, Kiron V. Exposure to Yeast Shapes the Intestinal Bacterial Community Assembly in Zebrafish Larvae. *Front Microbiol* (2018) 9:1868. doi: 10.3389/fmicb.2018.01868
21. Egerton S, Culloty S, Whooley J, Stanton C, Ross RP. The Gut Microbiota of Marine Fish. *Front Microbiol* (2018) 9:1–17. doi: 10.3389/fmicb.2018.00873
22. Xiao Joe JT, Tseng Y-C, Wu J-L, Lu M-W. The Alteration of Intestinal Microbiota Profile and Immune Response in Epinephelus Coioides During Pathogen Infection. *Life (Basel)* (2021) 11(2):99. doi: 10.3390/life11020099
23. Montalban-Arques A, De Schryver P, Bossier P, Gorkiewicz G, Mulero V, Gatlin DM, et al. Selective Manipulation of the Gut Microbiota Improves Immune Status in Vertebrates. *Front Immunol* (2015) 6:512. doi: 10.3389/fimmu.2015.00512
24. Cheesman SE, Neal JT, Mittge E, Seredick BM, Guillemin K. Epithelial Cell Proliferation in the Developing Zebrafish Intestine Is Regulated by the Wnt Pathway and Microbial Signaling *via* Myd88. *Proc Natl Acad Sci USA* (2011) 108 Suppl 1:4570–7. doi: 10.1073/pnas.1000072107
25. Sommer F, Bäckhed F. The Gut Microbiota–Masters of Host Development and Physiology. *Nat Rev Microbiol* (2013) 11:227–38. doi: 10.1038/nrmicro2974
26. Chen KL, Madak-Erdogan Z. Estrogen and Microbiota Crosstalk: Should We Pay Attention? *Trends Endocrinol Metab* (2016) 27:752–5. doi: 10.1016/j.tem.2016.08.001
27. Ervin SM, Li H, Lim L, Roberts LR, Liang X, Mani S, et al. Gut Microbial β-Glucuronidases Reactivate Estrogens as Components of the Estrobolome That Reactivate Estrogens. *J Biol Chem* (2019) 294:18586–99. doi: 10.1074/jbc.RA119.010950
28. Plottel CS, Blaser MJ. Microbiome and Malignancy. *Cell Host Microbe* (2011) 10:324–35. doi: 10.1016/j.chom.2011.10.003
29. Aguilera M, Gálvez-Ontiveros Y, Rivas A. Endobolome, A New Concept for Determining the Influence of Microbiota Disrupting Chemicals (MDC) in Relation to Specific Endocrine Pathogenesis. *Front Microbiol* (2020) 11:578007. doi: 10.3389/fmicb.2020.578007
30. Cabas I, Rodenas MC, Abellán E, Meseguer J, Mulero V, García-Ayala A. Estrogen Signaling Through the G Protein-Coupled Estrogen Receptor Regulates Granulocyte Activation in Fish. *J Immunol* (2013) 191:4628–39. doi: 10.4049/jimmunol.1301613
31. Liarte S, Chaves-Pozo E, Abellán E, Meseguer J, Mulero V, García-Ayala A. 17β-Estradiol Regulates Gilthead Seabream Professional Phagocyte Responses Through Macrophage Activation. *Dev Comp Immunol* (2011) 35:19–27. doi: 10.1016/j.dci.2010.07.007
32. Rodenas MC, Cabas I, Abellán E, Meseguer J, Mulero V, García-Ayala A. Tamoxifen Persistently Disrupts the Humoral Adaptive Immune Response of Gilthead Seabream (Sparus Aurata L.). *Dev Comp Immunol* (2015) 53:283–92. doi: 10.1016/j.dci.2015.06.014
33. Rodenas MC, Cabas I, García-Alcázar A, Meseguer J, Mulero V, García-Ayala A. Selective Estrogen Receptor Modulators Differentially Alter the Immune Response of Gilthead Seabream Juveniles. *Fish Shellfish Immunol* (2016) 52:189–97. doi: 10.1016/j.fsi.2016.03.041
34. Rodenas MC, Cabas I, Gómez-González NE, Arizcun M, Meseguer J, Mulero V, et al. Estrogens Promote the Production of Natural Neutralizing Antibodies in Fish Through G Protein-Coupled Estrogen Receptor 1. *Front Immunol* (2017) 8:736. doi: 10.3389/fimmu.2017.00736
35. Galindo-Villegas J, García-Alcazar A, Meseguer J, Mulero V. Aluminum Adjuvant Potentiates Gilthead Seabream Immune Responses But Induces Toxicity in Splenic Melanomacrophage Centers. *Fish Shellfish Immunol* (2019) 85:31–43. doi: 10.1016/j.fsi.2018.02.047
36. Cabas I, Liarte S, García-Alcázar A, Meseguer J, Mulero V, García-Ayala A. 17α-Ethynylestradiol Alters the Immune Response of the Teleost Gilthead Seabream (Sparus Aurata L.) Both *In Vivo* and *In Vitro*. *Dev Comp Immunol* (2012) 36:547–56. doi: 10.1016/j.dci.2011.09.011
37. Acosta F, Montero D, Izquierdo M, Galindo-Villegas J. High-Level Biocidal Products Effectively Eradicate Pathogenic γ-Proteobacteria Biofilms From Aquaculture Facilities. *Aquaculture* (2021) 532:736004. doi: 10.1016/j.aquaculture.2020.736004
38. Shved N, Berishvili G, D'Cotta H, Baroiller J-F, Segner H, Eppler E, et al. Ethinylestradiol Differentially Interferes With IGF-I in Liver and Extrahepatic Sites During Development of Male and Female Bony Fish. *J Endocrinol* (2007) 195:513–23. doi: 10.1677/JOE-07-0295
39. Angosto D, López-Muñoz A, García-Alcazar A, Meseguer J, Sepulcre MP, Mulero V. Aluminum Is a Powerful Adjuvant in Teleost Fish Despite Failing to Induce Interleukin-1β Release. *Dev Comp Immunol* (2018) 85:18–24. doi: 10.1016/j.dci.2018.03.017
40. López-Cánovas AE, Cabas I, Chaves-Pozo E, Ros-Chumillas M, Navarro-Segura L, López-Gómez A, et al. Nanoencapsulated Clove Oil Applied as an Anesthetic at Slaughtering Decreases Stress, Extends the Freshness, and Lengthens Shelf Life of Cultured Fish. *Foods* (2020) 9(12):1750. doi: 10.3390/foods9121750
41. Xu Z, Takizawa F, Parra D, Gómez D, von Gersdorff Jørgensen L, LaPatra SE, et al. Mucosal Immunoglobulins at Respiratory Surfaces Mark an Ancient Association That Predates the Emergence of Tetrapods. *Nat Commun* (2016) 7:10728. doi: 10.1038/ncomms10728
42. Rodríguez A, Esteban MA, Meseguer J. Phagocytosis and Peroxidase Release by Seabream (Sparus Aurata L.) Leucocytes in Response to Yeast Cells. *Anat Rec A Discovery Mol Cell Evol Biol* (2003) 272:415–23. doi: 10.1002/ar.a.10048
43. Chaves-Pozo E, Abellán E, Baixauli P, Arizcun M. An Overview of the Reproductive Cycle of Cultured Specimens of a Potential Candidate for Mediterranean Aquaculture, Umbrina Cirrosa. *Aquaculture* (2019) 505:137–49. doi: 10.1016/j.aquaculture.2019.02.039
44. Valero Y, López-Cánovas AE, Rodenas MC, Cabas I, García-Hernández P, Arizcun M, et al. Endocrine Disrupter Chemicals Affect the Humoral Antimicrobial Activities of Gilthead Seabream Males Even Upon the Cease of the Exposure. *Sci Rep* (2020) 10:7966. doi: 10.1038/s41598-020-64522-2
45. Haldar S, Maharajan A, Chatterjee S, Hunter SA, Chowdhury N, Hinenoya A, et al. Identification of Vibrio Harveyi as a Causative Bacterium for a Tail Rot Disease of Sea Bream Sparus Aurata From Research Hatchery in Malta. *Microbiol Res* (2010) 165:639–48. doi: 10.1016/j.micres.2009.12.001
46. Piazzon MC, Galindo-Villegas J, Pereiro P, Estensoro I, Calduch-Giner JA, Gómez-Casado E, et al. Differential Modulation of IgT and IgM Upon Parasitic, Bacterial, Viral, and Dietary Challenges in a Perciform Fish. *Front Immunol* (2016) 7:637. doi: 10.3389/fimmu.2016.00637
47. Pfaffl MW. A New Mathematical Model for Relative Quantification in Real-Time RT-PCR. *Nucleic Acids Res* (2001) 29:e45. doi: 10.1093/nar/29.9.e45
48. Yoon S-H, Ha S-M, Kwon S, Lim J, Kim Y, Seo H, et al. Introducing EzBioCloud: A Taxonomically United Database of 16S rRNA Gene Sequences and Whole-Genome Assemblies. *Int J Syst Evol Microbiol* (2017) 67:1613–7. doi: 10.1099/ijsem.0.001755
49. Langille MGI, Zaneveld J, Caporaso JG, McDonald D, Knights D, Reyes JA, et al. Predictive Functional Profiling of Microbial Communities Using 16S rRNA Marker Gene Sequences. *Nat Biotechnol* (2013) 31:814–21. doi: 10.1038/nbt.2676
50. Aramaki T, Blanc-Mathieu R, Endo H, Ohkubo K, Kanehisa M, Goto S, et al. KofamKOALA: KEGG Ortholog Assignment Based on Profile HMM and Adaptive Score Threshold. *Bioinformatics* (2020) 36(7):2251–2. doi: 10.1093/bioinformatics/btz859
51. Dhariwal A, Chong J, Habib S, King IL, Agellon LB, Xia J. MicrobiomeAnalyst: A Web-Based Tool for Comprehensive Statistical, Visual and Meta-Analysis of Microbiome Data. *Nucleic Acids Res* (2017) 45:W180–8. doi: 10.1093/nar/gkx295
52. Palacios-Flores K, García-Sotelo J, Castillo A, Uribe C, Morales L, Boege M, et al. Perfect Match Genomic Landscape Strategy: Refinement and Customization of Reference Genomes. *Proc Natl Acad Sci USA* (2021) 118 (14):e2025192118. doi: 10.1073/pnas.2025192118

53. Meng K-F, Ding L-G, Wu S, Wu Z-B, Cheng G-F, Zhai X, et al. Interactions Between Commensal Microbiota and Mucosal Immunity in Teleost Fish During Viral Infection With SVCV. *Front Immunol* (2021) 12:654758. doi: 10.3389/fimmu.2021.654758
54. Firmino JP, Galindo-Villegas J, Reyes-López FE, Gisbert E. Phytogenic Bioactive Compounds Shape Fish Mucosal Immunity. *Front Immunol* (2021) 12:695973. doi: 10.3389/fimmu.2021.695973
55. Chen Y, Li M, Yuan L, Xie Y, Li B, Xu W, et al. Growth, Blood Health, Antioxidant Status and Immune Response in Juvenile Yellow Catfish Pelteobagrus Fulvidraco Exposed to α-Ethinylestradiol (EE2). *Fish Shellfish Immunol* (2017) 69:1–5. doi: 10.1016/j.fsi.2017.08.003
56. Zheng Y, Houston KD. Glucose-Dependent GPER1 Expression Modulates Tamoxifen-Induced IGFBP-1 Accumulation. *J Mol Endocrinol* (2019) 63:103–12. doi: 10.1530/JME-18-0253
57. Waghulde H, Cheng X, Galla S, Mell B, Cai J, Pruett-Miller SM, et al. Attenuation of Microbiotal Dysbiosis and Hypertension in a Crispr/Cas9 Gene Ablation Rat Model of GPER1. *Hypertension* (2018) 72:1125–32. doi: 10.1161/HYPERTENSIONAHA.118.11175
58. Hosomi K, Kunisawa J. Impact of the Intestinal Environment on the Immune Responses to Vaccination. *Vaccine* (2020) 38:6959–65. doi: 10.1016/j.vaccine.2020.08.079
59. Lynn DJ, Pulendran B. The Potential of the Microbiota to Influence Vaccine Responses. *J Leukoc Biol* (2018) 103:225–31. doi: 10.1189/jlb.5MR0617-216R
60. Piazzon MC, Naya-Català F, Simó-Mirabet P, Picard-Sánchez A, Roig FJ, Calduch-Giner JA, et al. Sex, Age, and Bacteria: How the Intestinal Microbiota Is Modulated in a Protandrous Hermaphrodite Fish. *Front Microbiol* (2019) 10:2512. doi: 10.3389/fmicb.2019.02512
61. Panteli N, Mastoraki M, Nikouli E, Lazarina M, Antonopoulou E, Kormas KA. Imprinting Statistically Sound Conclusions for Gut Microbiota in Comparative Animal Studies: A Case Study With Diet and Teleost Fishes. *Comp Biochem Physiol Part D Genomics Proteomics* (2020) 36:100738. doi: 10.1016/j.cbd.2020.100738
62. Firmino JP, Vallejos-Vidal E, Balebona MC, Ramayo-Caldas Y, Cerezo IM, Salomón R, et al. Diet, Immunity, and Microbiota Interactions: An Integrative Analysis of the Intestine Transcriptional Response and Microbiota Modulation in Gilthead Seabream (Sparus Aurata) Fed an Essential Oils-Based Functional Diet. *Front Immunol* (2021) 12:625297. doi: 10.3389/fimmu.2021.625297
63. Stojanov S, Berlec A, Štrukelj B. The Influence of Probiotics on the Firmicutes/Bacteroidetes Ratio in the Treatment of Obesity and Inflammatory Bowel Disease. *Microorganisms* (2020) 8(11):1715. doi: 10.3390/microorganisms8111715
64. Maciuszek M, Pijanowski L, Pekala-Safinska A, Palichleb P, Błachut M, Verburg-van Kemenade BML, et al. 17α-Ethinylestradiol and 4-Tert-Octylphenol Concurrently Disrupt the Immune Response of Common Carp. *Fish Shellfish Immunol* (2020) 107:238–50. doi: 10.1016/j.fsi.2020.10.005
65. Balasch JC, Tort L. Netting the Stress Responses in Fish. *Front Endocrinol (Lausanne)* (2019) 10:62. doi: 10.3389/fendo.2019.00062
66. Benedek G, Zhang J, Nguyen H, Kent G, Seifert HA, Davin S, et al. Estrogen Protection Against EAE Modulates the Microbiota and Mucosal-Associated Regulatory Cells. *J Neuroimmunol* (2017) 310:51–9. doi: 10.1016/j.jneuroim.2017.06.007
67. Flores R, Shi J, Fuhrman B, Xu X, Veenstra TD, Gail MH, et al. Fecal Microbial Determinants of Fecal and Systemic Estrogens and Estrogen Metabolites: A Cross-Sectional Study. *J Transl Med* (2012) 10:253. doi: 10.1186/1479-5876-10-253
68. Jami M, Ghanbari M, Kneifel W, Domig KJ. Phylogenetic Diversity and Biological Activity of Culturable Actinobacteria Isolated From Freshwater Fish Gut Microbiota. *Microbiol Res* (2015) 175:6–15. doi: 10.1016/j.micres.2015.01.009
69. Triplett KD, Pokhrel S, Castleman MJ, Daly SM, Elmore BO, Joyner JA, et al. GPER Activation Protects Against Epithelial Barrier Disruption by Staphylococcus Aureus α-Toxin. *Sci Rep* (2019) 9:1343. doi: 10.1038/s41598-018-37951-3
70. Dhakal D, Pokhrel AR, Shrestha B, Sohng JK. Marine Rare Actinobacteria: Isolation, Characterization, and Strategies for Harnessing Bioactive Compounds. *Front Microbiol* (2017) 8:1106. doi: 10.3389/fmicb.2017.01106
71. Binda C, Lopetuso LR, Rizzatti G, Gibiino G, Cennamo V, Gasbarrini A. Actinobacteria: A Relevant Minority for the Maintenance of Gut Homeostasis. *Dig Liver Dis* (2018) 50:421–8. doi: 10.1016/j.dld.2018.02.012
72. Salwan R, Sharma V. Molecular and Biotechnological Aspects of Secondary Metabolites in Actinobacteria. *Microbiol Res* (2020) 231:126374. doi: 10.1016/j.micres.2019.126374
73. Ibero J, Galán B, Rivero-Buceta V, García JL. Unraveling the 17β-Estradiol Degradation Pathway in Novosphingobium Tardaugens NBRC 16725. *Front Microbiol* (2020) 11:588300. doi: 10.3389/fmicb.2020.588300
74. Hegedüs B, Kós PB, Bende G, Bounedjoum N, Maróti G, Laczi K, et al. Starvation- and Xenobiotic-Related Transcriptomic Responses of the Sulfanilic Acid-Degrading Bacterium, Novosphingobium Resinovorum SA1. *Appl Microbiol Biotechnol* (2018) 102:305–18. doi: 10.1007/s00253-017-8553-5
75. Kormas KA, Meziti A, Mente E, Frentzos A. Dietary Differences Are Reflected on the Gut Prokaryotic Community Structure of Wild and Commercially Reared Sea Bream (Sparus Aurata). *Microbiologyopen* (2014) 3:718–28. doi: 10.1002/mbo3.202
76. Jiang I, Yong PJ, Allaire C, Bedaiwy MA. Intricate Connections Between the Microbiota and Endometriosis. *Int J Mol Sci* (2021) 22(11):5644. doi: 10.3390/ijms22115644
77. Zhang R, Kang R, Klionsky DJ, Tang D. Ion Channels and Transporters in Autophagy. *Autophagy* (2021) 1–20. doi: 10.1080/15548627.2021.1885147
78. Galindo-Villegas J, Montalban-Arques A, Liarte S, de Oliveira S, Pardo-Pastor C, Rubio-Moscardo F, et al. TRPV4-Mediated Detection of Hyposmotic Stress by Skin Keratinocytes Activates Developmental Immunity. *J Immunol* (2016) 196:738–49. doi: 10.4049/jimmunol.1501729
79. Ramírez-Barrantes R, Carvajal-Zamorano K, Rodriguez B, Cordova C, Lozano C, Simon F, et al. TRPV1-Estradiol Stereospecific Relationship Underlies Cell Survival in Oxidative Cell Death. *Front Physiol* (2020) 11:444. doi: 10.3389/fphys.2020.00444
80. Huang N, Wang M, Peng J, Wei H. Role of Arachidonic Acid-Derived Eicosanoids in Intestinal Innate Immunity. *Crit Rev Food Sci Nutr* (2020) 61(14):2399–410. doi: 10.1080/10408398.2020.1777932
81. Wu J, Liu Y, Dou Z, Wu T, Liu R, Sui W, et al. Black Garlic Melanoidins Prevent Obesity, Reduce Serum LPS Levels and Modulate the Gut Microbiota Composition in High-Fat Diet-Induced Obese C57BL/6J Mice. *Food Funct* (2020) 11:9585–98. doi: 10.1039/d0fo02379e
82. Magalhães R, Guerreiro I, Coutinho F, Moutinho S. Effect of Dietary ARA/EPA/DHA Ratios on Growth Performance and Intermediary Metabolism of Gilthead Sea Bream (Sparus Aurata) Juveniles. *Aquaculture* (2020) 516:734644. doi: 10.1016/j.aquaculture.2019.734644

Conflict of Interest: The authors declare that the research was conducted in the absence of any commercial or financial relationships that could be construed as a potential conflict of interest.

Publisher's Note: All claims expressed in this article are solely those of the authors and do not necessarily represent those of their affiliated organizations, or those of the publisher, the editors and the reviewers. Any product that may be evaluated in this article, or claim that may be made by its manufacturer, is not guaranteed or endorsed by the publisher.

frontiers in Immunology

ORIGINAL RESEARCH
published: 20 October 2021
doi: 10.3389/fimmu.2021.693932

Essential Oils Improve the Survival of Gnotobiotic Brine Shrimp (*Artemia franciscana*) Challenged With *Vibrio campbellii*

Xiaoting Zheng[1,2], Biao Han[1,3], Vikash Kumar[1,4], Adam F. Feyaerts[5,6], Patrick Van Dijck[5,6] and Peter Bossier[1]**

[1] Laboratory of Aquaculture & Artemia Reference Center, Department of Animal Science and Aquatic Ecology, Faculty of Bioscience Engineering, Ghent University, Ghent, Belgium, [2] Key Laboratory of South China Sea Fishery Resources Exploitation & Utilization, Ministry of Agriculture and Rural Affairs, South China Sea Fisheries Research Institute, Chinese Academy of Fishery Sciences, Guangzhou, China, [3] Key Laboratory for Healthy and Safe Aquaculture, Institute of Modern Aquaculture Science and Engineering, School of Life Sciences, South China Normal University, Guangzhou, China, [4] Aquatic Environmental Biotechnology & Nanotechnology (AEBN), ICAR-Central Inland Fisheries Research Institute, Kolkata, India, [5] Vlaam Instituut voor Biotechnologie, Katholieke Univeriteit (VIB-KU) Leuven Center for Microbiology, Leuven, Belgium, [6] Laboratory of Molecular Cell Biology, Institute of Botany and Microbiology, Katholieke Univeriteit (KU) Leuven, Leuven, Belgium

OPEN ACCESS

Edited by:
Shoichiro Kurata, Tohoku University, Japan

Reviewed by:
Chengbo Sun, Guangdong Ocean University, China
Han-Ching Wang, National Cheng Kung University, Taiwan

***Correspondence:**
Peter Bossier
Peter.Bossier@ugent.be
Xiaoting Zheng
Xiaoting.Zheng@ugent.be

Specialty section:
This article was submitted to Comparative Immunology, a section of the journal Frontiers in Immunology

Received: *12 April 2021*
Accepted: *28 September 2021*
Published: *20 October 2021*

Citation:
Zheng X, Han B, Kumar V, Feyaerts AF, Van Dijck P and Bossier P (2021) Essential Oils Improve the Survival of Gnotobiotic Brine Shrimp (Artemia franciscana) Challenged With Vibrio campbellii. Front. Immunol. 12:693932. doi: 10.3389/fimmu.2021.693932

The halophilic aquatic bacterium *Vibrio campbellii* is an important aquatic pathogen, capable of causing vibriosis in shrimp and fish resulting in significant economic losses. In a previous work, essential oils (EOs) extracts from *Melaleuca alternifolia*, *Litsea citrata*, and *Eucalyptus citriodora* were found to inhibit the growth of *V. campbellii in vitro*. This study aimed to determine *in vivo* EOs' potential protective effect towards gnotobiotic brine shrimp *Artemia franciscana*, challenged with *V. campbellii*. The study showed that brine shrimp larvae supplemented with EOs of *M. alternifolia* (0.0008%) and *L. citrata* (0.002%) displayed significantly increased survival against *V. campbellii*. The results indicated that supplementation of these EOs increased the expression of immune-related genes (either in the presence or absence of the pathogen), probably contributing to enhanced protection. Furthermore, *in vitro* studies indicated that some EOs modulated the expression of virulence factors including swimming motility, biofilm formation, and gelatinase and lipase activity, while flow cytometry data and regrowth assay indicated that these EOs do not exhibit antimicrobial activity as *V. campbellii* grew at the tested concentrations [*M. alternifolia* (0.0008%) and *L. citrata* (0.002%)]. Our findings suggest that EOs extracted from *M. alternifolia* and *L. citrata*, can modulate virulence factor production and immunological responses and might hence become part of an intervention strategy to control vibriosis in a fish or shrimp aquaculture setting, a hypothesis that needs to be validated in the future.

Keywords: essential oil, *Vibrio campbellii*, *Artemia franciscana*, survival, immune gene, virulence factor

INTRODUCTION

The Gram-negative motile marine bacterium *Vibrio campbellii* is one of the most important pathogens in shrimp or fish culture, resulting in serious economic losses in aquaculture (1). The pathogenicity of *V. campbellii* is determined by its ability of biofilm formation, swimming motility, and the production of various degradative enzymes, such as hemolysins, gelatinases, lipases, and phospholipases (2). In many cases, *Vibrio* is an opportunistic pathogen. They cause disease only when the host organism is immune suppressed or otherwise physiologically stressed (3). Therefore, to prevent *V. campbellii*–based vibriosis in aquatic animals, an approach that focuses on understanding the host immune response of any potential mitigation strategy is warranted.

Traditionally, the non-judicious use or overuse of antibiotics and disinfectants applied to cure infections caused by *Vibrio* had limited success, resulting in the emergence of bacterial resistance (4). Because of such concerns, there is an urgent need for the development of plant-derived compounds or natural products that protect aquatic animals and enhance the immune reactivity towards *V. campbellii* infection. However, a major challenge in studying the biological activity of natural compounds *in vivo* is the difficulty to either eliminate or extricate the influence of the microbial communities that occur in the natural environment. Besides, in germ-associated conditions, natural components are not only metabolized by the microbial communities but also influence the physiology of the host-related microbes (5). Consequently, it is paramount to select an appropriate animal model system that permits better delineation of the biological effects of the natural components.

The brine shrimp *Artemia franciscana* is an aquatic invertebrate that can be reared under gnotobiotic conditions (a germ-free system that allows for full control over the host-associated microbial communities). This model allows for distinguishing the direct effect on the host (by pre-exposing axenic brine shrimp larvae to a compound of interest for a certain duration) from indirect effects (6).

The International Standard Organization (ISO) defines essential oils as concentrated relatively hydrophobic liquids containing relatively volatile chemical compounds. They can be obtained from different parts of the plant, such as seeds, roots, buds, leaves, flowers, peels, and fruits, by the methods of steam distillation or (cold) pression (7). Given their bactericidal and fungicidal properties, EO application in the aquaculture industry is becoming more and more widespread as an alternative in controlling pathogens. For instance, the EO of *Syzygium aromaticum* inhibits fish systemic bacteria (8). Oregano essential oil can not only act as a growth promoter but also improves resistance to *Aeromonas hydrophila* when supplied to channel catfish *(Ictalurus punctatus)* feed (9). The EOs extracted from the leaves of *Lippia sidoides* and *Mentha piperita* can kill the gill parasites of Nile tilapia (10).

Furthermore, in our previous work, 22 different EOs were screened for their possible anti–*V. campbellii* activity (11). The results demonstrated that EOs of *Melaleuca alternifolia*, *Litsea citrata*, and *Eucalyptus citriodora* were the three best candidates to inhibit the growth of *V. campbellii.* However, whether the selected EOs could modulate the *in vitro* production of *V. campbellii* BB120 virulence factors was not documented. Additionally, the immunomodulatory properties of these EOs that could lead to enhanced protection against pathogenic *V. campbellii* BB120 of the experimental animals have not been verified in this model. Hence, the present study aimed to investigate whether the selected EOs induce an innate immune response in brine shrimp larvae and/or regulate the virulence of pathogenic *V. campbellii in vitro*.

MATERIAL AND METHODS

Selected EOs and DMSO

EOs of *Melaleuca alternifolia*, *Litsea citrata*, and *Eucalyptus citriodora* were purchased from Pranarôm International S.A. (Ghislenghien, Belgium). Based on our previous study, the three essential oils mentioned above were selected to use in this study (11). The chemical composition of these three essential oils was characterized (**Supplementary Information 1**). All EOs were kept in the brown sterile glass vial and stored at 4°C. Dimethyl sulfoxide (DMSO) was purchased from VWR International (Leuven, Belgium).

Vibrio campbellii Strain and Growth Conditions

V. campbellii wild-type strain ATCC BAA-1116 (BB120), stored in 20% sterile glycerol at −80°C, was used in the challenge assays. This strain was reactivated by streaking from the stock solution onto Luria-Bertani agar plates (Carl Roth, Karlsruhe, Germany) containing 35 g/L of sodium chloride (LB_{35}). Subsequently, a pure colony was transferred to and cultured overnight in LB_{35} broth (Carl Roth, Karlsruhe, Germany) by incubation at 28°C with continuous shaking (120 rpm). Bacterial cell densities were measured by spectrophotometry at 600 nm.

Axenic Hatching of Brine Shrimp Larvae *Artemia franciscana*

Axenic brine shrimp larvae were obtained following the decapsulation and hatching process based on the method described before (12). Briefly, 200 mg of brine shrimp cysts originating from the Great Salt Lake, Utah, USA (EG Type, batch 1871, INVE Aquaculture, Dendermonde, Belgium) were hydrated in 18 ml of filter-sterilized distilled water for 1 h. Then, sterile cysts and larvae were obtained by decapsulation, adding 660 µl NaOH (32%) and 10 ml NaClO (50%). The decapsulation process was stopped after about 2 min by using 14 ml $Na_2S_2O_3$ at 10 g/L. Filtered aeration (0.22 µm) was provided during the reaction. The aeration was then terminated, and the decapsulated cysts were washed with filtered (0.2 µm) autoclaved artificial seawater (FASW) containing 35 g/L of instant ocean synthetic sea salt (Aquarium Systems, Sarrebourg, France). All manipulations were conducted under a laminar flow hood, and all tools were autoclaved at 121°C for 20 min. Afterwards, the cysts were

suspended in a 50 ml falcon tube containing 30 ml FASW and incubated for 28 h on a rotor at 6 rpm at 28°C with constant illumination of approximately 2,000 lux.

Evaluation of Selected EOs Toxicity in Brine Shrimp Larvae

After 28 h of hatching, the larvae at instar II stage (when they started ingesting particles) were randomly collected (n=20) and transferred to fresh, sterile 40 ml glass tubes containing 10 ml of FASW. The glass tubes with axenic larvae were added with increasing concentrations of essential oil from 0.0005 to 0.005%, in 1% of DMSO and fed once with 10^7 cells/ml autoclaved LVS3 (a feed for *Artemia*). The control group were supplemented with only 1% of DMSO. Afterwards, the tubes were put to the rotor and kept at 28°C. Survival of the larvae was recorded at 48 h after exposure to EOs. Four replicates were maintained for all treatments, and each experiment was repeated twice to verify the reproducibility. In each experiment, the sterility of the control and treatment groups was checked at the end of the toxicity assay by inoculating 1 ml of rearing water to 9 ml of LB_{35} and incubating the mixture for 2 days at 28°C (13).

Brine Shrimp Larvae Challenge Assay

The challenge test was performed as described by Yang et al. (12) with some modifications. Twenty larvae at development stage II were collected and transferred to fresh, sterile 40 ml glass tubes containing 10 ml of FASW as described above in the toxicity assay. A suspension of autoclaved LVS3 bacteria in each glass tubes was added as feed at the start of the challenge test at 10^7 cells/ml in all the treatments. Subsequently, the tubes were supplemented with increasing concentrations of selected EOs from 0.0001 to 0.001% (*M. alternifolia*), 0.003% (*L. citrata*), and 0.0008% (*E. citriodora*), respectively, in 1% of DMSO. The larvae not supplemented with EOs and challenged with *V. campbellii* served as the positive control, while non-supplemented larvae groups without challenge (but with 1% of DMSO supplemented) were used as the negative control. Afterwards, the larvae were challenged with *V. campbellii* at 10^7 cells/ml. The survival of larvae was scored after 48 h of *V. campbellii* challenge. Four replicates were maintained for all treatments, and the experiment was repeated twice to verify the reproducibility. In the experiment, the sterility of the negative control group was checked at the end of the survival assay by inoculating 1 ml of rearing water to 9 ml of LB_{35} and incubating the mixture for 2 days at 28°C (13). Relative percent of survival (%, RPS) was calculated by equation: = (1 − (% mortality in the EO treated group/% mortality in the control group)) × 100 (14).

Assay of Immune-Related Genes Expression in the Optimized Dose of EOs by Reverse Transcriptase Real-Time PCR

After 28 h incubation at 28°C, the instar II stage swimming *Artemia* nauplii were collected, counted volumetrically, and transferred to 1 L sterile glass bottles containing 500 ml FASW. The nauplii were fed once with 10^7 cells/ml of autoclaved LVS3. Afterwards, the nauplii were treated with an optimized dose of selected essential oils (based on the result of the dose-response study) and challenged with *V. campbellii* at 10^7 cells/ml. Non-challenged larvae groups (in 1% of DMSO) were used as control. Each treatment was carried out in triplicate. Samples containing 25 mg of live larvae were harvested from all treatments and control groups at 6, 12, and 24 h after addition of *V. campbellii*, rinsed in distilled water, immediately frozen in liquid nitrogen, and stored at −80°C.

Total RNA was extracted from control and treatment group larvae samples using the RNeasy Plus Mini Kit (Qiagen, Germany) according to the manufacturer's instructions. The genomic DNA was eliminated with a gDNA eliminator spin in the kit when isolating the RNA. The quality and quantity of RNA were confirmed by NanoDrop™ 2000 (Thermo Scientific, USA). Then 2 μg of total RNA was used to synthesize the first-strand cDNA using RevertAid H Minus First Strand cDNA Synthesis Kit (Thermo Scientific, USA) with an oligo (dT) primer. The reverse transcription quantitative PCR (RT-qPCR) assay was performed on Step One Plus Real-Time System (Applied Biosystems, USA) using Maxima SYBR Green/ROX qPCR Master Mix (2X) (Thermo Scientific, USA) in a total volume of 20 μl, containing 10 μl of 2X SYBR green master mix, 1 μl of forward and reverse primers (10 nM), 1 μl of template cDNA (10 ng), and 7 μl of nuclease-free water. The thermal cycling consisted of an initial denaturation at 95°C for 10 min followed by 40 cycles of denaturation at 95°C for 15 s and primer annealing and elongation at 60°C for 1 min. Dissociation curve analysis was performed to check for the amplification of untargeted fragments. Data acquisition was performed with the Rotor-Gene Q software version 2.0.2 (Qiagen, Germany). Two internal reference genes, *EF-1* and *GAPDH*, were introduced to normalize the qPCR data. Gene specific primers (designed by cross-exon strategy and the software PRIMER PREMIER version 5.0) were described by previous studies (15) and shown in **Table 1**.

The expression of the target genes was normalized to the endogenous control (Geomean of *EF-1* and *GAPDH*) by calculating ΔC_T:

$$\Delta C_T = C_{T,\text{ target}} - C_{T,\text{ Geomean of } EF-1 \text{ and } GAPDH}$$

and expressed relative to the calibrator sample by calculating $\Delta\Delta C_T$:

$$\Delta\Delta C_T = \Delta C_T - \Delta C_{T,\text{calibrator}}$$

The sample of unchallenged *Artemia* (1% of DMSO) at 6 h was used as a calibrator. The relative expression was then calculated as

$$\text{Relative expression} = 2^{-\Delta\Delta CT}$$

At each time point, the relative gene expression in the unchallenged control group was set at 1.0, and the gene expression of the remaining groups was normalized accordingly. If the fold change was significant and higher than 2, the EO was considered to have an immunostimulatory effect.

TABLE 1 | Specific primers used for reverse transcriptase qPCR.

Gene	Primer sequences (5'-3')
EF-1	TCGACAAGAGAACCATTGAAAA
	ACGCTCAGCTTTAAGTTTGTCC
GAPDH*	GTTGATGGCAAACTCGTCATA
	CCACCTTCCAAGTGAGCATTA
hsp70	CGATAAAGGCCGTCTCTCCA
	CAGCTTCAGGTAACTTGTCCTTG
sod	CAATCAGCATTGGGGTTTGTC
	GAATCTCTTCGTTGGTTGTAGGG
dscam	TCAAGAGGCTGAAAGAGAAGAAAT
	CAGTAGAAGCAGTGACCCAGAAAT
lgbp	CCGTGAAGATCCCAACGAAC
	GGAGGAGGTAATTGGGAGTTTCAAGG
hmgb	AGAGGCGGGAAAGGAAGC
	CCCACACCAAGACCAGGTTG
pxn	TTGGTGCTGCTGCTTTTCG
	CCCCATCGCTTGTCTTCGT
tgase 1	GCAAGGAGCTGGAATGGGT
	TGTTTGGGAGTTAATCGGACTGT
tgase 2	TTCTTTACACAGGCATTCCGTC
	GTTACATCAAATCCCAGCTCCA

*EF-1, elongation factor 1; GAPDH, glyceraldehyde-3-phosphate dehydrogenase; hsp70, heat shock protein 70; sod, superoxidase dismutase; dscam, down syndrome cell adhesion molecule; lgbp, lipopolysaccharide and β-1,3-glucan-binding protein; hmgb, high mobility group box protein; tgase 1, transglutaminase 1; tgase 2, transglutaminase 2. *Adapted from Chen et al. (16).*

Effect of Selected Essential Oils on Cell Viability and Growth Performance of *V. campbellii*

To determine the effect of selected essential oils on the viability of bacterial cells, the proportion of live or dead cells in the bacterial culture was investigated by flow cytometry and regrowth test. For that, the concentration of overnight *V. campbellii* culture was adjusted to 10^8 cells/ml and was subsequently diluted with FASW to 10^6 cells/ml. Then, the EOs of *M. alternifolia* (at the concentrations of 0.0005, 0.0008, 0.001, and 0.01%), *L. citrata* (at the concentrations of 0.001, 0.002, 0.003, and 0.01%), and *E. citriodora* (at the concentrations of 0.0003, 0.0005, 0.0008, and 0.01%) were dissolved in 1% DMSO and added to 1 ml of the acquired bacterial culture in Eppendorf tubes. The tubes containing only 1% DMSO with bacterial culture served as the negative control. Afterwards, all Eppendorf tubes were incubated at 28°C for 1 h on the rotor (6 rpm).

Later, 100 µl of the bacterial culture was placed into each well of the 96-well black microtiter plate with the flat bottom (SPL Life Sciences) together with 5 µl Thiazole Orange (17 mM) and 5 µl Propidium Iodide (0.15 mM). The mixture of 100 µl of FASW and dyes was used as the blank. The experiment was conducted in triplicate, corresponding to three wells of the plate. The plate was then covered by the lid for 10 min for the staining reaction. The amount of live and dead bacterial cells was then determined by the CytoFLEX instrument (Beckman Coulter, USA).

For the regrowth assay, 10 µl of the bacterial culture was added to 990 µl of LB_{35} broth. Then, 200 µl volume of this suspension was put in 96-well transparent plate with the flat bottom (VWR International) at 28°C with shaking for 48 h, and the cell density at 600 nm was monitored every hour using a Tecan Infinite 200 microplate reader (Tecan, Mechelen, Belgium) after resuspending the cells. Each concentration of EO had four replicates, and the growth curve was determined for three independent cultures.

Swimming Motility Assay

The swimming motility assay was performed on soft agar (LB_{35} plates containing 0.2% agar) as described previously (12) with some modification. The optimized doses of essential oils (based on the dose-response result) dissolved in 1% DMSO were added to the autoclaved agar, when the agar was cooled down to 40°C. Each plate was closed with a lid immediately after pouring the medium to maintain equal moisture in plates by preventing evaporation. *V. campbellii* was grown overnight in LB_{35} broth, and 2 µl aliquots (OD_{600} = 0.1) were spotted in the center of the soft agar plates. Plates were incubated at 28°C for 24 h, after which the diameters of the motility halos were measured. All assays were done with freshly prepared media in four replicates.

Biofilm Formation Assay

Biofilm formation assay was quantified by crystal violet staining, as described previously (12). In brief, *V. campbellii* was grown overnight and diluted to an OD_{600} of 0.1 in marine broth with or without essential oils, and 200 µl aliquots of these suspensions were pipetted into the wells of a 96-well plate. Then, the bacteria suspensions were incubated without agitation for 24 h at 28°C. After that, the cultures were removed, and the wells were washed three times with 300 µl sterile physiological saline to remove all non-adherent bacteria. The remaining attached bacteria were fixed with 200 µl/well of 99% methanol for 2 h, after which the methanol was removed and plates were air-dried overnight. Then, biofilms were stained for 20 min with 200 µl/well of a 0.1% crystal violet solution (Pro-lab Diagnostics, Richmond Hill, ON, Canada). Excess stain was rinsed off by placing the plate under running tap water, and washing was continued until the washings were free of the stain. After the plates were air dried, the dye bound to the adherent cells was resolubilized with 200 µl/well of 95% ethanol, and absorbance was measured at 570 nm with a Multi-reader (Infinite M200, TECAN, Austria). Five replicates of two independent bacteria cultures were maintained for all treatments in this test, and the experiment was repeated twice to verify the reproducibility.

Lytic Enzyme Activity Assays

All assays were conducted according to Natrah et al. (17). For each assay, an overnight culture of *V. campbellii* was diluted to an OD_{600} of 0.5, and 2 µl of the diluted culture was spotted in the middle of the test plates. The optimized doses of essential oils dissolved in 1% DMSO were added to the autoclaved agar, when the agar was cooled down to 40°C. All assays were done in quintuplicate. Similarly, the lipase and phospholipase activities were assessed on marine agar plates supplemented with 1% Tween 80 (Sigma-Aldrich) and 1% egg yolk emulsion (Sigma-Aldrich), respectively. The development of opalescent zones around the colonies was observed, and the diameters of the zones were measured after 2–4 days of incubation at 28°C. Gelatinase assay plates were prepared by mixing 0.5% gelatin

(Sigma-Aldrich) into the agar. After incubation for 2 days, saturated ammonium sulfate (80%) in distilled water was poured over the plates, and after 2 min, the diameters of the clearing zones around the colonies were measured. Hemolytic assay plates were prepared by supplementing Marine Agar with 5% defibrinated sheep blood (Oxoid), and clearing zones were measured after 2 days of incubation.

Statistical Analyses

Data were expressed as mean ± SEM. The *Artemia* survival data were arcsin transformed to satisfy normal distribution and homoscedasticity requirements as necessary. Lethal concentration in media (LC_{50}) was determined by interpolation to a 4PL-Sigmoidal standard curve. Log transformed gene expression data were shown. For each gene, the expression in control was set at 1, and the expression in different treatments was normalized accordingly using the $2^{-\Delta\Delta CT}$ method. In the interaction studies, statistical analysis was performed using two-way ANOVA followed by Tukey test. Unless stated otherwise, all other data were compared with one-way ANOVA, followed by Tukey's *post hoc* test. Statistical analysis was performed using the IBM statistical software SPSS (version 22.0, IBM Corp., Armonk, New York, USA), and the results were shown using GraphPad Prism software (version 7, GraphPad Software, Inc., San Diego, CA, USA) and included all biological repeats. The significance level was set at $P < 0.05$.

RESULTS

In Vivo Toxicity (Lethal Concentration, $LC_{50\text{-}48h}$) of EOs

Firstly, it was investigated whether the EOs have cytotoxic effects on axenic brine shrimp larvae. Therefore, the toxicity of three EOs was determined for *Artemia* as $LC_{50\text{-}48h}$ (**Figure 1**): (i) EO of *M. alternifolia* (2.2492×10^{-3}%) with a 95% confidence interval (CI) ranging from 2.0977×10^{-3} to 2.4016×10^{-3}%, $R^2 = 0.983$), (ii) EO of *L. citrata* (4.1563×10^{-3}%, 95% CI = 3.9812×10^{-3} to 4.3313×10^{-3}%, $R^2 = 0.987$), and (iii) EO of *E. citriodora* (0.8349×10^{-3}%, 95% CI from 0.813×10^{-3} to 0.857×10^{-3}%, $R^2 = 0.9866$). According to **Figure 1**, these results suggested that the exposure with EO *M. alternifolia*, *L. citrata*, and *E. citriodora*, at concentrations with no more than 0.001, 0.002, and 0.0005%, respectively, are non-toxic to brine shrimp larvae and considered as safe concentrations to *Artemia*, with the survival of *Artemia* is > 90%.

EOs Protect Brine Shrimp Larvae Against Subsequent *V. campbellii* Challenge

Secondly, it was determined whether the EOs at safe concentrations (EO *M. alternifolia*: 0.0001, 0.0003, 0.0005, 0.0008, and 0.001%; EO *L. citrata*: 0.0001, 0.0003, 0.0005, 0.0008, 0.001, 0.002, and 0.003%; EO *E. citriodora*: 0.0001, 0.0003, 0.0005, and 0.0008%) could protect *Artemia* nauplii against a *V. campbellii* challenge. Furthermore, the effect of two parameters (different concentrations, with/without a *V. campbellii* challenge) and their interaction on the survival of brine shrimp were analyzed. As shown in **Figure 2** and **Tables 2**, **3**, brine shrimp larvae that were treated with EOs at safe doses displayed a significant increase in their survival compared to the control when challenged with *V. campbellii*. As shown previously, the *Vibrio* challenge reduced the survival of brine shrimp larvae. A dose-dependent increase in the survival rate was recorded upon treatment with the EOs. In addition, a significant synergistic interaction between the two experimental factors (namely, EO at different doses and *Vibrio* challenge) was observed, indicating that the EOs protect against the *Vibrio*. The highest relative percent survival was observed in the *Vibrio*-exposed groups treated with *L. citrata* with concentrations of 0.0003–0.002%. However, with further increases in EO concentrations, the survival tended to decrease, probably a result of EO-related toxicity.

EO-Generated Immune Gene Expression Mediates *In Vivo* Protective Response in Brine Shrimp Larvae

Since the survival of *Vibrio*-challenged brine shrimp larvae treated with EOs at an optimized dose was significantly increased, we further investigated whether it was due to the stimulation of immune-related genes expression *in vivo*, either in the absence or presence of *Vibrio* challenge To address this, germ-free *Artemia* were treated with the EOs of *M. alternifolia*, *L. citrata*, and *E. citriodora* at a concentrations of 0.0008, 0.002, and 0.0005%, respectively, and analyzed for immune-related genes expression. The main function of the eight selected genes

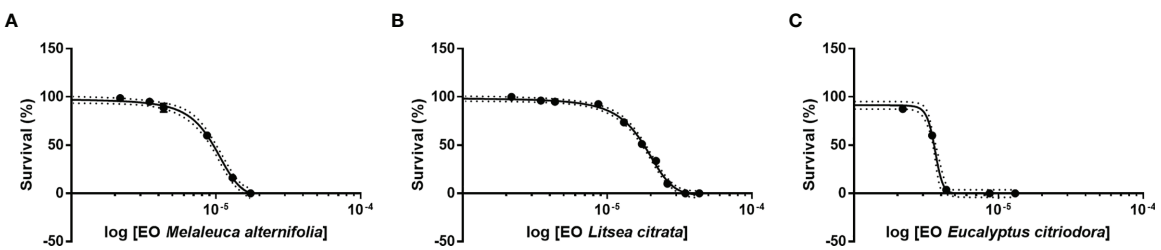

FIGURE 1 | Toxicity of three essential oils (*Melaleuca alternifolia, Litsea citrata,* and *Eucalyptus citriodora*) on *Artemia franciscana*. Survival was recorded 48 h after EOs treatment. **(A)** *Melaleuca alternifolia,* **(B)** *Litsea citrata,* **(C)** *Eucalyptus citriodora*. X axis represented log transformed concentrations data. The error bars represented the standard error of four replicates. Dotted line on charts represents 95% confidence intervals.

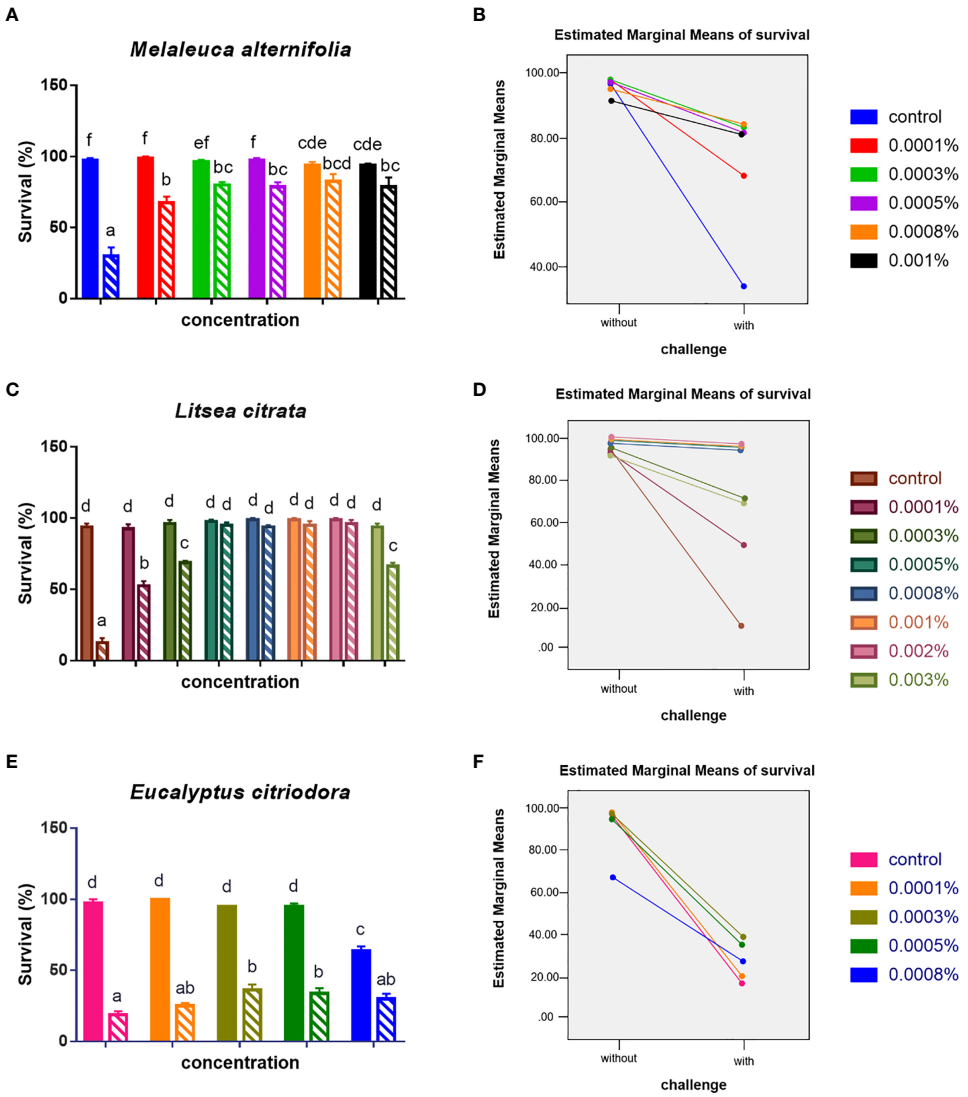

FIGURE 2 | Survival (mean ± SEM) of brine shrimp larvae 48 h after challenge with *Vibrio campbellii* BB120. **(A)** Treated with EO of *Melaleuca alternifolia*, **(C)** treated with EO of *Litsea citrata*, and **(E)** treated with EO of *Eucalyptus citriodora*. **(B, D, F)** showed the interaction plots between doses of each EO and with/without *V. campbellii* challenge, respectively, according to the output from two-way ANOVA. All treatments were carried out in four replicates. The bars without pattern were unchallenged groups; the opposite was challenged groups. Different letters indicated significant difference ($P < 0.05$). Control: no EO added but consisted of 1% of DMSO.

and their possible relationship with immunity in crustaceans are described in the supplementary information (**Supplementary Information 2**).

If the fold change (in one of the treatments) was higher than 2 and significant, the EO was considered to have an immunostimulatory effect. **Figure 3** showed that the expression level of *lgbp* is over two-fold higher at 12 and 24 h in the EO *M. alternifolia* group after the challenge. The *dscam* gene expression level was two-fold higher in the EO *M. alternifolia* group at 6 h, and in the EO *L. citrata* and *E. citriodora* groups at 12 h post challenge. The EO *L. citrata* group challenged with *V. campbellii* exhibited two-fold increase in the *hsp 70*, *sod*, and *pxn* gene expression level at 24 h time point. At 24 h after challenge, the *tgase 1* gene expression in all the EO groups was threefold higher than the control group.

In addition, **Figure 4** and **Table 4** showed a synergistic interaction of EO (*M. alternifolia*), and the challenge was observed at 6 h in the *dscam* and *hsp 70* gene expression. However, an antagonistic interaction of EO (*M. alternifolia*) and the challenge was observed at 6 h in the *hmgb*, *sod*, and *tagse1* gene expression. There was a significant antagonistic interaction between EO (*E. citriodora*) and the challenge at 6 h in the *hmgb*, *sod*, *tgase1*, and *tgase2* gene expression, and at 24 h in the *hmgb*, *pxn*, and *tgase2* gene expression. In addition, there were no interaction effects between *L. citrata* and challenge in the gene expression.

TABLE 2 | A summary table with EOs' lethal concentrations to 50% (LC50) value, 10% (LC10) value, and the EOs' concentration of relative precent of survival 50% (RPS 50) and 90% (RPS 90) of *Artemia*.

Essential oil of plant species	LC 50 (%)	LC 10 (%)	RPS 50 (%)	RPS 90 (%)
Melaleuca alternifolia	0.002	0.001	<0.0001	N
Litsea citrata	0.004	0.002	<0.0001	0.0003–0.002
Eucalyptus citriodora	0.0008	0.0005	N	N

Relative percent of survival (%, RPS) was calculated by equation: = (1 – (% mortality in the EO treated group/% mortality in the control group)) × 100 (14).
N, non-observed.

TABLE 3 | Two-way ANOVA showed main and interaction effects of indicated concentrations of essential oils and with or without *Vibrio campbellii* challenge on the survival of brine shrimp larvae.

Essential oil of plant species	Factors	*P* value	*P* value summary
Melaleuca alternifolia	concentrations	<0.0001	****
	challenge	<0.0001	****
	concentrations × challenge	<0.0001	****
Litsea citrata	concentrations	<0.0001	****
	challenge	<0.0001	****
	concentrations × challenge	<0.0001	****
Eucalyptus citriodora	concentrations	<0.0001	****
	challenge	<0.0001	****
	concentrations × challenge	<0.0001	****

*The larvae were treated with essential oils at indicated concentrations either alone or challenged with or without V. campbellii at 10^7 cells/ml of rearing water. Data represent the mean of four replicates. (Two-way ANOVA; ****P < 0.0001).*

EOs Regulate the *In Vitro* Virulence of Pathogenic *V. campbellii*

Finally, the effects of EOs on the virulence factors and the cell density of *V. campbellii* were investigated. The EOs of *M. alternifolia* at 0.0008%, *L. citrata* at 0.002%, and *E. citriodora* at 0.0005% significantly decreased biofilm formation, swimming motility, gelatinase activity, and lipase activity *in vitro* (**Figure 5** and **Supplementary Information 3**). However, there was no significant effect on phospholipase or hemolytic activity. There was no significant change in the number of total cells, live cells, and dead cells detected in the *V. campbellii* supplemented with the EOs of *M. alternifolia* (0.0008%), *L. citrata* (0.002%), and *E. citriodora* (0.0005%) (**Figure 6**, **Supplementary Information 4**, and **Table 5**). No significant regrowth was observed when *V. campbellii* was treated with *L. citrata* at 0.01% and *E. citriodora* at 0.01%, while the EO of *M. alternifolia* at 0.01% delayed the bacterial exponential growth phase. There is no significant difference in regrowth performance in other analyzed concentrations compared to the control group (**Figure 7**).

DISCUSSION

We observed that the EOs of *M. alternifolia* and *L. citrata* increase the survival of *Artemia* against the pathogenic *V. campbellii* BB120 strain *in vivo*. Our data implied that supplementation of EOs induced a protective response in *Artemia* when challenged with *V. campbellii*. EOs seemed to be responsible for stimulating the immune system of *Artemia in vivo*. Moreover, the EOs diminished the virulence factors production without inhibiting the growth of the pathogen *in vitro*.

The bacterial species *V. campbellii* is an important pathogen in the intensive rearing of aquatic animals, where mortality can be as high as 100% (1). The use of antibiotics and disinfectants has limited success in controlling this pathogen due to the emergence of bacterial resistance (18). Hence, an alternative approach is needed to control vibriosis. The EOs of *M. alternifolia*, *L. citrata*, and *E. citriodora* were previously observed to inhibit or decrease the growth of *V. campbellii* BB120 *in vitro*. This motivated us to investigate whether they can be applied as a disease-control agent in aquaculture. Therefore, using the axenic brine shrimp and *V. campbellii* as a host-pathogen model, the potential beneficial effect of the EOs was verified and the potential mode of action investigated.

To this end, the toxicity of each EO was firstly evaluated in brine shrimp larvae. The results showed that EOs of *M. alternifolia*, *L. citrata*, and *E. citriodora* below 0.001, 0.002, and 0.0005% concentration had no effect on the larvae survival, which indicated that *Artemia* was more tolerant to essential oil *L. citrata*, followed by *M. alternifolia* and *E. citriodora*. Hence, compared to the essential oil *M. alternifolia* and *E. citriodora*, there might be more flexibility in applying the EO of *L. citrata* in aquaculture.

Next, to evaluate the protective effect of EO in the brine shrimp, the optimized doses of each EO were applied to the standard *Artemia in vivo* challenge assay. The survival results indicated that the EOs of *M. alternifolia* at 0.0008% and *L. citrata* at 0.002% significantly improved the survival of brine shrimp challenged with *V. campbellii*, while the EO of *E. citriodora* had limited protection. To analyze this differential survival protection, it was tried to link survival with the influence of EO on the immune system of brine shrimp, especially the immune genes.

The *Artemia* group exposed to the EO *M. alternifolia* and challenged with *V. campbellii* exhibited a significant synergistic interaction in the *dscam* and *hsp 70* gene expression level at the 6 h time point, culminating for the latter gene in a more than two-fold higher expression at 24 h after *Vibrio* exposure. Previous studies showed that infected rats treated with *M. alternifolia* had increased levels of IgG (19), and treatment ameliorates the cytokine response of silver catfish during *Aeromonas hydrophila* infection (20). These studies were mainly focused on antibody and cytokine levels in serum. In the present study, significant antagonistic interaction was observed with the EO *M. alternifolia* treatment in combination with high expression of *tgase1*, indicating that *M. alternifolia* might protect *Artemia* by an enhanced immune response during the first 24 h of *Vibrio* exposure.

In the *Artemia* group treated with EO *E. citriodora*, a significant antagonistic interaction at 6 h in the expression of *hmgb*, *sod*, *tgase1*, and *tgase2* gene, and at 24 h in the *hmgb*, *pxn*, and *tgase2* gene expression was observed, culminating a two-fold higher expression of *hsp70* and *tgase1* after 24-h challenge in the presence of this EO. Yet, the *Artemia* group exposed to *E. citriodora* group only displayed a limited increase in survival after challenge. It was known that the

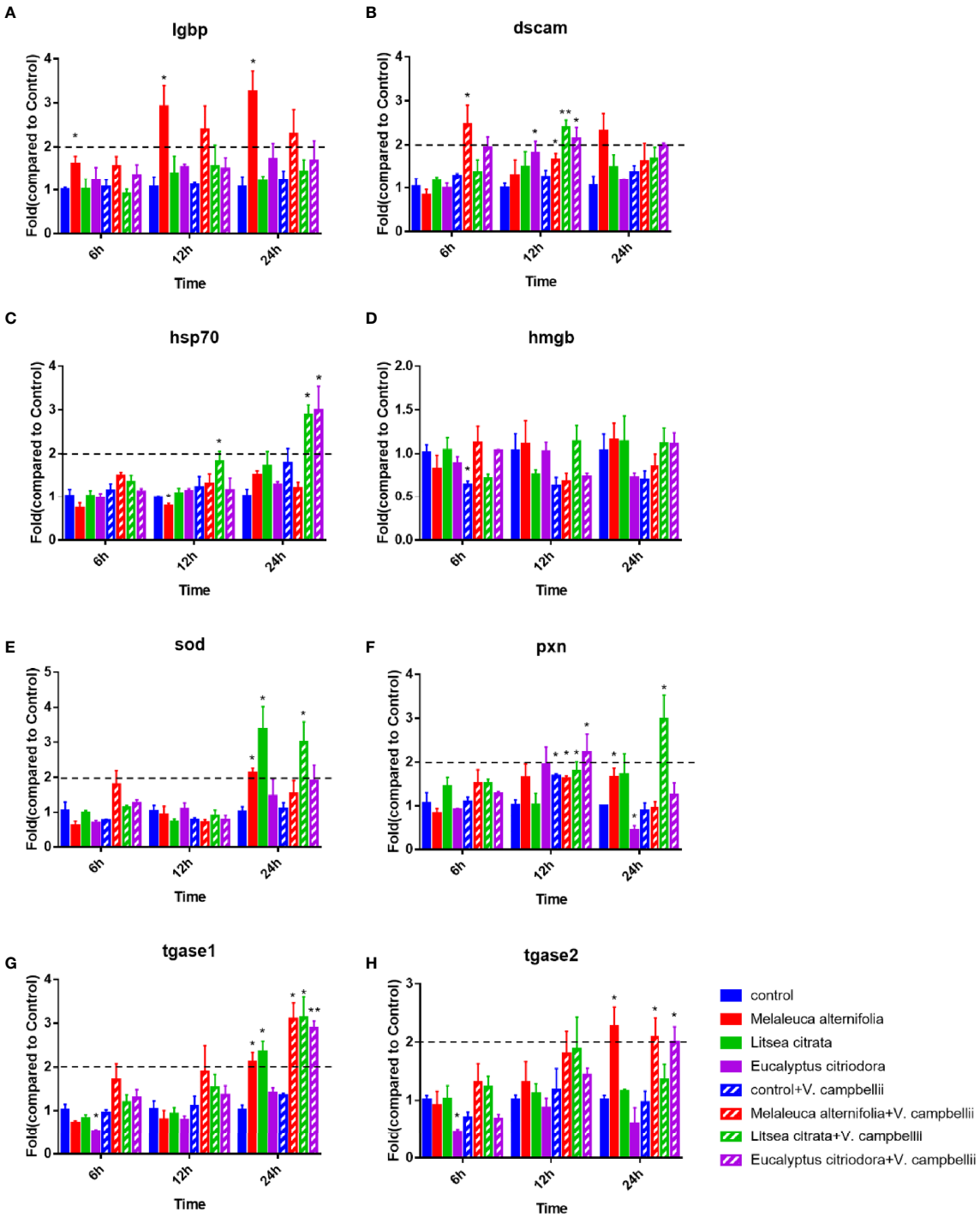

FIGURE 3 | Relative expression of *lgbp* **(A)**, *dscam* **(B)**, *hsp* 70 **(C)** and *hmgb* **(D)**, *sod* **(E)**, *pxn* **(F)**, *tgase 1* **(G)**, and *tgase 2* **(H)** genes in *Artemia* larvae. The unchallenged *Artemia* larvae served as control. For each gene, the expression in control was set at 1, and the expression in different treatments was normalized accordingly using the $2^{-\Delta\Delta CT}$ method. The geomean of the EF-1 and GAPDH was used as internal control. Data were average ± standard error of three replicates. Asterisks indicated a significant difference when compared to control (independent samples t-test; $^{*}P < 0.032$; $^{**}P < 0.0021$). EF-1, elongation factor 1; GAPDH, glyceraldehyde-3-phosphate dehydrogenase; *lgbp*, lipopolysaccharide and β-1,3-glucan-binding protein; *dscam*, down syndrome cell adhesion molecule; *hsp 70*, heat shock protein 70; *hmgb*, high mobility group box protein; *sod*, superoxidase dismutase; *pxn*, peroxinectin; *tgase 1*, transglutaminase 1; *tgase 2*, transglutaminase 2.

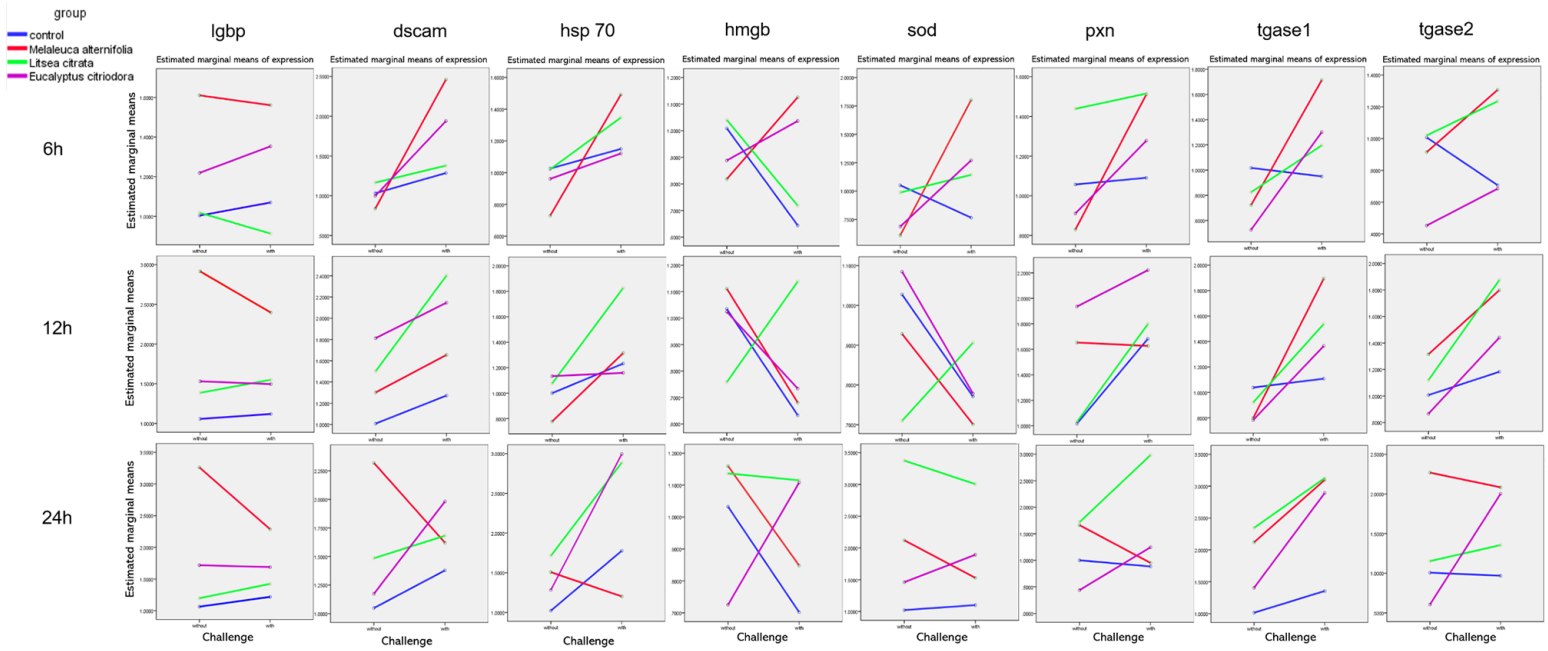

FIGURE 4 | The interaction plots between relative expression of *lgbp*, *dscam*, *hsp* 70, *hmgb*, *sod*, *pxn*, *tgase 1*, and *tgase 2* genes in *Artemia* larvae treated with EO of *Melaleuca alternifolia*, *Litsea citrata*, *Eucalyptus citriodora*, and the control group when challenged with/without *Vibrio campbellii* BB120, respectively, according to the output from two-way ANOVA. Control group: no EO added but consisted of 1% of DMSO.

TABLE 4 | Two-way ANOVA showing main and interaction effects of essential oils and with/without *Vibrio campbellii* challenge on the immune gene expressions of brine shrimp larvae at three different time points (6, 12, and 24 h).

A Time point	Gene	Factors	*P* value	*P* value summary	Interaction
6h	*lgbp*	EO (*Melaleuca alternifolia*)	0.0105	*	-
		challenge	0.9619	ns	
		Interaction	0.7353	ns	
	dscam	EO (*M. alternifolia*)	0.0842	ns	synergistic
		challenge	0.0055	**	
		Interaction	0.0253	*	
	hsp 70	EO (*M. alternifolia*)	0.8680	ns	synergistic
		challenge	0.0104	*	
		Interaction	0.0434	*	
	hmgb	EO (*M. alternifolia*)	0.3109	ns	antagonistic
		challenge	0.8372	ns	
		Interaction	0.0374	*	
	sod	EO (*M. alternifolia*)	0.2526	ns	antagonistic
		challenge	0.0965	ns	
		Interaction	0.0155	*	
	pxn	EO (*M. alternifolia*)	0.6615	ns	-
		challenge	0.1316	ns	
		Interaction	0.1670	ns	
	tgase1	EO (*M. alternifolia*)	0.2742	ns	antagonistic
		challenge	0.0490	*	
		Interaction	0.0291	*	
	tgase2	EO (*M. alternifolia*)	0.2633	ns	-
		challenge	0.8349	ns	
		Interaction	0.1402	ns	
12h	*lgbp*	EO (*M. alternifolia*)	0.0033	**	-
		challenge	0.5643	ns	
		Interaction	0.4659	ns	
	dscam	EO (*M. alternifolia*)	0.1460	ns	-
		challenge	0.1796	ns	
		Interaction	0.8368	ns	
	hsp 70	EO (*M. alternifolia*)	0.6845	ns	-
		challenge	0.0494	*	
		Interaction	0.3857	ns	
	hmgb	EO (*M. alternifolia*)	0.7357	ns	-
		challenge	0.0471	*	
		Interaction	0.9375	ns	
	sod	EO (*M. alternifolia*)	0.6114	ns	-
		challenge	0.1680	ns	
		Interaction	0.9285	ns	
	pxn	EO (*M. alternifolia*)	0.1248	ns	-
		challenge	0.0947	ns	
		Interaction	0.0745	ns	
	tgase1	EO (*M. alternifolia*)	0.4522	ns	-
		challenge	0.1306	ns	
		Interaction	0.1762	ns	
	tgase2	EO (*M. alternifolia*)	0.1888	ns	-
		challenge	0.3352	ns	
		Interaction	0.6450	ns	
24h	*lgbp*	EO (*M. alternifolia*)	0.0035	**	-
		challenge	0.3355	ns	
		Interaction	0.1960	ns	
	dscam	EO (*M. alternifolia*)	0.0450	*	-
		challenge	0.5783	ns	
		Interaction	0.1452	ns	
	hsp 70	EO (*M. alternifolia*)	0.8309	ns	antagonistic
		challenge	0.3049	ns	
		Interaction	0.0324	*	
	hmgb	EO (*M. alternifolia*)	0.4211	ns	-
		challenge	0.0818	ns	
		Interaction	0.9547	ns	
	sod	EO (*M. alternifolia*)	0.0112	*	-

(Continued)

TABLE 4 | Continued

A Time point	Gene	Factors	*P* value	*P* value summary	Interaction
		challenge	0.3028	ns	
		Interaction	0.1879	ns	
	pxn	EO (*M. alternifolia*)	0.0444	*	-
		challenge	0.0269	*	
		Interaction	0.0866	ns	
	tgase1	EO (*M. alternifolia*)	0.0002	***	-
		challenge	0.0173	*	
		Interaction	0.1867	ns	
	tgase2	EO (*M. alternifolia*)	0.0017	**	-
		challenge	0.6760	ns	
		Interaction	0.7809	ns	

B Time point	Gene	Factors	*P* value	*P* value summary	Interaction
6h	*lgbp*	EO (*Litsea citrata*)	0.6656	ns	-
		challenge	0.9053	ns	
		Interaction	0.6053	ns	
	dscam	EO (*L. citrata*)	0.5382	ns	-
		challenge	0.2184	ns	
		Interaction	0.9115	ns	
	hsp 70	EO (*L. citrata*)	0.5327	ns	-
		challenge	0.1660	ns	
		Interaction	0.5136	ns	
	hmgb	EO (*L. citrata*)	0.5772	ns	-
		challenge	0.0055	**	
		Interaction	0.8219	ns	
	sod	EO (*L. citrata*)	0.2664	ns	-
		challenge	0.6359	ns	
		Interaction	0.1313	ns	
	pxn	EO (*L. citrata*)	0.0545	ns	-
		challenge	0.7649	ns	
		Interaction	0.9075	ns	
	tgase1	EO (*L. citrata*)	0.8293	ns	-
		challenge	0.2389	ns	
		Interaction	0.1047	ns	
	tgase2	EO (*L. citrata*)	0.1274	ns	-
		challenge	0.7944	ns	
		Interaction	0.1445	ns	
12h	*lgbp*	EO (*L. citrata*)	0.2981	ns	-
		challenge	0.7485	ns	
		Interaction	0.8852	ns	
	dscam	EO (*L. citrata*)	0.0045	**	-
		challenge	0.0230	*	
		Interaction	0.1637	ns	
	hsp 70	EO (*L. citrata*)	0.0945	ns	-
		challenge	0.0241	*	
		Interaction	0.1816	ns	
	hmgb	EO (*L. citrata*)	0.4481	ns	antagonistic
		challenge	0.9420	ns	
		Interaction	0.0263	*	
	sod	EO (*L. citrata*)	0.5051	ns	-
		challenge	0.8230	ns	
		Interaction	0.1217	ns	
	pxn	EO (*L. citrata*)	0.7266	ns	-
		challenge	0.0039	**	
		Interaction	0.7825	ns	
	tgase1	EO (*L. citrata*)	0.4951	ns	-
		challenge	0.1562	ns	
		Interaction	0.2472	ns	
	tgase2	EO (*L. citrata*)	0.2764	ns	-
		challenge	0.2137	ns	

(Continued)

TABLE 4 | Continued

B Time point	Gene	Factors	*P* value	*P* value summary	Interaction
		Interaction	0.4248	ns	
24h	*lgbp*	EO (*L. citrata*)	0.4771	ns	-
		challenge	0.4263	ns	
		Interaction	0.8789	ns	
	dscam	EO (*L. citrata*)	0.1625	ns	-
		challenge	0.3050	ns	
		Interaction	0.7909	ns	
	hsp 70	EO (*L. citrata*)	0.0109	*	-
		challenge	0.0077	**	
		Interaction	0.4646	ns	
	hmgb	EO (*L. citrata*)	0.2385	ns	-
		challenge	0.4116	ns	
		Interaction	0.4688	ns	
	sod	EO (*L. citrata*)	0.0014	**	-
		challenge	0.7530	ns	
		Interaction	0.6294	ns	
	pxn	EO (*L. citrata*)	0.0053	**	-
		challenge	0.1603	ns	
		Interaction	0.1004	ns	
	tgase1	EO (*L. citrata*)	0.0005	***	-
		challenge	0.0738	ns	
		Interaction	0.4440	ns	
	tgase2	EO (*L. citrata*)	0.1593	ns	-
		challenge	0.6452	ns	
		Interaction	0.5054	ns	

C Time point	Gene	Factors	*P* value	*P* value summary	Interaction
6h	*lgbp*	EO (*Eucalyptus citriodora*)	0.2767	ns	-
		challenge	0.6524	ns	
		Interaction	0.8772	ns	
	dscam	EO (*E. citriodora*)	0.0964	ns	-
		challenge	0.0066	**	
		Interaction	0.0705	ns	
	hsp 70	EO (*E. citriodora*)	0.7276	ns	-
		challenge	0.3050	ns	
		Interaction	0.8937	ns	
	hmgb	EO (*E. citriodora*)	0.0694	ns	antagonistic
		challenge	0.1342	ns	
		Interaction	0.0042	**	
	sod	EO (*E. citriodora*)	0.6201	ns	antagonistic
		challenge	0.3071	ns	
		Interaction	0.0130	*	
	pxn	EO (*E. citriodora*)	0.8847	ns	-
		challenge	0.1854	ns	
		Interaction	0.2631	ns	
	tgase1	EO (*E. citriodora*)	0.5771	ns	antagonistic
		challenge	0.0188	*	
		Interaction	0.0082	**	
	tgase2	EO (*E. citriodora*)	0.0052	**	antagonistic
		challenge	0.6609	ns	
		Interaction	0.0079	**	
12h	*lgbp*	EO (*E. citriodora*)	0.0504	ns	-
		challenge	0.9434	ns	
		Interaction	0.7976	ns	
	dscam	EO (*E. citriodora*)	0.0032	**	-
		challenge	0.1783	ns	
		Interaction	0.8676	ns	
	hsp 70	EO (*E. citriodora*)	0.8764	ns	-
		challenge	0.5147	ns	
		Interaction	0.6000	ns	

(Continued)

TABLE 4 | Continued

C Time point	Gene	Factors	*P* value	*P* value summary	Interaction
	hmgb	EO (*Eucalyptus citriodora*)	0.7198	ns	-
		challenge	0.0215	*	
		Interaction	0.6577	ns	
	sod	EO (*E. citriodora*)	0.8301	ns	-
		challenge	0.0914	ns	
		Interaction	0.8695	ns	
	pxn	EO (*E. citriodora*)	0.0408	*	-
		challenge	0.1499	ns	
		Interaction	0.5417	ns	
	tgase1	EO (*E. citriodora*)	0.9968	ns	-
		challenge	0.1144	ns	
		Interaction	0.2009	ns	
	tgase2	EO (*E. citriodora*)	0.7905	ns	-
		challenge	0.1167	ns	
		Interaction	0.3772	ns	-
24h	*lgbp*	EO (*E. citriodora*)	0.1281	ns	-
		challenge	0.8545	ns	
		Interaction	0.7889	ns	
	dscam	EO (*E. citriodora*)	0.0344	*	-
		challenge	0.0041	**	
		Interaction	0.1328	ns	
	hsp 70	EO (*E. citriodora*)	0.0567	ns	-
		challenge	0.0059	**	
		Interaction	0.1879	ns	
	hmgb	EO (*E. citriodora*)	0.7132	ns	antagonistic
		challenge	0.8458	ns	
		Interaction	0.0250	*	
	sod	EO (*E. citriodora*)	0.1185	ns	-
		challenge	0.4891	ns	
		Interaction	0.6296	ns	
	pxn	EO (*E. citriodora*)	0.5817	ns	antagonistic
		challenge	0.0816	ns	
		Interaction	0.0292	*	
	tgase1	EO (*E. citriodora*)	0.0001	****	synergistic
		challenge	0.0001	****	
		Interaction	0.0010	**	
	tgase2	EO (*E. citriodora*)	0.1744	ns	antagonistic
		challenge	0.0125	*	
		Interaction	0.0096	**	

*The larvae were treated with either three different essential oils at an optimized concentration or challenged with/without V. campbellii at 10^7 cells/ml. Data represent the mean of four replicates. (Two-way ANOVA; ns, no significant differences; *, P < 0.05; **, P < 0.01; ***, P < 0.001; ****, P < 0.0001; no interaction); EO, essential oil.*

generation of protective immunity was an energy-consuming process (21). In invertebrates, each of the effector systems involved in the immune response may carry a different cost when activated, and their relative expression may shape the cost of the whole immune response to a standard challenge (6). Although *E. citriodora* activate, *e.g., tgase1*, known to be important for protection, it might be that this EO activated other immune-related genes not measured here, resulting in a high energetic cost. However, this mechanistic explanation is speculative at this stage and should be verified by, e.g., analyzing the complete immunological response in *Artemia* over a 24-h time span.

There were no interactive effects upon EO *L. citrata* exposure and challenge in the expression of immune-related genes (but a high *tgase1* exposure after 24-h challenge). Yet, the *L. citrata* group displayed a very high survival, and a protection closed to 100%. It was interesting to observe that there was a high *sod* gene expression (more than two-fold) in the *L. citrata* group at 24 h both with and without challenge (and not observed with the other two EOs). It has been reported that numerous short-lived and highly reactive oxygen species (ROS) such as superoxide (O_2^-), hydroxyl radical, and hydrogen peroxide were continuously generated *in vivo*, especially during an immune response (22). Oxidant/antioxidant imbalance was thought to be partially involved in the pathogenesis of the disorders (22). Maybe the EO *L. citrata* exposure helped to mount a balanced immune response in which radicals generated were neutralized by the expression of ROS-neutralizing genes such as SOD, contributing to a high survival under challenge. Summarizing, the EOs tested seemed to modulate the immune response in *Artemia*, each of them in their particular way. Only in two cases these seemed to contribute to a substantial increase in survival. It is possible that the panel of verified immune-related genes does not generate the complete picture of the immune

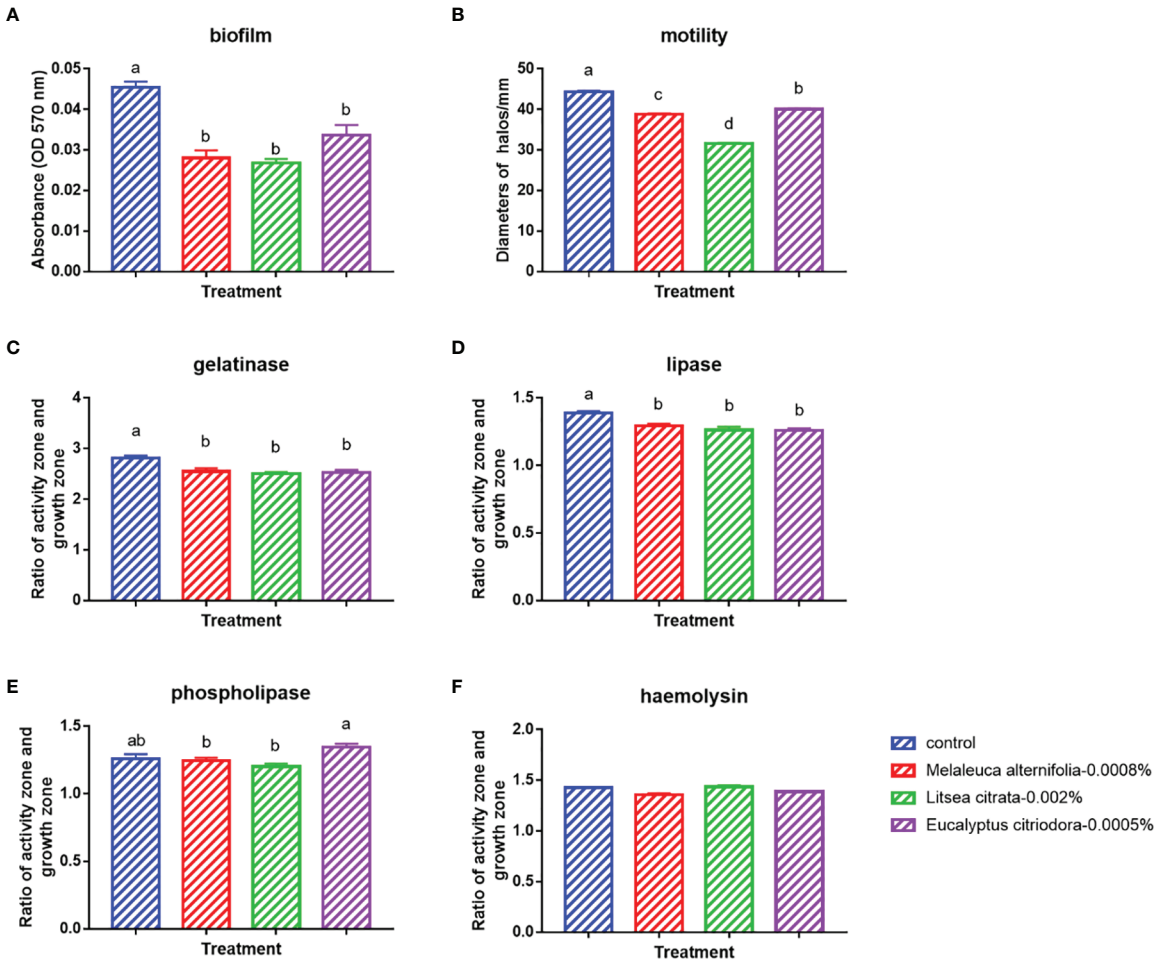

FIGURE 5 | *In vitro* tests on the bacterial virulence factors of *Vibrio campbellii* treated with the selected essential oils at an optimized dose. **(A)** Biofilm formation of *V. campbellii* in marine broth. **(B)** Swimming motility of *V. campbellii* on soft LB_{35} agar after 24 h of incubation at 28°C. **(C)** Gelatinase assay of *V. campbellii* on LB_{35} agar supplemented with 0.5% gelatin after 48 h of incubation at 28°C. **(D)** Lipase assay of *V. campbellii* on LB_{35} agar supplemented with 1% Tween 80 after 2–4 days of incubation at 28°C. **(E)** Phospholipase assay of *V. campbellii* on LB_{35} agar supplemented with 1% egg yolk after 2–4 days of incubation at 28°C. **(F)** Hemolytic assay of *V. campbellii* on LB_{35} agar supplemented with 5% defibrinated sheep blood after 48 h of incubation at 28°C. Control: no EO added but consisted of 1% of DMSO. The error bars of the graphs represented standard error. Different letters indicated significant difference ($P < 0.05$).

response upon exposure, and hence an unequivocal temporal picture between immune gene expression and *Artemia* survival for these three EOs could not be generated.

In addition to the effect of EO on the immune system of *Artemia in vivo*, the impact of the EOs on the pathogenic *V. campbellii* strain was also investigated in a series of *in vitro* assays. The flow cytometer results showed that the amount of live cell and dead cell of bacteria in the essential oil of *M. alternifolia* at 0.0008%, *L. citrata* at 0.002%, and *E. citriodora* at 0.0005% were the same magnitude as that in the control group, showing *V. campbellii* were not killed by the EOs at the tested concentrations. For the regrowth curve, bacteria in the essential oil of *M. alternifolia* at 0.0008%, *L. citrata* at 0.002%, and *E. citriodora* at 0.0005% exhibited the same growth curve as that in the control group, indicating that the growth performance of *V. campbellii* was not affected by the EOs at the tested concentrations. The EOs might act as a bacteriostatic or bactericidal agent. Bacteriostatic agents prevent the growth of bacteria, suppressing cellular division, while bactericidal agents kill the bacteria (23). The bacteriostatic action has a reversible character, and the microbial cells will recover their reproductive capacity (23) when the agent is removed. In contrast, the bactericidal effect is permanent, and the microbial cells are not able to regrow (23). Combined with the result from the flow cytometer and the regrowth performance, there was no bactericidal effect in the EOs at the tested concentrations. Bacterial swimming motility played a critical role in host-microbial interactions, which was also related to biofilm formation. In our study, all EOs at optimized concentration had a significant decrease in swimming motility and biofilm formation. Similar results have been reported by Domínguez-Borbor et al. (24), who observed that EOs have a profound effect on the virulence of *Vibrio* sp. The

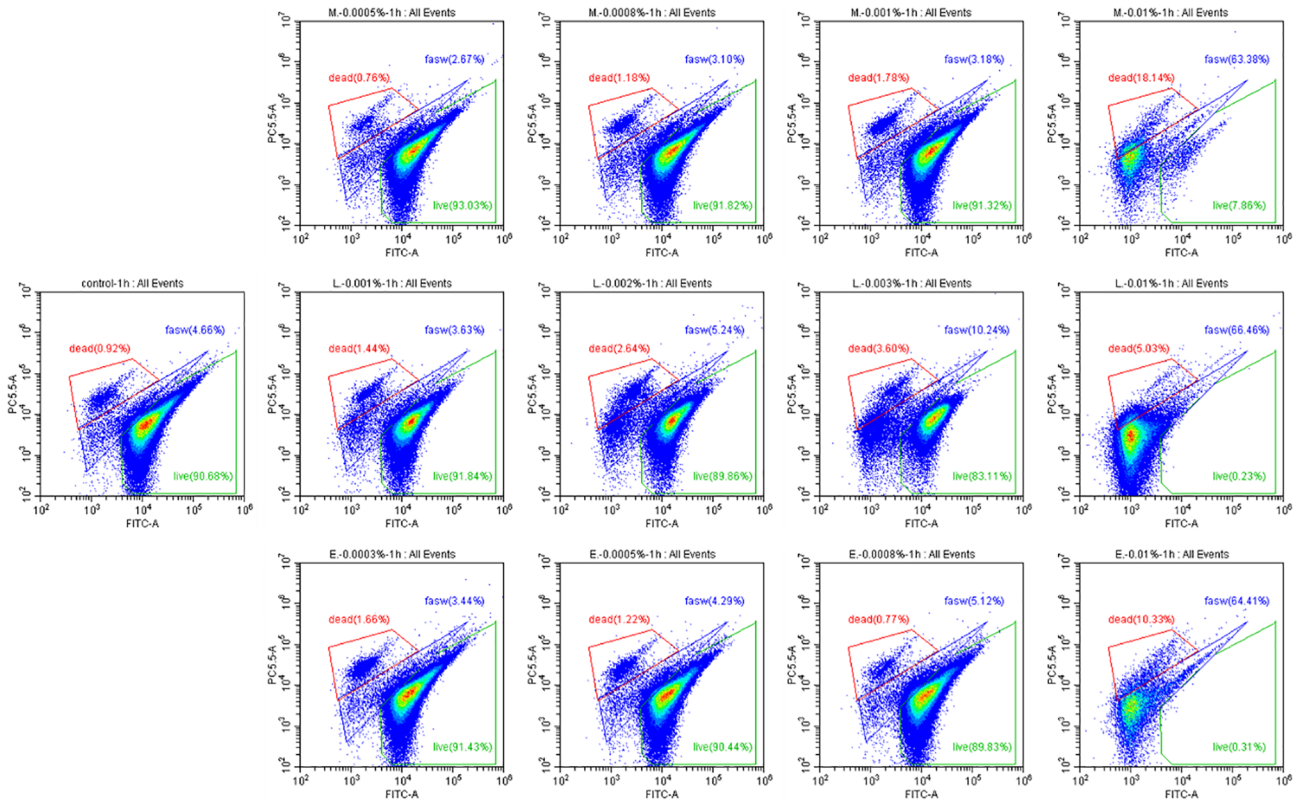

FIGURE 6 | Percentage of live and dead cells of *Vibrio campbellii* with or without the addition of essential oils. The first line from left to right was the group of essential oil *Melaleuca alternifolia* at the concentrations of 0.0005, 0.0008, 0.001, and 0.01%; the second line from left to right was control group, the group of essential oil *Litsea citrata* at the concentrations of 0.001, 0.002, 0.003, and 0.01%; and the third line from left to right was the group of essential oil *Eucalyptus citriodora* at the concentrations of 0.0003, 0.0005, 0.0008, and 0.01%. Control: no EO added but consisted of 1% of DMSO. The plot of live cells was in the green frame, dead cells was in the red frame, and damage cells or other were in the blue frame.

TABLE 5 | Average total cells count, live cells count, and dead cells count of *Vibrio campbellii* with or without essential oils at different concentrations, obtained from flow cytometer.

Group	Average total cells count (×10^3 cell/ml)	Live cells count (×10^3 cell/ml)	Dead cells count (×10^3 cell/ml)
Negative control	2,907.13 ± 7.56	2,645.69 ± 13.27	38.65 ± 10.84
Melaleuca alternifolia—0.0005%	2,643.05 ± 10.45	2,461.45 ± 7.50	25.87 ± 3.25
M. alternifolia—0.0008%	2,769.7 ± 26.08	2,589.03 ± 15.96	35.07 ± 4.06
M. alternifolia—0.001%	2,655.66 ± 11.82	2,453.48 ± 16.98	39.54 ± 4.84
M. alternifolia—0.01%	229.83 ± 2.74	18.68 ± 0.11	42.99 ± 0.19
Litsea citrata—0.001%	2,220.74 ± 18.12	2,053.67 ± 19.97	34.53 ± 3.71
L. citrata—0.002%	1,944.87 ± 4.05	1,757.44 ± 5.06	56.03 ± 2.44
L. citrata—0.003%	1,285.62 ± 20.30	1,078.70 ± 17.78	44.25 ± 1.97
L. citrata—0.01%	1,654.60 ± 24.84	3.94 ± 0.05	82.41 ± 0.51
Eucalyptus citriodora—0.0003%	2,731.842 ± 27.60	2,497.86 ± 20.99	34.29 ± 8.81
E. citriodora—0.0005%	2,847.15 ± 30.46	2,565.29 ± 21.95	31.33 ± 9.17
E. citriodora—0.0008%	2,789.38 ± 34.46	2,536.09 ± 26.24	36.84 ± 7.60
E. citriodora—0.01%	190.05 ± 4.59	0.8 ± 0.02	25.36 ± 0.37

results showed that EOs (*Organum vulgare* and *M. alternifolia*) significantly inhibited the biofilm formation in *V. harveyi*, *V. campbellii*, *V. parahaemolyticus*, and *V. vulnificus*. Additionally, the EOs from different ornamental plants have also been observed to be effective against biofilms formed by *Salmonella*, *Listeria*, *Pseudomonas*, *Staphylococcus*, and *Lactobacillus* spp (25, 26). *V. campbellii* excreted various virulence factors, such as extracellular products (gelatinase, lipase, phospholipase, hemolytic, and so on) that were involved in pathogenesis (17). The results revealed that essential oils significantly decreased the production of certain

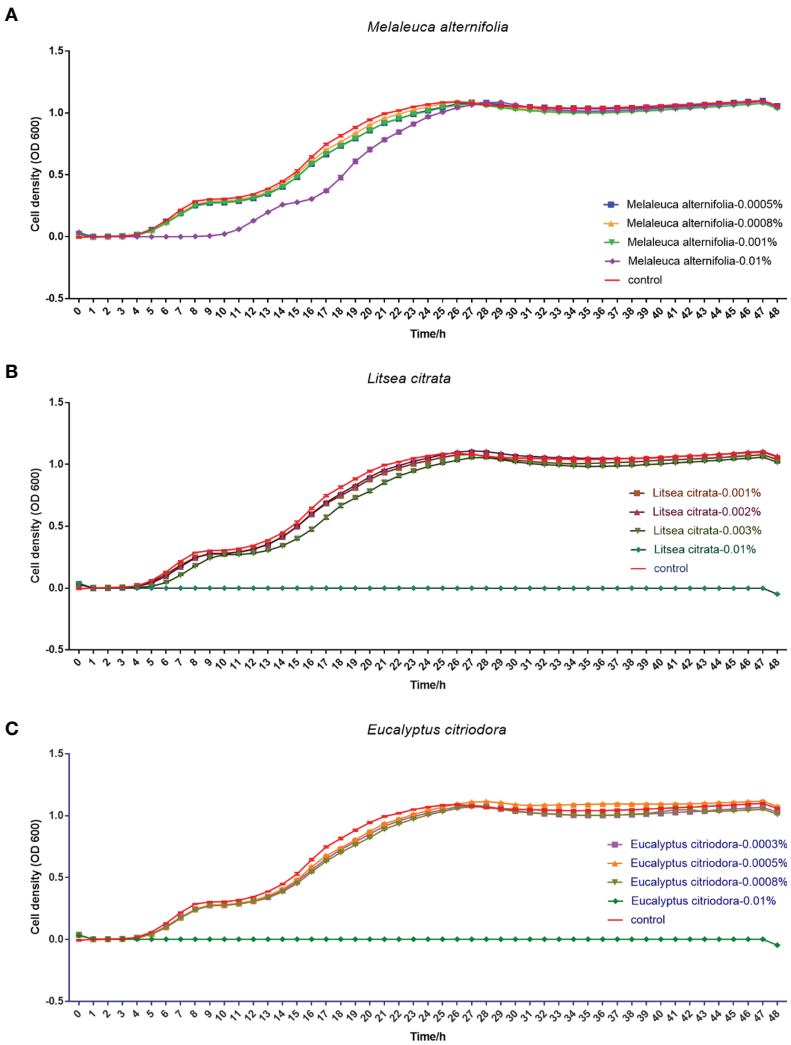

FIGURE 7 | Regrowth curve of *Vibrio campbellii* after incubation with or without essential oil *Melaleuca alternifolia* **(A)**, *Litsea citrata* **(B)**, and *Eucalyptus citriodora* **(C)** at different concentrations for 1 h. The group of essential oil *M. alternifolia* at the concentrations of 0.0005, 0.0008, 0.001, and 0.01%; the group of essential oil *L. citrata* at the concentrations of 0.001, 0.002, 0.003, and 0.01%; and the group of essential oil *E. citriodora* at the concentrations of 0.0003, 0.0005, 0.0008, and 0.01%. The control group contained 1% DMSO. Error bars represented the standard error of four replicates.

virulence factors (gelatinase, lipase), whereas they had no significant effect on phospholipase or hemolytic activity. This indicated that the inhibition of swimming motility, biofilm formation, and virulence factors was to a certain degree consistent with a bacteriostatic action of the EOs at the tested concentrations.

CONCLUSION

In conclusion, the results presented in this paper showed that essential oils of *M. alternifolia* at 0.0008% and *L. citrata* at 0.002% can significantly improve the survival of brine shrimp larvae when challenged with pathogenic *V. campbellii*. Our results indicated that supplementation of these two EOs enhanced immune gene expression (each of them in their particular way), possibly contributing to protective immunity in brine shrimp larvae against *V. campbellii*. Furthermore, the EOs-regulated expression of bacterial virulence factors, including decreased swimming motility and biofilm formation, might contribute in part to the protection of the brine shrimp larvae against pathogenic *V. campbellii*. However, further studies are needed to investigate the underlying protective mechanism of EOs, e.g., by analyzing the expression of a larger panel of immune-related genes. Taken together, the essential oils can be part of disease intervention strategies either based on their immunostimulatory properties or modulation of virulence factor production.

DATA AVAILABILITY STATEMENT

The original contributions presented in the study are included in the article/**Supplementary Material**. Further inquiries can be directed to the corresponding authors.

AUTHOR CONTRIBUTIONS

XZ: conceptualization, data curation, investigation, visualization, writing—original draft and writing—review and editing. BH: methodology and writing—review and editing. VK: methodology and writing—review and editing. AF: resources, methodology, and writing—review and editing. PD: resources, supervision, and writing—review and editing. PB: conceptualization, supervision, funding acquisition, and writing—review and editing.

FUNDING

This research was supported by the China Scholarship Council (CSC 201708440251) and the Special Research Fund of Ghent University (BOF-UGent 01SC7918).

ACKNOWLEDGMENTS

We thank Prof. Bonnie Bassler for providing *V. campbellii* wild-type strain ATCC BAA-1116.

SUPPLEMENTARY MATERIAL

The Supplementary Material for this article can be found online at: https://www.frontiersin.org/articles/10.3389/fimmu.2021.693932/full#supplementary-material

REFERENCES

1. Phuoc LH, Corteel M, Nauwynck HJ, Pensaert MB, Alday-Sanz V, Van den Broeck W, et al. Increased Susceptibility of White Spot Syndrome Virus-Infected *Litopenaeus Vannamei* to Vibrio Campbellii. *Environ Microbiol* (2008) 10(10):2718–27. doi: 10.1111/j.1462-2920.2008.01692.x
2. K. T, C. T. Isolation and Characterization of Vibrio Species From Shrimp and *Artemia* Culture and Evaluation of the Potential Virulence Factor. *Intellectual Property Rights: Open Access* (2016) 4(1):1–5. doi: 10.4172/2375-4516.1000153
3. Alderman DJ, Hastings TS. Antibiotic Use in Aquaculture: Development of Antibiotic Resistance – Potential for Consumer Health Risks*. *Int J Food Sci Technol* (1998) 33(2):139–55. doi: 10.1046/j.1365-2621.1998.3320139.x
4. Elmahdi S, DaSilva LV, Parveen S. Antibiotic Resistance of *Vibrio Parahaemolyticus* and *Vibrio Vulnificus* in Various Countries: A Review. *Food Microbiol* (2016) 57:128–34. doi: 10.1016/j.fm.2016.02.008
5. Baruah K, Huy TT, Norouzitallab P, Niu Y, Gupta SK, De Schryver P, et al. Probing the Protective Mechanism of Poly-Ss-Hydroxybutyrate Against Vibriosis by Using Gnotobiotic Artemia Franciscana and *Vibrio Campbellii* as Host-Pathogen Model. *Sci Rep* (9427) (2015) 5(1):1–8. doi: 10.1038/srep09427
6. Baruah K, Duy Phong HP, Norouzitallab P, Defoirdt T, Bossier P. The Gnotobiotic Brine Shrimp (*Artemia Franciscana*) Model System Reveals That the Phenolic Compound Pyrogallol Protects Against Infection Through its Prooxidant Activity. *Free Radic Biol Med* (2015) 89:593–601. doi: 10.1016/j.freeradbiomed.2015.10.397
7. Bakkali F, Averbeck S, Averbeck D, Idaomar M. Biological Effects of Essential Oils–A Review. *Food Chem Toxicol* (2008) 46(2):446–75. doi: 10.1016/j.fct.2007.09.106
8. Lee S, Najiah M, Wendy W, Nadirah M. Chemical Composition and Antimicrobial Activity of the Essential Oil of *Syzygium Aromaticum* Flower Bud (Clove) Against Fish Systemic Bacteria Isolated From Aquaculture Sites. *Front Agric China* (2009) 3(3):332–6. doi: 10.1007/s11703-009-0052-8
9. Zheng ZL, Tan JYW, Liu HY, Zhou XH, Xiang X, Wang KY. Evaluation of Oregano Essential Oil (*Origanum Heracleoticum* L.) on Growth, Antioxidant Effect and Resistance Against Aeromonas Hydrophila in Channel Catfish (*Ictalurus Punctatus*). *Aquaculture* (2009) 292(3-4):214–8. doi: 10.1016/j.aquaculture.2009.04.025
10. de Oliveira Hashimoto GS, Neto FM, Ruiz ML, Acchile M, Chagas EC, Chaves FCM, et al. Essential Oils of *Lippia Sidoides* and *Mentha Piperita* Against Monogenean Parasites and Their Influence on the Hematology of Nile Tilapia. *Aquaculture* (2016) 450:182–6. doi: 10.1016/j.aquaculture.2015.07.029
11. Zheng X, Feyaerts AF, Van Dijck P, Bossier P. Inhibitory Activity of Essential Oils Against Vibrio Campbellii and *Vibrio Parahaemolyticus*. *Microorganisms* (2020) 8(12):1946. doi: 10.3390/microorganisms8121946
12. Yang Q, Anh ND, Bossier P, Defoirdt T. Norepinephrine and Dopamine Increase Motility, Biofilm Formation, and Virulence of. *Vibrio harveyi. Front Microbiol* (2014) 5:584. doi: 10.3389/fmicb.2014.00584
13. Baruah K, Norouzitallab P, Phong H, Smagghe G, Bossier P. Enhanced Resistance Against *Vibrio Harveyi* Infection by Carvacrol and its Association With the Induction of Heat Shock Protein 72 in Gnotobiotic Artemia Franciscana. *Cell Stress Chaperones* (2017) 22(3):377–87. doi: 10.1007/s12192-017-0775-z
14. Amedn DF. Potency Testing of Fish Vaccines. International Symposium on Fish Biologics: Serodiagnostics and Vaccines. *Dev Biol Stand* (1981) 49:447–54.
15. Han B, Kaur VI, Baruah K, Nguyen VD, Bossier P. High Doses of Sodium Ascorbate Act as a Prooxidant and Protect Gnotobiotic Brine Shrimp Larvae (*Artemia Franciscana*) Against *Vibrio Harveyi* Infection Coinciding With Heat Shock Protein 70 Activation. *Dev Comp Immunol* (2019) 92:69–76. doi: 10.1016/j.dci.2018.11.007
16. Chen W-H, Ge X, Wang W, Yu J, Hu S. A Gene Catalogue for Post-Diapause Development of an Anhydrobiotic Arthropod Artemia Franciscana. *BMC Genomics* (2009) 10(1):52. doi: 10.1186/1471-2164-10-52
17. Natrah FM, Ruwandeepika HA, Pawar S, Karunasagar I, Sorgeloos P, Bossier P, et al. Regulation of Virulence Factors by Quorum Sensing in Vibrio Harveyi. *Vet Microbiol* (2011) 154(1-2):124–9. doi: 10.1016/j.vetmic.2011.06.024
18. Teo JW, Tan TM, Poh CL. Genetic Determinants of Tetracycline Resistance in Vibrio Harveyi. *Antimicrob Agents Chemother* (2002) 46(4):1038–45. doi: 10.1128/aac.46.4.1038-1045.2002
19. Baldissera MD, Da Silva AS, Oliveira CB, Vaucher RA, Santos RCV, Duarte T, et al. Effect of Tea Tree Oil (*Melaleuca Alternifolia*) on the Longevity and Immune Response of Rats Infected by Trypanosoma evansi. *Res Vet Sci* (2014) 96(3):501–6. doi: 10.1016/j.rvsc.2014.03.013
20. Baldissera MD, Souza CF, Júnior GB, de Vargas AC, Boligon AA, de Campos MMA, et al. *Melaleuca Alternifolia* Essential Oil Enhances the non-Specific Immune System and Prevents Oxidative Damage in Rhamdia Quelen Experimentally Infected by *Aeromonas Hydrophila*: Effects on Cholinergic and Purinergic Systems in Liver Tissue. *Fish Shellfish Immunol* (2017) 61:1–8. doi: 10.1016/j.fsi.2016.12.016
21. Sadd BM, Schmid-Hempel P. A Distinct Infection Cost Associated With Trans-Generational Priming of Antibacterial Immunity in Bumble-Bees. *Biol Lett* (2009) 5(6):798–801. doi: 10.1098/rsbl.2009.0458
22. Miao L, Clair DKS. Regulation of Superoxide Dismutase Genes: Implications in Disease. *Free Radic Biol Med* (2009) 47(4):344–56. doi: 10.1016/j.freeradbiomed.2009.05.018
23. Swamy MK, Akhtar MS, Sinniah UR. Antimicrobial Properties of Plant Essential Oils Against Human Pathogens and Their Mode of Action: An Updated Review. *Evid Based Complement Alternat Med* (2016) 2016:3012462. doi: 10.1155/2016/3012462
24. Domínguez-Borbor C, Sánchez-Rodríguez A, Sonnenholzner S, Rodríguez J. Essential Oils Mediated Antivirulence Therapy Against Vibriosis in Penaeus Vannamei. *Aquaculture* (2020) 529:735639. doi: 10.1016/j.aquaculture.2020.735639

25. Rossi C, Chaves-López C, Možina SS, Di Mattia C, Scuota S, Luzzi I, et al. Salmonella Enterica Adhesion: Effect of Cinnamomum Zeylanicum Essential Oil on Lettuce. *Lwt* (2019) 111:16–22. doi: 10.1016/j.lwt.2019.05.026
26. Kuhn D, Ziem R, Scheibel T, Buhl B, Vettorello G, Pacheco LA, et al. Antibiofilm Activity of the Essential Oil of *Campomanesia Aurea* O. Berg Against Microorganisms Causing Food Borne Diseases. *Lwt* (2019) 108:247–52. doi: 10.1016/j.lwt.2019.03.079

Conflict of Interest: The authors declare that the research was conducted in the absence of any commercial or financial relationships that could be construed as a potential conflict of interest.

Publisher's Note: All claims expressed in this article are solely those of the authors and do not necessarily represent those of their affiliated organizations, or those of the publisher, the editors and the reviewers. Any product that may be evaluated in this article, or claim that may be made by its manufacturer, is not guaranteed or endorsed by the publisher.

frontiers in Immunology

ORIGINAL RESEARCH
published: 23 November 2021
doi: 10.3389/fimmu.2021.766845

Sinomenine Hydrochloride Ameliorates Fish Foodborne Enteritis *via* α7nAchR-Mediated Anti-Inflammatory Effect Whilst Altering Microbiota Composition

Jiayuan Xie[1,2†], *Ming Li*[1,3†], *Weidong Ye*[1,2], *Junwei Shan*[1,3], *Xuyang Zhao*[1,3], *You Duan*[1,2], *Yuhang Liu*[1,3], *Bruno Hamish Unger*[1], *Yingyin Cheng*[1], *Wanting Zhang*[1], *Nan Wu*[1,2*] *and Xiao-Qin Xia*[1,3*]

[1] Institute of Hydrobiology, Chinese Academy of Sciences, Wuhan, China, [2] College of Advanced Agricultural Sciences, University of Chinese Academy of Sciences, Beijing, China, [3] College of Fisheries and Life Science, Dalian Ocean University, Dalian, China

OPEN ACCESS

Edited by:
Felipe E. Reyes-López, Universitat Autònoma de Barcelona, Spain

Reviewed by:
Julien Diana, Institut National de la Santé et de la Recherche Médicale (INSERM), France
Magdalena Chadzińska, Jagiellonian University, Poland

***Correspondence:**
Nan Wu
wunan@ihb.ac.cn
Xiao-Qin Xia
xqxia@ihb.ac.cn

[†]These authors share first authorhip

Specialty section:
This article was submitted to Nutritional Immunology, a section of the journal Frontiers in Immunology

Received: 30 August 2021
Accepted: 02 November 2021
Published: 23 November 2021

Citation:
Xie J, Li M, Ye W, Shan J, Zhao X, Duan Y, Liu Y, Unger BH, Cheng Y, Zhang W, Wu N and Xia X-Q (2021) Sinomenine Hydrochloride Ameliorates Fish Foodborne Enteritis via α7nAchR-Mediated Anti-Inflammatory Effect Whilst Altering Microbiota Composition. Front. Immunol. 12:766845. doi: 10.3389/fimmu.2021.766845

Foodborne intestinal inflammation is a major health and welfare issue in aquaculture. To prevent enteritis, various additives have been incorporated into the fish diet. Considering anti-inflammatory immune regulation, an effective natural compound could potentially treat or prevent intestinal inflammation. Our previous study has revealed galantamine's effect on soybean induced enteritis (SBMIE) and has highlighted the possible role of the cholinergic anti-inflammatory pathway in the fish gut. To further activate the intestinal cholinergic related anti-inflammatory function, α7nAchR signaling was considered. In this study, sinomenine, a typical agonist of α7nAChR in mammals, was tested to treat fish foodborne enteritis *via* its potential anti-inflammation effect using the zebrafish foodborne enteritis model. After sinomenine's dietary inclusion, results suggested that there was an alleviation of intestinal inflammation at a pathological level. This outcome was demonstrated through the improved morphology of intestinal villi. At a molecular level, SN suppressed inflammatory cytokines' expression (especially for *tnf-α*) and upregulated anti-inflammation-related functions (indicated by expression of *il-10*, *il-22*, and *foxp3a*). To systematically understand sinomenine's intestinal effect on SBMIE, transcriptomic analysis was done on the SBMIE adult fish model. DEGs (sinomenine *vs* soybean meal groups) were enriched in GO terms related to the negative regulation of lymphocyte/leukocyte activation and alpha-beta T cell proliferation, as well as the regulation of lymphocyte migration. The KEGG pathways for glycolysis and insulin signaling indicated metabolic adjustments of α7nAchR mediated anti-inflammatory effect. To demonstrate the immune cells' response, in the SBMIE larva model, inflammatory gatherings of neutrophils, macrophages, and lymphocytes caused by soybean meal could be relieved significantly with the inclusion of sinomenine. This was consistent within the sinomenine group as $CD4^+$ or $Foxp3^+$ lymphocytes were found with a higher proportion at the base of mucosal folds, which may suggest the Treg population. Echoing, the

sinomenine group's 16s sequencing result, there were fewer enteritis-related TM7, *Sphingomonas* and *Shigella*, but more *Cetobacterium*, which were related to glucose metabolism. Our findings indicate that sinomenine hydrochloride could be important in the prevention of fish foodborne enteritis at both immune and microbiota levels.

Keywords: SBMIE, zebrafish, sinomenine hydrochloride, α7nAChR, anti-inflammation, microbiota

INTRODUCTION

Currently, foodborne intestinal inflammation is a major health and welfare issue in aquaculture. As fishmeal remains an important source of dietary protein in aquaculture diets, its increasing price and decreasing availability have given birth to a replacement of feed made from plant sources of dietary protein, such as soybean meal (1). The side effects resulting from plant-sourced proteins have occurred in many fish species, from carnivorous to herbivorous, such as salmon (2), grouper (3), zebrafish (4, 5), and carp (6). Fish foodborne enteritis also is due to the dysregulation of oral tolerance, which is related to immunoregulation locally at the intestinal mucosa (7). Fish intestinal mucosal surfaces colonized by normal microbiota may elicit immune regulatory functions in gut-associated lymphoid tissues (GALT). Contrastingly, disturbances in these immuno-regulatory functions by an imbalanced microbiota may contribute to the development of disease (8). To prevent enteritis, various feed additives have been designed for modulating the host as well as intestinal bacteria. The effective ingratiates incorporated into the fish diet include probiotics, nutrients, and herbal medicine.

Since the effective components and long-term side-effects of herbal medicine cannot be easily determined, using a natural compound rather than herbal medicine to prevent fish disease may be a better solution for aquaculture (9). A traditional selection of the drugs or additives depends on the experimental result of field tests. Based on the exploration of an omics study, in aquaculture, the pursuit of discovering drugs or additives has developed novel methods, such as the reverse prediction of drugs or additives from the pathway enlightened by nutritionally transcriptomic study. Considering the anti-inflammatory effects of natural compounds, our previous transcriptomic study of grass carp soybean-induced enteritis (SBMIE) has indicated that the intestinal cholinergic anti-inflammatory pathway may work (6) and that the cholinesterase inhibitor galantamine can be used to prevent SBMIE (4). Thus, these findings have indicated the possible existence of the cholinergic anti-inflammatory pathway in the fish gut. Diet inclusion of galantamine could elicit a regulatory function on mucosal inflammation (10).

The preserved intestinal acetylcholine (4) in fish may enhance α7nAChR and had a mediating anti-inflammatory effect on immune cells, such as macrophages, neutrophils, and T cells (11–14). When considering effectors, fish SBMIE showed typical allergic cytokine profiles (15), similar to IBD in humans. For proinflammatory cytokines, TNF-α was highly expressed (especially in the epithelial cells) for accelerating intestinal inflammation (16, 17). The acute inflammation-related TNF-α, IL-1β, and allergic cytokine IL-17A/F have also been reported in fish SBMIE (4, 15, 18). Based on the existence of zebrafish nicotinic acetylcholine receptor α7nAChR (19) as well as α7 nicotinic agonist AR-R17779's protective effect on colitis (20), α7nAchR signaling would be a promising target to efficiently activate intestinal α7nAChR mediated anti-inflammatory function.

Sinomenine (SN), which is an agonist of α7nAChR (21), could insert into the active site of the α7nAchR structure in mammals (22) and has been identified as an effective component to treat swelling and pain during mucosal inflammation, such as enteritis (23). Sinomenine derivatives have also improved the immunosuppressive activity of its parent natural compound (24). For SN's effect on intestinal humoral immunity, sinomenine hydrochloride may suppress proinflammatory cytokines (such as TNF-α) and increase anti-inflammatory cytokine IL-10 during DSS-induced enteritis in mice (17). At a cellular level, sinomenine could either promote macrophage reprogramming toward M2-like phenotype (25) or induce the generation of Treg by upregulating the transcriptional factor Foxp3 (22). Recently, the gut microbiome was also found to be a target for regulatory T cell-based immunotherapy (26). In zebrafish, intestinal macrophages have been reported to have the ability to shape gut microbiota (27). These are in line with that SN-altered gut microbiota composition when treating DSS-induced colitis (17).

As an effective model organism, the zebrafish has been used to study enteritis in aquaculture (28, 29). SBMIE is the typical plant-sourced protein-induced inflammation, including in zebrafish, with the typical intestinal pathology (30, 31). To illustrate the immune mechanisms at a cellular level, the immune cell imaging using zebrafish larva provided important clues (28, 32, 33). Using zebrafish to model enteritis (34, 35) has revealed immune mechanisms that were not only the innate immune cells was involved (28, 30) during SBMIE, but also T cells played an important role, especially with a Th17 cytokine profile (15). Zebrafish has become a model for studying gastrointestinal tract-microbe interaction (36). In the zebrafish enteritis model, certain aquatic organisms, as well as natural compounds, have been proved to be effective in orally treating enteritis, such as microalga (28), lactoferrin (33), fucoidan (32). Therefore, zebrafish has become a model for testing ingredients, which could be potentially included in fish feeds.

In this study, sinomenine was tested for its anti-enteritis functions in the zebrafish SBMIE model. Using transcriptomic analysis of hindgut tissue and 16S sequencing of intestinal microbiota, the immune and metabolic processes involved have been revealed. The immune regulatory mechanisms have

been assessed by immune cell imaging and regulatory immune cell-related gene expression. Our findings indicate that sinomenine hydrochloride could be used as an effective additive for preventing diet-induced intestinal inflammation and even microbiota dysbiosis in fish.

MATERIALS AND METHODS

Zebrafish

Zebrafish, including both AB wild-type line and fluorescence-labeled lines, including Tg(lyz:DsRED2), Tg(mpeg1:EGFP), Tg (rag2:DsRed), and Tg(lck:lck-eGFP), were purchased from China Zebrafish Resource Center (http://en.zfish.cn/) and were maintained according to standard protocols (37). After crossing neutrophil and macrophage labeled lines, Tg(lyz:DsRED2/mpeg1:EGFP) were obtained, then together with Tg (rag2:DsRed) and Tg(lck:lck-eGFP), three lines of Tg fish were prepared for further experiments. The use of animals in this study was approved by the Animal Research and Ethics Committees of the Institute of Hydrobiology, Chinese Academy of Sciences. All experiments were conducted following the guidelines of the committees.

Diets and Feeding Trial

The formulation of the experimental diets is shown in **Table 1**. To model SBMIE in adult WT fish (3 mo), diets, as well as the 6-week feeding trial, followed a previously published method (4). For the SBMIE larva model, the feeding trials for both innate and adaptive immune cell imaging followed our recently published protocol (38). In brief, the innate model used 5 dpf larva of Tg (lyz:DsRED2/mpeg1:EGFP) to do a 4-day feeding trial with FM (negative control), SBM (positive control), and drug-included SBM diet (tested group). Afterwards, at 9 dpf, imaging of the hindgut was carried out. The adaptive model used 17 dpf larva of either Tg(rag2:DsRed) or Tg(lck:lck-eGFP) to do a 10-day feeding trial, and then larva at 27 dpf was conducted to imaging analysis. The sinomenine hydrochloride, which is the hydrochloride chemical form of sinomenine (39), was purchased from Xi'an Huilin Biotechnology Co., Ltd in China. Based on our previously researched effective concentration for preventing SBMIE, the dietary inclusion of sinomenine hydrochloride should be in the range of 15–60 ppm (40). Thus, in this study, 35 ppm sinomenine hydrochloride was included in the soybean meal diet to test if it could have any alleviating effect on SBMIE.

TABLE 1 | Formulation of experimental diets.

Raw Material g/kg	FM	SBM	SN
Fish meal	555	250	250
Soybean meal	0	500	500
Wheat meal	255	110	110
Starch	50	50	50
Fish oil	30	60	60
Mineral premix[a]	10	10	10
Vitamin premix[b]	10	10	10
Sinomenine	0	0	0.7
Cellulose	90	10	9.3
Gross weight (g)	1,000	1,000	1,000

[a]*Per kilogram of mineral premix (g kg−1): MnSO4·H2O (318 g kg−1 Mn), 1.640g; MgSO4·H2O (150 g kg−1 Mg), 60.530 g; FeSO4·H2O (300 g kg−1 Fe), 23.110 g; ZnSO4·H2O (345 g kg−1 Zn), 0.620 g; CuSO4·5H2O (250 g kg−1 Cu), 0.010 g; KI (38 g kg−1 I), 0.070 g; NaSeO3 (10 g kg−1 Se), 0.005 g. All ingredients were diluted with cornstarch to 1 kg.*

[b]*Per kilogram of vitamin premix (g kg−1): retinyl acetate (500,000 IU g−1), 2.40 g; cholecalciferol (500,000 IU g−1), 0.40 g; DL-a-tocopherol acetate (500 g kg−1), 12.55 g; menadione (230 g kg−1), 0.80 g; cyanocobalamin (10 g kg−1), 0.83 g; D-biotin (20 g kg−1), 4.91 g; folic acid (960 g kg−1), 0.40 g; thiamin hydrochloride (980 g kg −1), 0.05 g; ascorhyl acetate (930 g kg−1), 7.16 g; niacin (990 g kg−1), 2.24 g; meso-inositol (990 g kg−1), 19.39 g; calcium-D-pantothenate (980 g kg−1), 2.89 g; riboflavin (800 g kg−1), 0.55 g; pyridoxine (980 g kg−1), 0.59 g. All ingredients were diluted with corn starch to 1 kg.*

Analysis of Sinomenine's α7nAchR Binding Ability by Molecular Docking

To check if sinomenine could potentially activate zebrafish α7nAchR signaling, PROCHECK server and ProSA web were applied to test the potential binding ability of sinomenine to zebrafish α7nAChR protein, following a previously described method (41, 42).

Sampling

In adult zebrafish, the hindgut tissue, which is a third of the whole intestine from bend 2 to the anus (43), has been used for sampling. For gene expression analysis, including transcriptome, qPCR, and immunofluorescence (n = 6), the tissues used to isolate RNA for both transcriptomic and qPCR were cut into small pieces and soaked in a 10-fold volume of TRIzol (Invitrogen), and the tissues used to make frozen sections were soaked in a 10-fold volume of 4% PFA (Sigma). For all omics studies, the hindgut from one female and one male adult zebrafish were mixed for each sample (three repetitions) to avoid sex-biased differences for both transcriptome and 16S. The sampling of 16S sequencing analysis followed the method published in previous studies by Deng et al. (44). For the sampling of larvae, only 27 dpf larvae (n = 6) were sampled for HE staining at the meantime of imaging the adaptive immune cells.

Histological and Immunofluorescence Analyses

To demonstrate the basic pathology of intestinal mucosa, both hematoxylin eosin (HE) staining and immunofluorescence were performed using hindgut tissue slices of 10 μm. Then, the zebrafish anti-CD4-1 antibody (GeneTex), which can immune-stain the T helper cell, was applied during immunofluorescence analysis to further illustrate the inflammatory aggregation or infiltration of lymphocytes in different intestinal layers or villi locations in the hindgut (4). The zebrafish anti-foxp3 antibody (GeneTex) was also used to identify the regulatory lymphocytes in intestinal mucosal folds (45). Meanwhile, DAPI was used parallelly to stain the nucleus.

Library Preparation and Sequencing for Transcriptomic Data

For the hindgut's RNA (n = 6), transcriptomic analysis was completed to reveal the gene expression profile systematically in adult fish from all groups, including the negative control (FM group), the positive control (SBM group), and the tested drug

inclusion group (SN group). The procedure of the gene library preparation and sequencing for transcriptome followed previously published methods (46). Briefly, sequencing libraries were generated using NEBNext R UltraTM RNA Library Prep Kit for Illumina R (NEB, USA) following the manufacturer's recommendations, and the library quality was assessed on the Agilent Bioanalyzer 2100 system. The library preparations were sequenced on an Illumina platform (NovaSeq 6000), and 150 bp paired-end reads were generated.

Transcriptome Assembly, DEG Analysis, and Functional Annotation

After the clean data were mapped onto the reference genome by HISAT2 (version 2.1.0) (47), the transcript was assembled using StringTie (Version V1.3.1c) (48). Salmon (version 0.12.0) (49) was used to calculate the gene expression. $|\log2FoldChange| > 1$ and padj < 0.05 is considered to be differentially expressed genes (DEG), using DESeq2 1.24.0 (version) to analyze differential expression (50). For annotations, enrichment analysis of both GO terms and KEGG pathways was performed using clusterProfiler (version 3.12.0) (51), and $p < 0.05$ was considered to be a significant enrichment. In the case of the parameters used not being listed, default parameters were used.

RNA Extraction and qPCR Analysis

Principally, the RNA extraction and qPCR analysis of the zebrafish intestinal tissues were done according to previously published procedures (4, 6). In brief, TRIzol (Invitrogen) was used to extract RNA, and then the isolated RNA was reverse-transcribed into cDNA using HiScript III 1st Strand cDNA Synthesis Kit (Vazyme). In addition, all the RNA extraction was done immediately after sampling, or at the same time for sampling to do an omics study. Genes of interest, including both randomly selected DEGs and genes involved in α7nAChR, mediated anti-inflammatory function were validated for their expressional changes by qPCR. Specifically, genes of both intestinal pro-inflammatory factors (transcription factor *nf-κb*, cytokines *il-1β*, *tnf-α*, *il17a/f3*, and CD4) and anti-inflammatory factors (cytokines *tgf-β1a*, *il-10*, *il22* and transcription factor *foxp3a* and *foxp3b*) have been checked for SN-induced α7nAChR-mediated anti-inflammatory effect in intestine. Meanwhile, *rpl13a* was used as the internal reference. The primers used to amplify these genes are listed in **Table 2**.

In Vivo Imaging of Immune Cells in Zebrafish Larvae

In vivo imaging of immune cells was completed following previous studies of zebrafish larvae imaging (15, 28, 32), with some modified conditions, such as the incubating solution, exact time, and microscopy. Imaging of innate immune cells, including neutrophils (lyz labeled) and macrophages (mpeg labeled) in the hindgut (tail part) of Tg(lyz:DsRED2/mpeg1:EGFP) larvae (n = 10), was through referencing previously published methods (38). Larvae were fed with experimental diets (diets for FM, SBM, SB groups, which were crushed and passed through an 80-mesh sieve) between 5 to 8 dpf. At 9 dpf, the Tg(lyz:DsRED2/mpeg1:EGFP) larvae were anesthetized by MS222 and then embedded in 1% LMP Agarose (Invitrogen), dissolved in Danieau's solution (52) to conduct imaging analysis. For imaging adaptive immune cells, including immature (rag2 labeled) and mature lymphocytes (lck labeled) in the hindgut (tail part) of Tg(rag2:DsRed) and Tg(lck:lck-eGFP) larvae (N = 10), we followed previously published methods (38). After feeding 12 days of Larval AP100 Diet (Zeigler) from 5 to 16 dpf, as well as 10 days of experimental diets from 17 dpf, at 27 dpf the larvae were anesthetized and embedded in 1% LMP Agarose (Invitrogen), dissolved in Danieau's solution (52). The Tg(rag2:DsRed) or Tg(lck:lck-eGFP) larvae were observed under a Leica SP8 microscope. For the intestinal imaging of larvae, a composition of several stacks was merged to generate the picture for the whole tail part of the intestine.

16S rRNA Gene Sequencing of Intestinal Microbiota

The composition of bacterioplankton was analyzed using sequencing of 16S rRNA gene amplicons. DNAs from the six repetitions were extracted for each treated sample. Then the V3V4 regions of the 16S rRNA genes, which can yield accurate taxonomic information, were amplified with the primer set 338F (5'- ACTCCTACGGGAGGCAGCA-3')/806R (5'-GGACTAC HVGGGTWTCTAAT-3'). After the libraries were built, the paired-end 250-nucleotide reads were yielded using the Illumina NovaSeq platform, according to the manufacturer's instructions. Raw sequences were then trimmed, quality filtered, denoised, merged, chimera and dereplicated using the DADA2 plugin (53). Reads with 100% nucleotide sequence identity across all samples were assigned to operational taxonomic units (OTUs), and taxonomy was assigned to Non-singleton amplicon sequence variants (ASVs) using the classify-

TABLE 2 | qPCR primers used in enteritis-related cytokine gene expression analysis.

Gene Name	Forward sequence	Reverse sequence
il-1β	5'-TGGACTTCGCAGCACAAAATG-3'	5'-GTTCACTTCACGCTCTTGGATG-3'
nf-κb	5'-GATCATCGAGCAGCCTAAATC-3'	5'-CCCACTGTAGTTGTGAACCCT-3'
tnf-α	5'-GCGCTTTTCTGAATCCTACG-3'	5'-TGCCCAGTCTGTCTCCTTCT-3'
il-17a/f3	5'-AAGATGTTCTGGTGTGAAGAAGTG-3'	5'-ACCCAAGCTGTCTTTCTTTGAC-3'
tgf-β1a	5'-TGTACCCGCAATCCTTGACC-3'	5'-CCGACTGAGAAATCGAGCCA-3'
il-10	5'-CACTGAACGAAAGTTTGCCTTAAC-3'	5'-TGGAAATGCATCTGGCTTTG-3'
il22	5'-GATGACTGATACAGCACGAAA-3'	5'-CATTGATGCAGCAGGAACCT-3'
foxp3a	5'-GCCTCCATGATACGATGGGCAAT-3'	5'-CCTTCCTTCAACACGCACAA-3'
rpl13a	5'-TCTGGAGGACTGTAAGAGGTATGC-3'	5'-AGACGCACAATCTTGAGAGCAG-3'

sklearn naïve Bayes taxonomy classifier in the feature-classifier plugin (54) against the Greengenes reference database (version 13.8, http://greengenes.secondgenome.com/) (55).

Statistical Analysis

The HE-stained intestinal villi, immunofluorescence signals, as well as imaging results of immune cells in larvae were quantified by Image J software. T-tests were used to assess differences for most parameters for staining and imaging results, with a false discovery rate adjusted $p < 0.05$ or 0.01. For the quantification of immunofluorescence signals, the quantitative analysis method followed a previously published study (6, 56) with the modification to calculate the positive cell NO. per villi, which equaled to that the account of number was divided by the average length of intestinal villi. Then, the data were processed using Excel and SPSS 22.0. After eliminating abnormal data by Grubbs' test, one-way ANOVA was used to analyze the variance. The minimum significant difference method was used for multiple comparisons. Means ± Standard Deviation was used to generate bar. $p < 0.05$ was judged as significant difference, meanwhile $p < 0.01$ as extremely significant difference. The rearranged data from the pathological or immune analyses were applied to GraphPad Prism version 5.0 software for all graphs. For the correlation analysis to compare fold changes between results of qPCR and DEGs, data were processed in EXCEL. The plots and diagrams were displayed by ggplot2 (2.2.1) using R language.

RESULTS

The Validation of α7nAchR Binding Ability of Sinomenine

The results of molecular docking showed that sinomenine can bind to the same binding pocket of zebrafish α7nAChR as the positive control Epibatidine, a typical agonist of α7nAChR (**Figure S1**). In this pocket, sinomenine could form hydrogen bonds with several amino acids, including tryptophan, phenylalanine, and lysine. The binding energy of sinomenine to zebrafish α7nAChR was −29.62 kJ/mol, which was comparable to that of positive control Epibatidine (−37.15 kJ/mol).

Effect of Sinomenine on Intestinal Pathology in SBMIE Adult Model

The inclusion of sinomenine at 35 ppm significantly prevented pathological changes in the hindgut. The HE staining result demonstrated the relief of intestinal lesion at mucosal fold level upon sinomenine dietary inclusion, compared with the SBM group. Quantitative analyses of the histological parameters in the SBMIE adult model reflect that in the SN group the height of intestinal villi increased while the thickness of lamina propria (LP) decreased very significantly ($p < 0.01$) (**Figure 1A**). The increased height of intestinal villi ($p < 0.01$) in the SN group was revealed in the hindgut at 27 dpf in the larva model (**Figure 1B**), compared to the very shortened mucosal fold in the SB group. Specifically, in the LP layer of intestinal villi, the widened top with lymphocyte infiltration indicated by the blue hematoxylin-stained nuclei in SN group was reduced compared to that in the SBM group.

Lymphocyte-Related Intestinal Protein Expression

To reveal the mechanisms of the lymphomonocytes involved, T helper cells, which are at the nexus of the innate and adaptive arms of the immune system (57), have been checked for related protein expressions using immunofluorescent analysis. As the surface marker of T helper lymphocytes and expressed protein on certain populations of phagocytes in zebrafish (57), the immunofluorescence results of intestinal CD4-1 signals showed that the inflammatory aggregation in the widened LP layer of the hindgut, especially at the top of villi in the SBM group. While in the SN group, though that the positive cell NO. per villi of CD4 signals increased, there are fewer signals in the top of villi, but a large proportion of $CD4^+$ cells were found at the base of the mucosal fold (**Figure 2A**).

Further, to reveal the Treg's involvement, an immune-stained transcriptional factor reflected that there were brighter and more $Foxp3^+$ cells in the SN group, and a substantial proportion of $Foxp3^+$ cells was found at the base of the villi in the SN group, compared to SBM group (**Figure 2B**). In the SBM group, $Foxp3^+$ cells were also found at the edge of basal plasmacytosis (**Figure 2B**). While it was interesting to notice many vasally located $Foxp3^+$ cells in the SN group (**Figure S2**). Considering the recovered length of intestinal villi, the positive cell NO. per villi of Foxp3 in the SN group was lower compared to the SBM group, yet still higher than the FM group (**Figure 2B**).

qPCR Analysis of DEGs and Intestinal Pro- or Anti-Inflammatory Factors

The raw data of current transcriptomic analysis have been submitted to the Genome Sequence Archive (GSA) database (http://gsa.big.ac.cn/index.jsp) with the BioProject identifier <PRJCA005917> and data ID <CRA004582>. The close correlation ($R > 0.08$) of fold changes between fold changes of qPCR result and DEGs (**Figure 3A** and **Table S1**) proved the successful decoding of gene expression by the current transcriptomic analysis. Specifically, the immunoregulatory role of SN was reflected by the expression of pro-/anti-inflammatory factors (**Figure 3B**). The pro-inflammatory cytokine genes' result (**Figure 3B**, upper) showed that in the SN group *tnf-α* was very significantly downregulated compared to the SBM group, and even dropped to a similar level to the FM group. *il-1β* and *tnf-α* were downregulated with non-significant trends, yet, *nf-κb*, *il17a/f3*, and *cd4* were almost not changed compared to the SBM group. The anti-inflammatory factor genes' result (**Figure 3B**, lower) showed that except for the not significantly upregulated *tgf-β1a*, *il-10*, *il22*, *foxp3a*, and *foxp3b* were significantly upregulated.

Enriched GO Terms and KEGG Pathways of Intestinal DEGs

According to the enriched biological process GO terms of DEGs from a comparison between SN *vs* SBM groups (with details in **Table S2**), there were many immune cells or process-related terms (**Figure 4A** and **Table S3**). For immune cells, there were "leukocyte cell-cell adhesion," "negative regulation of lymphocyte activation," "negative regulation of leukocyte activation,"

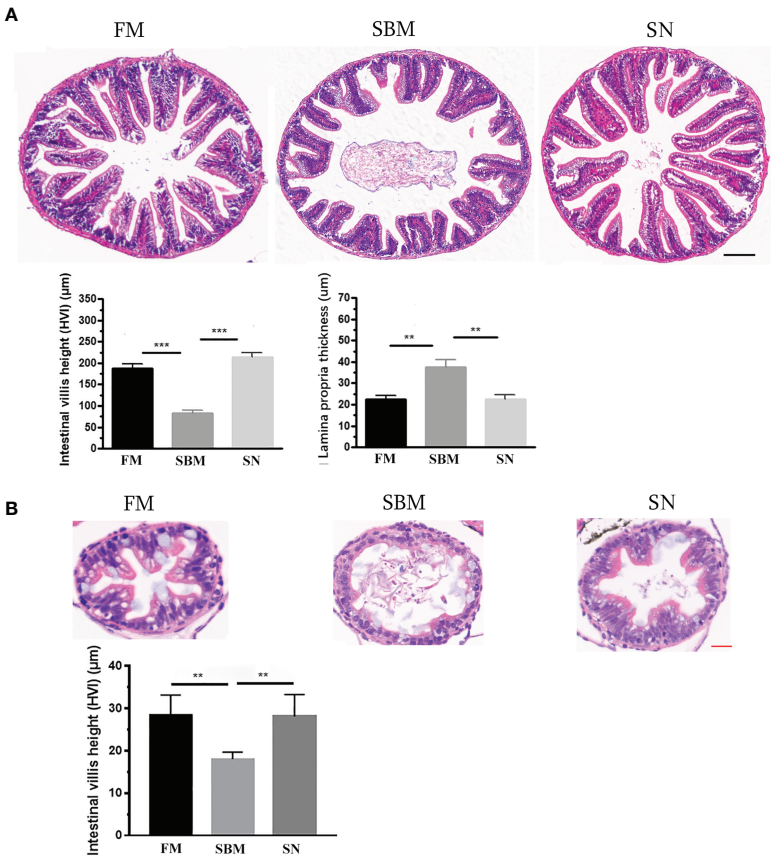

FIGURE 1 | Pathological analysis of sinomenine's effect on the intestinal mucosal fold. **(A)** HE staining of intestinal mucosa in adult fish fed with FM, SBM, and SN diets. Scale bar: 100 μm. **(B)** HE staining of intestinal mucosa in 27 dpf larva fed with FM, SBM, and SN diets. FM, fish meal diet; SBM, soybean meal diet; SN, sinomenine supplementary SBM diet. Scale bar: 20 μm. ** represented $p < 0.01$, and *** represented $p < 0.001$.

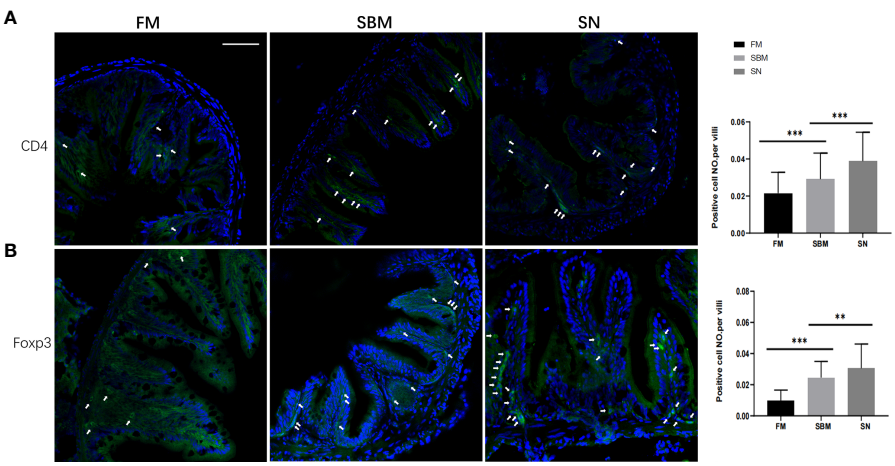

FIGURE 2 | Lymphocyte-related intestinal protein expression reflected by immunofluorescent signals. $CD4^+$ **(A)** or $Foxp3^+$ **(B)** immunofluorescence signals (green) in adult fish fed with FM, SBM, and SN diets. The quantification of the ratio, which was calculated by dividing positive cell number with intestinal villi's length, was shown beside the typical images (at the right side). Typical signals are indicated by arrows. The blue signals represented DAPI-stained cell nucleus. FM, fish meal diet; SBM, soybean meal diet; SN, sinomenine supplementary SBM diet. Scale bar: 100 μm. ** represented $p < 0.01$, and *** represented $p < 0.001$.

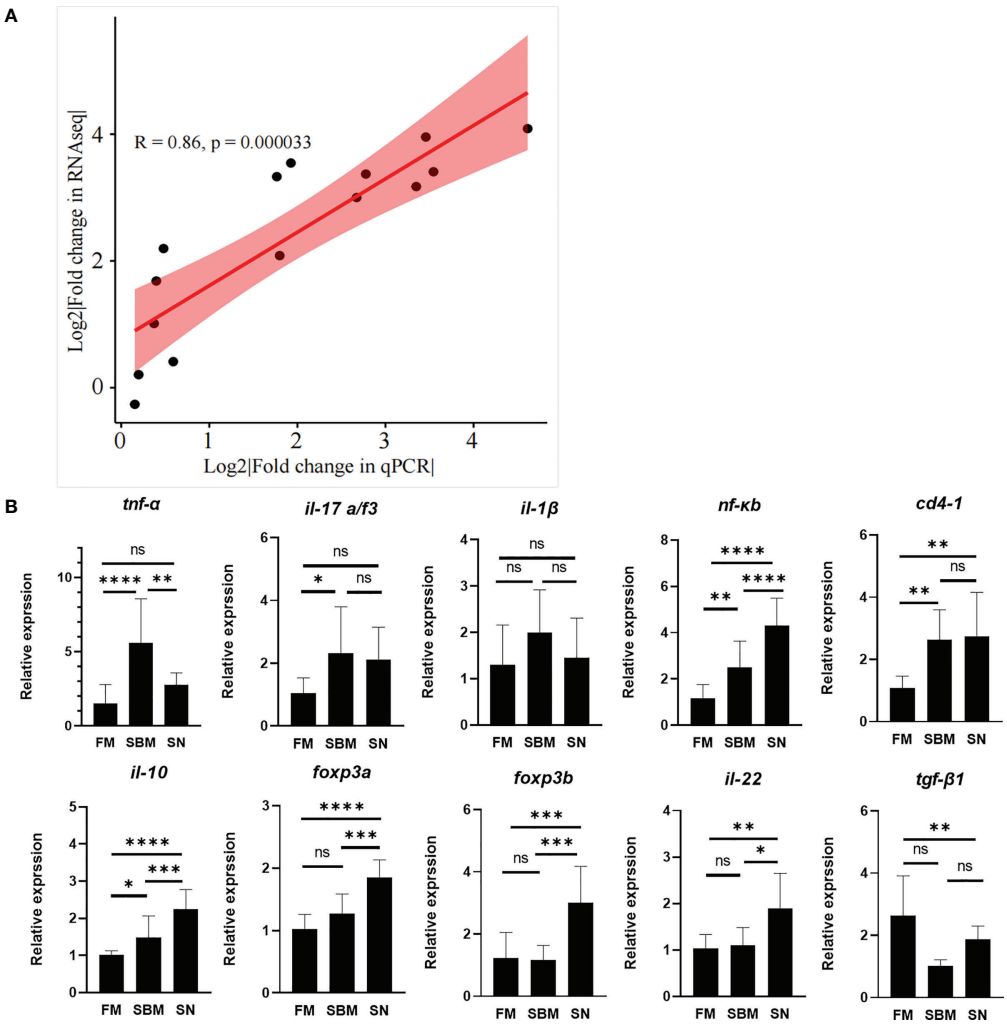

FIGURE 3 | qPCR validation. **(A)** qPCR validation of transcriptomic data; **(B)** qPCR analysis of enteritis-related pro-/anti-inflammatory factors, which could reflect α7nAchR-mediated anti-inflammatory effect in fish. "ns" represented p > 0.05, * represented $p < 0.05$, ** represented $p < 0.01$, and *** represented $p < 0.001$.

"negative regulation of alpha-beta T cell proliferation," "regulation of T cell migration," "regulation of alpha-beta T cell proliferation," "regulation of lymphocyte migration." For the immune process, there were "regulation of immune effector process," "positive regulation of production of molecular mediator of immune response," "regulation of cytokine production involved in immune response," and "cytokine production involved in immune response." Meanwhile, among revealed KEGG pathways (**Figure 4B**, **Table S4**), a high gene ratio existed in six pathways, which contained metabolic-related "glycolysis/gluconeogenesis" and "insulin signaling pathways."

Effect of Sinomenine on Intestinal Immune Cell in Zebrafish Larvae

At a cellular level, for innate immune cells, sinomenine could significantly ($p < 0.01$) relieve inflammatory aggregation for both neutrophils (lyz^+ cells) and macrophages ($mpeg^+$ cells) (**Figures 5A, B**) in the hindgut of the larva. For adaptive immune cells, sinomenine could significantly ($p < 0.01$) inhibit the inflammatory aggregation and immune synapse formation of both $rag2^+$ immature lymphocytes and lck^+ mature T lymphocytes (**Figures 5C, D**). Specifically, the formation of immune synapses of $mpeg^+$ and $rag2^+$ cells in the SBM group could be inhibited in the SN group.

Effect of Sinomenine on Microbiota OTU and Taxa Composition in Hindgut

The identified OTU in the hindgut of adult zebrafish for FM, SBM, and SN groups were 8,434, 5,976, and 5,895, respectively. As indicated by the Venn diagram (**Figure 6A**), the overlapping between the sinomenine and FM groups covered 635 OTUs, while the overlapping between the sinomenine and SBM groups contained 471 OTUs. To estimate the abundance of taxa, currently revealed OTUs could be identified by a lot of phyla. Among the most abundant 10 phyla, compared to the SBM groups, in the SN group,

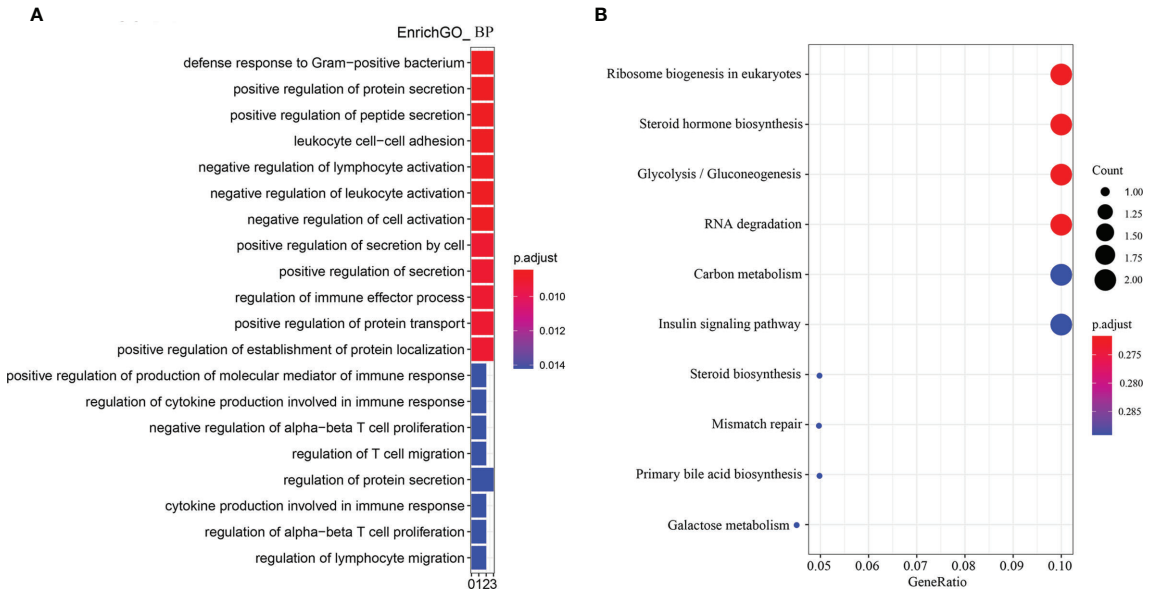

FIGURE 4 | Enriched GO terms and KEGG pathways for DEGs from the comparison between the SN and SBM groups in the zebrafish SBMIE adult model. **(A)** The GO terms of biological process; **(B)** the KEGG pathways. SBM, soybean meal diet; SN, sinomenine supplementary SBM diet.

the increased phyla included Proteobacteria, Actinabactieria, Acidobacteria, and Gemmatimonadetes, while decreased phyla included Firmicutes, Bacteroidetes, Fusobacteria, and TM7 (**Figure 6B**). Moreover, at a genus level (**Figure 6C**), among the 10 genera of most abundance, compared to SBM groups, in the SN group increased genera included *Aeromonas*, *Cetobacterium*, *Rhodobacter*, *Prevotella*, *Pelomonas*, and *Aquabacterium*, while decreased genera included *Sphingomonas*, *Acinetobacter*, and *Shigella*. The raw data of the current 16S sequencing analysis have been submitted to the Genome Sequence Archive (GSA) database (http://gsa.big.ac.cn/index.jsp) with the BioProject identifier <PRJCA005917> and data ID <CRA004611>.

DISCUSSION

In the present study, efforts were made to activate the intestinal local immune modulation by α7nAChR-mediated anti-inflammatory function to help treat fish foodborne enteritis. The results indicated sinomenine, which could closely bind to the zebrafish α7nAChR, reduced fish foodborne enteritis pathology at both the anti-inflammatory and metabolic levels paralleled by ameliorating dysbiosis of intestinal microbiota.

Enlightened by the structure-guided medicine discovery approach (58), the sinomenine's protective role against SBMIE was revealed in the fish foodborne enteritis model. Pathologically, the current data showed that sinomenine did work in the gut. Based on the successful modeling of SBMIE in adult or larval zebrafish as in our previously published papers (19, 20), the typical intestinal pathology, such as villus atrophy and basal cell hyperplasia, has also been observed in the positive control (SBM group) and was found to be relieved by the present results in the SN group. Although in mice, intestinal neutrophil recruitment could be inhibited *via* M2AChR (59), the currently used α7nAchR-specific agonist SN also suppressed fish neutrophil aggregation in the hindgut. This may be the downstream effect of suppressed TNF-α by SN. For the macrophage and T cell signals reflected by imaging analysis as well as immune-stained CD4-1 signals, this may result from SN-evoked α7nAChR-mediated anti-inflammatory macrophage and Treg's effects, as well as non-immune function, such as promoting local tissue repair (60) and preserving the integrity of the epithelial barrier (61). The tissue repair was also suggested by the upregulated trend of TGF-β. The current study revealed a large proportion of $Foxp3a^{+}$ cells are located in the basal part of LP and even in the intestinal vasal. This was in line with the HE results that in the SN group the lymphocytes infiltration mainly at the villi top was reduced compared to the SBM group.

At a molecular level, the revealed DEGs in transcriptomic analysis already provided signs for the involved mechanisms in SN's anti-inflammation effect. As for the upregulated genes, the peptidoglycan recognition protein may play a role similar to the pore-forming C-type lectin; thus, its higher expression was associated with enhanced intestinal mucosal immunity (36). The higher level of *intelectin 3*, which was reported to be involved in the protective mycobacterial immune response, may be a beneficial mucosa factor against dysbiosis. *Enolase*, a neuronal marker (62), may indicate enhanced participation of enteritic neurons upon sinomenine's stimulation. Significant upregulation of both *foxp3a* and *foxp3b*, which was responded to specifically in the fish intestine (63), may indicate both the impute and local differentiation of Treg in the hindgut. On the other hand, among the downregulated genes,

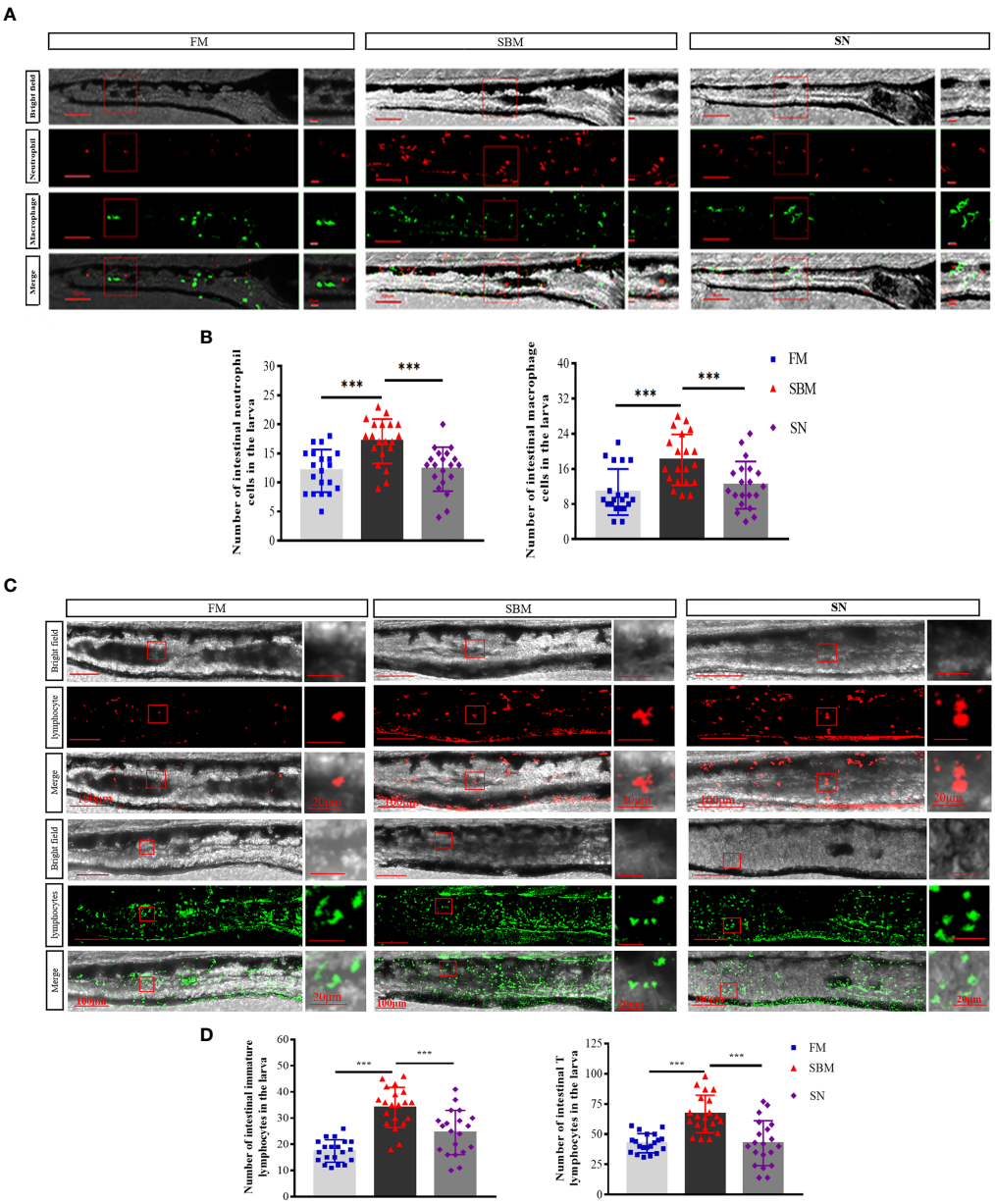

FIGURE 5 | Imaging analysis of immune cells in the hindgut of the zebrafish SBMIE larva model. **(A)** Hindgut innate immune cells, including neutrophils (lyz-DsRed labeled cells) and macrophages (mpeg-EGFP labeled cells); **(B)** the histogram of lyz or mpeg signals in the hindgut of larva. **(C)** Hindgut adaptive immune cells, including immature lymphocytes (rag2-DsRed-labeled red cells) and mature T lymphocytes (lck-EGFP-labeled green cells). **(D)** The histogram of rag2^{+} or lck $^{+}$ signals in the hindgut of larva. FM, fish meal diet; SBM, soybean meal diet; SN, sinomenine (35 ppm) supplementary SBM diet. The significant differences were indicated by p value, and *** represented $p < 0.001$. The scale bar in whole hindgut pictures was 100 μm, while the scale bar in the enlarged view was 20 μm.

there was a lower expression of TRIM9, which may suggest lower rates of macrophage migration (64). Downregulated Thy-1 in the SN group potentially suggested fewer gut intramucosal lymphocytes (65).

The currently revealed SN's immune effect was reflected at both innate and adaptive levels. Imaging of neutrophils and macrophages echoed with leukocyte-related GO terms; meanwhile, imaging of lymphocytes was coincident with lymphocyte-related terms. As to the enteritis-related cytokine, the significantly suppressed *tnf-α*, which is at the upstream of intestinal pro-inflammatory cytokines (66) (such as the currently revealed downregulated *il-1β* though not significantly), may play an important role in SN's ameliorating effect. Compared to the SBM group, the decreased number of both neutrophils and macrophages may result from the significantly restrained *tnf-α* expression. For macrophages, fewer immune synapse-like

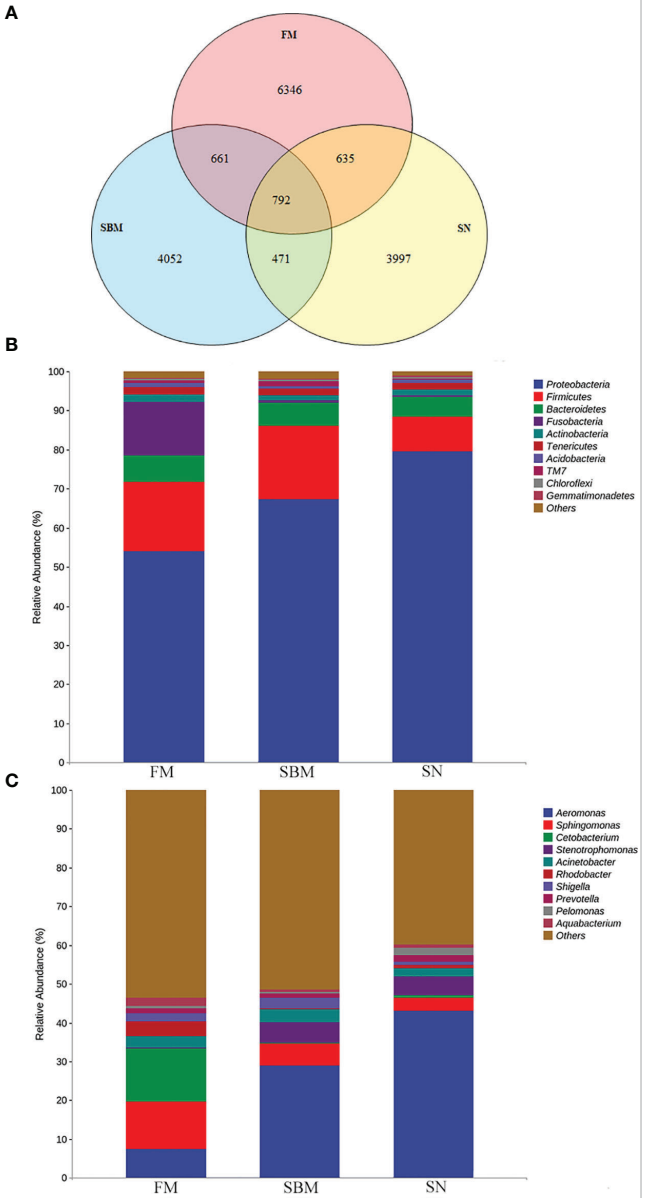

FIGURE 6 | Analysis of intestinal microbiota OTU and taxa composition influenced by sinomenine inclusion in zebrafish SBMIE adult model. **(A)** Venn diagram of OTU in the FM, SBM, and SN groups; **(B)** hindgut bacteria composition at phylum level; **(C)** hindgut bacteria composition at the genus level. FM, fish meal diet; SBM, soybean meal diet; SN, sinomenine supplementary SBM diet.

structures in the SN group may suggest the inhibition of innate immune cells' migration and phagocytic activity (67, 68), and the inhibition of the M1 phase at the mucosa (60). These results of fish macrophages were in line with the findings in mammals that the interaction with α7nAChR expressed on macrophages leads to a reduction of pro-inflammatory cytokines (13). In addition, for intestinal mucosa immunity, the significantly upregulated *il-22* (qPCR result) together with upregulated *muc2* in all DEGs (highlighted in **Table S2**) may indicate the protective function to maintain host epithelium integrity (69, 70).

From an adaptive view, hindgut lymphocytes were indicated as the SN's effective target, based on many lymphocytes (especially T cell) related biological process GO terms and imaging result of lymphocytes in comparison between SN and SBM groups. In general, hindgut lymphocytes' responses may be limited by SN, as that the number of lymphocytes was reduced and immune synapse like structure in Rag^+ cells in 27 dpf larvae's hindgut disappeared in the SN group. Yet, the increased intestinal CD4 at a protein level, but not RNA level, maybe due to the vesicular input caused by SN-induced systemic immune's response (71). The basal location of CD4 together with upregulated immune-regulated factors (*il-10*, *foxp3a*, and *foxp3b*) may be consistent with the location in the basal part of LP or mucosal fold was a feature of only Treg among Th populations (72). SN stimulated upregulated both TGF-β and Foxp3 echoed with that grass carp TGF-β1 could upregulate Foxp3 expression (73). Regarding the glucose metabolism and insulin-related KEGG pathways, as both the lower glucose values and insulin therapy seemed to be anti-inflammatory (74), these pathways could be considered as the metabolic effects of intestinal α7nAChR-mediated anti-inflammatory function in fish.

Coincident with recent findings that SN's effect could be limited by antibiotic's disturbing the intestinal microbiota (75), the current study used the immunomodulator SN in the fish diet, which caused an altered OTU and taxa composition in the hindgut. This actinobacterium could produce active metabolites against pathogenic microorganisms (76), increasing Actinabacteria and, as a result, indicating a protective factor in the SN group. Increased Acidobacteria in the SN group may indicate better protein utilization since that Acidobacteria was revealed as a major component of intestinal microbiota in carnivorous fish (77). The decreased Bacteroidetes, which was responsible for carbohydrate degrading in the intestine (78), may indicate less importance for starch utilization in the SN group. The decreased TM7 suggested less intestinal inflammation and that intestinal TM7 bacterial phylogenies may be a promoter of inflammation for IBD (enteritis in humans) (79). This finding was echoed with the result at a genus level, as that decreased *Sphingomonas*, which has been revealed as a disease biomarker in zebrafish (80), as well as *Shigella*, which has been found associated with CD (enteritis in humans) (81). Both of these results have indicated relief of enteritis. Upregulated probiotic *Rhodobacter* (82, 83) may be a protective factor. The increased *Cetobacterium*, which suggested improvement of fish carbohydrate utilization (84), was echoed with the KEGG pathway "glycolysis/gluconeogenesis" in the SN group.

In summary, dietary supplementation of sinomenine hydrochloride could enhance intestinal immune barrier function *via* both inhibiting aggregation of immune cells and changing immune cells' status possibly through glucose metabolism, whilst ameliorating microbiota dysbiosis to prevent foodborne enteritis in fish. The hypothetical

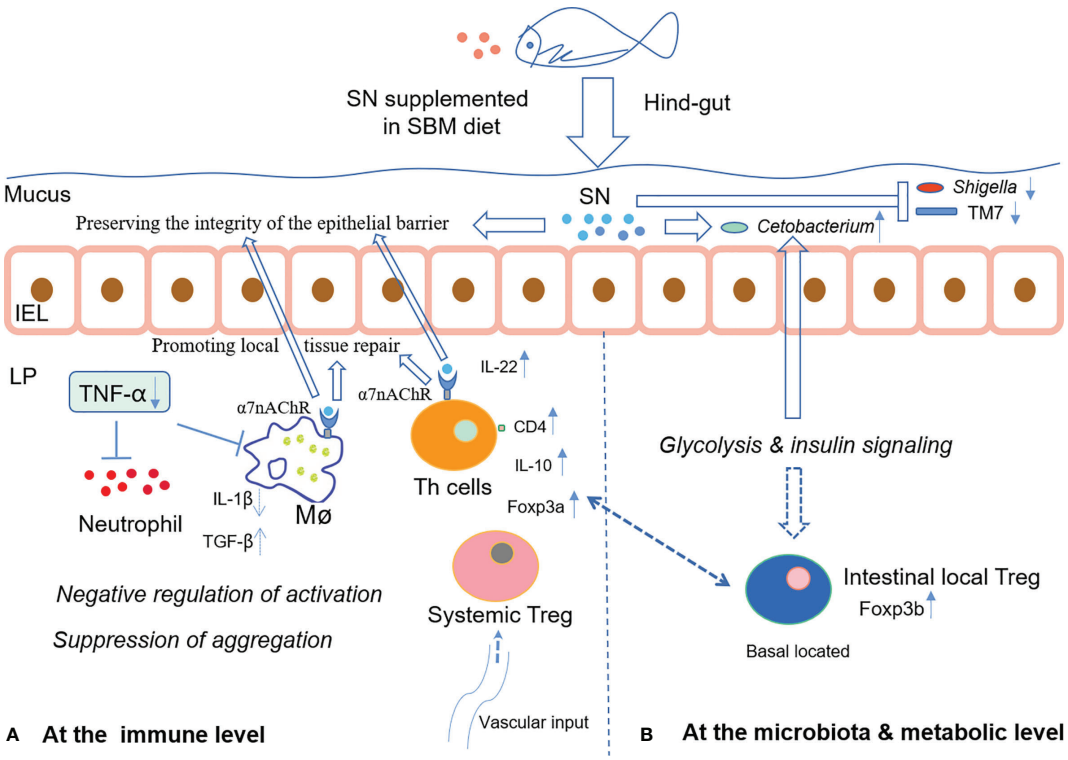

FIGURE 7 | The hypothetical mechanism of SN's α7nAchR-mediated anti-inflammatory effect on the intestinal immune barrier during foodborne enteritis in the fish hindgut **(A)** at the immune level; **(B)** at the microbiota and metabolic level. IEL, intestinal epithelial layer; LP, lamina propria layer; Mø, macrophage; Th, T helper; Treg, regulatory T cell.

mechanism of SN's α7nAchR-mediated anti-inflammatory effect on the intestinal immune barrier during foodborne enteritis in fish hindgut is shown in **Figure 7**. Since that in fish, the effective concentration for diet inclusion is very low and sinomenine hydrochloride is cheap, the commercial use of sinomenine hydrochloride could be expected to treat foodborne enteritis in cultured fish.

DATA AVAILABILITY STATEMENT

The data presented in the study are deposited in the Genome Sequence Archive (GSA) database (http://gsa.big.ac.cn/index.jsp) with the BioProject identifier PRJCA005917 and data ID CRA004582 and CRA004611.

ETHICS STATEMENT

The animal study was reviewed and approved by the Animal Research and Ethics Committees of the Institute of Hydrobiology, Chinese Academy of Sciences. Written informed consent was obtained from the owners for the participation of their animals in this study.

AUTHOR CONTRIBUTIONS

NW conceived the project. JX, NW, and XZ wrote the manuscript. ML, JX, JS, XZ, YL, and YC performed the experiments. JX, ML, WY, YD, NW, WZ, and YL did data analysis. BU did language proofreading. The manuscript was read and approved by X-QX. All authors contributed to the article and approved the submitted version.

FUNDING

This work was funded by grants from National Natural Science Foundation of China (31872592).

ACKNOWLEDGMENTS

We thank Ms. Guangxin Wang and Ms. Fang Zhou in the Analysis and Testing Center of Institute of Hydrobiology, Chinese Academy of Sciences for assisting us on confocal microscopy imaging, and Prof. Rui Wang from Wuhan

Polytechnic University for providing trainee to assist this study. We would like to thank Prof. Ming Jiang for helping us on making zebrafish feed. We also thank the Wuhan Branch, Supercomputing Center, Chinese Academy of Sciences, China, for support of the computation in this work.

SUPPLEMENTARY MATERIAL

The Supplementary Material for this article can be found online at: https://www.frontiersin.org/articles/10.3389/fimmu.2021.766845/full#supplementary-material

REFERENCES

1. Fowler EC, Poudel P, White B, St-Pierre B, Brown M. Effects of a Bioprocessed Soybean Meal Ingredient on the Intestinal Microbiota of Hybrid Striped Bass. *Morone Chrysops X M Saxatilis Microorg* (2021) 9:1032. doi: 10.3390/microorganisms9051032
2. Kiron V, Park Y, Siriyappagouder P, Dahle D, Vasanth GK, Dias J, et al. Intestinal Transcriptome Analysis Reveals Soy Derivative-Linked Changes in Atlantic Salmon. *Front Immunol* (2020) 11:596514. doi: 10.3389/fimmu.2020.596514
3. Yin B, Liu H, Tan B, Dong X, Chi S, Yang Q, et al. MHC II-PI3K/Akt/mTOR Signaling Pathway Regulates Intestinal Immune Response Induced by Soy Glycinin in Hybrid Grouper: Protective Effects of Sodium Butyrate. *Front Immunol* (2020) 11:615980. doi: 10.3389/fimmu.2020.615980
4. Wu N, Xu X, Wang B, Li XM, Cheng YY, Li M, et al. Anti-Foodborne Enteritis Effect of Galantamine Potentially *via* Acetylcholine Anti-Inflammatory Pathway in Fish. *Fish Shellfish Immunol* (2020) 97:204–15. doi: 10.1016/j.fsi.2019.12.028
5. Fehrmann-Cartes K, Coronado M, Hernandez AJ, Allende ML, Feijoo CG. Anti-Inflammatory Effects of Aloe Vera on Soy Meal-Induced Intestinal Inflammation in Zebrafish. *Fish Shellfish Immunol* (2019) 95:564–73. doi: 10.1016/j.fsi.2019.10.075
6. Wu N, Wang B, Cui ZW, Zhang XY, Cheng YY, Xu X, et al. Integrative Transcriptomic and Micrornaomic Profiling Reveals Immune Mechanism for the Resilience to Soybean Meal Stress in Fish Gut and Liver. *Front Physiol* (2018) 9:1154. doi: 10.3389/fphys.2018.01154
7. Rombout JH, Abelli L, Picchietti S, Scapigliati G, Kiron V. Teleost Intestinal Immunology. *Fish Shellfish Immunol* (2011) 31:616–26. doi: 10.1016/j.fsi.2010.09.001
8. Perez T, Balcazar JL, Ruiz-Zarzuela I, Halaihel N, Vendrell D, de Blas I, et al. Host-Microbiota Interactions Within the Fish Intestinal Ecosystem. *Mucosal Immunol* (2010) 3:355–60. doi: 10.1038/mi.2010.12
9. Ganeva VO, Korytar T, Peckova H, McGurk C, Mullins J, Yanes-Roca C, et al. Natural Feed Additives Modulate Immunity and Mitigate Infection With *Sphaerospora Molnari* (Myxozoa:Cnidaria) in Common Carp: A Pilot Study. *Pathogens* (2020) 9:1013. doi: 10.3390/pathogens9121013
10. Bai A, Guo Y, Lu N. The Effect of the Cholinergic Anti-Inflammatory Pathway on Experimental Colitis. *Scand J Immunol* (2007) 66:538–45. doi: 10.1111/j.1365-3083.2007.02011.x
11. Ren C, Tong YL, Li JC, Lu ZQ, Yao YM. The Protective Effect of Alpha 7 Nicotinic Acetylcholine Receptor Activation on Critical Illness and Its Mechanism. *Int J Biol Sci* (2017) 13:46–56. doi: 10.7150/ijbs.16404
12. Wang H, Foong JPP, Harris NL, Bornstein JC. Enteric Neuroimmune Interactions Coordinate Intestinal Responses in Health and Disease. *Mucosal Immunol* (2021). doi: 10.1038/s41385-021-00443-1
13. Han B, Li X, Hao J. The Cholinergic Anti-Inflammatory Pathway: An Innovative Treatment Strategy for Neurological Diseases. *Neurosci Biobehav Rev* (2017) 77:358–68. doi: 10.1016/j.neubiorev.2017.04.002
14. Inoue T, Abe C, Kohro T, Tanaka S, Huang L, Yao J, et al. Non-Canonical Cholinergic Anti-Inflammatory Pathway-Mediated Activation of Peritoneal Macrophages Induces Hes1 and Blocks Ischemia/Reperfusion Injury in the Kidney. *Kidney Int* (2019) 95:563–76. doi: 10.1016/j.kint.2018.09.020
15. Coronado M, Solis CJ, Hernandez PP, Feijoo CG. Soybean Meal-Induced Intestinal Inflammation in Zebrafish Is T Cell-Dependent and has a Th17 Cytokine Profile. *Front Immunol* (2019) 10:610. doi: 10.3389/fimmu.2019.00610
16. Marjoram L, Alvers A, Deerhake ME, Bagwell J, Mankiewicz J, Cocchiaro JL, et al. Epigenetic Control of Intestinal Barrier Function and Inflammation in Zebrafish. *Proc Natl Acad Sci USA* (2015) 112:2770–5. doi: 10.1073/pnas.1424089112
17. Zhou Y, Chen S, Gu WX, Sun X, Wang LX, Tang LM. Sinomenine Hydrochloride Ameliorates Dextran Sulfate Sodium-Induced Colitis in Mice by Modulating the Gut Microbiota Composition Whilst Suppressing the Activation of the NLRP3 Inflammasome. *Exp Ther Med* (2021) 22:1287. doi: 10.3892/etm.2021.10722
18. Zhu WQ, Yuan XQ, Luo HJ, Shao JC, Chen XH. High Percentage of Dietary Soybean Meal Inhibited Growth, Impaired Intestine Healthy and Induced Inflammation by TLR-MAPK/NF-KB Signaling Pathway in Large Yellow Croaker (*Larimichthys Crocea*). *Aquacult Rep* (2021) 20:100735. doi: 10.1016/j.aqrep.2021.100735
19. Papke RL, Ono F, Stokes C, Urban JM, Boyd RT. The Nicotinic Acetylcholine Receptors of Zebrafish and an Evaluation of Pharmacological Tools Used for Their Study. *Biochem Pharmacol* (2012) 84:352–65. doi: 10.1016/j.bcp.2012.04.022
20. Grandi A, Zini I, Flammini L, Cantoni AM, Vivo V, Ballabeni V, et al. Alpha7 Nicotinic Agonist AR-R17779 Protects Mice Against 2,4,6-Trinitrobenzene Sulfonic Acid-Induced Colitis in a Spleen-Dependent Way. *Front Pharmacol* (2017) 8:809. doi: 10.3389/fphar.2017.00809
21. Yi L, Luo JF, Xie BB, Liu JX, Wang JY, Liu L, et al. Alpha7 Nicotinic Acetylcholine Receptor Is a Novel Mediator of Sinomenine Anti-Inflammation Effect in Macrophages Stimulated by Lipopolysaccharide. *Shock* (2015) 44:188–95. doi: 10.1097/SHK.0000000000000389
22. Tong B, Yuan X, Dou Y, Wu X, Wang Y, Xia Y, et al. Sinomenine Induces the Generation of Intestinal Treg Cells and Attenuates Arthritis *via* Activation of Aryl Hydrocarbon Receptor. *Lab Invest* (2016) 96:1076–86. doi: 10.1038/labinvest.2016.86
23. Sun D, Zhou M, Ying X, Cheng B, Han Y, Nie Y, et al. Identification of Nuclear factor-kappaB Inhibitors in the Folk Herb Rhizoma Menispermi *via* Bioactivity-Based Ultra-Performance Liquid Chromatography/Quadrupole Time-of-Flight Mass Spectrometry Analysis. *BMC Complement Altern Med* (2014) 14:356. doi: 10.1186/1472-6882-14-356
24. Yan LC, Bi EG, Lou YT, Wu XD, Liu ZD, Zou J, et al. Novel Sinomenine Derivative 1032 Improves Immune Suppression in Experimental Autoimmune Encephalomyelitis. *Biochem Biophys Res Commun* (2010) 391:1093–8. doi: 10.1016/j.bbrc.2009.12.028
25. Ni P, Liu YQ, Man JY, Li W, Xue SS, Lu TH, et al. C16, a Novel Sinomenine Derivatives, Promoted Macrophage Reprogramming Toward M2-Like Phenotype and Protected Mice From Endotoxemia. *Int J Immunopathol Pharmacol* (2021) 35:20587384211026786. doi: 10.1177/20587384211026786
26. Ben Ya'acov A, Lichtenstein Y, Zolotarov L, Ilan Y. The Gut Microbiome as a Target for Regulatory T Cell-Based Immunotherapy: Induction of Regulatory Lymphocytes by Oral Administration of Anti-LPS Enriched Colostrum Alleviates Immune Mediated Colitis. *BMC Gastroenterol* (2015) 15:154. doi: 10.1186/s12876-015-0388-x
27. Earley AM, Graves CL, Shiau CE. Critical Role for a Subset of Intestinal Macrophages in Shaping Gut Microbiota in Adult Zebrafish. *Cell Rep* (2018) 25:424–36. doi: 10.1016/j.celrep.2018.09.025
28. Bravo-Tello K, Ehrenfeld N, Solis CJ, Ulloa PE, Hedrera M, Pizarro-Guajardo M, et al. Effect of Microalgae on Intestinal Inflammation Triggered by Soybean Meal and Bacterial Infection in Zebrafish. *PLoS One* (2017) 12:e0187696. doi: 10.1371/journal.pone.0187696
29. Randazzo B, Abbate F, Marino F, Mancuso M, Guerrera MC, Muglia U, et al. Induction of Mild Enterocolitis in Zebrafish *Danio Rerio via* Ingestion of Vibrio Anguillarum Serovar O1. *Dis Aquat Organ* (2015) 115:47–55. doi: 10.3354/dao02864
30. Fuentes-Appelgren P, Opazo R, Barros L, Feijoo CG, Urzua V, Romero J. Effect of the Dietary Inclusion of Soybean Components on the Innate Immune System in Zebrafish. *Zebrafish* (2014) 11:41–9. doi: 10.1089/zeb.2013.0934
31. Hedrera MI, Galdames JA, Jimenez-Reyes MF, Reyes AE, Avendano-Herrera R, Romero J, et al. Soybean Meal Induces Intestinal Inflammation in Zebrafish Larvae. *PLoS One* (2013) 8:e69983. doi: 10.1371/journal.pone.0069983

32. Ikeda-Ohtsubo W, Lopez Nadal A, Zaccaria E, Iha M, Kitazawa H, Kleerebezem M, et al. Intestinal Microbiota and Immune Modulation in Zebrafish by Fucoidan From Okinawa Mozuku (*Cladosiphon Okamuranus*). *Front Nutr* (2020) 7:67. doi: 10.3389/fnut.2020.00067
33. Ulloa PE, Solis CJ, de la Paz JF, Alaurent TG, Caruffo M, Hernandez AJ, et al. Lactoferrin Decreases the Intestinal Inflammation Triggered by a Soybean Meal-Based Diet in Zebrafish. *J Immunol Res* (2016) 2016:1639720. doi: 10.1155/2016/1639720
34. Ulloa PE, Medrano JF, Feijoo CG. Zebrafish as Animal Model for Aquaculture Nutrition Research. *Front Genet* (2014) 5:313. doi: 10.3389/fgene.2014.00313
35. Brugman S. The Zebrafish as a Model to Study Intestinal Inflammation. *Dev Comp Immunol* (2016) 64:82–92. doi: 10.1016/j.dci.2016.02.020
36. Flores EM, Nguyen AT, Odem MA, Eisenhoffer GT, Krachler AM. The Zebrafish as a Model for Gastrointestinal Tract-Microbe Interactions. *Cell Microbiol* (2020) 22:e13152. doi: 10.1111/cmi.13152
37. Renshaw SA, Loynes CA, Trushell DMI, Elworthy S, Ingham PW, Whyte MKB. A Transgenic Zebrafish Model of Neutrophilic Inflammation. *Blood* (2006) 108:3976–8. doi: 10.1182/blood-2006-05-024075
38. Li M, Xie J, Zhao X, Li X, Wang R, Shan J, et al. Establishing the Foodborne-Enteritis Zebrafish Model and Imaging the Involved Immune Cells' Response. *Acta Hydrobiol Sinica* (2021). doi: 10.7541/2022.2021.104
39. Liu Y, Sun Y, Zhou Y, Tang X, Wang K, Ren Y, et al. Sinomenine Hydrochloride Inhibits the Progression of Plasma Cell Mastitis by Regulating IL-6/JAK2/STAT3 Pathway. *Int Immunopharmacol* (2020) 81:106025. doi: 10.1016/j.intimp.2019.106025
40. Xia X-Q, Wu N, Li M, Shi M, Cheng Y, Zhang W. Application of Sinomenine in Prevention and Treatment of Enterohepatitis Induced by Soybean Meal. In.Edited by Administration CNIP. (2019) 201910847367.X. China:.
41. Chen X, Guo W, Lei L, Guo Y, Yang L, Han J, et al. Bioconcentration and Developmental Neurotoxicity of Novel Brominated Flame Retardants, Hexabromobenzene and Pentabromobenzene in Zebrafish. *Environ Pollut* (2021) 268:115895. doi: 10.1016/j.envpol.2020.115895
42. Patra P, Ghosh P, Patra BC, Bhattacharya M. Biocomputational Analysis and in Silico Characterization of an Angiogenic Protein (RNase5) in Zebrafish (*Danio Rerio*). *Int J Pept Res Ther* (2020) 26:1687–97. doi: 10.1007/s10989-019-09978-1
43. Lickwar CR, Camp JG, Weiser M, Cocchiaro JL, Kingsley DM, Furey TS, et al. Genomic Dissection of Conserved Transcriptional Regulation in Intestinal Epithelial Cells. *PLoS Biol* (2017) 15:e2002054. doi: 10.1371/journal.pbio.2002054
44. Deng Y, Zhang Y, Chen H, Xu L, Wang Q, Feng J. Gut-Liver Immune Response and Gut Microbiota Profiling Reveal the Pathogenic Mechanisms of *Vibrio Harveyi* in Pearl Gentian Grouper (*Epinephelus Lanceolatus* Male Symbol X *E. Fuscoguttatus* Female Symbol). *Front Immunol* (2020) 11:607754. doi: 10.3389/fimmu.2020.607754
45. Quintana FJ, Iglesias AH, Farez MF, Caccamo M, Burns EJ, Kassam N, et al. Adaptive Autoimmunity and Foxp3-Based Immunoregulation in Zebrafish. *PLoS One* (2010) 5:e9478. doi: 10.1371/journal.pone.0009478
46. Johnson KM, Hofmann GE. A Transcriptome Resource for the Antarctic Pteropod *Limacina helicina antarctica*. *Mar Genomics* (2016) 28:25–8. doi: 10.1016/j.margen.2016.04.002
47. Kim D, Paggi JM, Park C, Bennett C, Salzberg SL. Graph-Based Genome Alignment and Genotyping With HISAT2 and HISAT-Genotype. *Nat Biotechnol* (2019) 37:907–15. doi: 10.1038/s41587-019-0201-4
48. Pertea M, Pertea GM, Antonescu CM, Chang TC, Mendell JT, Salzberg SL. StringTie Enables Improved Reconstruction of a Transcriptome From RNA-Seq Reads. *Nat Biotechnol* (2015) 33:290–5. doi: 10.1038/nbt.3122
49. Patro R, Duggal G, Love MI, Irizarry RA, Kingsford C. Salmon Provides Fast and Bias-Aware Quantification of Transcript Expression. *Nat Methods* (2017) 14:417–9. doi: 10.1038/nmeth.4197
50. Love MI, Huber W, Anders S. Moderated Estimation of Fold Change and Dispersion for RNA-Seq Data With Deseq2. *Genome Biol* (2014) 15:550. doi: 10.1186/s13059-014-0550-8
51. Yu G, Wang LG, Han Y, He QY. Clusterprofiler: An R Package for Comparing Biological Themes Among Gene Clusters. *OMICS* (2012) 16:284–7. doi: 10.1089/omi.2011.0118
52. Van Dycke J, Cuvry A, Knickmann J, Ny A, Rakers S, Taube S, et al. Infection of Zebrafish Larvae With Human Norovirus and Evaluation of the *In Vivo* Efficacy of Small-Molecule Inhibitors. *Nat Protoc* (2021) 16:1830–49. doi: 10.1038/s41596-021-00499-0
53. Callahan BJ, McMurdie PJ, Rosen MJ, Han AW, Johnson AJ, Holmes SP. DADA2: High-Resolution Sample Inference From Illumina Amplicon Data. *Nat Methods* (2016) 13:581–3. doi: 10.1038/nmeth.3869
54. Bokulich NA, Kaehler BD, Rideout JR, Dillon M, Bolyen E, Knight R, et al. Optimizing Taxonomic Classification of Marker-Gene Amplicon Sequences With QIIME 2's Q2-Feature-Classifier Plugin. *Microbiome* (2018) 6:90. doi: 10.1186/s40168-018-0470-z
55. DeSantis TZ, Hugenholtz P, Larsen N, Rojas M, Brodie EL, Keller K, et al. Greengenes, a Chimera-Checked 16S rRNA Gene Database and Workbench Compatible With ARB. *Appl Environ Microbiol* (2006) 72:5069–72. doi: 10.1128/AEM.03006-05
56. Wu N, Rao X, Gao Y, Wang J, Xu F. Amyloid-Beta Deposition and Olfactory Dysfunction in an Alzheimer's Disease Model. *J Alzheimers Dis* (2013) 37:699–712. doi: 10.3233/JAD-122443
57. Dee CT, Nagaraju RT, Athanasiadis EI, Gray C, Fernandez Del Ama L, Johnston SA, et al. CD4-Transgenic Zebrafish Reveal Tissue-Resident Th2- and Regulatory T Cell-Like Populations and Diverse Mononuclear Phagocytes. *J Immunol* (2016) 197:3520–30. doi: 10.4049/jimmunol.1600959
58. Elmessaoudi-Idrissi M, Tsukiyama-Kohara K, Nourlil J, Kettani A, Windisch MP, Kohara M, et al. Structure-Guided Discovery Approach Identifies Potential Lead Compounds Targeting M(pro) of SARS-CoV-2. *Virusdisease* (2020) 31:1–5. doi: 10.1007/s13337-020-00627-6
59. Kimura H, Imura YK, Tomiyasu H, Mihara T, Kaji N, Ohno K, et al. Neural Anti-Inflammatory Action Mediated by Two Types of Acetylcholine Receptors in the Small Intestine. *Sci Rep* (2019) 9:5887. doi: 10.1038/s41598-019-41698-w
60. Li J, Tan J, Martino MM, Lui KO. Regulatory T-Cells: Potential Regulator of Tissue Repair and Regeneration. *Front Immunol* (2018) 9:585. doi: 10.3389/fimmu.2018.00585
61. Cosovanu C, Neumann C. The Many Functions of Foxp3(+) Regulatory T Cells in the Intestine. *Front Immunol* (2020) 11:600973. doi: 10.3389/fimmu.2020.600973
62. Bai Q, Wei X, Burton EA. Expression of a 12-Kb Promoter Element Derived From the Zebrafish Enolase-2 Gene in the Zebrafish Visual System. *Neurosci Lett* (2009) 449:252–7. doi: 10.1016/j.neulet.2008.10.101
63. Martin-Martin A, Simon R, Abos B, Diaz-Rosales P, Tafalla C. Rainbow Trout Mount a Robust Specific Immune Response Upon Anal Administration of Thymus-Independent Antigens. *Dev Comp Immunol* (2020) 109:103715. doi: 10.1016/j.dci.2020.103715
64. Tokarz DA, Heffelfinger AK, Jima DD, Gerlach J, Shah RN, Rodriguez-Nunez I, et al. Disruption of Trim9 Function Abrogates Macrophage Motility *In Vivo*. *J Leukoc Biol* (2017) 102:1371–80. doi: 10.1189/jlb.1A0816-371R
65. Schrader JW, Scollay R, Battye F. Intramucosal Lymphocytes of the Gut - Lyt-2 and Thy-1 Phenotype of the Granulated Cells and Evidence for the Presence of Both T-Cells and Mast-Cell Precursors. *J Immunol* (1983) 130:558–64. doi: 10.1073/pnas.79.13.4161
66. Treede I, Braun A, Jeliaskova P, Giese T, Fullekrug J, Griffiths G, et al. TNF-Alpha-Induced Up-Regulation of Pro-Inflammatory Cytokines Is Reduced by Phosphatidylcholine in Intestinal Epithelial Cells. *BMC Gastroenterol* (2009) 9:53. doi: 10.1186/1471-230X-9-53
67. Li M, Wang H, Li W, Xu XG, Yu Y. Macrophage Activation on "Phagocytic Synapse" Arrays: Spacing of Nanoclustered Ligands Directs TLR1/2 Signaling With an Intrinsic Limit. *Sci Advances* (2020) 6:eabc8482. doi: 10.1126/sciadv.abc8482
68. Goodridge HS, Reyes CN, Becker CA, Katsumoto TR, Ma J, Wolf AJ, et al. Activation of the Innate Immune Receptor Dectin-1 Upon Formation of a 'Phagocytic Synapse'. *Nature* (2011) 472:471–5. doi: 10.1038/nature10071
69. Hartmann P, Seebauer CT, Mazagova M, Horvath A, Wang L, Llorente C, et al. Deficiency of Intestinal Mucin-2 Protects Mice From Diet-Induced Fatty Liver Disease and Obesity. *Am J Physiol Gastrointest Liver Physiol* (2016) 310:G310–322. doi: 10.1152/ajpgi.00094.2015
70. Huo HJ, Chen SN, Laghari ZA, Li L, Hou J, Gan Z, et al. Specific Bioactivity of IL-22 in Intestinal Cells as Revealed by the Expression of IL-22RA1 in Mandarin Fish, Siniperca Chuatsi. *Dev Comp Immunol* (2021) 121:104107. doi: 10.1016/j.dci.2021.104107

71. Liu W, Zhang Y, Zhu W, Ma C, Ruan J, Long H, et al. Sinomenine Inhibits the Progression of Rheumatoid Arthritis by Regulating the Secretion of Inflammatory Cytokines and Monocyte/Macrophage Subsets. *Front Immunol* (2018) 9:2228. doi: 10.3389/fimmu.2018.02228
72. Gui X, Li J, Ueno A, Iacucci M, Qian J, Ghosh S. Histopathological Features of Inflammatory Bowel Disease Are Associated With Different CD4+ T Cell Subsets in Colonic Mucosal Lamina Propria. *J Crohns Colitis* (2018) 12:1448–58. doi: 10.1093/ecco-jcc/jjy116
73. Cui ZW, Zhang XY, Zhang XJ, Wu N, Lu LF, Li S, et al. Molecular and Functional Characterization of the Indoleamine 2,3-Dioxygenase in Grass Carp *(Ctenopharyngodon Idella*). *Fish Shellfish Immunol* (2019) 89:301–8. doi: 10.1016/j.fsi.2019.04.005
74. Collier B, Dossett LA, May AK, Diaz JJ. Glucose Control and the Inflammatory Response. *Nutr Clin Pract* (2008) 23:3–15. doi: 10.1177/011542650802300103
75. Chen Z, Zhijie C, Yuting Z, Shilin X, Qichun Z, Jinying O, et al. Antibiotic-Driven Gut Microbiome Disorder Alters the Effects of Sinomenine on Morphine-Dependent Zebrafish. *Front Microbiol* (2020) 11:946. doi: 10.3389/fmicb.2020.00946
76. Jami M, Ghanbari M, Kneifel W, Domig KJ. Phylogenetic Diversity and Biological Activity of Culturable Actinobacteria Isolated From Freshwater Fish Gut Microbiota. *Microbiol Res* (2015) 175:6–15. doi: 10.1016/j.micres.2015.01.009
77. Wei X, Huang L, Li J, Ni Y. Probiotic Characteristics of Intestinal Flora and Lactic Acid Bacteria of Cold Water Fish in High Latitudes of China. In: *The 16th Annual Meeting of CFST*. Wuhan, China (2019).
78. McKee LS, La Rosa SL, Westereng B, Eijsink VG, Pope PB, Larsbrink J. Polysaccharide Degradation by the Bacteroidetes: Mechanisms and Nomenclature. *Environ Microbiol Rep* (2021) 13:559–81. doi: 10.1111/1758-2229.12980
79. Kuehbacher T, Rehman A, Lepage P, Hellmig S, Folsch UR, Schreiber S, et al. Intestinal TM7 Bacterial Phylogenies in Active Inflammatory Bowel Disease. *J Med Microbiol* (2008) 57:1569–76. doi: 10.1099/jmm.0.47719-0
80. Ma C, Guo H, Chang H, Huang S, Jiang S, Huo D, et al. The Effects of Exopolysaccharides and Exopolysaccharide-Producing Lactobacillus on the Intestinal Microbiome of Zebrafish (*Danio Rerio*). *BMC Microbiol* (2020) 20:300. doi: 10.1186/s12866-020-01990-6
81. Zhang Z, Taylor L, Shommu N, Ghosh S, Reimer R, Panaccione R, et al. A Diversified Dietary Pattern Is Associated With a Balanced Gut Microbial Composition of *Faecalibacterium* and *Escherichia/Shigella* in Patients With Crohn's Disease in Remission. *J Crohns Colitis* (2020) 14:1547–57. doi: 10.1093/ecco-jcc/jjaa084
82. Ye Q, Feng Y, Wang Z, Zhou A, Xie S, Fan L, et al. Effects of Dietary Gelsemium Elegans Alkaloids on Intestinal Morphology, Antioxidant Status, Immune Responses and Microbiota of Megalobrama Amblycephala. *Fish Shellfish Immunol* (2019) 94:464–78. doi: 10.1016/j.fsi.2019.09.048
83. Liu WS, Chen MC, Chiu KH, Wen ZH, Lee CH. Amelioration of Dextran Sodium Sulfate-Induced Colitis in Mice by *Rhodobacter Sphaeroides* Extract. *Molecules* (2012) 17:13622–30. doi: 10.3390/molecules171113622
84. Wang A, Zhang Z, Ding Q, Yang Y, Bindelle J, Ran C, et al. Intestinal Cetobacterium and Acetate Modify Glucose Homeostasis *via* Parasympathetic Activation in Zebrafish. *Gut Microbes* (2021) 13:1–15. doi: 10.1080/19490976.2021.1900996

Conflict of Interest: The authors declare that the research was conducted in the absence of any commercial or financial relationships that could be construed as a potential conflict of interest.

Publisher's Note: All claims expressed in this article are solely those of the authors and do not necessarily represent those of their affiliated organizations, or those of the publisher, the editors and the reviewers. Any product that may be evaluated in this article, or claim that may be made by its manufacturer, is not guaranteed or endorsed by the publisher.

Advantages of publishing in Frontiers

OPEN ACCESS
Articles are free to read for greatest visibility and readership

FAST PUBLICATION
Around 90 days from submission to decision

HIGH QUALITY PEER-REVIEW
Rigorous, collaborative, and constructive peer-review

TRANSPARENT PEER-REVIEW
Editors and reviewers acknowledged by name on published articles

Frontiers
Avenue du Tribunal-Fédéral 34
1005 Lausanne | Switzerland

Visit us: www.frontiersin.org
Contact us: frontiersin.org/about/contact

REPRODUCIBILITY OF RESEARCH
Support open data and methods to enhance research reproducibility

DIGITAL PUBLISHING
Articles designed for optimal readership across devices

FOLLOW US
@frontiersin

IMPACT METRICS
Advanced article metrics track visibility across digital media

EXTENSIVE PROMOTION
Marketing and promotion of impactful research

LOOP RESEARCH NETWORK
Our network increases your article's readership